

**SECOND
EDITION**

COMBUSTION

COMBUSTION

Irvin Glassman

Glassman

SECOND EDITION



**ACADEMIC
PRESS**

Combustion

Second Edition

IRVIN GLASSMAN

*Department of Mechanical and Aerospace Engineering
Princeton University
School of Engineering and Applied Science
Princeton, New Jersey*

1987



ACADEMIC PRESS, INC.

Harcourt Brace Jovanovich, Publishers
Orlando San Diego New York Austin
Boston London Sydney Tokyo Toronto

COPYRIGHT © 1987 BY ACADEMIC PRESS, INC.
ALL RIGHTS RESERVED.
NO PART OF THIS PUBLICATION MAY BE REPRODUCED OR
TRANSMITTED IN ANY FORM OR BY ANY MEANS, ELECTRONIC
OR MECHANICAL, INCLUDING PHOTOCOPY, RECORDING, OR
ANY INFORMATION STORAGE AND RETRIEVAL SYSTEM, WITHOUT
PERMISSION IN WRITING FROM THE PUBLISHER.

ACADEMIC PRESS, INC.
Orlando, Florida 32887

United Kingdom Edition published by
ACADEMIC PRESS INC. (LONDON) LTD.
24-28 Oval Road, London NW1 7DX

Library of Congress Cataloging in Publication Data

Glassman, Irvin.
Combustion.

Includes index.

1. Combustion. I. Title.

QD516.G55 1986 541.3'61 86-13975

ISBN 0-12-285851-4 (alk. paper)

PRINTED IN THE UNITED STATES OF AMERICA

86 87 88 89 9 8 7 6 5 4 3 2 1

To
My Graduate Students
Past and Present
for the continual joy and pride they have given me

“No man can reveal to you aught but that which already lies half asleep in the dawning of your knowledge.

If he (the teacher) is wise he does not bid you to enter the house of his wisdom, but leads you to the threshold of your own mind.

The astronomer may speak to you of his understanding of space, but he cannot give you his understanding.

And he who is versed in the science of numbers can tell of the regions of weight and measures, but he cannot conduct you thither.

For the vision of one man lends not its wings to another man.”

Gibran, THE PROPHET



Contents

<i>Preface to Second Edition</i>	xv
<i>Acknowledgments to the Second Edition</i>	xvii
<i>Preface to First Edition</i>	xix
<i>Acknowledgments to the First Edition</i>	xxi

Chapter One **Chemical Thermodynamics and Flame Temperatures**

A. Introduction	1
B. Heats of Reaction and Formation	1
C. Free Energy and the Equilibrium Constants	6
D. Flame Temperature Calculations	15
Problems	27
References	30

Chapter Two **Chemical Kinetics**

A. Introduction	31
B. The Rates of Reactions and Their Temperature Dependency	32
1. The Arrhenius Rate Expression	33
2. Transition State and Recombination Rate Theories	36
C. Simultaneous Interdependent Reactions	40
D. Chain Reactions	41
E. Pseudo-First-Order Reactions and the "Fall-Off" Range	44
F. The Partial Equilibrium Assumption	47
G. Pressure Effect in Fractional Conversion	48
Problems	48
References	50

Chapter Three Explosive and General Oxidative Characteristics of Fuels

A. Introduction	51
B. Chain Branching Reactions and Criteria for Explosion	51
C. Explosion Limits and Oxidation Characteristics of Hydrogen	56
D. Explosion Limits and Oxidation Characteristics of Carbon Monoxide	63
E. Explosion Limits and Oxidation Characteristics of Hydrocarbons	67
1. Organic Nomenclature	68
2. Explosion Limits	72
a. The Negative Coefficients of Reaction Rate	73
b. Cool Flames	74
3. "Low-Temperature" Hydrocarbon Oxidation Mechanisms	75
a. Competition Between Chain Branching and Steady Reaction Steps	76
b. Importance of Isomerization in Large Hydrocarbon Radicals	78
F. The Oxidation of Aldehydes	81
G. The Oxidation of Methane	81
H. The Oxidation of Higher-Order Hydrocarbons	85
1. Aliphatic Hydrocarbons	85
a. Overall View	85
b. Paraffin Oxidation	87
c. Olefin and Acetylene Oxidation	90
2. Alcohols	94
3. Aromatic Hydrocarbons	96
a. Benzene Oxidation	96
b. Oxidation of Alkylated Aromatics	102
Problems	104
References	105

Chapter Four Flame Phenomena in Premixed Combustible Gases

A. Introduction	107
B. Laminar Flame Structure	111
C. The Laminar Flame Speed	114
1. The Theory of Mallard and Le Chatelier	117
2. The Theory of Zeldovich, Frank-Kamenetskii, and Semenov	119
3. The Laminar Flame and the Energy Equation	126
4. Flame Speed Measurements	126
a. Burner Method	130
b. Cylindrical Tube Method	131
c. Soap Bubble Method	132
d. Closed Spherical Bomb Method	132
e. Flat Flame Burner Method	133
5. Experimental Results—Physical and Chemical Effects	134
D. Stability Limits of Laminar Flames	141
1. Flammability Limits	142
2. Quenching Distance	148
3. Flame Stabilization (Low Velocity)	150

a. Flashback and Blowoff	151
b. Analysis and Results	151
4. Stability Limits and Design	156
E. Turbulent Reacting Flows and Turbulent Flames	159
1. The Rate of Reaction in a Turbulent Field	161
2. Regimes of Turbulent Reacting Flows	163
3. The Turbulent Flame Speed	175
F. Stirred Reactor Theory	178
G. Flame Stabilization in High-Velocity Streams	182
Problems	192
References	194

Chapter Five Detonation

A. Introduction	197
1. Premixed and Diffusion Flames	197
2. Explosion, Deflagration, and Detonation	198
3. The Onset of Detonation	198
B. Detonation Phenomena	201
C. Hugoniot Relations and the Hydrodynamic Theory of Detonations	202
1. Characterization of the Hugoniot Curve and the Uniqueness of the Chapman–Jouguet Point	203
2. Determination of the Speed of Sound in the Burned Gases for Conditions above the Chapman–Jouguet Point	211
a. Behavior of the Entropy along the Hugoniot Curve	211
b. The Concavity of the Hugoniot Curve	212
c. The Burned Gas Speed	214
3. Calculation of the Detonation Velocity	216
D. Comparison of Detonation Velocity Calculations with Experimental Results	220
E. The ZND Structure of Detonation Waves	223
F. The Structure of the Cellular Detonation Front and other Detonation Phenomena Parameters	226
1. The Cellular Detonation Front	226
2. The Dynamic Detonation Parameters	230
3. Detonation Limits	231
G. Detonations in Nongaseous Media	235
Problems	235
References	236

Chapter Six Diffusion Flames

A. Introduction	238
B. Gaseous Fuel Jets	239
1. Appearance	239
2. Structure	242
3. Theoretical Considerations	245
4. The Burke–Schumann Development	248
5. Turbulent Fuel Jets	254
C. Burning of Condensed Phases	255
1. General Mass Burning Considerations and the Evaporation Coefficient	256

2. Single Fuel Droplets in Quiescent Atmospheres	260
a. Heat and Mass Transfer without Chemical Reaction (Evaporation)— the Transfer Number B	262
b. Heat and Mass Transfer with Chemical Reaction (Droplet Burning Rates)	268
c. Refinements of the Mass Burning Rate Expression	275
D. Burning of Droplet Clouds	280
E. Burning in Convective Atmospheres	281
1. The Stagnant Film Case	281
2. The Longitudinally Burning Surface	283
3. The Flowing Droplet Case	285
4. Burning Rates of Plastics; The Small B Assumption and Radiation Effects	288
Problems	288
References	290

Chapter Seven Ignition

A. Concepts	292
B. Chain Spontaneous Ignition	295
C. Thermal Spontaneous Ignition	297
1. Semenov Approach to Thermal Ignition	298
2. Frank-Kamenetskii Theory of Thermal Ignition	303
a. The Stationary Solution—The Critical Mass and Spontaneous Ignition Problems	303
b. The Nonstationary Solution	305
D. Forced Ignition	308
1. Spark Ignition and Minimum Ignition Energy	309
2. Ignition by Adiabatic Compression and Shock Waves	315
Problems	316
References	316

Chapter Eight Environmental Combustion Considerations

A. Introduction	318
B. The Nature of Photochemical Smog	319
1. Primary and Secondary Pollutants	320
2. The Effect of NO_x	321
3. The Effect of SO_x	324
C. NO_x Formation and Reduction	326
1. The Structure of the Nitrogen Oxides	327
2. The Effect of Flame Structure	328
3. Atmospheric Nitrogen Kinetics	329
4. Fuel-Bound Nitrogen Kinetics	337
5. The Formation of NO_2	340
6. The Reduction of NO_x	342
D. SO_x Emissions	345
1. The Product Composition and Structure of Sulfur Compounds	346
2. Oxidative Mechanisms of Sulfur Fuels	348
a. H_2S	349

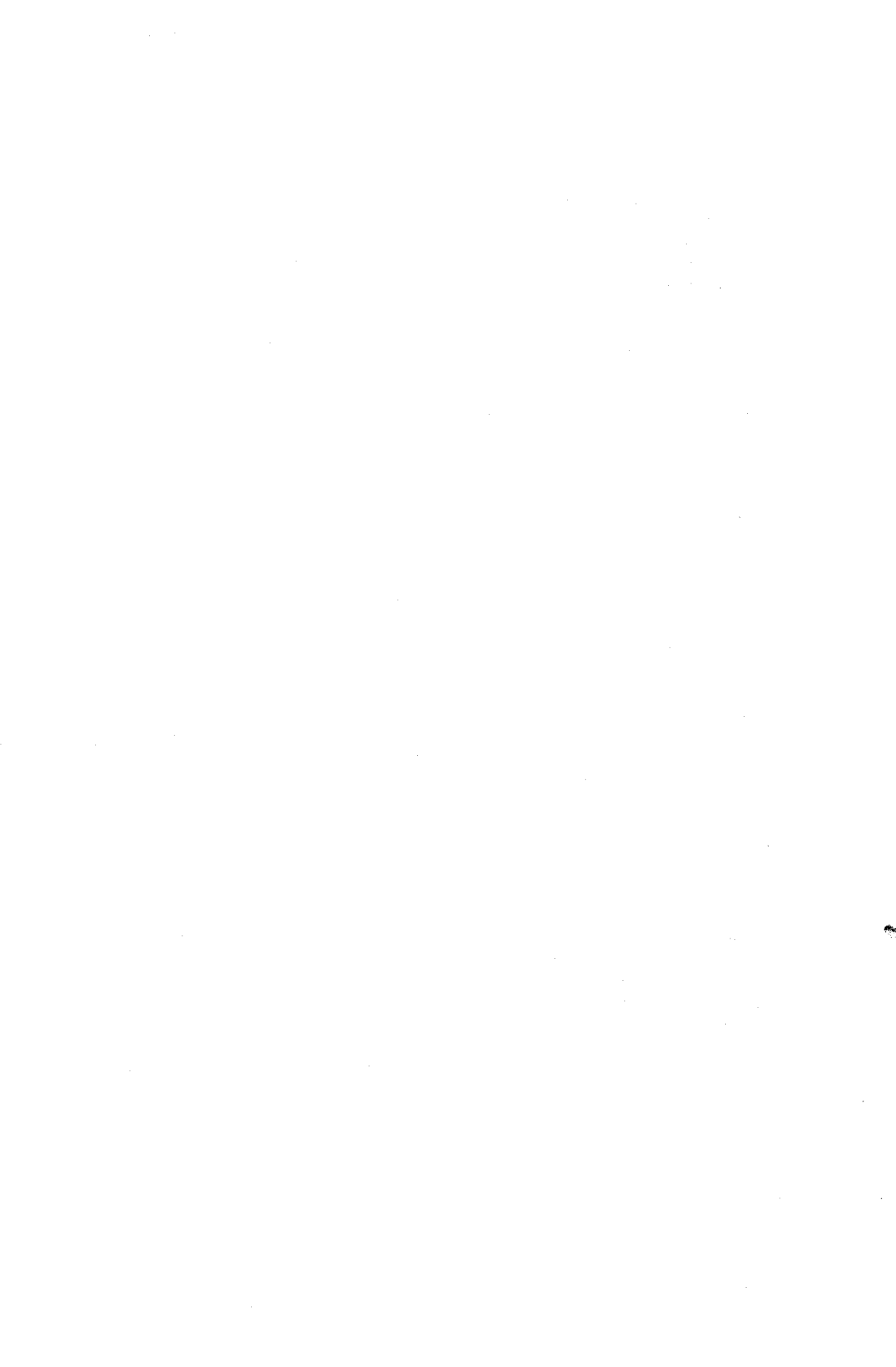
b. COS and CS ₂	353
c. Elemental Sulfur	354
d. Organic Sulfur Compounds	355
e. Sulfur Trioxide and Sulfates	357
f. SO _x -NO _x Interactions	360
E. Particulate Formation	360
1. Characteristics of Soot	361
2. Soot Formation Processes	362
3. The Use of Flames in Soot Formation Analyses	365
a. Premixed Flames	366
b. Diffusion Flames	369
4. The Influence of Physical and Chemical Parameters on Soot Formation	373
5. Particulates from Liquid Hydrocarbon Pyrolysis	375
F. Stratospheric Ozone	376
1. The HO _x Catalytic Cycle	376
2. The NO _x Catalytic Cycle	377
3. The ClO _x Catalytic Cycle	380
Problems	382
References	382

Chapter Nine The Combustion of Nonvolatile Fuels

A. Carbon Char and Metal Combustion	386
B. Diffusion Kinetics	388
C. Diffusion Controlled Burning Rate	390
1. The Burning of Carbon Char Particles	391
2. The Burning of Boron Particles	394
3. The Role of Gaseous Inerts in Heterogeneous Diffusion Burning	396
4. Oxidation of Very Small Particles—Pulverized Coal and Soot	397
D. The Burning of Porous Chars	404
E. The Burning Rate of Ash-Forming Coal	407
Problems	409
References	410

Appendixes	411
Appendix A. Thermochemical Data and Conversion Factors	413
Appendix B. Specific Reaction Rate Constants	448
Appendix C. Bond Dissociation Energies of Hydrocarbons	454
Appendix D. Laminar Flame Speeds	460
Appendix E. Flammability Limits in Air	465
Appendix F. Spontaneous Ignition Temperature Data	472
Appendix G. Minimum Spark Ignition Energies and Quenching Distances	486

<i>Indexes</i>	491
----------------	-----



Preface to the Second Edition

Motivations to write a second edition of *Combustion* were numerous. Great progress has been made in many areas of this field, and the original edition was being used as a text and therefore required problem sets and improved methods of explaining many of the basic concepts that had evolved over another decade of teaching. Every chapter of the original edition has been enlarged and, it is hoped, improved with new material, concepts, or methods of presentation.

Chapter One has been expanded with more detailed developments with respect to the relationship of the equilibrium constant to the basic thermodynamic properties. In addition, a method of rapidly estimating the flame temperature of any CH hydrocarbon in air is presented. Chapter Two now contains a more detailed discussion of chemical kinetics, particularly as it relates to transition state theory, chain reaction concepts, and the "fall-off" pressure effect. Chapter Three now provides a more extensive discussion of aliphatic and aromatic hydrocarbon oxidation processes at both low and high temperatures. The structure of a laminar flame and effects of turbulence on chemical systems such as flames are now considered in great detail in Chapter Four. The major modifications to Chapter Five consist of a completely revised discussion of the structure of the detonation front and the introduction of some discussion of the dynamic detonation parameters.

Buoyancy effects in gaseous diffusion flames, transient heating effects in droplet burning, and conceptual ideas in developing the Spalding B variables comprise the new material introduced in Chapter Six. Chapter Seven has been completely revised to integrate the concepts of both chain and thermal spontaneous ignition concepts. Discussion of forced ignition and, particularly, the minimum ignition energy concept has been added as well. Chapter Eight

contains extensive new material on SO_x , NO_x , and soot formation processes. Chapter Nine now considers the combustion of low volatile metals as well as carbon char. Also included is new material on the controlling elements in pulverized coal and soot oxidation.

The idea of adding appendixes first evolved in order to provide data required for the problem sets added to each chapter. However, various data collections have accumulated in the author's laboratory. Such data have proven to be of enormous convenience for many research purposes. Since no complete compilation of combustion data was known to exist, it was decided to expand the initial idea of the appendixes to meet a more general need and to include a large number which would provide a wide source of various data needed in combustion considerations. The author hopes this material will be as useful to the reader as it has been to the author in the past.

Acknowledgments to the Second Edition

Many people have contributed directly and indirectly to the content of this second edition. In particular, I must recognize the numerous stimulating discussions I have had with my colleagues F. A. Williams, F. L. Dryer, and K. Brezinsky. Professor Williams was very generous in making a draft of the second edition of his book *Combustion Theory* available to me during my writing. This draft was a stimulus to my thinking about many revisions I have made.

In much of the material added in the text, I drew heavily from the work of Westbrook and Dryer, Libby and Williams, Mulcahy and Smith, Bray and Lee. For the appendixes the major sources of data were from the compilers of the JANAF tables and the compilations of Westbrook and Dryer, McMillen and Golden, Gibbs and Calcote, Zebatakis, Mullins, Calcote, Gregory, and Barnett and Gilmer. I wish to express my appreciation to all these authors. K. Brezinsky, R. Yetter, C. Fernandez-Pello, M. Sichel, F. A. Williams, E. Dibora, D. Seery, and A. Sarofim each read a draft chapter of this revised edition and offered many helpful comments. To them, thanks are due as well.

One's research environment provides the stimulus and background for such an endeavor as writing a book. I must thank the Air Force Office of Scientific Research and the Mobil Research and Development Corporation for their continued support of my research program and J. A. Sivo, D. Peoples, and the late T. A. Bozowski for making that research program work.

Thanks are also due to Mrs. Memory J. Leleszi who typed the many drafts of this effort, and to Mrs. Norma-Jean Proscia who typed some of the first chapters. Mrs. Betty Adam ably assisted with the appendixes. As to be expected, my wife Beverly's support was always there.

Preface to the First Edition

During my twenty years of teaching combustion at Princeton, I had accumulated extensive lecture notes and developed my own approach to the subject matter. For years former students and associates have encouraged me to publish these notes. This book is the result.

My whole concept of teaching has been to stimulate the student to think, to learn the material on his own, and to understand how to use it in his own research and development endeavors. It is difficult to assess whether this concept will prevail in this book. Combustion is a most complex subject that involves primarily the disciplines of chemistry, physics, and fluid mechanics. However, it is important to understand that approaches to a complex subject can be made in a fundamental manner. One must gain the physical insight into underlying principles. Although many subjects are presented, I have tried to strip away the complexities and elaborate upon the physical insights essential to understanding. Chapter Nine on coal combustion epitomizes this approach. When I thought it necessary to cover this topic in class, I was surprised that there was not readily available in the literature some of the simple results developed in this chapter.

The subject matter which comprises the field of combustion is diverse. No attempt has been made to develop a unified approach to all material. Indeed, in my opinion, in order to gain the best insight the approach should vary with the subject matter.

Acknowledgments to the First Edition

My understanding of combustion came about from many associations. The one that I cherished the most has been with my own graduate students. Their contributions to this book are many. In particular, I must recognize and thank Dr. F. L. Dryer who chose to remain at Princeton and assume numerous responsibilities in our laboratory while I undertook other endeavors—such as writing this book.

The foundation for much of what I have written was developed during 25 years of research in the field. I had no previous experience or training in this prior to coming to Princeton. Practically all my Princeton research was sponsored by the U.S. government. Thus I would also like to recognize the confidence expressed in me by the technical monitors of my research contracts and grants. They deserve the thanks of many of us. In particular, I owe much to Dr. J. F. Masi of the Air Force Office of Scientific Research for his particular interest in the contributions he thought I could make by my approach to combustion. I hope this book is another such contribution.

Special thanks are due to my wife and children who gave me the love and happiness necessary to pursue this arduous, but enjoyable, career.

Chemical Thermodynamics and Flame Temperatures

A. INTRODUCTION

The most essential parameters necessary for the evaluation of combustion systems are the equilibrium product temperature and composition. If all the heat evolved in the reaction is employed solely to raise the product temperature, then this temperature is called the adiabatic flame temperature. Because of the importance of the temperature and gas composition in combustion considerations, it is useful to review those aspects of the field of chemical thermodynamics which deal with these subjects.

B. HEATS OF REACTION AND FORMATION

All chemical reactions are accompanied either by an absorption or evolution of energy, which usually manifests itself as heat. It is possible to determine this amount of heat and thus the temperature and product composition from very basic principles. Spectroscopic data and statistical calculations permit one to determine the internal energy of a substance. The internal energy of a given substance is found to be dependent upon its temperature, pressure, and state and is independent of the means by which

the state was attained. Likewise the change in internal energy, ΔE , of a system which results from any physical change or chemical reaction depends only on the initial and final state of the system. The total change in internal energy will be the same, whether or not the energy is evolved in any form of heat, energy, or work.

For a flow reaction proceeding with negligible changes in kinetic energy, potential energy, and with no form of work beyond that required for flow, the heat added is equal to the increase of enthalpy of the system

$$Q = \Delta H$$

where Q is the heat added and H is the enthalpy. For a nonflow reaction proceeding at constant pressure, the heat added is also equal to the gain in enthalpy

$$Q_p = \Delta H$$

and if heat is evolved,

$$Q_p = -\Delta H$$

Most thermochemical calculations are made for closed thermodynamic systems, and the stoichiometry is most conveniently represented in terms of the molar quantities as determined from statistical calculations. In dealing with compressible flow problems in which it is essential to work with open thermodynamic systems, it is best to employ mass quantities. Upper case symbols will be used for molar quantities, and lower case symbols will be used for mass quantities.

One of the most important thermodynamic facts to be known about a given chemical reaction is the change in energy or heat content associated with the reaction at some specified temperature, with each of the reactants and products in an appropriate standard state. This change is known either as the energy or heat of reaction at the specified temperature.

The standard state means that for each state a reference state of the aggregate exists. For gases, the thermodynamic standard reference state is taken equal to the ideal gaseous state at atmospheric pressure at each temperature. The ideal gaseous state is the case of isolated molecules which give no interactions and which obey the equation of state of a perfect gas. The standard reference state for pure liquids and solids at a given temperature is the real state of the substance at a pressure of one atmosphere.

The thermodynamic symbol which represents the property of the substance in the standard state at a given temperature is written, for example, as H_T° , E_T° , etc., where the superscript $^\circ$ specifies the standard state and the subscript T the specific temperature. Statistical calculations actually permit

the determination of $E_T - E_0$, which is the energy content at a given temperature referred to the energy content at 0 K. For one mole in the ideal gaseous state,

$$PV = RT \quad (1)$$

$$H^\circ = E^\circ + (PV)^\circ = E^\circ + RT \quad (2)$$

which at 0 K reduces to

$$H_0^\circ = E_0^\circ \quad (3)$$

Thus the heat content at any temperature referred to the heat or energy content at 0 K is known and

$$(H^\circ - H_0^\circ) = (E^\circ - E_0^\circ) + RT = (E^\circ - E_0^\circ) + PV \quad (4)$$

The value $(E^\circ - E_0^\circ)$ is determined from spectroscopic information and is actually the energy in the internal (rotational, vibrational, and electronic) and external (translational) degrees of freedom of the molecule. Enthalpy $(H^\circ - H_0^\circ)$ only has meaning when there is a group of molecules, a mole for instance, and is thus the ability of a group of molecules with internal energy to do PV work. In this sense then a single molecule can have internal energy but not enthalpy.

From the definition of the heat of reaction, Q_p will depend on the temperature T at which the reaction and product enthalpies are evaluated. The heat of reaction at one temperature T_0 can be related to that at another temperature T_1 . Consider the reaction configuration shown in Fig. 1. According to the First Law, the heat changes that proceed from reactants at temperatures T_0 to products at temperature T_1 by either Path A or Path B shown must be the same. Path A raises the reactants from temperature T_0 to T_1 and reacts at T_1 . Path B reacts at T_0 and raises the products from T_0 to T_1 .

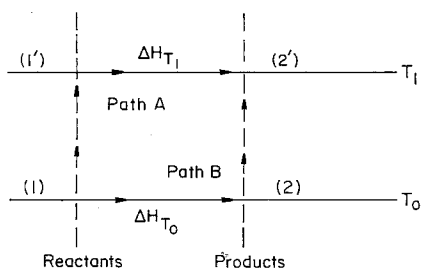


Fig. 1. Heats of reaction at different temperatures.

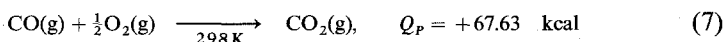
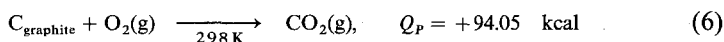
This energy equality, which relates the heats of reaction at the two different temperatures, is written as

$$\left\{ \sum_{j_{\text{react}}} n_j [(H_T^\circ - H_0^\circ) - (H_{T_0}^\circ - H_0^\circ)]_j \right\} + \Delta H_{T_1}$$

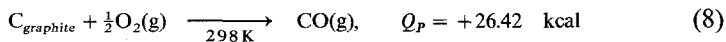
$$= \Delta H_{T_0} + \left\{ \sum_{i_{\text{prod}}} n_i [(H_{T_1}^\circ - H_0^\circ) - (H_{T_0}^\circ - H_0^\circ)]_i \right\} \quad (5)$$

Any phase changes can be included in the heat content terms. Thus, by knowing the difference in energy content at the different temperatures for the products and reactants, it is possible to determine the heat of reaction at one temperature from the heat of reaction at another.

If the heats of reaction at a given temperature are known for two separate reactions, the heat of reaction of a third reaction at the same temperature may be determined by simple algebraic addition. This statement is the Law of Heat Summation. For example, given below are two reactions that can be carried out conveniently in a calorimeter at constant pressure



Subtracting these two reactions one obtains



Since some of the carbon would burn to CO_2 and not solely CO , it is difficult to determine calorimetrically the heat released by reaction (8).

It is, of course, not necessary to have an extensive list of heats of reaction to determine the heat absorbed or evolved in every possible chemical reaction. A more convenient and logical procedure is to list what are known as the standard heats of formation of chemical substances. The standard heat of formation is the enthalpy of a substance in its standard state referred to its elements in their standard states at the same temperature. From this definition it is obvious that heats of formation of the elements in their standard states are zero.

The value of the heat of formation of a given substance from its elements may be the result of the determination of the heat of one reaction. Thus, from the calorimetric reaction for burning carbon to CO_2 [Eq. (6)], it is possible to write the heat of formation of carbon dioxide at 298 K as

$$(\Delta H_f^\circ)_{298, \text{CO}_2} = -94.05 \text{ kcal/mole}$$

The superscript to the heat of formation symbol ΔH_f represents the standard state and the subscript number the base or reference temperature. From the example for the Law of Heat Summation, it is apparent that the heat of formation of carbon monoxide from Eq. (8) is

$$(\Delta H_f^\circ)_{298, \text{CO}} = -26.42 \text{ kcal/mole}$$

It is evident that, by judicious choice, the number of reactions that must be measured calorimetrically will be about the same as the number of substances whose heats of formation are to be determined.

TABLE 1

Heats of formation at 298.1 K

Chemical symbol	Name	State	ΔH_f° (kcal/mole)	Δh_f° (kcal/gm)
C	Carbon	Vapor	126.36	10.530
N	Nitrogen atom	Gas	112.97	8.069
O	Oxygen atom	Gas	59.56	3.723
C ₂ H ₂	Acetylene	Gas	54.19	2.084
H	Hydrogen atom	Gas	52.09	52.090
O ₃	Ozone	Gas	34.00	0.708
NO	Nitric oxide	Gas	21.60	0.720
C ₆ H ₆	Benzene	Gas	19.80	0.254
C ₆ H ₆	Benzene	Liquid	11.71	0.150
C ₂ H ₄	Ethene	Gas	12.50	0.446
N ₂ H ₄	Hydrazine	Liquid	12.05	0.377
OH	Hydroxyl radical	Gas	10.06	0.592
O ₂	Oxygen	Gas	0	0
N ₂	Nitrogen	Gas	0	0
H ₂	Hydrogen	Gas	0	0
C	Carbon	Solid	0	0
NH ₃	Ammonia	Gas	-11.04	-0.649
C ₂ H ₄ O	Ethylene oxide	Gas	-12.19	-0.277
CH ₄	Methane	Gas	-17.89	-1.118
C ₂ H ₆	Ethane	Gas	-20.24	-0.675
CO	Carbon monoxide	Gas	-26.42	-0.944
C ₄ H ₁₀	Butane	Gas	-29.81	-0.518
CH ₃ OH	Methanol	Gas	-48.10	-1.503
CH ₃ OH	Methanol	Liquid	-57.04	-1.83
H ₂ O	Water	Gas	-57.80	-3.211
C ₈ H ₁₈	Octane	Liquid	-59.74	-0.524
H ₂ O	Water	Liquid	-68.32	-3.796
SO ₂	Sulfur dioxide	Gas	-71.00	-1.108
C ₁₂ H ₂₆	Dodecane	Liquid	-83.00	-0.519
CO ₂	Carbon dioxide	Gas	-94.05	-2.138
SO ₃	Sulfur trioxide	Gas	-94.45	-1.180

The logical consequence of the above is that, given the heats of formation of the substances which make up any particular reaction, one can determine directly the heat of reaction or heat evolved at the reference temperature T_0 as follows

$$\Delta H_{T_0} = \sum_{i \text{ prod}} n_i (\Delta H_f^\circ)_{T_0, i} - \sum_{j \text{ react}} n_j (\Delta H_f^\circ)_{T_0, j} = -Q_p \quad (9)$$

There exist extensive tables of standard heats of formation, but all are not at the same or reference temperature. The most convenient are the compilations known as the JANAF [1] and NBS Tables [2], both of which use 298 K as the reference temperature. Table 1 lists some values of the heat of formation taken from the JANAF Thermochemical Tables. Actual JANAF tables are reproduced in Appendix A. These tables are only a small selection from the JANAF volume and were chosen to aid in the problem sets throughout this book. Note as well that although the developments throughout this book take the reference state as 298.1 K the JANAF Tables also list ΔH_f° 's for all temperatures.

C. FREE ENERGY AND THE EQUILIBRIUM CONSTANTS

For those cases in which the products are measured at a different temperature T_2 than the reference temperature T_0 , and the reactants enter the reaction system as well as a different temperature T'_0 than the reference temperature, the heat of reaction becomes

$$\begin{aligned} \Delta H &= \sum_{i \text{ prod}} n_i [\{ (H_{T_2}^\circ - H_0^\circ) - (H_{T_0}^\circ - H_0^\circ) \} + (\Delta H_f^\circ)_{T_0, i}] \\ &\quad - \sum_{j \text{ react}} n_j [\{ (H_{T'_0}^\circ - H_0^\circ) - (H_{T_0}^\circ - H_0^\circ) \} + (\Delta H_f^\circ)_{T_0, j}] \\ &= -Q_p(\text{evolved}) \end{aligned} \quad (10)$$

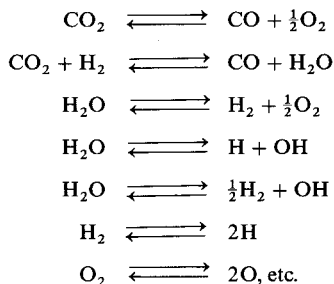
Most systems are considered to have the reactants enter at the standard reference temperature 298 K. Consequently the enthalpy terms in the braces for the reactants disappear. The JANAF Tables tabulate, as a supposed convenience, $(H_T^\circ - H_{298}^\circ)$ instead of $(H_T^\circ - H_0^\circ)$. This type of tabulation is unfortunate since for systems using cryogenic fuels and oxidizers, such as rockets, the reactants can enter the system at temperatures lower than the reference temperature. Indeed the fuel and oxidizer individually could enter at different temperatures, and the summation in Eq. (10) can be handled conveniently by realizing that T'_0 may vary with the substance j .

When all the heat evolved is used to heat up the product gases, ΔH and Q_p becomes zero. The product temperature T_2 in this case is called the adiabatic flame temperature and Eq. (10) becomes

$$\begin{aligned} & \sum_{i \text{ prod}} n_i [(H_{T_2}^\circ - H_0^\circ) - (H_{T_0}^\circ - H_0^\circ)] + (\Delta H_f^\circ)_{T_0}]_i \\ & = \sum_{j \text{ react}} n_j [(H_{T_0}^\circ - H_0^\circ) - (H_{T_0}^\circ - H_0^\circ)] + (\Delta H_f^\circ)_{T_0}]_j \end{aligned} \quad (11)$$

It is to be noted again that T_0 can be different for each reactant. Since the heats of formation throughout this text will always be considered as those evaluated at the reference temperature $T_0 = 298 \text{ K}$, the expression $[(H_T^\circ - H_0^\circ) - (H_T^\circ - H_0^\circ)] = (H_T^\circ - H_{T_0}^\circ)$, which is the value listed in the JANAF tables (see Appendix A).

If the products n_i of this reaction are known, then Eq. (11) can be solved for the flame temperature. For a reacting lean system whose product temperature is less than 1250 K, the products are the normal stable species CO_2 , H_2O , N_2 , and O_2 , whose molar quantities can be determined from simple mass balances. However most combustion systems reach temperatures appreciably greater than 1250 K, and dissociation of the stable species occurs. Since the dissociation reactions are quite endothermic, a few percent dissociation can lower the flame temperature substantially. The stable products from a C-H-O reaction system can dissociate by any of the following reactions:



Each of these dissociation reactions also specifies a definite equilibrium concentration of each product at a given temperature; consequently, the reactions are written as equilibrium reactions. Whereas in heat of reaction experiments or low-temperature combustion experiments, the products could be specified from the chemical stoichiometry, one sees now that with dissociation the specification of the product concentrations becomes much more complex and the n_i 's in the flame temperature equation [Eq. (11)] are as unknown as the flame temperature itself. In order to solve the equation for the n_i 's and T_2 , it is apparent that more than mass balance equations are

needed. The necessary equations are found in the equilibrium relationships which exist among the product composition in the equilibrium system.

The conditions for equilibrium are determined from the combined form of the first and second laws of thermodynamics, i.e.,

$$dE = T dS - P dV \quad (12)$$

where S is the entropy. This condition applies to any change affecting a system of constant mass in the absence of gravitational, electrical, and surface forces. However, the energy content of the system can be changed by introducing more mass. Consider the contribution to the energy of the system on adding one molecule i to be μ_i . The introduction of a small number dn_i of the same type contributes a gain in energy of the system of $\mu_i dn_i$. All the possible reversible increases in the energy of the system due to each type molecule i can be summed to give

$$dE = T dS - P dV + \sum_i \mu_i dn_i \quad (13)$$

It is apparent from the definition of enthalpy H and the introduction of the concept of Gibbs free energy F

$$F \equiv H - TS \quad (14)$$

that

$$dH = T dS + V dP + \sum_i \mu_i dn_i \quad (15)$$

and

$$dF = -S dT + V dP + \sum_i \mu_i dn_i \quad (16)$$

It is to be recalled that P and T are intensive properties and are independent of the size or mass of the system; whereas E , H , F , and S (also V and n) are extensive properties and, thus, increase in proportion to mass or size. By writing the general relation for the total derivative with respect to Eq. (16), one obtains

$$dF = \left(\frac{\partial F}{\partial T} \right)_{P, n_i} dT + \left(\frac{\partial F}{\partial P} \right)_{T, n_i} dP + \sum_i \left(\frac{\partial F}{\partial n_i} \right)_{P, T, n_j (j \neq i)} dn_i \quad (17)$$

Thus,

$$\mu_i = \left(\frac{\partial F}{\partial n_i} \right)_{T, P, n_j} \quad (18)$$

or more generally from dealing with the equations for E and H

$$\mu_i = \left(\frac{\partial F}{\partial n_i} \right)_{T, P, n_j} = \left(\frac{\partial E}{\partial n_i} \right)_{S, V, n_i} = \left(\frac{\partial E}{\partial n_i} \right)_{S, P, n_i} \quad (19)$$

where μ_i is called the chemical potential or the partial molal free energy. The condition of equilibrium is that the entropy of the system has a maximum value for all possible configurations that are consistent with constancy of energy and volume. If the entropy of any system at constant volume and temperature is at its maximum value, the system is at equilibrium and, therefore, in any change from its equilibrium state dS is zero. It follows then from Eq. (13) that the condition for equilibrium is

$$\sum \mu_i dn_i = 0 \quad (20)$$

The introduction of the concept of the chemical potential is due to the importance this property plays in reacting systems. In this context one may consider that a reaction moves in the direction of decreasing chemical potential and reaches equilibrium only when the potential of the reactants equals that of the products [3].

Thus, from Eq. (16) the criteria for equilibrium for combustion products of a chemical system at constant T and P is

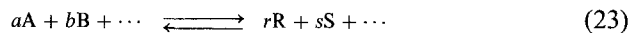
$$(dF)_{T, P} = 0 \quad (21)$$

and it becomes possible to determine the relationship between the Gibbs free energy and the equilibrium partial pressures of a combustion product mixture.

One deals with perfect gases so that there are no forces of interactions between the molecules except at the instant of reaction, and, thus, each gas acts as if it were in a container alone. Let F the total free energy of a product mixture be represented by

$$F = \sum n_i F_i, \quad i = A, B, \dots, R, S \quad (22)$$

for an equilibrium reaction among arbitrary products:



It is important to stress that A, B, \dots, R, S, \dots represent substances in the products only and a, b, \dots, r, s, \dots are the stoichiometric coefficients that govern the proportions by which different substances appear in the arbitrary equilibrium system chosen. The n_i 's are the instantaneous number of each compound. Under the ideal gas assumption the free energies are additive as shown above. This assumption permits one to neglect the free energy of mixing. Thus, as stated earlier

$$F(p, T) = H(T) - TS(p, T) \quad (24)$$

Since the standard state pressure for a gas is $p_0 = 1$ atm, one may write

$$F^\circ(p_0, T) = H^\circ - TS^\circ(p_0, T) \quad (25)$$

Subtracting the last two equations, one obtains

$$F - F^\circ = (H - H^\circ) - T(S - S^\circ) \quad (26)$$

Since H is not a function of pressure, $H - H^\circ$ must be zero and then

$$F - F^\circ = -T(S - S^\circ) \quad (27)$$

Equation (27) relates the difference in free energy for a gas at any pressure and temperature to the standard state condition at constant temperature. Here $dH = 0$ and from Eq. (15) the relationship of the entropy to the pressure is found to be

$$S - S^\circ = -R \ln(p/p_0) \quad (28)$$

Hence, one finds that

$$F(T, p) = F^\circ + RT \ln(p/p_0) \quad (29)$$

An expression can now be written for the total free energy of a gas mixture. In this case p is the partial pressure p_i of a particular gaseous component and obviously has the following relationship to the total pressure P :

$$p_i = \left(n_i / \sum_i n_i \right) P \quad (30)$$

where $(n_i / \sum_i n_i)$ is the mole fraction of gaseous species i . Equation (29) thus becomes

$$F(T, P) = \sum_i n_i \{ F_i^\circ + RT \ln(p_i/p_0) \} \quad (31)$$

As determined earlier [Eq. (21)] the criteria for equilibrium is $(dF)_{T,P} = 0$. Taking the derivative of F in Eq. (31), one obtains

$$\sum_i F_i^\circ dn_i + RT \sum_i (dn_i) \ln(p_i/p_0) + RT \sum_i n_i (dp_i/p_i) = 0 \quad (32)$$

Evaluating the last term of Eq. (32) one has

$$\sum_i n_i \frac{dp_i}{p_i} = \sum_i \left(\frac{\sum_i n_i}{P} \right) dp_i = \frac{\sum_i n_i}{P} \sum_i dp_i = 0 \quad (33)$$

since the total pressure is constant and thus $\sum_i dp_i = 0$. Now consider the first term in Eq. (32):

$$\sum_i F_i^\circ dn_i = (dn_A)F_A^\circ + (dn_B)F_B^\circ + \cdots - (dn_R)F_R^\circ - (dn_S)F_S^\circ + \cdots \quad (34)$$

By definition of the stoichiometric coefficients:

$$dn_i \sim a_i, \quad dn_i = \kappa a_i \quad (35)$$

where κ is a proportionality constant. Hence

$$\sum_i F_i^\circ dn_i = \kappa \{ aF_A^\circ + bF_B^\circ + \dots - rF_R^\circ - sF_S^\circ \dots \} \quad (36)$$

Similarly the proportionality constant κ will appear as a multiplier in the second term of Eq. (32). Since Eq. (32) must equal zero, the third term already has been shown equal to zero and κ cannot be zero, one obtains

$$-(aF_A^\circ + bF_B^\circ + \dots - rF_R^\circ - sF_S^\circ - \dots) = RT \ln \left\{ \frac{(p_R/p_0)^r (p_S/p_0)^s}{(p_A/p_0)^a (p_B/p_0)^b} \right\} \quad (37)$$

One then defines

$$\Delta F^\circ = aF_A^\circ + bF_B^\circ + \dots - rF_R^\circ - sF_S^\circ - \dots \quad (38)$$

where ΔF° is called the standard state free energy change. This name is reasonable since ΔF° is the change of free energy if the reaction (23) took place at standard conditions and went to completion to the right. Since the standard state pressure p_0 is one atmosphere, the condition for equilibrium becomes

$$-\Delta F^\circ = RT \ln(p_R^r p_S^s / p_A^a p_B^b) \quad (39)$$

where the partial pressures are measured in atmospheres. One then defines the equilibrium constant at constant pressure from Eq. (39) as

$$K_p \equiv p_R^r p_S^s / p_A^a p_B^b$$

Then

$$-\Delta F^\circ = RT \ln K_p, \quad K_p = \exp(-\Delta F^\circ / RT) \quad (40)$$

where K_p is not a function of total pressure but is a function of temperature alone. It is a little surprising that the free energy change at the standard state pressure (1 atm) determines the equilibrium condition at all other pressures. Equations (39) and (40) can be modified to account for nonideality in the product state; however, because of the high temperatures reached in combustion systems, ideality can be assumed even under rocket chamber pressures.

The energy and mass conservation equations used in the determination of the flame temperature are more conveniently written in terms of moles, and thus it is best to write the partial pressure in K_p in terms of moles and the total pressure P . This conversion is accomplished through the relationship between partial pressure p and total pressure P , as given by Eq. (30).

Substituting this expression for p_i [Eq. (30)] in the definition of the equilibrium constant [Eq. (40)], one obtains

$$K_p = (n_R^r n_S^s / n_A^a n_B^b) (P / \sum n_i)^{r+s-a-b} \quad (41)$$

which is sometimes written as

$$K_p = K_N (P / \sum n_i)^{r+s-a-b} \quad (42)$$

where

$$K_N \equiv n_R^r n_S^s / n_A^a n_B^b \quad (43)$$

When

$$r + s - a - b = 0 \quad (44)$$

the equilibrium reaction is said to be pressure insensitive. Again, however, it is worthy to repeat that K_p is not a function of pressure, but then Eq. (42) shows that K_N can be a function of pressure.

The equilibrium constant based on concentration (moles/cm³) is sometimes used particularly in chemical kinetic analyses to be discussed in the next chapter. This constant is found by recalling the perfect gas law, which states that

$$PV = \sum n_i RT \quad (45)$$

or

$$(P / \sum n_i) = (RT / V) \quad (46)$$

where V is the volume. Substituting for $(P / \sum n_i)$ in Eq. (42) gives

$$K_p = (n_R^r n_S^s) / (n_A^a n_B^b) (RT / V)^{r+s-a-b} \quad (47)$$

or

$$K_p = \frac{(n_R / V)^r (n_S / V)^s}{(n_A / V)^a (n_B / V)^b} (RT)^{r+s-a-b} \quad (48)$$

Equation (48) can be written as

$$K_p = (C_R^r C_S^s / C_A^a C_B^b) (RT)^{r+s-a-b} \quad (49)$$

where $C = n/V$. From Eq. (49) it is seen that the definition of the equilibrium constant for concentration is

$$K_C \equiv C_R^r C_S^s / C_A^a C_B^b \quad (50)$$

Given a temperature and pressure all the equilibrium constants (K_p , K_N ,

and K_C) can be determined thermodynamically from ΔF° for the equilibrium reaction chosen.

How the equilibrium constant varies with temperature can be of importance. Consider first the simple derivative

$$\frac{d(F/T)}{dT} = \frac{T(dF/dT) - F}{T^2} \quad (51)$$

Recall that Gibbs free energy may be written as

$$F + E + PV - TS \quad (52)$$

or, at constant pressure,

$$\frac{dF}{dT} = \frac{dE}{dT} + P \frac{dV}{dT} - S - T \frac{dS}{dT} \quad (53)$$

At equilibrium from Eq. (12) for the constant pressure condition

$$T \frac{dS}{dT} = \frac{dE}{dT} + P \frac{dV}{dT} \quad (54)$$

Combining Eqs. (53) and (54) gives

$$dF/dT = -S \quad (55)$$

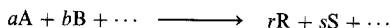
Hence Eq. (51) becomes

$$\frac{d(F/T)}{dT} = \frac{-TS - F}{T^2} = -\frac{H_2}{T^2} \quad (56)$$

This expression is valid for any substance under constant pressure conditions. Applied to a reaction system with each substance in its standard state, one obtains

$$d(\Delta F^\circ/T) = -(\Delta H^\circ/T^2) dT \quad (57)$$

where ΔH° is the standard state heat of reaction for any arbitrary reaction:



at temperature T (and, of course, pressure is 1 atm). Substituting the expression for ΔF° given by Eq. (39) into Eq. (57), one obtains

$$d \ln K_p/dT = \Delta H^\circ/RT^2 \quad (58)$$

If it is assumed that ΔH° is a slowly varying function of T , one obtains

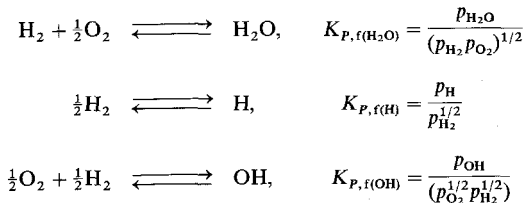
$$\ln \left(\frac{K_{p_2}}{K_{p_1}} \right) = -\frac{\Delta H^\circ}{R} \left(\frac{1}{T_2} - \frac{1}{T_1} \right) \quad (59)$$

Thus for small changes in T

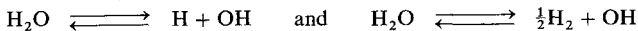
$$(K_{P_2}) > (K_{P_1}) \quad \text{when} \quad T_2 > T_1$$

In the same context as the heat of formation, the JANAF Tables have tabulated most conveniently the equilibrium constants of formation for practically every substance of concern in combustion systems. The equilibrium constant of formation ($K_{P,f}$) is based on the equilibrium equation of formation of a species from its elements in their normal states. Thus by algebraic manipulation it is possible to determine the equilibrium constant of any reaction. In flame temperature calculations, by dealing only with equilibrium constants of formation, there is no chance of choosing a redundant set of equilibrium reactions. Of course, the equilibrium constant of formation for elements in their normal state is zero.

Consider the following three equilibrium reactions of formation



The equilibrium reaction is always written for the formation of one mole of the substances other than the elements. Now if one desires to calculate the equilibrium constant for reactions such as



then the respective K_P is found from

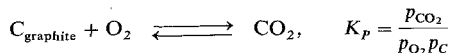
$$K_P = \frac{p_{\text{H}} p_{\text{OH}}}{p_{\text{H}_2\text{O}}} = \frac{K_{P,f(\text{H})} K_{P,f(\text{OH})}}{K_{P,f(\text{H}_2\text{O})}}, \quad K_P = \frac{p_{\text{H}}^{1/2} p_{\text{OH}}}{p_{\text{H}_2\text{O}}} = \frac{K_{P,f(\text{OH})}}{K_{P,f(\text{H}_2\text{O})}}$$

Because of this type of result and the thermodynamic expression

$$\Delta F^\circ = -RT \ln K_P$$

the JANAF Tables list $\log K_{P,f}$. Note the base 10 logarithm.

For those compounds that contain carbon and a combustion system in which solid carbon is found, the thermodynamic handling of the K_P is somewhat more difficult. The equilibrium reaction of formation for CO_2 would be



However, since the standard state of carbon is the condensed state, carbon graphite, the only partial pressure it exerts is its vapor pressure (p_{vp}), a known thermodynamic property that is also a function of temperature. Thus, the above formation expression is written as

$$K_p(T)p_{vp,c}(T) = \frac{p_{CO_2}}{p_{O_2}} = K'_p$$

The $K_{p,f}$'s for substances containing carbon tabulated by JANAF are in reality K'_p , and the condensed phase is simply ignored in evaluating the equilibrium expression. The number of moles of carbon (or any other condensed phase) is not included in the $\sum n_i$ since this summation is for the gas phase components contributing to the total pressure.

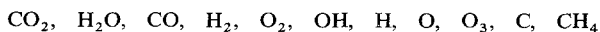
D. FLAME TEMPERATURE CALCULATIONS

If one examines the equation for the flame temperature [Eq. (11)], an interesting observation can be made. The values in Table 1 and the realization that many moles of product form for each mole of the reactant fuel will show that the sum of the molar heats of the products will be substantially greater than the sum of the molar heats of the reactants; i.e.,

$$\sum_{i, \text{prod}} n_i(\Delta H_f^\circ)_i \gg \sum_{j, \text{react}} (\Delta H_f^\circ)_j$$

Consequently it would appear that the flame temperature is not determined by the specific reactants, but only by the atomic ratios and the specific atoms that are introduced. It is the atoms that determine what products will form. Only ozone and acetylene have high enough positive molar heats of formation to cause a noticeable variation (rise) in flame temperature. Ammonia has a low enough negative heat of formation to lower the final flame temperature. One can normalize for the effects of total moles of products formed by considering the heats of formation per gram (Δh_f°) and these values are given for some fuels and oxidizers in Table 1. The variation of Δh_f° among most hydrocarbon fuels is very small. This fact will be used later in correlating the flame temperatures of hydrocarbons in air.

One can draw the further conclusion that the product concentrations also are only functions of temperature, pressure, and the C/H/O ratio and not the original source of atoms. Thus, for any C-H-O system, the products will be the same, i.e., they will be CO_2 , H_2O , and their dissociated products. The dissociation reactions listed earlier give some of the possible "new" products. A more complete list would be

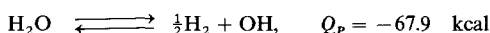
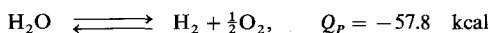
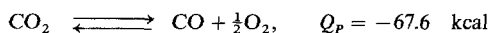


For a C, H, O, N system, the following could be added:



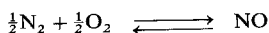
Nitric oxide has a very low ionization potential and will ionize at flame temperatures. For a normal composite solid propellant that contains C, H, O, N, Cl, and Al, many more products would have to be considered. In fact if one listed all the possible number of products for this system, the solution to the problem becomes most difficult and advanced computers are necessary for exact results. However, knowledge of thermodynamic equilibrium constants and kinetics allows one to eliminate many possible product species.

Consider a C, H, O, N system. For an over-oxidized case, there is an excess of oxygen to convert all the carbon and hydrogen present to CO_2 and H_2O . The term stoichiometric mixture ratio specifies exactly the ratio of the oxygen to fuel to just burn all the C and H to CO_2 and H_2O . The principal products for an over-oxidized case are CO_2 , H_2O , O_2 , and N_2 . As the temperature of the flame increases, dissociation begins; and, if $T_2 > 2200$ K at $P = 1$ atm or $T_2 > 2500$ K at 20 atm, one must take into account the dissociation of CO_2 and H_2O by the following reactions:



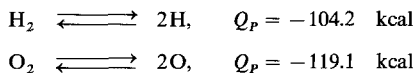
where the Q_p 's are calculated at 298 K. This heuristic rule is based upon the fact that under these temperatures and pressures at least 1% dissociation takes place. The pressure enters through Le Chatelier's principle that the equilibrium concentrations will shift with the pressure. The equilibrium constant, although independent of pressure, can be expressed in a form that contains the pressure. A variation in pressure shows that the molar quantities change. Since the reactions noted above are quite endothermic, even small concentration changes must be considered. If one initially assumes that certain products of dissociation were absent and calculates a temperature that would indicate 1% dissociation of the species noted, then the flame temperature must be reevaluated by including in the product mixture the products of dissociation, i.e., the presence of CO, H_2 , and OH as products is now indicated.

Since concern about emissions from power plant sources has arisen, there is concern of concentrations of certain products much less than 1%, even though such concentrations do not affect the temperature even in a minute way. The major pollutant of concern in this regard is nitric oxide NO. To make an estimate of the amount of NO found in a system at equilibrium, one would use the equilibrium reaction of formation of NO

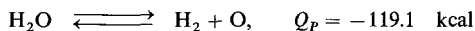


A rule of thumb is that any temperature above 1800 K gives sufficient NO to be of concern. The NO formation reaction is pressure insensitive, so there is no need to specify the pressure.

If in the over-oxidized case $T_2 > 2400$ K at $P = 1$ atm and $T_2 > 2800$ K at $P = 20$ atm, then the dissociation of O_2 and H_2 becomes important, namely



Although these dissociation reactions are written to show one mole of the molecule dissociating, recall that the $K_{p,i}$'s are written for one mole of the radical forming. These dissociation reactions are highly endothermic, and even very small percentages can affect the final temperature. The new products are H and O atoms. Actually the presence of O atoms could come about from the dissociation of water at this higher temperature according to the equilibrium step

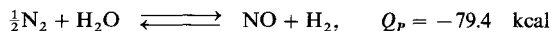


Since the heat absorption is about the same in each case, from Le Chatelier's principal there is basically no preference in the reactions leading to O. Thus in an over-oxidized flame, water dissociation introduces the species H_2 , O_2 , OH, H, and O.

At even higher temperatures, the nitrogen begins to take part in the reactions and to affect the system thermodynamically. At $T > 3000$ K, NO forms mostly from the reaction given before



rather than



If $T_2 > 3500$ K at $P = 1$ atm or $T > 3600$ K at 20 atm, N_2 starts to dissociate by another highly endothermic reaction:

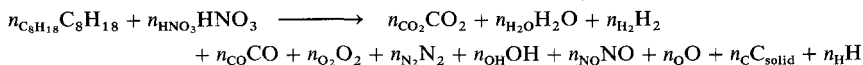


Thus the complexity in solving for the flame temperature depends on the number of product species chosen. If one has a system whose approximate temperature range is known, then by the approach indicated above, the complexity of the system can be reduced. Computer programs and machines are now available that can handle the most complex systems, and sometimes little thought is given to reducing the complexity and thus the machine time.

Equation (11) is now examined closely. If the n_i 's (products) total a number μ , one needs $(\mu + 1)$ equations to solve for the μn_i 's and T_2 . The energy equation is available as one equation. Furthermore, one has a mass balance

equation for each atom in the system. If there are α atoms, then $(\mu - \alpha)$ additional equations are required to solve the problem. These $(\mu - \alpha)$ equations came from the equilibrium equations. These equations are basically nonlinear. For the CHON system it is necessary to solve five linear equations and $(\mu - 4)$ nonlinear equations simultaneously, in which one of the unknowns T_2 is not even present explicitly. It is present in terms of the enthalpies of the products. This set of equations is a difficult one to solve and can be done only with modern computational machinery.

Consider the reaction between octane and nitric acid taking place at a pressure P as an example. The stoichiometric equations is written as



Since the mixture ratio is not specified explicitly for this general expression, no effort is made to eliminate products and $\mu = 11$. The new mass balance equations then are ($\alpha = 4$)

$$N_H = 2n_{H_2} + 2n_{H_2O} + 2n_{OH} + n_H$$

$$N_O = 2n_{O_2} + n_{H_2O} + 2n_{CO_2} + n_{CO} + n_{OH} + n_O + n_{NO}$$

$$N_N = 2n_{N_2} + n_{NO}$$

$$N_C = n_{CO_2} + n_{CO} + n_C$$

where

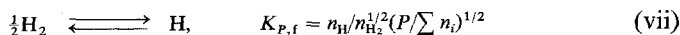
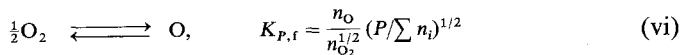
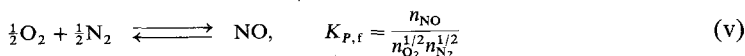
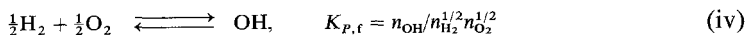
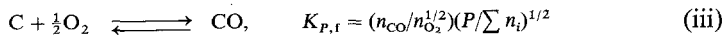
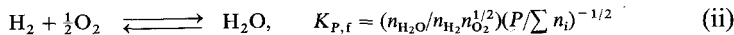
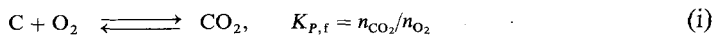
$$N_H = 18n_{C_8H_{18}} + n_{HNO_3}$$

$$N_O = 3n_{HNO_3}$$

$$N_C = 8n_{C_8H_{18}}$$

$$N_N = n_{HNO_3}$$

The seven ($\mu - \alpha = 11 - 4 = 7$) equilibrium equations needed would be



In these equations $\sum n_i$ includes only the gaseous products; that is, it does not include n_C ; n_C is determined from the equation for N_C .

The reaction between the reactants and products is considered nonreversible, so that only the products exist in the system being analyzed. Thus, if the reactants were H_2 and O_2 , H_2 and O_2 would appear on the product side as well. In dealing with the equilibrium reactions, the molar quantities of the reactants H_2 and O_2 are ignored. They are given or known quantities. The amounts of H_2 and O_2 in the product mixture would be unknowns. This point should be considered carefully, even though obvious. It is one of the major sources of error in first attempts to solve flame temperature problems.

There are various mathematical approaches for solving these equations by numerical methods [3,4,5]. The most commonly used program is that of Gordon and McBride [4].

As stated, to solve explicitly for the temperature T_2 and the product composition, one must consider α mass balance equations, $(\mu - \alpha)$ nonlinear equilibrium equations, and an energy equation in which one of the unknowns T_2 is not even present explicitly. Since numerical procedures are used to solve the problem on computers, the thermodynamic functions are represented in terms of power series with respect to temperature.

The general iterative approach used is to determine the equilibrium state for the product composition at an initially assumed value of the temperature and pressure and then to examine whether the energy equation is satisfied. Chemical equilibrium is usually described by either of two equivalent formulations—equilibrium constants or minimization of free energy. For simple problems such as determining the decomposition temperature of a monopropellant whose exhaust products may be very few or for examining the variation of a specific species with temperature or pressure, it is most convenient to deal with equilibrium constants. For complex problems using either equilibrium constants or minimization of free energy the problem reduces to the same number of iteration equations; however, use of equilibrium constants causes more computational bookkeeping, numerical difficulties with use of components, more difficulty in testing for presence of some condensed species, and more difficulty in extending the generalized methods used to condition, which require nonideal equations of state [3, 4].

The condition for equilibrium may be described by any of several thermodynamic functions, such as the minimization of the Gibbs free energy or the Helmholtz free energy or the maximization of entropy. If one wishes to use temperature and pressure to characterize a thermodynamic state, the Gibbs free energy is most easily minimized, inasmuch as temperature and pressure are its natural variables. Similarly, the Helmholtz free energy is most easily minimized if the thermodynamic state is characterized by temperature and volume (density) [4].

The most versatile procedure and computer program and that most commonly used for temperature and composition calculations is that of Gordon and McBride [4] who use the minimization of the Gibbs free energy technique and a descent Newton–Raphson method to solve the equations iteratively. A similar method for solving the equations when equilibrium constants are used is shown in Ref. [5].

In combustion calculations, one primarily wants to know the variation of the temperature with the oxidizer to fuel ratio. Therefore in solving flame temperature problems, it is normal to take the number of moles of fuel as one and the number of moles of oxidizer as that given by the oxidizer to fuel ratio. In this manner the coefficients are one and a number normally larger than one. Plots of flame temperature versus oxidizer to fuel ratio peak about the stoichiometric mixture ratio. If the system is over oxidized, there is excess oxygen that must be heated to the product temperature; thus, the product temperature drops from the stoichiometric value. If too little oxidizer is present, that is the system is under oxidized, then there is not sufficient oxygen to burn all the carbon and hydrogen to their most oxidized state, the energy released is less, and the temperature drops as well. More generally the flame temperature is plotted as a function of equivalence ratio (Fig. 2), where the equivalence ratio is defined as the fuel/oxidizer ratio divided by the stoichiometric fuel/oxidizer ratio. The equivalence ratio is given the symbol ϕ . For fuel-rich systems, there is more than the stoichiometric amount of fuel, and $\phi > 1$. For over-oxidized, or fuel-lean systems, $\phi < 1$. Obviously at the stoichiometric ratio, $\phi = 1$.

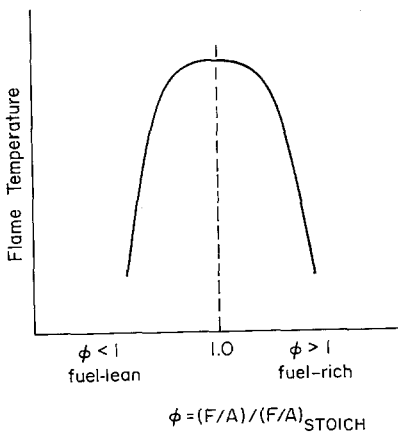


Fig. 2. Variation of flame temperature with equivalence ratio.

Most combustion systems deal with air as the oxidizer and it is desirable to be able to conveniently determine the flame temperature of any fuel with air at any equivalence ratio. This objective is possible on the background built in this chapter. As discussed earlier, Table 1 is similar to a potential energy diagram in that movement from the top of the table to products at the bottom indicates energy release. It should be noted, as well, that as the size of most hydrocarbon fuel molecules increases so does its negative heat of formation. Thus, it is possible to have fuels with negative heats of formation that approach that of carbon dioxide. It would appear then that there would be very little heat release. Heats of formation of hydrocarbons range from 54.2 kcal/mole for acetylene to -108.9 kcal/mole for *n*-erosane ($C_{20}H_{42}$). However, the greater the number of carbon atoms there are in a hydrocarbon fuel, the greater the number of moles of CO_2 , H_2O , and, of course, their formed dissociation products. Thus, even though a fuel may have a large negative heat of formation, it will form many moles of combustion products and will not necessarily have a low flame temperature. Thus, in order to estimate the contribution of the heat of formation of the fuel to the flame temperature it is more appropriate to examine the heat of formation on a unit mass basis rather than on a molar basis. With this consideration, one finds that practically every hydrocarbon fuel has a heat of formation between -1.5 and 1.0 kcal/gm. In fact most fall in the range -0.5 to $+0.5$ kcal/gm. Acetylene and methyl acetylene are the only exceptions with values of 2.08 and 1.11 kcal/gm, respectively.

In considering the flame temperatures of fuels in air, it becomes quite apparent that the major effect on flame temperature is the equivalence ratio and of almost equal importance is the H/C ratio, which determines the ratio of water vapor, CO_2 , and their formed dissociation products. Since the heats of formation per unit mass of the olefins do not vary much and the H/C is the same for all, it is not surprising that there is very little variation in flame temperature among the monoolefins. When discussing fuel-air mixture temperatures, one must always recall the presence of large number of moles of nitrogen.

With these conceptual ideas it is possible to develop simple graphs that give the adiabatic flame temperature of any hydrocarbon fuel in air at any equivalence ratio [6]. Such graphs are shown in Figs. 3, 4, and 5. These graphs depict the flame temperatures for a range of hypothetical hydrocarbons that have heats of formation ranging from -1.5 to 1.0 kcal/gm. The hydrocarbons chosen have the formulae, CH_4 , CH_3 , $CH_{2.5}$, CH_2 , $CH_{1.5}$, and CH_1 ; that is, they have H/C ratios of 4, 3, 2.5, 2.0, 1.5, and 1.0. These values include every conceivable hydrocarbon, except the acetylenes mentioned. The values listed were calculated from the standard Gordon and McBride computer program and were determined for all species entering at

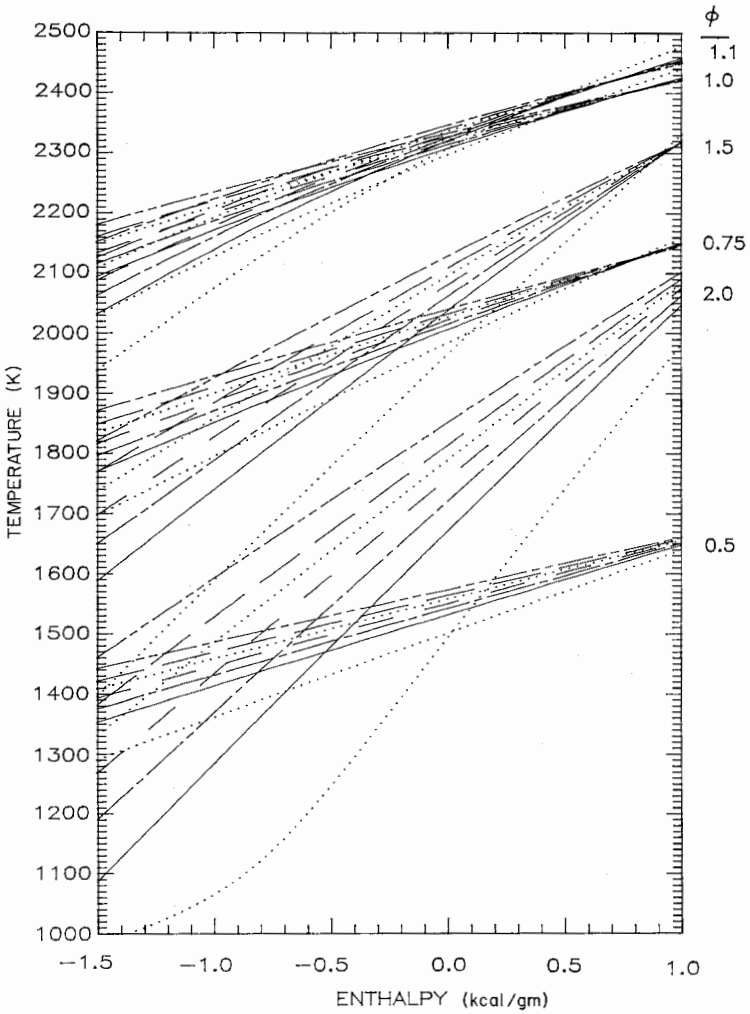


Fig. 3. Flame temperatures in kelvin of hydrocarbons and air as a function of the total enthalpy content of reactions in kilocalories/gram for various equivalence and H/C ratios at 1-atm pressure. Reference sensible enthalpy related to 298 K. H/C ratios in the order

- H/C = 4
- H/C = 3
- H/C = 2.5
- · - · H/C = 2.0
- - - - H/C = 1.5
- H/C = 1.0
- H/C = 0.0

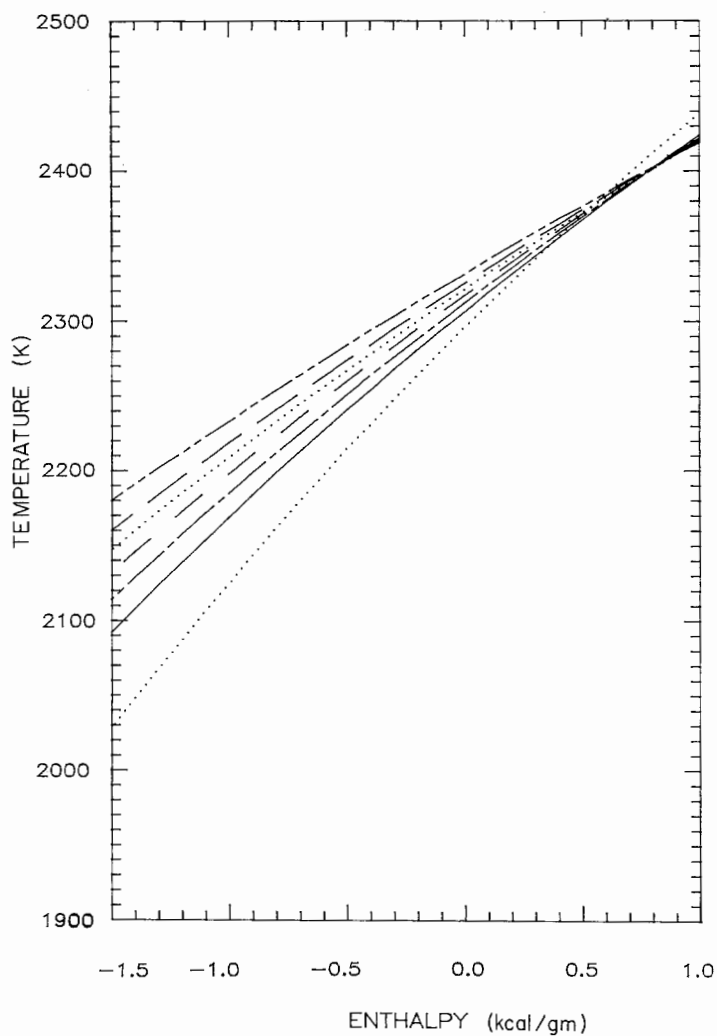


Fig. 4. Equivalence ratio, $\Phi = 1.0$ values of Fig. 3 on an expanded scale.

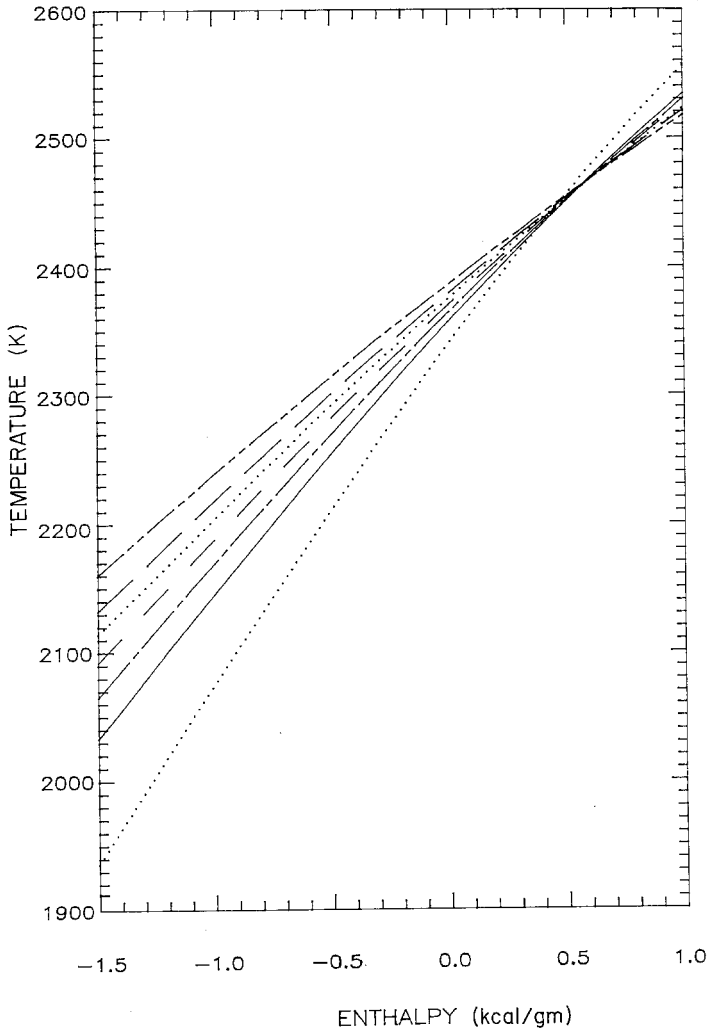


Fig. 5. Equivalence ratio, $\Phi = 1.1$ values of Fig. 3 on an expanded scale.

298 K and a pressure of 1 atm. As a matter of interest, also plotted in the figures are the values of CH_0 , or a H/C ratio of zero. Since the only possible species with this H/C ratio is carbon, the only meaningful points from a physical point of view are those for a heat of formation of zero.

The results are plotted in the figures as flame temperature, in kelvins, as function of the chemical enthalpy content of the reacting system in kilocalories per gram of reactant fuel. In the figures there are lines of constant H/C ratio grouped according to the equivalence ratio ϕ . For most systems the enthalpy used as the abscissa will be the heat of formation of the fuel in kilocalories per gram, but there is actually greater versatility in using this enthalpy. For example, in a cooled flat flame burner, the measured heat extracted by the water can be converted on a unit fuel flow basis to a reduction in the heat of formation of the fuel. This lower enthalpy value is then used in the graphs to determine the adiabatic flame temperature. The same kind of adjustment can be made to determine the flame temperature when either or both the fuel or air enter the system at a temperature different from 298 K.

If a temperature is desired at an equivalence ratio other than that listed, then it is best obtained from a plot of T versus ϕ for the given values. The errors in extrapolating in this manner or from the graph are trivial, less than 1%. The reason for Figs. 4 and 5 is that the values for $\phi = 1.0$ and $\phi = 1.1$ overlap to a great extent. For Fig. 5 $\phi = 1.1$ was chosen because the flame

TABLE 2

Approximate flame temperatures of various stoichiometric mixtures, critical temperature 298 K

Fuel	Oxidizer	Pressure (atm)	T (K)
Acetylene	Air	1	2600 ^a
Acetylene	Oxygen	1	3410 ^b
Carbon monoxide	Air	1	2400
Carbon monoxide	Oxygen	1	3220
Heptane	Air	1	2290
Heptane	Oxygen	1	3100
Hydrogen	Air	1	2400
Hydrogen	Oxygen	1	3080
Methane	Air	1	2210
Methane	Air	20	2270
Methane	Oxygen	1	3030
Methane	Oxygen	20	3460

^a This maximum exists at $\phi = 1.3$.

^b This maximum exists at $\phi = 1.7$.

temperature for many fuels peaks not at the stoichiometric value, but between $\phi = 1.0$ and 1.1 due to lower mean specific heats of the richer products. The maximum temperature for acetylene-air peaks, for example, at a value of $\phi = 1.3$ (see Table 2).

The flame temperature values reported in Fig. 3 show some interesting trends. The H/C ratio has a greater effect in rich systems. This trend is due to the fact that there is less nitrogen in the rich cases and a greater effect of the mean specific heat of the combustion products exists. For richer systems the mean specific heat of the product composition is lower due to the greater preponderance of CO and H₂. For a given enthalpy content of reactants, the lower the mean specific heat of the product mixture, the greater the final flame temperature. At a given chemical enthalpy content of reactants, the larger the H/C ratio, the higher the temperature. This effect also comes about from the lower specific heat of water and its dissociation products compared to that of CO₂ and the higher endothermicity of CO₂ dissociation. As one

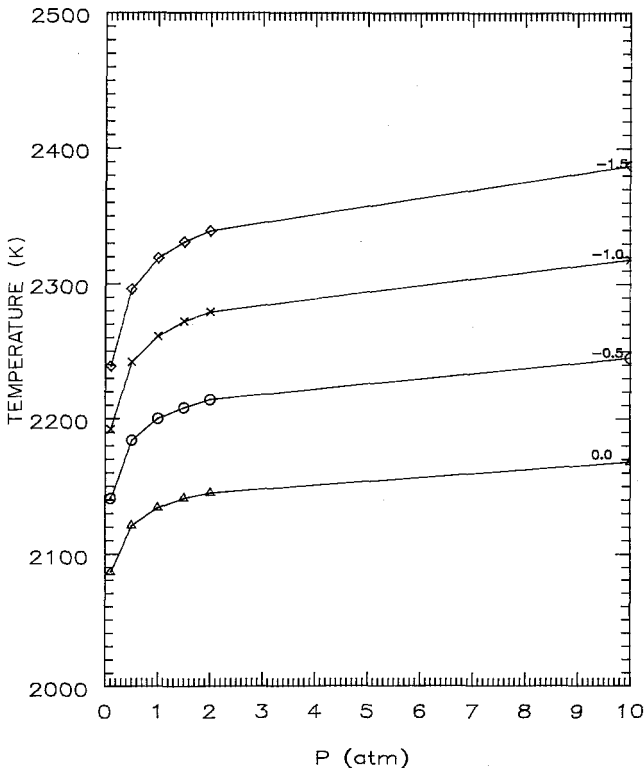


Fig. 6. Variation of the stoichiometric temperature as a function of pressure for various total enthalpy contents in kilocalories/gram of reactants.

proceeds to more energetic reactants, the dissociation of CO_2 increases and the differences diminish. At the highest temperatures and reaction enthalpies, the dissociation of the water is so complete the system does not benefit from the heat of formation of the combustion product water. There is still a benefit from the heat of formation of CO , the major dissociation product of CO_2 , so that the lower the H/C ratio, the higher the temperature. Thus for equivalence ratios around unity and very high energy content, the lower the H/C ratio, the greater the temperature; that is, the H/C curves cross.

Figure 6 reports the calculated stoichiometric flame temperatures as a function of pressure. One can conclude that the degree of dissociation at 1 atm is small. For zero reactant enthalpy content there is only a 1.5% change from 1.0 to 10 atm and a 2.2% change from 1.0 to 0.10 atm. The role of the large amount of nitrogen present is again evident. The effect of nitrogen as a diluent is also noted in Table 2 where the maximum flame temperatures of various fuels in air and pure oxygen are compared. One should compare the results for methane in particular. The change in methane-air temperatures from 1–20 atm is just about 2.7%, whereas the change in methane-oxygen temperatures over the same pressure range is about 14.2%. This variation is due to the differences in the degree of dissociation.

PROBLEMS

1. Calculate the heat of reaction when methane and air in stoichiometric proportions are brought into a calorimeter at 500 K. The product composition is brought to the ambient temperature (298 K) by the cooling water. The pressure in the calorimeter is assumed to remain at 1 atm, but the water formed has condensed.
2. Calculate the flame temperature of normal octane (liquid) burning in air at an equivalence ratio of 0.5. For this problem assume there is no dissociation of the stable products formed. All reactants are at 298 K and the system operates at 1-atm pressure. Compare the results with those given by the graphs in the text. Explain any differences.
3. Carbon monoxide is oxidized to carbon dioxide in an excess of air (1 atm) in an afterburner so that the final temperature is 1300 K. Under the assumption of no dissociation, determine the air-fuel ratio required. Report the results on both a molar and mass basis. For the purposes of this problem assume that air has the composition of 1 mole of oxygen to 4 moles of nitrogen. The carbon monoxide and air enter the system at 298 K.
4. The exhaust of a carbureted automobile engine, which is operated slightly fuel rich, has an efflux of unburned hydrocarbons entering the exhaust manifold. One can assume that all the hydrocarbons are equivalent to ethylene (C_2H_4) and all the remaining gases are equivalent to inert nitrogen (N_2). On a molar basis there are 40 moles of nitrogen for every mole of ethylene. The hydrocarbons are to be burned over an oxidative catalyst and converted to carbon dioxide and water vapor only.

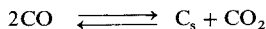
In order to accomplish this objective, ambient (298 K) air must be injected into the manifold before the catalyst. If the catalyst is to be maintained at 1000 K, how many moles of air per mole of ethylene must be added? Take the temperature of the manifold gases before air injection as 400 K. Assume the composition of air to be 1 mole of oxygen to 4 moles of nitrogen.

5. A combustion test was performed at 20-atm pressure in a hydrogen-oxygen system. Analysis of the combustion products, which were considered to be in equilibrium, was as follows

Compound	Mole fraction
H ₂ O	0.493
H ₂	0.498
O ₂	0
O	0
H	0.020
OH	0.005

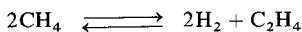
What must the combustion temperature have been in the test?

6. Whenever carbon monoxide is present in a reacting system it is possible for it to disproportionate into carbon dioxide according to the equilibrium



Assume that such an equilibrium can exist in some crevice in an automotive cylinder or manifold. Determine whether raising the temperature decreases or increases the amount of carbon present. Determine the K_p for the reactant and the effect of raising the pressure on the amount of carbon formed.

7. Determine the equilibrium constant K_p at 1000 K for the following reaction



8. The atmosphere of Venus is said to contain 5% carbon dioxide and 95% nitrogen by volume. It is possible to simulate this atmosphere for Venus reentry studies by burning gaseous cyanogen (C₂N₂) and oxygen and diluting with nitrogen in the stagnation chamber of a continuously operating wind tunnel. If the stagnation pressure is 20 atm, what is the maximum stagnation temperature that could be reached and still have Venus atmosphere conditions? If the stagnation pressure were 1 atm, what would be the maximum temperature? Assume all gases enter the chamber at 298 K. Take the heat of formation of cyanogen as $(\Delta H_f^\circ)_{298} = 91.2$ kcal/mole.

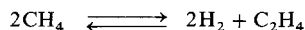
9. A mixture of 1 mole of N₂ and 0.5 mole O₂ is heated to 4000 K at 0.5 atm pressure and results in an equilibrium mixture of N₂, O₂, and NO only. If the O₂ and N₂ were initially at 298 K and the process is one of steady heating, how much heat was required to bring the final mixture to 4000 K on the basis of one initial mole of N₂?

10. Calculate the adiabatic decomposition temperature of benzene under the constant pressure condition of 20 atm. Assume that benzene enters the decomposition chamber in the liquid state at 298 K and decomposes into the following products: carbon (graphite), hydrogen, and methane.

11. Calculate the flame temperature and product composition of liquid ethylene oxide decomposing at 20-atm pressure by the irreversible reaction:



The four products are as specified. The equilibrium known to exist is

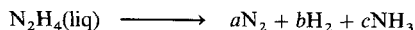


The heat of formation of liquid ethylene oxide is

$$\Delta H_{f,298} = -18.3 \text{ kcal/mole}$$

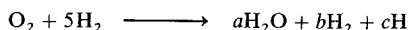
It enters the decomposition chamber at 298 K.

12. Liquid hydrazine (N_2H_4) decomposes exothermically in a monopropellant rocket operating at 100-atm chamber pressure. The products formed in the chamber are N_2 , H_2 , and ammonia (NH_3) according to the irreversible reaction



Determine the adiabatic decomposition temperature and the product composition a , b , and c . Take the standard heat of formation of liquid hydrazine as 11.95 kcal/mole. The hydrazine enters the system at 298 K.

13. Gaseous hydrogen and oxygen are burned at 1-atm pressure under the rich conditions designated by the following combustion reaction:



The gases enter at 298 K. Calculate the adiabatic flame temperature and the product composition a , b , and c .

14. The liquid propellant combination nitrogen tetroxide (N_2O_4) and UDMH (unsymmetrical dimethyl hydrazine) has optimum performance at an oxidizer to fuel weight ratio of 2 at a chamber pressure of 67 atm. Assume that the products of combustion of this mixture are N_2 , CO_2 , H_2O , CO , H_2 , O , H , OH , and NO .

Set down the equations necessary to calculate the adiabatic combustion temperature and the actual product composition under these conditions. These equations should contain all the numerical data in the description of the problem and in the tables in the appendices. The heats of formation of the reactants are

$$\begin{array}{ll} \text{N}_2\text{O}_4(\text{liq}), & \Delta H_{f,298} = -0.50 \text{ kcal/mole} \\ \text{UDMH}(\text{liq}), & \Delta H_{f,298} = +12.7 \text{ kcal/mole} \end{array}$$

The propellants enter the combustion chamber at 298 K.

REFERENCES

1. JANAF Thermochemical Tables, Second Edition, NSRDS-NBS37, U.S. National Bureau of Standards, 1971.
2. National Bureau of Standards Circular C461 (1947).
3. Huff, V. N., and Morell, V. E. NACA TN 1113 (1950).
4. Gordon, S., and McBride, B. J. NASA SP-273 (1971).
5. Glassman, I., and Sawyer, R. F., "The Performance of Chemical Propellants," Chap. II. Technivision, London, 1970.
6. Glassman, I., and Clark, G., East. States Combust. Inst. Meet., Paper No. 12, Providence, Rhode Island (November 1983).

Chemical Kinetics

A. INTRODUCTION

Flames will propagate through only those chemical mixtures that are capable of reacting sufficiently fast to be considered explosive in character. Indeed the expression “explosive” essentially specifies very rapid reaction. From the standpoint of combustion, the interest in chemical kinetic phenomena is directed, generally, towards considering the conditions under which chemical systems would undergo explosive reaction. More recently, however, great interest has developed in the rates and mechanisms of steady (nonexplosive) chemical reactions, for most of the known complex pollutants form in zones of steady, usually lower temperature, reactions during the combustion process.

These essential features of chemical kinetics, which occur frequently in combustion phenomena, are reviewed in this chapter. For a more detailed understanding of any of these aspects and a thorough coverage of the subject, one should refer to any of the books on chemical kinetics, such as those listed in Ref. [1].

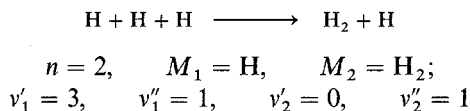
B. THE RATES OF REACTIONS AND THEIR TEMPERATURE DEPENDENCY

All chemical reactions, whether of the hydrolysis, acid–base, or combustion type, take place at a definite rate and depend on the conditions of the system. The most important of these conditions are the concentration of the reactants, the temperature, radiation effects, and the presence of a catalyst or inhibitor. The rate of the reaction may be expressed in terms of the concentration of any of the substances reacting or any product of the reaction; i.e., the rate may be expressed as the rate of decrease of the concentration of a reactant or the rate of increase of a product of reaction.

A stoichiometric relation describing a one-step chemical reaction of arbitrary complexity can be represented by the equation [2, 3]

$$\sum_{j=1}^n v_j M_j = \sum_{j=1}^n v_j'' M_j \quad (1)$$

where v_j' is the stoichiometric coefficient of the reactants, v_j'' the stoichiometric coefficients of the products, M an arbitrary specification of all chemical species, and n the total number of species involved. If a species represented by M_j does not occur as a reactant or product, its v_j equals zero. Consider, as an example, the recombination of H atoms in the presence of H atoms; that is, the reaction



The reason for following this complex notation will become apparent shortly.

The law of mass action, which is confirmed experimentally, states that the rate of disappearance of a chemical species i , defined as RR_i , is proportional to the product of the concentrations of the reacting chemical species, each concentration raised to a power equal to the corresponding stoichiometric coefficient, i.e.,

$$RR_i \sim \prod_{j=1}^n (M_j)^{v_j'}, \quad RR_i = k \prod_{j=1}^m (M_j)^{v_j''} \quad (2)$$

where k is the proportionality constant called the specific reaction rate coefficient. In Eq. (2) $\sum v_j'$ is also given the symbol n , which is called the overall order of the reaction; v_j' itself would be the order of the reaction with respect to species j . In an actual reacting system, the rate of change of the

concentration of a given species i is given by

$$\frac{d(M_i)}{dt} = [v_i'' - v_i']RR = [v_i'' - v_i']k \prod_{j=1}^m (M_j)^{v_j} \quad (3)$$

since v_i'' moles of M_i are formed for every v_i' moles of M_i consumed. For the previous example, $d(\text{H})/dt = -2k(\text{H})^3$. The use of this complex representation prevents error in sign and eliminates confusion when stoichiometric coefficients are different from one.

In many systems M_i can be formed not only from a single-step reaction such as that represented by Eq. (3), but also from many different such steps leading to a rather complex formulation of the overall rate. However, for a single-step reaction such as Eq. (3), $\sum v_i'$ not only represents the overall order of the reaction, but also the molecularity, which is defined as the number of molecules that interact in the reaction step. Generally the molecularity of most reactions of interest will be 2 or 3. For a complex reaction scheme the concept of molecularity is not appropriate and the overall order can take various values including fractional ones.

1. The Arrhenius Rate Expression

Most chemical reactions that take place have their rates dominated by collisions of two species that may have the capability to react. Thus, most simple reactions are second order. Other reactions are dominated by a loose bond breaking step and thus are first order. Most of these latter type reactions fall in the class of decomposition processes. Isomerization reactions are also found to be first order. According to Lindemann's theory [1, 4] of first-order processes, first-order reactions occur as a result of a two-step process. This point will be discussed in a subsequent section.

An arbitrary second-order reaction may be written as



where a real example would be the reaction of oxygen atoms with nitrogen molecules



For the arbitrary reaction (4), the rate expression takes the form

$$RR = \frac{d(\text{A})}{dt} = -k(\text{A})(\text{B}) = -\frac{d(\text{C})}{dt} \quad (5)$$

The convention used throughout this book is that parenthesis around a chemical symbol refers to the concentration of that species in moles or mass

per cubic centimeter. Specifying the reaction in the manner above does not mean every collision of the reactants A and B would lead to products or cause the disappearance of an amount of either. Arrhenius [5] put forth a simple theory that accounts for this fact and gives a temperature dependency of k . Arrhenius stated that only molecules that possess energy greater than a certain amount E will react. Molecules acquire the additional energy necessary from collisions induced by the thermal condition that exists. These high-energy activated molecules lead to products. Arrhenius' postulate may be written as

$$RR = Z_{AB} \exp(-E/RT) \quad (6)$$

where Z_{AB} is the gas kinetic collision frequency and $\exp(-E/RT)$ is the Boltzmann factor. Kinetic theory shows that the Boltzmann factor gives the fraction of all collisions that have an energy greater than E .

The energy term in the Boltzmann factor may be considered as the size of the barrier along a potential energy surface for a system of reactants going to products and is represented schematically in Fig. 1. The state of the reacting species at this activated energy can be thought of as some intermediate complex that leads to the products. This energy is referred to as the activation energy of the reaction and is generally given the symbol E_A . In Fig. 1, this energy is given the symbol E_f to distinguish it from the condition in which the product species can revert to reactants by a backward reaction. The activation energy of this backward reaction is represented by E_b and is obviously much larger than E_f . Figure 1 shows an exothermic condition for reactants going to products. The relationship between the activation energy and the heat of reaction has been developed (cf. Laidler [1]). Generally, the more exothermic a reaction is, the smaller the activation energy. In complex systems energy release from one reaction can sustain other endothermic reactions, such as that represented in Fig. 1 for products reverting to reactants. As a practical example, once initiated, acetylene will decompose to the elements in a monopropellant rocket in a sustained fashion because the

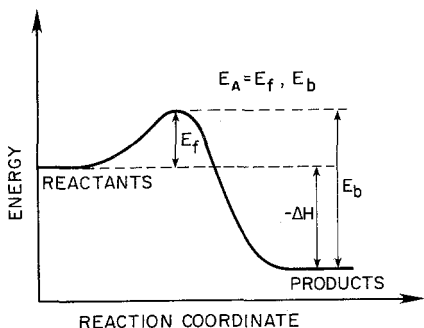


Fig. 1. Energy as a function of a reaction coordinate for a reacting system.

energy release of the decomposition process is greater than the activation of the process. Although a calculation of the decomposition of benzene shows the process to be exothermic, the activation energy of the benzene decomposition process is so large that it will not sustain monopropellant decomposition. Indeed for this reason acetylene is considered an unstable species and benzene a stable one.

Considering again Eq. (6) and referring to E as an activation energy, attention is focused on the collision rate Z_{AB} , which from simple kinetic theory can be represented by

$$Z_{AB} = (A)(B)\sigma_{AB}^2[8\pi k_B T/\mu]^{1/2} \quad (7)$$

where σ_{AB} is the hard sphere collision diameter, k_B the Boltzmann constant, μ the reduced mass [$m_A m_B / (m_A + m_B)$], and m the mass of the species. Z_{AB} may be written in the form

$$Z_{AB} = Z'_{AB}(A)(B)$$

Thus, the Arrhenius form for the rate is

$$RR = Z'_{AB}(A)(B) \exp(-E/RT)$$

When compared to the reaction rate written from the law of mass action [reaction (2)], one finds that

$$k = Z'_{AB} \exp(-E/RT) = Z''_{AB} T^{1/2} \exp(-E/RT) \quad (8)$$

Thus, the important conclusion is that the specific reaction rate constant k is dependent on temperature alone and is independent of concentration. Actually, when complex molecules are reacting, not every collision has the proper steric orientation for the specific reaction to take place. To include the steric probability k is written as

$$k = Z''_{AB} T^{1/2} [\exp(-E/RT)] \mathcal{P} \quad (9)$$

where \mathcal{P} is a steric factor, which at times can be a very small number. Most generally, however, the Arrhenius form of the reaction rate constant is written as

$$k = \text{const } T^{1/2} \exp(-E/RT) = A \exp(-E/RT) \quad (10)$$

where the constant A takes into account the steric factor and the terms in the collision frequency other than the concentrations and is referred to as the kinetic pre-exponential A factor. The factor A as represented in Eq. (10) has a very mild $T^{1/2}$ temperature dependency that is generally ignored when plotting data. The form of Eq. (10) holds well for many reactions and shows an increase in k with T and permits convenient straight line correlations of data on $\ln k$ versus $(1/T)$ plots. Data that correlate as a straight line on a $\ln k$ versus $(1/T)$ plot are said to follow Arrhenius kinetics, and plots of the logarithm of rates or rate constants as a function of $(1/T)$ are referred to as

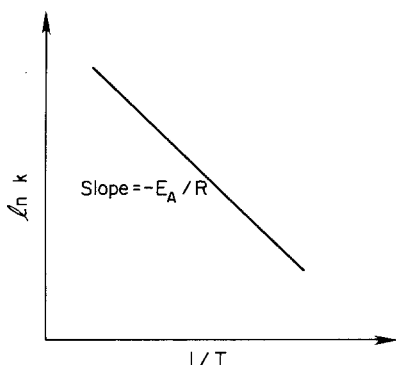


Fig. 2. Arrhenius plot of the specific reaction rate constant as a function of the reciprocal temperature.

Arrhenius plots. The slope of lines on these plots are equal to $(-E/R)$ and thus the activation energy may be determined readily (see Fig. 2). Low activation energy processes proceed faster than high activation energy processes at low temperatures and have much less temperature sensitivity. At high temperatures, high-activation energy reactions can prevail, because of this temperature sensitivity.

2. Transition State and Recombination Rate Theories

There are two classes of reactions for which Eq. (10) is not suitable. For low activation-energy free radical reactions, the temperature dependence in the pre-exponential takes on more importance. In this case the approach known as absolute or transition state theory of reaction rates gives a more appropriate correlation of reaction rate data with temperature. In this theory the reactants are assumed to be in equilibrium with an activated complex. One of the vibrational modes in the complex is considered loose and permits the complex to dissociate to products. Figure 1 is again an appropriate representation with reactants in equilibrium with the activated complex. When the equilibrium constant for this situation is written in terms of partition functions and the frequency of the loose vibration is allowed to approach zero, a rate constant can be derived in the following fashion.

The concentration of the activated complex may be calculated by statistical thermodynamics in terms of the reactant concentrations and an equilibrium constant [1, 6]. If the reaction scheme is written as



then the equilibrium constant with respect to the reactants may be written as

$$K_\ddagger = \frac{(ABC)^\ddagger}{(A)(BC)} \quad (12)$$

The symbol # refers to the activated complex. Statistical thermodynamics relate equilibrium constants to partition functions, and for the case in question one finds [6]

$$K_{\#} = \frac{(Q_T)_{\#}}{(Q_T)_A(Q_T)_{BC}} \exp\left(-\frac{E}{RT}\right) \quad (13)$$

where Q_T is the total partition function of each species in the reaction, and can be considered separable into vibrational, rotational, and translation partition functions.

According to the theory, one of the terms in the vibrational partition function part of $Q_{\#}$ is of a different character than the rest since it corresponds to a very loose vibration that allows the complex to dissociate into products. The complete vibrational partition function is written as

$$Q_{\text{vib}} = \prod_i [1 - \exp(-hv_i/k_B T)]^{-1} \quad (14)$$

where h is Planck's constant and ν_i the vibrational frequency of the i th mode. For the loose vibration, one term of the complete vibrational partition function can be separated and its value employed when ν tends to zero,

$$\lim_{\nu \rightarrow 0} [1 - \exp(h\nu/k_B T)] = (k_B T/h\nu) \quad (15)$$

Thus

$$(ABC)_{\#}/[(A)(BC)] = [(Q_{T-1})_{\#}(k_B T/h\nu)]/[(Q_T)_A(Q_T)_{BC}] \exp(-E/RT) \quad (16)$$

which rearranges to

$$\nu(ABC)_{\#} = (A)(BC)(k_B T/h)(Q_{T-1})_{\#}/[(Q_T)_A(Q_T)_{BC}] \exp(-E/RT) \quad (17)$$

where $(Q_{T-1})_{\#}$ is the partition function of the activated complex evaluated for all vibrational frequencies except the loose one. The term $\nu(ABC)_{\#}$ on the left-hand side of Eq. (17) is the frequency of the activated complex in the degree of freedom corresponding to its decomposition mode and is therefore the frequency of decomposition. Thus,

$$k = (k_B T/h)[(Q_{T-1})_{\#}/(Q_T)_A(Q_T)_{BC}] \exp(-E/k_B T) \quad (18)$$

is the expression for the specific reaction rate as derived from transition state theory.

If A is only a diatomic molecule, the reaction scheme can be represented by



Thus $(Q_{T-1})_{\#}$ goes to 1. There is only one bond in A, so

$$Q_{\text{vib},A} = [1 - \exp(-h\nu_A/k_B T)]^{-1} \quad (20)$$

Then

$$k = (k_B T/h)[1 - \exp(-h\nu_A/k_B T)]^{-1} \exp(-E/RT) \quad (21)$$

If ν_A of the stable molecule is large, which it normally is in decomposition systems, then the term in square brackets goes to one and

$$k = (k_B T/h) \exp(-E/RT) \quad (22)$$

Note that the term $(k_B T/h)$ gives a general order of the pre-exponential term for these dissociation processes.

Whereas the rate constant will increase monotonically with T for Arrhenius' collision theory, examination of Eqs. (18) and (22) reveals that for the low activation energy processes represented by transition state theory a nonmonotonic trend can be found [7]. Thus, data that show curvature on an Arrhenius plot probably represent a reacting system in which an intermediate complex forms and which is of low activation energy. The earliest representation of an important combustion reaction that showed curvature was by Dryer *et al.* [7] who by application of transition state theory correlated a wide temperature range of data for the CO + OH reaction. Since then consideration of transition state theory has been given to many other reactions important to combustion [8].

The use of transition state theory as a convenient expression of rate data is obviously complex due to the presence of the temperature dependent partition functions. Most researchers working in the area of chemical kinetic modeling have found it necessary to adopt a uniform means of expressing the temperature variation of rate data and consequently have adopted a modified Arrhenius form [9]

$$k = AT^n \exp(-E/RT) \quad (23)$$

where the power of T accounts for all the pre-exponential temperature dependent terms in Eqs. (10), (18), and (20). Since most elementary binary reactions exhibit Arrhenius behavior over modest ranges of temperature, usually the temperature dependence can be incorporated with sufficient accuracy into the exponential alone; thus for most data $n = 0$ is adequate, as will be noted for the extensive listing in the appendices [9]. However, for the large temperature ranges found in combustion, "non-Arrhenius" behavior of rate constants is more likely the rule rather than the exception, particularly for processes that have a small energy barrier. It should be noted that for these processes the pre-exponential factor that contains the ratios of partition functions (which are weak functions of temperature compared to an exponential) corresponds roughly to a T^n dependency with n in the $\pm 1-2$ range [10]. Indeed the values of n for the rate data expressions reported in the appendices fall within this range.

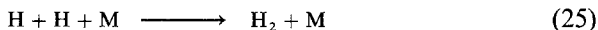
The units for the reaction rate constant k when the reaction is of order n (different from the n power of T) will be $[(\text{conc})^{n-1} (\text{time})]^{-1}$. Thus, for a first-order reaction the units of k are (sec^{-1}) and for a second-order reaction process, $\text{cm}^3 \text{ moles}^{-1} \text{ sec}^{-1}$.

Radical recombination is another class of reactions in which the Arrhenius expression will not hold. When simple radicals recombine to form a product, the energy liberated in the process is sufficiently great to cause the product to decompose into the original radicals. A third body is ordinarily necessary to remove this energy to complete the recombination. If the molecule formed in a recombination process has a large number of internal (generally vibrational) degrees of freedom, it can redistribute the energy of formation among these degrees and a third body is not necessary. In some cases the recombination process can be stabilized by the formed molecule radiatively dissipating some energy (chemiluminescence) or colliding with a surface and dissipating energy in this manner.

If one follows the approach of Landau and Teller [11], who in dealing with vibrational relaxation developed an expression by averaging a transition probability based on the relative molecular velocity over the Maxwellian distribution, the following expression for the recombination rate constant is obtained [6]

$$k \sim \exp(-T^{-1/3}) \quad (24)$$

Thus, for radical recombination, the reaction rate constant decreases mildly with the temperature, as one would intuitively expect. In dealing with the recombination of radicals in nozzle flow, this mild temperature dependency should be kept in mind. Recall the example of H atom recombination given earlier. If one writes M as any (or all) third body in the system, then the equation takes the form



The rate of formation of H_2 is third order and given by

$$d(\text{H}_2)/dt = k(\text{H})^2(\text{M}) \quad (25a)$$

Thus, in expanding dissociated gases through a nozzle, the velocity increases and the temperature and pressure decrease. The rate constant for this process thus increases, but only slightly. The pressure affects the concentrations and since the reaction is third order it enters the rate as a cubed term. In all, then, the rate of recombination in the high velocity expanding regions decreases due to the pressure term. The point to be made is that third-body recombination reactions are mostly pressure sensitive, generally favored at higher pressure, and rarely occur at very low pressures.

C. SIMULTANEOUS INTERDEPENDENT REACTIONS

In complex reacting systems, such as those which exist in combustion processes, a simple one-step rate expression will not suffice. More generally one finds simultaneous, interdependent reactions or chain reactions.

The most frequently occurring simultaneous, interdependent reaction mechanism is the case in which the product, as its concentration is increased, begins to dissociate into the reactants. The classical example is the hydrogen-iodine reaction:



The rate of formation of HI is then affected by two rate constants, k_f and k_b , and is written as

$$d(\text{HI})/dt = 2k_f(\text{H}_2)(\text{I}_2) - 2k_b(\text{HI})^2 \quad (27)$$

At equilibrium, the rate of formation of HI is zero, and one finds that

$$2k_f(\text{H}_2)_{\text{eq}}(\text{I}_2)_{\text{eq}} - 2k_b(\text{HI})_{\text{eq}}^2 = 0 \quad (28)$$

where the subscript eq designates the equilibrium concentrations. Thus,

$$\frac{k_f}{k_b} = \frac{(\text{HI})_{\text{eq}}^2}{(\text{H}_2)_{\text{eq}}(\text{I}_2)_{\text{eq}}} \equiv K_C \quad (29)$$

i.e., the forward and backward rate constants are related to the equilibrium constant K based on concentrations (K_C). The equilibrium constants are calculated from basic thermodynamic principles as discussed in Section 1B and the relationship $(k_f/k_b) \equiv K_C$ holds for any reacting system. The calculation of the equilibrium constant is much more accurate than experimental measurements of specific reaction rate constants. Thus given a measurement of a specific reaction rate constant, the reverse rate constant is determined from the relationship $K_C \equiv (k_f/k_b)$.

With this equilibrium consideration the rate expression for the formation of HI becomes

$$\frac{d(\text{HI})}{dt} = 2k_f(\text{H}_2)(\text{I}_2) - 2k_b(\text{HI})^2 = 2k_f(\text{H}_2)(\text{I}_2) - 2\frac{k_f}{K_C}(\text{HI})^2 \quad (30)$$

which shows there is only one independent rate constant in the problem.

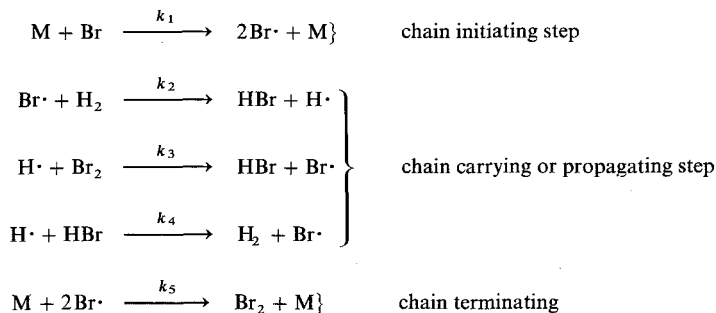
D. CHAIN REACTIONS

In most instances, two reacting molecules do not react directly as H_2 and I_2 do, but, in fact, react by one dissociating first to form radicals. These radicals then initiate a chain of steps. Interestingly, this procedure occurs in the reaction of H_2 with another halogen Br_2 . Experimentally, Bodenstein [12] found that the rate of formation of HBr obeys the expression

$$\frac{d(HBr)}{dt} = \frac{k'_{\text{exp}}(H_2)(Br_2)^{1/2}}{1 + k''_{\text{exp}}[(HBr)/(Br_2)]} \quad (31)$$

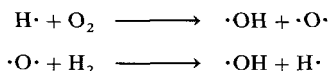
This expression shows that HBr is inhibiting to its own formation.

Bodenstein explained this result by suggesting that the H_2 - Br_2 reaction was chain in character and initiated by a radical (Br). He proposed the following steps:



The Br_2 bond energy is 46 kcal/mole and the H_2 is 104 kcal/mole. Consequently, over all the temperatures but the very highest, Br_2 dissociation will be the initiating step.

There exists another chain step that is perhaps the most important of the various chain types in that it is necessary to achieve nonthermal explosions. This chain step is one in which two radicals are created for each radical consumed. It is called chain branching, and two typical chain branching steps that occur in the H_2 - O_2 reaction system are



where the dot next to a species is the convention for designating a radical. Such branching will usually occur when the monoradical (such as $H\cdot$) formed by breaking a single bond reacts with a species containing a double bond type structure (such as that in O_2) or when a biradical (such as $\cdot O\cdot$) formed by

breaking a double bond reacts with a saturated molecule (such as H_2 or RH where R is any organic radical). For an extensive discussion of chain reactions reference should be made to the monograph by Dainton [13].

As shown in the H_2-Br_2 example radicals are produced by dissociation of a reactant in the initiation process. These types of dissociation reactions are highly endothermic and therefore are quite slow. Activation energy of these processes would be in the range of 40–110 kcal/mole. Propagation reactions similar to those of reactions (2)–(4) in the H_2-Br_2 example are important because they determine the rate at which the chain continues. For most propagation reactions of importance in combustion, activation energies normally lie between 0 and 10 kcal/mole. Obviously branching chain steps are a special case of propagating steps and as mentioned these will be the steps that lead to explosion. Since branching steps need not necessarily occur rapidly because of the multiplication effect, their activation energies may be higher than that of the linear propagation reactions with which they compete [14].

Termination occurs when two radicals recombine; they need not be similar, as shown in the H_2-Br_2 case. Termination can also occur when a radical reacts with a molecule to give either a molecular species or a radical of lower activity that cannot propagate a chain. Since recombination processes are exothermic, the energy developed must be removed by another source as discussed previously. The source can be another gaseous molecule M , as shown in the example, or a wall. For the gaseous case, a termolecular or third-order reaction is required and consequently except at high pressures these reactions are slower than other types.

In writing chain mechanisms note that many times backward reactions are written as an individual step; that is, reaction (4) of the H_2-Br_2 scheme is the backward step of reaction (2). The inverse of reaction (3) proceeds very slowly, is therefore not important in the system and usually is omitted for the H_2-Br_2 example.

From the five chain steps written for the H_2-Br_2 reaction, one can write an expression for the HBr formation rate:

$$\frac{d(HBr)}{dt} = k_2(Br)(H_2) + k_3(H)(Br_2) - k_4(H)(HBr) \quad (32)$$

In experimental systems, it is usually very difficult to measure the concentration of the radicals that are important intermediates. One would like to be able to relate the radical concentrations to other known or measurable quantities. It is possible to achieve this objective by the so-called steady-state approximation for the reaction's radical intermediates. The assumption is that the radicals form and react very rapidly so that the radical concentration changes only very slightly with time and approximates a steady-state

concentration. Thus, the equations for the rate of change of the radical concentration are written and then set equal to zero. For the H_2 - Br_2 system, then one has for (H) and (Br)

$$\frac{d(H)}{dt} = k_2(Br)(H_2) - k_3(H)(Br_2) - k_4(H)(HBr) \cong 0 \quad (33)$$

$$\frac{d(Br)}{dt} = 2k_1(Br_2) - k_2(Br)(H_2) + k_3(H)(Br_2) + k_4(H)(HBr) - 2k_5(Br)^2 \cong 0 \quad (34)$$

Writing these two equations equal to zero does not imply that equilibrium conditions exist as was the case for Eq. (28). It is important to realize that the steady-state approximation also does not imply that the rate of change of the radical concentration is necessarily zero, but that the rate terms for the expressions of radical formation and disappearance are much greater than the radical concentration rate term; that is, the sum of the positive terms and the sum of the negative terms on the right-hand side of the equality in Eqs. (33) and (34) are in absolute magnitude very much greater than the term on the left of the equality [3].

Thus it is assumed in the H_2 - Br_2 experiment that steady-state concentrations of radicals are approached and the concentrations for H and B are found to be

$$(Br) = (k_1/k_5)^{1/2}(Br_2)^{1/2} \quad (35)$$

$$(H) = \frac{k_2(k_1/k_5)^{1/2}(H_2)(Br_2)^{1/2}}{k_3(Br_2) + k_4(HBr)} \quad (36)$$

By substituting these values in the rate expression for the formation of HBr [Eq. (32)], one obtains

$$\frac{d(HBr)}{dt} = \frac{2k_2(k_1/k_5)^{1/2}(H_2)(Br_2)^{1/2}}{1 + [k_4(HBr)/k_3(Br_2)]} \quad (37)$$

which is the exact form found experimentally [Eq. (31)]. Thus,

$$k'_{\text{exp}} = 2k_2(k_1/k_5)^{1/2}, \quad k''_{\text{exp}} = k_4/k_3$$

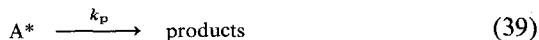
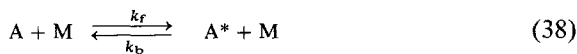
Thus, it is seen that, from the measurement of the overall reaction rate and the steady-state approximation, values of the rate constants of the intermediate radical reactions can be determined without any measurement of radical concentrations. Values k'_{exp} and k''_{exp} evolve from the experimental measurements and the form of Eq. (31). Since (k_1/k_5) is the inverse of the equilibrium constant for Br_2 dissociation and this value is known from thermodynamics, k_2 can be found from k'_{exp} . Value k_4 is found from k_2 and

the equilibrium constant that represents reactions (2) and (4), as written in the H_2 -Br reaction scheme. From the experimental value of k''_{exp} and k_4 , k_3 can be calculated.

The steady-state approximation, found to be successful in application to this straight chain process, can be applied to many other straight chain processes, chain reactions with low degrees of branching, and other types of nonchain systems. Because the rates of the propagating steps greatly exceed those of the initiation and termination steps in most, if not practically all, of the straight chain systems, the approximation always works well. However, the use of the approximation in the initiation or termination phase of a chain system, at which the radical concentrations are rapidly building or being destroyed, can lead to substantial errors.

E. PSEUDO-FIRST-ORDER REACTIONS AND THE "FALL-OFF" RANGE

As mentioned earlier, practically all reactions are initiated by bimolecular collisions; however, certain bimolecular reactions exhibit first-order kinetics. Whether a reaction is first or second order is particularly important in combustion because of the presence of large radicals that decompose into a stable species and a smaller radical (primarily the hydrogen atom). A prominent combustion example would be a paraffinic radical decaying to an olefin and a H atom. The order of such reactions and therefore the appropriate rate constant expression can change with the pressure. Thus, the application of a rate expression developed from one pressure and temperature range may not be applicable to another range. This question of order was first addressed by Lindemann [4] who proposed that first-order processes occurred as a result of a two-step reaction sequence in which the reacting molecule is activated by collisional processes and then the activated species decomposes to products. Similarly the activated molecule could be deactivated by another collision before it decomposes. If A is considered the reactant molecule and M its nonreacting collision partner, the Lindemann scheme can be represented as follows:



The rate of decay of A is given by

$$\frac{d(A)}{dt} = -k_f(A)(M) + k_b(A^*)(M) \quad (40)$$

and the rate of change of the activated species A^* by

$$\frac{d(A^*)}{dt} = k_f(A)(M) - k_b(A^*)(M) - k_p(A^*) \quad (41)$$

Applying the steady-state assumption to the activated species equation gives

$$A^* = \frac{k_f(A)(M)}{k_b(M) + k_p} \quad (42)$$

Substituting this value of A^* into Eq. (41), one obtains

$$-\frac{1}{(A)} \frac{d(A)}{dt} = \frac{k_f k_p(M)}{k_b(M) + k_p} = k_{\text{diss}} \quad (43)$$

where k_{diss} is a function of the rate constants and the collision partner concentration that is a direct function of the total pressure if the effectiveness of all collision partners is considered the same. Due to size, complexity, and the possibility of resonance energy exchange, the effectiveness of a collision partner (third body) can vary. Normally collision effectiveness is not a concern, but for some reactions specific molecules may play an important role [15].

At high pressures, $k_b(M) \gg k_p$ and

$$k_{\text{diss}, \infty} = \frac{k_f k_p}{k_b} = K k_p \quad (44)$$

where $k_{\text{diss}, \infty}$ becomes the high-pressure limit rate constant and K is the equilibrium constant (k_f/k_b). Thus at high pressures the decomposition process becomes overall first order. At low pressure $k_b(M) \ll k_p$ as the concentrations drop and

$$k_{\text{diss}, 0} = k_f(M) \quad (45)$$

where $k_{\text{diss}, 0}$ is the low-pressure limit rate constant. The process is then second order. Note the presence of the concentration (A) in the manner that Eq. (43) is written.

Many systems fall in a region of pressures (and temperatures) between the high- and low-pressure limits. This region is called the "fall-off range" and its importance to combustion problems has been very adequately discussed by Troe [16]. The question then is how to treat rate processes in the "fall-off range." Troe proposed that the "fall-off range" between the two limiting rate constants be represented using a dimensionless pressure scale

$$(k_{\text{diss}, 0}/k_{\text{diss}, \infty}) = k_b(M)/k_p \quad (46)$$

Substituting Eq. (44) into Eq. (43), one obtains

$$\frac{k_{\text{diss}}}{k_{\text{diss}, \infty}} = \frac{k_{\text{b}}(\text{M})}{k_{\text{b}}(\text{M}) + k_{\text{p}}} = \frac{k_{\text{b}}(\text{M})/k_{\text{p}}}{[k_{\text{b}}(\text{M})/k_{\text{p}}] + 1} \quad (47)$$

or, from Eq. (46)

$$\frac{k_{\text{diss}}}{k_{\text{diss}, \infty}} = \frac{k_{\text{diss}, 0}/k_{\text{diss}, \infty}}{1 + (k_{\text{diss}, 0}/k_{\text{diss}, \infty})} \quad (48)$$

For a pressure (or concentration) in the center of the "fall-off range," $(k_{\text{diss}, 0}/k_{\text{diss}, \infty}) = 1$ and

$$k_{\text{diss}} = 0.5k_{\text{diss}, \infty} \quad (49)$$

Since it is possible to write the products designated in Eq. (39) as two species that could recombine, it is apparent that recombination reactions can have a pressure sensitivity, and an expression for the recombination rate constant similar to Eq. (48) can be developed [16].

The preceding discussion stresses the importance of properly handling rate expressions for thermal decomposition of polyatomic molecules, a condition that prevails in many hydrocarbon oxidation processes. For a detailed discussion on evaluation of low- and high-pressure rate constants, one is again referred to Ref. [16].

Another example in which a pseudo-first-order condition can arise in evaluating experimental data is one in which one of the reactants (generally the oxidizer in a combustion system) is in large excess. Consider the arbitrary process



where $(\text{B}) \gg (\text{A})$. The rate expression is

$$\frac{d(\text{A})}{dt} = -\frac{d(\text{D})}{dt} = -k(\text{A})(\text{B}) \quad (51)$$

Since $(\text{B}) \gg (\text{A})$, the concentration of (B) does not change appreciably and $k(\text{B})$ would appear as a constant. The Eq. (51) becomes

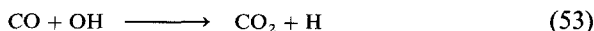
$$\frac{d(\text{A})}{dt} = -\frac{d(\text{D})}{dt} = -k'(\text{A}) \quad (52)$$

where $k' = k(\text{B})$. Equation (52) could represent experimental data because little dependence would be found on variations in the concentration of the excess component (B) . It, of course, appears overall first order. One should keep in mind however that k' contains a concentration and is pressure dependent. This pseudo-first-order concept arises in many practical combustion systems that are very fuel lean; i.e., O_2 is in large excess.

F. THE PARTIAL EQUILIBRIUM ASSUMPTION

As will be discussed in the following chapter, most combustion systems entail oxidation mechanisms with numerous individual reaction steps. Under certain circumstances a group of reactions will proceed rapidly and reach a quasi-equilibrium state. Concurrently, one or more reactions may proceed slowly. If the rate or rate constant of this slow reaction is to be determined and if the reaction contains a species difficult to measure, it is possible through a partial equilibrium assumption to express the unknown concentrations in terms of other measurable quantities. Thus, the partial equilibrium assumption is very much like the steady-state approximation discussed earlier. The difference is that in the steady-state approximation one is concerned with a particular species and in the partial equilibrium assumption one is concerned with particular reactions. Essentially then, partial equilibrium comes about when forward and backward rates are very large and the contribution that a particular species makes to a given slow reaction of concern can be compensated for by very small differences in the forward and backward rates of those reactions in partial equilibrium.

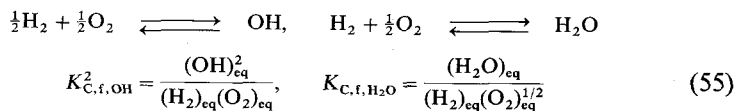
A specific example can illustrate the use of the partial equilibrium assumption. Considering, for example, a complex reacting hydrocarbon in an oxidizing medium. By the measurement of the CO and CO₂ concentrations it is desired to obtain an estimate of the rate constant of the reaction



The rate expression is

$$\frac{d(\text{CO}_2)}{dt} = -\frac{d(\text{CO})}{dt} = k(\text{CO})(\text{OH}) \quad (54)$$

Then the question is how to estimate the rate constant k without a measurement of the OH concentration. If one assumes there is equilibrium between the H₂-O₂ chain species, then the following equilibrium reactions of formation would develop from the complete reaction scheme



Solving the two latter expressions for the (OH)_{eq} concentration; one obtains

$$(\text{OH})_{\text{eq}} = (\text{H}_2\text{O})^{1/2}(\text{O}_2)^{1/4} [K_{\text{C},\text{f},\text{OH}}^2 / K_{\text{C},\text{f},\text{H}_2\text{O}}]^{1/2} \quad (56)$$

and the rate expression becomes

$$\frac{d(\text{CO}_2)}{dt} = -\frac{d(\text{CO})}{dt} = k [K_{\text{C},\text{f},\text{OH}}^2 / K_{\text{C},\text{f},\text{H}_2\text{O}}]^{1/2} (\text{CO})(\text{H}_2\text{O})^{1/2} (\text{O}_2)^{1/4} \quad (57)$$

Thus, one observes that the rate expression can be written in terms of readily measurable stable species. Care must be exercised in applying this assumption. Equilibria do not always exist among the H_2 - O_2 reactions in a hydrocarbon combustion system, and, indeed, there is a question if equilibrium exists during CO oxidation in a hydrocarbon system. Nevertheless it is interesting to note that there is experimental evidence that shows the rate of formation of CO_2 is $\frac{1}{4}$ order with respect to O_2 , $\frac{1}{2}$ order with respect to water and first order with respect to CO [17,18].

G. PRESSURE EFFECT IN FRACTIONAL CONVERSION

In combustion problems, one is interested in the rate of energy conversion or utilization. Thus it is more convenient to deal with the fractional change of a particular substance rather than the absolute concentration. If (M) is used to denote the concentrations in a chemical reacting system of arbitrary order n , then the rate expression is

$$\frac{d(M)}{dt} = -k(M)^n \quad (58)$$

Since (M) is a concentration, it may be written in terms of the total density ρ and the mole or mass fraction ε ,

$$(M) = \rho\varepsilon \quad (59)$$

It follows then that at constant temperature

$$\rho(d\varepsilon/dt) = -k(\rho\varepsilon)^n \quad (60)$$

$$(d\varepsilon/dt) = -k\varepsilon^n \rho^{n-1} \quad (61)$$

For a constant temperature system, $\rho \sim P$ and

$$(d\varepsilon/dt) \sim P^{n-1} \quad (62)$$

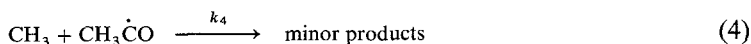
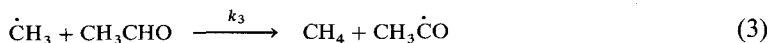
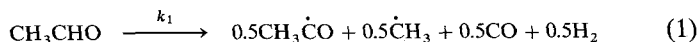
The fractional change is proportional to the pressure to the reaction order minus one. This result is important in determining the pressure dependency of laminar flame speeds to be discussed in Chapter 4.

PROBLEMS

1. For a temperature of 1000 K calculate the pre-exponential factor in the specific reaction rate constant for (a) any simple bimolecular reaction and (b) any simple unimolecular decomposition reaction.

2. The decomposition of acetaldehyde is found to be overall first order with respect to the acetaldehyde and to have an overall activation energy of 60 kcal/mole.

Assume the following sequence to be the chain decomposition mechanism of acetaldehyde:



For these conditions

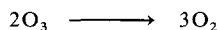
- List the type of chain reaction and the molecularity of each of the four reactions
- Show that these reaction steps would predict an overall reaction order of one with respect to the acetaldehyde
- Estimate the activation energy of Reaction 2, if $E_1 = 80$, $E_3 = 10$, and $E_4 = 5$ kcal/mole.

Hint: E_1 is much larger than E_2 , E_3 , and E_4 .

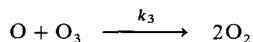
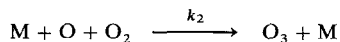
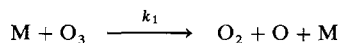
3. Many early investigators interested in determining the rate of decomposition of ozone performed their experiments in mixtures of ozone and oxygen. Their observations led them to write the following rate expression

$$d(\text{O}_3)/dt = k_{\text{exp}}[(\text{O}_3)^2/(\text{O}_2)]$$

The overall thermodynamic equation for ozone conversion to oxygen is



The inhibiting effect of the oxygen led many to expect that the decomposition followed the following chain mechanism:



- If the chain mechanisms postulated were correct and if the rate constants k_2 and k_3 were nearly equal, would the initial concentration of oxygen have been much less than or much greater than that of ozone?
- What is the effective overall order of the experimental result under these conditions?
- Given that k_{exp} was determined as a function of temperature, which of the three elementary rate constants is determined? Why?
- What type of additional experiment should be performed in order that all the elementary rate constants be determined?

REFERENCES

1. (a) Benson, S. W., "The Foundations of Chemical Kinetics," McGraw-Hill, New York, 1960.
(b) Weston, R. E., and Schwartz, H. A., "Chemical Kinetics," Prentice-Hall, Englewood Cliffs, New Jersey, 1972. (c) Smith, I. W. M., "Kinetics and Dynamics of Elementary Reactions," Butterworth, London, 1980. (d) Laidler, K. J., "Theories of Chemical Reaction Rates," McGraw-Hill, New York, 1969.
2. Penner, S. S., "Introduction to the Study of the Chemistry of Flow Processes," Chapter 1, Butterworth, London, 1955.
3. Williams, F. A., "Combustion Theory," 2nd ed., Appendix B, Benjamin-Cummings, Menlo, California, 1985.
4. Lindemann, F. A., *Trans. Faraday Soc.*, **17**, 598 (1922).
5. Arrhenius, S., *Phys. Chem.* **4**, 226 (1889).
6. Vincenti, W. G., and Kruger, C. H., Jr., "Introduction to Physical Gas Dynamics," Chapter VII, Wiley, New York, 1965.
7. Dryer, F. L., Naegeli, D. W., and Glassman, I., *Combust. Flame* **17**, 270 (1971).
8. Fontijn, A., and Zellner, R., Influence of temperature on rate coefficients of bimolecular reactions, in "Reactions of Small Transient Species" (A. Fontijn and M. A. A. Clyne, eds.), Academic Press, Orlando, 1983.
9. Westbrook, C. K., and Dryer, F. L., *Prog. Energy Combust. Sci.* **10**, 1 (1984).
10. Kaufman, F., *Int. Symp. Combust.*, 15th p. 752, Combustion Inst., Pittsburgh, Pennsylvania, 1974.
11. Landau, L., and Teller, E., *Phys. Z. Sowjet.* **10**, 1, 34 (1936).
12. Bodenstein, M., *Phys. Chem.* **85**, 329 (1913).
13. Dainton, F. S., "Chain Reactions: An Introduction," Methuen, London, 1956.
14. Bradley, J. N., "Flame and Combustion Phenomena," Chapter 2, Methuen, London, 1969.
15. Yetter, R. A., Dryer, F. L., and Rabitz, H., *Int. Symp. Gas Kinetics*, 7th, Gottingen, 1982.
16. Troe, J., *Int. Symp. Combustion*, 15th, p. 667, Combustion Inst., Pittsburgh, Pennsylvania, 1974.
17. Dryer, F. L., and Glassman, I., *Int. Symp. Combustion*, 14th, p. 987, Combustion Inst., Pittsburgh, Pennsylvania, 1972.
18. Williams, G. C., Hottel, H. C., and Morgan, A. G., *Int. Symp. Combustion*, 12th, Combustion Inst., Pittsburgh, Pennsylvania, 1968.

Explosive and General Oxidative Characteristics of Fuels

A. INTRODUCTION

In the previous chapters, the fundamental areas of thermodynamics and chemical kinetics were reviewed. These areas provide the background for the study of very fast reacting systems, termed explosions. In order for flames (deflagrations) or detonations to propagate, the reaction kinetics must be fast; i.e., the mixture must be explosive.

B. CHAIN BRANCHING REACTIONS AND CRITERIA FOR EXPLOSION

Consider, for example, a mixture of hydrogen and oxygen stored in a vessel in stoichiometric proportions and at a total pressure of 1 atm. The vessel is immersed in a thermal bath kept at 500°C, as shown in Fig. 1.

If the vessel shown in Fig. 1 is evacuated to a few millimeters of mercury (torr) pressure, there is an explosion. Similarly, if the system is pressurized to 2 atm pressure, there is also an explosion. These facts suggest explosive limits.

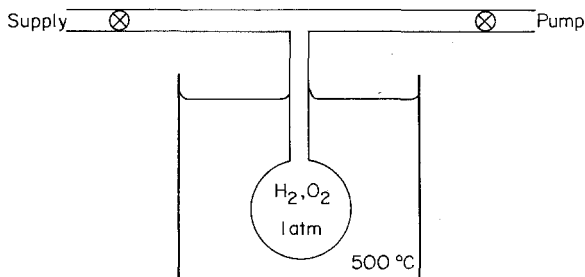
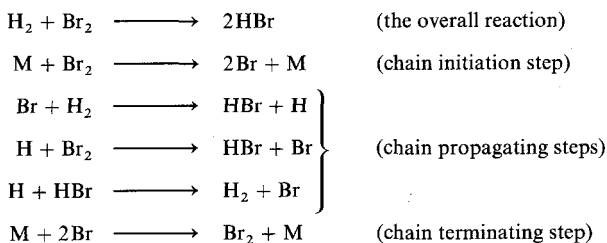


Fig. 1. Experimental configuration for the determination of explosion limits.

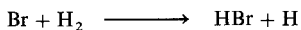
If H_2 and O_2 react to form explosive combustion, it is possible that such processes could occur in a flame, which indeed they do. A fundamental question is what governs the conditions that give explosive mixtures. In order to answer this question, it is well to consider again the chain reaction as it occurs in the H_2 and Br_2 reaction:



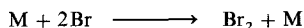
There are two means by which the reaction can be initiated—thermally or photochemically. If the H_2 - Br_2 mixture is at room temperature, a photochemical experiment can be performed by using light of short wavelength; i.e., high enough $h\nu$ to rupture the Br—Br bond through a transition to a higher electronic state. In an actual experiment, the light source can be made as weak as possible and the actual energy measured. Then, one can estimate the number of bonds broken and measure the number of HBr molecules formed. The ratio of HBr molecules formed per Br atom created is called the photoyield. It is found in the room temperature experiment that

$$\text{HBr}/\text{Br} \sim 0.01 \ll 1$$

and, of course, no explosive characteristic is observed. The reason no explosive characteristic is found in the photolysis experiment at room temperature is that the reaction

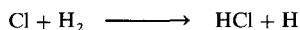


is quite endothermic and thus slow. Since the reaction is slow, the chain effect is overtaken by the recombination reaction



Thus, there are competitive reactions that appear to determine the overall character of the reacting system and one observes that a chain reaction is possible without an explosion.

For the H_2-Cl_2 system, the photoyield is of the order 10^4 to 10^7 . In this case, the chain step is much faster, in that the reaction



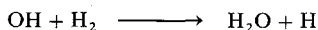
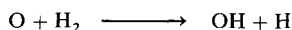
has an activation energy of only 6 kcal/mole compared to 18 kcal/mole for the corresponding bromine reaction. The fact that in the iodine reaction the corresponding step has an activation energy of 33 kcal/mole gives credence to the fact that the iodine reaction does not proceed through a chain mechanism, whether initiated thermally or by photolysis.

From the above discussion, it is obvious, then, that only the H_2-Cl_2 reaction can be exploded photochemically, that is, at low temperatures. The H_2-Br_2 and H_2-I_2 systems can only support thermal (high-temperature) explosions. A thermal explosion occurs when a chemical system undergoes an exothermic reaction, sufficient heat is not removed from the system and it becomes self-heating. Since the rate of reaction, and thus rate of heat release, will both increase exponentially with temperature, the reaction rapidly runs away; that is, the system explodes. This phenomenon is the same as that involved in ignition processes and is treated in detail in the chapter on thermal ignition (Chapter 7).

Recall that in the discussion of kinetic processes it was emphasized that the H_2-O_2 reaction contains an important characteristic chain branching step, namely,



which leads to a further chain branching system,



The first two of the above three steps are branching, in that two radicals are formed for each one consumed. Since all three steps are necessary in the chain system, the multiplication factor, usually designated α , is seen to be greater than 1, but less than 2. The first of the above three reactions is strongly endothermic and thus will not proceed rapidly at low temperatures. So, at low temperatures an H atom can survive many collisions and can find its way to a surface to be destroyed. This result explains why there is steady reaction

in some H_2-O_2 systems where H radicals are introduced. Explosion occurs only at the higher temperatures, where the first step proceeds more rapidly.

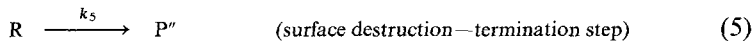
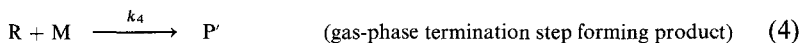
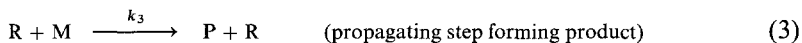
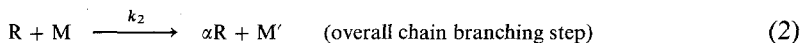
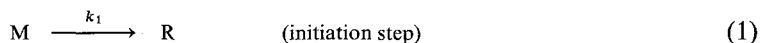
It is interesting to consider the effect of the multiplication factor. In a particular straight chain reaction, assume there are 10^8 collisions/sec, 1 chain particle/cm³, and 10^{19} molecules/cm³. Thus, all molecules will be consumed in 10^{11} sec or approximately 30 years.

In a particular branched chain reaction, the same basic conditions as before are assumed. However, the multiplication factor is taken as 2. Thus,

$$2^N = 10^{19}, \quad N = 62$$

All the molecules are consumed in 62 generations, and the time for completion is 62×10^{-8} sec or approximately a microsecond. For $\alpha = 1.01$, the time is only 10^{-4} sec, or 10 msec; consequently one may conclude that as long as α is greater than 1, the reaction proceeds rapidly. These two previous results hold only for the case in which no radicals are destroyed; that is, there are no termination steps. The explicit value of α necessary for explosion is determined by the rate of the termination steps as shown in the subsequent paragraphs.

In order to illustrate the conditions under which chain branching can lead to an explosion, a simplified generalized kinetic model is chosen and written as



where M and M' are reactant molecules in the system, R represents all radicals that are chain carriers, and P, P', and P'' are products formed in the system. According to this generalized scheme M' must be different from M because of Reaction 2, but essentially becomes another M since it can react with a radical. A radical is consumed and formed in reaction (3) and since R represents any radical chain carrier it is written on both sides of this equation; that is reaction (3) is a typical chain propagating step, a chain carrier is neither gained nor lost. The reactions leading to P and P' are the principal product formation steps and P and P' are meant to represent different products; P'' represents minor products formed on walls or surfaces.

Now the question to be considered is what value of α is necessary for the system to be explosive. The steady-state analysis is used again. The explosion condition is determined by the rate of formation of a major product and for purposes here P from reaction (3) is selected. Thus,

$$d(P)/dt = k_3(R)(M) \quad (3a)$$

The steady-state condition for the chain carrier concentration (R) is

$$d(R)/dt = k_1(M) + k_2(\alpha - 1)(R)(M) - k_4(M)(R) - k_5(R) = 0 \quad (6)$$

and one finds

$$(R) = \frac{k_1(M)}{k_4(M) + k_5 - k_2(\alpha - 1)(M)} \quad (7)$$

Substituting Eq. (7) into Eq. (3a), one obtains

$$\frac{d(P)}{dt} = \frac{k_1 k_3 (M)^2}{k_4(M) + k_5 - k_2(\alpha - 1)(M)} \quad (8)$$

The rate of formation of the product P becomes infinite, or the system explodes, when the denominator of Eq. (8) equals zero. Notice that k_1 , that is the initiation step, determines the rate of formation of P, but does not affect the condition for explosion. Solving for α when the denominator is zero gives the critical value for explosion, namely,

$$\alpha_{\text{crit}} = 1 + \frac{k_4(M) + k_5}{k_2(M)} \quad (9)$$

Thus, for a temperature and pressure condition for which $\alpha_{\text{react}} > \alpha_{\text{crit}}$, the system becomes explosive; for the reverse, the products form by slow reaction. For most purposes (M) can be considered proportional to the total pressure, and one readily can understand the pressure effect observed for the $\text{H}_2\text{-O}_2$ experiment discussed at the beginning of this section. When $\alpha_{\text{react}} > \alpha_{\text{crit}}$, the radical pool continues to increase rapidly, the steady-state assumption can no longer hold and, thus, Eq. (7) has no physical significance. If the system were written for the rate of formation of product P', the determination of α_{crit} would have been the same since the denominator of the new rate expression would be the same.

Since a most generalized scheme was considered above, from a practical point of view, it is well to point out that you cannot reach an explosive condition even if there is chain branching if the reacting radical for the chain branching step is not regenerated in the propagating steps and this radical's only source is the initiation step.

It is also interesting to note that, if the general mechanism [Eqs. (1)–(5)] were a propagating system with $\alpha = 1$, the rate of change of product P would be

$$[d(P)/dt] = [k_1 k_3 (M)^2] / [k_4 (M) + k_5]$$

Thus, the condition for fast reaction is

$$k_1 k_3 (M)^2 \gg k_4 + k_5$$

and an explosion is obtained at high pressure and/or high temperature (where the rates of propagation reactions exceed the rates of termination reactions). In the photochemical experiments described earlier, the explosive condition would not be dependent on k_1 , but on the initial perturbed concentration of radicals.

In most systems of interest in combustion there are numerous chain steps and it is important to introduce the concept of a chain length that is defined as the average number of product molecules formed in a chain cycle or the product reaction rate divided by the system initiation rate [1]. Thus, for the previous scheme, one has the chain length (cl) equal to Eq. (8) divided by the rate expression for Eq. (1); i.e.,

$$cl = \frac{k_3 (M)}{k_4 (M) + k_5 - k_2 (\alpha - 1) (M)} \quad (10)$$

or if the system contains only propagating steps, $\alpha = 1$, and

$$cl = \frac{k_3 (M)}{k_4 (M) + k_5} \quad (11)$$

Considering that for a steady-system termination and initiation steps must be in balance, the definition of chain length could have been defined, as well, as the rate of product formation divided by the rate of termination. When chains are long, the types of products formed are determined by the propagating reactions alone and one can ignore the initiation and termination steps.

C. EXPLOSION LIMITS AND OXIDATION CHARACTERISTICS OF HYDROGEN

Many of the early contributions to the understanding of hydrogen–oxygen oxidation mechanisms developed from the study of explosion limits. There were many extensive treatises written on the subject of the hydrogen–oxygen reaction and, in particular, much attention had been given to the effect of walls on radical destruction (a chain termination step) [2]. Such effects are

not important in the combustion processes of most interest here. More recently thorough reviews of this system have appeared [3,4].

Flames of hydrogen in air or oxygen show little or no visible radiation and what radiation is normally observed is due to trace impurities. Considerable amounts of OH can be detected, however, in the ultraviolet region of the spectrum. In stoichiometric flames, the maximum temperature reached in air is about 2400 K and in oxygen 3100 K. The burned gas composition in air shows about 57% conversion to water and the radicals H, O, and OH comprise about one-quarter of the remainder [5]. In static systems practically no reactions occur below 675 K and above 850 K explosion occurs spontaneously at all pressures. Between these temperatures, three separate explosion limits have been identified (Fig. 2). Any H_2-O_2 reaction mechanism must be able to explain these explosion limits.

It is now important to stress some points in order to eliminate possible confusion with previously held concepts and certain subjects to be discussed later. The explosive limits are not flammability limits. Explosion limits are the pressure-temperature boundaries for a specific mixture ratio of fuel and oxidizer and separate the regions of slow and fast reaction. For a given temperature and pressure, flammability limits specify the lean and rich fuel-oxidizer mixture ratio beyond which no flame will propagate. One must have fast reactions for a flame to propagate. A stoichiometric mixture of H_2 and O_2 , at standard conditions, will support a flame because an ignition source initially brings a local mixture into the explosive regime, and the established flame by diffusion heats fresh mixture to high enough temperatures to be explosive. Thus, in the early parts of any flame, the fuel-air

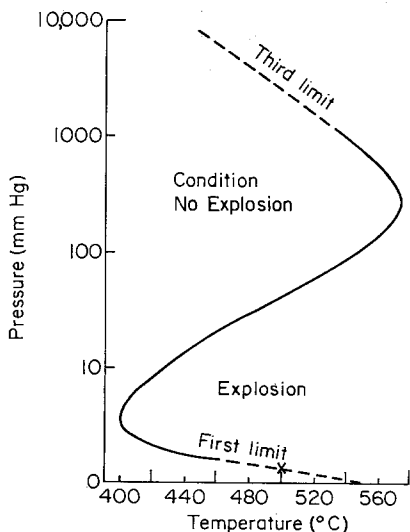


Fig. 2. Explosion limits of a stoichiometric hydrogen-oxygen mixture (after Lewis and von Elbe [2]).

mixture may follow a low-temperature steady reaction system and in the latter parts, an explosive reaction system. This point is significant, particularly in hydrocarbon combustion, because it is in the low-temperature regime where particular compounds that lead to pollutants are formed.

Figure 2 depicts the explosion limits of a stoichiometric mixture of hydrogen and oxygen. Explosion limits can be found for many different mixture ratios. The point *X* on Fig. 2 marks the conditions (500°C; 1 atm) described at the very beginning of this chapter in Fig. 1. It now becomes obvious that increasing or decreasing the pressure at constant temperature can cause an explosion.

Certain general characteristics of this curve can be stated. The third limit portion of the curve is as one would expect from simple density considerations. Any discussion of the first, or lower limit, will be related to wall effects and its role in chain destruction.

The expression developed for α_{crit} [Eq. (9)] applies to the lower limit only when the wall effect is considered as a first-order reaction of chain destruction, since $R \xrightarrow[k_{wall}]{} \text{destruction}$ was written. Although, in general, the features of the movement of the boundaries are not explained fully, the three limits can be explained by reasonable hypotheses of mechanisms.

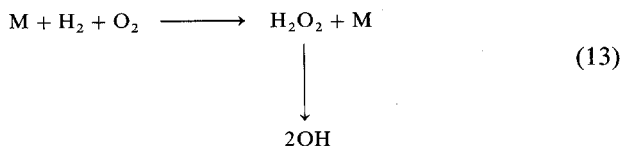
The manner in which the reaction is initiated to give the front designated by the curve in Fig. 2 suggests, as was inferred earlier, that the explosion is in itself a branched chain phenomenon. Thus, possible branched chain mechanisms to explain the limits must be considered.

Basically, only thermal, and not photolysis, mechanisms are considered. The dissociation energy of hydrogen is less than oxygen, so that the initiation can be related to hydrogen dissociation. Only a few radicals are required to initiate the explosion in the region of temperature of interest, i.e., about 400°C. If hydrogen dissociation is the chain's initiating step, then it proceeds by the reaction

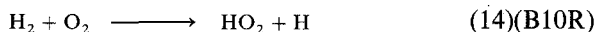


which requires about 106 kcal/mole. The second equation number refers to the rate data for the reaction in question as given in Appendix B. When R appears after the number it means that the reaction is the backward one of that referenced in Appendix B.

The early modelling literature suggested the following initiation step

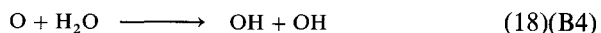
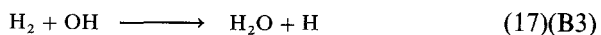
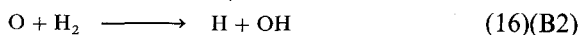


because this reaction required only 51 kcal/mole, but this trimolecular reaction has been evaluated to have only a very small rate [6]. Because in modelling it accurately reproduces experimental ignition delay measurements under shock tube and detonation conditions [7], the most probable initiation step, except at the very highest temperature at which Eq. (12) would prevail, could be



where HO_2 is the relatively stable hydroperoxy radical that has been identified by mass spectroscopic analysis.

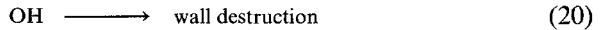
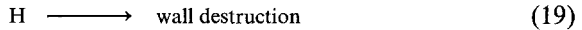
The essential feature of the initiation step is to provide a radical for the chain system and, as discussed in the previous section, the actual initiation step is not important in determining the explosive condition, nor is it important in determining the products formed. Either Eq. (12) or (14) provides an H radical that develops a radical pool of OH, O, and H by the chain reactions



Equation (15) is chain branching and 16 kcal/mole endothermic. Equation (16) is also chain branching and 2 kcal/mole exothermic. Note that the H radical is regenerated in the chain system and there is no chemical mechanism barrier to prevent the system from becoming explosive. Since, as discussed previously, radicals react rapidly, their concentration levels in many systems are very small; consequently the reverse of reactions (15), (16), and (18) can be neglected. Normally reactions between radicals are not considered, except in termination steps late in the reaction when the concentrations are high and only stable product species exist. Thus, the reverse reactions (15), (16), and (18) are not important for the determination of the second limit [i.e., $(M) = 2k_{15}/k_{21}$], nor are they important for the steady-slow H_2/O_2 and $\text{CO}/\text{H}_2\text{O}/\text{O}_2$ reactions; however, they are generally important in all explosive H_2/O_2 and $\text{CO}/\text{H}_2\text{O}/\text{O}_2$ reactions. The importance of these radical-radical reaction in these cases is verified by the existence of superequilibrium radical concentrations and the validity of the partial equilibrium assumption.

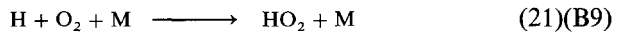
The sequence [Eqs. (15)–(18)] is of great importance in the oxidation reaction mechanisms of any hydrocarbon in that it provides the essential chain branching and propagating steps as well as the radical pool for fast reaction.

The important chain termination steps in the static explosion experiments (Fig. 1) are



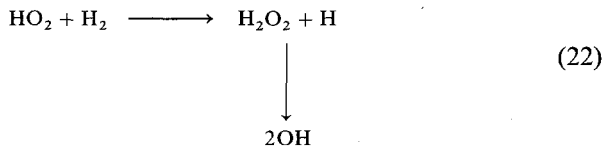
Either, or both, explain the lower limit of explosion since it is apparent that wall collisions become much more predominant at lower pressure than molecular collisions. The fact that the limit is found experimentally to be a function of the containing vessel diameter is further evidence of this type of wall destruction step.

The second explosion limit must be explained by gas-phase production and destruction of radicals. This limit is found to be independent of vessel diameter. For it to exist, the most effective chain branching reaction [(reaction (15))] must be overridden by another reaction step. Since at a fixed temperature as one moves from a lower to higher pressure the system goes from an explosive to steady reaction condition, then the reaction step that overrides the chain branching step must be more pressure sensitive. This reasoning leads one to propose a third-order reaction in which the species involved are in large concentration [2]. The accepted reaction that satisfies these prerequisites is



where M is the usual third body that takes away the energy necessary to stabilize the combination of H and O₂. At higher pressures it certainly is possible to obtain proportionally more of this trimolecular reaction than the binary system represented by reaction (15). The hydroperoxy radical HO₂ is considered to be relatively unreactive so that it is able to diffuse to the wall and thus become a means for effectively destroying H radicals.

The upper (third) explosion limit is due to a reaction that overtakes the stability of the HO₂ and is possibly the system

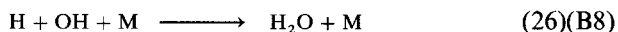
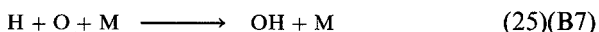
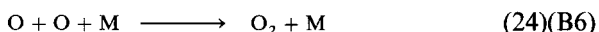
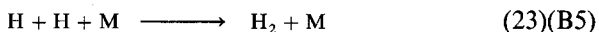


Water vapor tends to inhibit explosion due to the effect of reaction (21) in that water has a high third-body efficiency, which is most probably due to some resonance energy exchange with the HO₂ formed.

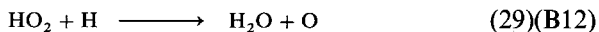
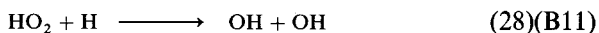
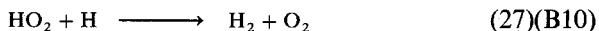
Since reaction (21) is a recombination step requiring a third body, its rate decreases with increasing temperature, whereas the rate of reaction (15) increases with temperature. One then can come to the general conclusion that

reaction (15) will dominate at higher temperatures and lower pressures, and reaction (21) will be more effective at higher pressures and lower temperatures. Thus, in order to explain the limits in Fig. 2 it becomes apparent that at temperatures above 875 K, reaction (15) always prevails and the mixture is explosive for the complete pressure range covered.

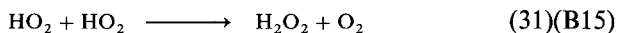
In this higher temperature regime and in atmospheric pressure flames, the eventual fate of the radicals formed is by recombination. The principal gas-phase termination steps are



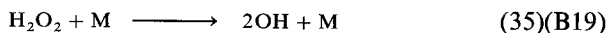
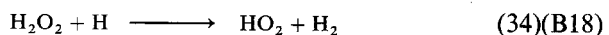
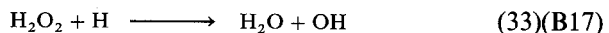
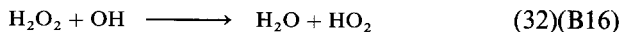
In combustion systems, there are usually ranges of temperature and pressure in which the rates of reactions (15) and (21) have comparable rates. Thus, to be complete, reactions of HO_2 also must be considered. Sometimes HO_2 is called a metastable species because it is relatively unreactive as a radical. Its concentrations can build up in a reacting system. Thus, HO_2 may be consumed in the H_2 - O_2 system by various radicals according to the reactions [4]



The recombination of HO_2 radicals by

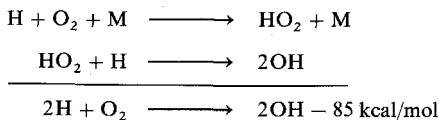


yields hydrogen peroxide (H_2O_2), which is consumed by reactions with radicals and by thermal decomposition according to

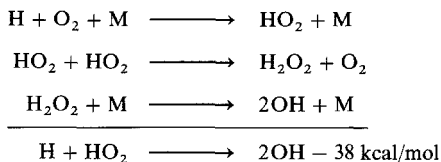


From the above sequence of reactions one finds that although reaction (21) terminates the chain under some conditions, under other conditions it is part of a chain propagating path consisting essentially of reactions (21) and (28)

or reactions (21), (31), and (35). It is also interesting to note that, as are most HO_2 reactions, these two sequences of reactions are very exothermic, i.e.,



and



and hence they can significantly affect the temperature of an (adiabatic) system and thus move the system into an explosive regime. The point to be emphasized is that slow competing reactions can become important if they are very exothermic.

It is apparent that the fate of the H atom (radical) is crucial in determining the rate of the $\text{H}_2\text{-O}_2$ reaction, or for that matter the rate of any hydrocarbon oxidation mechanism. From observations of the data in Appendix B one will observe that at temperatures encountered in flames the rates of reaction between H atoms and many hydrocarbon species are considerably larger than the rate of reaction (15). Note the comparisons in Table 1. Thus, these reactions compete very effectively with reaction (15) for H atoms and reduce the chain branching rate. For this reason, hydrocarbons are found to act as inhibitors for the $\text{H}_2\text{-O}_2$ system [4]. At highly elevated pressures ($P \geq 20$ atm) and at relatively low temperatures ($T \cong 1000$ K), reaction (21) will dominate over reaction (15), and the sequence of reactions (21), (31), and (35)

TABLE 1
Rate constants of specific radical reactions

Rate constant	1000 K	2000 K
$k(\text{C}_3\text{H}_8 + \text{OH})$	5.0×10^{12}	1.6×10^{13}
$k(\text{H}_2 + \text{OH})$	1.6×10^{12}	6.0×10^{12}
$k(\text{CO} + \text{OH})$	1.7×10^{11}	3.5×10^{11}
$k(\text{H} + \text{C}_3\text{H}_8) \longrightarrow i\text{C}_3\text{H}_7$	7.1×10^{11}	9.9×10^{12}
$k(\text{H} + \text{O}_2)$	4.7×10^{10}	3.2×10^{12}

has been found to provide the chain propagation. Also, at higher temperatures, when $\text{H} + \text{O}_2 = \text{OH} + \text{O}$ is microscopically balanced, reaction (21) ($\text{H} + \text{O}_2 + \text{M} \rightarrow \text{HO}_2 + \text{M}$) can compete favorably with reaction (15) for H atoms since the net removal of H atoms from the system by reaction (15) may be small due to its equilibration. In contrast the sequence of reaction (21) followed by the reaction of the fuel with HO_2 to form a radical and hydrogen peroxide, and then reaction (35) results in chain branching. Under these conditions increased fuel will result, therefore, in an accelerated overall rate of reaction and as stated at lower pressures will act as an inhibitor due to competition with reaction (15) [4].

D. EXPLOSION LIMITS AND OXIDATION CHARACTERISTICS OF CARBON MONOXIDE

The understanding of the oxidation of carbon monoxide from early experimental evidence was confused by the presence of any hydrogen containing impurity. The rate of CO oxidation in the presence of species such as water is substantially faster than the "bone dry" condition. It is very important to realize that very small quantities of hydrogen, even of the order of 20 ppm, will increase the rate of CO oxidation substantially [8]. Generally, the mechanism with hydrogen-containing compounds present is referred to as the "wet" carbon monoxide condition. Obviously in most practical systems, CO will proceed through this so-called "wet" route.

It is informative, however, to consider the possible mechanisms for dry CO oxidation. Again the approach is to consider the explosion limits of a stoichiometric, dry CO-O_2 mixture. The explosion limits shown in Fig. 3 and the reproducibility of these limits are not well defined, principally because the extent of dryness in the various experiments determining the limits may not be the same. Thus, typical results for explosion limits for "dry" CO would be as depicted in Fig. 3.

Figure 3 reveals that the low-pressure ignition of CO-O_2 is characterized by an explosion peninsula very much like the case of $\text{H}_2\text{-O}_2$. Outside this peninsula a pale-blue glow is often observed and its limits determined as well. A third limit has not been defined, and if it exists, it lies well above 1 atm.

As in the case of $\text{H}_2\text{-O}_2$ limits, certain general characteristics of the defining curve in Fig. 3 may be stated. The lower limit meets all the requirements of wall destruction of a chain propagating species. The effect of vessel diameter and surface character and condition has been well established by experiment [2].

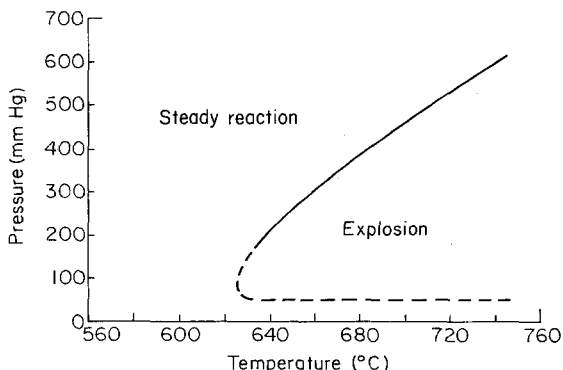
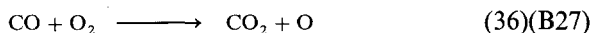
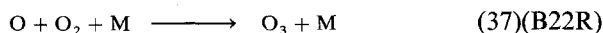


Fig. 3. Explosion limits of a carbon monoxide-oxygen mixture (after Lewis and von Elbe [2]).

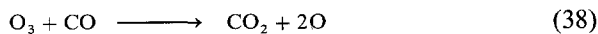
Under dry conditions the chain initiating step is



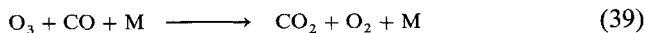
which is mildly exothermic, but slow at combustion temperatures. The further steps in this oxidation process involve O atoms, but the exact nature of these steps is not fully established. Lewis and von Elbe [2] suggested that chain branching would come about from the step



This reaction is slow, but could build up in supply. Ozone O_3 is the metastable species in the process (like HO_2 in H_2 - O_2 explosions) and could initiate chain branching and, thus, explain the explosion limits. The branching arises from the reaction

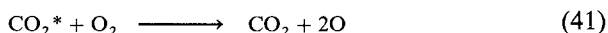


Ozone destruction at the wall to form oxygen molecules would explain the lower limit. Lewis and von Elbe explain the upper limit by the third-order reaction

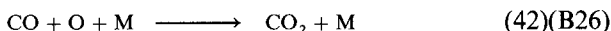


However, O_3 does not appear to react with CO below 523 K. Since CO is apparently oxidized by the oxygen atoms formed by the decomposition of ozone [the reverse of reaction (37)], the reaction must have a high activation energy (> 30 kcal/mole). This oxidation of CO by O atoms was thought to be rapid in the high-temperature range, but one must recall that it is a three-body recombination reaction.

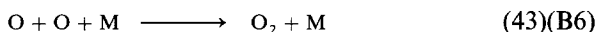
Analysis of the glow and emission spectra of the CO-O₂ reaction suggests that excited carbon dioxide molecules could be present. If it is argued that O atoms cannot react with oxygen (to form ozone), then they must react with the CO. A suggestion of Semenov was developed further by Gordon and Knipe [9] to give the following alternate scheme for chain branching



where CO₂* is the excited molecule from which the glow appears. This process is exothermic and might be expected to occur. Gordon and Knipe counter the objection that CO₂* is short-lived in that through system crossing in excited states its lifetime may be sufficient to sustain the process. In this scheme the competitive three-body reaction to explain the upper limit is the aforementioned one

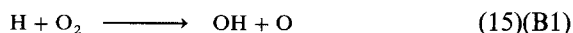
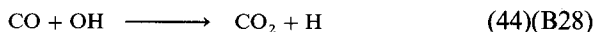
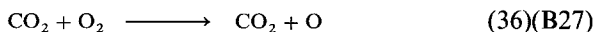


Due to the fact that the above mechanisms did not explain shock tube rate data, Brokaw [8] proposed that the mechanism consisted of reaction (36) as the initiation step with subsequent large energy release through the three-body reaction (42) and

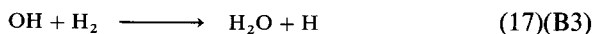


The rates of reactions (36), (42), and (43) are very small at combustion temperatures, so that the oxidation of CO in the absence of any hydrogen containing material is very slow. Indeed it is extremely difficult to ignite and have a flame propagate through a bone dry, impurity free CO-O₂ mixture.

Very early, from the analysis of ignition, flame speed, and detonation velocity data, investigators realized that small concentrations of hydrogen-containing materials would catalyze appreciably the kinetics of CO-O₂. The H₂O catalyzed reaction essentially proceeds in the following manner:

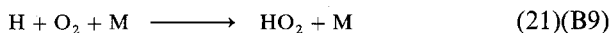


If H₂ were the catalyst, then the steps

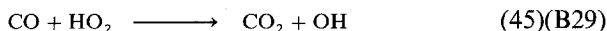


should be included. It is evident then in the so-called "wet" mechanism of CO oxidation that all the steps of H₂-O₂ reaction scheme should be included. As

discussed in the previous section the reaction



enters and provides another route for the conversion of CO to CO₂ by



Although at high pressures or in the initial stages of hydrocarbon oxidation, the high concentrations of HO₂ can make reaction (45) competitive to reaction (44), reaction (45) is rarely as important as reaction (44) in most combustion situations [4]. In developing an understanding of hydrocarbon oxidation, it is important to realize that any high-temperature hydrocarbon mechanism involves H₂ and CO oxidation kinetics, and that most, if not all, of the CO₂ that is formed results from reaction (44).

The very important reaction (44) actually proceeds through a four-atom activated complex [10,11] and is not a simple elementary reaction step. As

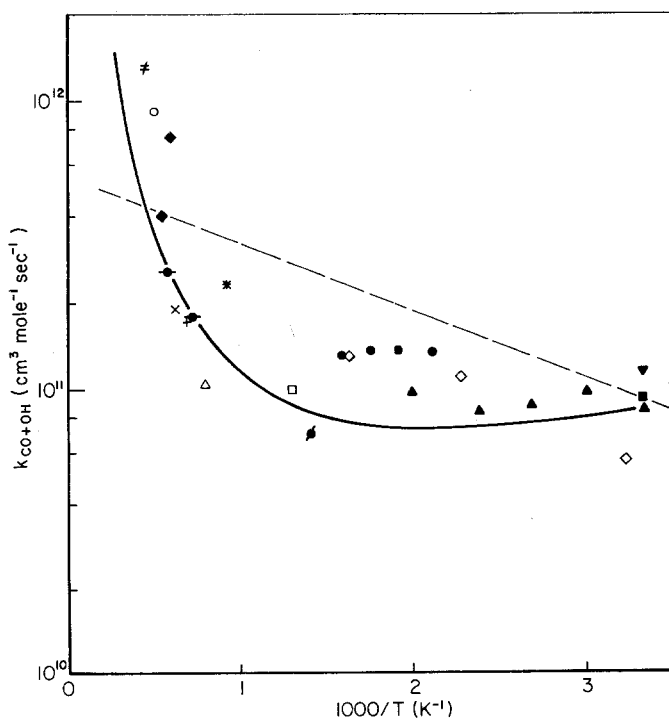


Fig. 4. Reaction rate constant for the CO + OH reaction as a function of reciprocal temperature based on transition state (—) and Arrhenius (---) theories compared with experimental data (after Dryer *et al.* [10]).

shown in Fig. 4 there is curvature on an Arrhenius plot [10]. As a result, the reaction rate exhibits some pressure dependence.

Just as the fate of H radicals is crucial in determining the rate of the H_2-O_2 reaction sequence in any hydrogen-containing combustion system, the concentration of hydroxyl radicals is also important in the rate of CO oxidation. Again similar to H_2-O_2 reaction, rate data reveal that reaction (44) is slower than the reaction of hydroxyl radicals and typical hydrocarbon species and one can conclude correctly that hydrocarbons inhibit the oxidation of CO (see Table 1).

It is apparent that in any hydrocarbon oxidation process, that CO is the primary product and forms in substantial amounts. However there is substantial experimental evidence that reveals that the oxidation of CO to CO_2 comes late in the reaction scheme [12]. The conversion to CO_2 is retarded until all the original fuel and intermediate hydrocarbon fragments have been consumed [4,12]. When these species have disappeared the hydroxyl concentration rises to high levels and converts CO to CO_2 . Further examination of Fig. 4 reveals that the rate of reaction (44) does not begin to rise appreciably until the reaction reaches temperatures above 1100 K. Thus in practical hydrocarbon combustion systems in which temperatures are of the order of 1100 K and below, the complete conversion of CO to CO_2 may not take place.

E. EXPLOSION LIMITS AND OXIDATION CHARACTERISTICS OF HYDROCARBONS

It is interesting to note that the combustion mechanism of methane, the most simple of all the hydrocarbons, was for a long period of time the least understood. In recent years, however, there have been many studies of methane, and its specific oxidation mechanisms are known over various ranges of temperatures. These mechanisms are now some of the best understood, and the details will be discussed later in this chapter.

The higher-order hydrocarbons, particularly propane and above, oxidize much slower than hydrogen and are known to form metastable molecules that are important in explaining the explosion limits of hydrogen and carbon monoxide. The existence of these metastable molecules makes it possible to explain qualitatively the unique explosion limits of the complex hydrocarbons and to gain some insights into what the oxidation mechanisms are likely to be.

Mixtures of hydrocarbons and oxygen react very slowly at temperatures below 200°C; as the temperature increases a variety of oxygen-containing compounds can begin to form. As the temperature is increased further, CO

and H_2O begin to predominate in the products and H_2O_2 (hydrogen peroxide), CH_2O (formaldehyde), CO_2 , and other compounds begin to appear. At 300–400°C a faint light often appears, and this light may be followed by one or more blue flames that successively traverse the reaction vessel. These light emissions are called cool flames and can be followed by an explosion. Generally, the presence of aldehydes are revealed.

In discussing the mechanisms of hydrocarbon oxidation and, later, in reviewing the chemical reactions in photochemical smog, it becomes necessary to identify compounds that may appear complex in structure and nomenclature to those not familiar with organic chemistry. One need not have a background in organic chemistry in order to follow the combustion mechanisms; one should, however, study the following section to obtain an elementary knowledge of organic nomenclature and structure.

1. Organic Nomenclature

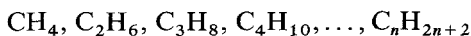
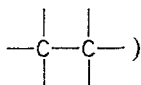
No attempt is made to cover all the complex organic compounds that exist. The classes of organic compounds reviewed are those that occur most frequently in combustion process and photochemical smog.

Alkyl Compounds

Paraffins

(alkanes)

(single bonds,



methane, ethane, propane, butane, ... straight chain
iso-butane ... branched chain

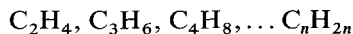
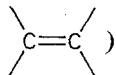
all are saturated (i.e., no more hydrogen can be added
to any of the compounds)

radicals deficient in one H atom take the names
methyl, ethyl, propyl, etc.

Olefins

(alkenes)

(contain double
bonds,

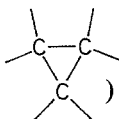


ethene, propene, butene
(ethylene, propylene, butylene)

di-olefins contain two double bonds

the compounds are unsaturated, since C_nH_{2n} can be
saturated to C_nH_{2n+2}

Cycloparaffins
(cycloalkanes)
single bond



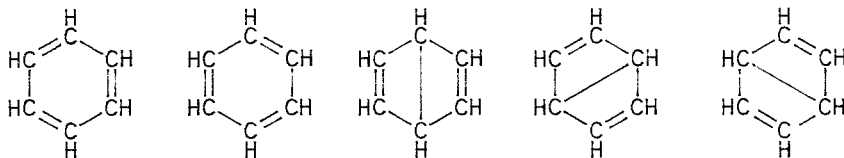
C_nH_{2n} —no double bonds
cyclopropane, cyclobutane, cyclopentane
compounds are unsaturated since ring can be broken
 $C_nH_{2n} + H_2 \rightarrow C_nH_{2n+2}$

Acetylenes
(alkynes)
(contain triple
bonds, $-C\equiv C-$)

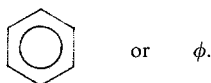
$C_2H_2, C_3H_4, C_4H_6, \dots C_nH_{2n-2}$
ethyne, propyne, butyne
(acetylene, methyl acetylene, ethyl acetylene)
unsaturated compounds

Aromatics

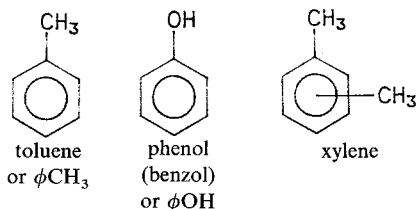
The building block for the aromatics is the ring structured benzene C_6H_6 , which has many resonance structures and is therefore very stable:



The ring structure of benzene is written in shorthand as either



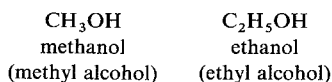
Thus



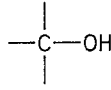
xylene being ortho, meta, or para according to whether methyl groups are separated by one, two, or three carbon atoms, respectively.

Alcohols

Those organic compounds that contain a hydroxyl group ($-OH$) are called alcohols and follow the simple naming procedure.

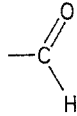


The bonding arrangement is always

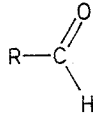


Aldehydes

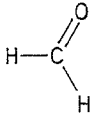
The aldehydes contain the characteristic group (formyl radical)



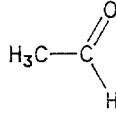
and



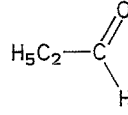
where R can be a hydrogen atom or an organic radical. Thus,



formaldehyde



acetaldehyde



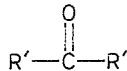
propionaldehyde

Ketones

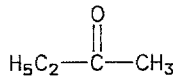
The ketones contain the characteristic group



and can be written more generally as



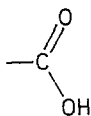
where R' is an organic radical only. Thus,



would be methyl ethyl ketone.

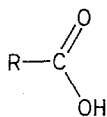
Acids

Organic acids contain the groups

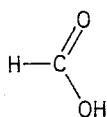


carboxyl radical

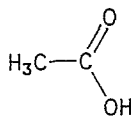
or more generally



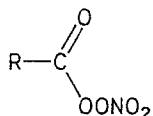
where R can be a hydrogen atom or an organic radical



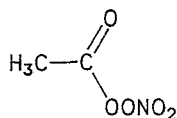
formic acid



acetic acid

Organic Salts

peroxyacyl nitrate



peroxyacetyl nitrate
PAN

Other

The ethers take the form $\text{R}^1\text{—O—R}^1$, where R^1 is an organic radical. The peroxides take the form $\text{R}^1\text{—O—O—R}^1$ or $\text{R}^1\text{—O—O—H}$, in which case the term hydroperoxide is used.

2. Explosion Limits

At temperatures around 300–400°C and slightly higher, explosive reaction in hydrocarbon–air mixtures can take place. Thus, explosion limits exist in hydrocarbon oxidation. A general representation of the explosion limits of hydrocarbons is shown in Fig. 5.

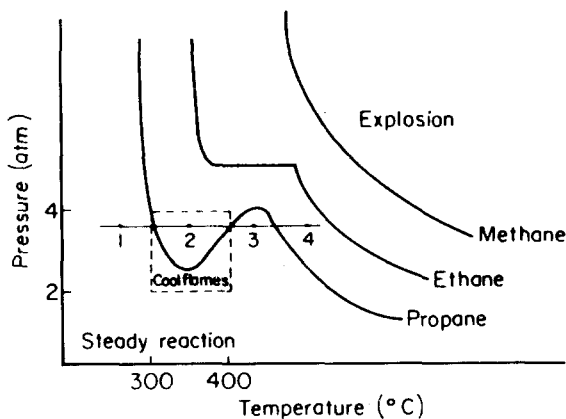


Fig. 5. General explosion limit characteristics of hydrocarbon-air mixtures. Dashed box denotes approximate cool flame region.

One would expect the shift of curves, as shown in Fig. 5, since the larger fuel molecules and their intermediates tend to break down more readily to form radicals that initiate fast reactions. The shape of the propane curve suggests that branched chain mechanisms are possible for hydrocarbons. One can conclude that the character of the propane mechanisms must be different from the $\text{H}_2\text{-O}_2$ reaction when one compares the explosion curve with the $\text{H}_2\text{-O}_2$ pressure peninsula. The island in the propane-air curve drops and goes slightly to the left for higher-order paraffins; e.g., for hexane it occurs at 1 atm. For the reaction of propane with pure oxygen, the curve drops to about 0.5 atm.

Hydrocarbons exhibit certain experimental combustion characteristics that are consistent with the explosion limit curves and practical considerations and are worth reviewing:

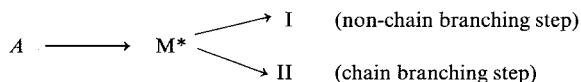
- (a) They exhibit induction intervals that are followed by a very rapid reaction rate. Below 300°C these intervals are of the order of 60 sec and below 400°C they are of the order of 1 sec or a fraction thereof.
- (b) Their rate of reaction is inhibited strongly by adding surface (therefore, an important part of the reaction mechanism must be of the free radical type).
- (c) Aldehyde groups form and appear to have an influence. They accelerate and shorten the ignition lags (formaldehyde is the strongest).
- (d) One finds the presence of so-called cool flames, except for methane and ethane.
- (e) They exhibit negative temperature coefficients of reaction rate.

(f) Two-stage ignition is observed and is related, perhaps, to the cool-flame phenomena.

(g) Explosion occurs without appreciable self-heating (branched chain explosion without steady temperature rise) and usually occurs passing from region 1 to region 2 in Fig. 5. Explosions may occur in other regions, but the reactions are so fast one cannot tell whether they are self heating or not.

a. The Negative Coefficient of Reaction Rate

Semenov [13] explained the long induction period on the basis of the hypothesis that there are unstable but long-lived species that form as intermediates and then undergo different reactions according to the temperature. This concept can be represented in the form of the following competing reaction routes after the formation of the unstable intermediate M^* :



Route I is controlled by an activation energy process larger than that of II.

Figure 6 shows the variation of the reaction rate of each step as a function of temperature. The numbers of Fig. 6 correspond to the same temperature position designation in Fig. 5. At point 1 in Fig. 6 one has a chain branching system, but $\alpha < \alpha_{crit}$ and the system is nonexplosive. As the temperature is increased (point 2), the rate constant of the chain steps in the system increase

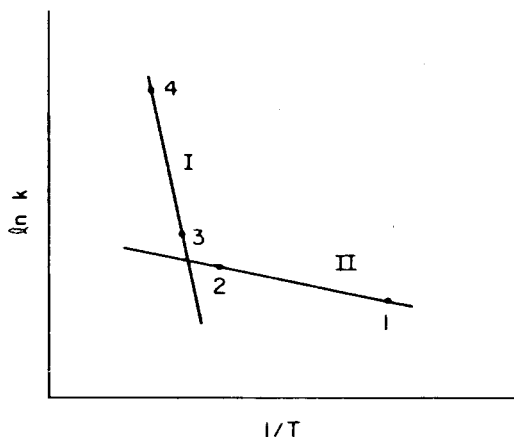


Fig. 6. Arrhenius plot of the Semenov steps in hydrocarbon oxidation. Points 1-4 correspond to same points in Fig. 5.

so that $\alpha > \alpha_{\text{crit}}$ and the system explodes. At a still higher temperature (point 3), the non-chain branching route I becomes faster. Although this step is faster, α is always < 1 and thus the system cannot explode. Raising temperatures along route I still further leads to a reaction so fast that it becomes self-heating and thus explosive again (point 4).

The temperature domination, as shown above, explains the peninsula in the P - T diagram (Fig. 5) and the negative coefficient of reaction rate appears because of the shift from point 2 to 3.

b. Cool Flames

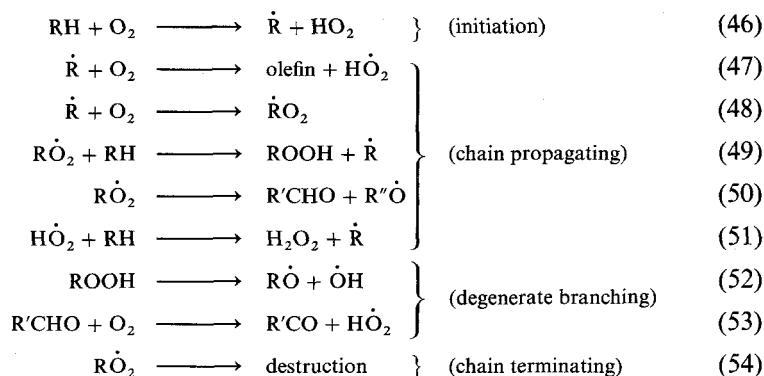
The phenomenon known as cool flames [14] is generally a result of the type of experiment performed to determine the explosion limits and the negative temperature coefficient feature of the explosion limits. The chemical mechanisms used to explain these phenomena are now usually referred to as cool-flame chemistry.

Most explosion limit experiments are performed in vessels contained in isothermal liquid baths (Fig. 1). Such systems are considered to be isothermal within the vessel itself. However, the cool gases that must enter will become hotter at the walls than in the center. The reaction starts at the walls and then propagates to the center of the vessel. The initial reaction volume, which is the hypothetical outermost shell of gases in the vessel, reaches an explosive condition (point 2). However, due to the exothermicity of the reaction, the shell's temperature rises and moves the reacting system to the steady condition point 3, and because the reaction is slow at this condition all the reactants are not consumed. Each successive inner (shell) zone is initiated by the previous zone and progresses through the steady reaction phase in the same manner. Since there is some chemiluminescence during the initial reaction stages, it appears as if a flame propagates through the mixture. Indeed, the events that occur meet all the requirements of an ordinary flame, except that the reacting mixture loses its explosive characteristic. Thus there is no chance for the mixture to react completely and reach its adiabatic flame temperature. The reactions in the system are exothermic and the temperatures are known to rise about 200°C. Thus the phenomena has been called "cool flames."

After the complete vessel moves into the slightly higher temperature zone, it begins to be cooled by the liquid bath. The mixture temperature drops, the system at the wall can move into the explosive regime again, and the phenomenon can repeat itself since all the reactants have not been consumed. According to the specific experimental conditions and mixtures under study, as many as five cool flames have been known to propagate through a given single mixture. Cool flames have been observed in flow systems as well [15].

3. "Low-Temperature" Hydrocarbon Oxidation Mechanisms

It is essential to establish the specific mechanisms that explain the cool-flame phenomenon and, as well, the hydrocarbon combustion characteristics mentioned earlier. Semenov [13] was the first to propose the general mechanism that formed the basis of the latter research, which clarified the processes taking place. This mechanism is written in the following manner:

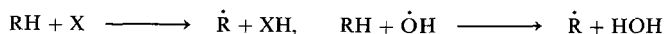


and is sufficient for all hydrocarbons with a few carbon atoms. When consideration is given to many carbon atoms (>5) species, as will be shown later, other intermediate steps must be added.

Since the system requires the buildup of ROOH and R'CHO before chain branching occurs to a sufficient degree to dominate the system, Semenov termed these steps degenerate branching. This buildup time, indeed, appears to account for the experimental induction times noted in hydrocarbon combustion systems.

Controversy had existed as to the relative importance of ROOH versus aldehydes as the important intermediates; however, recent work would indicate that the hydroperoxide step dominates. Aldehydes are quite important as fuels in the cool-flame region, but they do not lead to the important chain branching step as readily.

Due to its high endothermicity, the chain initiating reaction, as one realizes, is not the important route to formation of the radical $\dot{\text{R}}$ once the reaction system has created other radicals. Obviously the important generation step is a radical attack on the fuel, and the fastest rate of attack is by the hydroxyl radicals since this reaction step is highly exothermic due to the creation of water as a product. So the system for obtaining R comes from the reactions



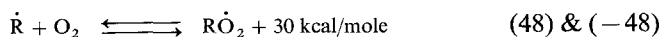
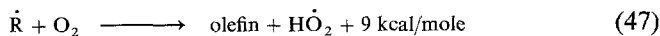
(primarily from the second reaction) where X represents any radical. It is the fate of the hydrocarbon radical that determines the existence of the negative temperature coefficient and cool flames. The alkyl peroxy radical forms via reaction (48). The structure of this radical can be quite important. The H abstracted to form the radical R comes from a preferential position. The weakest C—H bonding is on a tertiary carbon and, if such C atoms exist, the O₂ will preferentially attack this position. If no tertiary carbon atoms exist, then the next weakest C—H bonds are those on the second carbon atoms from the ends of the chain. The reader should refer to Appendix C for all bond strengths. As the hydroxyl radical pool builds, as noted, it becomes the predominate attacker of the fuel. Because of the energetics of the hydroxyl step [reaction (56)], for all intent and purposes, it is relatively nonselective in hydrogen abstraction.

It is known that when O₂ attaches to the radical it forms about a 90° angle with the carbon atoms. The realization of this steric condition will facilitate understanding of certain reactions to be depicted later. The peroxy radical abstracts an H from any fuel molecule or other hydrogen donor to form the hydroperoxide (ROOH) [reaction (49)]. Tracing the steps, one realizes that the amount of hydroperoxy radical that will form depends on the competition of reaction (48) with reaction (47), which forms the stable olefin and HO₂·. The HO₂·, which forms from reaction (47), then forms the peroxide H₂O₂ through reaction (51). At high temperatures H₂O₂ dissociates into two hydroxyl radicals; however, at temperatures of concern here, this dissociation does not occur and the fate of the H₂O₂ (usually heterogeneous) is to form water and oxygen. Thus, reaction (47) essentially leads only to steady reaction. To repeat, then, under low-temperature conditions it is the competition between reactions (47) and (48) that determines whether the fuel-air mixture will become explosive or not. If explosive, then it depends on whether the chain system formed is sufficiently branching to have an α greater than α_{crit} .

a. Competition between Chain Branching and Steady Reaction Steps

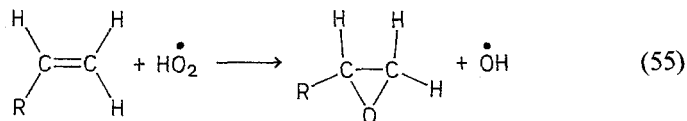
In determining the relative importance of reactions (2) and (3) the work of Benson [16] is closely followed.

The two reactions can be written as



in which the notation reaction (−48) is the reverse of reaction (48). The important distinction between the two sets of reactions is that reaction (48) is rapidly reversible above 200°C and reaction (47) is effectively irreversible.

The reason is that the reaction between $\text{HO}_2\cdot$ and an olefin has two paths: Reaction (-47), the reverse reaction of (47), and the addition reaction to form $\text{RCH}-\text{CHO}_2\text{H}$. The latter is appreciably faster because of its lower activation energy and leads to what is known as epoxidation:



Although reaction (48) is much faster than reaction (47) at all temperatures, reaction (48) begins to reverse as the temperature increases and permits the irreversible reaction (47) to dominate in depleting the hydrocarbon radical.

Still following Benson [16] explicitly, a steady-state analysis of the rates of production of ROOH and the olefin is developed and found to give the ratio

$$\frac{d(\text{olefin}/dt)}{d(\text{ROOH})/dt} = \frac{d(\text{olefin})}{d(\text{ROOH})} = \frac{k_{47}(\dot{\text{R}})(\text{O}_2)}{k_{49}(\dot{\text{R}}\text{O}_2)(\text{RH})} \quad (56)$$

Under cool-flame conditions, it has been shown that $(\dot{\text{R}}\text{O}_2)$ and $(\dot{\text{R}})$ are in equilibrium via reaction (48), so that it is possible to write

$$(\dot{\text{R}}\text{O}_2)/(\text{R}) = K_{48}(\text{O}_2) \quad (57)$$

where K_{48} is the equilibrium constant for reaction (48). Equation (57) is often used to define the "ceiling temperature," which is a simple measure of the extent of equilibration of reaction (48). For a particular oxygen concentration, the "ceiling temperature" is that at which the ratio $[(\text{RO}_2)/(\text{R})] = 1$.

Combining Eqs. (56) and (57) results in

$$\frac{d(\text{olefin})}{d(\text{ROOH})} = \frac{k_{47}}{k_{49}K_{48}(\text{RH})} \quad (58)$$

a somewhat paradoxical result since O_2 and all radical concentrations have disappeared from the ratio. By assuming that the H was abstracted from a secondary carbon atom and assigning values to the constants in Eq. (58), Benson found

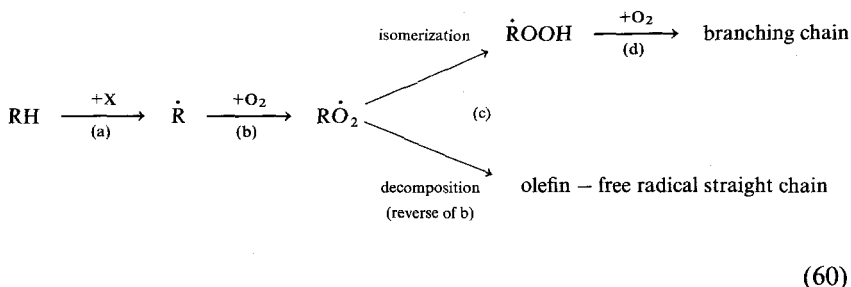
$$\frac{d(\text{olefin})}{d(\text{ROOH})} = \frac{10^{(5.7 - (8.47/RT))}}{(\text{RH})} \quad (59)$$

where R is the universal gas constant (kcal/mole K), and T the temperature (K), 8.47 in units of kcal/mole, and (RH) in moles/liter.

Equation (59) predicts that the olefin production does indeed become more important than the ROOH production as the temperature rises. Thus, when a cool flame begins and its temperature rises, the olefin production begins to dominate and destroys the flame by overtaking the step leading to degenerate branching.

b. Importance of Isomerization in Large Hydrocarbon Radicals

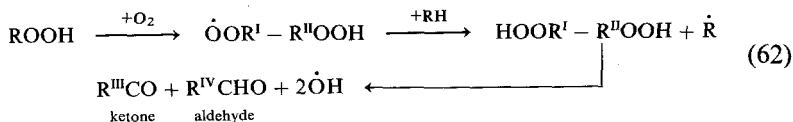
With large hydrocarbon molecules an important isomerization reaction will occur, and Benson has noted that with six or more carbon atoms, this reaction becomes a dominant feature in the chain mechanism. Since most practical fuels contain large paraffinic molecules, one can generalize the new competitive mechanisms as



The isomerization step is

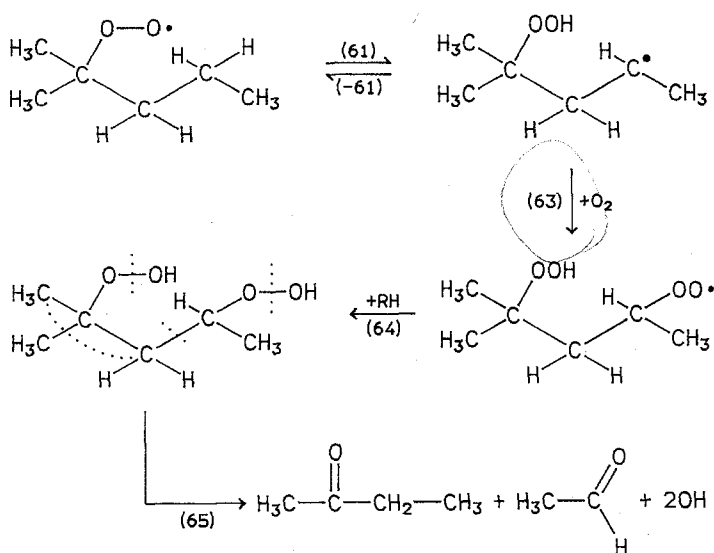


(For clarity, an example of this type of isomerization is shown below in the discussion of the oxidation of 2-methyl-pentane.) The general sequence of Step (d) is



where R with Roman number superscripts represent different hydrocarbon radicals of smaller chain length than RH. It is the isomerization concept that requires the introduction of additional reactions to the Semenov mechanism to make this mechanism most general.

The oxidation reactions of 2-methyl-pentane provide a good example for showing how the hydroperoxy states are formed and the importance of molecular structure in establishing a mechanism. The C—C bond angles in hydrocarbons are about 108°. The reaction scheme is then



Here one notices that it is the structure of the 90° (COO) bonding that determines the intermediate ketone, aldehyde, and hydroxyl radicals that are formed.

Although reaction (61) is endothermic and the reverse step reaction (-61) is faster, the competing step reaction (63) can be faster still so that the isomerization [reaction (61)] controls the overall rate of formation of $\text{R}\dot{\text{O}}$ and subsequent chain branching. This sequence essentially negates the extent of reaction (-48). Thus the competition between $\text{RO}\dot{\text{O}}$ and olefin production becomes more severe and it is more likely that $\text{RO}\dot{\text{O}}$ would form at the higher temperatures.

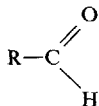
It has been suggested [16] that the greater tendency for long-chain hydrocarbons to knock as compared to smaller and branched chain molecules would appear to be a result of this internal, isomerization branching mechanism.

F. THE OXIDATION OF ALDEHYDES

The low-temperature hydrocarbon oxidation mechanism discussed in the previous section is incomplete because the reactions leading to CO were not included. Water formation is primarily by reaction (56). The CO forms by the conversion of aldehydes and their acetyl (and formyl) radicals, $\text{R}\dot{\text{C}}\text{O}$. The same type of conversion takes place at high temperatures and, thus, it is

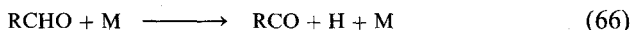
appropriate, prior to considering high-temperature hydrocarbon oxidation schemes, to develop an understanding of the aldehyde conversion process.

As shown in Section D1, aldehydes have the structure

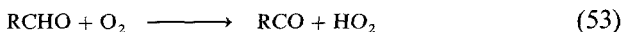


where R is either an organic radical or a H atom; $\dot{\text{H}}\text{C}\text{O}$ is the formyl radical.

The initiation step for the high-temperature oxidation of aldehydes is the pyrolysis reaction

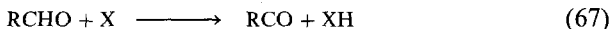


The CH bond on the formyl group is the weakest of all CH bonds in the molecule (see Appendix C) and is the predominant one broken. The R—C bond is substantially stronger than the CH bonds, so cleavage of this bond as an initiation step need not be considered. As before, at lower temperatures, high pressures and under lean conditions, the abstraction initiation step must be considered



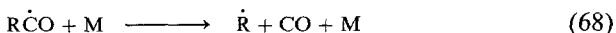
Hydrogen labeling studies show conclusively that the formyl H is the one abstracted and this finding is consistent with the bond energies.

The H atom introduced by reaction (66) and the OH, which arises from the $\text{H} + \text{O}_2$, initiate the H radical pool that comes about from reactions (15)–(18). The subsequent decay of the aldehyde is then given by



where X is chosen to represent the dominant radicals OH, O, H, and CH_3 . The methyl radical CH_3 is included not only because of its slow reactions with O_2 , but also because many methyl radicals are formed during the oxidation of practically all aliphatic hydrocarbons. The general effectiveness of each radical is in the order OH, O, H, CH_3 , which has the hydroxyl radical reacting the fastest with the aldehyde. Since in a general hydrocarbon oxidation system H radicals arise from steps other than reaction (66) or those which could follow reaction (55), for combustion concerns the aldehyde oxidation process begins with reaction (67).

When R is an organic element, the radical RCO is much more unstable than HCO, which would arise if R were a hydrogen atom, and only the decomposition of RCO need be considered in combustion systems; namely



Similarly HCO will decompose via



but under the usual conditions the following abstraction reaction must be considered to play some small part in the process

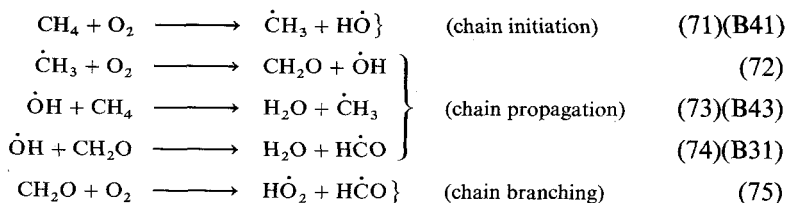


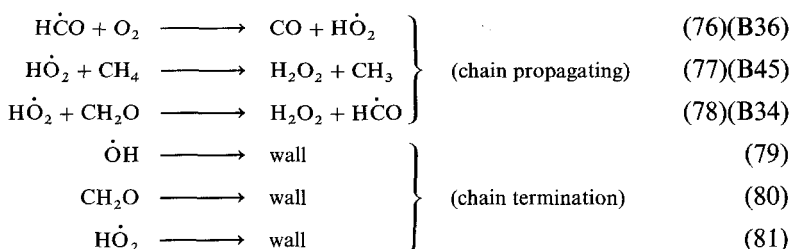
The formyl radical reacts very rapidly with the OH, O, and H radicals; however radical concentrations are much lower than those of stable reactants and intermediates, and thus formyl reactions with these radicals are considered insignificant as compared to the other formyl reactions. As will be seen in a later section in which the oxidation of large hydrocarbon molecules is discussed, R is most likely a methyl radical, and the highest-order aldehydes to arise in high-temperature combustion are acetaldehyde and propionaldehyde. The acetaldehyde is the dominant form. Essentially then the sequence above was developed with the consideration that R was a methyl group.

G. THE OXIDATION OF METHANE

Methane exhibits certain oxidation characteristics that are different from all other hydrocarbons. Tables of bond energy list the first broken C—H bond in methane to be kilocalories more than the others, and certainly more than the C—H bonds in longer-chain hydrocarbons. Thus, it is not surprising to find various kinds of experimental evidence to lead one to believe that it is more difficult to ignite methane/air (oxygen) mixtures than it is with other hydrocarbons. At low temperatures, even oxygen radical attack is slow. Indeed, in discussing exhaust emissions with respect to pollutants, the terms total hydrocarbons and reactive hydrocarbons are used. The difference between the two terms is simply methane, which in this context is considered to react so slowly with oxygen radicals at atmospheric temperatures that it is called unreactive.

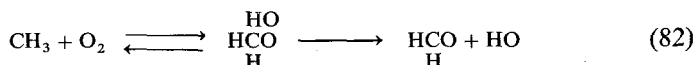
The simplest scheme that will explain the lower temperature results of methane oxidation is





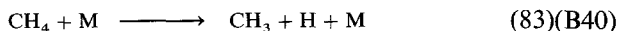
As before, reaction (71) is slow. Reactions (72) and (73) are faster since they involve a radical and one of the initial reactants. The same is true for reactions (75), (76), and (77). Reaction (75) represents the necessary chain branching step. Reactions (74) and (78) introduce the formyl radical known to exist in the low-temperature combustion scheme. Carbon monoxide is formed by reaction (76); water by reaction (73) and the subsequent decay of the peroxides formed. A conversion step of CO to CO₂ is not considered because the rate of conversion by reaction (44) is too slow at the temperatures of concern here.

It is important to examine more closely reaction (72) which precedes [17,18] through a metastable intermediate complex, the methyl peroxy radical, in the following manner



At lower temperatures the equilibrium step is shifted strongly towards the complex and the formaldehyde and hydroxyl radical form. The structure of the complex represented in reaction (82) is well established. Recall when O₂ adds to the carbon atom in a hydrocarbon radical, it forms a 90° bond angle. Perhaps what is more important to note, however, is that at temperatures of the order of 1000 K and above, the equilibrium step in reaction (82) shifts strongly towards the reactants and the overall reaction to form formaldehyde and hydroxyl cannot proceed [17]. This condition poses a restriction on the rapid oxidation of methane at high temperatures.

In contrast to reaction (71), at high temperatures the thermal decomposition of the methane provides the chain initiation step, namely



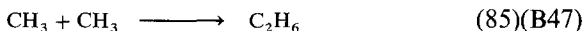
With the presence of H atoms the H₂-O₂ branching and propagating scheme proceeds and a pool of OH, O, and H develops. These radicals, together with HO₂, which would form if the temperature range were to include reaction (71) and an initiating step, abstract hydrogen from CH₄ according to



where again X represents any of the radicals. The abstraction rates by the radicals OH, O, and H are fast and the order of effectiveness is again as

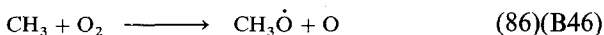
written with OH abstraction the fastest; however, these reactions are now known to exhibit substantial non-Arrhenius temperature behavior over the temperature range of interest to combustion. The rate of abstraction by O compared to H is somewhat faster, but the order could change according to the stoichiometry; that is, under fuel-rich conditions the hydrogen rate will be faster than the O rate due to the much larger hydrogen atom concentrations under these conditions.

The fact that reaction (82) does not proceed at high temperatures explains why methane oxidation is slow compared to other hydrocarbon fuels and why substantial concentrations of ethane are found [4] during the methane oxidation process. The processes now known to consume methyl radicals are slow, so the methyl concentration builds up and ethane forms through simple recombination:

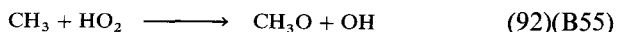
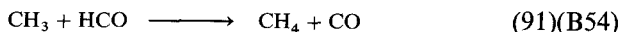
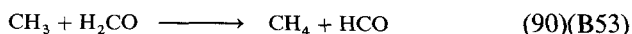
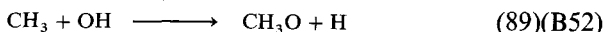
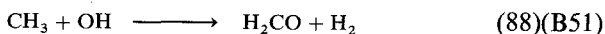
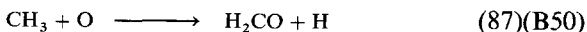


Thus methyl radicals are consumed by other methyl radicals to form ethane, which must then be oxidized. The characteristics of the oxidation of ethane and the higher-order aliphatics are substantially different than those of methane and will be discussed in the next section. For this reason, methane should not be used to typify hydrocarbon oxidation processes in combustion experiments. A third body generally is not written for reaction (85) because the ethane molecule's numerous internal degrees of freedom can redistribute the energy created by the formation of the new bond.

Evidence [4] is now such that the following reaction path initially suggested by Brabbs and Brokaw [19] appears to be the main oxidation destruction path of methyl radicals

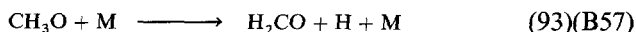


where $\text{CH}_3\dot{\text{O}}$ is the methoxy radical. Reaction (86) is very endothermic, has a relatively large activation energy (~ 29 kcal/mole) [4] and is, thus, quite slow for a chain step. Other methyl radical reactions [4] are as follows:



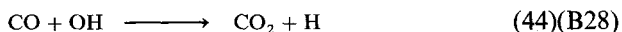
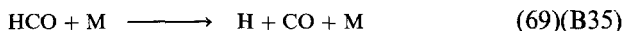
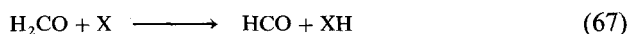
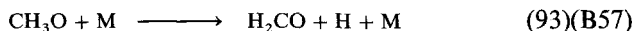
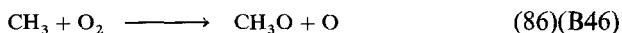
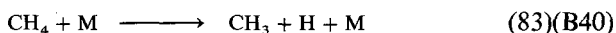
however, these are radical-radical reactions or reactions of methyl radicals with a product of a radical-radical reaction and due to concentration effects are much less important than reaction (86).

The methoxy radical formed by reaction (86) decomposes primarily and rapidly via



Although reactions with radicals could be included to give formaldehyde and another product, they would have only a very minor role. They have large rate constants, but concentration factors in reacting systems keep these rates slow.

Reaction (86) is relatively slow for a chain step, nevertheless it is followed by the very rapid decay reaction for the methoxy [reaction (93)] and the products of this two-step process are formaldehyde and two very reactive radicals, O and H. These radicals provide more chain branching than the low-temperature step represented by reaction (72) which produces formaldehyde and a single hydroxyl radical. The added chain branching from the reaction path [reactions (86) and (93)] is what produces a reasonable overall oxidation rate for methane at high temperatures. In summary, the major reaction paths for the high-temperature oxidation of methane are



Of course, all the appropriate higher-temperature reaction paths for H_2 and CO discussed in the previous sections must be included. Again, note that H_2 and water would form from reaction (84). The system is not complete because sufficient ethane forms so that its oxidation path must be a consideration. For example, in atmospheric pressure methane-air flames, Warnatz [20,21] has estimated that for lean or stoichiometric systems about 30% of methyl radicals recombine to form ethane and for fuel-rich systems the percentage rises as high as 80%. Essentially then there are two parallel oxidation paths in the methane system: one via the oxidation of methyl radicals and the other via the oxidation of ethane. Again it is worthy to note that reaction (84) with hydroxyl is faster than reaction (44) so that early in the methane system CO accumulates, later when the CO concentration rises it effectively competes with methane for hydroxyl radicals and the fuel consumption rate is slowed.

H. THE OXIDATION OF HIGHER ORDER HYDROCARBONS

1. Aliphatic Hydrocarbons

The understanding of the high-temperature oxidation of paraffins larger than methane is somewhat complicated by the greater instability of the higher-order alkyl radicals and the great variety of minor species that can form (see Table 2). Nevertheless it is possible to develop a general framework of important steps that would give one an understanding of this complex subject.

a. Overall View

It is interesting to review a general pattern for oxidation of hydrocarbons in flames, as initially suggested by Fristrom and Westenberg [22]. They suggested two essential thermal zones: the primary zone in which the initial hydrocarbons are attacked and reduced to products (CO , H_2 , H_2O) and radicals (H , O , OH) and the secondary zone in which CO and H_2 are oxidized. The intermediates are said to form in the primary zone. In oxygen-rich saturated hydrocarbon flames, they suggest that initially hydrocarbons of lower order than the initial fuel form according to



Because hydrocarbon radicals of higher order than ethyl are unstable, the initial radical $\text{C}_n\text{H}_{2n+1}$ usually splits off CH_3 and forms the next lower-order olefinic compound, as shown. With hydrocarbons of higher order than C_3H_8 , there is fission into an olefinic compound and a lower-order radical. The radical alternately splits off CH_3 . The formaldehyde that forms in the oxidation of the fuel and radicals is rapidly attacked in flames by O , H , and OH , so that formaldehyde is usually only found as a trace in flames.

TABLE 2
Relative importance of intermediates in hydrocarbon combustion

Fuel	Relative hydrocarbon intermediate concentrations
ethane	ethene \gg methane
propane	ethene > propene \gg methane > ethane
butane	ethene > propene \gg methane > ethane
hexane	ethene > propene > butene > methane \gg pentene > ethane
2-methyl pentane	propene > ethene > butene > methane \gg pentene > ethane

In fuel-rich saturated hydrocarbon flames, Fristrom and Westenberg state that the situation is more complex, although the initial reaction is simply the H abstraction analogous to the preceding OH reaction; e.g.,



Under these conditions the concentrations of H and other radicals are large enough that their recombination becomes important, and hydrocarbons of higher order than the original fuel are formed as intermediates.

The general features suggested by Fristrom and Westenberg have been confirmed at Princeton [12] by high-temperature flow-reactor studies. However, this new work permits more detailed understanding of the high-temperature oxidation mechanism. This work shows that under oxygen-rich conditions the initial attack by O atoms must be considered as well as the primary OH attack. More importantly, however, it has been established that the paraffin reactants produce intermediate products that are primarily olefinic, and the fuel is consumed, to a major extent, before significant energy release occurs. The higher the initial temperature the greater the energy release, as the fuel is being converted. This observation leads one to conclude that the olefin oxidation rate simply increases more appreciably with temperature; i.e., the olefins are being oxidized while they are being formed from the fuel. Typical flow-reactor data for the oxidation of ethane are shown in Fig. 7.

The evidence [12] is [see Fig. 7] that there are three distinct but coupled zones in hydrocarbon combustion:

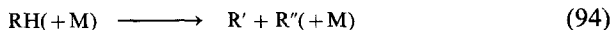
(1) Following ignition, primary fuel disappears with little or no energy release and produces unsaturated hydrocarbons and hydrogen. A little of the hydrogen is concurrently oxidized to water.

(2) Subsequently, the unsaturated compounds are further oxidized to carbon monoxide and hydrogen. Simultaneously the hydrogen present, and formed, is oxidized to water.

(3) Lastly, the large amounts of carbon monoxide formed are oxidized to carbon dioxide and most of the heat released from the overall reaction is obtained.

b. Paraffin Oxidation

Since the oxidation of large paraffin molecules is being considered in this section, it is apparent that the chain initiation step is one in which a CC bond is broken to form hydrocarbon radicals; namely



This step will undoubtedly dominate since the CC bond is substantially weaker than any of the CH bonds in the molecule. As mentioned in the

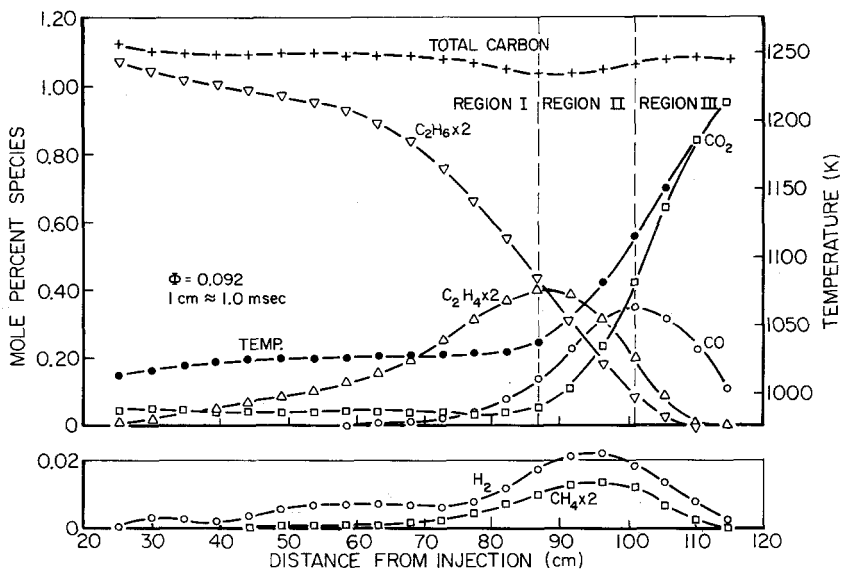
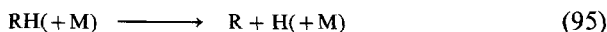
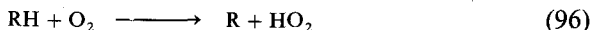


Fig. 7. Oxidation of ethane in a turbulent flow reactor showing intermediate and final product formation (after Dwyer and Glassman [12]).

previous section the radicals R' and R'' (fragments of the original hydrocarbon molecule RH) decay into an olefin and a H atom. At any reasonable combustion temperature, some CH bonds are broken and H atoms appear due to the initiation step

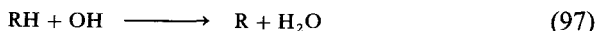


For completeness, one could include a lower-temperature, abstraction-initiation step



The essential point is that the initiation steps provide H atoms that react with the oxygen in the system to begin the chain branching propagating sequence that nourishes the radical reservoir of OH , O , and H ; that is, the reaction sequences for the complete H_2-O_2 system must be included in any high-temperature hydrocarbon mechanism. Similarly when CO forms, its reaction mechanism must be included as well.

Once the radical pool forms, the disappearance of the fuel is controlled by the reaction



where, again, X is any radical and for the high-temperature condition is primarily OH , O , H , and CH_3 . Since the RH under consideration is a

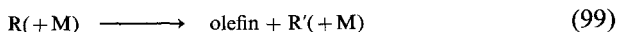
multicarbon atom compound, the character of the radical R formed depends on which hydrogen in the molecule is abstracted. Furthermore, it is important to consider how the rate of reaction (98) varies as X varies, since the formation rates of the alkyl isomeric radicals can possibly vary.

Data for the specific rate coefficients for abstraction from CH bonds have been derived from experiments with hydrocarbons with different distributions of primary, secondary, and tertiary CH bonds. A primary CH bond is one on a carbon in which the carbon atom is only connected to one other carbon; that is the end carbon in a chain or a branch of a chain of carbon atoms. A secondary CH bond is one on a carbon atom connected to two others and a tertiary, the carbon atom is connected to three others. In a chain the CH bond strength on the carbons second from the ends is a few kilocalories less than other secondary atoms. The tertiary CH bond strength is still less and the primary the greatest. Assuming additivity of these rates one can derive specific reaction rate constants for abstraction from the higher-order hydrocarbons by H, O, OH, and HO₂ [23].

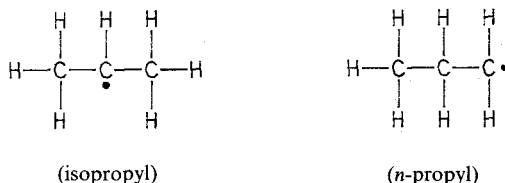
From the rates given in Ref. [23], the relative magnitudes of rate constants for abstraction of H by H, O, OH, and HO₂ species from single tertiary, secondary, and primary CH bonds at 1080 K have been determined [24]. These relative magnitudes should not vary substantially over modest ranges of temperatures and were found to be

Tertiary : Secondary : Primary					
H	13	:	4	:	1
O	10	:	5	:	1
OH	4	:	3	:	1
HO ₂	10	:	3	:	1

Note that OH abstraction reaction, which is more exothermic than others, is the least selective of H atom position in its attack on large hydrocarbon molecules. There is great selectivity by H, O, and HO₂ between tertiary and primary CH bonds. Furthermore, estimates of rate constants at 1080 K [23] and radical concentrations for a reacting hydrocarbon system [25] reveals that *k* values for H, O, and OH are practically the same and during early part of the reactions when concentrations of fuel are large the radical species concentrations are of the same order of magnitude. Only the HO₂ rate constant is lower than the other three. Consequently, knowing the structure of a paraffin hydrocarbon, it is quite possible to make estimates of the proportions of various radicals that would form from a given fuel molecule [from the abstraction reaction (98)]. The radicals then decay further according to



where R' is a H atom or another hydrocarbon radical. The ethyl radical will thus become ethene and a H atom. Propane leads to a normal propyl and an isopropyl radical:



These radicals decompose according to the so-called β -scission rule, which implies that the bond that will break is one removed from the radical site, because in this manner an olefin can form without both a proton and hydrogen atom shift. Thus in the case of the isopropyl radical, propene and a H atom form, and in the case of the *n*-propyl radical, ethene, and a methyl radical form. Since the CC single bond is weaker than a CH bond, in applying the β scission rule when there is a choice between these two bonds, the CC bond is normally the one which breaks. Considering that there are six primary CH bonds in propane and only two secondary ones, one would expect to find substantially more ethene as an intermediary in the oxidation process than propene. The experimental results [12] shown in Fig. 8 verify this conclusion. The same experimental effort found the olefin trends shown

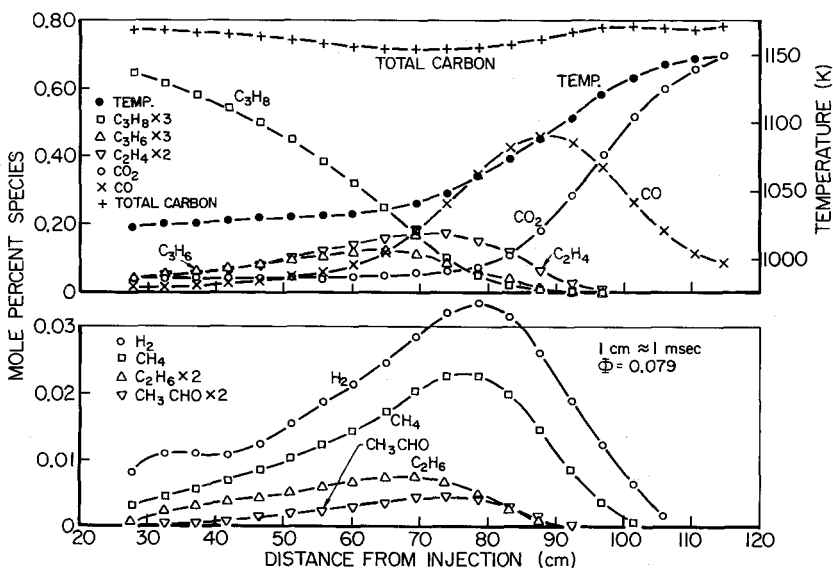
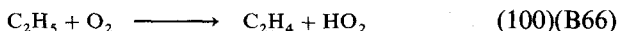


Fig. 8. Oxidation of propane in a turbulent flow reactor showing intermediate and final product formation (after Dryer and Glassman [12]).

in Table 2 and it is possible to estimate the order reported from the principles just described.

If the initial intermediate or the original fuel is a large monoolefin, the radicals will abstract H from those carbon atoms, which are singly bonded because of the large CH bond strengths when the carbons are doubly bonded (see Appendix C). Thus, the evidence [12,24] is building that during oxidation all nonaromatic hydrocarbons primarily form ethene and propene (and some butene and isobutene) and that the oxidative attack that eventually leads to CO is almost solely from these small intermediates. Thus, the study of ethene oxidation is crucially important for all alkyl hydrocarbons.

Reactions (94), (95), and (99) contain parentheses around the collision partner M. When RH in reactions (94) and (95) is ethane and R in reaction (99) is the ethyl radical, the reaction order depends on the temperature and pressure range. Reactions (94), (95), and (99) for the ethane system are in the fall-off regime for most typical combustion conditions. Reactions (94) and (95) for propane possibly could lie in the fall-off regime for some combustion conditions; however, around 1-atm pressure, butane and larger molecules pyrolyze near their high-pressure limit [26] and essentially follow first-order kinetics. Furthermore, for the formation of the olefin an ethyl radical in reaction (99) must compete with the abstraction reaction

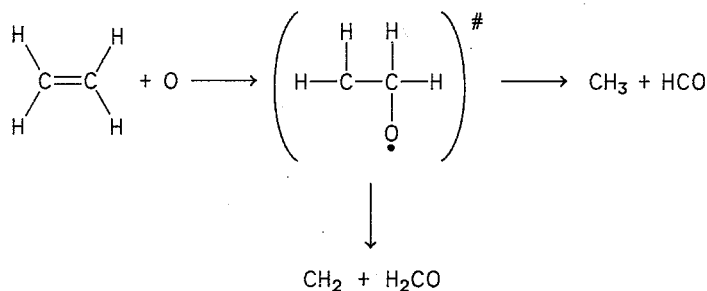


Due to the great instability of the radicals formed from propane and larger molecules, reaction (99) is fast and for all purposes first-order and, thus, competitive reactions similar to the one above need not be considered. Thus, the M in reactions (94) and (95) only has to be included for ethane, and to a small degree propane, and in reaction (99) only for ethane. Thus, ethane is unique among all paraffin hydrocarbons in its combustion characteristics and for experimental purposes, similar to methane, should not be chosen as a typical hydrocarbon fuel.

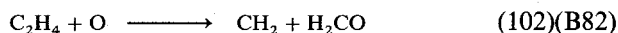
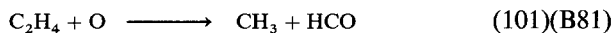
c. Olefin and Acetylene Oxidation

Following the discussion from the preceding section, consideration will be given (when a radical pool already exists) to the oxidation of ethene and propene, and since acetylene is a product of this oxidation process, acetylene as well. This condition then would be that which develops in the oxidation of a paraffin or any large olefin.

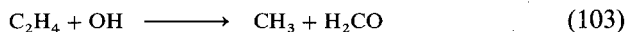
The primary attack on ethene is by addition of the biradical O, although abstraction by H and OH can play some small role. In adding to ethene, O forms an adduct [27] that fragments according to the scheme



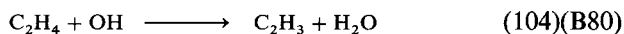
The primary products are methyl and formyl radicals [28,29] due to the fact that there is at combustion temperatures potential energy surface crossing that leads to a H shift [27]. Thus the two primary addition reactions that can be written are



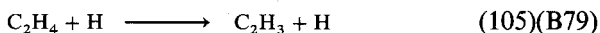
Due to the high endothermicity of forming an adduct with OH [30], there is some question if the following reaction can proceed as others [4] have quoted



OH abstraction via

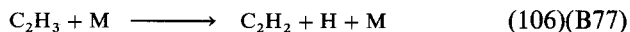


could have a rate comparable to the preceding three and H abstraction

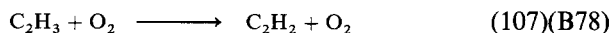


could play a minor role. Addition reactions generally have smaller activation energies than abstraction reactions, so at low temperatures the abstraction reaction is negligibly slow, but at high temperatures the abstraction reaction can dominate. Hence, the temperature dependence of the net rate of disappearance of reactants can be quite complex.

The vinyl radical (C_2H_3) decays to acetylene primarily by



but, again under particular conditions the abstraction reaction

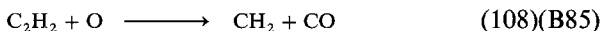


must be included.

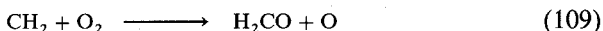
Since the oxidation mechanisms of CH_3 , H_2CO (formaldehyde), and CO have been discussed, only the fate of C_2H_2 and CH_2 (methylene) remains to be determined.

The most important means of consuming acetylene for lean, stoichiometric and even slightly rich conditions is again by reaction with the biradical O

[29,31] to form a methylene radical and CO,



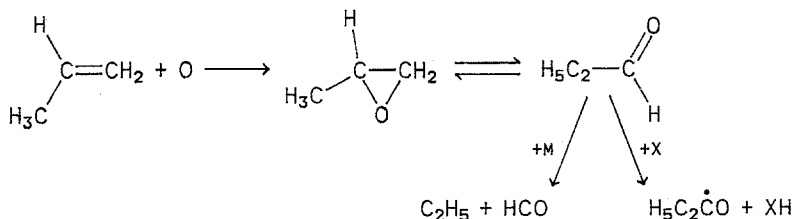
The rate constant for reaction (108) would not be considered large in comparison with that for reaction of O with either an olefin or a paraffin. Mechanistically, reaction (108) is of significance. Since the C_2H_2 reaction with H atoms is slower than $\text{H} + \text{O}_2$, the oxidation of acetylene does not significantly inhibit the radical pool formation. Also, since its rate with OH is comparable to CO with OH, C_2H_2 unlike the other fuels discussed will not inhibit CO oxidation and therefore substantial amounts can be found in the high-temperature regimes of flames. Reaction (108) states that acetylene consumption is dependent on events that control the O atom concentration. As discussed in Chapter 8, this fact has ramifications for acetylene as the soot growth species in premixed flames. Acetylene-air-flame speeds and detonation velocities are fast primarily because of the high temperatures that evolve, not necessarily because acetylene reaction mechanisms contain steps with favorable rate constants. The primary candidate to oxidize methylene is O_2 via



however, there is some uncertainty with the products as specified.

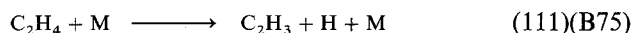
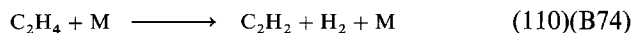
There are numerous other possible reactions that can be included in a very complete mechanism of any of the oxidation schemes of any of the hydrocarbons discussed. Indeed it is evident from the fact that hydrocarbon radicals form that higher-order hydrocarbon species can develop during an oxidation process. All these reactions play only a very minor, and sometimes interesting role, but inclusion here would detract from the major important steps and the insights thought necessary.

With respect to propene, the suggestion has been [27] that O atom addition is the most dominant decay route through an intermediate complex in the following manner



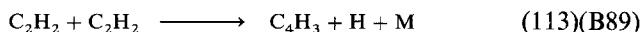
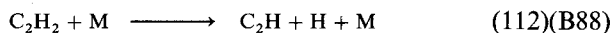
For the large activated propionaldehyde molecule, the pyrolysis step would appear to be favored and the equilibrium with the propylene oxide shifts in its direction. The products given for this scheme appear to be consistent with experimental results [30]. The further reaction history of the products have already been discussed.

Whereas the oxidation chemistry of the aliphatics higher than C_2 essentially has been discussed since the initiation step is mainly CC bond or some CH bond cleavage, the initiation steps for pure ethene or acetylene oxidation are somewhat different. For ethene the major initiation steps are [4]

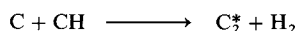
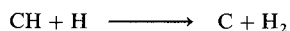
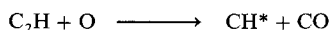


Reaction (110) is the fastest, but reaction (111) would start the chain.

Similarly, acetylene initiation steps [4] are

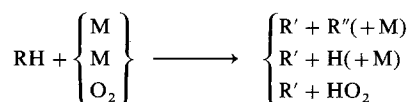


Reaction (112) dominates under dilute conditions and reaction (113) is more important at high fuel concentrations [4]. The subsequent history of C_2H and C_4H_3 is not important for the oxidation scheme once the chain system develops. Nevertheless, the oxidation of C_2H could lead to chemiluminescent reactions that form CH and C_2 , the species responsible for the blue-green appearance of hydrocarbon flames. Steps leading to these species that have been proposed [32] are

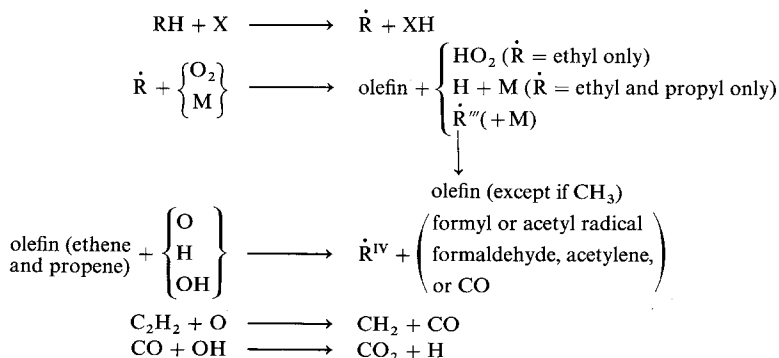


where * represents electronically excited species.

With all the above considerations it is possible to postulate a general mechanism for the oxidation of aliphatic hydrocarbons; namely



where H creates the radical pool (H, O, and OH = X)



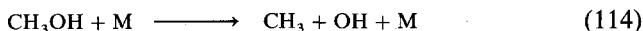
As a matter of interest the oxidation of the diolefin butadiene would appear to occur through O atom addition to a double bond and through abstraction reactions involving OH, and H. Oxygen addition leads to 3-butenal and finally allyl radicals and CO. The allyl radical is oxidized by O atoms through acrolein to form CO, acetylene, and ethene. The abstraction reactions lead to a butadienyl radical and then vinyl acetylene. The butadienyl radical is now thought to be important in aromatic ring formation processes in soot formation [32-35]. Details of butadiene oxidation are presented in Ref. [36].

2. Alcohols

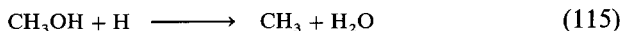
Work at Princeton by Norton and Dryer [37] on the oxidation of alcohol fuels has provided the foundation for the review of this subject and is followed directly here.

The presence of the OH group in alcohols makes alcohol combustion chemistry an interesting variation of the analogous paraffin hydrocarbon. Two fundamental pathways can exist in the initial attack on alcohols. In one the OH group can be displaced and an alkyl radical also remain as a product. In the other the alcohol is attacked at a different site and forms an intermediate oxygenated species, typically an aldehyde. The dominant pathway depends on the bond strengths in the particular alcohol molecule and on the overall stoichiometry that determines the relative abundance of the reactive radicals.

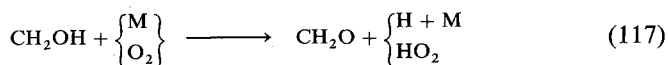
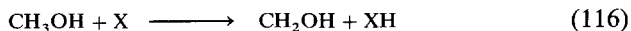
For methanol, the alternative initiating mechanisms are well established [38-41]. The dominant initiation step is the high-activation process.



which contributes little to the products in the intermediate (~ 1000 K) temperature range [40]. Aders [42] by means of deuterium labelling has demonstrated the occurrence of OH displacement by H atoms



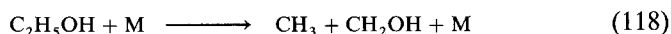
This reaction may account for as much as 20% of the methanol disappearance under fuel-rich conditions [40]. The major oxidation route as in many hydrocarbon processes is by radical abstraction and in the case of methanol yields the hydroxymethyl radical and ultimately formaldehyde via



where as before X represents the radicals in the system.

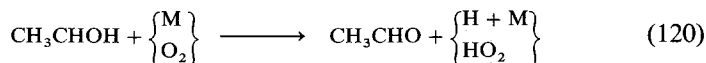
The mechanism of ethanol oxidation is less well established, but it appears that there are two mechanistic pathways of approximately equal importance that lead to acetaldehyde and ethene as major intermediate species. Although in flow reactor studies [37] acetaldehyde appears earlier in the reaction than does ethene, both species are assumed to form directly from ethanol. Studies of acetaldehyde oxidation [43] do not indicate any direct mechanism for the formation of ethene from acetaldehyde.

Because C—C bonds are weaker than the C—OH bond, ethanol, unlike methanol, does not displace the OH group in an initiation step. The dominant initial step is

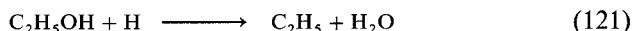


As in all long-chain-length fuel processes, this initiation step does not appear to contribute significantly to the product distribution and indeed no formaldehyde is observed experimentally as a reaction intermediate.

It would appear that the reaction sequence leading to acetaldehyde would appear to be



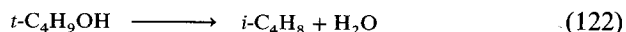
By analogy with methanol, the major source of ethene may be the displacement reaction



with the ethyl radical decaying into ethene.

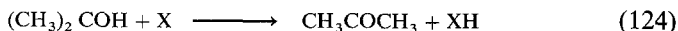
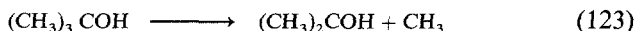
Because the initial oxygen concentration determines the relative abundance of specific abstracting radicals, ethanol like methanol oxidation shows a variation in the relative concentration of intermediate species according to the overall stoichiometry. The ratio of acetaldehyde to ethene increases for lean mixtures.

As the chain length of the primary alcohols increase, thermal decomposition through fracture of C—C bonds become more prevalent. In the pyrolysis of *n*-butanol, following the rupture of the C₃H₇—CH₂OH bond, the species found are primarily formaldehyde and small hydrocarbons. However, because of the relative weak C—OH bond at a tertiary site, tertiary butyl alcohol displaces its OH group quite readily. In fact, the reaction



is used as a classical example of a unimolecular thermal decomposition.

In the oxidation of *t*-butanol, acetone, and isobutene appear [37] as intermediate species. Acetone can arise from two possible sequences:



and H abstraction leading to β scission and an H shift as

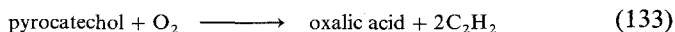
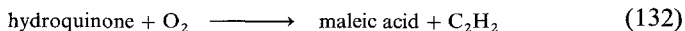
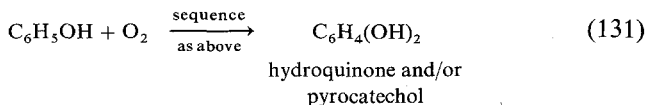
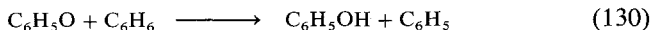
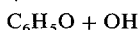
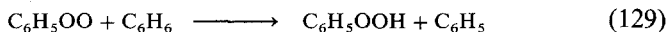
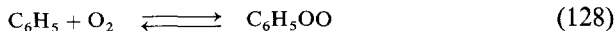
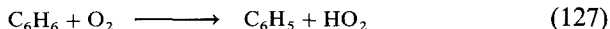


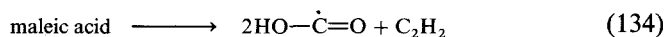
Reaction (123) may be fast enough at temperatures above 1000 K to be competitive with reaction (122) [44].

3. Aromatic Hydrocarbons

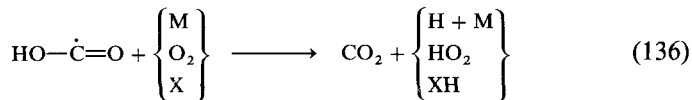
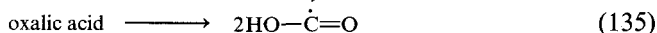
a. Benzene Oxidation

Based on the early work of Norris and Taylor [45] and Barnard and Ibberson [46], who confirmed the theory of multiple hydroxylation, a general low-temperature oxidation scheme for benzene was proposed [47,48], namely





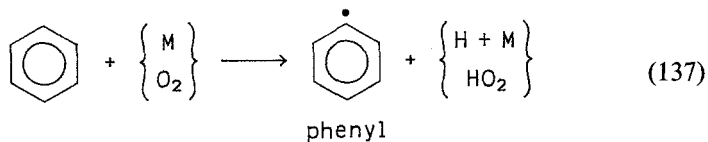
↑
carboxyl radical



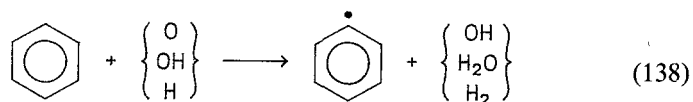
Although many of the intermediates were detected in low-temperature oxidation studies, Benson [32] determined that the ceiling temperature for the bridging peroxide molecules formed from aromatics was of the order of 300°C; that is, the reverse of reaction (128) was favored at higher temperatures.

High-temperature flow-reactor studies [41] on benzene oxidation revealed a sequence of intermediates, which followed the order phenol, cyclopentadiene, vinylacetylene, butadiene, ethene, and acetylene (Fig. 9). Since the sampling techniques used in these experiments could not distinguish between unstable species, the intermediates could have been radicals that reacted to form a stable compound most likely by H addition in the probe. The relative time order of the maximum concentrations, while not the only criteria for establishing a mechanism, has been helpful in modeling of many oxidation systems [12].

The benzene molecule is stabilized by strong resonance, consequently removal of a H by pyrolysis or O₂ abstraction is difficult and therefore slow. It is not surprising then that the induction period for benzene oxidation is longer than that for alkylated aromatics. The high-temperature initiation step is similar to all cases written before:



but probably plays a small role once the radical pool builds from the H obtained. Subsequent formation of the phenyl radical arises from the propagating step



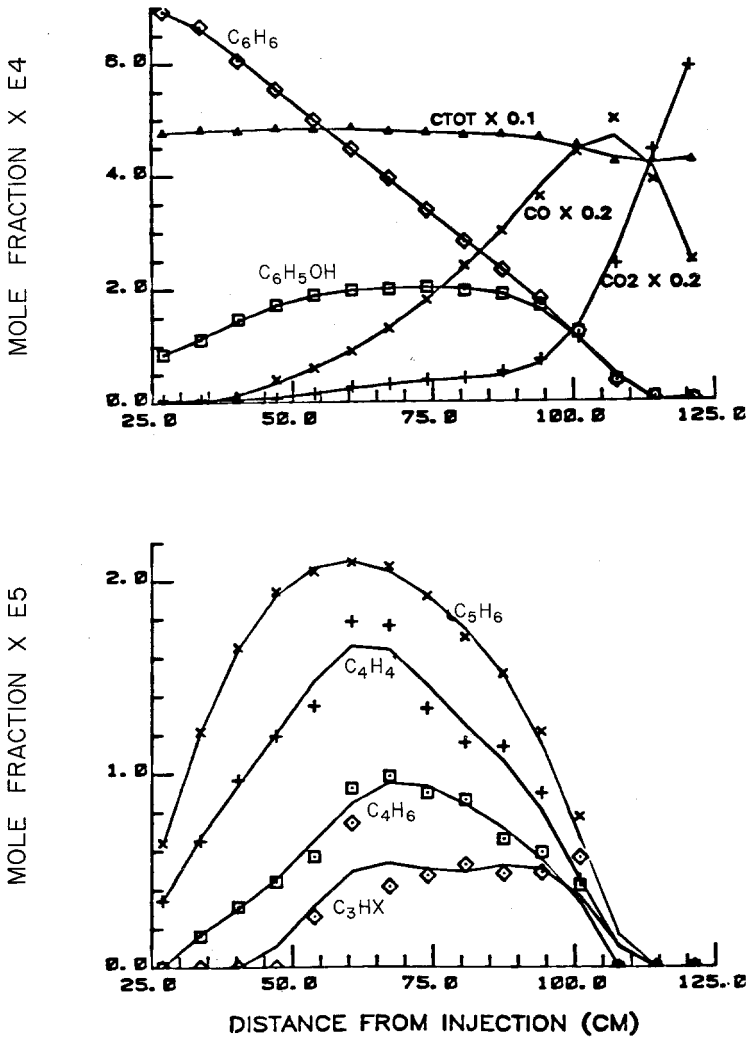


Fig. 9. The oxidation of benzene in a turbulent flow reactor ($\phi = 0.39$) showing intermediate product formation (after Vandooran and van Tiggelen [41]).

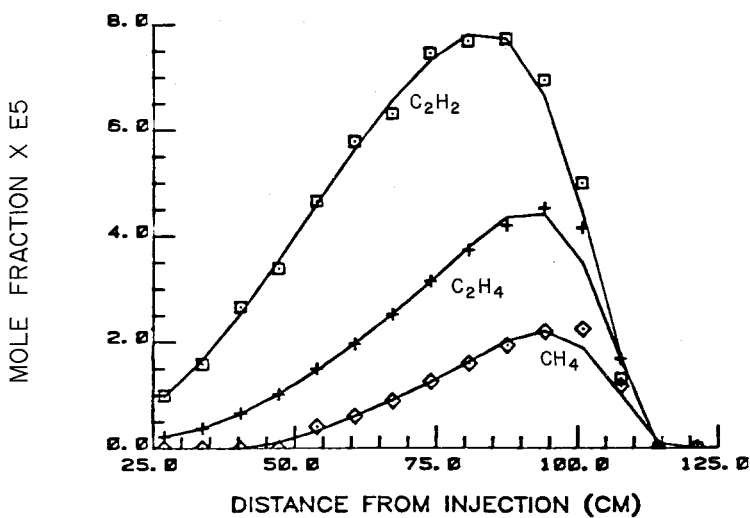
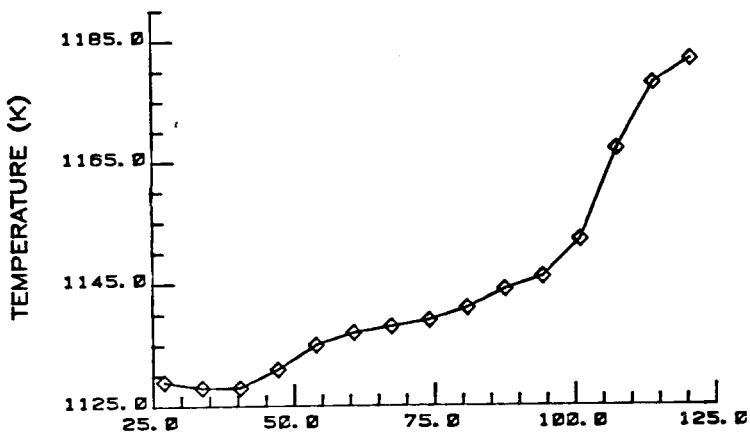
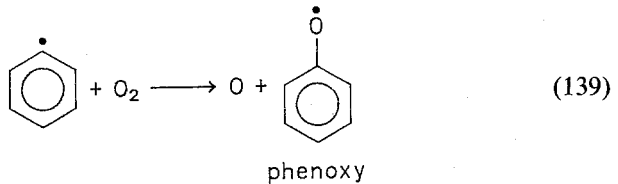
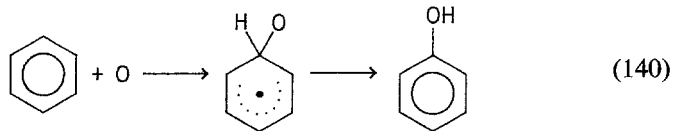


Fig. 9. (continued)

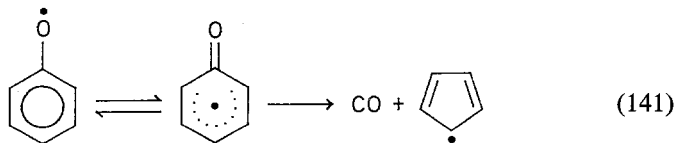
The fate of the phenyl radical is not known with great certainty. The large presence of phenol in flow-reactor studies led [35] to the suggestion of



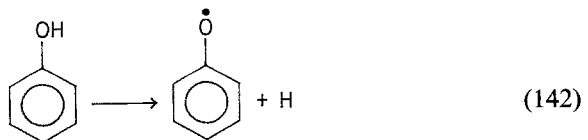
because this chain branching step was found [49] to be exothermic to the extent of approximately 10 kcal/mole, to have a low activation energy and to be relatively fast. It is interesting that the main chain branching step [reaction (15)] in the $\text{H}_2\text{-O}_2$ system is endothermic to about 16 kcal/mole. This rapid reaction (139) could explain the large amount of phenol found in flow-reactor studies. In studies [50] of near sooting benzene flames, the low mole fraction of phenyl found could have required an unreasonable high rate for reaction (139). The difference could be due to the higher temperatures, and thus large O atom concentrations in the flame studies. A possible important reaction for the formation of phenol could be direct O addition to benzene via



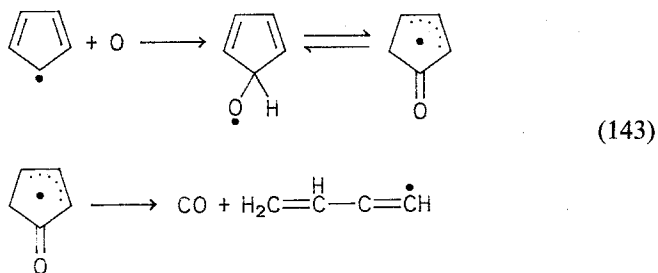
much the same as the biradical added to double bonds in the oxidation of olefins. The cyclopentadienyl radical apparently could form [43] from the phenoxy radical by



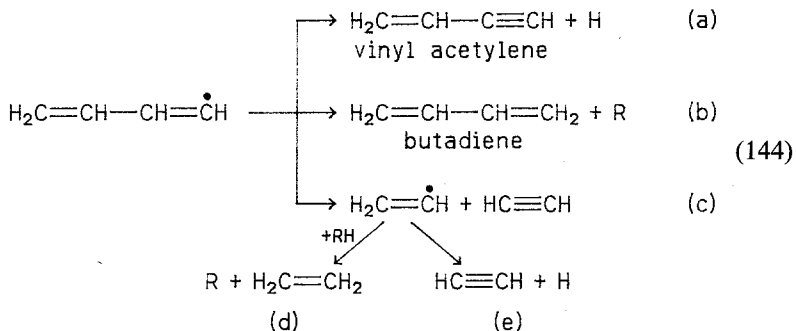
Or, as has been shown [43] the phenol could dissociate according to



which would be followed by reaction (141). The expulsion of CO from ketocyclohexadienyl radical is reasonable not only in view of the data given in Fig. 9 but also in view of other pyrolysis studies [51]. The expulsion indicates the early formation of CO in aromatic oxidation, whereas in aliphatic oxidation CO does not form until later in the reaction after the small olefins form (see Figs. 7 and 8). Since due to resonance the cyclopentadienyl radical is also very stable and its reaction with an O₂ molecule has a large endothermicity, a feasible step is reaction with O atoms; namely



The butadienyl radical found in reaction (143) then decays along various paths [41]:



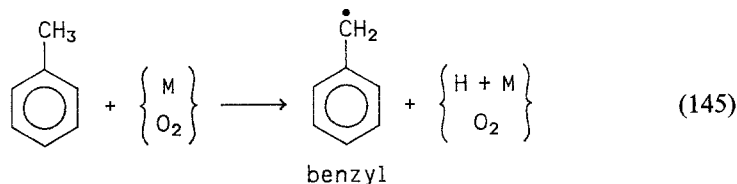
It is interesting to note that all the products of reaction (144) are considered important intermediates in soot formation [47,48] and reaction (144) may be an important reason why aromatics have a high propensity to soot.

Although there is no reported work on vinylacetylene oxidation, oxidation by O would probably lead primarily to the formation of CO, H₂, and acetylene (via an intermediate methyl acetylene) [29]. The oxidation of vinyl acetylene, or cyclopentadienyl radical shown earlier, requires the formation of an adduct [as shown in reaction (143)]. The high exothermicity when OH forms the adduct drives the system back to the initial reacting species. Thus,

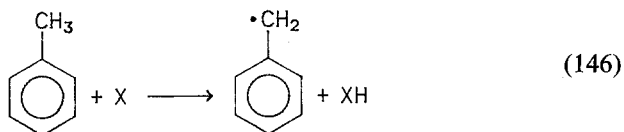
O atoms become the primary oxidizing species in the reaction steps. This factor may be the reason that for rich and lean oxidation experiments the fuel decay and intermediate species formed follow the same trend, although rich experiments show much slower rates [52] due to lower concentrations of oxygen atoms.

b. Oxidation of Alkylated Aromatics

The initiation step in the high-temperature oxidation of toluene would be the pyrolytic cleavage of a hydrogen atom from the methyl side chain and at lower temperatures by O_2 abstraction of an H from the side chain, namely

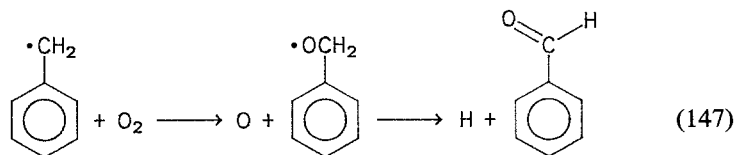


The radical pool that then develops begins the reactions that cause the fuel concentration to decay according to

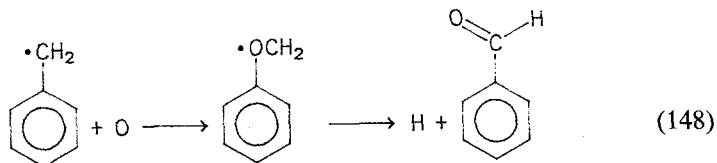


A significant proportion of the fuel can decay through displacement of the methyl side chain by a hydrogen atom to form benzene and a methyl radical [53]. Such displacement reactions are a characteristic step in alkylated aromatic mechanisms.

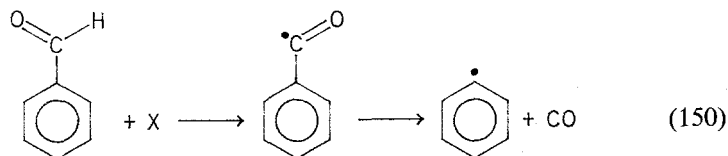
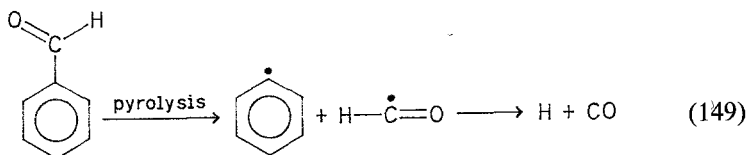
Flow-reactor studies [25] have shown that the primary product of benzyl radical decay is benzaldehyde. The reaction of benzyl radicals with O_2 through an intermediate adduct again is not possible as was found for reaction of methyl radicals and O_2 . Indeed one may think of benzyl to be a methyl radical with one H replaced by a phenyl group. However, it is to be noted that the reaction



is very endothermic and would not proceed as readily as reaction (139). Even though O atom concentrations in oxidation systems are substantially lower than O₂ concentrations, the reaction

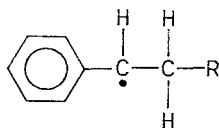


has been shown [25] to be orders of magnitude faster than reaction (147). The fate of benzaldehyde is the same as any aldehyde in an oxidizing system and the following reactions lead to phenyl radicals and CO, whose oxidation has been discussed:

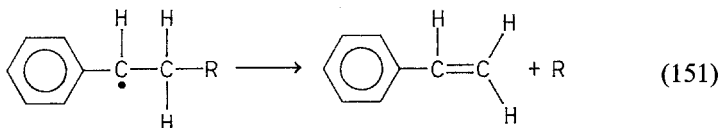


Reaction (148) is the dominant means of oxidizing benzyl radicals and as a slow step causes the oxidation of toluene to be overall slower than benzene, even though the induction period for toluene is shorter [54].

The first step of other high-order alkylated aromatics proceeds through pyrolytic cleavage of a CC bond. The radicals formed soon decay to give H atoms that initiate the H₂-O₂ radical pool. The decay of the initial fuel is dominated by radical attack. What is to be noted, however, is that the benzylic carbon has the weakest bond, selectivity of attack sets in and the resulting radical for the *n*-alkylated species is of the form



which due to the β scission rule decays to styrene and a radical [52]



where R, of course, can be a H or a hydrocarbon radical. If the side chain is in an iso form, then a more complex aromatic olefin forms. Isopropyl benzene leads to α methyl styrene [55].

In combustion systems the styrene formed would appear [49,52] to undergo predominantly displacement reactions by H atoms to give benzene and an alkyl radical, both of whose oxidation characteristics have been enumerated.

PROBLEMS

- In hydrocarbon oxidation there is the possibility of a negative reaction rate coefficient. What does this statement mean and when does the negative rate occur? What is the dominant chain branching step in the high-temperature oxidation of hydrocarbons? What are the four dominant overall steps in the oxidative conversion of aliphatic hydrocarbons to fuel products?
- Explain in a concise manner what the essential differences in the oxidative mechanisms of hydrocarbons are:
 - When the temperature is such that the reaction is taking place at a slow (measurable) rate; i.e., a steady reaction.
 - When the temperature is such that the mixture has just entered the explosive regime.
 - When the temperature is very high, such as that which is obtained in the latter part of a flame or in a shock tube.

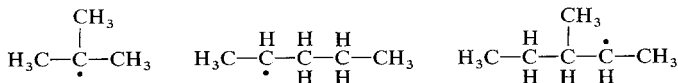
The pressure is assumed the same in all three cases.

- In the text the following relation was taken

$$\frac{d(\text{olefin})}{d(\text{ROOH})} = \frac{k_{47}(\dot{\text{R}})(\text{O}_2)}{k_{49}(\text{RO}_2)(\text{RH})}$$

Show that a steady-state analysis gives this relationship.

- Draw the chemical structure of heptane, 3-octene, and isopropyl benzene.
- What are the first two species to form during the thermal dissociation of each of the following radicals?



- Toluene is easier to ignite than benzene, yet its overall burning rate is slower. Explain why.

REFERENCES

1. Dainton, F. S., "Chain Reactions: An Introduction," 2nd ed., Methuen, London, 1966.
2. Lewis, B., and von Elbe, G., "Combustion, Flames and Explosions of Gases," 2nd ed., Part 1, Academic Press, New York, 1961.
3. Gardiner, W. C., Jr., and Olson, D. B., *Ann. Rev. Phys. Chem.* **31**, 377 (1980).
4. Westbrook, C. K., and Dryer, F. L., *Prog. Energy Combust. Sci.* **10**, 1 (1984).
5. Bradley, J. N., "Flame and Combustion Phenomena," Chapter 2, Methuen, London, 1969.
6. Baulch, D. L., et al., "Evaluated Kinetic Data for High Temperature Reactions," Vols. 1, 2, and 3, Butterworth, London, 1973, 1976.
7. Westbrook, C. K., *Combust. Sci. Technol.* **29**, 67 (1982).
8. Brokaw, R. S., *Int. Symp. Combust.*, 11th, p. 1063, Combustion Inst., Pittsburgh, Pennsylvania, 1967.
9. Gordon, A. S., and Knipe, R., *J. Phys. Chem.* **59**, 1160 (1955).
10. Dryer, F. L., Naegeli, D. W., and Glassman, I., *Combust. Flame* **17**, 270 (1971).
11. Smith, I. W. M., and Zellner, R., *J. Chem. Soc. Faraday. Trans.* **2** **69**, 1617 (1973).
12. Dryer, F. L., and Glassman, I., *Prog. Astronaut. Aeronaut.* **62** (1978).
13. Semenov, N. N., "Some Problems in Chemical Kinetics and Reactivity," Chapter VII, Princeton Univ. Press, Princeton, New Jersey, 1958.
14. Minkoff, G. J., and Tipper, C. F. H., "Chemistry of Combustion Reactions," Butterworth, London, 1962.
15. Williams, F. W., and Sheinson, R. S., *Combust. Sci. Technol.* **7**, 85 (1973).
16. Benson, S. W., *Prog. Energy Combust. Sci.* **7**, 125 (1981).
17. Benson, S. W., *Nat. Bur. Stand. Spec. Publ.* **359**, 101 (1972).
18. Baldwin, A. C., and Golden, D. M., *Chem. Phys. Lett.* **55**, 350 (1978).
19. Brabbs, T. A., and Brokaw, R. S., *Int. Symp. Combust.*, 15th, p. 893, Combustion Inst., Pittsburgh, Pennsylvania, 1975.
20. Warnatz, J., *Int. Symp. Combust.*, p. 369, Combustion Inst., Pittsburgh, Pennsylvania, 1981.
21. Warnatz, J., *Prog. Astronaut. Aeronaut.* **76**, 501 (1981).
22. Fristrom, R. M., and Westenberg, A. A., "Flame Structure." Chapter XIV, McGraw-Hill, New York, 1965.
23. Warnatz, J. "Combustion Chemistry" (W. C. Gardiner, Jr., ed.), Chapter 5, Springer-Verlag, New York, 1984.
24. Dryer, F. L., and Brezinsky, K., *West. States Sect. Combust. Inst.*, Pap. No. 84-88 (1984).
25. Brezinsky, K., Litzinger, T. A., and Glassman, I., *Int. J. Chem. Kinet.* **16**, 1053 (1984).
26. Golden, D. M., and Larson, C. W., *Int. Symp. Combust.*, 20th, p. 595, Combustion Inst., Pittsburgh, Pennsylvania, 1985.
27. Hunziker, H. E., Knepe, H., and Wendt, H. R., *J. Photochem.* **17**, 377 (1981).
28. Peters, J., and Mahnen, G., "Combustion Institute European Symposium," p. 53, Academic Press, New York (1973).
29. Blumenberg, B., Hoyermann, K., and Sievert, R., *Int. Symp. Combust.*, 16th, p. 841, Combustion Inst., Pittsburgh, Pennsylvania, 1977.
30. Tully, F. P., *Phys. Chem. Lett.* **96**, 148 (1983).
31. Miller, J. A., Mitchell, R. E., Smooke, M. D., and Kee, R. J., *Int. Symp. Combust.*, 19th, p. 181, Combustion Inst., Pittsburgh, Pennsylvania, 1982.
32. Grebe, J., and Homann, R. H., *Ber. Busen-Ges. Phys. Chem.* **86**, 587 (1982).
33. Glassman, I., Mech. Aerospace Eng. Rep. No. 1450 Princeton Univ., Princeton, New Jersey (1979).
34. Cole, J. A., M.S. Thesis, Dept. of Chem. Eng., MIT, Cambridge, Massachusetts (1982).

35. Frenklach, M., Clary, D. W., Gardiner, W. C., Jr., and Stein, S. E., *Int. Symp. Combust.*, 20th, p. 887, Combustion Inst. Pittsburgh, Pennsylvania, 1985.
36. Brezinsky, K., Burke, E. J., and Glassman, I., *Int. Symp. Combust.*, 20th, p. 613, Combustion Inst., Pittsburgh, Pennsylvania, 1985.
37. Norton, T. S., and Dryer, F. L., *East. States Sect. Combust. Inst. Meet.*, Paper No. 36 (1985).
38. Aronowitz, D., Santoro, R. J., Dryer, F. L., and Glassman, I., *Int. Symp. Combust.*, 17th, p. 633, Combustion Inst., Pittsburgh, Pennsylvania, 1978.
39. Bowman, C. T., *Combust. Flame* **25**, 343 (1975).
40. Westbrook, C. K., and Dryer, F. L., *Combust. Sci. Technol.* **20**, 125 (1979).
41. Vandooren, J., and van Tiggelen, P. J., *Int. Symp. Combust.*, 18th, p. 473, Combustion Inst., Pittsburgh, Pennsylvania, 1981.
42. Aders, W. K., "Combustion Institute European Symposium," Academic Press, New York (1973).
43. Colket, M. B., III, Naegeli, D. W., and Glassman, I., *Int. Symp. Combust.*, 16th, p. 1023, Combustion Inst., Pittsburgh, Pennsylvania, 1977.
44. Tsiang, W., *J. Chem. Phys.* **40**, 1498 (1964).
45. Norris, R. G. W., and Taylor, G. W., *Proc. R. Soc. London A* **153**, 448 (1936).
46. Barnard, J. A., and Ibberson, V. J., *Combust. Flame* **9**, 81, 149 (1965).
47. Glassman, I., Mech. and Aerosp. Eng. Rep. No. 1446 Princeton Univ., Princeton, New Jersey (1979).
48. Santoro, R. J., and Glassman, I., *Combust. Sci. Technol.* **19**, 161 (1979).
49. Venkat, C., Brezinsky, K., and Glassman, I., *Int. Symp. Combust.*, 19th, p. 143, Combustion Inst., Pittsburgh, Pennsylvania, 1982.
50. Bittner, J. D., and Howard, J. B., *Int. Symp. Combust.*, 19th, p. 211, Combustion Inst., Pittsburgh, Pennsylvania, 1982.
51. Cypres, R., and Bettens, B., *Tetrahedron* **30**, 1253 (1974).
52. Litzinger, T. A., Brezinsky, K., and Glassman, I., *Combust. Flame* **63**, 251 (1986).
53. Astholz, D. C., Durant, J., and Troe, J., *Int. Symp. Combust.*, 18th, p. 885, Combustion Inst., Pittsburgh, Pennsylvania, 1981.
54. Venkat, C., M.S., Thesis, Chem. Eng. Dept., Princeton Univ., Princeton, New Jersey, (1980).
55. Litzinger, T. A., Brezinsky, K., and Glassman, I., *J. Phys. Chem.* **90**, 508 (1986).

Flame Phenomena in Premixed Combustible Gases

A. INTRODUCTION

In the previous chapter, the conditions under which a fuel and oxidizer would undergo explosive reaction were discussed. Such conditions were found to be strongly dependent on the pressure and temperature. Given a premixed fuel-oxidizer system at room temperature and ambient pressure, the mixture is essentially unreactive. However, if an ignition source applied locally raises the temperature substantially, or causes a high concentration of radicals to form, a region of explosive reaction can propagate through the gaseous mixture provided that the composition of the mixture is within certain limits. These limits are called flammability limits and will be discussed later in this chapter. Ignition phenomena will be covered in a later chapter.

If a premixed gaseous fuel and oxidizer mixture within the flammability limits is contained in a long tube and an ignition source is applied at one end, a combustion wave will propagate down the tube. When the tube is opened at both ends, the velocity of the combustion wave can be observed to fall in the range of 20–200 cm/sec and for most hydrocarbon–air mixtures about 45 cm/sec. The velocity of this wave is controlled by transport processes, mainly simultaneous heat conduction and diffusion of radicals, and it is not

surprising to find that the velocities observed are much less than the sound speed in the unburned gaseous mixture. In this propagating combustion wave, subsequent reaction, after the ignition source is removed, is induced in the layer of gas ahead of the flame front by two mechanisms that are closely analogous to the thermal and chain branching mechanisms discussed in the preceding chapter for static systems [1]. This combustion wave is normally referred to as a flame and, since it can be treated as a flow entity; it is also called a deflagration.

When the tube is closed at one end and ignited there, the propagating wave undergoes a transition from a subsonic wave to one travelling at supersonic speeds. This supersonic wave is called a denotation. Rather than heat conduction and radical diffusion controlling the velocity, the shock wave structure of the developed supersonic wave raises the temperature and pressure substantially to cause explosive reaction and energy release that sustains the wave propagation.

The fact that subsonic and supersonic waves can be obtained under almost the same conditions leads one to believe that more can be learned by considering the phenomena as overall fluid mechanical in nature. Consider that the wave propagating in the tube is opposed by the unburned gases flowing at a velocity exactly equal to the wave propagation velocity. The wave then becomes fixed with respect to the containing tube (Fig. 1). This description of wave phenomena is readily treated analytically by the integrated conservation equations shown in the following paragraph.

If the subscript 1 specifies the unburned gas conditions and subscript 2 the burned gas conditions, the conservation equations generally written are

$$\rho_1 u_1 = \rho_2 u_2 \quad (\text{continuity}) \quad (1)$$

$$p_1 + \rho_1 u_1^2 = p_2 + \rho_2 u_2^2 \quad (\text{momentum}) \quad (2)$$

$$c_p T_1 + \frac{1}{2} u_1^2 + q = c_p T_2 + \frac{1}{2} u_2^2 \quad (\text{energy}) \quad (3)$$

$$p_1 = \rho_1 R T_1 \quad (\text{state}) \quad (4)$$

$$p_2 = \rho_2 R T_2 \quad (\text{state}) \quad (5)$$

Equation (4) connects the known variables, unburned gas pressure, temperature, and density, and thus is not an independent equation. In the coordinate system chosen, u_1 is the velocity fed into the wave and u_2 is the velocity coming out of the wave. In the laboratory coordinate system, the velocity ahead of the wave is zero, the wave velocity is u_1 , and $(u_1 - u_2)$ is

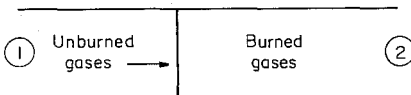


Fig. 1. Combustion wave fixed with respect to a containing tube.

the velocity of the burned gases with respect to the tube. The unknowns in the system are u_1 , u_2 , ρ_2 , T_2 , and p_2 . The chemical energy release is q and the stagnation adiabatic combustion temperature is T_2 .

Notice that there are five unknowns and only four independent equations. Nevertheless, one can proceed by analyzing the equations at hand. Simple algebraic manipulation (detailed in Chapter 5) results in two new equations

$$\frac{\gamma}{\gamma - 1} \left(\frac{p_2}{\rho_2} - \frac{p_1}{\rho_1} \right) - \frac{1}{2}(p_2 - p_1) \left(\frac{1}{\rho_1} + \frac{1}{\rho_2} \right) = q \quad (6)$$

and

$$\gamma M_1^2 = \left(\frac{p_2}{p_1} - 1 \right) / \left[1 - \frac{(1/\rho_2)}{(1/\rho_1)} \right] \quad (7)$$

where γ is the ratio of specific heats and M is the wave velocity divided by $(\gamma RT_1)^{1/2}$, or the Mach number of the wave. For simplicity the specific heats are assumed constant; i.e., $c_{p1} = c_{p2}$.

Equation (6) is referred to as the Hugoniot relationship and states for given initial conditions $(p_1, 1/\rho_1, q)$ a whole family of solutions $(p_2, 1/\rho_2)$ is possible. The family of solutions lie on a curve on a plot of P_2 versus $1/\rho_2$ as shown in Fig. 2. Plotted on the graph represented by Fig. 2 is the initial point $(p_1, 1/\rho_1)$ and the two tangents through this point to the curve representing the family of solutions. One obtains a different curve for each fractional values of q . Indeed, a curve is obtained for $q = 0$; that is, no energy release. This curve goes through the point representing the initial condition and is referred to as the shock Hugoniot since it gives the solution for simple shock waves.

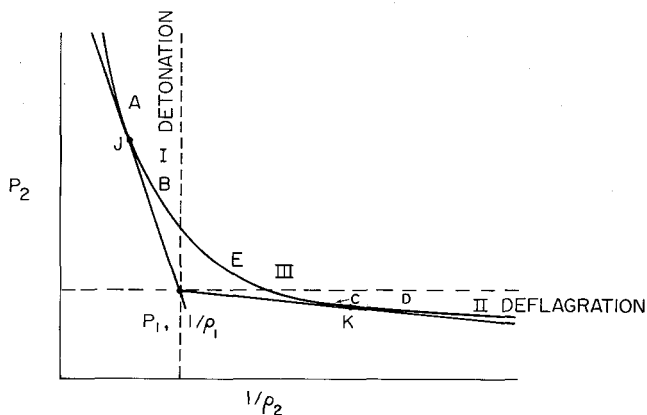


Fig. 2. Hugoniot plot divided in five regions A-E.

A horizontal line and vertical line are drawn through the initial condition point, as well. These lines, of course, represent the conditions of constant pressure and constant specific volume ($1/\rho$), respectively. They further break the curve into three sections. Sections I and II are further divided into sections by the tangency point (J and K) and the other letters defining particular points.

Examination of Eq. (7) reveals the character of M_1 for regions I and II. In region I, P_2 is much greater than P_1 , and thus the difference is a number much larger than 1. Furthermore, in this region $(1/\rho_2)$ is a little less than $(1/\rho_1)$, and thus the ratio is a number close to, but a little less than 1. Therefore the denominator is very small, much less than 1. Consequently the right-hand side of Eq. (7) is very much larger than one, certainly greater than 1.4. Conservatively one assumes $\gamma = 1.4$, then M_1^2 and M_1 are greater than 1. Thus, region I gives supersonic waves and is called the detonation region. Consequently, a detonation can be defined as a supersonic wave supported by energy release (combustion).

Similarly in region II, since P_2 is a little less than P_1 , the numerator of Eq. (7) is a small negative number less than 1. $(1/\rho_2)$ is much greater than $(1/\rho_1)$, and thus the denominator is a negative number greater than 1. The right-hand side of Eq. (7) for region II is less than 1, consequently M_1 is less than 1. Thus region II gives subsonic waves and is called the deflagration region. Thus deflagration waves in this context are defined as subsonic waves supported by combustion.

In region III, $P_2 > P_1$ and $1/\rho_2 > 1/\rho_1$; the numerator of Eq. (7) is positive and the denominator is negative. Thus M_1 is imaginary in region III and therefore does not represent a physically real solution.

It will be shown in Chapter 5 that the velocity of sound in the burned gases for points on the Hugoniot higher than J is greater than the velocity of the detonation wave relative to the burned gases. Consequently in any real physical situation in a tube, wall effects cause a rarification. This rarification wave will catch up to the detonation front, reduce the pressure, and cause the final values of P_2 and $1/\rho_2$ to drop to point J , the so-called Chapman-Jouguet point. Points between J and B are eliminated by considerations of the structure of the detonation wave or by entropy. Thus, the only steady-state solution in region II is given by point J . This unique solution has been found strictly by fluid dynamic and thermodynamic considerations.

Furthermore, the velocity of the burned gases at J and K can be shown to equal the sound speed there, and thus $M_2 = 1$ is a condition at both J and K . An expression similar to Eq. (7) for M_2 reveals that M_2 is greater than 1 as values past K are assumed. Such a condition cannot be real for it would mean that the velocity of the burned gases would increase by heat addition. It is well known that it is not possible by heat addition to increase the flow of

gases in a constant area duct past the sonic velocity. Thus region *KD* is ruled out. Unfortunately there are no means by which to reduce the range of solutions that is given by region *CK*. In order to find a unique deflagration velocity for a given set of initial conditions, another equation must be obtained. This equation comes about from the examination of the structure of the deflagration wave and deals with the rate of chemical reaction, or more specifically the rate of energy release.

The Hugoniot curve shows that in the deflagration region the pressure change is very small. Indeed, approaches seeking the unique deflagration velocity assume the pressure to be constant and drop the momentum equation.

The gases that flow in a Bunsen tube are laminar. Since in the horizontal tube experiment, the wave created is so very similar to the Bunsen flame, it too is laminar. The deflagration velocity under these conditions is called the laminar flame velocity, and it is the subject of laminar flame propagation that is treated in the remainder of this section.

For those who have not studied fluid mechanics, the definition of a deflagration as a subsonic wave supported by combustion may sound oversophisticated, nevertheless it is the only precise definition. Others describe flames in a more relative context. A flame can be considered a rapid, self-sustaining chemical reaction occurring in a discrete reaction zone. Reactants may be introduced into this reaction zone, or the reaction zone may move into the reactants depending on whether the unburned gas velocity is greater than or less than the flame (deflagration) velocity.

B. LAMINAR FLAME STRUCTURE

Much is to be learned by analyzing the structure of a flame in more detail. Consider, for example, a flame anchored on top of a single Bunsen burner as shown in Fig. 3. Recall that the fuel gas entering the burner induces air into the tube from its surroundings. As the fuel and air flow up the tube, they mix and, before the top of the tube is reached, the mixture is completely homogeneous. The flow velocity in the tube is considered to be laminar and the velocity across the tube parabolic in nature. Thus the flow velocity near the tube wall is very low and is a major factor along with heat losses to the burner rim in stabilizing the flame at the top. This type of stabilization will also be discussed later in this chapter.

The dark zone designated in Fig. 3 is simply the unburned premixed gases before they enter the area of the luminous zone where reaction and heat release take place. The luminous zone is less than 1-mm thick. More

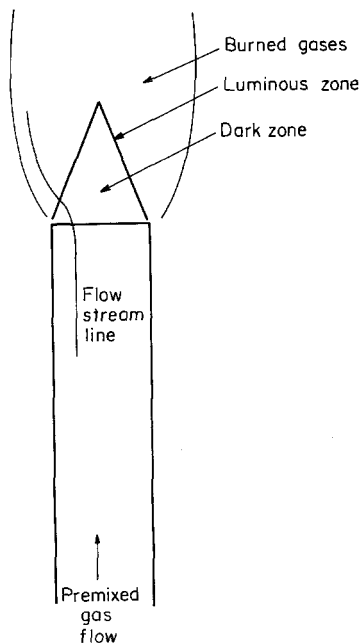


Fig. 3. Characteristic laminar Bunsen burner flame.

specifically the luminous zone is that portion of the reacting zone in which the temperature is the highest and indeed is the zone in which much of the reaction and heat release takes place. The color of the luminous zone changes with fuel-air ratio. For hydrocarbon-air mixtures that are fuel lean, a deep violet radiation due to excited CH radicals appears. When the mixture is fuel rich, the green radiation found is due to excited C_2 molecules. The high-temperature burned gases usually show a reddish glow which arises from CO_2 and water vapor radiation. When the mixture is adjusted to be very rich, carbon particles form and an intense yellow radiation can appear. This radiation is continuous and due to the presence of the solid carbon particles. Although Planck's black body curve peaks in the infrared for the temperatures that normally exist in these flames, the response of the human eye favors the yellow part of the electromagnetic spectrum. However, non-carbon containing hydrogen-air flames are nearly invisible.

With the background on hydrocarbon oxidation mechanisms developed, it is possible to characterize [1] the flame as existing of three zones: a preheat zone, a reaction zone, and a recombination zone. Conceptually this configuration is presented in Fig. 4, which shows a temperature profile taken normal to the flame front and the corresponding general composition changes in relation to this profile. The general structure of the reaction zone can be

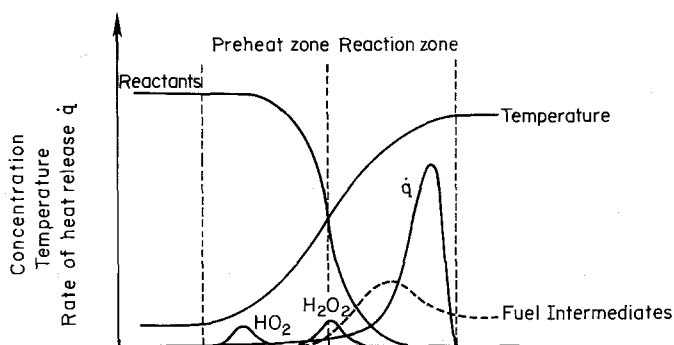


Fig. 4. Structure of a laminar flame characterized by reactant disappearance, product formation, temperature rise, rate of heat release, and position of intermediates HO_2 and H_2O_2 .

considered to be made up of early pyrolysis reactions and a zone in which the intermediates, CO and H_2 , are consumed. For a very stable molecule like methane, little or no pyrolysis can occur within the short residence time within the flame. With the majority of the other saturated hydrocarbons, considerable degradation occurs, and the fuel fragments that leave this part of the reaction zone consist of mainly olefins, hydrogen, and the lower hydrocarbons. Since the flame temperature of the saturated hydrocarbons would also be very nearly the same for reasons discussed in Chapter 1, it is not surprising then that their burning velocities, which will be shown to be very dependent on reaction rate, would all be of the same order (~ 40 cm/sec for a stoichiometric mixture in air).

The actual characteristics of the reaction zone and the composition changes throughout the flame are determined by the convective flow of unburned gases toward the flame zone and the diffusion of radicals from the high-temperature reaction zone against the convective flow into the preheat region. This diffusion is dominated by H atoms and consequently significant amounts of HO_2 form in the lower-temperature preheat region. Because of the lower temperatures in the preheat zone, reaction (21) (Chapter 2) proceeds readily to form the HO_2 . At these temperatures the chain branching reaction [Eq. (2), Chapter 2] does not proceed. The HO_2 subsequently forms hydrogen peroxide. Since the peroxide does not dissociate at the temperatures in the preheat zone, it is convected into the reaction zone and then forms OH radicals at the higher temperatures that prevail there [2].

Thus a relatively large OH concentration with respect to that of O and H exists in the early part of the reaction zone and OH is the primary reason for the fuel decay. Since the OH rate constant for abstraction from the fuel is of the same order as those for H and O , its abstraction reaction must dominate.

The latter part of the reaction zone forms the region where the intermediate fuel molecules are consumed and where the CO is converted to CO_2 . As discussed in Chapter 3, the CO conversion results in the major heat release in the system and is the reason the rate of heat release curve in Fig. 4 peaks near the maximum temperature. This curve falls off quickly because of the rapid disappearance of CO and the remaining fuel intermediates. The temperature follows a more smooth exponential-like rise because of the diffusion of heat back to the cooler gases.

The recombination zone falls into the burned gas or post-flame zone. Although recombination reactions are very exothermic, the radicals recombining have such low concentrations that the temperature profile is depicted as not being affected by this phase of the overall flame system.

C. THE LAMINAR FLAME SPEED

The flame velocity, which is also called the burning velocity, normal combustion velocity, or laminar flame speed, is more precisely defined as the velocity at which unburned gases move through the combustion wave in the direction normal to the wave surface.

The theoretical analyses for the determination of the laminar flame speed fall into three categories: thermal theories, diffusion theories, and comprehensive theories. The historical development followed approximately the same order.

The thermal theories date back to Mallard and Le Chatelier [3] who proposed that it is propagation of heat back through layers of gas that is the controlling mechanism in flame propagation. As one would expect, a form of the energy equation is the basis for the development of the thermal theory. Mallard and Le Chatelier postulated (as shown in Fig. 5) that a flame consists

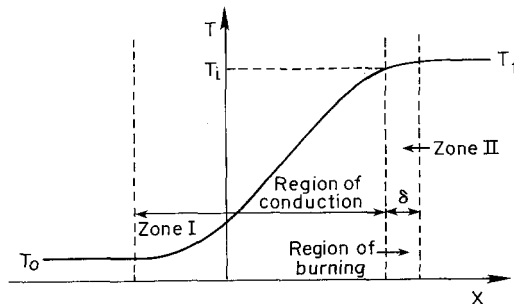


Fig. 5. Mallard-LeChatelier description of a laminar flame temperature wave.

of two zones separated at the point where the next layer ignites.

Unfortunately, this thermal theory requires the concept of an ignition temperature. Neither adequate means exist for the determination of ignition temperatures, nor does an actual ignition temperature exist in a laminar flame.

Later there were improvements in the thermal theories, probably the most significant of which is that due to Zeldovich and Frank-Kamenetskii, whose derivation was presented in detail by Semenov [4] and is commonly called the Semenov theory. These authors included the diffusion of molecules as well as heat, but not of free radicals or atoms. As a result, their approach emphasized thermal mechanism and it has been widely used in correlations of experimental flame velocities. As in the theory of Mallard and Le Chatelier, Semenov assumed an ignition temperature but by approximations eliminated it from the final equation to make the final result more useful.

The theory was advanced further when it was postulated that not only can heat control the reaction mechanism, but also the diffusion of certain active species such as radicals. As described in the preceding section, light particles can readily diffuse back and initiate further reactions.

The theory of particle diffusion was first put forth in 1934 by Lewis and von Elbe [5] in dealing with the ozone reaction. Tanford and Pease [6] carried this concept further by postulating that it is the diffusion of radicals that is all important and not the temperature gradient as required by the thermal theories. They proposed a diffusion theory that was quite different in physical concept than the thermal theory. However, one should recall that equations that govern mass diffusion are the same as those that govern thermal diffusion.

After these theories were put forth, there was a great deal of experimentation in order to determine the effect of temperature and pressure on the flame velocity and thus to verify which of the theories were correct. In the thermal theory, the higher the ambient temperature the higher the final temperature and therefore the faster the reaction rate and flame velocity. Similarly for the diffusion theory, the higher the temperature, the greater the dissociation, the greater the concentration of radicals to diffuse back, and therefore the faster the velocity. Consequently data obtained from temperature and pressure effects did not give conclusive results.

There appeared to be some evidence to support the diffusion concept, for this theory seemed to best explain the effect of H_2O on the experimental flame velocities of $\text{CO}-\text{O}_2$. As described in the previous chapter, at high temperature it is known that water provides the source of hydroxyl radicals to facilitate rapid reaction of CO and O_2 .

Hirschfelder *et al.* [7] reasoned that in the cyanogen-oxygen flame there is no dissociation. The products of this reaction are CO and N_2 , no intermediate species form, and the $\text{C}=\text{O}$ and $\text{N}\equiv\text{N}$ bonds are difficult to break. In

this system it is apparent that the concentration of radicals is not important for flame propagation, and one must conclude that thermal effects predominate. Hirschfelder *et al.* [7] essentially concluded that one should follow the thermal theory concept and include the diffusion of all particles, both into and out of the flame zone.

In developing the equations governing the thermal and diffusional processes, Hirschfelder obtained a set of complicated nonlinear equations, which could be solved only by numerical methods. In order to solve the set of equations, Hirschfelder had to assume some heat sink for a boundary condition on the cold side. This sink was required because of the use of the Arrhenius expressions for reaction rate. The complexity is that the Arrhenius expression requires a finite reaction rate even at $\chi = -\infty$, where the temperature is that of the unburned gas.

Friedman and Burke [8] in order to simplify the Hirschfelder solution modified the Arrhenius reaction rate equation so the rate was zero at $T = T_0$, but Friedman and Burke also required numerical calculations.

It was possible by certain physical principles to simplify the complete equations so that they could be solved relatively easily. The simplification was first carried out by von Karman and Penner [9]. This approach was considered one of the more significant advances in laminar flame propagation, but it could not have been developed and verified if it were not for the extensive work of Hirschfelder and his collaborators. The major simplification that von Karman and Penner introduced is the fact that the eigenvalue solution of the equations was the same for all ignition temperatures whether it be near T_f or not. More recently asymptotic analyses which provide formulae with greater accuracy and further clarification of the wave structure have been developed. These developments are described in detail in three books [10–12].

It is easily recognized that any exact solution of laminar flame propagation must make use of the basic equations of fluid dynamics modified to account for the liberation and conduction of heat and for changes of chemical species within the reaction zones. By certain physical assumption and mathematical techniques the equations have been simplified. Such assumptions have led to many formulations in Refs. [10–12], but the theories that will be considered here are an extended development of the simple Mallard–Le Chatelier approach and the Semenov approach. The Mallard–Le Chatelier development is given because of its historical significance and because this very simple thermal analysis permits the establishment of the important parameters in laminar flame propagation that are more difficult to interpret in the complex analyses. The Zeldovich–Frank–Kaminetskii–Semenov theory is reviewed because certain approximations related to the ignition temperature that are employed are useful in other problems in the combustion field.

1. The Theory of Mallard and Le Chatelier

Conceptually, Mallard and Le Chatelier stated that the heat conducted from zone I in Fig. 5 equalled that necessary to raise the unburned gases to the ignition temperature (the boundary between zones I and II). If it is assumed that the slope of the temperature curve were linear, then the slope could be approximated by the expression $[(T_f - T_i)/\delta]$, where T_f is the final or flame temperature, T_i the ignition temperature, and δ the thickness of the reaction zone. The enthalpy balance then becomes

$$\dot{m}c_p(T_i - T_0) = \lambda \frac{(T_f - T_i)}{\delta} A \quad (8)$$

where λ is the thermal conductivity, \dot{m} the mass rate into the combustion wave, T_0 the temperature of the unburned gases, and A the cross-sectional area taken as unity. Since the problem as described is fundamentally one dimensional,

$$\dot{m} = \rho Au = \rho S_L A \quad (9)$$

where ρ is the density and u the velocity of the gases. Because the unburned gases enter normal to the wave, by definition

$$S_L = u \quad (10)$$

Equation (8) then becomes

$$\rho S_L c_p (T_i - T_0) = \lambda (T_f - T_i) / \delta \quad (11)$$

or

$$S_L = \frac{(\lambda) (T_f - T_i)}{\rho c_p (T_i - T_0)} \frac{1}{\delta} \quad (12)$$

Equation (12) is the expression for the flame speed obtained by Mallard and Le Chatelier. Unfortunately, in this expression δ is not known and, therefore, a better representation is required.

Since δ is the reaction zone thickness it is possible to relate δ to S_L . Thus

$$\delta = S_L \cdot \tau = S_L \frac{1}{(d\varepsilon/dt)} = \frac{S_L}{RR} \quad (13)$$

where τ is the reaction time and $(d\varepsilon/dt)$ is the reaction rate in terms of fractional conversion as described in Chapter 2, Section E. Substituting this expression into Eq. (12), one obtains

$$S_L = \left(\frac{\lambda}{\rho c_p} \frac{T_f - T_0}{T_i - T_0} \frac{d\varepsilon}{dt} \right)^{1/2} \sim (\alpha RR)^{1/2} \quad (14)$$

where α ($= \lambda/\rho c_p$) is the thermal diffusivity and RR the reaction rate. Substituting Eq. (14) into Eq. (13) in order to eliminate RR , one finds that

$$\delta = \alpha/S_L \quad (15)$$

Most hydrocarbon flames have a speed of about 40 cm/sec. Using a value of thermal diffusivity evaluated at a mean temperature of about 1300 K, a value of δ close to 0.1 cm is found. Thus, as depicted in Fig. 5 hydrocarbon flames have a characteristic length of the order of 1 mm. The characteristic time is (α/S_L^2) and for hydrocarbon flames this value is of the order of a few milliseconds.

This adaptation of the simple Mallard-Le Chatelier approach is most significant in that the result

$$S_L \sim (\alpha RR)^{1/2}$$

is very useful in predicting laminar flame spread phenomena. It is a result that one should commit to memory. In fact one could question whether the more complex theories reveal much more. Comparisons between actual calculated values of flame speed and experimental results are few and far between. The only published comparisons are for the most simple decomposition flames, and even there one could argue that the agreement could be fortuitous. In any of the theories, in order to calculate the laminar flame speed one must know the thermophysical properties of a complex mixture at high temperatures and have accurate reaction rate data. But for flames to propagate the reaction system must be explosive. Thus, all flame systems contain a very complex set of basic reaction steps. These property and reaction data are just not known in the detail required. The worth of the more advanced theories rests solely in the fact that they can obtain a quantitative result that compares within an order of magnitude to the experimental flame speed. In his sense they give validation to all the physical models based on heat and mass diffusion.

To examine how Eq. (15) predicts experimental trends, first recall that

$$d\varepsilon/dt = k\varepsilon^n p^{n-1} = Ae^{-E/RT} \varepsilon^n p^{n-1} \quad (16)$$

where n is the overall reaction order. Thus, it is possible to calculate the pressure dependence. Since for gases only the density term in α is pressure dependent and

$$S_L \sim \{(1/\rho)p^{n-1}\}^{1/2} \sim (p^{n-2})^{1/2} \quad (17)$$

which states that the flame speed is independent of pressure for second-order reactions. Most hydrocarbon oxygen reactions have an overall reaction order close to 2, and, thus, flame speeds for hydrocarbons generally are pressure independent, as has been found experimentally. There are some deviation from this pressure dependency that will be discussed in Section C.5.

Even though it is not possible to evaluate T_i , the temperature dependence in the flame speed expression is dominated by the exponential; thus, it is possible to assume

$$S_L \sim \{\exp(-E/RT)\}^{1/2} \quad (18)$$

Since physical reasoning states that most of the reaction and heat release must occur close to the highest temperature if Arrhenius kinetics control, the temperature to be used in the above expression is T_f and one obtains

$$S_L \sim \{\exp(-E/RT_f)\}^{1/2} \quad (19)$$

Thus, the effect of varying the initial temperature is found in the degree it alters the flame temperature. Recall a 100° rise in initial temperature results in a rise of flame temperature that is much smaller. These trends due to temperature have been verified experimentally.

2. The Theory of Zeldovich, Frank-Kamenetskii, and Semenov

These Russian investigators derived an expression for the laminar flame speed by an important extension of the very simplified Mallard-Le Chatelier approach. Their basic equation included diffusion of species as well as heat. Since their initial insight was that flame propagation was fundamentally a thermal mechanism, they were not concerned with the diffusion of radicals and their effect on the reaction rate. They were concerned with the energy transported by the diffusion of species.

As in the Mallard-Le Chatelier approach, an ignition temperature arises in this development; but, it is used only as a mathematical convenience for computation. Because the chemical reaction rate is an exponential function of temperature according to the Arrhenius equation, Semenov assumed that the ignition temperature, above which nearly all reaction occurs, is very near the flame temperature. With this assumption, the ignition temperature can be eliminated in the mathematical development. Since the energy equation is the one to be solved in this approach, the assumption is physically correct. As described in the previous section for hydrocarbon flames, most of the energy release is due to CO oxidation, which takes place very late in the flame where there is great availability of hydroxyl radicals.

For the initial development, although these restrictions are partially removed in further developments, two other important assumptions are made. The assumptions are the c_p and λ are constant and that

$$(\lambda/c_p) = D\rho \quad (20)$$

where D is the mass diffusivity. This assumption is essentially that

$$\alpha = D$$

Simple kinetic theory gives

$$\alpha - D = \nu \tag{21}$$

where ν is kinetic viscosity (momentum diffusivity). The ratios of these three diffusivities give some of the familiar dimensionless similarity parameters,

$$\text{Pr} = \nu/\alpha, \quad \text{Sc} = \nu/D, \quad \text{Le} = D/\alpha \tag{22}$$

where Pr, Sc, and Le are the Prandtl, Schmidt, and Lewis numbers, respectively. The Prandtl number is the ratio of momentum to thermal diffusion, the Schmidt number, momentum to mass diffusion, and the Lewis number, thermal to mass diffusion. Elementary kinetic theory then also gives as a first approximation

$$\text{Pr} = \text{Sc} = \text{Le} = 1 \tag{23}$$

In addition, this theory gives as a first approximation

$$(\lambda/c_p) = D\rho \neq f(P) \tag{24}$$

Consider the thermal wave given in Fig. 5. If a differential control volume is taken within this one-dimensional wave and the variations as given in the figure are in the x -direction, then the thermal and mass balances are as shown in Fig. 6. In Fig. 6, a is the number of moles of reactant per cubic centimeter, \dot{w} is the rate of reaction, and Q is the heat of reaction per mole of reactant. Since the problem is a steady one, there can be no accumulation of species or heat

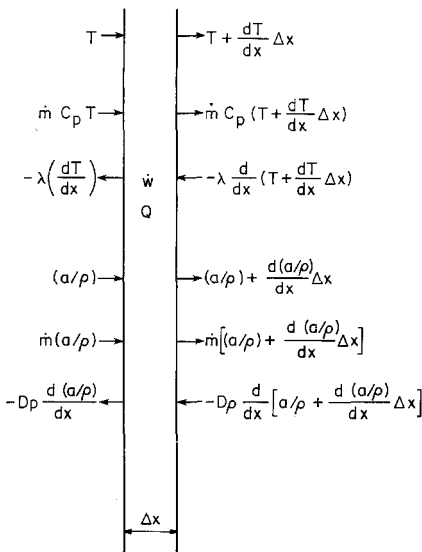


Fig. 6. Balances across a differential element in a thermal wave.

with respect to time, and the balance of the energy terms and the species terms must each be equal to zero.

The amount of mass convected into the volume $A \Delta x$ (where A is the area usually taken as unity) is

$$\dot{m} \left[\left(\frac{a}{\rho} \right) + \frac{d(a/\rho)}{dx} \Delta x \right] A - \dot{m} \left(\frac{a}{\rho} \right) A = \dot{m} \frac{d(a/\rho)}{dx} A \Delta x \quad (25)$$

The amount of mass diffusing into the volume is

$$- \frac{d}{dx} \left[D\rho \left(\frac{a}{\rho} + \frac{d(a/\rho)}{dx} \Delta x \right) \right] A - \left(-D\rho \frac{d(a/\rho)}{dx} \right) A = -(D\rho) \frac{d^2(a/\rho)}{dx^2} A \Delta x \quad (26)$$

The amount of mass reacting (disappearing) in the volume is

$$\dot{w} A \Delta x \quad (27)$$

and it is to be noted that \dot{w} is a negative quantity. Thus the continuity equation for the reactant is

$$-D\rho \frac{d^2(a/\rho)}{dx^2} + \dot{m} \frac{d(a/\rho)}{dx} + \dot{w} = 0 \quad (28)$$

(diffusion term) (convective term) (generation term)

The energy equation is determined similarly and is

$$-\lambda \frac{d^2 T}{dx^2} + \dot{m} c_p \frac{dT}{dx} - \dot{w} Q = 0 \quad (29)$$

Because \dot{w} is negative and the overall term must be positive since there is heat release, the third term has a negative sign. The state equation is written as

$$(\rho/\rho_0) = (T_0/T) \quad (30)$$

New variables are defined as

$$\tilde{T} = \frac{c_p(T - T_0)}{Q} \quad (31)$$

$$\tilde{a} = (a_0/\rho_0) - (a/\rho) \quad (32)$$

where the subscript 0 designates initial conditions. Substituting the new variables in Eqs. (28) and (29), two new equations are obtained

$$D\rho \frac{d^2 \tilde{a}}{dx^2} - \dot{m} \frac{d\tilde{a}}{dx} + \dot{w} = 0 \quad (33)$$

$$\frac{\lambda}{c_p} \frac{d^2 \tilde{T}}{dx^2} - \dot{m} \frac{d\tilde{T}}{dx} + \dot{w} = 0 \quad (34)$$

The boundary conditions for these equations are

$$\begin{aligned} x = -\infty, \quad \tilde{a} = 0, \quad \tilde{T} = 0 \\ x = +\infty, \quad \tilde{a} = a_0/\rho_0, \quad \tilde{T} = [c_p(T_f - T_0)]/Q \end{aligned} \quad (35)$$

where T_f is the final or flame temperature. For the condition $D\rho = (\lambda/c_p)$, Eqs. (33) and (34) are identical in form. If the equations and boundary conditions for \tilde{a} and \tilde{T} coincide, i.e., if $\tilde{a} = \tilde{T}$ over the entire interval, then

$$c_p T_0 + (a_0 Q/\rho_0) = c_p T_f = c_p T + (aQ/\rho) \quad (36)$$

The meaning of Eq. (36) is that the sum of the thermal and chemical energies per unit mass of the mixture is constant in the combustion zone; i.e., the relation between the temperature and the composition of the gas mixture is the same as that for the adiabatic behavior of the reaction at constant pressure.

Thus, the variable defined in Eq. (36) can be used to develop a new equation in the same manner as Eq. (28) and the problem reduces to the solution of only one differential equation. Indeed either Eq. (28) or (29) can be solved; however Semenov chose to work with the energy equation.

In the first approach it is assumed, as well, that the reaction proceeds by zero order. Since the rate term \dot{w} is not a function of concentration, the continuity equation is not required and one can deal with the more convenient energy equation. The Russian investigators, similar to Mallard-Le Chatelier, examined the thermal wave as if it were made up of two parts. The unburned gas part is considered to be a zone of no chemical reaction, and the reaction part is considered to be the zone in which the reaction and diffusion terms dominate and the convective term can be dropped. Thus, in the first zone (I), the energy equation reduces to

$$\frac{d^2 T}{dx^2} - \frac{\dot{m}c_p}{\lambda} \frac{dT}{dx} = 0 \quad (37)$$

with the boundary conditions

$$x = -\infty, \quad T = T_0; \quad x = 0, \quad T = T_i$$

It is apparent from the latter boundary condition that the coordinate system is so chosen that T_i is at the origin. The reaction zone extends a small distance d , so that in the reaction zone (II), the energy equation is written as

$$\frac{d^2 T}{dx^2} + \frac{\dot{w}Q}{\lambda} = 0 \quad (38)$$

with the boundary conditions

$$x = 0, \quad T = T_i; \quad x = d, \quad T = T_f$$

The added condition, which permits the determination of the solution (eigenvalue), is the requirement of the continuity of heat flow at the interface of the two zones:

$$\lambda \left(\frac{dT}{dx} \right)_{x=0,I} = \lambda \left(\frac{dT}{dx} \right)_{x=0,II} \quad (39)$$

The solution to the problem is obtained by initially considering Eq. (38). First, recall that

$$\frac{d}{dx} \left(\frac{dT}{dx} \right)^2 = 2 \left(\frac{dT}{dx} \right) \frac{d^2T}{dx^2} \quad (40)$$

Now, Eq. (38) is multiplied by $2(dT/dx)$ to obtain

$$2 \left(\frac{dT}{dx} \right) \frac{d^2T}{dx^2} = -2 \frac{\dot{w}Q}{\lambda} \left(\frac{dT}{dx} \right) \quad (41)$$

$$\frac{d}{dx} \left(\frac{dT}{dx} \right)^2 = -2 \frac{\dot{w}Q}{\lambda} \left(\frac{dT}{dx} \right) \quad (42)$$

Integrating Eq. (42) one obtains

$$-\left(\frac{dT}{dx} \right)_{x=0}^2 = -2 \frac{Q}{\lambda} \int_{T_i}^{T_r} \dot{w} dT \quad (43)$$

since $(dT/dx)^2$ evaluated at $x = d$ or $T = T_r$ is equal to zero. But from Eq. (37), one has

$$\frac{d}{dx} \left(\frac{dT}{dx} \right) = \frac{\dot{m}c_p}{\lambda} \frac{dT}{dx} \quad (44)$$

Integrating Eq. (44),

$$dT/dx = (\dot{m}c_p/\lambda)T + \text{const}$$

Since at $x = -\infty$, $T = T_0$ and $(dT/dx) = 0$,

$$\text{const} = -(\dot{m}c_p/\lambda)T_0 \quad (45)$$

and

$$dT/dx = [\dot{m}c_p(T - T_0)]/\lambda \quad (46)$$

Evaluating the expression at $x = 0$ where $T = T_i$,

$$(dT/dx)_{x=0} = \dot{m}c_p(T_i - T_0)/\lambda \quad (47)$$

The continuity of heat flux permits this expression to be combined with Eq. (43) to obtain

$$\frac{\dot{m}c_p(T_i - T_0)}{\lambda} = \left(\frac{2Q}{\lambda} \int_{T_i}^{T_r} \dot{w} dT \right)^{1/2}$$

Since Arrhenius kinetics dominate, it is apparent that T_i is very close to T_f , so the last expression is rewritten as

$$\frac{\dot{m}c_p(T_f - T_0)}{\lambda} = \left(\frac{2Q}{\lambda} \int_{T_i}^{T_f} \dot{w} dT \right)^{1/2} \quad (48)$$

For $\dot{m} = S_L \rho_0$ and $(a_0/\rho_0) Q$ can be taken equal to $c_p(T_f - T_0)$ [from Eq. (36)], one obtains

$$S_L = 2 \left(\frac{\lambda}{\rho c_p} \right) \left(\frac{I}{T_f - T_0} \right)^{1/2} \quad (49)$$

where

$$I = \frac{1}{a_0} \int_{T_i}^{T_f} \dot{w} dT \quad (50)$$

and \dot{w} is a function of T and not of concentration for a zero-order reaction and it may be expressed as

$$\dot{w} = Z' e^{-E/RT} \quad (51)$$

where Z' is the pre-exponential term in the Arrhenius expression.

For sufficiently large energy of activation such as one has for hydrocarbon-oxygen mixtures where E is of the order of 40 kcal/mole, $(E/RT) \gg 1$. Thus most of the reaction will be near the flame temperature, T_i will be very near the flame temperature, and zone II a very narrow region. Consequently it is possible to define a new variable σ such that

$$\sigma = (T_f - T) \quad (52)$$

The values of σ will vary from

$$\sigma_i = (T_f - T_i) \quad (53)$$

to zero. Since

$$\sigma \ll T_f$$

then

$$\begin{aligned} (E/RT) &= [E/R(T_f - \sigma)] = [E/RT_f(1 - (\sigma/T_f))] \\ &= (E/RT_f)[1 + (\sigma/T_f)] = (E/RT_f) \left(\frac{E\sigma/RT_f^2}{1} \right) \end{aligned}$$

Thus the integral I becomes

$$I = \frac{Z' e^{-E/RT_f}}{a_0} \int_{T_i}^{T_f} e^{-E\sigma/RT_f^2} dT = - \frac{Z' e^{-E/RT_f}}{a_0} \int_{\sigma_i}^0 e^{-E\sigma/RT_f^2} d\sigma \quad (54)$$

Defining still another variable β as

$$\beta = E\sigma/RT_f^2 \quad (55)$$

the integral becomes

$$I = \frac{Z' e^{-E/RT_f}}{a_0} \left[\int_0^{\beta_i} e^{-\beta} d\beta \right] \frac{RT_f^2}{E} \quad (56)$$

With sufficient accuracy one may write

$$j = \int_0^{\beta_i} e^{-\beta} d\beta = 1 - e^{-\beta_i} \cong 1 \quad (57)$$

since $(E/RT_f) \gg 1$ and $(\sigma_i/T_f) \cong 0.25$. Thus,

$$I = \left(\frac{Z'}{a_0} \right) \left(\frac{RT_f^2}{E} \right) e^{-E/RT_f} \quad (58)$$

and

$$S_L = \left(\frac{2\lambda}{c_p \rho_0 a_0} \frac{Z' e^{-E/RT_f} RT_f^2}{(T_f - T_0) E} \right)^{1/2} \quad (59)$$

In the preceding development, it was assumed that the number of moles did not vary during reaction. This restriction can be removed to allow the number to change in the ratio (n_r/n_p) , which is the number of moles of reactant to product. Furthermore, the Lewis number equal to one restriction can be removed to allow

$$(\lambda/c_p)/D\rho = A/B$$

where A and B are constants. With these restrictions removed, then the result for a first-order reaction becomes

$$S_L = \left\{ \frac{2\lambda_f(c_p)_f Z'}{\rho_0 \bar{c}_p^2} \left(\frac{T_0}{T_f} \right) \left(\frac{n_r}{n_p} \right) \left(\frac{A}{B} \right) \left(\frac{RT_f^2}{E} \right)^2 \frac{e^{-E/RT_f}}{(T_f - T_0)^2} \right\}^{1/2} \quad (60)$$

and for a second-order reaction

$$S_L = \left\{ \frac{2\lambda c_{pr}^2 Z' a_0}{\rho_0 (\bar{c}_p)^3} \left(\frac{T_0}{T_f} \right)^2 \left(\frac{n_r}{n_p} \right) \left(\frac{A}{B} \right)^2 \left(\frac{RT_f^2}{E} \right)^3 \frac{e^{-E/RT_f}}{(T_f - T_0)^3} \right\}^{1/2} \quad (61)$$

c_{pr} is the specific heat evaluated at T_f and \bar{c}_p is the average specific heat between T_0 and T_f .

Notice that since a_0 and ρ_0 are both functions of pressure, S_L is independent of pressure. Furthermore, this complex development shows that

$$S_L \sim \left(\frac{\lambda c_{pr}^2}{\rho_0 (\bar{c}_p)^3} a_0 Z' e^{-E/RT_f} \right)^{1/2}, \quad S_L \sim \left(\frac{\lambda}{\rho_0 c_p} RR \right)^{1/2} \sim (\alpha RR)^{1/2}$$

as was obtained from the simple Mallard-Le Chatelier approach.

3. The Laminar Flame and the Energy Equation

An important point about laminar flame propagation not previously discussed is worth stressing. It has become the practice to state that in the case of premixed homogeneous combustible gaseous mixtures that reaction rate phenomena control and in initially unmixed fuel-oxidizer systems that diffusion phenomena control. The subject of diffusion flames will be discussed in Chapter 6. In the case of laminar flames, and indeed in most aspects of turbulent flame propagation, it should be emphasized that it is the diffusion of heat (and mass) that causes the flame to propagate, i.e., flame propagation is a diffusional mechanism. The reaction rate determines the thickness of the reaction zone and, thus, the temperature gradient. The temperature effect indeed is a strong one, but, nevertheless, it is diffusion of heat and mass that causes the flame to propagate. The expression $S_L \sim (\alpha RR)^{1/2}$ says it well—the propagation rate is proportional to the square root of the diffusivity and the reaction rate.

4. Flame Speed Measurements

For a long period of time there has been no interest in flame speed measurements. Sufficient data and understanding were thought to be at hand. As lean burn conditions became popular in spark ignition engines, interest in flame speed of lean limits has rekindled this interest in measurement techniques. Some techniques are discussed in the following paragraphs.

The flame velocity has been defined as the velocity at which the unburned gases move through the combustion wave in a direction normal to the wave surface. If, in an infinite plane flame, the flame is regarded as stationary and a particular flow tube of gas considered, the area of the flame enclosed by the tube is not dependent on how the term “flame surface or wave surface” in which the area is measured is defined. The areas of all parallel surfaces are the same whatever property (e.g., particularly temperature) is chosen to define the surface, and these areas are all equal to each other and to that of the inner surface of the luminous part of the flame. The definition is more difficult in any other geometric system. Consider, for example, an experiment in which gas is supplied at the center of a sphere and flows radially outwards in a laminar manner to a spherical flame that is stationary. The inward movement of the flame is balanced by the outward flow of gas. The experiment takes place in an infinite volume at constant pressure. The area of the surface of the wave will depend on where the surface is located. The area of the sphere for which $T = 500^\circ\text{C}$ will be less than that of one for which $T = 1500^\circ\text{C}$. So, if the burning velocity is defined as the volume of unburned gas consumed per

second divided by the surface area of the flame, the result obtained will depend on the particular surface selected. The only quantity that does remain constant in this system is $u_r \rho_r A_r$, where u_r is the velocity of flow at the radius r where the surface area is A_r and the gas density is ρ_r . This product equals \dot{m} , the mass flowing through the layer at r per unit time, and must be constant for all values of r . Thus u_r varies with r , the distance from the center, in the manner shown in Fig. 7.

It is apparent from Fig. 7 that it is difficult to select a particular linear flow rate of unburned gas up to the flame and regard this velocity as the burning velocity.

If an attempt is made to define burning velocity strictly for such a system, it is found that no definition free from all possible objections can be formulated. Moreover, it is impossible to construct a definition which will, of necessity, lead to the same value being determined as that in an experiment using a plane flame. The essential difficulties are that over no range of r values does the linear velocity of the gas have even an approximately constant value and that, in this ideal system, the temperature varies continuously from the center of the sphere outwards and approaches the flame surface asymptotically as r approaches infinity. So no spherical surface can be considered to have a significance greater than any other.

In Fig. 7, u_x , the velocity of gas flow at x for a plane flame, is plotted on the same scale against x , the space coordinate measured normal to the flame front. It is assumed that over the main part of the rapid temperature rise u_r and u_x coincide. This correspondence is likely to be true if the curvature of the flame is large compared with the flame thickness. The burning velocity is then, strictly speaking, the value to which u_x approaches asymptotically as x approaches minus infinity. However, because the temperature of the unburned gas varies exponentially with x , the value of u_x becomes effectively

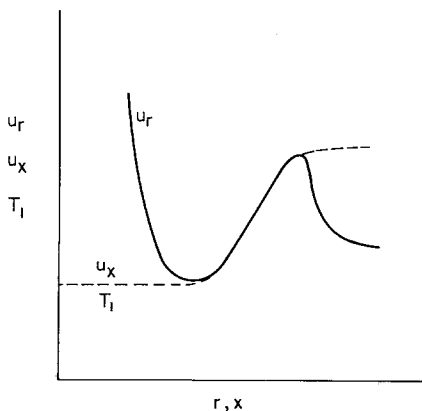


Fig. 7. Velocity and temperature variations through non-one-dimensional flame systems.

constant only a very short distance from the flame. The value of u_r on the low-temperature side of the spherical flame will not at any point be as small as the limiting value of u_x , which one calls the burning velocity. However, the value of u_r at the point where it is a minimum is likely for all ordinary flames (for which the flame zone is thin) to be very little more than the limiting value of u_x . In fact, the difference, although not zero, will probably be inappreciable for such flames. This value of u_r could be determined using the formula

$$u_r = \dot{m}/\rho_r A_r$$

Since the layer of interest is immediate on the unburned side of the flame, ρ_r will be close to ρ_u , the density of the unburned gas, and \dot{m}/ρ_r will be close to the volume flow rate of unburned gas.

So, to obtain, in practice, a value for burning velocity, which is close to that for the plane flame, it is necessary to locate and measure an area as far on the unburned side of the flame as possible. Systems such as Bunsen flames are in many ways more complicated than either the plane case or the spherical case.

Before proceeding, consider the methods of observation. The following methods have been most widely used to observe the flame:

- (a) The luminous part of the flame is observed and the side of this zone, which is toward the unburned gas, is used for measurement (direct photography).
- (b) A shadowgraph picture is taken.
- (c) A Schlieren picture is taken.
- (d) Interferometry (another less frequently used method).

Which surface in the flame does each method give? Again consider the temperature distribution through the flame as given in Fig. 8. The luminous zone comes late in the flame and, thus, is generally not satisfactory.

A shadowgraph picture measures the derivative of the density gradient ($\partial\rho/\partial x$) or $(-1/T^2)(\partial T/\partial x)$, i.e., it evaluates $\{\partial[(-1/T^2)(\partial T/\partial x)]/\partial x\} = (2/T^3)(\partial T/\partial x)^2 - (1/T^2)(\partial^2 T/\partial x^2)$. Shadowgraphs, thus, measure the earliest variational front and are not a precisely defined surface. Actually one could define two shadowgraph surfaces, one at the unburned side and one on the burned side. The inner term is much brighter than the outer value, since the absolute value for the expression above is greater when evaluated at T_0 than at T_f .

Schlieren photography gives $(\partial\rho/\partial x)$ or $(-1/T^2)(\partial T/\partial x)$, which has the greatest value about the inflection point of the temperature curve and which corresponds more closely to the ignition temperature. This surface lies quite early in the flame, is more readily definable than most images, and is recommended and preferred by many workers. Interferometry, which measures density or temperature directly, is much too sensitive and can be used

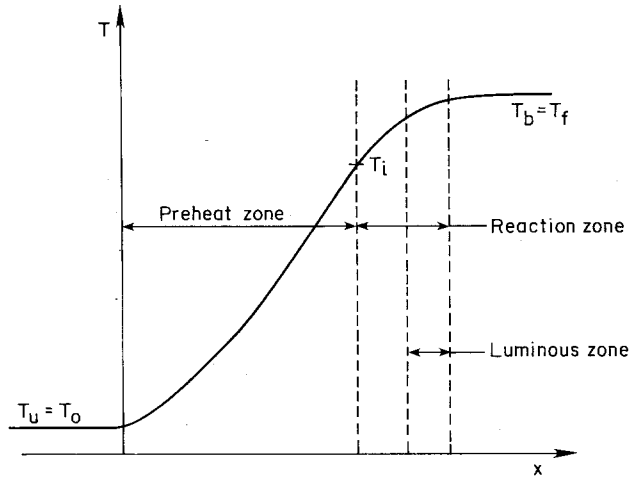


Fig. 8. Temperature regimes in a laminar flame.

only on two-dimensional flames. In an exaggerated picture of a Bunsen tube flame the surfaces would lie as shown in Fig. 9.

The various experimental configurations used for flame speeds may be classified under the following headings:

- (a) Conical stationary flames on cylindrical tubes and nozzles.
- (b) Flame in tubes.
- (c) Soap bubble method.
- (d) Constant volume explosion in spherical vessel.
- (e) Flat flame methods.

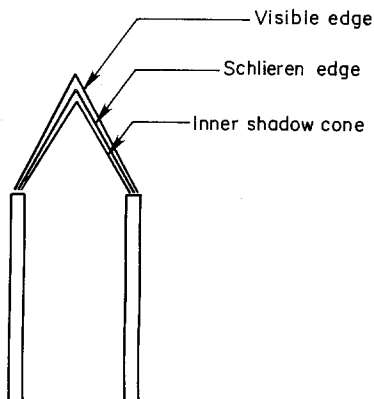


Fig. 9. Optical fronts in a Bunsen flame.

The methods are listed in order of decreasing complexity of flame surface and correspond to an increasing complexity of experimental arrangement. Each has certain advantages that bring about their usage.

a. Burner Method

In this method premixed gases flow up a cylindrical jacketed tube long enough to insure streamline flow at the mouth. The gas burns at the mouth of the tube and the shape of the Bunsen cone is recorded and measured by various means and in various ways. When shaped nozzles are used instead of long tubes, the flow is uniform instead of parabolic and the cone has straight edges. Because of the complicated flame surface, the different procedures used for measuring the flame cone have led to different results.

The burning velocity is not constant over the cone. The velocity near the tube wall is lower because of cooling by the walls. Thus, there are lower temperatures; therefore, lower reaction rates and, consequently, lower flame speeds. The top of the cone is crowded due to the presence of large energy release, and, therefore, reaction rates are too high.

It has been found that 30% of the internal portion of the cone gives a constant flame speed when related to the proper velocity vector and, thus, gives results comparable with other methods. Actually, if S_L is measured at each point one will see that it varies along every point for each velocity vector and that it is not really constant. This variation is the major disadvantage of the method.

The earliest procedure of calculating flame speed by this method was to divide the volume flow rate by the area of flame cone:

$$S_L = \frac{Q \text{ cm}^3/\text{sec}}{A \text{ cm}^2} = \text{cm/sec}$$

so that it is apparent then that the choice of cone will give widely different results. Experiments with fine magnesium oxide particles dispersed in the gas stream have shown that the flow streamlines remain relatively unaffected until the Schlieren cone and then diverge from the Burner axis before reaching the visible cone. These experiments have led many investigators to use the Schlieren cone as the most suitable one for flame speed evaluation.

The shadow cone is used by many experimenters because of the much greater simplicity than the Schlieren techniques. The shadow being on the cooler side certainly gives more correct results than the visible cone. The fact that the flame cone can act as a lens in shadow measurements causes uncertainties as to the proper cone size.

Some investigators have used the central portion of the cone only and used the volume flow through tube radii corresponding to this portion. The proper choice of cone is of concern here also.

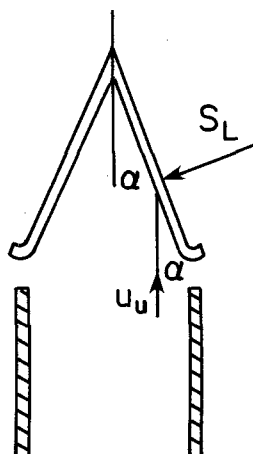


Fig. 10. Velocity vectors in a Bunsen cone.

The angle of cone slant makes with the burner axis can also be used to determine S_L (see Fig. 10). This angle should be measured only at the central portion of the cone. Thus $S_L = u_u \sin \alpha$.

Two of the disadvantages of the Burner methods are:

- (1) One can never completely eliminate wall effects.
- (2) One needs a steady source of supply of gas, which for rare or pure gases can be a severe problem.

The next three methods to be discussed make use of small amounts of gas.

b. Cylindrical Tube Method

A gas mixture in a horizontal tube opened at one end is ignited at the open end. The rate of progress of the flame into the unburned gas is the flame speed.

The difficulty with this method is that due to buoyancy effects the flame front is curved. Then the question arises as to which flame area to use.

The flame area is no longer a geometric image of the tube; if hemispherical, $S_L A_f = u_m \pi R^2$. Closer observation will also reveal quenching at the wall. Therefore, there is mixing of the unaffected center with an affected peripheral area.

Because a pressure wave is established by the burning (heating causing pressure change), the statement that gas ahead of flame is not affected by the flame is not correct. This pressure wave causes a velocity in the unburned gases and one must account for this movement. Therefore, since the flame is in a moving gas, one must subtract this velocity from the measured value. Friction effects downstream cause a greater pressure wave and, therefore,

length can have an effect. One can cap the end of the tube, drill a small hole in the cap and measure the efflux with a soap solution [13]. The rate of growth of the soap bubble is used to obtain the velocity exiting the tube and, thus, the velocity of unburned gas. A restriction at the open end minimizes effects due to the back flow of the expanding burned gases.

These adjustments permit relatively good values to be obtained, but still there are errors due to wall effects and distortion due to buoyancy. This buoyancy effect can be remedied by turning the tube vertically.

c. Soap Bubble Method

In an effort to eliminate wall effects, two spherical methods were developed. In the one to be discussed here, the gas mixture is contained in a soap bubble and ignited at the center by a spark so that a spherical flame spreads radially through the flame. Because the gas is enclosed in a soap film, the pressure remains constant. The growth of the flame front along a diameter is followed by some photographic means. Because, at any stage of the explosion, the burned gas behind the flame occupies a larger volume than it did as unburned gas, the fresh gas into which the flame is burning moves outwards. Then

$$S_L \times A \times \rho_0 = u_r \times A \times \rho_f$$

amount of material that must go into flame to increase volume

$$S_L = u_r(\rho_f/\rho_0)$$

The great disadvantage is the large uncertainty in the temperature ratio T_0/T_f necessary to obtain ρ_f/ρ_0 . Other disadvantages are

- (1) the method can only be used for fast flames to avoid the convective effect of hot gases, and
- (2) the method cannot work with dry mixtures.

d. Closed Spherical Bomb Method

The bomb method is quite similar to the bubble method except that the constant volume condition causes a variation in pressure. One must, therefore, follow the pressure simultaneously with the flame front.

Similar to the soap bubble method, because the adiabatic compression of the unburned gases must be measured in order to calculate the flame speed, only fast flames can be used. Also, the gas into which the flame is moving is always changing and consequently both the burning velocity and flame speed vary through the explosion. These features make the treatment complicated

and, to a considerable extent, uncertain. The following expression has been derived for the flame speed [14]:

$$S_L = \left[1 - \frac{R^3 - r^3}{3p\gamma_u r^2} \frac{dp}{dr} \right] \frac{dr}{dt}$$

where R is the sphere radius and r the radius of spherical flames at any moment. The fact that the second term in the brackets is close to one makes it difficult to attain high accuracy.

e. Flat Flame Burner Method

The flat flame burner method is usually attributed to Powling [15]. Because it offers the most simple flame front and one in which the area of shadow, Schlieren, and visible fronts are all the same, probably the most accurate.

Either by placing a porous metal disk or a series of small tubes of 1-mm diameter or less at the exit of the larger flow tube, one can create suitable conditions for flat flames. The flame is usually ignited with too high a flow rate and the flow or composition adjusted until the flame is flat. The diameter of the flame is then measured and the area divided into the volume flow rate of unburned gas. If the velocity emerging is greater than the flame speed, one obtains a cone due to the larger flame required. If velocity is too slow, the flame tends to flash back and is quenched. In order to accurately define the edges of the flame, an inert gas usually is flowed around the burners. By controlling the rate of efflux of burned gases with a grid, a more stable flame is obtained. This experimental apparatus would appear as shown in Fig. 11.

This method as originally developed by Powling was applicable only to mixtures having low burning velocities of the order of 15 cm/sec and less. At higher burning velocities, the flame front positions itself too far from the burner and takes a multiconical form.

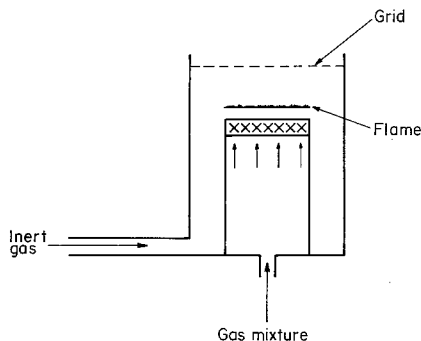


Fig. 11. Flat flame apparatus.

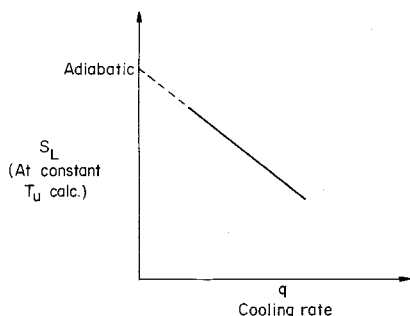


Fig. 12. Cooling effect in flat flame burners.

Spalding and Botha [16] extended the flame burner method to higher flame speeds by cooling the plug. The cooling draws the flame front closer to the plug and stabilizes it. Operationally, the procedure is as follows: a flow rate giving a velocity greater than the flame speed is set and the cooling controlled until a flat flame is obtained. For a given mixture ratio many cooling rates are used. A plot of flame speed versus cooling rate is made and is extrapolated to zero cooling rate (Fig. 12). At this point the adiabatic flame speed S_L is obtained. This procedure can be used for all mixture ratios within the flammability limits. The reason this procedure is preferable over the other methods is that the heat that is generated is leaking to the porous plug and not to the unburned gases as in the other model. Thus, there is quenching all along the plug and not just at the walls.

The temperature at which the flame speed is measured is calculated as follows. For the approach gas temperature one calculates what the initial temperature would have been if there were no heat extraction. Then the velocity of the mixture, which would give the measured mass flow rate at this temperature, is determined. This velocity is S_L at the calculated temperature. Detailed descriptions of various burned systems and techniques are to be found in Ref. [17].

5. Experimental Results—Physical and Chemical Effects

The Mallard–LeChatelier development for the laminar flame speed permits one to determine the general trends with pressure and temperature. When one approximates real hydrocarbon oxidation kinetics experimental results with an overall rate expression, the activation energy of the overall process is found to be quite high, of the order of 40 kcal/mole. Thus, the exponential in the flame speed equation is quite sensitive to variations in the flame temperature. This sensitivity is the dominant temperature effect on flame speed. There is, of course, an effect as well of temperature on the

diffusivity and generally the diffusivity is considered to vary with the temperature to the 1.75 power.

The pressure dependency of flame speed as developed from the thermal approaches was given by the expression.

$$S_L \sim P^{n-2}$$

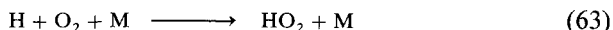
where n was the overall order of reaction. Thus, for second-order reactions the flame speed is essentially independent of pressure. In observing experimental measurements of flame speed as a function of pressure, one must determine whether the temperature was kept constant with inert dilution. As the pressure is increased, dissociation decreases and the temperature rises. This effect must be considered in the experiment. However for hydrocarbon-air systems the temperature varies little from atmospheric pressure and above due to a minimal amount of dissociation. There is a more pronounced temperature effect at subatmospheric pressures.

To a first approximation one could perhaps assume that hydrocarbon-air reactions are second order. Although it is impossible to develop a single overall rate expression for the complete experimental range of temperatures and pressures used by various investigators, values have been reported and hold for the limited experimental ranges of temperature and pressure from which the expression was derived. The overall reaction orders reported range from 1.5 to 2.0 and most results are around 1.75 [2,18]. Thus, it is not surprising that experimental results show a decline in flame speed with increasing pressure [2].

With the background developed in the detailed studies of hydrocarbon oxidation, it is possible to explain this pressure trend more thoroughly. Recall it was found that the key chain branching reaction in any hydrogen containing system was reaction (62) [Chapter 3, Reaction (15)],



Any process that reduces the H atom concentration and any reaction that competes with reaction (62) for H atoms will tend to reduce the overall oxidation rate; that is, it will inhibit combustion. As discussed in Chapter 3 [reaction (21)], reaction (63)



competes directly with reaction (62). Reaction (63) is third order and therefore much more pressure dependent than reaction (62). Consequently, as pressure is increased reaction (63) essentially inhibits the overall reaction and reduces the flame speed. Figure 13 reports the results of some analytical calculations of flame speeds in which detailed kinetics were included; the results obtained are quite consistent with recent measurements [2]. For

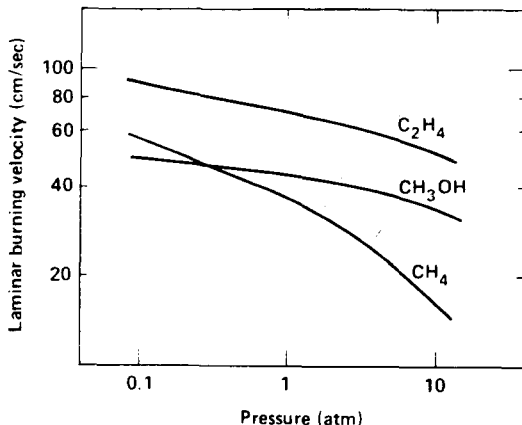


Fig. 13. Variation in laminar flame speeds with pressure for some stoichiometric fuel-air mixtures (after Westbrook and Dryer [2]).

pressures below atmospheric, there is only a very small decrease in flame speed as the pressure is increased and at higher pressures (1–5 atm) the decline in S_L with increasing pressure becomes more pronounced. The reason for this change of behavior is two fold. Below atmospheric pressure reaction (63) does not compete effectively with reaction (62) and any decrease due to this reaction is compensated by a rise in temperature. Above 1 atm reaction (63) competes very effectively with reaction (62), temperature variation with pressure in this range is slight, and thus a steeper decline in S_L with pressure is found. Since the kinetic and temperature trends with pressure exist for all hydrocarbons, the same pressure effect on S_L will exist for all such fuels.

The variation of flame speed with equivalence ratio follows the variation with temperature. Since, as discussed in Chapter 1, flame temperatures for hydrocarbon-air systems peak slightly on the fuel-rich side of stoichiometric, as do the flame speeds. In the case of hydrogen-air systems, since excess hydrogen increases the thermal diffusivity substantially, the maximum S_L falls well on the fuel-rich side of stoichiometric. Hydrogen gas with a maximum value of 325 cm/sec has the highest flame speed in air of any other fuel.

Reported flame speed results for most fuels vary somewhat with the measurement technique used. Most results however are internally consistent. Plotted in Fig. 14 are some typical flame speed results as a function of the stoichiometric mixture ratio. Detailed data are given in recent combustion symposia and in the extensive tabulations of Refs. [19–21]. The flame speed for many fuels in air have been summarized from these references and are listed in Appendix D. Since most paraffins, except methane, have approxi-

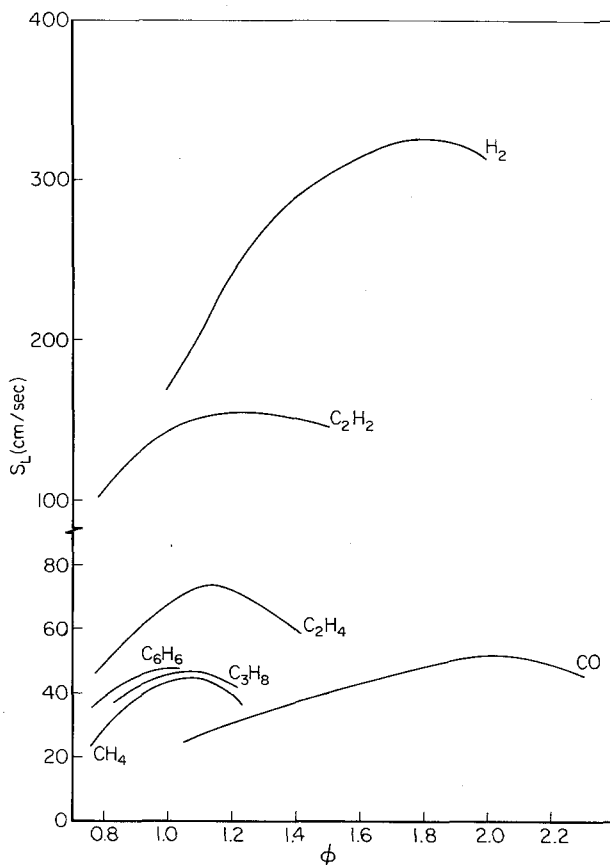


Fig. 14. Variation in laminar flame speeds with equivalence ratio for various fuel-air systems at standard conditions.

mately the same flame temperature in air, it is not surprising that their flame speeds are about the same (~ 45 cm/sec). Methane has a somewhat lower speed (~ 40 cm/sec). Attempts [19] have been made to correlate flame speed with hydrocarbon fuel structure and chain length, but these correlations appear to follow the general trends of temperature. Olefins, having the same C/H ratio, have the same flame temperature, except for ethene, which is slightly higher, and have flame speeds approximately 50 cm/sec. In this context ethene has a flame speed of approximately 75 cm/sec. Due to its high flame temperature acetylene has a maximum flame speed of about 160 cm/sec.

The variation of flame speed with oxygen concentration poses further considerations of the factors that govern the flame speed. Shown in Fig. 15 is

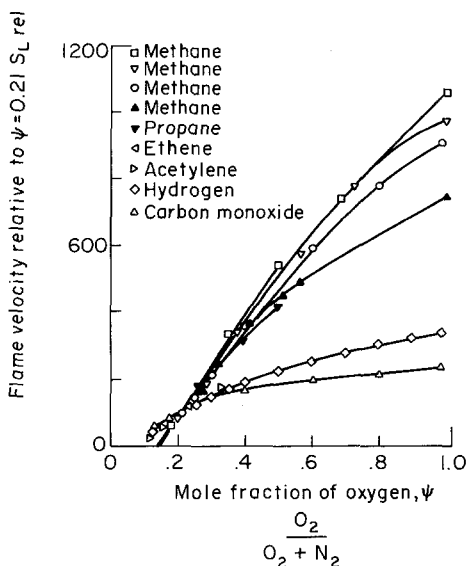


Fig. 15. Relative effect of oxygen concentration on flame speed for various fuel-air systems at standard conditions (after Zebatakis [20]).

the flame speed of a fuel in various oxygen–nitrogen mixtures relative to its value in air. One will note a 10-fold increase for methane between pure oxygen and air, 7.5-fold increase for propane, a 3.4-fold increase for hydrogen, and a 2.4-fold increase for carbon monoxide. From the effect of temperature on the overall rates and diffusivities, one would expect about a 5-fold increase for all these fuels. Since the CO results contain a fixed amount of hydrogen additives [19], the fact that the important OH radical concentration does not increase as much as one would expect is a factor for the lower rise. Perhaps for general considerations the hydrogen values are near enough to a general estimate. Indeed there is probably a sufficient radical pool at all oxygen concentrations. For the hydrocarbons, undoubtedly the radical pool concentration increases substantially as one goes to pure oxygen for two reasons—increased temperature and no nitrogen dilution. Thus applying the same general rate expression for air and oxygen just does not suffice.

The maximum flame speed for hydrocarbon–pure oxygen systems increases with pressure [20] rather than decreases as was found for air. For pure oxygen systems, the temperature effect must override the competition between reactions (62) and (63).

The effect of the initial temperature of a premixed fuel–air mixture on the flame propagation rate again appears to be reflected through the final flame temperature. Since the chemical energy release is always so much greater

than the sensible energy of the reactants, small changes of initial temperature generally have little effect on the flame temperature. Nevertheless, the flame propagation expression contains the flame temperature in an exponential term; thus, as discussed many times previously, small changes in flame temperature can give noticeable changes in flame propagation rates. If the initial temperatures are substantially higher than normal ambient, then reaction (63) can be affected in the preheat zone. Since reaction (63) is one of recombination, its rate decreases with increasing temperature and thus the flame speed will be attenuated even further.

Perhaps the most interesting set of experiments to elucidate the dominant factors in flame propagation was performed by Clingman *et al.* [22]. Their results clearly shown the effect of the thermal diffusivity and reaction rate terms. These investigators measured the flame propagation rate of methane in various oxygen-inert gas mixtures. The mixtures of oxygen to inert gas were 0.21/0.79 on a volumetric basis, the same as that which exists for air. The inerts chosen were nitrogen (N_2), helium (He), and argon (Ar). The results of these experiments are shown in Fig. 16.

The trends of the results in Fig. 16 can be readily explained. Argon and nitrogen have thermal diffusivities that are approximately equal. However, Ar is a monoatomic gas that has a specific heat lower than N_2 . Since the heat release in all systems is the same, the final (or flame) temperature will be higher in the Ar mixture than in the N_2 mixture. Thus, S_L will be higher for Ar than N_2 . Argon and helium are both monoatomic and thus their final temperatures are equal. However, the thermal diffusivity of He is much greater than that of Ar. Helium has a higher thermal conductivity and a much lower density than argon. Consequently, S_L for He is much greater than that for Ar.

The effect of chemical additives on the flame speed has also been explored extensively. Leason [23] has reported the effects on flame velocity of small

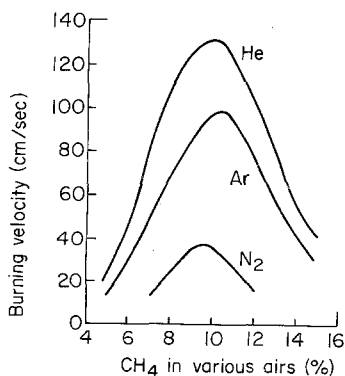


Fig. 16. Methane flame velocities in various airs (after Clingman *et al.*, [22]).

concentrations of additives (<3%) and other fuels. He studied the propane-air flame. Considered were compounds such as acetone, acetaldehyde, benzaldehyde, diethyl ether, benzene, and carbon disulfide, and many others were chosen from those classes of compounds that were oxidation intermediates in low-temperature studies and, hence, were expected to decrease the induction period and, thus, increase the flame velocity. Despite differences in apparent oxidation properties, all compounds changed the flame velocity in exactly the same way that dilution with excess fuel would on the basis of oxygen requirement. These results support the contention that the laminar flame speed is controlled by the high-temperature reaction region. The high temperatures generate more than ample radicals via chain branching so that it is not likely that any additive could contribute any reaction rate accelerating feature.

There is, of course, a chemical effect in carbon monoxide flames. This point was mentioned in the discussion of carbon monoxide explosion limits. Studies have shown that CO flame velocities increase appreciably when small amounts of hydrogen, hydrogen containing fuels, or water are added. For 45% CO in air, the flame velocity passes through a maximum after approximately 5% by volume of water has been added. At this point the flame velocity is 2.1 times the value with 0.7% H₂O added. After 5%, a dilution effect begins to cause a decrease in flame speed. The effect and the maximum arise due to the necessity of establishing a sufficient steady-state concentration of OH radicals for the most effective explosive condition.

Although it may be expected that the common antiknock compounds would decrease the flame speed, no effects of antiknocks have been found in constant pressure combustion. The effect of the inhibition of the preignition reaction on flame speed is of negligible consequence. Although there is not universal agreement as to the mechanism of antiknock, many believe they serve to decrease the radical concentrations by absorption on particle surfaces. The reduction of the radical concentration in the preignition reactions or near the flammability limits can have severe consequences on the ability to initiate combustion. In these cases the radical concentrations are such that the chain branching factor is very close to the critical value for explosion. Any reduction could prevent the explosive condition from being reached. Around the stoichiometric mixture ratio the radical concentrations are normally so great that it would appear most difficult to add any small amounts of additives that would capture sufficient amounts of radicals to alter the reaction rate and the flame speed.

Certain halogen compounds such as the Freons are known to alter the flammability limits of hydrocarbon-air mixtures. The accepted mechanism is that the halogen atoms trap hydrogen radicals necessary for the chain branching step. Near the flammability limits, conditions exist in which the

radical concentrations are such that α is just above α_{crit} . Any reduction in radicals and the chain branching effects these radicals may have could eliminate the explosive (fast reaction rate and larger energy release rate) regime. However, small amounts of halogen compounds do not seem to affect the flame speed in a large region around the stoichiometric mixture ratio. The reason is, again, that in this region the temperatures are so high and radicals so abundant that elimination of some radicals does not affect the reaction rate.

It has been found that some of the larger halons (the generic name for the halogenated compounds sold under commercial names such as the Freons) are effective as flame suppressants. Also, some investigators have found that inert powders are effective in fire fighting. Fundamental experiments to evaluate the effectiveness of the halons and powders have been performed with various types of apparatus that measure the laminar flame speed. Results have been reported that the halons and the powders reduce flame speeds even around the stoichiometric air-fuel ratio. The investigators performing these experiments have argued that those agents are effective by reducing the radical concentrations. However, this explanation could be questioned. The quantities of these agents added are great enough that they could absorb sufficient amounts of heat to reduce the temperature and thus the flame speed. Both halons and powders have large total heat capacities.

D. STABILITY LIMITS OF LAMINAR FLAMES

There are two types of stability criteria associated with laminar flames. The first is concerned with the ability of the combustible fuel-oxidizer mixture to support flame propagation and is strongly related to the chemical rates in the system. A point can be reached for a given limit mixture ratio in which the rate of reaction and its subsequent heat release are not sufficient to sustain reaction and, thus, propagation. This type of stability limit includes (1) flammability limits in which gas-phase losses of heat from limit mixtures reduce the temperature, rate of heat release and the heat feed back, and do not permit the flame to propagate and (2) quenching distances in which the loss of heat to a wall and radical quenching at the wall reduce the reaction rate to a point when it cannot sustain a flame in a confined situation such as propagation in a tube.

The other type of stability limit is associated with the mixture flow and its relationship to the laminar flame itself. This stability limit includes the phenomena of flashback, blow off, and the onset of turbulence and describes the limitations of stabilizing a laminar flame in a real experimental situation.

1. Flammability Limits

Explosion limit curves presented earlier and most of which appear in the open literature are for a definite fuel-oxidizer mixture ratio, usually stoichiometric. For the stoichiometric case, if an ignition source were introduced into the mixture even at a very low temperature and at reasonable pressures, such as around atmospheric, the gases about the ignition source reach a sufficient temperature so that the local mixture moves into the explosive region and a flame propagates. This flame, of course, continues to propagate even after the ignition source is removed. There are mixture ratios, however, that will not self-support the flame after the ignition source is removed. These mixture ratios fall at the lean and rich end of the concentration spectrum. The leanest and richest concentrations, which will just self-support a flame, are called the lean and rich flammability limit, respectively. Essentially what determines the flammability limit is a competition between the rate of heat generation, which is controlled by the rate of reaction and the heat of reaction for the limit mixture rates, and the external rate of heat loss by the flame. In the literature one will find flammability limits in both air and oxygen. The lean limit rarely differs for air or oxygen, as the excess oxygen in the lean condition has the same thermophysical properties as nitrogen.

There have been attempts to standardize the determination of inflammability limits. Coward and Jones [24] recommended that a 2-in. glass tube be employed, which should be about 4-ft long and ignited by a spark a few millimeters long or by a small naked flame. The high-energy starting conditions are such that weak mixtures will be sure to ignite. The large tube diameter is selected because the most consistent results are obtained with tubes of this diameter. Quenching effects may interfere in tubes of small diameter. Large diameters create some disadvantages since the quantity of gas is a hazard and the possibility of cool flames exists. The 4-ft length is chosen in order to allow an observer to truly judge whether the flame will propagate indefinitely or not.

It is important to specify the direction of flame propagation. Since it may be assumed as an approximation that a flame cannot propagate downward in a mixture contained within a vertical tube if the convection current it produces is faster than the speed of the flame, the limits for upward propagation are usually slightly wider than for downward propagation or if the containing tube were in a horizontal position.

Table 1 lists some upper and lower inflammability limits (in air) taken from Refs. [19] and [20] for some typical combustible compounds. Data for other fuels are given in Appendix E.

In view of the accelerating effect of temperature on chemical reactions, it is reasonable to expect that limits of inflammability should be broadened if the

TABLE 1

Flammability limits of some fuels in air-fuel, volume percent

	Lower (lean)	Upper (rich)	Stoichiometric
Methane	5	15	9.47
Heptane	1	6.7	1.87
Hydrogen	4	75	29.2
Carbon Monoxide	12.5	74.2	29.5
Acetaldehyde	4.0	60	7.7
Acetylene	2.5	100	7.7
Carbon disulfide	1.3	50	—
Ethylene oxide	3.6	100	—

temperature is increased. This trend is confirmed experimentally. The increase is only slight and it appears to give a linear variation for hydrocarbons.

As noted from the data in Appendix E, the upper limit is about three times stoichiometric and the lower limit is about 50% of stoichiometric. Generally the upper limit is higher than that for detonation. The lower (lean) limit of a gas is the same in oxygen as in air due to the fact that the excess oxygen has the same heat capacity as if it were nitrogen. The higher (rich) limit of all flammable gases is much greater in oxygen than in air, due to higher temperature, which comes about from the absence of any nitrogen. Hence, the range of flammability is always greater in oxygen. Table 2 shows this effect.

TABLE 2

Comparison of oxygen and air flammability limits, fuel volume percent

	Lean		Rich	
	Air	O ₂	Air	O ₂
H ₂	4	4	75	94
CO	12	16	74	94
NH ₃	15	15	28	79
CH ₄	5	5	15	61
C ₃ H ₈	2	2	10	55

As increasing amounts of an incombustible gas or vapor are added to the atmosphere, the flammability limits of a gaseous fuel in the atmosphere approach one another and finally meet. Inert diluents such as CO_2 , N_2 , or Ar merely replace part of the O_2 in the mixture, but they do not have the same extinction power. It is found that the order of efficiency is of the same order of the heat capacities of these three gases:

$$\text{CO}_2 > \text{N}_2 > \text{Ar (or He)}$$

For example, the minimum percent oxygen that will permit flame propagation in mixtures of CH_4 , O_2 , and CO_2 is 14.6%; if N_2 were the diluent, the minimum percent oxygen is less and equals 12.1%. In the case of Ar, the value is 9.8%. As discussed, a higher specific heat gas present in sufficient quantities will reduce the final temperature, and in this sense reduces the rate of energy release that must sustain the rate of propagation over other losses.

It is interesting to examine in more detail the effect of additives as shown in Fig. 17 [20]. As discussed, the general effect of the nonhalogenated additives

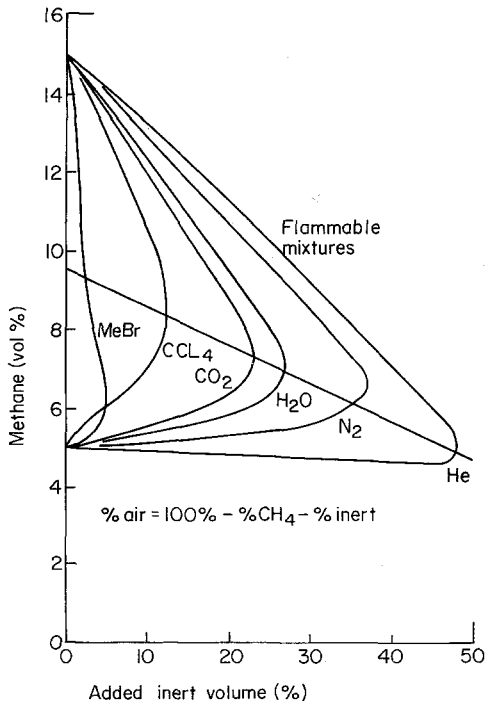
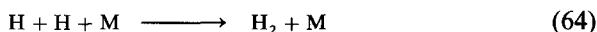


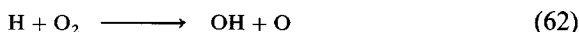
Fig. 17. Limits of flammability of various methane-inert gas-air mixtures at standard conditions (after Zebatakis [20]).

follows the variation in the molar specific heat; that is, the greater the specific heat of an inert additive, the greater the effectiveness. Again, this effect is strictly one of lowering the temperature to a greater extent and was verified as well by flammability measurements in air where the nitrogen was replaced by carbon dioxide and argon. Figure 17 however represents the condition in which additional species were added to the air in the fuel-air mixture. As noted in Fig. 17 rich limits are more sensitive to inert diluents than lean limits; however, species such as halogenated compounds affect both limits and this effect is one greater than that expected from heat capacity alone. Helium additions extends the lean limit somewhat due to the increase in the thermal diffusivity and, thus, the flame speed.

That the rich limit is affected by additives more than the lean limit can be explained by the important competing steps for possible chain branching. In the case where the system is rich [Chapter 3, reaction (23)]

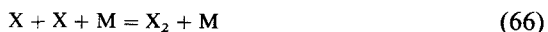


competes with [Chapter 3, reaction (15)]

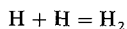


The recombination [reaction (64)] increases with decreasing temperature and increasing concentration of the third body M. Thus, the more diluent added the faster this reaction is compared to the chain branching step [reaction (62)]. This aspect is also reflected in the overall activation energy found for rich systems compared to lean systems. Rich systems have a much higher overall activation energy and therefore a greater temperature sensitivity.

The effect of all halogen compounds on flammability limits is substantial. The addition of only a few percent can make some systems nonflammable. These observed results support the premise that effect of the addition of halogens is not one of dilution alone, but one in which the halogens act as a catalyst in reducing the H atom concentration in the system necessary for the chain branching reaction scheme. Any halogen added either as the element, hydrogen halide, or bound in an organic compound will act in the same manner. Halogenated hydrocarbons have weak carbon-halogen bonds that are readily broken in flames of any respectable temperature and place the halogen atom in the reacting system. This halogen atom rapidly abstracts a hydrogen from the hydrocarbon fuel to form the hydrogen halide and the following reaction system, in which X represents any of the halogens F, Cl, Br, or I, occurs



Reactions (65)-(67) total overall to



and thus it is seen that X is a homogeneous catalyst for recombination of the important H atoms. What is important in the present context is that the halide reactions above are fast compared to the other important H atom reactions such as



or

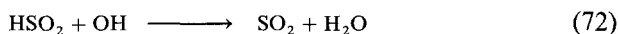


This competition for H atoms reduces the rate of chain branching in the important $\text{H} + \text{O}_2$ reaction. The real key to this type of inhibition is the regeneration of X_2 , which permits the entire cycle to be catalytic.

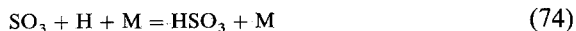
Because it essentially removes O atoms catalytically by the mechanism,



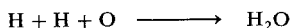
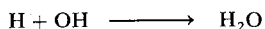
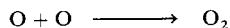
and also by H radical removal by the system



and by



SO_2 is similarly a known inhibitor that affects flammability limits. The above catalytic cycles [reactions (69)-(70), reactions (71)-(72), reactions (73)-(75)] are equivalent to



The behavior of the limits at elevated pressures can be explained somewhat satisfactorily. For simple hydrocarbons (ethane, propane, . . . , pentane), it appears that the rich limits extend almost linearly with increasing pressure at a rate of about 0.13 vol. %/atm.; the lean limits, on the other hand, are at first extended slightly and are thereafter narrowed as pressure is increased to 6 atm. In all, the lean limit is not affected appreciably by the pressure. Figure 18 for natural gas in air shows the pressure effect for conditions above atmospheric.

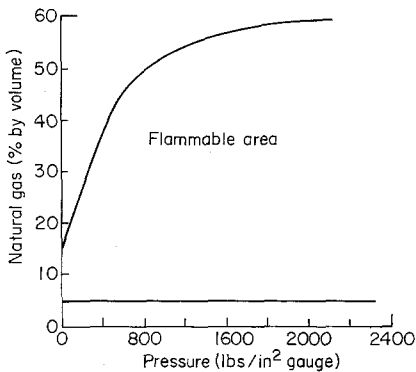


Fig. 18. Effect of pressure increase above atmospheric pressure on flammability limits of natural gas-air mixtures (from Lewis and von Elbe [5]).

For flammability limits at reduced pressures, most of the older work indicated that the rich and lean limits converge as the pressure is reduced until a pressure is reached below which no flame will propagate. However, this behavior appears to be due to wall quenching by the tube in which the experiments were performed. As shown in Fig. 19, the limits are actually as wide at low pressure as at 1 atm, provided the tube is sufficiently wide and provided an ignition source can be found to ignite the mixtures. Consequently the limits obtained at reduced pressures are not generally true limits of flammability, since they are influenced by the tube diameter and are, therefore, not physicochemical constants of a given fuel. These low-pressure limits might better be termed limits of flame propagation in a tube of specified diameter.

As stated earlier, what determines the flammability limit is a critical value of the rate of heat loss to the rate of heat development by chemical reaction. Consider, for example, a flame anchored on a Bunsen tube. The loss to the

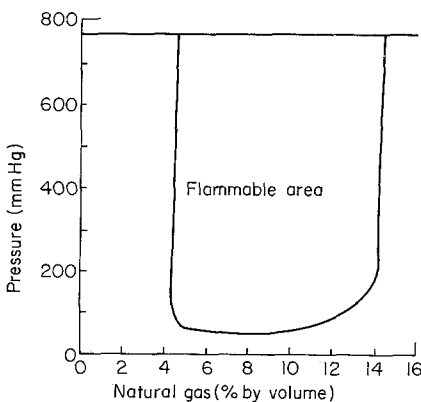


Fig. 19. Effect of reduction of pressure below atmospheric pressure on flammability limits of natural gas-air mixtures (from Lewis and von Elbe [5]).

anchoring position is small and, thus, the radiative loss from the flame gases must be the major heat loss condition. This radiative loss is in the infrared due primarily to the bond radiation of CO_2 , H_2O , and CO . The amount of dissociation at the flammability limits is indeed small so there is essentially no increase in temperature with increase in pressure. The radiant heat loss in a vibrational spectral band system varies as T^5 . This variation should be compared with the rate of reaction variation with temperature, which is $e^{-E/RT}$. But for most hydrocarbon systems the activation energy and temperature range are such that $e^{-E/RT}$, as a function of temperature, is very much like a variation T^5 [25]. However the radiation equation contains an emissivity term and the emissivity is approximately proportional to the total pressure for gaseous systems. So as one raises the pressure the emissivity and heat loss increase linearly. On the lean side the system is effectively first order due to the large excess of air, the overall reaction rate then varies essentially as pressure to the first power, and thus the rate of heat loss and rate of heat development increase the same for a variation in pressure; therefore, there is no change in the lean flammability limit with pressure. On the fuel-rich side the reaction rate is second order and, thus, increases faster than the heat loss and one can increase the richness of the system before there is extinction [25].

2. Quenching Distance

Wall quenching not only affects flammability limits, but also plays a role in ignition phenomena, which will be discussed in Chapter 7. The quenching diameter, which is the parameter given the greatest consideration and the symbol d_T , is generally determined experimentally in the following manner. A premixed flame is established on a burner port and the gas flow is suddenly stopped. If the flame propagates down the tube into the gas supply source, a smaller tube is substituted. The tube diameter is decreased until the flame cannot propagate back to the source. The diameter of the tube, which just prevents flashback, is the quenching distance or diameter d_T .

A flame is quenched in a tube by affecting the two mechanisms that permit flame propagation, i.e., diffusion of species and of heat. Tube walls extract heat, the smaller the tube the greater the surface area to volume ratio within the tube and thus the greater volumetric heat loss. Similarly, the smaller the tube, the greater the number of collisions of the active radical species that are destroyed. Since the condition and the material of construction of the tube wall affect the rate of destruction of the active species [5], a specific analytical determination of the quenching distance is not feasible.

Intuition would suggest that there would be an inverse correlation between flame speed and quenching diameter. Since S_L varies with equivalence ratio

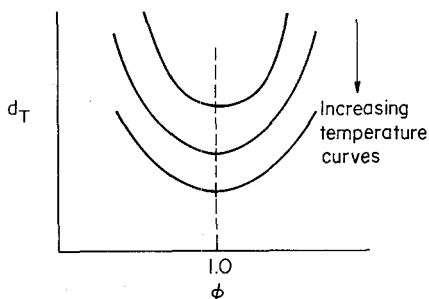


Fig. 20. Variation of quenching diameter as a function of equivalence ratio and various initial temperatures.

ϕ , so should d_T vary with ϕ ; however, the curve of d_T would be inverted compared to S_L , as shown in Fig. 20.

One would also expect, and it is found experimentally, that increasing the temperature would decrease the quenching distance. This trend arises because the heat losses are reduced and species are not as readily deactivated. Sufficient data are not available to develop any specific correlation, but trend of d_T with temperature would be as depicted in Fig. 20 as well.

It has been concretely established and derived theoretically [25] that quenching distance increases as pressure decreases; in fact the correlation is almost exactly

$$d_T \sim 1/P$$

for many compounds. For various fuels, P sometimes has an exponent somewhat less than one. An exponent close to one in the above relationship can be explained with the following reasoning. The mean fuel path of gases increases as pressure decreases, thus there are more collisions with the walls and more species are deactivated. Pressure results are generally represented in the form given in Fig. 21, which also establishes that when measuring flammability limits as a function of subatmospheric pressures, the tube diameter must be chosen so that it is greater than the d_T given for the

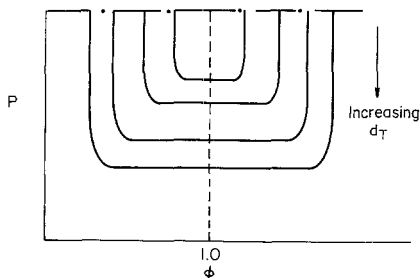


Fig. 21. Effect of pressure on quenching diameter.

pressure. The horizontal dot-dash in Fig. 21 specifies the various flammability limits that would be obtained at a given subatmospheric pressure in tubes of different diameters.

3. Flame Stabilization (Low Velocity)

In the introduction to this chapter a combustion wave was considered to be propagating in a tube. When the cold premixed gases flow in a direction opposite to the wave propagation and at a velocity equal to the propagation velocity, i.e., the laminar flame speed, the wave (flame) becomes stationary with respect to the containing tube. Such a flame would only possess neutral stability and its actual position would drift [1]. If the velocity of the unburned mixture is increased the flame will leave the tube and in most cases fix itself in some form at the tube exit. If the tube were considered to be in a vertical position, then one realizes that a simple burner configuration, as shown in Fig. 3, is obtained. In essence, such burners stabilize the flame. As described earlier these burners are so configured that the fuel and air become a homogeneous mixture before they exit the tube. The length of the tube and physical characteristics of the system are such that the gas flow is laminar in nature. In the context to be discussed here a most important aspect of the burner is that it acts as a heat and radical sink, which under many conditions stabilizes the flame at its exit. As will be described in detail later, it is the burner rim and the area close to the tube wave that provides the stabilization position.

When the flow velocity is increased to a value greater than the flame speed, the general shape of the flame becomes conical. The greater the flow velocity, the smaller is the cone angle of the flame. This angle decreases so that the velocity component of the flow normal to the flame is equal to the flame speed. However near the burner rim, the flow velocity is lower than that in the center of the tube, at some point in this area the flame speed and flow velocity become equal and the flame is anchored by this point. The flame is quite close to the burner rim and its actual speed is controlled by heat and radical loss to the wall. As the flow velocity is increased, the flame edge moves further from the burner, there is less losses to the rim, the flame speed increases and another stabilization point is reached. When the flow is such that the flame edge moves far from the rim, outside air is entrained, the mixture is diluted, the flame speed drops, and the flame reaches its blowoff limit.

If the flow velocity is gradually reduced, a condition is reached in this burner configuration where the flame speed is greater than the flow velocity at some point across the burner. Under this condition the flame will propagate down into the burner and the so-called flashback limit is reached. Somewhat before the flashback limit is reached, tilted flames may occur. This

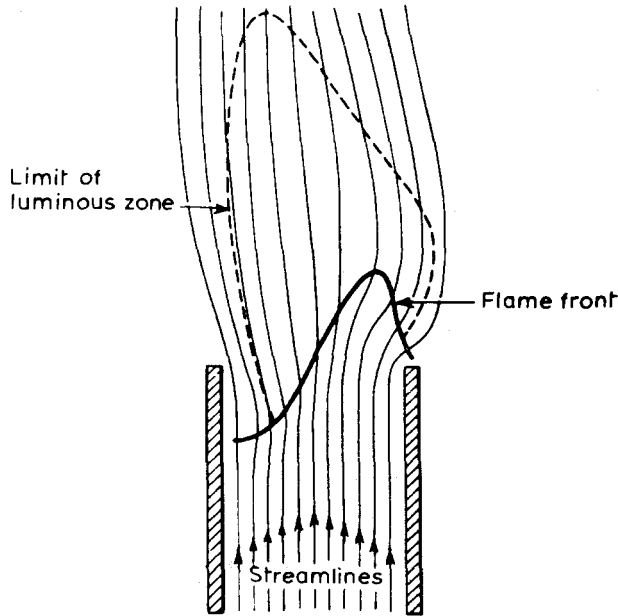


Fig. 22. Formation of a tilted flame (after Bradley [1]).

situation occurs because the back pressure of the flame causes a disturbance in the flow and only in the region where the flow velocity is reduced does the flame enter the burner. Because of the constraint provided by the burner tube, the flow there is less prone to distortion so that further propagation is prevented and a tilted flame such as that shown in Fig. 22 is established [1].

Thus it is seen that the laminar flame is stabilized on burners only within certain flow velocity limits. The following subsections treat the physical picture given above in more detail.

a. Flashback and Blowoff

Assume Poiseuille flow in the burner tube. The gas velocity is zero at the stream boundary (wall) and increases to a maximum in the center of the stream. The linear dimensions of the wall region of interest are usually very small. In slow-burning mixtures such as methane and air, they are of the order of 1 mm. Since usually the burner tube diameter is large in comparison, as shown in Fig. 23, the gas velocity near the wall can be represented by an approximately linear vector profile. Figure 24 represents the conditions in the area where the flame is anchored by the burner rim. It is further assumed that the flow lines of the fuel jet are parallel to the tube axis, that a combustion

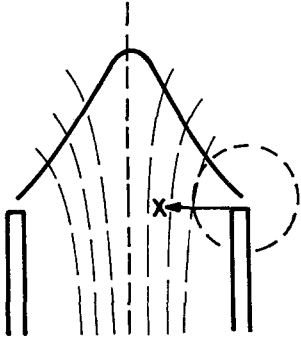


Fig. 23. Streamlines through a Bunsen cone flame.

wave is formed in the stream, and that the fringe of the wave approaches the burner rim closely. Along the flame wave profile the burning velocity attains its maximum values S_L^0 . Toward the fringe the burning velocity decreases as heat and chain carriers are lost to the rim. If the wave fringe is very close to the rim (position 1 in Fig. 24), the burning velocity in any flow line is smaller than the gas velocity, and the wave is driven back by the gas flow. As the distance from the rim increases as described, the loss of heat and chain carriers decrease and the burning velocity becomes larger. Eventually, a position is reached (position 2 in Fig. 24) in which at some point of the wave profile the burning velocity is equal to the gas velocity. The wave is now in equilibrium with respect to the solid rim. If the wave is displaced to a larger distance (position 3 in Fig. 24), the burning velocity at the indicated point becomes larger than the gas velocity and the wave moves back to the equilibrium position.

Consider a graph of flame velocity S_L , as a function of distance, for a wave inside a tube (Fig. 25). The consideration is then that the flame has entered the tube. The distance from the burner wall is called the penetration distance (half the quenching diameter d_T). If \bar{u}_1 is the mean velocity of the gas flow in the tube and the line labeled \bar{u}_1 is the graph of the velocity near the tube wall,

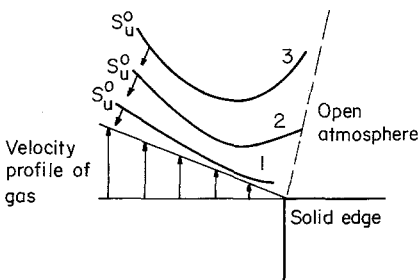


Fig. 24. Stabilization position of a Bunsen flame (after Lewis and von Elbe [5]).

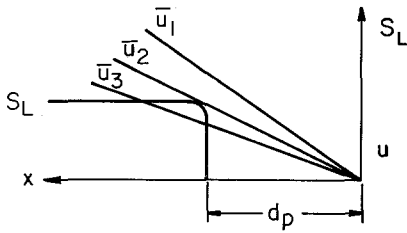


Fig. 25. Burning velocity and gas velocity inside a Bunsen tube (after Lewis and von Elbe [5]).

then there is no place where the local flame velocity is greater than the local gas velocity; therefore, any flame that finds itself inside the tube will then blow out of the tube. Then \bar{u}_2 is the minimum mean velocity before flashback occurs. The line for the mean velocity \bar{u}_3 indicates a region in which the flame does flashback.

The gradient for flashback, g_F , is S_L/d_p . Analytical developments [25] show that

$$d_p \approx (\lambda/c_p \rho)(1/S_L)$$

Similar reasoning can apply to blowoff, but the arguments are somewhat different and less exact because nothing similar to a boundary layer exists. However, a free boundary does exist.

When the gas flow in the tube is increased, the equilibrium position shifts away from the rim. It is noted that with increasing distance from the rim the gas mixture becomes progressively diluted by interdiffusion with the surrounding atmosphere, and the burning velocity in the outermost stream lines decreases correspondingly. This effect is indicated by the increasing retraction of the wave fringe for flame positions 1 to 3 in Fig. 26. But, as the wave moves further from the rim it loses less heat and radicals to the rim so it can extend closer to the hypothetical edge. However, an ultimate equilibrium position of the wave exists beyond which the effect everywhere on the burning

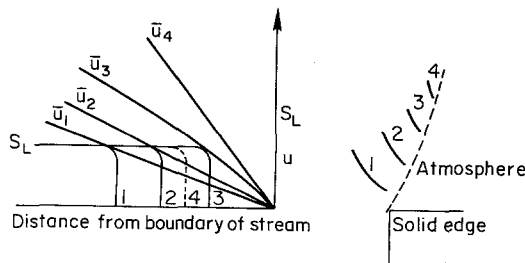


Fig. 26. Burning velocity and gas velocity above a Bunsen tube rim (after Lewis and von Elbe [5]).

velocity of increased distance from the burner rim is overbalanced by the effect of dilution. If the boundary layer velocity gradient is so large that the combustion wave is driven beyond this position, the gas velocity exceeds the burning velocity in every streamline and the combustion wave blows off. These trends are represented diagrammatically in Fig. 26.

The diagram follows the postulated trends in which S_L^0 is the flame velocity after the gas has been diluted due to the flame front having moved slightly past \bar{u}_3 . Thus, there is blowoff and \bar{u}_3 is the blowoff velocity.

b. Analysis and Results

Since the topic of concern is the stability of laminar flames fixed to burner tubes, the flow profile of the premixed gases flowing up the tube must be parabolic; that is, Poiseuille flow exists. The gas velocity along any streamline is given then by

$$u = n(R^2 - r^2)$$

where R is the tube radius. Since the volumetric flow rate, Q (cm³/sec) is given by

$$Q = \int_0^R 2\pi r u \, dr$$

then n must equal

$$n = 2Q/\pi R^4$$

The gradient for blow off or flashback is defined as

$$g_{F,B} \equiv - \lim_{r \rightarrow R} (du/dr)$$

then

$$g_{F,B} = \frac{4Q}{\pi R^3} = 4 \frac{\bar{u}_{av}}{R} = 8 \frac{\bar{u}_{av}}{d}$$

where d is the diameter of the tube.

Most experimental data on flashback were plotted as a function of the average flashback velocity, $u_{av,F}$, as shown in Fig. 27. It is possible to estimate penetration distance (quenching thickness) from the burner wall in figures such as Fig. 27 by observing the cut-off radius for each mixture.

The development for the gradients of flashback and blowoff suggests a more appropriate plot of g versus ϕ , as shown in Figs. 28 and 29. Examination of these figures reveals that the blowoff curve is much steeper than that

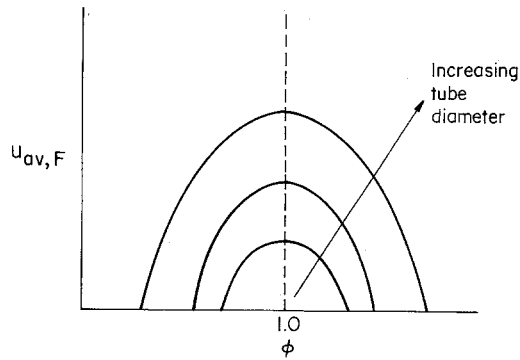


Fig. 27. Critical flow for flashback as a function of equivalence ratio.

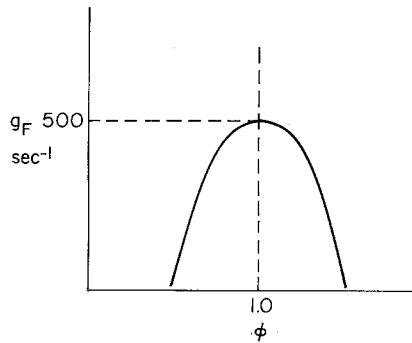


Fig. 28. Typical curve of the gradient of flashback as a function of equivalence ratio. The value at $\phi = 1$ is for natural gas.

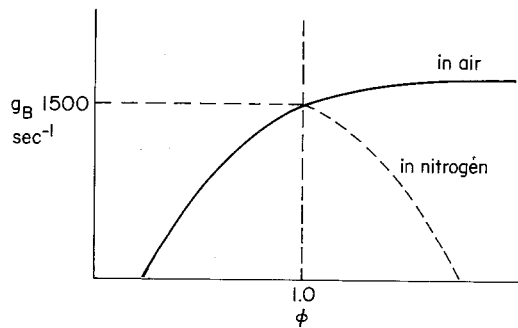


Fig. 29. Typical curves of the gradient of blowoff as a function of equivalence ratio. The value at $\phi = 1$ is for natural gas.

for flashback. For rich mixtures the blowoff curves continue to rise instead of decreasing after the stoichiometric value is reached. The reason for this trend is that experiments are performed in air, and the diffusion of air into the mixture as the flame lifts off the burner wall increases the local flame speed of the initially fuel-rich mixture. Experiments in which the surrounding atmosphere was not air, but nitrogen, verify this explanation and show that the g_B would peak at stoichiometric.

The characteristics of the lifted flame are worthy of note as well and there are limits similar to the seated flame [1]. When a flame is in the lifted position and then the gas velocity is reduced, the so-called dropback takes place and the flame takes up its normal position on the burner rim. When instead the gas velocity is increased, a condition is reached in which the flame will blowout. The instability requirements of both the seated and lifted flames are shown in Fig. 30.

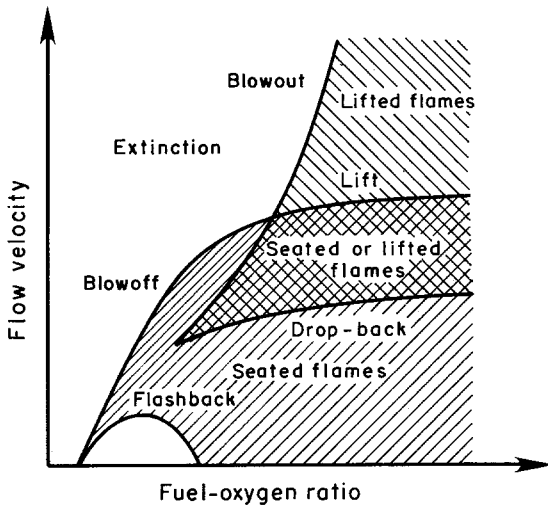


Fig. 30. Seated and lifted flame regimes for Bunsen type burners.

4. Stability Limits and Design

The practicality of understanding the stability limits is uniquely obvious when one considers the design of Bunsen tubes and cooking stoves using gaseous fuels.

In the design of a Bunsen burner, it is desirable to have the maximum range of volumetric flow without encountering stability problems. The question arises as to what is the optimum size tube for maximum flexibility. First, the tube must be at least twice the penetration distance, that is greater than the quenching distance. Secondly, the average velocity must be at least twice S_L or a precise Bunsen cone would not form. Experimental evidence shows further that if the average velocity is five times S_L , the fuel penetrates the Bunsen cone tip. If the Reynold's number of the combustible gases in the tube exceeds 2000, the flow can become turbulent and the laminar characteristics of the flame destroyed. Of course, there are the limitations of the gradients of flashback and blowoff. If one plots u_{av} versus d for these various limitations, a plot such as that shown in Fig. 31 is obtained. In this figure the dotted region is that in which one has the greatest flow variability without some stabilization problem, and it is interesting to note that this region is about $d = 1$ cm; consequently the tube diameter of Bunsen burners is always about 1 cm.

The burners on cooking stoves are very much like Bunsen tubes. The fuel induces air and the two premix prior to reaching the burner ring with its flame holes. It is possible to idealize this situation as an ejector. For an ejector, the total gas mixture flow rate can be related to the rate of fuel admitted to the system through continuity of momentum

$$m_m u_m = m_f u_f$$

$$u_m (\rho_m A_m u_m) = (\rho_f A_f u_f) u_f$$

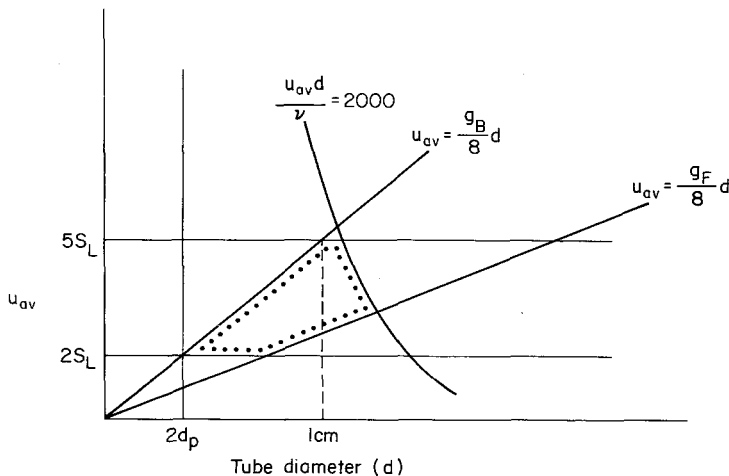


Fig. 31. Stability and operation limits of a Bunsen burner.

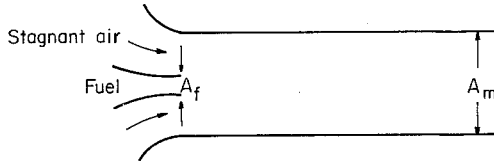


Fig. 32. Fuel-jet ejector system for burners.

where the subscript m represents the conditions for the mixture (A_m is the total area) and the subscript f represents conditions for the fuel. The ejector is depicted in Fig. 32. The momentum expression can be written as

$$\rho_m u^2 = \alpha \rho_f u_f^2$$

where α is the area ratio.

If one examines the g_F and g_B on the same graph as shown in Fig. 32, some interesting observations can be made. The burner port diameter is fixed such that a rich-mixture ratio is obtained and at a value represented by the dashed line on Fig. 33. When the mixture ratio is set at this value, the flame can never flashback into the stove and burn without the operator noticing the situation. If the fuel is changed, as the gas industry did when it switched from manufacturer's gas to natural gas, difficulties could arise. Such difficulties could arise again if the industry felt compelled to switch to synthetic gas or to use synthetic or petroleum gas as an additive to natural gas to increase supplies.

The volumetric fuel-air ratio in the ejector is given by

$$(F/A) = (u_f A_f)/(u_m A_m)$$

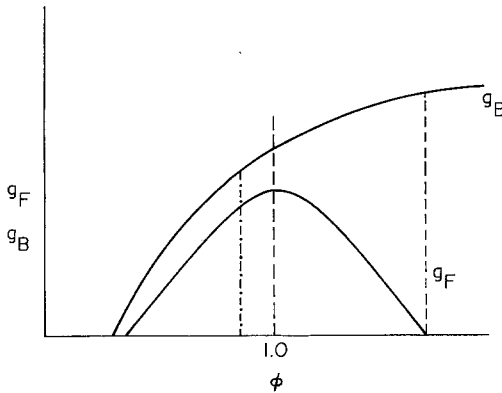


Fig. 33. Flame stability diagram for a gas-air mixture.

It is assumed here that the fuel-air mixture is essentially air; that is, the density of the mixture does not change as the amount of fuel changes. From the momentum equation, this fuel-air mixture ratio becomes

$$(F/A) = (\rho_m/\rho_f)^{1/2}\alpha^{1/2}$$

The stoichiometric molar (volumetric) fuel-air ratio is strictly proportional to the molecular weight of the fuel for two common hydrocarbon fuels, i.e.,

$$(F/A_{\text{stoich}}) \sim 1/MW_f \sim 1/\rho_f$$

The equivalence ratio then is

$$\phi = \frac{(F/A)}{(F/A_{\text{stoich}})} \sim \frac{\alpha^{1/2}(\rho_m/\rho_f)^{1/2}}{(1/\rho_f)} \sim \alpha^{1/2}\rho_f^{1/2}\rho_m^{1/2}$$

Examining Fig. 33, one observes that as one converts from a heavier fuel to a lighter fuel, the equivalence ratio drops and the dot-dash operating line is obtained. Someone adjusting the same burner with the new lighter fuel would have a very consistent flashback-blowoff problem. Thus, when the gas industry switched to natural gas, it was required that every fuel port in every burner on every stove be drilled open so that α could become larger to compensate for the decreased ρ_f . Synthetic gases of the future will certainly be heavier than methane (natural gas). They will probably be mostly methane with some heavier components, particularly ethane. Consequently, present burners will not give a stability problem, but will operate more fuel rich and thus be more wasteful of energy. It would be logical to make the fuel ports smaller by caps so that the operating line would be moved next to the rich flashback cut-off line.

E. TURBULENT REACTING FLOWS AND TURBULENT FLAMES

In the preceding sections of this chapter it was tactly assumed that in laminar flames the flow conditions did not alter the chemical mechanism or the associated chemical energy release rate. However in many flow configurations there can be an interaction between the character of the flow and the reaction chemistry. If the flow becomes turbulent, there are fluctuating components of velocity, temperature, density, pressure, and concentration. The degree that such components affect the chemical reactions, heat release rate, and flame structure in a combustion system depends upon the relative characteristic times associated with each of the individual elements. In a general sense, if the characteristic time (τ_c) of the chemical reaction is much

shorter than a characteristic time (τ_m) associated with the fluid-mechanical fluctuations, then the chemistry is essentially not influenced by the flow field. If the contrary condition ($\tau_c > \tau_m$) is true, then the fluid mechanics could have an effect on the chemical reaction rate, energy release rates, and flame structure.

The interaction of turbulence and chemistry constitutes the field of turbulent reacting flows and is of importance whether flame structures exist or not. The concept of turbulent reacting flows can have many different meanings and depends on the interaction range, which is governed by the overall character of the flow environment. Associated with various flows are different characteristic times, or, as more commonly used, different characteristic lengths.

There are many different aspects to the field of turbulent reacting flows. Consider, for example, the effect of turbulence on the rate of an exothermic reaction such as that which would occur in a turbulent flow reactor. Here, the fluctuating temperatures and concentrations could affect the chemical reaction and heat release rates. Then there is the situation in which combustion products are rapidly mixed with reactants in a time much shorter than the chemical reaction time. This later example is the so-called stirred reactor to be discussed in more detail in the next section. In both examples no flame structure is considered to exist.

Turbulence-chemistry interactions related to premixed flames comprise another major category. A turbulent flow field dominated by large-scale, low-intensity turbulence will affect a premixed laminar flame so that it appears as a wrinkled laminar flame. The flame would be contiguous throughout the front. As the intensity of turbulence increases the contiguous flame front is destroyed and laminar flamelets exist within turbulent eddies. Finally at very high-intensity turbulence all laminar flame structure disappears and one has a distributed reaction zone. Time-averaged photographs of these three flames would show a very bushy flame front that would look very thick in comparison to the smooth thin zone that characterizes a laminar flame. However, if a very fast response thermocouple were inserted into these three flames, the fluctuating temperatures in the first two cases would show a bimodal probability density function with well-defined peaks at the temperatures of the unburned and completely burned mixtures. But, for the distributed reaction case, a bimodal function would not be found.

Since under premixed fuel-oxidizer conditions the turbulent flow field causes a mixing between the different fluid elements, the characteristic time was given the symbol τ_m . In general with increasing turbulence intensity this time approaches the chemical time, and the associated length approaches the flame or reaction zone thickness. Essentially the same is true with respect to non-premixed flames. The fuel and oxidizer (reactants) in non-premixed

flames are not in the same flow stream, and, since different streams can have different velocities, a gross shear effect can take place and coherent structures (eddies) can develop throughout this mixing layer. These eddies enhance the mixing of fuel and oxidizer. The same type of shear can occur under turbulent premixed conditions when large velocity gradients exist.

The complexity of the turbulent reacting flow problem is such that it is best to deal first with the effect of a turbulent field on an exothermic reaction in a plug flow reactor. Then the different turbulent reacting flow regimes will be described more precisely in terms of appropriate characteristic lengths, which will be developed from a general discussion of turbulence. And, lastly the turbulent premixed flame will be examined in detail.

1. The Rate of Reaction in a Turbulent Field

An excellent simple example to examine how fluctuating parameters can affect a reacting system is to examine how the mean rate of a reaction would differ from the rate evaluated at the mean properties when there are no correlations among these properties. In flow reactors, time-averaged concentrations and temperatures are usually measured and rates are determined from these quantities. Only by optical techniques or very fast response thermocouples could the proper instantaneous values be measured and they would fluctuate with time.

The fractional rate of change of a reactant can be written as

$$\dot{w} = -k\rho^{n-1}Y_i^n = -Ae^{-E/RT}(P/R)^{n-1}T^{1-n}Y_i^n$$

where Y_i are the mass fractions of the reactants. The instantaneous change in rate is given by

$$\begin{aligned} d\dot{w} = & -A(P/R)^{n-1}[(E/RT^2)e^{-E/RT}T^{1-n}Y_i^n dT \\ & + (1-n)T^{-n}e^{-E/RT}Y_i^n dT \\ & + ne^{-E/RT}T^{1-n}Y_i^{n-1} dY_i] \end{aligned}$$

$$d\dot{w} = (E/RT)\dot{w}(dT/T) + (1-n)\dot{w}(dT/T) + \dot{w}n(dY_i/Y_i)$$

or

$$d\dot{w}/\dot{w} = \{E/RT + (1-n)\}(dT/T) + n(dY_i/Y_i)$$

For most hydrocarbon flame or reacting systems the overall order of reaction is about 2, the activation energy approximately 40 kcal/mole, and the flame temperature about 2000 K. Thus,

$$(E/RT) + (1-n) \cong 9$$

and it would appear that the temperature variation would be dominant factor. Since the temperature effect comes into this problem through the specific reaction rate constant, then the problem simplifies to whether the mean rate constant can be represented by the rate constant evaluated at the mean temperature.

In the hypothetical simplified problem one assumes further that the temperature T fluctuates with time around some mean represented by the form

$$T(t)/\bar{T} = 1 + a_n f(t)$$

where a_n is the amplitude of the fluctuation and $f(t)$ is some time-varying function in which

$$-1 \leq f(t) \leq +1$$

and

$$\bar{T} = \frac{1}{\tau} \int_0^\tau T(\tau) d\tau$$

$T(t)$ can be considered to be composed of $\bar{T} + T'(t)$, where T' is the fluctuating component around the mean. Ignoring the temperature dependency in the pre-exponential, one writes the instantaneous-rate constant as

$$k(T) = A \exp(-E/RT)$$

and the rate constant evaluated at the mean temperature as

$$k(\bar{T}) = A \exp(-E/R\bar{T})$$

Dividing the two expressions, one obtains

$$k(T)/k(\bar{T}) = \exp\{(E/R\bar{T})[1 - (\bar{T}/T)]\}$$

Obviously then for small fluctuations

$$1 - (\bar{T}/T) = [a_n f(t)]/[1 + a_n f(t)] \approx a_n f(t)$$

The expression for the mean rate is written as

$$\begin{aligned} \frac{\overline{k(T)}}{k(\bar{T})} &= \frac{1}{\tau} \int_0^\tau \frac{k(T)}{k(\bar{T})} dt = \frac{1}{\tau} \int_0^\tau \exp\left(\frac{E}{R\bar{T}} a_n f(t)\right) dt \\ &= \frac{1}{\tau} \int_0^\tau \left[1 + \frac{E}{R\bar{T}} a_n f(t) + \frac{1}{2} \left(\frac{E}{R\bar{T}} a_n f(t)\right)^2 + \dots \right] dt \end{aligned}$$

But recall

$$\int_0^\tau f(t) dt = 0 \quad \text{and} \quad 0 \leq f^2(t) \leq 1$$

Examining the third term, it is apparent

$$\frac{1}{\tau} \int_0^{\tau} a_n^2 f^2(t) dt \leq a_n^2$$

since the integral of the function can never be greater than 1. Thus,

$$\frac{\overline{k(T)}}{k(\bar{T})} \leq 1 + \frac{1}{2} \left(\frac{E}{R\bar{T}} a_n \right)^2 \quad \text{or} \quad \Delta = \frac{\overline{k(T)} - k(\bar{T})}{k(\bar{T})} \leq \frac{1}{2} \left(\frac{E}{R\bar{T}} a_n \right)^2$$

If the amplitude of the temperature fluctuations is of the order of 10% of the mean temperature, then one can take $a_n \approx 0.1$, and if the fluctuations are considered sinusoidal, then

$$\frac{1}{\tau} \int_0^{\tau} \sin^{-2} t = \frac{1}{2}$$

and for the example being discussed

$$\Delta = \frac{1}{4} \left(\frac{E}{R\bar{T}} a_n \right)^2 = \frac{1}{4} \left(\frac{40000 \times 0.1}{2 \times 2000} \right)^2, \quad \Delta \cong \frac{1}{4}$$

or a 25% difference in the two rate constants.

Instead of a simple sinusoidal fluctuation, the result could be improved by assuming a more appropriate distribution function of T' ; however, the example chosen even with its assumptions well exemplifies the problem. Normally, probability distribution functions are chosen; these functions will be described later. If the concentrations and temperatures were correlated, the rate expression becomes very complicated. Bilger [26] has presented a form of a two-component mean-reaction rate when it is expanded about the mean states as

$$\begin{aligned} -\bar{w} = & \bar{\rho}^2 \bar{Y}_i \bar{Y}_j \exp(-E/R\bar{T}) \{ 1 + (\bar{\rho}'^2/\bar{\rho}^2) + (Y_i' Y_j' / \bar{Y}_i' \bar{Y}_j') \\ & + 2(\bar{\rho}' Y_i' / \bar{\rho} \bar{Y}_i) + 2(\bar{\rho}' Y_j' / \bar{\rho} \bar{Y}_j) \\ & + (E/R\bar{T})(Y_i' T' / \bar{Y}_i \bar{T})(Y_j' T' / \bar{Y}_j \bar{T}) \\ & + [(E/2R\bar{T}) - 1](\bar{T}'^2/\bar{T}^2) \\ & + \dots \end{aligned}$$

2. Regimes of Turbulent Reacting Flows

The previous example epitomizes how a reacting media can be affected by a turbulent field. To understand the detailed effect one must understand the elements of the field of turbulence. When considering turbulent combustion systems in this regard a suitable starting point is the consideration of the

quantities that determine the fluid characteristics of the system. The material presented subsequently has been synthesized from Refs. [27,28].

Most flows have at least one characteristic velocity U and characteristic length scale L of the device in which the flow takes place. In addition there is at least one representative density ρ_0 and T_0 , usually the unburned condition when considering combustion situations. Thus, a characteristic kinematic viscosity $\nu_0 \equiv \mu_0/\rho_0$ can be defined, where μ_0 is the coefficient of viscosity at the characteristic temperature T_0 . The Reynold's number for the system is then $Re = UL/\nu_0$. It is interesting to note that ν is approximately proportional to T^2 . Thus, a change in temperature by a factor of 3 or more, quite modest by combustion standards, means a drop in Re by an order of magnitude. Thus, energy release can dampen any turbulent fluctuations. Viscosity ν is inversely proportional to the pressure p , and changes in p are usually small, the effects of such changes in ν typically are much less than those of changes in T .

Even though the Reynold's number gives some measure of turbulent phenomena, flow quantities characteristic of turbulence itself are of more direct relevance to modelling turbulent reacting systems. The turbulent kinetic energy \tilde{q} may be assigned a representative value \tilde{q}_0 at a suitable reference point. The relative intensity of the turbulence is then characterized by either $\tilde{q}_0/(\frac{1}{2}U^2)$ or U'/U , where $U' = (2\tilde{q}_0)^{1/2}$ is a representative root-mean-square velocity fluctuation. Weak turbulence corresponds to $U'/U \ll 1$ and intense turbulence has U'/U of the order unity.

Although there is a continuous distribution of length scales associated with the turbulent fluctuations of velocity components and of state variables (p, ρ, T), it is useful to focus on two widely disparate lengths that determine separate effects in turbulent flows. First, there is a length l_0 which characterizes the large eddies, those of low frequencies and long wavelengths. Experimentally l_0 can be defined as a length beyond which various fluid-mechanical quantities become essentially uncorrelated; typically l_0 is less than L but of the same order of magnitude. This length can be used in conjunction with U' to define a turbulent Reynolds number,

$$R_l = U'l_0/\nu_0$$

which has more direct bearing on structure of turbulence in flows than does Re . Large values of R_l can be achieved by intense turbulence, large-scale turbulence and small values of ν produced, for example, by low temperatures or high pressures. The cascade view of turbulence dynamics is restricted to large values of R_l . Generally $R_l < Re$.

The second length scale characterizing turbulence is that over which molecular effects are significant and can be introduced in terms of a representative rate of dissipation of velocity fluctuations, essentially the rate

of dissipation of the turbulent kinetic energy. This rate of dissipation is given by the symbol ε_0 and is

$$\varepsilon_0 = \frac{\bar{q}_0}{t} \approx \frac{(U')^2}{t} \approx \frac{(U')^2}{(l_0/U')} \approx \frac{(U')^3}{l_0}$$

This rate estimate corresponds to the idea that the time scale over which velocity fluctuations (turbulent kinetic energy) decay by a factor of $(1/e)$ is the order of the turning time of a large eddy. The rate ε_0 increases with turbulent kinetic energy (which is due principally to the large-scale turbulence) and decreases with increasing size of the large-scale eddies. At the small scales at which the molecular dissipation occurs, the relevant parameters are the kinematic viscosity, which causes the dissipation and the rate of dissipation. The only length scale that can be constructed from these two parameters is the so-called Kolmogorov length

$$l_k = \left(\frac{v^3}{\varepsilon_0} \right)^{1/4} = \left[\frac{\text{cm}^6/\text{sec}^3}{(\text{cm}^3/\text{sec}^3)(1/\text{cm})} \right]^{1/4} = (\text{cm}^4)^{1/4} = \text{cm}$$

However note then that

$$\begin{aligned} l_k &= [v^3 l_0 / (U')^3]^{1/4} \\ &= [(v^3 l_0^4) / (U')^3 l_0^3]^{1/4} = (l_0^4 / R_l^3)^{1/4} \end{aligned}$$

Therefore,

$$l_k = l_0 / R_l^{3/4}$$

This length is representative of the dimension at which dissipation occurs and defines a cutoff of the turbulence spectrum. For large R_l there is a large spread of the two extreme lengths characterizing turbulence. This spread is reduced with increasing temperature because of the consequent increase in v_0 .

Considerations analogous to those for velocity apply to scalar fields as well, and lengths analogous to l_k have been introduced for these fields. They differ from l_k by factors involving the Prandtl and Schmidt numbers, which differ relatively little from unity for representative gas mixtures. Therefore, to a first approximation for gases, l_k may be used for all fields and there is no need to introduce any new corresponding lengths.

An additional length, intermediate in size between l_0 and l_k , which often arises in formulations of equations for average quantities in turbulent flows is the Taylor length (λ), which is representative of the dimension over which strain occurs in a particular viscous medium. The strain can be written as (U'/l_0) . As before, the length that can be constructed between the strain and the viscous forces is

$$\begin{aligned} \lambda &= [v / (U'/l_0)]^{1/2} \\ \lambda^2 &= (vl_0 / U') = (vl_0^2 / U'l_0) = (l_0^2 / R_l) \end{aligned}$$

or

$$\lambda = l_0/R_t^{1/2}$$

In a sense the Taylor microscale is similar to an average of the other scales, l_0 and l_k , but heavily weighted towards l_k .

Recall that there are length scales associated with laminar flame structures in reacting flows. One is the characteristic thickness of a premixed flame, δ_L , given by

$$\delta_L \approx \left(\frac{\alpha}{\dot{w}}\right)^{1/2} \approx \left(\frac{\text{cm}^2/\text{sec}}{1/\text{sec}}\right)^{1/2} = \text{cm}^2$$

The derivation is, of course, consistent with the characteristic velocity in the flame speed problem. This velocity is obviously the laminar flame speed itself, so that

$$S_L \approx \frac{v}{\delta_L} = \frac{\text{cm}^2/\text{sec}}{\text{cm}} = \text{cm}/\text{sec}$$

More detailed analysis has shown that δ_L is the characteristic scale of the thermal preheat region and the rapid chemical reaction rate and heat release are confined to a narrower zone at the high-temperature end of the flame.

The characteristic time of the chemical reaction in this context is

$$\tau_c = (1/\dot{w}) = \delta_L/S_L$$

It may be expected then that the nature of the turbulent reacting flows may differ considerably and would depend on the comparison of these chemical and flow scales; that is, whether

$$\begin{array}{ccc} \delta_L < l_k; & l_k < \delta_L < \lambda; & \lambda < \delta_L < l_0; \\ \text{wrinkled flame} & \text{severe wrinkling} & \text{flamelets in eddies} \end{array} \quad \text{OR} \quad \begin{array}{c} l_0 < \delta_L \\ \text{distributed front} \end{array}$$

Wrinkled flames may occur when $\delta_L < l_k$ and broadly distributed reactions when $l_0 < \delta_L$. The nature of turbulent flames implied by these various inequalities has not been completely explored. In theories it is often assumed that $\delta_L < l_k$.

As indicated, a characteristic time for chemical reaction can be called τ_c . Indeed this time, which was defined earlier, would be appropriate whether a flame existed or not. Generally in consideration of turbulent reacting flows, chemical lengths are constructed to be $U\tau_c$ or $U'\tau_c$. Comparison of an appropriate chemical length with a fluid dynamical length provides a nondimensional parameter that has a bearing on the relative rate of reaction. Nondimensional numbers of this type are conventionally called Damkohler numbers and are given the symbol Da. An example appropriate to the

considerations here is

$$Da = (l_0/U'\tau_c) = (\tau_m/\tau_c) = (l_0S_L/U'\delta_L)$$

where τ_m is a mixing time defined (l_0/U') and the last equality in the expression applies when there is a flame structure.

For large Damkohler numbers, chemistry is fast (reaction time is short) and reaction sheets of various wrinkled types may occur. For small Da 's, chemistry is slow and well-stirred flows may occur.

There are two other nondimensional numbers relevant to the chemical reaction aspect part of this problem [27]. They have been introduced by Frank-Kamenetskii and others. These Frank-Kamenetskii numbers are the nondimensional heat release $FK_1 \equiv Q_p/c_p T_f$, where Q_p is the chemical heat release of the mixture and T_f the flame (or reaction) temperature, and the nondimensional activation energy $FK_2 = (T_a/T_f)$, where $T_a = (E_a/R)$. Combustion, in general, and turbulent combustion, in particular, typically are characterized by large values of these numbers. When FK_1 is large, chemistry is likely to have a large influence on turbulence. When FK_2 is large, the rate of reaction depends strongly on the temperature. It is usually true that the larger the FK_2 , the thinner will be the region in which the principal chemistry occurs. Thus, irrespective of the value of the Damkohler number, reactions tend to be found in thin, convoluted sheets in turbulent flows, for both premixed and non-premixed systems having large FK_2 . In premixed flames it is known that the thickness of the reaction region is of the order δ_L/FK_2 . Different relative sizes of δ_L/FK_2 and fluid-mechanical lengths, therefore, may introduce additional classes of turbulent reacting flows.

The flames themselves can alter the turbulence. In simple open Bunsen flames whose tube Reynold's number were such that the flow would be considered in the turbulent regime, there have been results that indicate that the temperature effects on the viscosity are such that the resulting flame structure is completely laminar. Similarly for a completely laminar flow in which a simple wire is oscillated near the flame surface, a wrinkled flame can be obtained (Fig. 34). Nevertheless, most open flames created by a turbulent fuel jet exhibit a wrinkled flame type of structure. Indeed short-duration schlieren photographs appear to indicate these flames to have continuous surfaces. Measurements of flames such as that shown in Figs. 35(a) and (b) have been taken at different time intervals and the instantaneous flame shapes verify the continuous wrinkled flame structure. A plot of these instantaneous surface measurements are shown in Fig. 36. One can visualize that a larger number of these measurements would result in a thick flame region just as the eye would visualize. Indeed turbulent premixed flames are described as bushy flames. The thickness of this turbulent flame zone appears to be related to the scale of turbulence.

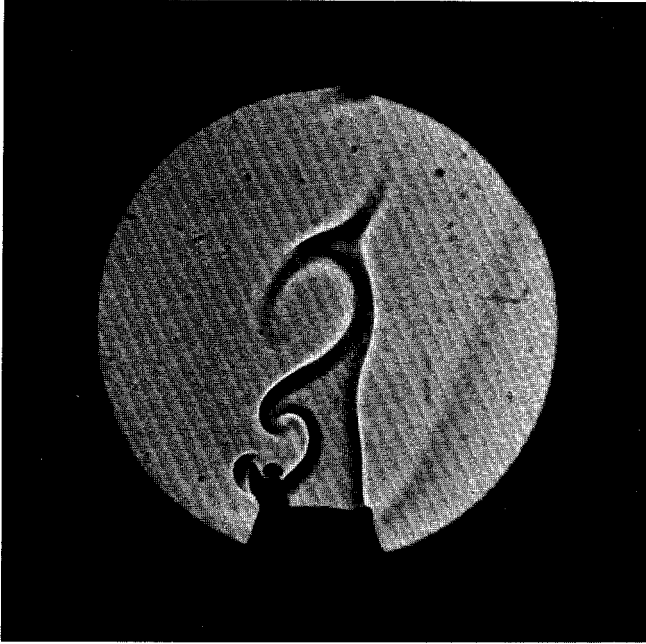


Fig. 34. Flow turbulence induced by a vibrating wire. Spark shadow-graph of 5:6% propane-air flame (after Markstein, *Int. Symp. Combust.*, 7th).

In turbulent Bunsen flames it has been found that the axial component of the mean velocity along the centerline remains almost constant with height above the burner, but away from the centerline the axial mean velocity increases with height. The radial outflow component increases with distance from the centerline and reaches a peak outside the flame. Both axial and radial components of turbulent velocity fluctuations show a complex variation with position and include peaks and troughs in the flame zone. Thus, there are indications of both generation and removal of turbulence within the flame. With increasing height above the burner, the Reynolds shear stress decays from that corresponding to an initial pipe flow profile.

In all flames there is a large increase in velocity as the gases enter the burned gas state. Thus, it should not be surprising that the heat release itself can play a role in inducing turbulence. Such velocity changes in a fixed combustion configuration can cause shear effects which can contribute to the turbulence phenomenon. There is no better example of some of these aspects than in turbulent flames stabilized in ducted systems. The mean axial velocity field of ducted flames involves considerable acceleration resulting from gas expansion due to heat release. Typically the axial velocity of the unburned gas doubles before it is entrained into the flame and the velocity at the center

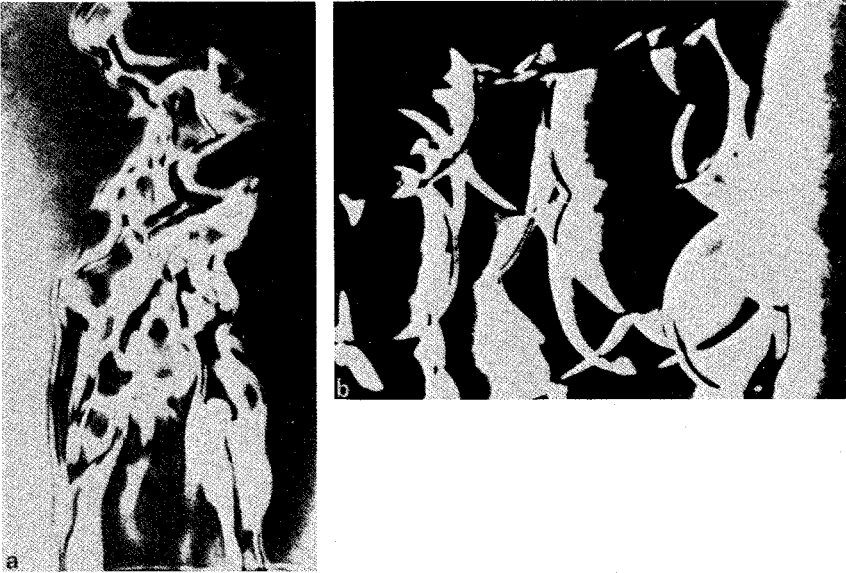


Fig. 35. Short durations in Schlieren photographs of open turbulent flames [after Fox and Weinberg, *Proc. R. Soc. London A* 268, 222 (1962)].

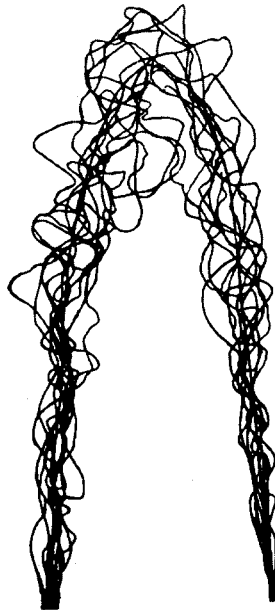


Fig. 36. Superimposed contours of instantaneous flame boundaries [after Fox and Weinberg, *Proc. R. Soc. London A* 268, 222 (1962)].

line at least doubles again. Large mean velocity gradients are therefore produced. The streamlines in the unburnt gas are deflected away from the flame.

The growth of axial turbulence in the flame zone of these ducted systems is attributed to the mean velocity gradient resulting from the combustion. The production of turbulence energy by shear depends on the product of the mean velocity gradient and the Reynolds stress. Such stresses provide the most plausible mechanism for the modest growth in turbulence observed.

Whereas laminar flame speed is a unique aerothermochemical property of a fuel-oxidizer mixture ratio, a turbulent flame speed is not only a function of the fuel-oxidizer mixture ratio, but also a function of the flow characteristics and experimental configuration. Thus, there is great difficulty in correlating the experimental data of various investigators. In a sense there is no flame speed in a turbulent stream. Essentially as a flow field is made turbulent for a given experimental configuration, the mass consumption rate (and thus rate of energy release) of the fuel-oxidizer mixture increases. Thus, some have found it convenient to define a turbulent flame speed S_T as the mean mass flux per unit area, in a coordinate system fixed to the time-averaged motion of the flame, divided by the unburned gas density ρ_0 . The area chosen is the smoothed surface of the time-averaged flame zone. However, this zone is thick and curved and thus the choice of an area near the unburned gas edge can give quite a different result than a flame position taken in the center or burned gas side of the bushy flame. Thus, there is a great deal of uncertainty with respect to the various experimental values of S_T reported. Nevertheless there do appear to be definite trends reported. These trends can be summarized as follows:

(1) S_T is always greater than S_L . This trend would be expected since the increased area of the turbulent flame allows greater total mass consumption.

(2) S_T increases with increasing intensity of turbulence ahead of the flame. Many have found the relationship to be approximately linear. This point will be discussed later.

(3) Some experiments show S_T to be insensitive to the scale of the approach flow turbulence.

(4) In open flames, the variation of S_T with composition is generally much the same as for S_L , and S_T has a well-defined maximum close to stoichiometric. Thus, many report turbulent flame speed data as the ratio of S_T/S_L .

(5) Very large values of S_T may be observed in ducted burners at high approach flow velocities. Under these conditions S_T increases in proportion to the approach flow velocity, but is insensitive to approach flow turbulence and composition. It is believed that these effects result from the dominant influence of turbulence generated within the stabilized flame by the large-velocity gradients.

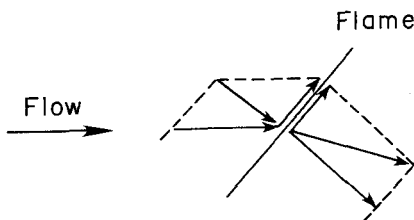


Fig. 37. Deflection of velocity vector through oblique flame.

The definition of the flame speed as the mass flux through the flame per unit area of the flame divided by the unburned gas density ρ_0 is useful for laminar nonstationary and oblique flames as well.

Consider a plane oblique flame. Because of the increase in velocity demanded by continuity, a streamline through such an oblique flame is deflected towards the direction of the normal to the flame surface. The velocity vector may be broken up into a component normal to the flame wave and a component tangential to the wave (Fig. 37). Because of the energy release, the continuity of mass requires that the normal component increase on the burned gas side and, of course, the tangential component remains the same. A consequence of the tangential velocity is that fluid elements in the oblique flame surface move along this surface. If the surface is curved, adjacent points travelling along the flame surface may either move further apart (which is known as flame stretch) or they may come closer together (flame compression).

An oblique flame is curved if the velocity U of the approach flow varies in a direction y perpendicular to the direction of the approach flow. Strehlow has shown that the quantity

$$K_1 = (\delta_L/U)(\delta U/\delta y)$$

which is known as the Karlovitz flame stretch factor, is approximately equal to the ratio of the flame thickness δ_L to the flame curvature. The Karlovitz school has argued that excessive stretching can lead to local quenching of the reaction. Klimov, and later Williams, analyzed the propagation of a laminar flame in a shear flow with velocity gradient in terms of a more general stretch factor

$$K_2 = (\delta_L/S_L)(1/\Lambda) d\Lambda/dt$$

where Λ is the area of an element of flame surface, $d\Lambda/dt$ is its rate of increase, and δ_L/S_L is a measure of the transit time of the gases passing through the flame. Stretch ($K_2 > 0$) is found to reduce the flame thickness and to increase reactant consumption per unit area of the flame and large stretch ($K_2 \gg 0$) may lead to extinction. On the other hand, compression ($K_2 < 0$) increases

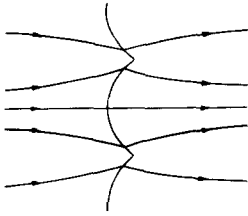


Fig. 38. Convergence-divergence of flow streamlines due to wrinkle in laminar flame.

flame thickness and reduces reactant consumption per unit incoming reactant area. These findings are relevant to laminar flamelets in a turbulent flame structure.

Since the concern here is with the destruction of a contiguous laminar flame in a turbulent field, consideration must also be given to certain inherent instabilities in laminar flames themselves. There is a fundamental hydrodynamic instability and also one due to the fact that mass and heat can diffuse at different rates; i.e., the Lewis number is nonunity. In the latter mechanism, when the Le number (D/α) is less than one, then a flame instability can occur. Consider initially the instability due to the flow, first described by Darrieus [29], Landau [30], and Markstein [31]. If a minor wrinkle occurs in a laminar flame, the approach flow streamlines will either diverge or converge as shown in Fig. 38. If the wrinkle did not incur in the flame, then the flame speed S_L would be equal to the upstream unburned gas velocity U_0 . Considering the two upper streamlines one notes that, because of the curvature due to the wrinkle, the normal component of the velocity, with respect to the flame, is less than U_0 . Thus, the streamlines diverge as they enter the wrinkled flame front. Since there must be continuity of mass between the streamlines, the unburned gas velocity at the front must decrease due to the increase of area. Since S_L is now greater than the unburned approaching gas, the flame moves further downstream and the wrinkle is accentuated. For similar reasons, between another pair of streamlines as the first, the unburned gas velocity increases near the flame front and the flame bows in the upstream direction. It is not clear why these instabilities do not keep growing. Some have attributed the growth limit to nonlinear effects that arise in the hydrodynamics.

When the Lewis number is nonunity, then mass diffusivity can be greater than the thermal diffusivity. This discrepancy in diffusivities is important with respect to the reactant that limits the reaction. Ignoring the hydrodynamic instability and again considering the condition between a pair of streamlines entering a wrinkle in a laminar flame, but looking more closely at the flame structure that these streamlines encompass, one will note that more of the limiting reactant will diffuse into the flame zone than heat will diffuse from the flame zone into the unburned mixture. Thus, the flame temperature will

rise, the flame speed increases, and the flame wrinkles bows further in the downstream direction. The flame will then look very much like the flame depicted for the hydrodynamic instability in Fig. 38. The flame surface breaks up continuously into new cells in a chaotic manner as was photographed by Markstein. There would appear to be a higher-order stabilizing effect. The fact that the phenomenon is controlled by a limiting reactant means that this cellular condition can occur when the unburned premixed gas mixture is either fuel rich or fuel lean. It should not be surprising then that the most evident mixture would be a lean hydrogen-air system.

Earlier it was stated that the structure of a turbulent velocity field may be presented in terms of two parameters, the scale and intensity of turbulence. The intensity was defined as the square root of the turbulent kinetic energy, which essentially gave a root-mean-square velocity fluctuation U' . Three length scales were defined: the integral scale l_0 , which characterizes the large eddies; the Taylor microscale λ obtained from the rate of strain; and the Kolmogorov microscale l_k , which typifies the smallest dissipative eddies. These length scales and the intensity can be combined to form not one but three turbulent Reynolds numbers: $R_l = U'l_0/\nu$, $R_\lambda = U'\lambda/\nu$, and $R_k = U'l_k/\nu$. From the relationship between l_0 , l_k , and λ previously derived it is found that $R_k^4 \approx R_\lambda^2 \approx R_l$.

There is now sufficient information to relate the Damkohler number Da and the length ratios l_0/δ_L , l_k/δ_L and l_0/l_k to a nondimensional velocity ratio U'/S_L and the three turbulence Reynolds numbers. The complex relationships are given in Fig. 39 and are very informative. The right-hand side of the figure has $R_\lambda > 100$ and ensures the length-scale separation that is characteristic of high Reynolds number behavior. The largest Damkohler numbers are found in the bottom right corner of the figure.

This graph and the relationship it contains permits one to address the question whether and under what conditions a laminar flame can exist in a turbulent flow. As before, if allowance is made for flame front curvature effects, a laminar flame can be considered stable to disturbances of sufficiently short wavelength, but that intense shear can lead to its extinction. From solutions of the laminar flame equations in an imposed shear flow Klimov [32] and Williams [33] showed that a conventional propagating flame may exist only if the stretch factor K_2 is less than a critical value of unity. Modelling the area change term in the stretch expression as

$$(1/\Lambda) d\Lambda/dt \approx U'/\lambda$$

and recalling

$$\delta_L \approx \nu/S_L$$

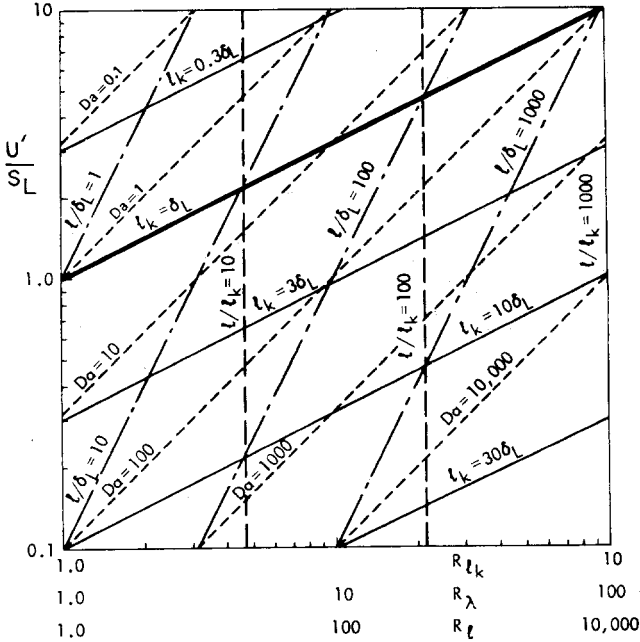


Fig. 39. Characteristic parameters of premixed turbulent combustion. The Klimov-Williams criterion is satisfied above the line $l_k = \delta_L$.

One finds

$$K_2 \approx \frac{\delta_L U'}{S_L \Lambda} = \frac{\delta_L^2 U'}{v \lambda} = \frac{\delta_L^2 U'}{v l_0} R_{l_0}^{1/2} \cdot \frac{l_0}{l_0} = \frac{\delta_L^2}{l_0^2} Re_i^{3/2}$$

But as shown earlier

$$l_k = l_0 / Re^{3/4} \quad \text{or} \quad l_0^2 = l_k^2 Re^{3/2}$$

$$K_2 = \delta_L^2 / l_k^2 = (\delta_L / l_k)^2$$

Thus, the criterion to be satisfied if a laminar flame is to exist in a turbulent flow is that the laminar flame thickness δ_L must be less than the Kolmogorov microscale l_k of the turbulence.

The heavy line in Fig. 39 indicates the condition $\delta_L = l_k$. This line is drawn in this fashion since

$$K_2 \approx \frac{\delta_L U'}{S_L \lambda} \approx \frac{v U'}{S_L^2 \lambda} \approx \frac{v U'}{S_L^2 \lambda} \cdot \frac{U'}{U'} \approx \frac{(U')^2}{S_L^2} \frac{1}{R_\lambda} \approx 1 \quad \text{or} \quad \left(\frac{U'}{\delta_L}\right)^2 \approx R_\lambda$$

Thus for $(U'/\delta_L) = 1$, $R_\lambda = 1$, and for $(U'/\delta_L) = 10$, $R_\lambda = 100$. The other Reynold's numbers follow from $R_k^4 = R_\lambda^2 = R_l$.

Below and to the right of this line the Klimov-Williams criterion is satisfied and wrinkled laminar flames may occur. The figure shows that this region includes both large and small values of turbulence Reynolds numbers and velocity ratios (U'/S_L) $\gg 1$, but predominately large Da.

Above and to the left of the criterion line is the region in which $l_k < \delta_L$. According to the Klimov-Williams criterion, the turbulent velocity gradients in this region, or perhaps in a region defined with respect to any of the characteristic lengths, are sufficiently intense so that they may destroy a laminar flame. The figure shows $U' \geq S_L$ in this region and Da is predominately small. At the highest Reynolds numbers the region is entered only for very intense turbulence $U' \gg S_L$. The region has been considered as that of a distributed reaction zone in which reactants and products are found somewhat uniformly dispersed throughout the flame front. Reactions are still fast everywhere so that unburned mixture near the burned gas side of the flame is completely burned before it leaves what would be considered the flame front. An instantaneous temperature measurement in this flame would yield a normal probability density function, more importantly one that is not bimodal.

3. The Turbulent Flame Speed

As stated earlier, unlike one's ability to assign to a laminar flame a flame speed S_L that is a physicochemical and chemical kinetic property of the unburned gas mixture alone, for turbulent flames, the turbulent flame speed S_T , is in reality a mass consumption rate per unit area divided by the unburned gas density and must depend also on the properties of the turbulent flow and the method of flame stabilization. As pointed out even with this definition of S_T a difficulty arises because the time-averaged turbulent flame is bushy (thick) and there is a large difference between the area on the unburned gas side and that on the burned gas side. Nevertheless much data are reported as turbulent flame speeds.

In attempts to analyze the early experimental data Damkohler considered that large-scale, low-intensity turbulence simply distorted (wrinkled) the laminar flame, but that the transport properties would remain the same and thus the laminar flame speed would not be affected. Figure 36 depicts how a planar-laminar flame would be distorted by the turbulence. It is apparent from this figure that the area of the flame increases due to the turbulent field. Thus Damkohler [34] proposed for large-scale, small-intensity turbulence so that

$$S_T/S_L = A_L/A_T$$

where A_L is the total area of laminar surface contained within an area of turbulent flame whose time-averaged area is A_T . Damkohler further proposed that the area ratio could be approximated by

$$A_L/A_T = 1 + (U'_0/S_L)$$

which leads to the result

$$S_T = S_L + U'_0, \quad S_T/S_L = (U'_0/S_L) + 1$$

where U'_0 is the turbulent intensity of the unburned gases ahead of the flame. Many groups of experimental data had been correlated by semi-empirical correlations of the type

$$S_T/S_L = A(U'_0/S_L) + B$$

and

$$S_T = A \text{Re} + B$$

The first expression above is very similar to the Damkohler result except that A and B are 1 in the Damkohler result. Since the turbulent exchange coefficient (eddy diffusivity) $\varepsilon \cong l_0 U'$ for tube flow and, indeed, l_0 is essentially constant for tube flow, it follows that

$$U' \sim \varepsilon \sim \text{Re}$$

where Re is the tube Reynolds number. Thus, the later expression has the same form as the Damkohler result except for the constants that would have to equal 1 and S_L , respectively, for exact similarity.

For small-scale, high-intensity turbulence, Damkohler reasoned that the transport properties of the flame were altered from the laminar kinetic theory viscosity ν_0 to the turbulent exchange coefficient ε so that

$$(S_T/S_L) = (\varepsilon/\nu)^{1/2}$$

Recall $S_L \sim (\alpha)^{1/2} \sim (\nu)^{1/2}$. Again realizing that $\varepsilon \sim U' l_0$, then

$$S_T/S_L \sim R_t^{1/2}$$

To assume, when there is small-scale, high-intensity turbulence of such order, that the transport properties are altered and that the chemical reactions are not altered is questionable from a physical point of view. Summerfield *et al.* [35] extended the Damkohler concept to include the effect of the turbulence on both the transport and chemistry and wrote

$$(S_T/S_L) = (\varepsilon/\tau_T)^{1/2}/(\nu/\tau_L)^{1/2}$$

where τ_T and τ_L are the characteristic chemical times for the laminar and turbulent condition, respectively. In this context the times can be represented

by

$$\tau_L = \delta_L/S_L, \quad \tau_T = \delta_T/S_T$$

where δ_T is turbulent flame thickness. This approach essentially considers the turbulent flame to be a distributed reaction zone. With the expressions for τ , it follows then that

$$(S_T^2/S_L^2) = (\varepsilon S_T/\delta_T)/(v S_L/\delta_L)$$

or cross multiplying to obtain a form of the Peclet number

$$(S_T \delta_T/\varepsilon) = (S_L \delta_L/v)$$

Experimental data on laminar flames give

$$(S_L \delta_L/v) \approx 10$$

Thus

$$(S_T \delta_T/\varepsilon) = (S_L \delta_L/v) \approx 10$$

so that δ_T may be approximated from the turbulent flame thickness and the eddy diffusivity.

In an early kinetic approach Schelkin [36] also extended Damkohler's model by starting from the fact that the transport in a turbulent flame could be made up of molecular movements (laminar λ_L) and eddy movements turbulent (λ_T) so that one could write

$$S_T \sim [(\lambda_L + \lambda_T)/\tau_c]^{1/2} \sim \{(\lambda_L/\tau_c)[1 + (\lambda_T/\lambda_L)]\}^{1/2}$$

where λ is the thermal conductivity. Since in this context

$$(\lambda_T/\tau_c)^{1/2} \sim S_L$$

it follows that

$$S_T = S_L[1 + (\lambda_T/\lambda_L)]^{1/2}$$

or essentially

$$S_T/S_L = 1 + (v_T/v_L)^{1/2}$$

Schelkin also considered large-scale, small-intensity turbulence. He assumed that flames surfaces distorted into cones whose base was proportional to the square of the average eddy diameter (i.e., proportional to l_0). The height of the cone was assumed proportional to U' and to the time t which an element of the wave is associated with an eddy. Thus, time can then be taken as equal to l_0/S_L . Schelkin then proposed that the ratio of S_T to S_L (average)

equals the ratio of the average cone area to the cone base. From the geometry, thus, visualized

$$A_C = A_B(1 + 4h^2/l_0^2)$$

where A_C is the area of the cone, A_B the area of the base, and h the cone height. But,

$$h = U't = U'l_0/S_L$$

Therefore,

$$S_T = S_L[1 + (2U'/S_L)^2]^{1/2}$$

For large values of (U'/S_L) the preceding expression reduces to that developed by Damkohler, i.e., $S_T \sim U'$. A rigorous development of wrinkled turbulent flames led Clavin and Williams [37] to a result that if isotropic turbulence is assumed S_T can be written as

$$S_T \sim \{1 + [(\overline{U'})^2/S_L^2]\}^{1/2}$$

which only differs from the heuristic approach by a factor of two in the second term.

F. STIRRED REACTOR THEORY

In the discussion on premixed turbulent flames, the case of infinitely fast mixing of the reactants and products was introduced. Generally this concept is referred to as a stirred reactor, and many have applied stirred reactor theory not only to turbulent flame phenomena, but also to determine overall reaction kinetic rates [18] and to understand stabilization in high-velocity streams [38]. Stirred reactor theory is important in its own right because from a practical point of view it predicts the maximum energy release rate possible in a fixed volume at a particular pressure.

Consider a fixed volume V into which fuel and air are injected at a fixed total mass flow rate \dot{m} and temperature T_0 . The fuel and air react in the volume and the injection of reactants and outflow of products (also equal to \dot{m}) are so oriented that within the volume there is instantaneous mixing of the unburned gases and the reaction products (burned gases). The reactor volume attains some steady temperature T_R and pressure P . The temperature of the gases leaving the reactor is, thus, T_R as well. The pressure differential between the reactor and the exit is generally considered to be small. The mass leaving the reactor contains the same concentrations as those within the reactor and thus contains products as well as fuel and air. Within the reactor

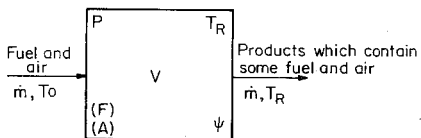


Fig. 40. Variables in a stirred reactor system of fixed volume.

there exists a certain concentration of fuel (F) and air (A), and also a fixed unburned mass fraction, ψ . Throughout the reactor volume, T_R , P , (F), (A), and ψ are constant and fixed; i.e., the reactor is so completely stirred that all elements are uniform everywhere. Figure 40 depicts the stirred reactor concept in a generalized manner.

The stirred reactor is to be compared to a plug flow reactor in which premixed fuel-air mixtures flow through the reaction tube. The unburned gases enter at temperature T_0 and leave the reactor at the flame temperature T_f . The system is assumed to be adiabatic. Only completely burned products leave the reactor. This reactor is depicted in Fig. 41.

The volume required to convert all the reactants to products for the plug flow reactor is greater than for the stirred reactor. The final temperature is, of course, higher than the stirred reactor temperature.

It is relatively straightforward to develop the controlling parameters of a stirred reactor process; ψ has been defined as the unburned mass fraction. Then it must follow that the fuel-air mass rate of burning \dot{R}_B is

$$\dot{R}_B = \dot{m}(1 - \psi)$$

and the rate of heat evolution q is

$$\dot{q} = q\dot{m}(1 - \psi)$$

where q is the heat reaction per unit mass of reactants for the given fuel-air ratio. If it is assumed that the specific heat of the gases in the stirred reactor can be represented by some average quantity \bar{c}_p , then an energy balance may be written as

$$\dot{m}q(1 - \psi) = \dot{m}\bar{c}_p(T_R - T_0)$$

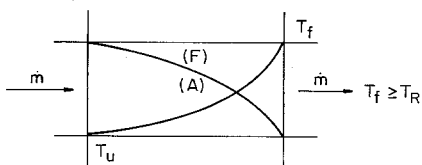


Fig. 41. Variables in a plug flow reactor.

For the plug flow reactor or any similar adiabatic system, it is also possible to define an average specific heat that takes its explicit definition from

$$\bar{c}_p \equiv q/(T_f - T_0)$$

To a very good approximation the two average specific heats can be assumed equal. Thus, it follows that

$$(1 - \psi) = T_R - T_0/T_f - T_0, \quad \psi = T_f - T_R/T_f - T_0$$

The mass burning rate is determined from the ordinary expression for chemical kinetic rates; i.e., the fuel consumption rate is given by

$$d(F)/dt = -(F)(A)Z'e^{-E/RT_R} = -(F)^2(A/F)Z'e^{-E/RT_R}$$

where (A/F) represents the air-fuel ratio. The concentration of the fuel can be written in terms of the total density and unburned mass fraction

$$(F) = \frac{(F)}{(A) + (F)} \rho\psi = \frac{1}{(A/F) + 1} \rho\psi$$

which permits the rate expression to be written as

$$\frac{d(F)}{dt} = -\frac{1}{[(A/F) + 1]^2} \rho^2 \psi^2 \left(\frac{A}{F}\right) Z' e^{-E/RT_R}$$

Now the great simplicity in stirred reactor theory is realizable. Since (F) , (A) , and T_R are constant in the reactor, the rate of conversion is constant. It is now possible to represent the mass rate of burning in terms of the above chemical kinetic expression:

$$\dot{m}(1 - \psi) = +V \frac{(A) + (F)}{(F)} \frac{d(F)}{dt}$$

or

$$\dot{m}(1 - \psi) = -V \left[\left(\frac{A}{F}\right) + 1 \right] \frac{1}{[(A/F) + 1]^2} \left(\frac{A}{F}\right) \rho^2 \psi^2 Z' e^{-E/RT_R}$$

From the equation of state, by defining

$$B = \frac{Z'}{[(A/F) + 1]}$$

and substituting for $(1 - \psi)$ is this last expression, one obtains

$$\left(\frac{\dot{m}}{V}\right) = \left(\frac{A}{F}\right) \left(\frac{P}{RT_R}\right)^2 \left[\frac{(T_f - T_R)^2}{T_f - T_0} \right] \frac{Be^{-E/RT_R}}{T_R - T_0}$$

By dividing through by P^2 , one observes that

$$(\dot{m}/VP^2) = f(T_R) = f(A/F)$$

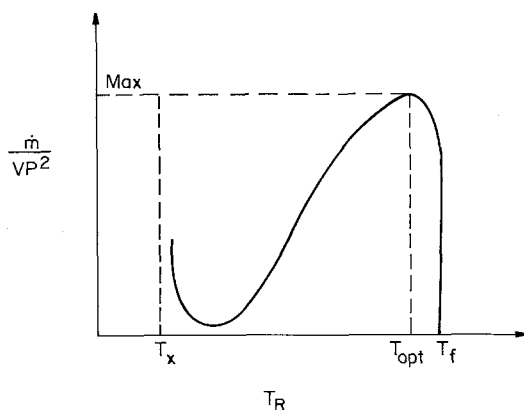


Fig. 42. Stirred reaction parameter (\dot{m}/VP^2) as a function of reactor temperature T_R .

This derivation was made as if the overall order of the air-fuel reaction were two. In reality, this order is found to be closer to 1.8. The development could have been carried out for arbitrary overall order n , which would give the result

$$(\dot{m}/VP^n) = f(T_R) = f(A/F)$$

A plot of (\dot{m}/VP^2) versus T_R reveals a multivalued graph that exhibits a maximum as shown in Fig. 42. The part of the curve in Fig. 42 that approaches the value T_x asymptotically cannot exist physically since the mixture could not be ignited at temperatures this low. In fact, the major part of the curve, which is to the left of T_{opt} , has no physical meaning. At fixed volume and pressure it is not possible for both the mass flow rate and temperature of the reactor to rise. The only stable region exists between T_{opt} to T_f . Since it is not possible to mix some unburned gases with the product mixture and still obtain the adiabatic flame temperature, the reactor parameter must go to zero when $T_R = T_f$.

The value of T_R , which gives the maximum value of (\dot{m}/VP^2), is obtained by maximizing the last equation. The result is

$$T_{R,opt} = \frac{T_f}{1 + (2RT_f/E)}$$

For hydrocarbons, the activation energy falls within a range of 30–40 kcal/mole and the flame temperature in a range of 2000–3000 K. Thus,

$$T_{R,opt}/T_f \sim 0.75$$

Stirred reactor theory reveals a fixed maximum mass loading rate for a fixed reactor volume and pressure. Any attempts to overload the system will

quench the reaction. Attempts have been made to determine chemical kinetic parameters from stirred reactor measurements; however, the usefulness of such measurements must be considered limited in nature. Firstly, the analysis is based on the assumption that a hydrocarbon-air system can be represented by a simple one-step overall order kinetic expression. Recent evidence would indicate that such an assumption is not realistic. Secondly, the analysis is based on the assumption of complete instantaneous mixing, which is impossible to achieve experimentally.

In a positive sense, however, it is worthy to note that the analysis does give the maximum overall energy release rate that is possible for a fuel-oxidizer mixture in a fixed volume and at a given pressure.

G. FLAME STABILIZATION IN HIGH-VELOCITY STREAMS

The values of laminar flame speeds for hydrocarbon fuels in air are rarely greater than 40 cm/sec. Hydrogen is unique in its flame velocity, which approaches 240 cm/sec. If one could attribute a turbulent flame speed to hydrocarbon mixtures, it would at most a few hundred centimeters per second. However, in many practical devices, such as ramjet and turbojet combustors in which high volumetric heat release rates are necessary, the flow velocities of the fuel-air mixture are of the order 50 m/sec. Furthermore for such velocities the boundary layers are too thin in comparison to the quenching distance for there to be stabilization by the same means as that which occurs in Bunsen burners. Thus, some other means for stabilization is necessary. In practice, the stabilization is accomplished by causing some of the combustion products to recirculate and to continually ignite the fuel mixture. Of course, the continuous ignition could be obtained by inserting small pilot flames. Since pilot flames are an added inconvenience and by themselves can blow out, they are generally not used in fast flowing turbulent streams.

Recirculation of combustion products can be obtained by inserting solid obstacles in the stream as pursued in ramjet technology (*bluff-body stabilization*); by directing part of the flow or one of the flow constituents, usually air, opposed or normal to the main stream, as in gas turbine combustion chambers (*aerodynamic stabilization*); or by a step in the wall enclosure, as used in the so-called dump combustors. These modes of stabilization are depicted in Fig. 43. Complete reviews of flame stabilization of premixed turbulent gases appear in Refs. [39,40].

Photographs of ramjet-type burners, which use rods as bluff obstacles, show that the regions behind the rods recirculate part of the flow that react to

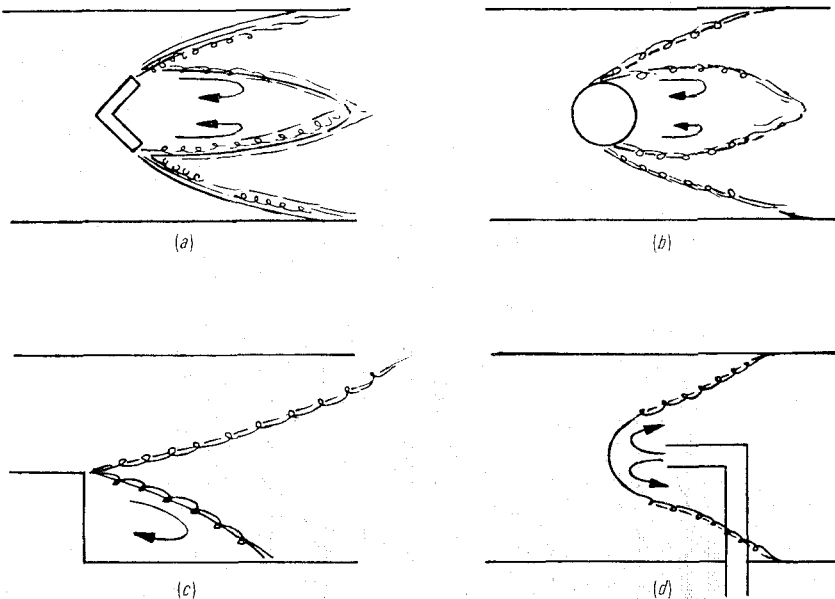


Fig. 43. Stabilization methods for high-velocity streams (a) vee gutter, (b) rod or sphere, (c) sudden expansion, and (d) opposed jet (after Strehlow, "Combustion Fundamentals," McGraw-Hill, New York, 1985).

form hot combustion products and, indeed, the wake region of the rod acts as a pilot flame. Nicholson and Field [41] very graphically showed this effect by placing small aluminum particles in the flow (Fig. 44). The wake pilot condition initiates flame spread. The flame spread process for a fully developed turbulent wake has been depicted [39] as shown in Fig. 45. The theory of flame spread in a uniform laminar flow downstream from a laminar mixing zone has been fully developed [12,39] and reveals that the angle of flame spread is $\sin^{-1}(S_L/U)$, where U is the main stream flow velocity. For a turbulent flame one approximates the spread angle by replacing S_L by an appropriate turbulent flame speed S_T . The limitations in defining S_T in this regard are described in Section D.

The types of obstacles used in stabilization of flames in high-speed flows could be rods, V gutters, toroids, disks, strips, etc. But in choosing the bluff body stabilizer, the designer must not only consider the maximum blow-off velocity the obstacle will permit for a given flow, but also pressure drop, cost, ease of manufacture, etc.

Since the combustion chamber should be of minimum length, it is rare that a single rod, toroid, etc., is used. In Fig. 46, a schematic of flames spreading from the flame holders is given. One can readily see that multiple units can

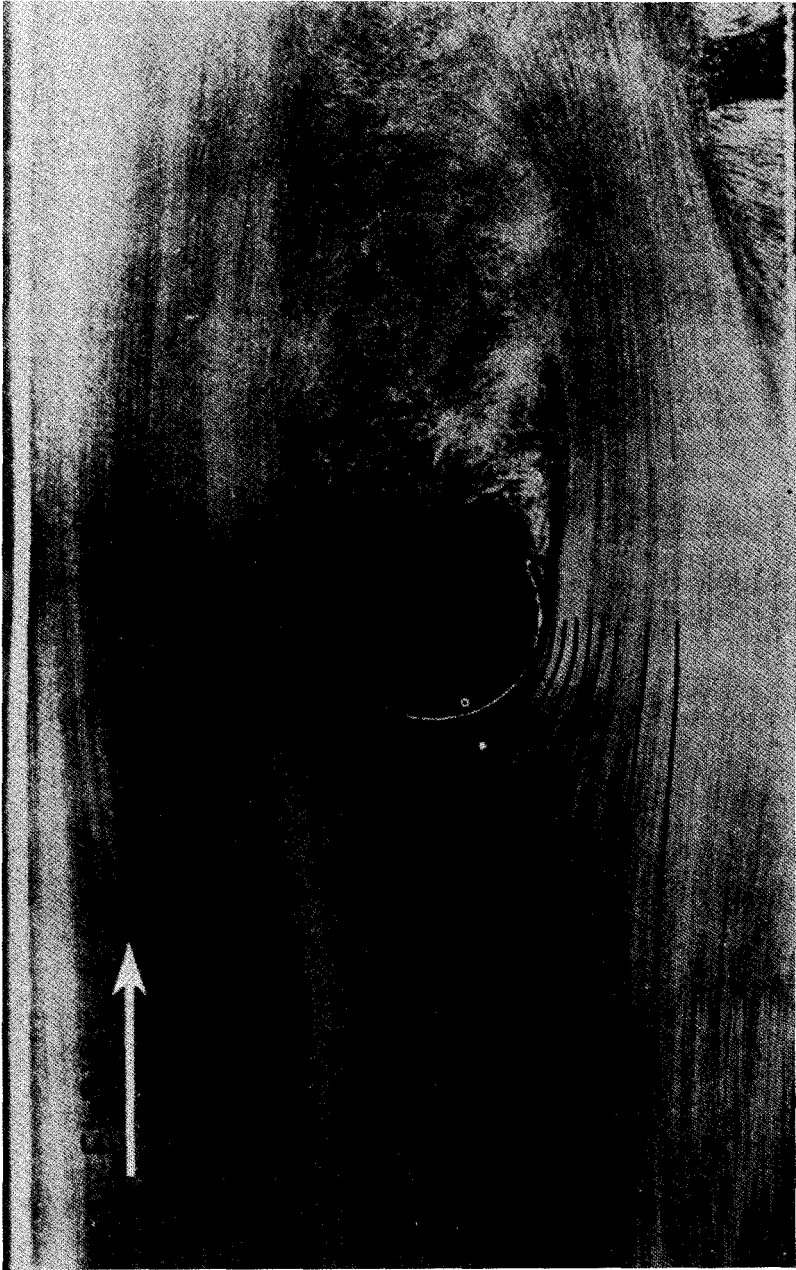


Fig. 44. Flow past a 0.5-cm rod at a velocity of 50 ft/sec as depicted by aluminum powder technique. Solid lines are flow streamlines of experimenters [41].

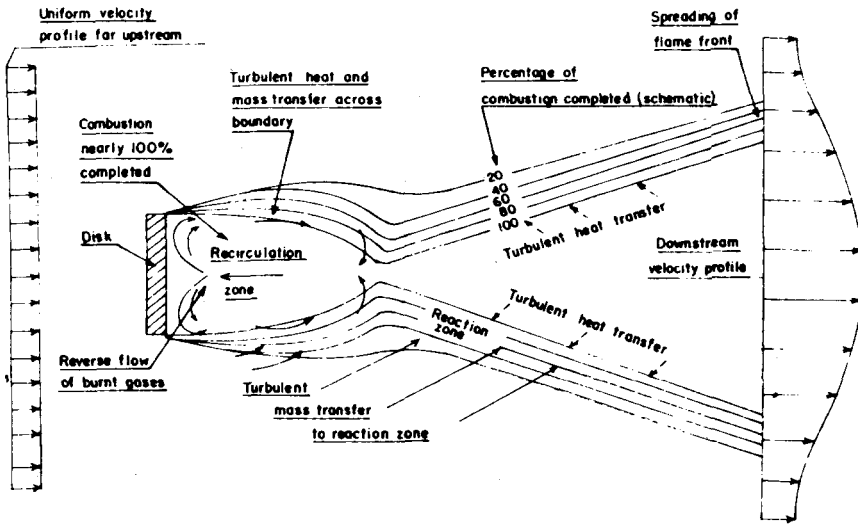


Fig. 45. Recirculation zone and flame-spreading region for a fully developed turbulent wake behind a bluff body (after Williams [39]).

appreciably shorten the length of the combustion chamber. However, flame holders cause a stagnation pressure loss across the burner, and this pressure loss must be added to the large-pressure drop due to burning. Thus, there is an optimum between the number of flame holders and pressure drop. It is sometimes difficult to use aerodynamic stabilization when large chambers are involved because the flow creating the recirculation would have to penetrate too far across the main stream. Bluff-body stabilization is not used in gas turbine systems because of the required combustor shape and the short lengths. In gas turbines a high weight penalty is paid for even the slightest increase in length. Because of reduced pressure losses, step stabilization is commanding current attention. A wall heating problem associated with this technique would appear solvable by some transpiration cooling.

In either case, bluff-body or aerodynamic, the primary concern is that of blowout. In ramjets, the smallest frontal dimension for the highest flow velocity to be used is desirable; in turbojets, it is the smallest volume of the

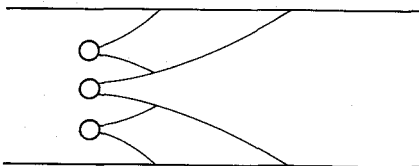


Fig. 46. Flame spreading interaction behind multiple bluff bodies.

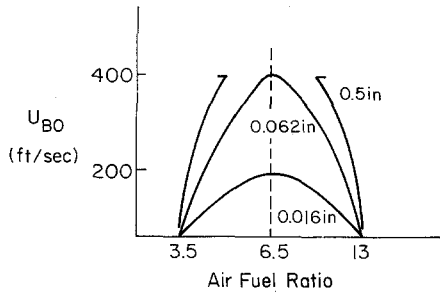


Fig. 47. Blowoff velocities for various rod diameters as a function of air-fuel ratio. Short duct using premixed fuel-air mixtures. Large-diameters data limited by choking of duct (after Scurlock [42]).

primary recirculation zone that is of concern; and in dump combustors, it is the least severe step.

There were many early experimental investigations of bluff-body stabilization. Most of this work [42] used premixed gaseous fuel-air systems and typically plotted the blowoff velocity as a function of the air-fuel ratio for various stabilizer sizes, as shown in Fig. 47. Early attempts to correlate the data appeared to indicate that the dimensional dependency of blow-off velocity was different for different bluff-body shapes. Later it was shown that the Reynold's number range of the experiments were different and that a simple independent dimensional dependency did not exist. Furthermore, the state of turbulence, the temperature of the stabilizer, incoming mixture temperature, etc., also had secondary effects. All these facts suggest that fluid mechanics play a significant role in the process.

Considering that fluid mechanics do play an important role, it is worth considering the cold flow field behind a bluff body (rod) in the region called the wake. Figure 48 depicts the various stages in the development of the wake as the Reynold's number of the flow is increased. In region (1), there is only a slight slowing behind the rod and a very slight region of separation. The heavy dot specifies the stagnation point. In region (2), eddies start to form and the stagnation points are as indicated. As the Reynold's number increases, the eddy (vortex) size increases and the downstream stagnation point moves farther away from the rod. In region (3), the eddies become unstable, shed alternately, as shown in the figure, and $(h/a) \sim 0.3$. As the velocity u increases, the frequency N of shedding increases; $N \sim 0.3 (u/d)$. In region (4), it is important to note that there is a complete turbulent wake behind the body. The stagnation point must pass 90° to about 80° and the boundary layer is also turbulent. The turbulent wake behind the body is eventually destroyed downstream by jet mixing.

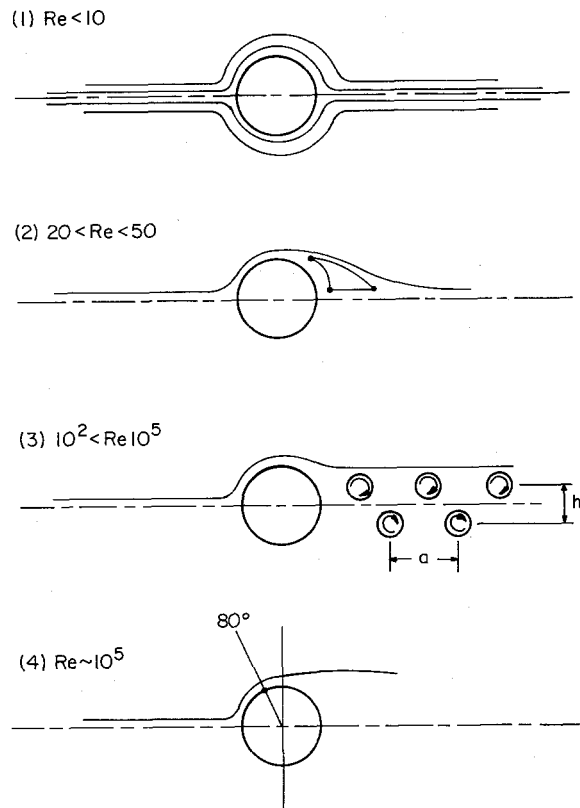


Fig. 48. Flow fields past rod obstacles.

The flow fields described in Fig. 48 are very specific in that they apply to cold flow over a cylindrical body. When spheres are immersed in a flow, region (3) does not exist. More striking however, is that when combustion exists over this Reynolds number range of practical interest, the shedding eddies disappear and a well-defined, steady vortex is established. The reason for this change in flow pattern between cold flow and a combustion situation is believed to be due to the increase in kinematic viscosity caused by the rise in temperature. Thus, the Reynold's number affecting the wake is drastically reduced, as discussed in the section of premixed turbulent flow. Thus, it would be expected that region (2) would extend from $10 < Re < 10^5$. Flame holding studies by Zukoski and Marble [43,44] showed that the ratio of the length of the wake (recirculation zone) to the diameter of the cylindrical flame holder was independent of the approach flow Reynold's number above a critical value of about 10^4 . These Reynold's numbers are based on the critical

dimension of the bluff body; that is, the diameter of the cylinder. Thus, it would appear that one could assume for approach flow Reynold's number greater 10^4 that a fully developed turbulent wake would exist during combustion.

Experiments [41] have shown that any original ignition source located upstream, near or at the flame holder, appears to establish a steady ignition position from which a flame spreads in the wake region immediately behind the stabilizer. This ignition position is created by the recirculation zone that contains hot combustion products near the adiabatic flame temperature [44]. The hot combustion products cause ignition by transferring heat across the mixing layer between the free-stream gases and the recirculation wake. Based on these physical concepts two early theories developed and correlated the existing data well. One was due to Spalding [45] and the other to Zukoski and Marble [43,44]. Another early theory of flame stabilization was due to Longwell *et al.* [46], who considered the wake behind the bluff-body as a stirred reactor zone.

Considering the wake of a flame holder as a stirred reactor may be inconsistent with experimental data. As blowoff is approached it has been shown [44] that the temperature of the recirculating gases remains essentially constant and further their composition is practically all products. Both of these observations are contrary to what one would expect from stirred reactor theory. The primary zone of a gas turbine combustor could possibly be considered to approach a state that could be considered completely stirred. Nevertheless, as will be shown, all three theories give essentially the same correlation.

Zukoski and Marble [43,44] considered the wake of a flame holder to establish a critical ignition time. Their experiments as indicated earlier established that the length of the recirculating zone was determined by the characteristic dimension of the stabilizer. At the blowoff condition, they assumed that the free-stream combustible mixture flowing past the stabilizer had a contact time equal to the ignition time associated with the mixture; i.e., $\tau_c = \tau_i$, where τ_c is the flow contact time and τ_i is the ignition time. Since the flow contact time is given by

$$\tau_c = L/U_{BO}$$

where L is the length of the recirculating wake and U_{BO} is the velocity at blowoff, they essentially postulated that blow off occurs when the Damkohler number has the critical value of 1; i.e.

$$Da = (L/U_{BO})(1/\tau_i) = 1$$

Since the length of the wake is proportional to the characteristic dimension of the stabilizer, the diameter d in the case of a rod, then

$$\tau_c \sim (d/U_{BO})$$

Thus it must follow that

$$(U_{BO}/d) \sim (1/\tau_i)$$

For second-order reactions, the ignition time is inversely proportional to the pressure. Writing the relation between pressure and time by referencing them to a standard pressure P_0 and time τ_0 , one has

$$(\tau_0/\tau_i) = (P/P_0)$$

where P is the actual pressure in the system of concern.

The ignition time is a function of the combustion (recirculating) zone temperature, which, in turn, is a function of the air-fuel ratio (A/F). Thus,

$$(U_{BO}/dP) \sim (1/\tau_0 P_0) = f(T) = f(A/F)$$

Spalding [45] considered the wake region as one of the steady-state heat transfer with chemical reaction. The energy equation with chemical reaction was developed and nondimensionalized. The solution for the temperature profile along the outer edge of the wake zone, which essentially heats the free stream through a mixing layer, was found to be a function of two nondimensional parameters that are functions of one another. Extinction or blowout was considered to exist when these dimensionless groups were not of the same order. Thus, the functional extinction condition could be written as

$$(U_{BO}d/\alpha) = f(Z'P^{n-1}d^2/\alpha)$$

where d is, again, the critical dimension, α the thermal diffusivity, Z' the pre-exponential in the Arrhenius rate constant, and n the overall reaction order.

From laminar flame theory, the relationship

$$S_L \sim (\alpha RR)^{1/2}$$

was obtained, so that the expression above could be modified by the relation

$$S_L \sim (\alpha Z'P^{n-1})^{1/2}$$

Since the final correlations have been written in terms of the air-fuel ratio, which also specifies the temperature, the temperature dependencies were omitted. Thus, a new proportionality could be written as

$$(S_L^2/\alpha) \sim Z'P^{n-1}$$

$$(Z'P^{n-1}d^2/\alpha) = (S_L^2d^2/\alpha^2)$$

and the original functional relation would then be

$$(U_{BO}d/\alpha) \sim f(S_Ld/\alpha) \sim (U_{BO}d/\nu)$$

Both correlating parameters are in the form of Peclet numbers and the air-fuel ratio dependency is in S_L . Figure 49 shows the excellent correlation

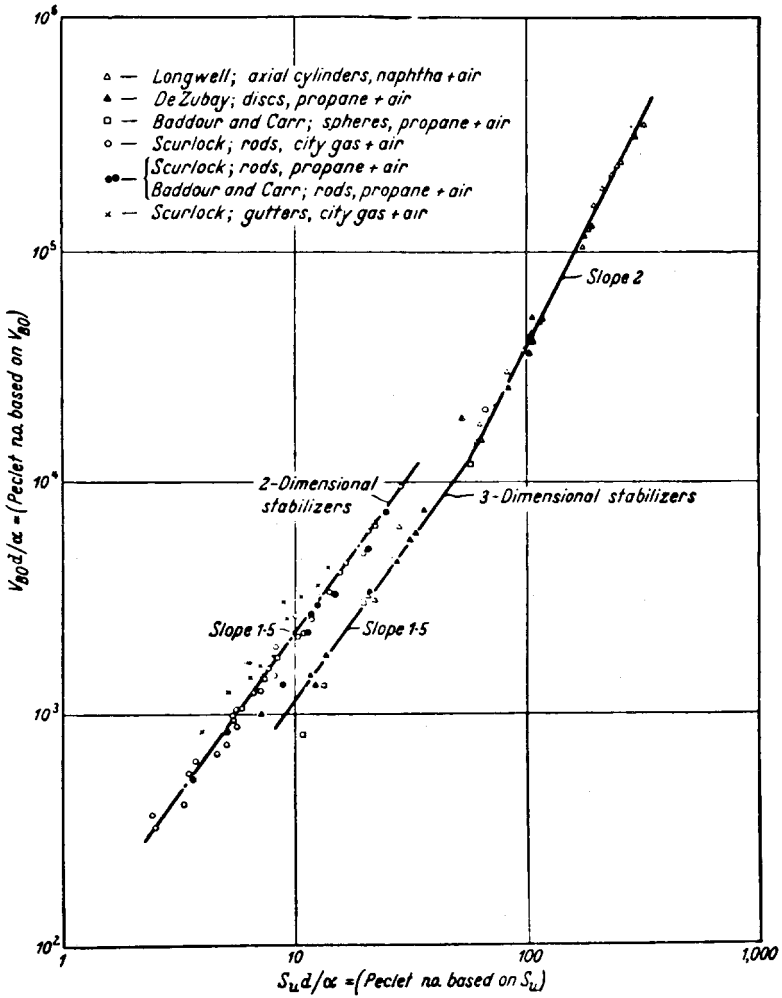


Fig. 49. Correlation of various blow-off velocity data by Spalding [45]; $V_{BO} = V_{BO}$, $S_u = S_L$.

of data by the above expression developed from the Spalding analysis. Indeed the power dependency of d with respect to blowoff velocity can be developed from the slopes of the lines in Fig. 49. Notice that the slope is two for values $(U_{BO}d/\alpha) > 10^4$, which was found experimentally to be the range in which a fully developed turbulent wake exists. The correlation in this region is that to be compared to the correlation developed from the work of Zukoski and Marble.

Stirred reactor theory was initially applied to stabilization in gas turbine combustor cans in which the primary zone was treated as a completely stirred

region. This theory has been sometimes extended to bluff-body stabilization even though aspects of the theory appear inconsistent with experimental measurements made in the wake of a flame holder. Nevertheless, it would appear that stirred reactor theory would give the same functional dependency as the other correlations developed. In the previous section, it was found from stirred reactor considerations that

$$(\dot{m}/VP^2) = f(A/F)$$

for second-order reactions. If \dot{m} is considered to be the mass entering the work and V its volume, then the following proportionalities can be written

$$\dot{m} = \rho AU \sim Pd^2U_{BO}, \quad V \sim d^3$$

where A is an area. Substituting these proportionalities in the stirred reactor result, one obtains

$$[(Pd^2U_{BO})/(d^3P^2)] = f(A/F) = (U_{BO}/dP)$$

which is the same result as that obtained by Zukoski and Marble. Indeed in the turbulent regime, Spalding's development also gives the same form since in this regime the correlation can be written as the equality

$$(U_{BO}d/\alpha) = \text{const}(S_L d/\alpha)^2$$

Then it follows that

$$(U_{BO}/d) \sim (S_L^2/\alpha) \sim P^{n-1}f(T) \quad \text{or} \quad (U_{BO}/dP^{n-1}) \sim f(T)$$

Thus, for a second-order reaction

$$(U_{BO}/dP) \sim f(T) \sim f(A/F)$$

From these correlations it would be natural to expect that the maximum blow-off velocity as a function of air-fuel ratio would occur at the stoichiometric mixture ratio. For premixed gaseous fuel-air systems, the maxima do occur at this mixture ratio as shown in Fig. 47. However, in real systems in order to allow for mixing liquid fuels are injected upstream of the bluff-body flame holder. Results [47] for such liquid injection systems show that the maximum blow-off velocity is obtained on the fuel-lean side of stoichiometric. This trend is readily explained by the fact that liquid droplets impinge on the stabilizer and enrich the wake. Thus, a stoichiometric wake undoubtedly occurs for a lean upstream liquid-fuel injection system. That the wake can be modified to alter blow-off characteristics was proven by experiments due to Fetting *et al.* [47]. The trends of these experiments can be explained by the correlations developed in this section.

Recesses in combustor walls when designed to have sharp leading edges cause flow separation as shown in Fig. 43. During combustion the separated regions establish recirculation zones of hot combustion products much like the wake of bluff-body stabilizers. Studies [48] of turbulent propane-air mixtures stabilized by wall recesses in a rectangular duct showed stability limits significantly wider than a gutter bluff-body flame holder and lower-pressure drops. The observed blowoff limits for a variety of symmetrically located wall recesses showed [39] substantially the same results provided: (1) the recess was of sufficient depth to support an adequate amount of recirculating gas, (2) the slope of the recess at the upstream end was sharp enough to produce separation, and (3) the geometric construction of the recess lip was such that flow oscillations were not induced.

The criterion for blow off from recesses is essentially the same as that developed for bluff bodies and L is generally taken to be the length of the recess [48]. The length of the recess essentially serves the same function as the length of the bluff-body recirculation zone unless the length is large enough for flow attachment to occur within the recess and then the recirculation length depends on the depth of the recess [12]. This latter condition applies to the so-called dump combustor, in which a duct with a small cross-sectional area exhausts coaxially with a right-angle step into a duct with a larger cross section. The recirculation zone forms at the step.

There appears to be two major disadvantages with recess stabilization. The first is due to the large increase in heat transfer in the step area and the second to flame spread angles smaller than those obtained with bluff bodies. Smaller flame spread angles demand longer combustion chambers.

Establishing a criteria for blowoff during opposed jet stabilization is difficult due to the sensitivity of the recirculation region formed to its stoichiometry. This stoichiometry is well defined only if the main stream and opposed jet compositions are the same. Since the combustor pressure drop is of the same order as that found with bluff bodies [49], the utility of this means of stabilization is questionable.

PROBLEMS

1. A stoichiometric fuel-air mixture flowing in a Bunsen burner forms a well-defined conical flame. The mixture is then made leaner. For the same flow velocity in the tube, how does the cone angle change for the leaner mixture; that is, does it become larger or smaller than the angle for the stoichiometric mixture? Explain.
2. Sketch a temperature profile that would exist in a one-dimensional laminar flame. Superimpose on this profile a relative plot of what the rate of energy release would be through the flame

as well. Below the inflection point in the temperature profile, large amounts of HO_2 are found. Explain why. If flame was due to a first-order, one-step decomposition reaction, could rate data be obtained directly from the existing temperature profile?

3. In which of the two cases would the laminar flame speed be greater: (1) oxygen in a large excess of a wet equal molar $\text{CO}-\text{CO}_2$ mixture or (2) oxygen in a large excess of a wet equal molar $\text{CO}-\text{N}_2$ mixture? Both cases are ignitable, contain the same amount of water and have the same volumetric oxygen-fuel ratio. Discuss the reasons for the selection made.

4. A gas mixture is contained in a soap bubble and ignited by a spark in the center so that a spherical flame spreads radially through the mixture. It is assumed that the soap bubble can expand. The growth of the flame front along a radius is followed by some photographic means. Relate the velocity of the flame front as determined from the photographs to the laminar flame speed as defined in the text. If this method were used to measure flame speeds, what would be its advantages and disadvantages?

5. On what side of stoichiometric would you expect the maximum flame speed of hydrogen-air mixtures? Why?

6. A laminar flame propagates through a combustible mixture in a horizontal tube 3 cm in diameter. The tube is open at both ends. Due to buoyancy effects the flame tilts at a 45° angle to the normal and is planar. The normal laminar flame speed for the combustible mixture is 40 cm/sec. If the unburned gas mixture has a density of 0.015 gm/cm^3 , what is the mass burning rate of the mixture in grams per second under this laminar flow condition?

7. The flame speed for a combustible hydrocarbon-air mixture is known to be 30 cm/sec. The activation energy of such hydrocarbon reactions is generally assumed to be 40 kcal/mole. The true adiabatic flame temperature for this mixture is known to be 1600 K. An inert diluent is added to the mixture to lower the flame temperature to 1450 K. Since the reaction is of second order, the addition of the inert can be considered to have no other effect on any property of the system. Estimate the flame speed after the diluent is added.

8. A horizontal long tube 3 cm in diameter is filled with a mixture of methane and air in stoichiometric proportions at 1 atm pressure and 27°C . The column is ignited at the left end and a flame propagates at uniform speed from left to right. At the left end of the tube there is a convergent nozzle which has a 2-cm diameter opening. At the right end there is a similar nozzle 0.3 cm in diameter at the opening. Calculate the velocity of the flame with respect to the tube in cm/sec. Assume the following:

- The effect of pressure increase on the burning velocity can be neglected; similarly, the small temperature increase due to adiabatic compression has a negligible effect.
- The entire flame surface consumes combustible gases at the same rate as an ideal one-dimensional flame.
- The molecular weight of the burned gases equals that of the unburned gases.
- The flame temperature is 2100 K.
- The normal burning velocity at stoichiometric is 40 cm/sec.

Hint: Assume that the pressure in the burned gases is essentially 1 atm. In calculating the pressure in the cold gases make sure the value is correct to many decimal places.

9. A continuous flow stirred reactor operates off the decomposition of gaseous ethylene oxide fuel. If the fuel injection temperature is 300 K, the volume of the reactor 1500 cm^3 , and the operating pressure is 20 atm, calculate the maximum rate of heat evolution possible in the

reactor. Assume that the ethylene oxide follows homogeneous first-order reaction kinetics and that values of the reaction rate constant k are

$$\begin{aligned}k &= 3.5 \text{ sec}^{-1} \text{ at } 890 \text{ K} \\k &= 50 \text{ sec}^{-1} \text{ at } 1000 \text{ K} \\k &= 600 \text{ sec}^{-1} \text{ at } 1150 \text{ K}\end{aligned}$$

Develop any necessary rate data from these values. You are given that the adiabatic decomposition temperature of gaseous ethylene oxide is 1300 K. The heat of formation of gaseous ethylene oxide at 300 K is -12.2 kcal/mole.

10. What are the essential physical processes that determine the flammability limit? Why is the lean limit essentially pressure insensitive?

11. It is desired to measure the laminar flame speed at 273 K of a homogeneous gas mixture by the burner tube method. If the mixture to be measured is 9% natural gas in air, what size would you make the tube diameter? Natural gas is mostly methane. The laminar flame speed of the mixture can be taken to be 34 cm/sec at 298 K. Other required data can be found in standard reference books.

12. A ramjet has a flame stabilized in its combustion chamber by a single rod whose diameter is 1.25 cm. The mass flow of the unburned fuel-air mixture entering the combustion chamber is 22.5 kg/sec, which is the limit amount that can be stabilized at a combustor pressure of 3 atm for the cylindrical configuration. The ramjet is redesigned to fly with the same fuel-air mixture and a mass flow rate twice the original mass flow in the same size (cross section) combustor. The inlet diffusion is such that the temperature entering the combustor is the same as in the original case, but the pressure has dropped to 2 atm. What is the minimum size rod that will stabilize the flame under these new conditions?

13. A laminar flame propagates through a combustible mixture at 1 atm pressure, has a velocity of 50 cm/sec and a mass burning rate of 0.1 gm/sec cm². The overall chemical reaction rate is second order in that it depends only on the fuel and oxygen concentrations. Now consider a turbulent flame propagating through the same combustible mixture at a pressure of 10 atm. In this situation the turbulent intensity is such that the thermal diffusivity is ten times the laminar diffusivity. Estimate the turbulent flame propagation and mass burning rates.

14. Discuss the difference between explosion limits and flammability limits. Why is the lean flammability limit the same for both air and oxygen?

15. Explain briefly why halogen compounds are effective in altering flammability limits.

REFERENCES

1. Bradley, J. N., "Flame and Combustion Phenomena," Chapter 3, Methuen, London, 1969.
2. Westbrook, C. K., and Dryer, F. L., *Prog. Energy Combust. Sci.* **10**, 1 (1984).
3. Mallard, E., and Le Chatelier, H. L., *Ann. Mines* **4**, 379 (1983).
4. Semenov, N. N., *NACA Tech. Memo.* No. 1282 (1951).
5. Lewis, B., and von Elbe, G., "Combustion, Flames and Explosion of Gases," 2nd ed., Chapter 5, Academic Press, New York (1961).
6. Tanford, C., and Pease, R. N., *J. Chem. Phys.* **15**, 861 (1947).
7. Hirschfelder, J. O., Curtiss, C. F., and Bird, R. B., "The Molecular Theory of Gases and Liquids," Chapter 11, Wiley, New York, 1954.

8. Friedman, R., and Burke, E., *J. Chem. Phys.* **21**, 710 (1953).
9. Von Karman, T., and Penner, S. S., "Selected Combustion Problems" (AGARD Combust. Colloq.), p. 5, Butterworth, London, 1954.
10. Zel'dovich, Y. B., Barenblatt, G. I., Librovich, V. B., and Makviladze, G. M., "The Mathematical Theory of Combustion and Explosions," Nauka, Moscow, 1980.
11. Buckmaster, J. D., and Ludford, G. S. S., "The Theory of Laminar Flames," Cambridge Univ. Press, Cambridge, Massachusetts, 1982.
12. Williams, F. A., "Combustion Theory," 2nd ed., Benjamin-Cummings, Menlo Park, California, 1985.
13. Gerstein, M., Levine, O., and Wong, E. L., *J. Am. Chem. Soc.* **73**, 418 (1951).
14. Flock, E. S., Marvin, C. S., Jr., Caldwell, F. R., and Roeder, C. H., *NACA Rep.* No. 682 (1940).
15. Powling, J., *Fuel* **28**, 25 (1949).
16. Spalding, D. B., and Botha, J. P., *Proc. R. Soc. London A* **225**, 71 (1954).
17. Fristrom, R. M., and Westenberg, A. A., "Flame Structure," Chapters VI and VII, McGraw-Hill, New York, 1965.
18. Hottel, H. C., Williams, G. C., Nerheim, N. M., and Schneider, G. R., *Int. Symp. Combust.* p. 111, Combustion Inst., Pittsburgh, Pennsylvania, 1965.
19. *NACA Rep.* No. 1300, Chapter IV (1959).
20. Zebatakis, K. S., *U. S. Bur. Mines Bull.* No. 627 (1965).
21. Gibbs, G. J., and Calcote, H. F., *J. Chem. Eng. Data* **5**, 226 (1959).
22. Clingman, W. H., Jr., Brokaw, R. S., and Pease, R. D., *Int. Symp. Combust.* 24th, p. 310, Williams and Wilkins, Baltimore, 1953.
23. Leason, D. B., *Int. Symp. Combust.* 4th, p. 369, Williams and Wilkins, Baltimore, 1953.
24. Coward, H. F., and Jones, O. W., *U. S. Bur. Mines Bull.* No. 503 (1951).
25. Spalding, D. B., *Proc. R. Soc. London A* **240**, 83 (1957).
26. Bilger, R. W., Turbulent flows with nonpremixed reactants in "Turbulent Reacting Flows" (P. A. Libby and F. A. Williams, eds.), p. 65, Springer-Verlag, Berlin, 1980.
27. Libby, P. A., and Williams, F. A., Fundamental aspects, *ibid.*, p. 1.
28. Bray, K. N. C., Turbulent flows with premixed reactants, *ibid.*, p. 115.
29. Darrieus, G., "Propagation d'un Front de Flamme," Congrès de Mécanique Appliquée, Paris, 1945.
30. Landau, L. D., *Acta Physicochem. URSS* **19**, 77(1944).
31. Markstein, G. H., *J. Aeronaut. Sci.* **18**, 199 (1951).
32. Klimov, A. M., *Zh. Prikl. Mekh. Tekh. Fiz.* **3**, 49 (1963).
33. Williams, F. A., *Combust. Flame* **26**, 269 (1976).
34. Damkohler, G., *Z. Elektrochem.* **46**, 601 (1940).
35. Summerfield, M., Reiter, S. H., Kibeley, V., and Mascolo, R. W., *Jet Propul.* **25**, 377 (1955).
36. Schelkin, K. I., *NACA Tech. Memo.* No. 1110 (1947).
37. Clavin, P., and Williams, F. A., *J. Fluid Mech.* **90**, 589 (1979).
38. Longwell, J. P., and Weiss, M. A., *Ind. Eng. Chem.* **47**, 1634 (1955).
39. Williams, F. A., Flame stabilization in premixed turbulent gases, in "Applied Mechanics Surveys" (N. N. Abramson, H. Liebowitz, J. M. Crowley, and S. Juhasz, eds.), p. 1158, Spartan Books, Washington, D.C., 1966.
40. Edelman, R. B., and Harsha, P. T., *Prog. Energy Combust. Sci.* **4**, 1 (1978).
41. Nicholson, H. M., and Fields, J. P., *Int. Symp. Combust.*, 3rd, p. 44, Combustion Inst. Pittsburgh, Pennsylvania, 1949.
42. Scurlock, A. C., *M.I.T. Fuel Res. Lab. Meterol. Rep.* No. 19 (1948).
43. Zukoski, E. E., and Marble, F. E., "Combustion Research and Reviews," p. 167, Butterworth, London, 1955.

44. Zukoski, E. E., and Marble, F. E., *Proc. Gas Dyn. Symp. Aerothermochem.*, p. 205, Northwestern Univ., Evanston, Illinois, 1956.
45. Spalding, D. B., "Some Fundamentals of Combustion," Chapter 5, Butterworth, London, 1955.
46. Longwell, J. P., Frost, E. E., and Weiss, M. A., *Ind. Eng. Chem.* **45**, 1629 (1953).
47. Fetting, F., Choudbury, A. P. R., and Wilhelm, R. H., *Int. Symp. Combust., 7th*, p. 621, Combustion Inst., Pittsburgh, Pennsylvania, 1959.
48. Choudbury, P. R., and Cambel, A. B., *Int. Symp. Combust.*, p. 743, Williams and Wilkins, Baltimore, 1953.
49. Putnam, A. A., *Jet Propul.* **27**, 177 (1957).

Detonation

A. INTRODUCTION

Established usage of certain terms related to combustion phenomena can be misleading, for what appear to be synonyms are not really so. Before proceeding with the topic of detonation, there will be a slight discourse into the semantics of combustion, with some brief mention of subjects to be covered later.

1. Premixed and Diffusion Flames

The previous chapter covered primarily laminar flame propagation. By inspecting the details of the flow, particularly, high-speed or higher Reynold's number flow, it was possible to consider the subject of turbulent flame propagation. These subjects (laminar and turbulent flames) are concerned with gases in the premixed state only. The material presented, generally, is not adaptable to the consideration of the combustion of liquids, solids, or systems in which the gaseous reactants diffuse towards a common reacting front.

Diffusion flames can best be described as the combustion state controlled by mixing phenomena, i.e., the diffusion of fuel into oxidizer, or vice versa, until some flammable mixture ratio is reached. According to the flow state of the individual diffusing species, the situation may be either laminar or

turbulent. It will be shown later that there are gaseous diffusion flames, that liquid burning proceeds by a diffusion mechanism and that the combustion of solids and of some solid propellants falls in this category as well.

2. Explosion, Deflagration, and Detonation

Explosion is a term that corresponds to rapid heat release (or pressure rise). An explosive gas or gas mixture is one which will permit rapid energy release, as compared to most steady, low-temperature reactions. Certain gas mixtures (fuel and oxidizer) will not propagate a burning zone or combustion wave. These gas mixtures are said to be outside the flammability limits of the explosive gas.

Depending upon whether the combustion wave is a deflagration or detonation, there are limits of flammability or detonation.

In general, the combustion wave is considered as a deflagration only, although the detonation wave is another class of the combustion wave. The detonation wave is in all essence a shock wave that is sustained by the energy of the chemical reaction in the highly compressed explosive medium existing in the wave. Thus, a deflagration is a subsonic wave sustained by a chemical reaction and a detonation is a supersonic wave sustained by chemical reaction. In the normal sense, it is the general practice to call a combustion wave a flame, so combustion wave, flame, and deflagration have been used interchangeably.

It is a very common error to confuse a pure explosion and a detonation. An explosion does not necessarily require the passage of a combustion wave through the exploding medium, whereas an explosive gas mixture must exist in order to have either a deflagration or a detonation. That is, deflagrations and detonations require rapid energy release, but explosions do not require the presence of a waveform.

The difference between deflagration and detonation is described qualitatively, but extensively, by Table 1 (from Friedman [1]).

3. The Onset of Detonation

Depending upon various conditions an explosive medium may support either a deflagration or a detonation wave. The most obvious conditions are confinement, mixture ratio, and ignition source.

Original studies of gaseous detonation have shown no single sequence of event due primarily to what is now known to be the complex cellular

TABLE 1

Qualitative differences between
detonations and deflagration in gases

Ratio	Usual magnitude of ratio	
	Detonation	Deflagration
u_w/c_u^a	5-10	0.0001-0.03
u_b/u_u	0.4-0.7	4-16
P_b/P_u	13-55	0.98-0.976
T_b/T_u	8-21	4-16
ρ_b/ρ_u	1.4-2.6	0.06-0.25

^a c_u is the acoustic velocity in the unburned gases. u_w/c_u is the Mach number of the wave.

structure of a detonation wave. The primary result of an ordinary thermal initiation always appears to be a flame that propagates with subsonic speed. When conditions are such that the flame causes adiabatic compression of the still unreacted mixture ahead of it, the flame velocity increases. In some early observations, the speed of the flame seems to rise gradually until it equals that of a detonation wave. Normally, a discontinuous change of velocity is observed from the low flame velocity to the high speed of detonation. In still other observations, the detonation wave has been observed to originate apparently spontaneously some distance ahead of the flame front. The place of origin appeared to coincide with the location of a shock wave sent out by the expanding gases of the flame. Modern experiments and analysis have shown that these seemingly divergent observations were in part due to the mode of initiation. In detonation phenomena one can consider that two modes of initiation exist: a slow mode, in which there is transition from deflagration, and sometimes called thermal initiation, and a fast mode brought about by an ignition blast or strong shock wave. Some [2] refer to these modes as self-ignition and direct ignition, respectively.

A tube containing an explosive gas mixture and having one or both ends open will permit a combustion wave to propagate when ignited at the open end. This wave attains a steady velocity and does not accelerate to a detonation wave.

If the mixture is ignited at the closed end, a combustion wave is formed and, if the tube is long enough, this wave can accelerate and lead to a detonation. This thermal initiation mechanism is described as follows. The burned gas products from the initial deflagration have a specific volume of

the order of 5–15 times that of the unburned gases ahead of the flame. Since each preceding compression wave tends to heat the unburned gas mixture somewhat, the sound velocity increases and the succeeding waves catch up with the initial one. Furthermore, the preheating tends to increase the flame speed, which then accelerates the unburned gas mixture even further to a point where turbulence is developed in the unburned gases. Then, a still greater velocity, acceleration of the unburned gases and compression waves are obtained. This sequence of events forms a shock that is strong enough to ignite the gas mixture ahead of the front. The reaction zone behind the shock sends forth a continuous compression wave that keeps the shock front from decaying and a detonation is obtained. At the point of shock formation a detonation forms and propagates back into the burned gases [2,3]. Transverse vibrations associated with the onset of detonation have been noticed and contributed to known cellular structure of the detonation wave. Photographs of the onset of detonation have been taken by Oppenheim and co-workers [3] using a stroboscopic-laser schlieren technique.

The reaction zone in a detonation wave is no different from that in other flames, in that it supplies the sustaining energy. A difference does exist in that the detonation front initiates chemical reaction by compression, both by diffusion of heat and species, and, thus, inherently maintains itself. A further, but not essential, difference worth noting is that the reaction takes place in highly compressed and preheated gases with extreme rapidity.

The transition length for deflagration to detonation is of the order of a meter for highly reactive fuels such as acetylene, hydrogen, and ethylene, but many orders of magnitudes larger for most other hydrocarbon–air mixtures. Consequently, one finds most laboratory results for detonation reported for acetylene and hydrogen. Obviously this transition length is governed by many physical and chemical aspects of the experiments. Such elements of overall chemical composition, physical aspects of the detonation tube, initiation/ignition characteristics can all play a role. Interestingly there is some question whether methane will detonate at all.

According to Lee [2] direct initiation of a detonation can occur only when a strong shock wave is generated by a source and this shock retains a certain minimum strength for some required duration. Under these conditions “the blast and reaction front are always coupled in form of a multiheaded detonation wave that starts at the (ignition) source and expands at about the detonation velocity [2].” Because of the coupling phenomena necessary, it is apparent that reaction rates play a role in whether a detonation is established or not. Thus, initiation energy is one of the dynamic detonation parameters discussed in the next section. However no clear quantitative or qualitative analysis exists for determining this energy and this aspect of the detonation problem will not be discussed further.

B. DETONATION PHENOMENA

Scientific studies of detonation phenomena date back to the end of the last century and persist as an active field to the time of this writing. A wealth of literature has developed over this period and no detailed reference list will be presented. For details and extensive references the reader is referred to books on detonation phenomena [4], Williams' book on combustion [5], and the review by Lee [6].

Since the detonation phenomena to be considered here will deal extensively with premixed combustible gases, it is appropriate to introduce much of the material initially by comparison with deflagration phenomena. As will be noted from the data in Table 1, deflagration speeds are orders of magnitude less than those of detonation. The simple solution for laminar flame speeds given in Chapter 4 were obtained by essentially starting with the integrated conservation and state equations. However, by establishing the Hugoniot relations and developing a Hugoniot plot, it was shown that deflagration waves were in the very low Mach number regime and then it was assumed that the momentum equation degenerates and the situation through the wave is one of essentially uniform pressure. The degeneration of the momentum equation assures that the wave velocity to be obtained from the integrated equations used will be small. In order to obtain a deflagration solution, it was necessary to have some knowledge of the wave structure and the chemical reaction rates that affected this structure.

As will be shown the steady solution for the detonation velocity does not involve any knowledge of the structure of the wave. The Hugoniot plot discussed in Chapter 4 established that detonation is a large Mach number phenomenon. It is apparent then that the integrated momentum equation is included in obtaining a solution for the detonation velocity. However, it was also noted that the integrated conservation and state equations were four in number and there were five unknowns. Thus, other considerations were necessary to solve for the velocity. Concepts put forth by Chapman [7] and Jouget [8] provided the additional insights that permitted the mathematical solution to the detonation velocity problem. The solution from the integrated conservation equations are obtained by assuming the detonation wave to be steady, planar, and one dimensional, and the approach is called Chapman-Jouget theory. Chapman and Jouget established for these conditions that the flow behind the supersonic detonation is sonic and the point on the Hugoniot that represents this condition and the other physical conditions of this state are called Chapman-Jouget point and conditions, respectively. What is unusual about the Chapman-Jouget solution is that, unlike the deflagration problem, no knowledge of the structure of the detonation wave

is necessary and equilibrium thermodynamic calculations for the Chapman-Jouguet state suffice. As will be shown, the detonation velocities which result from this theory agree very well with experimental observations, and even in near limit conditions when the flow structure near the flame front is highly three dimensional [6].

Reasonable models for the detonation wave structure had been presented by Zeldovich [9], von Neumann [10], and Döring [11]. Essentially they constructed the detonation wave to be a planar shock followed by a reaction zone initiated after an induction delay. This structure is generally referred to as the ZND model and will be discussed further in a later section.

As in consideration of deflagration phenomena, there are other parameters that are of import in detonation research. These parameters are detonation limits, initiation energy, critical tube diameter, quenching diameter, and thickness of the supporting reaction zone, and they require just as in deflagration theory, a knowledge of the wave structure and, thus, chemical reaction rates. Lee [6] refers to these parameters as "dynamic" to distinguish them from the equilibrium "static" detonation states, which permit the calculation of the detonation velocity by Chapman-Jouguet theory.

Calculation of the dynamic parameters using a ZND wave structure model are not in agreement with experimental measurements due mainly to the fact that the ZND structure is unstable and is never observed experimentally except under transient conditions. This disagreement is not surprising since there are numerous experimental observations which show that all self-sustained detonations have a three-dimensional cell structure that comes about because reacting blast "wavelets" collide with each other to form a series of waves transverse to the direction of propagation. There presently are no suitable theories that define this three-dimensional cell structure.

The next section deals with the calculation of the detonation velocity based on Chapman-Jouguet theory. The subsequent section discusses the ZND model in detail and the last deals with the dynamic detonation parameters.

C. HUGONIOT RELATIONS AND THE HYDRODYNAMIC THEORY OF DETONATIONS

If one is to consider the approach to calculating the steady, planar, one-dimensional gaseous detonation velocity, then a system configuration similar to that given in Chapter 4 should be considered. For the configuration given there, it is important to establish an understanding of the various velocity symbols used. Reference should then be made here to Fig. 1, which defines the appropriate velocities. With these velocities the integrated conservation and

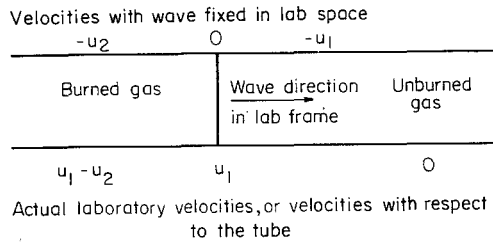


Fig. 1. Velocities in the detonation problem.

state equations are, as before, written as

$$\rho_1 u_1 = \rho_2 u_2 \quad (1)$$

$$P_1 + \rho_1 u_1^2 = P_2 + \rho_2 u_2^2 \quad (2)$$

$$c_p T_1 + \frac{1}{2} u_1^2 + q = c_p T_2 + \frac{1}{2} u_2^2 \quad (3)$$

$$P_1 = \rho_1 R T_1, \quad (\text{connects known variables}) \quad (4)$$

$$P_2 = \rho_2 R T_2$$

This type of representation considers that all combustion events are collapsed into discontinuity (the wave). Thus, the unknowns are u_1 , u_2 , ρ_2 , T_2 , and P_2 . Since there are four equations and five unknowns, an eigenvalue cannot be obtained. Experimentally it is found that the detonation velocity is uniquely constant for a given mixture. In order to determine all unknowns, it is necessary to know something about the internal structure (rate of reaction), or to obtain another necessary condition.

1. Characterization of the Hugoniot Curve and the Uniqueness of the Chapman-Jouguet Point

The method of obtaining a unique solution, or the elimination of many of the possible solutions, will be deferred at present. In order to establish the argument for the nonexistence of various solutions, it is best to pinpoint or define the various velocities that arise in the problem and then to develop certain relationships that will prove convenient.

First, one proceeds to calculate expressions for the velocities u_1 and u_2 . From Eq. (1),

$$u_2 = (\rho_1/\rho_2)u_1$$

Substituting in Eq. (2), we have

$$\rho_1 u_1^2 - (\rho_1^2/\rho_2)u_1^2 = (P_2 - P_1)$$

Dividing by ρ_1^2 , we obtain

$$u_1^2 \left(\frac{1}{\rho_1} - \frac{1}{\rho_2} \right) = \frac{P_2 - P_1}{\rho_1^2}, \quad u_1^2 = \frac{1}{\rho_1^2} \left[(P_2 - P_1) / \left(\frac{1}{\rho_1} - \frac{1}{\rho_2} \right) \right] \quad (5)$$

It is to be noted that Eq. (5) is the equation of the Rayleigh line and can also be derived without involving any equation of state. Since $(\rho_1 u_1)^2$ is always a positive value, it follows that if $\rho_2 > \rho_1$, $P_2 > P_1$, and vice-versa. Since the sound speed c can be written as

$$c_1^2 = \gamma R T_1 = \gamma P_1 (1/\rho_1)$$

where γ is the ratio of specific heats,

$$\gamma M_1^2 = \left(\frac{P_2}{P_1} - 1 \right) / \left[1 - \frac{(1/\rho_2)}{(1/\rho_1)} \right] \quad (5')$$

Substituting Eq. (5) into Eq. (1), one obtains

$$u_2^2 = \frac{1}{\rho_2^2} \left[(P_2 - P_1) / \left(\frac{1}{\rho_1} - \frac{1}{\rho_2} \right) \right] \quad (6)$$

and

$$\gamma M_2^2 = \left(1 - \frac{P_1}{P_2} \right) / \left[\frac{(1/\rho_1)}{(1/\rho_2)} - 1 \right] \quad (6')$$

A relationship, which is used throughout these developments, is called the Hugoniot equation and is developed as follows. Recall

$$c_p/R = \gamma/(\gamma - 1), \quad c_p = R[\gamma/(\gamma - 1)]$$

Substituting in Eq. (3), one obtains

$$R[\gamma/(\gamma - 1)]T_1 + \frac{1}{2}u_1^2 + q = R[\gamma/(\gamma - 1)]T_2 + \frac{1}{2}u_2^2$$

Implicit in writing the equation in this form is the assumption that c_p and γ are constant throughout. Since $RT = P/\rho$, then

$$\frac{\gamma}{\gamma - 1} \left(\frac{P_2}{\rho_2} - \frac{P_1}{\rho_1} \right) - \frac{1}{2}(u_1^2 - u_2^2) = q \quad (7)$$

One then obtains from Eqs. (5) and (6)

$$\begin{aligned} u_1^2 - u_2^2 &= \left(\frac{1}{\rho_1^2} - \frac{1}{\rho_2^2} \right) \left[\frac{P_2 - P_1}{(1/\rho_1) - (1/\rho_2)} \right] = \frac{\rho_2^2 - \rho_1^2}{\rho_1^2 \rho_2^2} \left[\frac{(P_2 - P_1)}{(1/\rho_1) - (1/\rho_2)} \right] \\ &= \left(\frac{1}{\rho_1^2} - \frac{1}{\rho_2^2} \right) \left[\frac{(P_2 - P_1)}{(1/\rho_1) - (1/\rho_2)} \right] = \left(\frac{1}{\rho_1} + \frac{1}{\rho_2} \right) (P_2 - P_1) \end{aligned} \quad (8)$$

Substituting Eq. (8) into Eq. (7), one obtains the Hugoniot equation

$$\frac{\gamma}{\gamma - 1} \left(\frac{P_2}{\rho_2} - \frac{P_1}{\rho_1} \right) - \frac{1}{2} (P_2 - P_1) \left(\frac{1}{\rho_1} + \frac{1}{\rho_2} \right) = q \quad (9)$$

This relationship, of course, will hold for a shock wave when q is placed equal to zero. The Hugoniot equation is also written in terms of the enthalpy and internal energy changes. The expression with internal energies is particularly useful in the actual solution for the detonation velocity u_1 . If a total enthalpy (sensible plus chemical) in unit mass terms is defined such that

$$h \equiv c_p T + h^\circ$$

where h° is the heat of formation in the standard state and per unit mass, then a simplification of the Hugoniot equation evolves. Since by this definition

$$q = h_1^\circ - h_2^\circ$$

Equation (3) becomes

$$\frac{1}{2} u_1^2 + c_p T_1 + h_1^\circ = c_p T_2 + h_2^\circ + \frac{1}{2} u_2^2 \quad \text{or} \quad \frac{1}{2} (u_1^2 - u_2^2) = h_2 - h_1$$

Or further from Eq. (8), the Hugoniot equation can also be written as

$$\frac{1}{2} (P_2 - P_1) \left[\left(\frac{1}{\rho_1} \right) + \left(\frac{1}{\rho_2} \right) \right] = h_2 - h_1 \quad (10)$$

To develop the Hugoniot equation in terms of the internal energy, one proceeds by first writing

$$h = e + RT = e + (P/\rho)$$

where e is the total internal energy (sensible plus chemical) per unit mass. Substituting for h in Eq. (10) one obtains

$$\begin{aligned} \frac{1}{2} \left[\left(\frac{P_2}{\rho_1} + \frac{P_2}{\rho_2} \right) - \left(\frac{P_1}{\rho_1} + \frac{P_1}{\rho_2} \right) \right] &= e_2 + \frac{P_2}{\rho_2} - e_1 - \frac{P_1}{\rho_1} \\ \frac{1}{2} \left(\frac{P_2}{\rho_1} - \frac{P_2}{\rho_2} + \frac{P_1}{\rho_1} - \frac{P_1}{\rho_2} \right) &= e_2 - e_1 \end{aligned}$$

Factoring, another form of the Hugoniot equation is obtained:

$$\frac{1}{2} (P_2 + P_1) \left[\left(\frac{1}{\rho_1} \right) - \left(\frac{1}{\rho_2} \right) \right] = e_2 - e_1 \quad (11)$$

If the energy equation [Eq. (3)] were written in the form

$$h_1 + \frac{1}{2} u_1^2 = h_2 + \frac{1}{2} u_2^2$$

then the Hugoniot relations [Eqs. (10) and (11)] are derivable without the perfect gas assumption and are, thus, valid for shocks and detonations in gases, metals, etc.

There is also interest in the velocity of the burned gases with respect to the tube since as the wave proceeds into the medium at rest it is not known

whether the burned gases proceed in the direction of the wave (follow) or proceed away from the wave. From Fig. 1 it is apparent that this velocity, which is also called the particle velocity (Δu), is

$$\Delta u = u_1 - u_2$$

and from Eq. (8)

$$\Delta u = \{[(1/\rho_1) - (1/\rho_2)](P_2 - P_1)\}^{1/2} \tag{12}$$

Before proceeding further, it must be established which values of the velocity of the burned gases are valid. Thus, it is now best to make a plot of the Hugoniot equation for an arbitrary q . The Hugoniot equation is essentially a plot of all the possible values of $(1/\rho_2, P_2)$ for a given value of $(1/\rho_1, P_1)$ at the given q . This point $(1/\rho_1, P_1)$ called A is also plotted on the graph.

The regions of possible solutions are constructed by drawing the tangents to the curve that go through $A[(1/\rho_1), P_1]$. Since the form of the Hugoniot equation obtained is a hyperbola, there are two tangents to the curve through A as shown in Fig. 2. The tangents and horizontal and vertical lines through the initial condition A divide the Hugoniot curve into five regions, as specified by the roman numerals. The horizontal and vertical through A are, of course, the lines of constant P and $1/\rho$. A pressure difference for a final condition can be determined very readily from the Hugoniot relation [Eq. (9)] by considering the conditions along the vertical through A ; i.e., the condition of constant $(1/\rho)$ or constant volume heating:

$$\begin{aligned} \frac{\gamma}{\gamma - 1} \left(\frac{P_2 - P_1}{\rho} \right) - \left(\frac{P_2 - P_1}{\rho} \right) &= q \\ \left[\left(\frac{\gamma}{\gamma - 1} \right) - 1 \right] \left(\frac{P_2 - P_1}{\rho} \right) &= q, \quad (P_2 - P_1) = \rho(\gamma - 1)q \end{aligned} \tag{13}$$

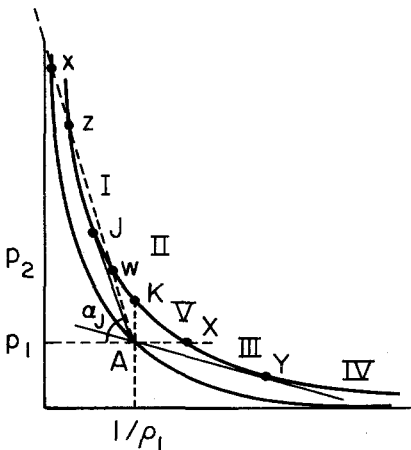


Fig. 2. Hugoniot plot divided in five regions (I-V).

From Eq. (13), it can be concluded that the pressure differential generated is proportional to the heat release q . If there is no heat release ($q = 0$), $P_2 = P_1$ and the Hugoniot curve would pass through the initial point A . As inferred before, the shock Hugoniot curve must pass through A . For differential values of q , one obtains a whole family of Hugoniot curves.

The Hugoniot diagram also defines an angle α_J such that

$$\tan \alpha_J = \frac{(P_2 - P_1)}{(1/\rho_1) - (1/\rho_2)}$$

From Eq. (5) then

$$u_1 = 1/\rho_1(\tan \alpha_J)^{1/2}$$

Any other value of α obtained, say by taking points along the curve from J to K and drawing a line through A , is positive and the velocity u_1 is real and possible. However, from K to X , one does not obtain a real velocity due to negative α_J . Thus, region V does not represent real solutions and can be eliminated. A result in this region would require a compression wave to move in the negative direction—an impossible condition.

Regions III and IV give expansion waves, which are the low-velocity waves already classified as deflagrations. That these waves are subsonic can be established from the relative order of magnitude of the numerator and denominator of Eq. (6') and as has already been done in Chapter 4.

Regions I and II give compression waves, high velocities, and are the regions of detonation (also as established in Chapter 4).

One can verify that region II gives compression waves and region III expansion waves, by examining the ratio of Δu to u_1 obtained by dividing Eq. (12) by the square root of Eq. (5)

$$\frac{\Delta u}{u_1} = \frac{(1/\rho_1) - (1/\rho_2)}{(1/\rho_1)} = 1 - \frac{(1/\rho_2)}{(1/\rho_1)} \quad (14)$$

In regions I and II, the detonation branch of the Hugoniot curve, $1/\rho_2 < 1/\rho_1$ and the right-hand side of Eq. (14) is positive. Thus, in detonations, the hot gases follow the wave. In regions III and IV, the deflagration branch of the Hugoniot curve, $1/\rho_2 > 1/\rho_1$, and the right-hand side of Eq. (14) is negative. Thus, in deflagrations the hot gases move away from the wave.

To this point in the development, the deflagration and detonation branches of the Hugoniot curve have been characterized and region V has been eliminated. There are some specific characteristics of the tangency point J that were initially postulated by Chapman [7] in 1889. Chapman established that the slope of adiabat is exactly the slope through J , i.e.,

$$\left[\frac{(P_2 - P_1)}{(1/\rho_1) - (1/\rho_2)} \right]_J = - \left\{ \left[\frac{\partial P_2}{\partial (1/\rho_2)} \right]_s \right\}_J \quad (15)$$

The proof of Eq. (15) is a very interesting one and is verified in the following development. From thermodynamics one can write for every point along the Hugoniot curve

$$T_2 ds_2 = de_2 + P_2 d(1/\rho_2) \quad (16)$$

where s is the entropy per unit mass. Differentiating Eq. (11), the Hugoniot equation in terms of e is

$$de_2 = -\frac{1}{2}(P_1 + P_2) d(1/\rho_2) + \frac{1}{2}[(1/\rho_1) - (1/\rho_2)] dP_2$$

since the initial conditions e_1 , P_1 , and $(1/\rho_1)$ are constant. Substituting this result in Eq. (16),

$$\begin{aligned} T_2 ds_2 &= -\frac{1}{2}(P_1 + P_2) d(1/\rho_2) + \frac{1}{2}[(1/\rho_1) - (1/\rho_2)] dP_2 + P_2 d(1/\rho_2) \\ &= -\frac{1}{2}(P_1 - P_2) d(1/\rho_2) + \frac{1}{2}[(1/\rho_1) - (1/\rho_2)] dP_2 \end{aligned} \quad (17)$$

It follows from Eq. (17) that along the Hugoniot curve,

$$T_2 \left[\frac{ds_2}{d(1/\rho_2)} \right]_{\text{H}} = \frac{1}{2} \left(\frac{1}{\rho_1} - \frac{1}{\rho_2} \right) \left\{ -\frac{P_1 - P_2}{(1/\rho_1) - (1/\rho_2)} + \left[\frac{dP_2}{d(1/\rho_2)} \right]_{\text{H}} \right\} \quad (18)$$

The subscript H is used to emphasize that derivatives are along the Hugoniot curve. Now somewhere along the Hugoniot curve, the adiabatic curve passing through the same point has the same slope as the H curve. There ds_2 must be zero and Eq. (18) becomes

$$\left\{ \left[\frac{dP_2}{d(1/\rho_2)} \right]_{\text{H}} \right\}_s = \frac{(P_1 - P_2)}{(1/\rho_1) - (1/\rho_2)} \quad (19)$$

The right-hand side of Eq. (19) is the value of the tangent that also goes through point A ; therefore, the tangency point along the H curve is J . Since the order of differentiation on the left-hand side of Eq. (19) can be reversed, it is obvious that Eq. (15) has been developed.

Equation (15) is useful in developing another important condition at point J . The velocity of sound in the burned gas can be written as

$$c_2^2 = \left(\frac{\partial P_2}{\partial \rho_2} \right)_s = -\frac{1}{\rho_2^2} \left[\frac{\partial P_2}{\partial (1/\rho_2)} \right]_s \quad (20)$$

Cross-multiplying and comparing with Eq. (15), one obtains

$$\rho_2^2 c_2^2 = - \left[\frac{\partial P_2}{\partial (1/\rho_2)} \right]_s = \left[\frac{(P_2 - P_1)}{(1/\rho_1) - (1/\rho_2)} \right]_J$$

or

$$[c_2^2]_J = \frac{1}{\rho_2^2} \left[\frac{(P_2 - P_1)}{(1/\rho_1) - (1/\rho_2)} \right]_J = [u_2^2]_J$$

Therefore

$$[u_2]_J = [c_2]_J \quad \text{or} \quad [M_2]_J = 1$$

Thus, the important result is obtained that at J the velocity of the burned gases (u_2) is equal to the speed of sound in the burned gases. Furthermore, an exact similar analysis would show, as well that

$$[M_2]_Y = 1$$

Recall that the velocity of the burned gas with respect to the tube (Δu) is written as

$$\Delta u = u_1 - u_2$$

or at J

$$u_1 = \Delta u + u_2 = \Delta u + c_2 \quad (21)$$

Thus, at J the velocity of the unburned gases moving into the wave, i.e., the detonation velocity, equals the velocity of sound in the gases behind the detonation wave plus the mass velocity of these gases (the velocity of the burned gases with respect to the tube). It will be shown presently that this solution at J is the only solution that can exist along the detonation branch of the Hugoniot curve for actual experimental conditions.

Although the complete solution of u_1 at J will not be attempted at this point, it can be shown readily that the detonation velocity has a simple expression now that u_2 and c_2 have been shown to be equal. The conservation of mass equation is rewritten to show that

$$\rho_1 u_1 = \rho_2 u_2 = \rho_2 c_2 \quad \text{or} \quad u_1 = \frac{\rho_2}{\rho_1} c_2 = \frac{(1/\rho_1)}{(1/\rho_2)} c_2$$

Then from Eq. (20) for c_2 , it follows that

$$u_1 = \frac{(1/\rho_1)}{(1/\rho_2)} (1/\rho_2) \left\{ - \left[\frac{\partial P_2}{\partial(1/\rho_2)} \right]_s \right\}^{1/2} = \left(\frac{1}{\rho_1} \right) \left\{ - \left[\frac{\partial P_2}{\partial(1/\rho_2)} \right]_s \right\}^{1/2} \quad (22)$$

With the condition that $u_2 = c_2$ at J , it is possible to characterize the different branches in the following manner:

Region I: strong detonation since $P_2 > P_J$ (supersonic flow to subsonic)

Region II: weak detonation since $P_2 < P_J$ (supersonic flow to supersonic)

Region III: weak deflagration since $P_2 > P_Y$ ($1/\rho_2 < 1/\rho_Y$) (subsonic flow to subsonic)

Region IV: strong deflagration since $P_2 < P_Y$ ($1/\rho_2 > 1/\rho_Y$) (subsonic flow to supersonic)

At points above J , $P_2 > P_J$, and, thus, $u_2 < u_{2,J}$. Since the temperature increases somewhat at higher pressures, then $c_2 > c_{2,J}$ [$c = (\gamma RT)^{1/2}$]. Thus, M_2 above J must be less than 1. Similar arguments show that points between J and K show that $M_2 > M_{2,J}$ and thus supersonic flow behind the wave. At points past Y , $1/\rho_2 > 1/\rho_Y$, or the velocities are greater than $u_{2,Y}$. Also past Y , the sound speed is about equal to the value at Y . Thus, past Y , $M_2 > 1$. A similar argument shows that $M_2 < 1$ between X and Y . Thus, past Y , the density decreases, and therefore the heat addition prescribes that there be supersonic outflow. But, in a constant area duct, it is not possible to have heat addition and proceed past the sonic condition. Thus, region IV is not a physically possible region of solutions and is ruled out.

Region III (weak deflagration) encompasses the laminar flame solutions that were treated in Chapter 4.

There is no condition by which one can rule out strong detonation, but Chapman stated that in this region only velocities corresponding to J were valid. Jouguet [8] gave the following analysis.

If the final values of P and $1/\rho$ correspond to a point on the Hugoniot curve higher than the point J , it can be shown (next section) that the velocity of sound in the burned gases is greater than the velocity of the detonation wave relative to the burned gases. (It can also be shown that the entropy is a minimum at J and that M_J is greater than values above J .) Consequently, if a rarefaction wave due to any reason whatsoever starts behind the wave, it will catch up with the detonation front. The rarefaction will then reduce the pressure and cause the final value of P_2 and $1/\rho_2$ to drop and move down the curve toward J . Thus, points above J are not stable. Heat losses, turbulence, friction, etc., can start the rarefaction. At the point J , the velocity of the detonation wave is equal to the velocity of sound in the burned gases plus the mass velocity of these gases, so that the rarefaction will not overtake it and, thus, J corresponds to a "self-sustained" detonation. The point and conditions at J are referred to as the Chapman-Jouguet results.

Thus, it appears that solutions in region I are possible, but only in the transient state, since external effects quickly break down this state. Some have claimed to have measured strong detonations in the transient state. There also exist standing detonations that are strong. Overdriven detonations have been generated by pistons and some investigators have observed oblique detonations which are overdriven.

The argument that is used to exclude points on the Hugoniot curve below J is based on the structure of the wave. If a solution in region II were possible, then there would be an equation that would give results in both region I and region II. The broken line in Fig. 2 representing this equation would go through A and some point, say Z , in region I and another point, say W , in region II. Both Z and W must correspond to the same detonation velocity. The same line would cross the shock Hugoniot curve at point X . As will be

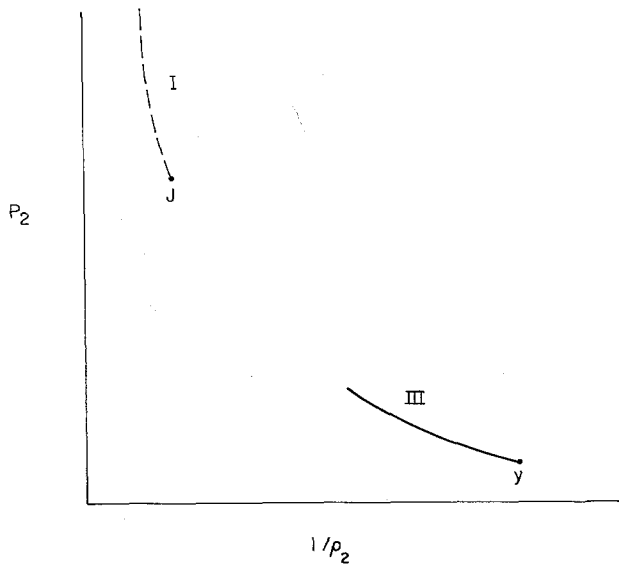


Fig. 3. The only physically possible steady results along the Hugoniot—the point J and region III. The broken line represents transient conditions.

discussed in Section C, the structure of the detonation is a shock wave followed by chemical reaction. Thus, to detail the structure of the detonation wave on Fig. 2, the pressure could rise from A to X , and then be reduced along the broken line to Z as there is chemical energy release. To proceed to the weak detonation solution at W , there would have to be further energy release. However, all the energy is expended for the initial mixture at point Z . Hence, it is physically impossible to reach the solution given by W as long as the structure requires a shock wave followed by chemical energy release. Therefore, the condition of tangency at J provides the additional condition necessary to specify the detonation velocity uniquely. The physically possible solutions represented by the Hugoniot curve, thus, are only those shown in Fig. 3.

2. Determination of the Speed of Sound in the Burned Gases for Conditions above the Chapman-Jouguet Point

a. Behavior of the Entropy along the Hugoniot Curve

Equation (18) was written as

$$T_2 \left[\frac{ds_2}{d(1/\rho_2)} \right]_{\text{H}} = \frac{1}{2} \left(\frac{1}{\rho_1} - \frac{1}{\rho_2} \right) \left\{ \left[\frac{dP_2}{d(1/\rho_2)} \right]_{\text{H}} - \frac{P_1 - P_2}{(1/\rho_1) - (1/\rho_2)} \right\}$$

with the further consequence that $[ds_2/d(1/\rho_2)] = 0$ at points Y and J (the latter is the Chapman–Jouguet point).

Differentiating again and taking into account the fact that

$$[ds_2/d(1/\rho_2)] = 0$$

at point J , one obtains

$$\left[\frac{d^2s}{d(1/\rho_2)^2} \right]_{\text{H at } J \text{ or } Y} = \frac{(1/\rho_1) - (1/\rho_2)}{2T_2} \left[\frac{d^2P_2}{d(1/\rho_2)^2} \right] \quad (23)$$

Now $[d^2P_2/d(1/\rho_2)^2] > 0$ everywhere, since the Hugoniot curve has its concavity directed toward the positive ordinates (see formal proof later).

Therefore, at point J , $(1/\rho_1) - (1/\rho_2) > 0$, and, hence, the entropy is minimum at J . At point Y , $(1/\rho_1) - (1/\rho_2) < 0$, and hence s_2 goes through a maximum.

When $q = 0$, the Hugoniot curve represents an adiabatic shock. Point 1 ($P_1, 1/\rho_1$) is then on the curve and Y and J are 1. Then $(1/\rho_1) - (1/\rho_2) = 0$, and the classical result of the shock theory is found; i.e., the shock Hugoniot curve osculates the adiabat at the point representing the conditions before the shock.

Along the detonation branch of the Hugoniot curve the variation of the entropy is as given in Fig. 4. For the adiabatic shock, the entropy variation is as shown in Fig. 5.

b. The Concavity of the Hugoniot Curve

Solving for P_2 in the Hugoniot relation, one obtains

$$P_2 = \frac{a + b(1/\rho_2)}{d + d(1/\rho_2)}$$

where

$$a = q + \frac{\gamma + 1}{2(\gamma - 1)} \frac{P_1}{\rho_1}, \quad b = -\frac{1}{2}P_1, \quad c = -\frac{1}{2}\rho_1^{-1}, \quad d = \frac{\gamma + 1}{2(\gamma - 1)} \quad (24)$$

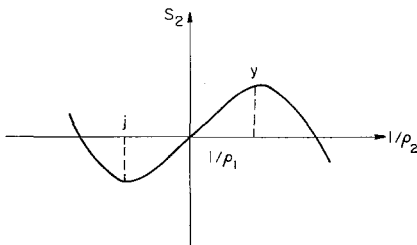


Fig. 4. Variation of entropy along the Hugoniot curve.

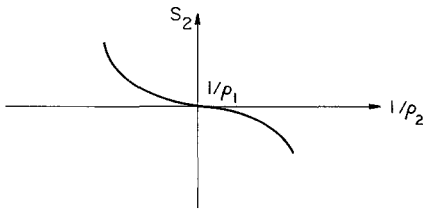


Fig. 5. Entropy variation for an adiabatic shock.

From this equation for the pressure, it is obvious that the Hugoniot curve is a hyperbola. Its asymptotes are the lines

$$\frac{1}{\rho_2} = \left(\frac{\gamma - 1}{\gamma + 1}\right)\left(\frac{1}{\rho_1}\right) > 0, \quad P_2 = -\frac{\gamma - 1}{\gamma + 1} P_1 < 0$$

The slope is

$$\left[\frac{dP_2}{d(1/\rho_2)} \right]_H = \frac{bc - ad}{[c + d(1/\rho_2)]^2}$$

where

$$bc - ad = -\left[\frac{\gamma + 1}{2(\gamma - 1)} q + \frac{P_1}{\rho_1} \frac{\gamma}{(\gamma - 1)^2} \right] < 0 \quad (25)$$

since $q > 0$, $P_1 > 0$, and $\rho_1 > 0$. A complete plot of the Hugoniot curves with its asymptotes would be as shown in Fig. 6. From Fig. 6 it is seen, as could be seen from earlier figures, that the part of the hyperbola representing the strong detonation branch has its concavity directed upwards. It is also possible to determine directly the sign of

$$\left[\frac{d^2 P_2}{d(1/\rho_2)^2} \right]_H$$

By differentiating Eq. (24)

$$\frac{d^2 P_2}{d(1/\rho_2)^2} = \frac{2d(ad - bc)}{[c + d(1/\rho_2)]^3}$$

Now, $d > 0$, $ad - bc > 0$ [Eq. (25)], and

$$c + d\left(\frac{1}{\rho_2}\right) = \frac{1}{2} \left[\frac{\gamma + 1}{\gamma - 1} \left(\frac{1}{\rho_2}\right) - \left(\frac{1}{\rho_1}\right) \right] > 0$$

The solutions lie on the part of the hyperbola situated on the right-hand side of the asymptote

$$(1/\rho_2) = [(\gamma - 1)/(\gamma + 1)](1/\rho_1)$$

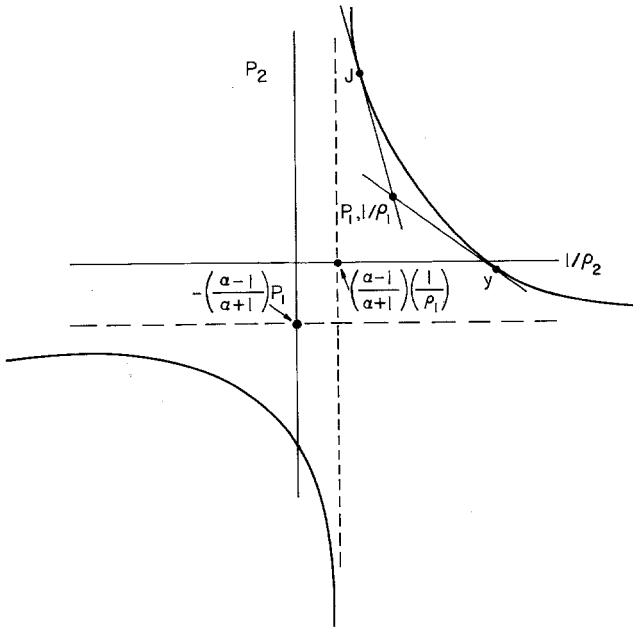


Fig. 6. Asymptotes to the Hugoniot curve.

Hence

$$[d^2 P_2 / d(1/\rho_2)^2] > 0$$

c. The Burned Gas Speed

Here

$$ds = \left(\frac{\partial s}{\partial (1/\rho)} \right)_P d\left(\frac{1}{\rho}\right) + \left(\frac{\partial s}{\partial P} \right)_{1/\rho} dP \tag{26}$$

Since $ds = 0$ for the adiabat Eq. (26) becomes

$$0 = \left[\frac{\partial s}{\partial (1/\rho)} \right]_P + \left(\frac{\partial s}{\partial P} \right)_{1/\rho} \left[\frac{\partial P}{\partial (1/\rho)} \right]_s \tag{27}$$

Differentiating Eq. (26) along the Hugoniot curve,

$$\left[\frac{ds}{d(1/\rho)} \right]_H = \left[\frac{\partial s}{\partial (1/\rho)} \right]_P + \left(\frac{\partial s}{\partial P} \right)_{1/\rho} \left[\frac{dP}{d(1/\rho)} \right]_H \tag{28}$$

Subtracting and transposing Eqs. (27) and (28)

$$\left[\frac{dP}{d(1/\rho)} \right]_{\text{H}} - \left[\frac{\partial P}{\partial(1/\rho)} \right]_{\text{s}} = \frac{[ds/d(1/\rho)]_{\text{H}}}{(\partial s/\partial P)_{1/\rho}} \quad (29)$$

A thermodynamic expression for the enthalpy is

$$dh = T ds + dP/\rho \quad (30)$$

With the conditions of constant c_p and an ideal gas, the expressions

$$dh = c_p dT, \quad T = P/R\rho, \quad c_p = [\gamma/(\gamma - 1)]R$$

are developed and substituted in

$$dh = \left(\frac{\partial h}{\partial P} \right) dP + \frac{\partial h}{\partial(1/\rho)} d\left(\frac{1}{\rho}\right)$$

to obtain

$$dh = \left(\frac{\gamma}{\gamma - 1} \right) R \left[\left(\frac{1}{R\rho} \right) dP + \frac{P}{R} d\left(\frac{1}{\rho}\right) \right] \quad (31)$$

Combining Eqs. (30) and (31),

$$\begin{aligned} ds &= \frac{1}{T} \left[\left(\frac{\gamma}{\gamma - 1} \right) \frac{1}{\rho} dP - \frac{dP}{\rho} + \left(\frac{\gamma}{\gamma - 1} \right) P d\left(\frac{1}{\rho}\right) \right] \\ &= \frac{1}{T} \left[\left(\frac{1}{\gamma - 1} \right) \frac{dP}{\rho} + \left(\frac{\gamma}{\gamma - 1} \right) \rho R T d\left(\frac{1}{\rho}\right) \right] \\ &= \frac{dP}{(\gamma - 1)\rho T} + \left(\frac{\gamma}{\gamma - 1} \right) R \rho d\left(\frac{1}{\rho}\right) \end{aligned}$$

Therefore,

$$(\partial s/\partial P)_{1/\rho} = 1/(\gamma - 1)\rho T \quad (32)$$

Then substituting in the values of Eq. (32) into Eq. (29), one obtains

$$\left[\frac{\partial P}{\partial(1/\rho)} \right]_{\text{H}} - \left[\frac{\partial P}{\partial(1/\rho)} \right]_{\text{s}} = (\gamma - 1)\rho T \left[\frac{\partial s}{\partial(1/\rho)} \right]_{\text{H}} \quad (33)$$

Equation (18) may be written as

$$\left[\frac{\partial P}{\partial(1/\rho)} \right]_{\text{H}} - \frac{P_1 - P_2}{(1/\rho_1) - (1/\rho_2)} = \frac{2T_2}{(1/\rho_1) - (1/\rho_2)} \left[\frac{\partial s_2}{\partial(1/\rho)} \right]_{\text{H}} \quad (34)$$

Combining Eqs. (33) and (34) gives

$$\begin{aligned} & \left[-\frac{dP_2}{\partial(1/\rho_2)} \right]_s - \frac{P_2 - P_1}{(1/\rho_1) - (1/\rho_2)} \\ &= \left[\frac{\partial s_2}{\partial(1/\rho_2)} \right]_H \left[-\frac{2T_2}{(1/\rho_1) - (1/\rho_2)} + (\gamma - 1)\rho_2 T_2 \right] \end{aligned}$$

or

$$\rho_2^2 c_2^2 - \rho_2^2 u_2^2 = \frac{P_2}{R} \left[\gamma - \frac{1 + (\rho_1/\rho_2)}{1 - (\rho_1/\rho_2)} \right] \left[\frac{\partial s_2}{\partial(1/\rho_2)} \right]_H \quad (35)$$

Since the asymptote is given by

$$1/\rho_2 = [(\gamma - 1)/(\gamma + 1)](1/\rho_1)$$

values of $(1/\rho_2)$ on the right-hand side of the asymptote must be

$$1/\rho_2 > [(\gamma - 1)/(\gamma + 1)](1/\rho_1)$$

which leads to

$$\left[\gamma - \frac{1 + (\rho_1/\rho_2)}{1 - (\rho_1/\rho_2)} \right] < 0$$

Since also $[\partial s/\partial(1/\rho_2)] < 0$, then the right-hand side of Eq. (35) is the product of two negative numbers, or a positive number. If the right-hand side of Eq. (35) is positive, then c_2 must be greater than u_2 , i.e.,

$$c_2 > u_2$$

3. Calculation of the Detonation Velocity

With the background provided, it is now possible to calculate the detonation velocity for an explosive mixture at given initial conditions. Equation (22)

$$u_1 = \left(\frac{1}{\rho_1} \right) \left[-\frac{dP_2}{d(1/\rho_2)} \right]_s^{1/2}$$

shows the strong importance of density of the initial gas mixture, which is reflected more properly in the molecular weight of the products, as will be derived later.

For ideal gases, the adiabatic expansion law is

$$PV^\gamma = \text{const} = P_2(1/\rho_2)^{\gamma_2}$$

Differentiating this expression, one obtains

$$(1/\rho_2)^{\gamma_2} dP_2 + P_2(1/\rho_2)^{\gamma_2-1} \gamma_2 d(1/\rho_2) = 0$$

which gives

$$-\left[\frac{dP_2}{d(1/\rho_2)} \right]_s = \frac{P_2}{(1/\rho_2)} \gamma_2 \quad (36)$$

Substituting Eq. (36) into Eq. (22), one obtains

$$u_1 = \frac{(1/\rho_1)}{(1/\rho_2)} [\gamma_2 P_2 (1/\rho_2)]^{1/2} = \frac{(1/\rho_1)}{(1/\rho_2)} (\gamma_2 RT_2)^{1/2}$$

If one defines

$$\mu = (1/\rho_1)/(1/\rho_2)$$

then

$$u_1 = \mu (\gamma_2 RT_2)^{1/2} \quad (37)$$

Rearranging Eq. (5), it is possible to write

$$P_2 - P_1 = u_1^2 \frac{(1/\rho_1) - (1/\rho_2)}{(1/\rho_1)^2}$$

Substituting for u_1^2 from above

$$(P_2 - P_1) \frac{(1/\rho_2)}{\gamma_2 P_2} = \left(\frac{1}{\rho_1} - \frac{1}{\rho_2} \right) \quad (38)$$

Now Eq. (11) was

$$e_2 - e_1 = \frac{1}{2} (P_2 + P_1) [(1/\rho_1) - (1/\rho_2)]$$

Substituting Eq. (38) into Eq. (11)

$$e_2 - e_1 = \frac{1}{2} (P_2 + P_1) \frac{(P_2 - P_1)(1/\rho_2)}{\gamma_2 P_2}$$

or

$$e_2 - e_1 = \frac{1}{2} \frac{(P_2^2 - P_1^2)(1/\rho_2)}{\gamma_2 P_2}$$

Since $P_2^2 \gg P_1^2$

$$e_2 - e_1 = \frac{1}{2} \frac{P_2^2 (1/\rho_2)}{\gamma_2 P_2} = \frac{1}{2} \frac{P_2 (1/\rho_2)}{\gamma_2}$$

Recall all expressions are in mass units, therefore the gas constant R is not the universal gas constant and, indeed, should now be written R_2 to indicate this condition. Thus,

$$e_2 - e_1 = \frac{1}{2} \frac{P_2(1/\rho_2)}{\gamma_2} = \frac{1}{2} \frac{R_2 T_2}{\gamma_2} \quad (39)$$

Recall, as well, that e is the sum of the sensible internal energy plus the internal energy of formation. Equation (39) is the one to be solved in order to obtain T_2 and, thus, u_1 . However, it is more convenient to solve this expression on a molar basis, because the available thermodynamic data and stoichiometric equations are in molar terms.

Equation (39) may be written in terms of the universal gas constant R' as

$$e_2 - e_1 = \frac{1}{2}(R'/MW_2)(T_2/\gamma_2) \quad (40)$$

where MW_2 is the average molecular weight of the products. The gas constant R used throughout this chapter must be the engineering gas constant since all the equations developed were in terms of unit mass, not moles. If one multiplies through Eq. (40) with MW_1 , the average molecular weight of the reactants

$$(MW_1/MW_2)e_2(MW_2) - (MW_1)e_1 = \frac{1}{2}(R'T_2/\gamma_2)(MW_1/MW_2)$$

or

$$n_2 E_2 - E_1 = \frac{1}{2}(n_2 R' T_2 / \gamma_2) \quad (41)$$

where the E 's are the total internal energies per mole of total reactants or products and n_2 is (MW_1/MW_2) , which is the number of moles of the product per mole of reactant. Usually there are more than one product and one reactant; thus, the E 's are the molar sums.

Now to solve to T_2 , first assume a T_2 and estimate γ_2 and MW_2 , which do not vary substantially for burned gas mixtures. For these approximations, it is possible to determine $1/\rho_2$ and P_2 .

If Eq. (38) is multiplied by $(P_1 + P_2)$,

$$(P_1 + P_2)\{(1/\rho_1) - (1/\rho_2)\} = (P_2^2 - P_1^2)(1/\rho_2)/\gamma_2 P_2$$

Again $P_2^2 \gg P_1^2$, so that

$$\begin{aligned} \frac{P_1}{\rho_1} - \frac{P_1}{\rho_2} + \frac{P_2}{\rho_1} - \frac{P_2}{\rho_2} &= \frac{P_2(1/\rho_2)}{\gamma_2} \\ \frac{P_2}{\rho_1} - \frac{P_1}{\rho_2} &= \frac{P_2(1/\rho_2)}{\gamma_2} + \frac{P_2}{\rho_2} - \frac{P_1}{\rho_1} \end{aligned}$$

or

$$\frac{P_2 \rho_2}{\rho_2 \rho_1} - \frac{P_1 \rho_1}{\rho_1 \rho_2} = \frac{R_2 T_2}{\gamma_2} + R_2 T_2 - R_1 T_1$$

$$R_2 T_2 \left[\frac{(1/\rho_1)}{(1/\rho_2)} \right] - R_1 T_1 \left[\frac{(1/\rho_2)}{(1/\rho_1)} \right] = \frac{R_2 T_2}{\gamma_2} + R_2 T_2 - R_1 T_1$$

In terms of μ ,

$$R_2 T_2 \mu - R_1 T_1 (1/\mu) = [(1/\gamma_2) + 1] R_2 T_2 - R_1 T_1$$

which gives

$$\mu^2 - [(1/\gamma_2) + 1 - (R_1 T_1 / R_2 T_2)] \mu - (R_1 T_1 / R_2 T_2) = 0 \quad (42)$$

This quadratic equation can be solved for μ ; thus, for the initial condition $(1/\rho_1)$, $(1/\rho_2)$ is known. It is possible to find P_2 , as

$$P_2 = \mu (R_2 T_2 / R_1 T_1) P_1$$

Thus, for the assumed T_2 , P_2 is known. Then it is possible to determine the equilibrium composition of the burned gas mixture in the same fashion as described in Chapter 1. For this mixture and temperature, both sides of Eq. (39) or (41) are deduced. If the correct T_2 was assumed, both sides of the equation will be equal. If not, reiterate the procedure until T_2 is found. The correct γ_2 and MW_2 will be determined readily. For the correct values, u_1 is determined from Eq. (37) written as

$$u_1 = \mu \left(\frac{\gamma_2 R' T_2}{MW_2} \right)^{1/2}$$

The solution is simpler if the assumption $P_2 \gg P_1$ is made. Then from Eq. (38)

$$\left(\frac{1}{\rho_1} - \frac{1}{\rho_2} \right) = (P_2 - P_1) \frac{(1/\rho_2)}{\gamma_2 P_2} = \frac{P_2 (1/\rho_2)}{\gamma_2 P_2}$$

$$\left(\frac{1}{\rho_1} - \frac{1}{\rho_2} \right) = \frac{1}{\gamma_2} \left(\frac{1}{\rho_2} \right), \quad \left(\frac{1}{\rho_2} \right) = \frac{\gamma_2}{1 + \gamma_2} \left(\frac{1}{\rho_1} \right)$$

Since an excellent guess usually can be made of γ_2 , one obtains μ immediately and, thus, P_2 .

Gordon and McBride [12] present a more detailed computational scheme and the associated computational program.

D. COMPARISON OF DETONATION VELOCITY CALCULATIONS WITH EXPERIMENTAL RESULTS

In the previous discussion of laminar and turbulent flames, the effects of the physical and chemical parameters on flame speeds were considered and the trends were compared with the experimental trends measured. It is of interest here to recall that it was not possible to calculate these flame speeds explicitly, but as stressed throughout this chapter, it is possible to calculate the detonation velocity accurately. Indeed, the accuracy of the theoretical calculations and the ability to measure the detonation velocity precisely as well has permitted some investigators to calculate thermodynamic properties (such as the bond strength of nitrogen and heat of sublimation of carbon) from experimental measurements of the detonation velocity.

In their book, Lewis and von Elbe [13] have made numerous comparisons between calculated detonation velocities and experimental values. This book is one of the better sources of such data. Most of the data available for comparison purposes unfortunately were calculated long before the advent of digital computers. Consequently, the theoretical values do not account for all the dissociation that would normally take place. The data presented in Table 2 were abstracted from Lewis and von Elbe and were so chosen to emphasize some important points about the factors that affect the detonation velocity. Although the agreement between the calculated and experimental values in Table 2 can be considered quite good, there is no doubt that the agreement would be much better if dissociation of all possible species was allowed for the final conditions. These early data are quoted here because there have been no recent similar comparisons in which the calculated values were determined for equilibrium dissociation concentrations using modern computational techniques. Shown in Table 3 are some data from Strehlow [14], which

TABLE 2

Detonation velocities of stoichiometric hydrogen-oxygen mixture^a

Mixture	P_2 (atm)	T_2 (K)	u_1 (m/sec)	
			Calculated	Experimental
$(2\text{H}_2 + \text{O}_2)$	18.05	3583	2806	2819
$(2\text{H}_2 + \text{O}_2) + 5\text{O}_2$	14.13	2620	1732	1700
$(2\text{H}_3 + \text{O}_2) + 5\text{N}_2$	14.39	2685	1850	1822
$(2\text{H}_2 + \text{O}_2) + 4\text{H}_2$	15.97	2975	3627	3527
$(2\text{H}_2 + \text{O}_2) + 5\text{He}$	16.32	3097	3617	3160
$(2\text{H}_2 + \text{O}_2) + 5\text{Ar}$	16.32	3097	1762	1700

^a $P_0 = 1$ atm, $T_0 = 291$ K.

TABLE 3

Detonation velocities of various mixtures^a

	Measured velocity (m/sec)	Calculated		
		Velocity (m/sec)	P_2 (atm)	T_2 (K)
$4\text{H}_2 + \text{O}_2$	3390	3408	17.77	3439
$2\text{H}_2 + \text{O}_2$	2825	2841	18.56	3679
$\text{H}_2 + 3\text{O}_2$	1663	1737	14.02	2667
$\text{CH}_4 + \text{O}_2$	2528	2639	31.19	3332
$\text{CH}_4 + 1.5\text{O}_2$	2470	2535	31.19	3725
$0.7\text{C}_2\text{N}_2 + \text{O}_2$	2570	2525	45.60	5210

^a $P_0 = 1/\text{atm}$, $T_0 = 298 \text{ K}$

are a comparison of measured and calculated detonation velocities. The experimental data in both tables have not been corrected for the infinite tube diameter condition for which the calculations hold. This small correction would make the general agreement shown to be even better. The calculated results in Table 3 are the more accurate ones in that Gordon and McBride [12] computational program was used and this program properly accounts for dissociation in the product composition.

Variations in the initial temperature and pressure should not affect the detonation velocity for a given initial density. A rise in the initial temperature could only cause a much smaller rise in the final temperature. In laminar flame theory, a small rise in final temperature was important since the temperature was in an exponential term. For detonation theory, recall

$$u_1 = \mu(\gamma_2 R_2 T_2)^{1/2}$$

The subscript 2 has been added in the square root to emphasize that the γ and T are evaluated at the Chapman-Jouguet point and that R is the engineering gas constant.

Also, a change in initial pressure does not affect too severely the final results, since the effect would be in μ , which is a specific volume ratio and, thus, is little affected by the pressure. In fact, recall that

$$\mu \cong (\gamma_2 + 1)/\gamma_2$$

γ_2 does not vary significantly.

Examination of Table 2 would lead one to expect that the major factor affecting u_1 would be the initial density. Indeed many have stated that the initial density is one of the most important parameters in determining the detonation velocity. This point is best seen by comparing the results for the

mixtures in which the helium and argon inerts are added. The lower-density helium mixture gives a much higher detonation velocity than the higher-density argon mixture, but identical values of P_2 and T_2 are obtained.

Notice as well that the addition of excess H_2 gives a larger detonation velocity than the stoichiometric mixture. The temperature of the stoichiometric mixture is higher throughout. Again, one could conclude that this variation is a result of the initial density of the mixture. The addition of excess oxygen lowers both detonation velocity and temperature. Again, it is possible to argue that excess oxygen increases the initial density.

Whether it is the initial density that is the important parameter should be questioned. The initial density appears in the parameter μ . A change in the initial density by species addition also causes a change in the final density as well, so that, overall, μ does not change appreciably. However, recall that

$$R_2 = R'/MW_2 \quad \text{or} \quad u_1 = \mu(\gamma_2 R' T_2 / MW_2)^{1/2}$$

where R' is the universal gas constant and MW_2 is the average molecular weight of the burned gases. It is really MW_2 that is affected by initial diluents, whether the diluent is an inert or a light-weight fuel such as hydrogen. Indeed the ratio of the detonation velocities for the excess helium and argon can be predicted almost exactly, if one takes the square root of the inverse of the ratio of the molecular weights. If it is assumed that there is little dissociation in these two burned gas mixtures, then the reaction products in each case are two moles of water and five moles of helium. In the helium case, the average molecular weight is 9; in the argon case, the average molecular weight is 33.7. The square root of the ratio of the molecular weights is 2.05. The detonation velocity calculated for the argon mixtures is 1762. The estimated velocity for helium would be $2.05 \times 1762 = 3617$, which is very close to the calculated result of 3617.

The variation of detonation velocity with mixture ratio is most interesting. Figure 7 shows the variation for acetylene-oxygen mixtures. One notices

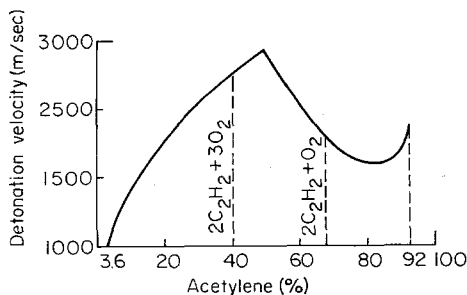


Fig. 7. Detonation velocities of acetylene-oxygen mixtures [after Breton, *Ann. Office Nat. Combust. Liquids* 11, 4871 (1936)].

from Fig. 7 that the maximum detonation velocity is not obtained at the stoichiometric mixture ratio, but the maximum occurs closer to the mixture ratio that would correspond [13] to a stoichiometry for the products to be carbon monoxide and water vapor. Indeed the maximum occurs at an even richer mixture ratio. The argument generally given has been that the conversion of CO to CO₂ is too slow to affect the detonation. However, the data of Dryer *et al.* [15] show that the CO oxidation rates are much faster at high temperatures than originally expected. If the previous reasoning were correct, the maximum should occur at the mixture ratio that gives the largest T_2/MW_2 . The mixture ratio for acetylene-oxygen, which gives a product stoichiometry for CO and H₂ only, is 50% and, indeed, the maximum in Fig. 7 occurs at this value. For propane, the maximum does not occur quite so rich. For the hydrogen-oxygen system, the maximum occurs very near the fuel-rich limit.

It is rather interesting to note that the maximum specific impulse of a rocket propellant system occurs when $(T_2/MW_2)^{1/2}$ is maximized, even though the rocket combustion process is not one of detonation [16].

E. THE ZND STRUCTURE OF DETONATION WAVES

Zeldovich [9], von Neumann [10], and Döring [11] independently arrived at a theory for the structure of the detonation wave. This theory states that the detonation wave consists of a planar shock moving at the detonation velocity and leaving heated and compressed gas behind it. After an induction period the chemical reaction starts and as the reaction progresses the temperature rises and the density and pressure fall until they reach the Chapman-Jouguet values and the reaction attains equilibrium. A rarefaction wave whose steepness depends on the distance traveled by the wave then sets in. Thus, behind the *C-J* shock, energy is generated by thermal reaction.

In the previous section in which the detonation velocity was calculated, the conservation equations were used and it was found that no knowledge of the chemical reaction rate or structure was necessary. The wave was assumed to be a discontinuity. This assumption is satisfactory since these equations placed no restriction on the distance between a shock and the seat of the generating force.

But to look somewhat more closely at the structure of the wave one must deal with the kinetics of the chemical reaction. The kinetics and mechanism of reaction give the time and spatial separation of the front and the *C-J* plane.

The distribution of pressure, temperature, and density behind the shock depends upon the fraction of material reacted. If the reaction rate is

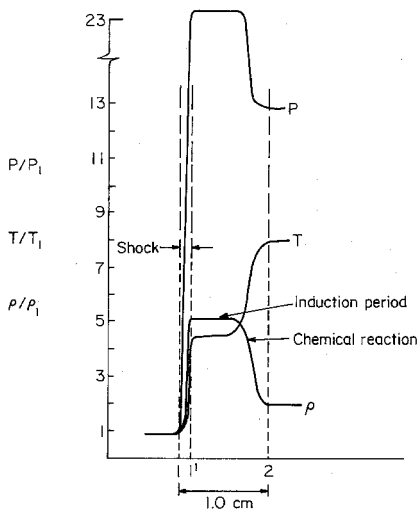


Fig. 8. Variation of physical parameters through a typical detonation wave (see Table 4).

exponentially accelerating (follows an Arrhenius law and has a relatively large overall activation energy as that normally associated with hydrocarbon oxidation), then the fraction reacted changes very little initially and the pressure, density, and temperature profiles are very flat for a distance behind the shock front and then change sharply as the reaction goes to completion at a high rate.

Figure 8 is a graphical representation of the ZND theory and shows the variation of the important physical parameters as a function of spatial distribution. Plane 1 is the shock front, plane 1' is that immediately after the shock, and plane 2 is the Chapman-Jouguet plane. In the previous section, the conditions for plane 2 were calculated and u_1 obtained. From u_1 and the shock relationships or tables, it is possible to determine the conditions at plane 1'. Typical results for 20% H_2 in air are shown in Table 4. Note from this table that $(\rho_2/\rho_1) = 1.8$. Thus, generally for many situations the approximation that u_1 is twice c_2 can be used.

Thus, as the gas passes from the shock front to the *C-J* state, its pressure drops about a factor of two, the temperature rises about a factor of two, and the density drops by a factor of three. It is interesting to follow the model on a Hugoniot plot as shown in Fig. 9.

There are two alternate paths by which a mass element passing through the wave from $\epsilon = 0$ to $\epsilon = 1$ may satisfy the conservation equations and at the same time change its pressure and density continuously, not discontinuously, with distance of travel.

The element may enter the wave in the state corresponding to the initial point and move directly to the *C-J* point. However, this path would demand

TABLE 4

Calculated values of the physical parameters in a 20% H_2 -air detonation

	1	1'	2
M	4.5	0.42	1.0
u (m/sec)	1524	305	549
P (atm)	1	23	13
T (K)	298	1350	2415
ρ/ρ_1	1	5	1.8

that this reaction occur everywhere along the path. Since there is little compression along this path, there cannot be sufficient temperature to initiate any reaction. Thus, there is no energy release to sustain the wave. If on another path a jump is made to the upper point (1'), the pressure and temperature conditions for initiation of reaction are met. In proceeding from 1 to 1', the pressure does not follow the points along the shock Hugoniot curve.

The general features of the model in which a shock, or at least a steep pressure and temperature rise, creates conditions for reaction and in which the subsequent energy release causes a drop in pressure and density, have been verified by measurements in a detonation tube [16]. Most of these experiments were measurements of density variation by x-ray absorption.

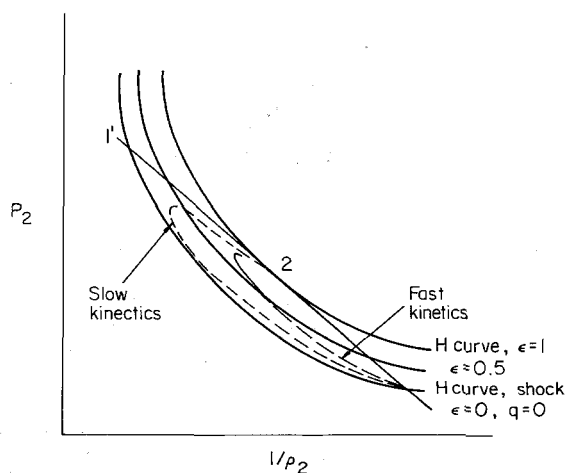


Fig. 9. Effect of kinetic reaction rates on detonation structures as viewed on a Hugoniot curve; ϵ is the fractional amount of chemical energy converted.

The above ZND concepts consider the structure of the wave to be one dimensional and are adequate for determining the "static" parameters u , ρ_2 , T_2 , and P_2 . The evidence now exists that all self-sustaining detonations have a three-dimensional cellular structure.

F. THE STRUCTURE OF THE CELLULAR DETONATION FRONT AND OTHER DETONATION PHENOMENA PARAMETERS

1. The Cellular Detonation Front

An excellent description of the cellular detonation front and its relation to chemical rates and their effect on the dynamic parameters has been given by Lee [6]. With permission this description is reproduced almost verbatim here.

Figure 10 shows the pattern made by the normal reflection of a detonation on a glass plate coated lightly with carbon soot, which may be from either a wooden match or a kerosene lamp. The cellular structure of the detonation front is quite evident. If a similarly soot-coated polished metal (or mylar) foil is inserted into a detonation tube, the passage of the detonation wave will leave a characteristic "fish-scale" pattern on the smoked foil. Figure 11 is a sequence of laser-schlieren records of a detonation wave propagating in a rectangular tube. One of the side windows has been coated with smoke, and the fish-scale pattern formed by the propagating detonation front is very well illustrated. The detailed shock configuration of the cellular detonation front itself is illustrated by the interferogram shown in Fig. 12. The direction of propagation of the detonation is toward the right. As can be seen in the sketch at the top left corner, there are two triple points. At the first triple point A , AI and AM represent the incident shock and Mach stem of the leading front, while AB is the reflected shock. Point B is the second triple point of another three-shock Mach configuration on the reflected shock AB : the entire shock pattern represents what is generally referred to as a double Mach reflection. The hatched lines denote the reaction front, while the dash-dot lines represent the shear discontinuities or slip lines associated with the triple-shock Mach configurations. The entire front $ABCDE$ is generally referred to as the transverse wave, and it propagates normal to the direction of the detonation motion (down in the present case) at about the sound speed of the hot product gases. It has been shown conclusively that it is the triple-point regions at A and B that "write" on the smoked foil. The exact mechanics of how the triple-point region does the writing is not clear. It has been postulated that the high shear at the slip discontinuity causes the soot particles to be erased. Figure 12 shows a schematic of the motion of the detonation front. The fish-scale pattern is a record of the trajectories of the triple points. It is important to note the cyclic motion of the detonation front. Starting at the apex of the cell at A , the detonation shock front is highly overdriven, propagating at about 1.6 times the equilibrium Chapman-Jouguet detonation velocity. Toward the end of the cell at D , the shock has decayed to about 0.6 times the Chapman-Jouguet velocity before it is impulsively accelerated back to its highly overdriven state when the transverse waves collide to start the next cycle again. For the first half of the propagation from A to BC , the wave serves as the Mach stem to the incident shocks of the adjacent cells. During the second half from BC to D , the wave then becomes the incident shock to

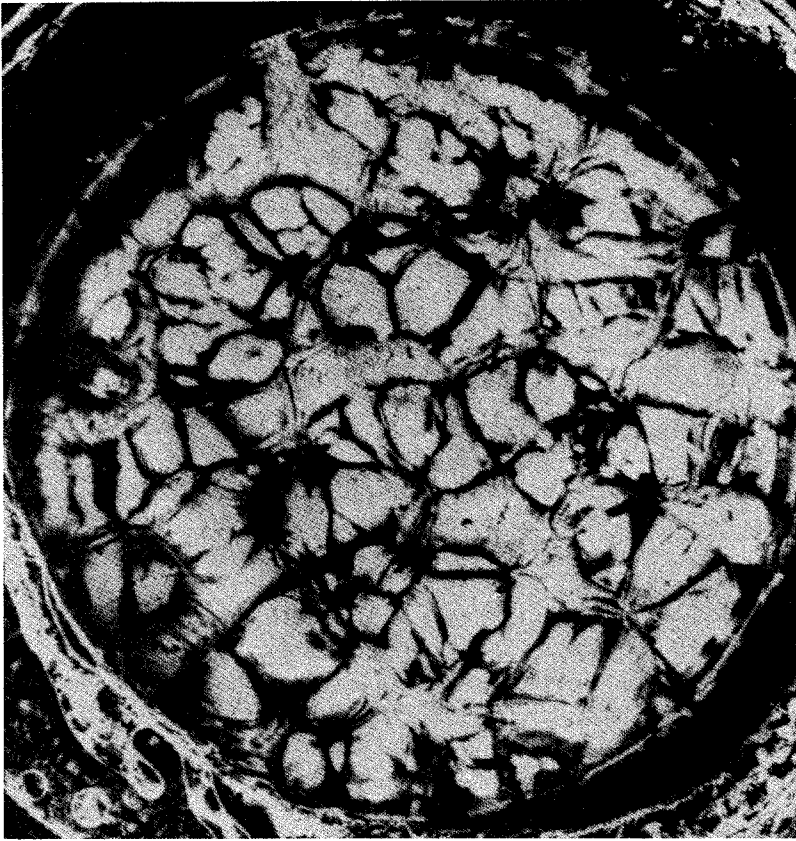


Fig. 10. End-on pattern from the normal reflection of a cellular detonation on a smoked glass plate (after Lee [2]).

the Mach stems of the neighboring cells. Details of the variation of the shock strength and chemical reactions inside a cell can be found in a paper by Libouton *et al.* [18]. AD is usually defined as the length L_c of the cell, and BC denotes the cell diameter (also referred to as the cell width or the transverse-wave spacing). The average velocity of the wave is close to the equilibrium Chapman-Jouguet velocity.

We thus see that the motion of a real detonation front is far from the steady and one-dimensional motion given by the ZND model. Instead, it proceeds in a cyclic manner in which the shock velocity fluctuates within a cell about the equilibrium Chapman-Jouguet value. Chemical reactions are essentially complete within a cycle or a cell length. However, the gas dynamic flow structure is highly three dimensional, and full equilibration of the transverse shocks, so that the flow becomes essentially one dimensional, will probably take an additional distance of the order of a few more cell lengths.

From both the cellular end-on or the axial fish-scale smoke foil, the average cell size λ can be measured. The end-on record gives the cellular pattern at one precise instant. The axial record,

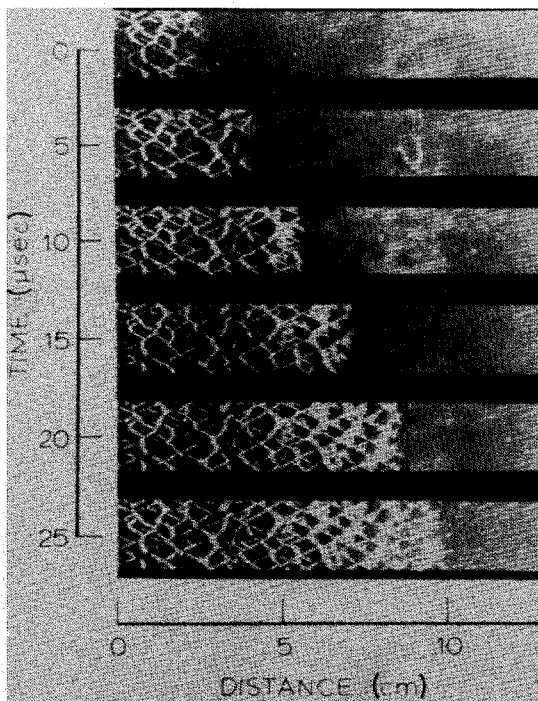


Fig. 11. Laser-schlieren cinematography of a propagating detonation in low-pressure mixtures with fish-scale pattern on a soot-covered window (courtesy of A. K. Oppenheim).

however, permits the detonation to be observed as it travels along the length of the foil. It is much easier by far to pick out the characteristic cell size λ from the axial record; thus, the end-on pattern is not used, in general, for cell-size measurements.

Early measurements of the cell size have been carried out mostly in low-pressure fuel-oxygen mixtures diluted with inert gases such as He, Ar, and N_2 [19]. The purpose of these investigations is to explore the details of the detonation structure and to find out the factors that control it. It was not until very recently that Bull *et al.* [20] made some cell-size measurements in stoichiometric fuel-air mixtures at atmospheric pressure. Due to the fundamental importance of the cell size in the correlation with the other dynamic parameters, a systematic program has been carried out by Knystautas to measure the cell size of atmospheric fuel-air detonations in all the common fuels (e.g., H_2 , C_2H_2 , C_2H_4 , C_3H_6 , C_2H_6 , C_3H_8 , C_4H_{10} , and the welding fuel MAPP) over the entire range of fuel composition between the limits [21]. Stoichiometric mixtures of these fuels with pure oxygen, and with varying degrees of N_2 dilution at atmospheric pressures, were also studied (Knystautas *et al.* [22]). To investigate the pressure dependence, Knystautas *et al.* [22] have also measured the cell size in a variety of stoichiometric fuel-oxygen mixtures at initial pressures $10 \leq p_0 \leq 200$ torr. The minimum cell size usually occurs at about the most detonable composition ($\phi = 1$). The cell size λ is representative of the sensitivity of the mixture. Thus, in descending order of sensitivity, we have C_2H_2 , H_2 , C_2H_4 , and the alkanes C_3H_8 , C_2H_6 , and C_4H_{10} . Methane (CH_4), although belonging to the same alkane family, is exceptionally insensitive to detonation, with an estimated cell size $\lambda \approx 33$ cm for stoichiometric composition as

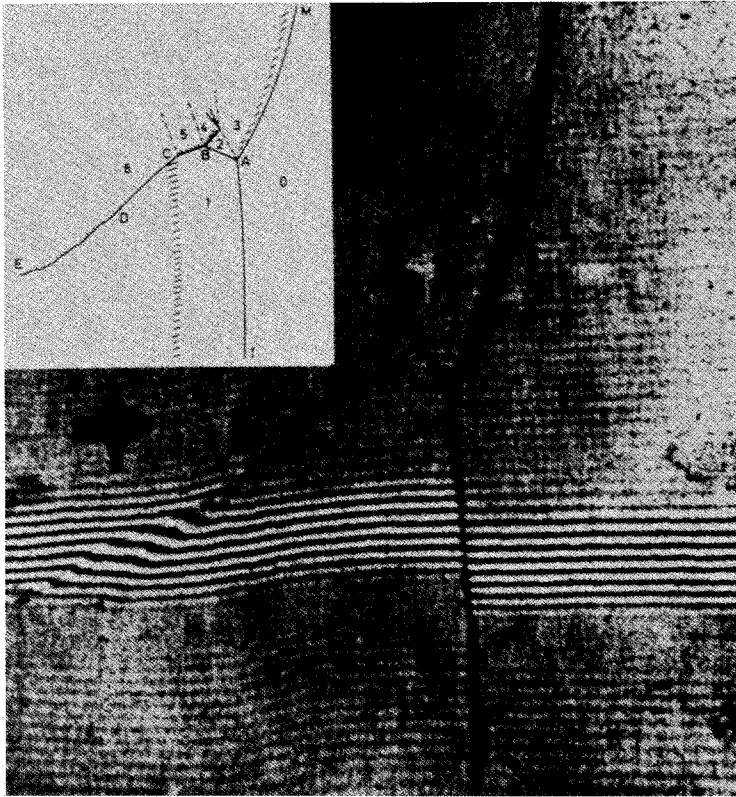


Fig. 12. Interferogram of the detailed double Mach-reflection configurations of the structure of a cellular front (courtesy of D. H. Edwards).

compared with the corresponding value of $\lambda \approx 5.35$ cm for the other alkanes. That the cell size λ is proportional to the induction time of the mixture had been suggested by Shchelkin and Troshin [23] long ago. However, to compute an induction time requires that the model for the detonation structure be known, and no theory exists as yet for the real three-dimensional structure. Nevertheless, one can use the classical ZND model for the structure and compute an induction time or, equivalently, an induction-zone length l . While this is not expected to correspond to the cell size λ (or cell length L_c), it may elucidate the dependence of λ on l itself (e.g., a linear dependence $\lambda = Al$, as suggested by Shchelkin and Troshin). Westbrook [24,25] has made computations of the induction-zone length l using the ZND model, but his calculations are based on a constant-volume process after the shock, rather than integration along the Rayleigh line. Very detailed kinetics of the oxidation processes are employed. By matching with one experimental point, the proportionality constant A can be obtained. The constant A differs for different gas mixtures (e.g., $A = 10.14$ for C_2H_4 , $A = 52.23$ for H_2); thus, the three-dimensional gas dynamic processes cannot be represented by a single constant alone over a range of fuel composition for all the mixtures. The chemical reactions in a detonation wave are strongly coupled to the details of the transient gas dynamic processes, with the end product of the

coupling being manifested by a characteristic chemical length scale λ (or equivalently L_c) or time scale $t_c = \lambda/C_1$ (where C_1 denotes the sound speed in the product gases, which is approximately the velocity of the transverse waves) that describes the global rate of the chemical reactions. Since $\lambda \simeq 0.6L_c$ and $C_1 \simeq 0.5D$, where D is the Chapman–Jouguet detonation velocity, we have $t_c \simeq L_{cD}$, which corresponds to the fact that the chemical reactions are essentially completed within one-cell length (or one cycle).

2. The Dynamic Detonation Parameters

The extent to which a detonation will propagate from one experimental configuration into another determines the dynamic parameter called critical tube diameter. “It has been found that if a planar detonation wave propagating in a circular tube emerges suddenly into an unconfined volume containing the same mixture, the planar wave will transform into a spherical wave if the tube diameter d exceeds a certain critical value d_c (i.e., $d \geq d_c$). If $d < d_c$, the expansion waves will decouple the reaction zone from the shock, and a spherical deflagration wave results [6].”

Rarefaction waves are generated circumferentially at the tube as the detonation leaves, propagate toward the tube axis, cool the shock heated gases, and, consequently, increase the reaction induction time. This induced delay decouples the reaction zone from the shock and a deflagration persists. The tube diameter must be large enough so that a core near the tube axis is not quenched and can support the development of a spherical detonation wave.

Some analytical and experimental estimates show that the critical tube diameter is 13 times the detonation cell size ($d_c \simeq 13 \lambda$) [6]. This result is extremely useful in that only laboratory tube measurements are necessary to obtain an estimate of d_c . It is a value, however, that could change somewhat as more measurements are made.

As in the case of deflagrations, a quenching distance exists for detonations, i.e., a detonation will not propagate in a tube whose diameter is below a certain size or between infinitely large parallel plates whose separation distance is again below a certain size. This quenching diameter or distance appears to be associated with the boundary layer growth in the retainer configuration [5]. According to Williams [5] the boundary layer growth has the effect of an area expansion on the reaction zone that tends to reduce the Mach number in the burned gases and the quenching distance arises due to the competition of this effect with the heat release that increases this Mach number. For the detonation to exist the heat release effect must exceed the expansion effect at the C - J plane otherwise the subsonic Mach number and the associated temperature and reaction rate will decrease further behind the shock front, and the system will not be able to recover to reach the C - J state.

The quenching distance is that at which the two effects are equal. This concept leads to the relation [5]

$$\delta^* \approx (\gamma - 1)H/8$$

where δ^* is the boundary layer thickness at the *C-J* plane and H is the hydraulic diameter (four times the ratio of the area to the periment of a duct, which is the diameter of a circular tube or twice the height of a chemical). Order-of-magnitude estimates of quenching distance may be obtained from the above expression if boundary layer theory is employed to estimated δ^* ; namely, $\delta^* \approx l/\sqrt{\text{Re}}$ where Re is $\rho l (u_1 - u_2)/\mu$ and l is the length of the reaction zone; μ is evaluated at the *C-J* plane. Typically $\text{Re} \geq 10^5$ and l can be found experimentally and approximated as 6.5 times the cell size λ [26].

3. Detonation Limits

Again as in the case of deflagrations, there exist mixture ratio limits outside of which it is not possible to propagate a detonation. Because of the quenching distance problem one could argue that two sets of possible detonation limits can be determined. One is based on chemical-rate-thermodynamic considerations and would give the widest limits since infinite confinement distance is inherently assumed and the other follows extension of the arguments with respect to quenching distance given in the preceding paragraph.

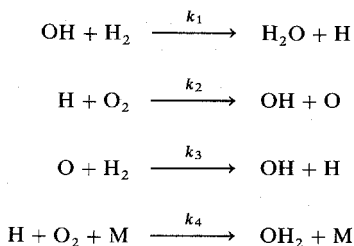
The quenching distance detonation limit comes about if the induction period or reaction zone length increase greatly as one proceeds away from the stoichiometric mixture ratio. Then the variation of δ^* or l will be so great that no matter how large the containing distance, the quenching condition will be achieved for the given mixture ratio. This mixture is the detonation limit.

Belles [27] essentially established the pure chemical-kinetic-thermodynamic approach to estimating detonation limits. Questions have been raised about the approach, but the line of reasoning developed is worth considering. It is a fine example of coordinating various fundamental elements discussed to this point and used to obtain an estimate of a complex phenomenon.

The Belles' prediction of the limits of detonability takes the following course. He deals with the hydrogen-oxygen case. Initially the chemical kinetic conditions for branched chain explosion in this system are defined in terms of the temperature, pressure, and mixture composition. The standard shock wave equations are used to express, for a given mixture, the temperature and pressure of the shocked gas before reaction is established (condition 1'). The shock Mach number is determined from the detonation velocity. These results are then combined with the explosion condition in terms of M and the mixture composition in order to specify the critical shock strengths

for explosion. The mixtures are then examined to determine whether they can support the shock strength necessary for explosion. Some cannot and they define the limit.

The set of reactions that determine the explosion condition of the hydrogen-oxygen system are



The steady-state solution shows that

$$d(\text{H}_2\text{O})/dt = \text{various terms}/[k_4(M) - 2k_2]$$

consequently the criterion for explosion is

$$k_4(M) = 2k_2 \quad (43)$$

Using rate constant for k_2 and k_4 and expressing the third body concentration (M) in terms of the temperature and pressure by means of the gas law, Belles rewrites Eq. (43) in the form

$$3.11 T e^{-8550/T}/f_x P = 1 \quad (44)$$

where f_x is the effective mole fraction of the third bodies in the formation reaction for HO_2 . Lewis and von Elbe [13], give the following empirical relationship for f_x :

$$f_x = f_{\text{H}_2} + 0.35 f_{\text{O}_2} + 0.43 f_{\text{N}_2} + 0.20 f_{\text{Ar}} + 1.47 f_{\text{CO}_2} \quad (45)$$

This expression gives a weighting for the effectiveness of other species as a third body, as compared to H_2 as a third body. Equation (44) is then written as a logarithmic expression

$$(3.710/T) - \log_{10}(T/P) = \log_{10}(3.11/f_x) \quad (46)$$

This equation suggests that if a given hydrogen-oxygen mixture, which could have a characteristic value of f dependent on the mixture composition, is raised to a temperature and pressure that satisfy the equation, then the mixture will be explosive.

For the detonation waves, the following relationships for the temperature and pressure can be written for the condition (1') behind the shock front. It is

these conditions which initiate the deflagration state in the detonation wave:

$$P_1/P_0 = (1/\alpha)[(M^2/\beta) - 1] \quad (47)$$

$$T_1/T_0 = [(M^2/\beta) - 1][\beta M^2 + (1/\gamma)]/\alpha^2 \beta M^2 \quad (48)$$

where M is the Mach number, $\alpha = (\gamma + 1)/(\gamma - 1)$, and $\beta = (\gamma - 1)/2\gamma$. Shock strengths in hydrogen mixtures are sufficiently low so that one does not have to be concerned with the real gas effects on the ratio of specific heats γ , and γ can be evaluated at the initial conditions.

From Eq. (46) it is apparent that many combinations of pressure and temperature will satisfy the explosive condition. However, if the condition is specified that the ignition of the deflagration state must come from the shock wave, Belles argues that there is only one Mach number that will satisfy the explosive condition. This Mach number is called the critical Mach number and is found by substituting Eqs. (47) and (48) into Eq. (46) to give:

$$\frac{3.710\alpha^2\beta M^2}{T_0[(M^2/\beta) - 1][\beta M^2 + (1/\gamma)]} - \log_{10} \left[\frac{T_0[\beta M^2 + (1/\gamma)]}{P_0\alpha\beta M^2} \right] = f(T_0, P_0, \gamma, M) \\ = \log_{10}(3.11f_x) \quad (49)$$

This equation is most readily solved by plotting the left-hand side as a function of M for the initial conditions. The logarithm term on the right-hand side is calculated for the initial mixture and M found from the plot.

The final criterion that establishes the detonation limits is imposed by energy considerations. The shock provides the mechanism whereby the combustion process is continually sustained; however, the energy to drive the shock, i.e., to heat up the unburned gas mixture, comes from the ultimate energy release in the combustion process. But if the enthalpy increase across the shock which corresponds to the critical Mach number is greater than the heat of combustion, an impossible situation arises. No explosive condition can be reached, and the detonation cannot propagate. Thus the criterion for the detonation of a mixture is

$$\Delta h_s \leq \Delta h_c$$

where Δh_c is the heat of combustion per unit mass for the mixture and Δh_s is the enthalpy rise across the shock for the critical number (M_c).

$$h_{T_1} - h_{T_0} = \Delta h_s \quad \text{where} \quad T_1 = T_0 \left[1 + \frac{1}{2}(\gamma - 1)M_c^2 \right]$$

The plot of Δh_c and Δh_s for the hydrogen-oxygen case as given by Belles is shown in Fig. 13. Where the curves cross in Fig. 13, $\Delta h_c = \Delta h_s$ and the limits specified. The comparisons with experimental data are very good as is shown in Table 5.

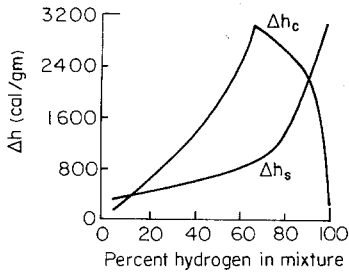


Fig. 13. Heat combustion per unit mass (Δh_c) and enthalpy rise across detonation shock (Δh_s) as a function of present hydrogen in oxygen (after Belles [27]).

Questions have been raised about this approach to calculate detonation limits, and some believe the general agreement between experiments and the theory as shown in Table 5 is fortuitous. One of the criticisms is that a given Mach number specifies a particular temperature and a pressure behind the shock. The expression representing the explosive condition also specifies a particular pressure and temperature. It is unlikely that there would be a direct correspondence of the two conditions from the different shock and explosion relationships. Equation (36) must give a unique result for the initial conditions because of the manner in which it was developed.

Detonation limits have been measured for various fuel-oxidizer mixtures. These values and comparison with the deflagration (flammability) limits are given in Table 6. It is interesting to note that the detonation limits are always

TABLE 5

Hydrogen detonation limits in oxygen and air

System	Lean limit (vol %)		Rich limit (vol %)	
	Experimental	Calculated	Experimental	Calculated
H ₂ -O ₂	15	16.3	90	92.3
H ₂ -Air	18.3	15.8	59.9	59.7

TABLE 6

Comparison of deflagration and detonation limits

	Lean		Rich	
	Deflagration	Detonation	Deflagration	Detonation
H ₂ -O ₂	4	15	94	90
H ₂ -Air	4	18	74	59
CO-O ₂	16	38	94	90
NH ₃ -O ₂	15	25	79	75
C ₃ H ₈ -O ₂	2	3	55	37

narrower than the deflagration limit. But for H_2 and the hydrocarbons, one should recall that because of the product molecular weight the detonation velocity has its maximum near the rich limit. The deflagration velocity maximum is always very near the stoichiometric value and indeed has its minimum values at the limits. Indeed, the experimental definition of the deflagration limits would require this result.

G. DETONATIONS IN NONGASEOUS MEDIA

Detonations can be generated in solid propellants and solid and liquid explosives. Such propagation through these condensed phase media make up another important aspect of the overall subject of detonation theory. The general Hugoniot relations developed are applicable, but a major difficulty exists in obtaining appropriate solutions due to the lack of good equations of state necessary due to the very high (10^5 atm) pressures generated. For details on this subject the reader is referred to a number of books [28].

Detonations will also propagate through liquid fuel droplet dispersions (sprays) in air and through solid-gas mixtures such as dust dispersions. Volatility of the liquid fuel plays an important role in characterizing the detonation developed. For low volatile fuels, fracture and vaporization of the fuel droplets become an important element in the propagation mechanism and it is not surprising that the velocities obtained are less than the theoretical maximum. Recent reviews of this subject can be found in Refs. [29] and [30]. Dust explosions and subsequent detonation generally occur when the dust particle size becomes sufficiently small that the heterogeneous surface reactions occur rapidly enough that the energy release rates will nearly support Chapman-Jouguet conditions. The mechanism of propagation of this type of detonation is not well understood. Some reported results of detonations in dust dispersions can be found in Refs. [31] and [32].

PROBLEMS

1. A mixture of hydrogen, oxygen, and nitrogen, having partial pressures in the ratio 2:1:5 in the order listed, is observed to detonate and produce a detonation wave that travels at 1890 m/sec when the initial temperature is 292 K and the initial pressure is 1 atm. Assuming fully relaxed conditions, calculate the peak pressure in the detonation wave and the pressure and temperature just after the passage of the wave. Prove that u_2 corresponds to the Chapman-Jouguet condition. Reasonable assumptions should be made for this problem; that is assume no dissociation, the pressure after the wave passes is much greater than the initial pressure, that one can use existing gas dynamic tables designed for air to analyze processes inside the wave and specific heats independent of pressure.

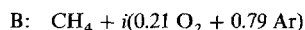
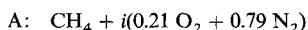
2. Calculate the detonation velocity in a gaseous mixture of 75% ozone (O_3) and 25% oxygen (O_2) initially at 298 K and 1 atm pressure. The only products after detonation are oxygen molecules and atoms. Take the $\Delta H_f^\circ(O_3) = 34.0$ kcal/mole and all other thermochemical data from the JANNAF tables in the appendices.

Report the temperature and pressure of the Chapman–Jouget point as well.

For the same mixture as the previous problem, calculate the adiabatic (deflagration) temperature when the initial cold temperature is 298 K and the pressure the same as that calculated for the Chapman–Jouget point.

Compare and discuss the results for these deflagration and detonation temperatures.

3. There exists two mixtures (A and B) that will propagate both a laminar flame and a detonation wave under the appropriate conditions.



Which mixture will have the higher flame speed? Which will have the higher detonation velocity? Very brief explanations should support your answers. The stoichiometric coefficient i is the same for both mixtures.

4. What would be the most effective diluent to a detonable mixture to lower, or prevent, detonation possibility: carbon dioxide, helium, nitrogen, or argon? Order the expected effectiveness.

REFERENCES

1. Friedman, R., *J. Am. Rocket Soc.* **23**, 349 (1953).
2. Lee, J. H., *Ann. Rev. Phys. Chem.* **28**, 75 (1977).
3. Urtiew, P. A., and Oppenheim, A. K., *Proc. R. Soc. London A* **295**, 13 (1966).
4. Fickett, W., and Davis, W. C., "Detonation," Univ. of California Press, Berkeley, California, 1979.
5. Zeldovich, Y. B., and Kompaneets, A. S., "Theory of Detonation," Academic Press, New York, 1960.
6. Williams, F. A., "Combustion Theory," Chapter 6, Benjamin-Cummings, Menlo Park, California, 1985.
7. Lee, J. H., *Ann. Rev. Fluid Mech.* **16**, 311 (1984).
8. Chapman, D. L., *Philos. Mag.* **47**, 90 (1899).
9. Jouguet, E., "Mécaniques des Explosifs," Dorn, Paris, 1917.
10. Zeldovich, Y. B., *NACA Tech. Memo.* No. 1261 (1950).
11. Von Neumann, J., *OSRD Rep.* No. 549 (1942).
12. Döring, W., *Ann. Phys.* **43**, 421 (1943).
13. Gordon, S., and McBride, B. V., *NASA SP-273* (1971).
14. Lewis, B., and von Elbe, G., "Combustion, Flames and Explosions of Gases," 2nd ed., Chapter VIII, Academic Press, New York, 1961.
15. Strehlow, R. A., "Fundamentals of Combustion," Intention Textbook Co., Scranton, Pennsylvania, 1984.
16. Dryer, F. L., Naegeli, D. W., and Glassman, I., *Combust. Flame* **17**, 270 (1971).
17. Glassman, I., and Sawyer, R., "The Performance of Chemical Propellants," Technivision, Ltd., Slough, England, 1971.

17. Hirschfelder, J. O., Curtiss, C. F., and Bird, R. B., "The Molecular Theory of Gases and Liquids," Wiley, New York, 1954.
18. Libouton, J. C., Dormal, M., and van Tiggelen, P. J., *Prog. Astronaut. Aeronaut.* **75**, 358 (1981).
19. Strehlow, R. A., and Engel, C. D., *AIAA J.* **7**, 492 (1969).
20. Bull, D. C., Elsworth, J. E., Shuff, P. J., and Metcalfe, E., *Combust. Flame* **45**, 7 (1982).
21. Kynstantas, R., Guirao, C., Lee, J. H. S., and Sulmistras, A., *Int. Colloq. Dyn. Explos. React. Syst. 9th*, Poitiers, France.
22. Kynstantas, R., Lee, J. H. S., and Guirao, C., *Combust. Flame* **48**, 63 (1982).
23. Shchelkin, K. I., and Troshin, Y. K., "Gasdynamics of Combustion," Mono Book Corp., Baltimore, 1965.
24. Westbrook, C., *Combust. Flame* **46**, 191 (1982).
25. Westbrook, C., and Urtiew, P., *Int. Symp. Combust., 19th*, p. 615, Combustion Inst., Pittsburgh, Pennsylvania, 1982.
26. Edwards, D. H., Jones, A. J., and Phillips, P. E., *J. Phys. D* **9**, 1331 (1976).
27. Belles, F. E., *Int. Symp. Combust.*, p. 745, Butterworth, London, (1959).
28. Bowden, F. P., and Yoffee, A. D., "Limitation and Growth of Explosions in Liquids and Solids," Cambridge Univ. Press, Cambridge, England, 1952.
Cook, M. A., The Science of High Explosives, *ACS Monogr.* No. 39 (1958).
29. Dabora, E. K., in "Fuel-Air Explosions" (J. H. S. Lee and C. M. Guirao, eds.), p. 245, Univ. of Waterloo Press, Waterloo, Canada, 1982.
30. Sichel, M., in "Fuel-Air Explosions" (J. H. S. Lee and C. M. Guirao, eds.), p. 265, Univ. of Waterloo Press, Waterloo, Canada, 1982.
31. Strauss, W. A., *AIAA J.* **6**, 1753 (1968).
32. Palmer, K. N., and Tonkin, P. S., *Combust. Flame* **17**, 159 (1971).

Diffusion Flames

A. INTRODUCTION

Earlier chapters were concerned with flames in which the fuel and oxidizer were homogeneously mixed. Even if in the initial stages of a combustion event the fuel and oxidizer are separate entities and mixing occurs rapidly compared to combustion reactions, or if mixing occurs well ahead of the flame zone (as in a Bunsen Burner), the burning process may be considered in terms of homogeneous premixed conditions. There are systems in which the mixing rate is slow compared to the reaction rate of the fuel and oxidizer and, thus, the mixing controls the burning rate. Most practical systems fall in the category of mixing rate controlling and lead to the so-called diffusion flames in which fuel and oxidizer come together in a reaction zone through molecular and turbulent diffusion. The fuel may be in the form of a gaseous fuel jet or a condensed medium (either liquid or solid) and the oxidizer may be a flowing gas stream or the simple quiescent atmosphere. The distinctive characteristic of a diffusion flame is that the burning (or fuel consumption) rate is determined by the rate at which the fuel and oxidizer are brought together in proper proportions for reaction.

Since diffusion rates vary with pressure and the rate of overall combustion reactions vary approximately with the pressure squared, at very low pressures, even though the fuel and oxidizer may be separate concentric gaseous streams, the flame formed will exhibit premixed combustion characteristics. Figure 1 details how the flame structure varies with pressure for such

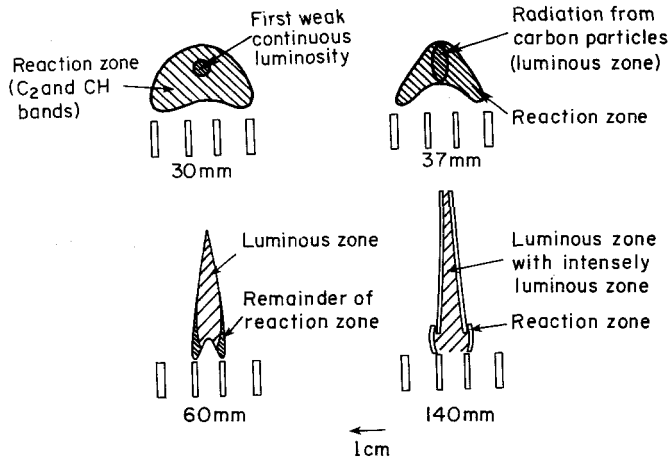


Fig. 1. Structure of an acetylene-air diffusion flame at various pressures (after Gaydon and Wolfhard [1]).

a configuration in which the fuel is a simple higher-order hydrocarbon. Normally, the concentric fuel-oxidizer configuration is typical of diffusion flame processes.

B. GASEOUS FUEL JETS

Until recently gaseous diffusion flames have received less research attention than premixed flames, despite the fact that diffusion flames have far greater practical application. Perhaps the lack has been due to the fact that gaseous diffusion flames, unlike premixed flames, have no fundamental characteristic property such as flame velocity, which can be measured readily; even initial mixture strength has no practical meaning. Indeed a mixture strength does not exist for a gaseous fuel jet issuing into a quiescent atmosphere. Certainly no mixture strength exists for a single, small fuel droplet burning in the infinite reservoir of a quiescent atmosphere.

1. Appearance

Only the shape of the burning laminar fuel jet depends on the mixture strength, i.e., the quantity of air supplied. If in a concentric configuration the volumetric flow rate of air flowing in the outer annulus is in excess of the stoichiometric amount required for the volumetric flow rate of the inner fuel jet, the flame that develops takes a closed, elongated form. A similar flame

forms when a fuel jet issues into the quiescent atmosphere. Such flames are referred to as being overventilated. If in the concentric configuration the air supply in the outer annulus is reduced below an initial mixture strength that would correspond to the stoichiometric required amount, a fan-shaped, underventilated flame is produced. The general shapes of the underventilated and overventilated flame are shown in Fig. 2. As will be shown later in this chapter, the actual heights vary with the flow conditions.

The axial symmetry of the concentric configuration shown in Fig. 2 is not conducive to experimental analyses, particularly when some optical diagnostic tools or thermocouples are used. There are parametric variations in the r and y coordinates shown in Fig. 2. To facilitate experimental measurements on diffusion flames, the so-called Wolfhard–Parker two-dimensional gaseous fuel jet burner is used. Such a configuration is shown in Fig. 3 taken from Smyth *et al.* [2]; the screens shown in the figure are used to stabilize the flame. As can be seen in this figure, ideally there are no parametric variations along the length of the slot.

Another type of gaseous diffusion flame is created by opposed jets of fuel and oxidizer. The types most frequently used are shown in Fig. 4. Although these configurations are somewhat more complex to establish experimentally, they have definite advantages. The opposed jet configuration in which the fuel stream is injected through a porous cylinder has two major advantages compared to the concentric fuel jet or Wolfhard–Parker burners. First, there is no possibility of oxidizer diffusion to the fuel side through the quench zone at the jet-tube lip; and secondly, the flow configuration is very amenable to analysis. Although the aerodynamic analysis of the configuration, which produces the flat diffusion flame, is somewhat more complex and stability a little more sensitive to flow conditions, the creation of a flat flame is a definite experimental advantage when immersion or optical instrumentation is used.

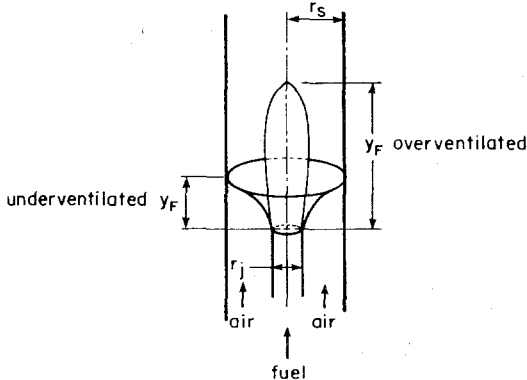


Fig. 2. Appearance of cylindrical gaseous fuel jet flames.

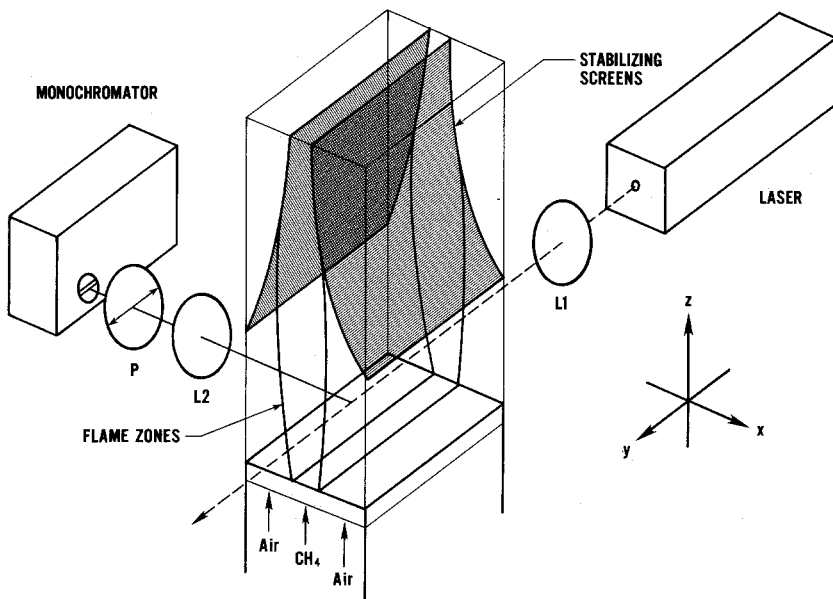


Fig. 3. Two-dimensional Wolfhard-Parker gaseous fuel jet burner (after Smyth *et al.* [2]).

The color of a hydrocarbon-air diffusion flame is distinctively different than its premixed counterpart. Whereas a premixed hydrocarbon-air flame is violet or blue-green in color, the corresponding diffusion flame varies from a bright yellow to an orange color. The color of the diffusion flame arises because of the formation of soot on the fuel side of the flame. Soot particles, which flow through the reaction zone, reach the flame temperature and are usually burned in the reaction zone. Due to the flame temperatures that exist and the sensitivity of the eye to various wavelengths in the visible region of the electromagnetic spectrum, the hydrocarbon-air diffusion flame appears to be yellow or orange in color. In Wolfhard-Parker and opposed jet burners, some soot escapes without entering the flame zone and appears as black smoke. In the concentric jet configuration, if the volumetric flow rate of the fuel is increased substantially, the top of the flame will appear to open and a soot smoke trail appears. The presence of soot also confuses the selection of the actual height of a concentric diffusion flame. Many early investigators assumed that the diffusion flame height coincided with the height of the visible tip. However, soot particles penetrate the actual diffusion flame around its apex, burn and radiate. Thus, the luminous height of most hydrocarbon diffusion flames is greater than the actual diffusion flame height [3-6]. The actual flame height thus must be determined from measurement of the flame gas composition. Non soot-forming diffusion flames, such as those

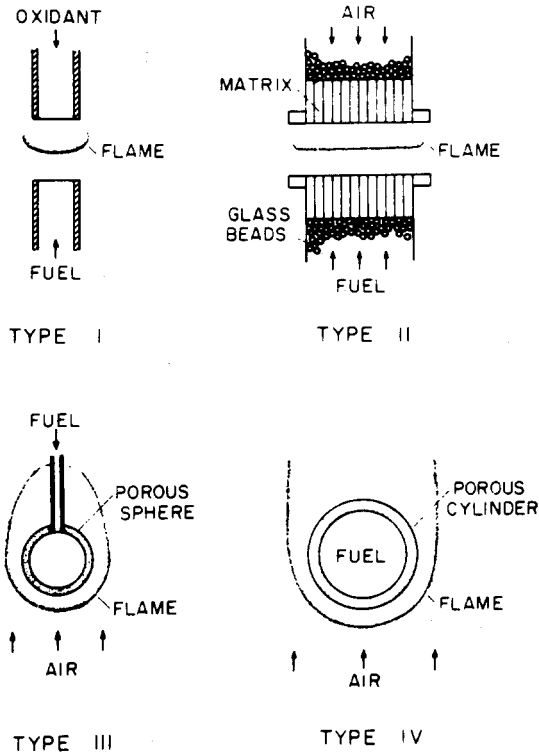


Fig. 4. Various counterflow diffusion flames.

found with H_2 , CO , and methanol, are mildly visible and look very much like their premixed counterparts. Their heights can be estimated visibly.

2. Structure

Unlike premixed flames that have a very narrow reaction zone, diffusion flames have a wider region over which the composition changes and chemical reaction can take place. Obviously, these changes are due principally to some interdiffusion of reactants and products. Hottel and Hawthorne [7] were the first to make detailed measurements of species distributions in a concentric laminar H_2 -air diffusion flame. The type of results they obtained for a radial distribution at a height corresponding to the broken line on Fig. 2 is shown in Fig. 5. More recently Smyth *et al.* [2] made very detailed and accurate measurements of temperature and species variation across a Wolfhard-Parker burner in which methane was the fuel. Their results are shown in Figs. 6 and 7.

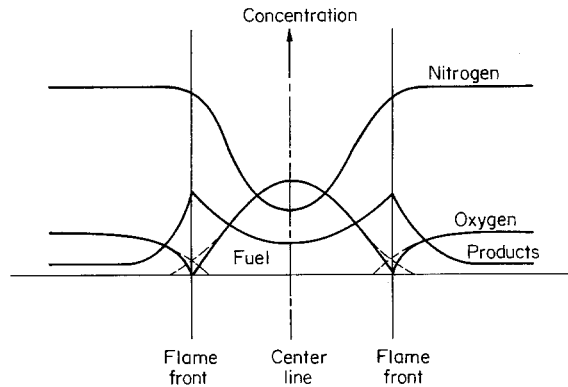


Fig. 5. Species variations through a diffusion flame at a fixed height above the fuel jet tube.

The flame front can be assumed to exist at the point of maximum temperature and indeed this point corresponds to that at which the maximum concentrations of major products (CO_2 and H_2O) exist. The same type of profiles would exist for a simple fuel jet issuing into a quiescent air. The maxima arise due to diffusion of reactants in a direction normal to the flowing streams. It is most important to realize that for the concentric configuration the diffusion establishes a bulk velocity component in the normal direction. In the steady state the flame front produces a flow outward,

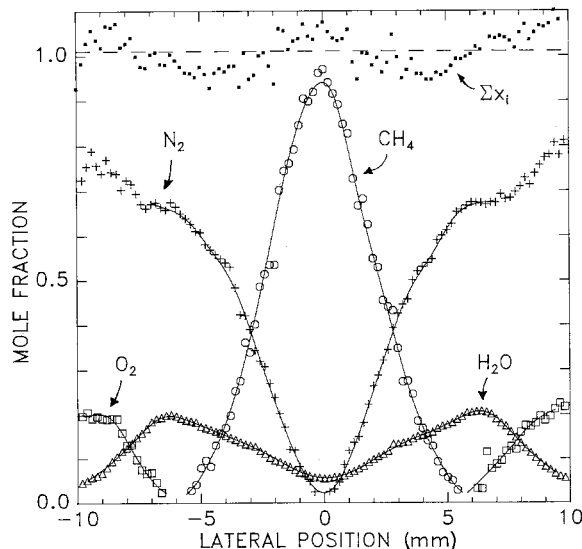


Fig. 6. Species variations throughout a Wolfhard-Parker methane-air diffusion flame (after Smyth *et al.* [2]).

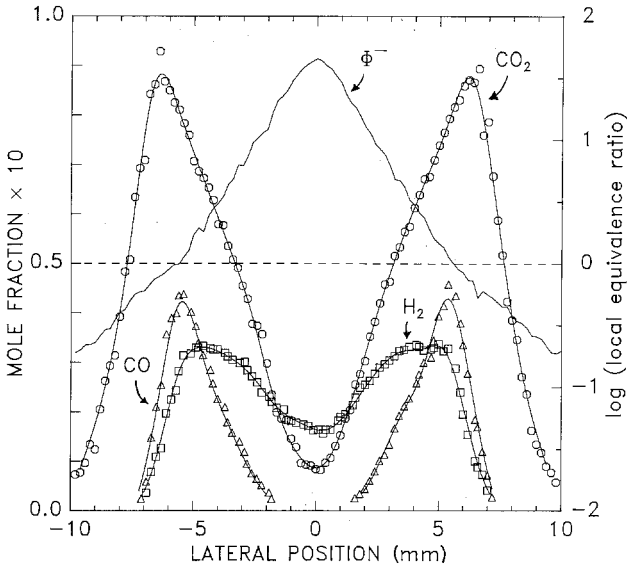


Fig. 7. Additional species variations for conditions of Fig. 6 (after Smyth *et al.* [2]).

and oxygen and a little nitrogen flow inward toward the centerline. Normally in the steady state the total mass rate of products is greater than the sum of the other two. Thus, the bulk velocity that one would observe moves from the flame front outward. The oxygen flow that arises due to diffusion and the concentration gradient of oxygen between the outside stream and the flame front is then in the opposite direction to the bulk flow. Between the centerline and the flame front, the bulk velocity must, of course, flow from the centerline outward. There is no sink at the centerline. In the steady state, the concentration of the products reaches a definite value at the centerline. This value is established by the diffusion rate of products inward and the amount transported outward by the bulk velocity.

Since total disappearance of reactants at the flame front would indicate infinitely fast reaction rates, it is more likely that a graphical representation of the radial distribution of reactants should be as that given by the dashed lines in Fig. 5. To stress this point, the dashed lines are drawn to grossly exaggerate the thickness of the flame front. Even with finite reaction rates, the flame front is quite thin. The experimental results shown in Figs. 6 and 7 indicate that in diffusion flames the fuel and oxidizer diffuse toward each other at rates that are in stoichiometric proportions. Since the flame front is a sink for both the fuel and oxidizer, intuitively one would have expected this most important observation. Independent of the overall mixture strength, since fuel and oxidizer diffuse together in stoichiometric proportions, the flame temperature

closely approaches the adiabatic stoichiometric flame temperature. Probably it is somewhat lower due to finite reaction rates, i.e., approximately 90% of the adiabatic stoichiometric value [8] whether it is a hydrocarbon fuel or not. This observation establishes an interesting aspect of practical diffusion flames in that for an adiabatic situation two fundamental temperatures exist for a fuel: one that corresponds to its stoichiometric value and occurs at the flame front and one that occurs after the products mix with the excess air to give an adiabatic temperature that corresponds to the initial mixture strength.

3. Theoretical Considerations

The theory of premixed flames consisted essentially of an analysis of factors such as mass diffusion, heat diffusion, and the reaction mechanisms as they affected the rate of homogeneous reactions taking place. Inasmuch as the primary mixing processes of fuel and oxidizer appear to dominate the burning processes in diffusion flames, the theories emphasize the rates of mixing (diffusion) in deriving the characteristics of such flames.

It can be verified easily by experiments that in an ethylene-oxygen premixed flame, the average rate of consumption of reactants is about 4 moles/cm³ sec, whereas for the diffusion flame (by measurement of flow, flame height, and thickness of reaction zone—a crude but approximately correct approach), the average rate of consumption is only 6×10^{-5} moles/cm³ sec. Thus, the consumption and heat release rates of premixed flames are much larger than those of pure mixing controlled diffusion flames.

The theoretical solution to the diffusion flame problem is best approached in the overall sense of a steady flowing gaseous system in which both the diffusion and chemical processes play a role. Even in the burning of liquid droplets, a fuel flow due to evaporation exists. The approach is very much the same as that presented in Chapter 4, Section A.2, except that the fuel and oxidizer are diffusing in opposite directions and in stoichiometric proportions relative to each other. If one picks a differential element along the x direction of diffusion, then the conservation balances for heat and mass may be obtained for the fluxes, as shown in Fig. 8.

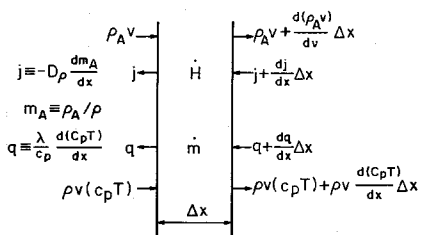


Fig. 8. Balances across a differential element within a diffusion flame.

In Fig. 8, j is the mass flux as given by a representation of Fick's law when there is bulk movement. From Fick's law

$$j = -D(\partial\rho_A/\partial x)$$

As will be shown in Section 6.B.2, the following form of j is exact; however, the same form can be derived if it is assumed that the total density does not vary with the distance x , as, of course, it actually does:

$$j = -D\rho \frac{\partial(\rho_A/\rho)}{\partial x} = -D\rho \frac{\partial m_A}{\partial x}$$

where m_A is the mass fraction of species A . q is the heat flux as given by Fourier's law of heat conduction; \dot{m}_A is the rate of decrease of mass A in the volumetric element $(\Delta x.1)(g/cm^3 \text{ sec})$ and \dot{H} is the rate of chemical energy release in the volumetric element $(\Delta x.1)(\text{cal/cm}^3 \text{ sec})$ (see Fig. 8).

With the above definitions, for the one-dimensional problem defined in Fig. 8, the expression for conservation of a species A (say the oxidizer) is

$$\frac{\partial\rho_A}{\partial t} = \frac{\partial}{\partial x} \left[(D\rho) \frac{\partial m_A}{\partial x} \right] - \frac{\partial(\rho_A v)}{\partial x} - \dot{m}_A \quad (1)$$

where ρ is the total mass density, ρ_A the partial density of species A , and v the bulk velocity in direction x . Solving this time-dependent diffusion flame problem is outside the scope of this text. Indeed most practical combustion problems have a steady fuel mass input. Thus, for the steady problem, which infers steady mass consumption and flow rates, not only may $\partial\rho_A/\partial t$ be taken as zero, but also the following substitution used:

$$\frac{d(\rho_A v)}{dx} = \frac{d[(\rho v)(\rho_A/\rho)]}{dx} = (\rho v) \frac{dm_A}{dx} \quad (2)$$

The term (ρv) is a constant in the problem since there are no sources or sinks. With the further assumption from simple kinetic theory that $D\rho$ is independent of temperature and, thus, of x , Eq. (1) becomes

$$D\rho \frac{d^2 m_A}{dx^2} - (\rho v) \frac{dm_A}{dx} = \dot{m}_A \quad (3)$$

Obviously, the same type of expression must hold for the other diffusing species B (say the fuel) even if its gradient is opposite to that of A so that

$$D\rho \frac{d^2 m_B}{dx^2} - (\rho v) \frac{dm_B}{dx} = \dot{m}_B = i\dot{m}_A \quad (4)$$

where \dot{m}_B is the rate of decrease of species B in the volumetric element $(\Delta x.1)$ and i is the mass stoichiometric coefficient

$$i \equiv \dot{m}_B/\dot{m}_A$$

The energy equation evolves as it did in Chapter 4, Section A.2 to give

$$\frac{\lambda}{c_p} \frac{d^2(c_p T)}{dx^2} - (\rho v) \frac{d(c_p T)}{dx} = + \dot{H} = -i\dot{m}_A H \quad (5)$$

where \dot{H} is the rate of chemical energy release per unit volume and H is the heat release per unit mass of fuel consumed, (cal/g); i.e.,

$$-\dot{m}_B H = \dot{H}, \quad -i\dot{m}_A H = \dot{H} \quad (6)$$

since \dot{m}_B must be negative for there to be heat release (exothermic reaction).

Although the form of Eqs. (3), (4), and (5) is the same as that obtained in dealing with premixed flames, there is an important difference in the boundary conditions which exist. Furthermore, in comparing Eqs. (3) and (4) with Eqs. (28) and (29) (in Chapter 4) it must be realized that in Chapter 4, the mass change symbol \dot{w} was defined as always being a negative quantity.

Multiplying Eq. (3) by $i\dot{H}$ and then combining it with Eq. (5) for the condition $Le = 1$ or $D\rho = (\lambda/c_p)$, one obtains

$$D\rho \frac{d^2}{dx^2} (c_p T + im_A H) - (\rho v) \frac{d}{dx} (c_p T + im_A H) = 0 \quad (7)$$

This procedure is sometimes referred to as the Schvab-Zeldovich formulation. Mathematically what has been accomplished is that the nonhomogeneous terms (\dot{m} and \dot{H}) have been eliminated and a homogeneous differential equation [Eq. (7)] has been obtained.

The equations could have been developed for a generalized coordinate system. In a generalized coordinate system, they would have the form

$$\nabla \cdot [(\rho v)(c_p T) - (\lambda/c_p)\nabla(c_p T)] = -\dot{H} \quad (8)$$

$$\nabla \cdot [(\rho v)(m_j) - \rho D\nabla m_j] = +\dot{m}_j \quad (9)$$

These equations could be generalized even further (see Williams [9]) by simply writing $\sum h_j^0 \dot{m}_j$ instead of \dot{H} , where h_j^0 is the heat of formation per unit mass at the base temperature of each species j . However, for notation simplicity and since for most combustion and propulsion systems it is the energy release which is of importance, an overall rate expression for a reaction of the type which follows will suffice:

$$F + \phi O = P \quad (10)$$

where F is the fuel, O the oxidizer, P the product, and ϕ the molar stoichiometric index. Then Eqs. (8) and (9) may be written as

$$\nabla \cdot \left[(\rho v) \frac{\dot{m}_j}{MW_j v_j} - (\rho D) \nabla \frac{\dot{m}_j}{MW_j v_j} \right] = \dot{M} \quad (11)$$

$$\nabla \cdot \left[(\rho v) \frac{c_p T}{HMW_j v_j} - (\rho D) \nabla \frac{c_p T}{HMW_j v_j} \right] = \dot{M} \quad (12)$$

where MW is the molecular weight, $\dot{M} = \dot{m}_j / MW_j v_j$; $v_j = \phi$ for the oxidizer, and $v_j = 1$ for the fuel. Both equations have the form

$$\nabla \cdot [(\rho v)\alpha - (\rho D)\nabla\alpha] = \dot{M} \quad (13)$$

where $\alpha_T = c_p T / HMW_j v_j$ and $\alpha_j = \dot{m}_j / MW_j v_j$. They may be expressed as

$$L(\alpha) = \dot{M} \quad (14)$$

where the linear operator $L(\cdot)$ is defined as

$$L(\alpha) = \nabla \cdot [(\rho v)\alpha - (\rho D)\nabla\alpha] \quad (15)$$

The nonlinear term may be eliminated from all except one of the relationships $L(\alpha) = \dot{M}$. For example,

$$L(\alpha_1) = \dot{M} \quad (16)$$

can be solved for α_1 , then the other flow variables can be determined from the linear equations for a simple coupling function Ω so that

$$L(\Omega) = 0 \quad (17)$$

where $\Omega = (\alpha_T - \alpha_1) \equiv \Omega_T$ or $\Omega = (\alpha_j - \alpha_1) \equiv \Omega_j$ ($j \neq 1$). Obviously if $1 =$ fuel and there is a fuel-oxidizer system only, $j = 1$ gives $\Omega = 0$ and shows the necessary redundancy.

4. The Burke-Schumann Development

With the development in the previous section, it is now possible to approach the classical problem of determining the shape and height of a burning gaseous fuel jet in a coaxial stream as first described by Burke and Schumann and presented in detail in Lewis and von Elbe [10].

This description is given by the following particular assumptions:

1. At the port position, the velocities of the air and fuel are considered constant, equal, and uniform across their respective tubes. Experimentally this condition could be obtained by varying the radii of the tubes (see Fig. 1). The molar fuel rate is then given by the radii ratio:

$$r_j^2 / (r_s^2 - r_j^2)$$

2. The velocity of the fuel and air up the tube in the region of the flame is the same as the velocity at the port.

3. The coefficient of interdiffusion of the two gas streams is constant.

Burke and Schumann [11] suggested that the effects of assumptions 2 and 3 compensate for each other and thus minimize errors. However, D increases

as $T^{1.67}$ and velocity increases as $T^{1.00}$, but this disparity should not be the main objection. The main objection should be the variation of D with T in the horizontal direction due to heat conduction from the flame.

4. Interdiffusion is entirely radial.
5. Mixing is by diffusion only; i.e., there are no radial velocity components.
6. Of course, the general stoichiometric relation prevails.

With these assumptions it is possible to readily solve the coaxial jet problem. The only differential equation that one is obliged to consider is

$$L(\Omega) = 0 \quad \text{with} \quad \Omega = \alpha_F - \alpha_o$$

where $\alpha_F = +m_F/MW_F v_F$ and $\alpha_o = +m_o/MW_o v_o$.

In cylindrical coordinates the general equation becomes

$$(v/D)(\partial\Omega/\partial y) - (1/r)(\partial/\partial r)(r \partial\Omega/\partial r) = 0 \quad (18)$$

The terms in $\partial/\partial\theta$ are set equal to zero because of the symmetry. The boundary conditions become

$$\begin{aligned} \Omega &= \frac{m_{F,0}}{MW_F v_F} & \text{at } y = 0, & \quad 0 \leq r \leq r_j \\ &= -\frac{m_{o,0}}{MW_o v_o} & \text{at } y = 0, & \quad r_j \leq r \leq r_s \end{aligned}$$

and $\partial\Omega/\partial r = 0$ at $r = r_s$, $y > 0$.

It is convenient to introduce dimensionless coordinates

$$\xi \equiv r/r_s, \quad \eta \equiv yD/vr_s^2$$

and to define parameters $c \equiv r_j/r_s$ and

$$v \equiv m_{o,0} MW_F v_F / m_{F,0} MW_o v_o$$

and the reduced variable

$$\gamma \equiv \Omega(MW_F v_F / m_{r,0})$$

Equation (18) and the boundary condition then become

$$\partial\gamma/\partial\eta = (1/\xi)(\partial/\partial\xi)(\xi \partial\gamma/\partial\xi) \quad (19)$$

$$\gamma = 1 \quad \text{at } \eta = 0, \quad 0 \leq \xi < c; \quad \gamma = -v \quad \text{at } \eta = 0, \quad c \leq \xi < 1$$

and

$$\partial\gamma/\partial\xi = 0 \quad \text{at } \xi = 1, \quad \eta > 0$$

Equation (19) with these new boundary conditions has the known solution:

$$\gamma = (1 + \nu)c^2 - \nu + 2(1 + \nu)c \sum_{n=1}^{\infty} (1/\phi_n) \{J_1(c\phi_n)/[J_0(\phi_n)]^2\} \\ \times J_0(\phi_n \xi) \exp(-\phi_n^2 \eta) \quad (20)$$

where J_0 and J_1 are Bessel functions of the first kind (of order zero and one, respectively) and the ϕ_n represent successive roots of the equation $J_1(\phi) = 0$ (with ordering convention $\phi_n > \phi_{n-1}$, $\phi_0 = 0$). This equation gives the solution for Ω in the present problem.

The flame shape is defined at the point where the fuel and oxidizer disappear and that specifies the place where $\Omega = 0$. Hence, setting $\gamma = 0$ provides a relation between ξ and η that defines the locus of the flame surface.

The equation for the flame height is obtained by solving Eq. (20) for η after setting $\xi = 0$ for the overventilated flame and $\xi = 1$ for the underventilated flame (also $\gamma = 0$).

The resulting equation is still very complex. Since flame heights are large enough to cause the factor $\exp(-\phi_n^2 \eta)$ to decrease rapidly as n increases at these values of η , it usually suffices to retain only the first few terms of the sum in the basic equation for this calculation. Neglecting all terms except $n = 1$, one obtains the rough approximation

$$\eta = (1/\phi_1^2) \ln\{2(1 + \nu)cJ_1(c\phi_1)/[\nu - (1 + \nu)c]\phi_1 J_0(\phi_1)\} \quad (21)$$

for the dimensionless height of the overventilated flame. The first zero of $J_1(\phi)$ is $\phi_1 = 3.83$.

The flame shapes and heights predicted by such expressions (see Fig. 9) are shown by Lewis and von Elbe [10] to be in good agreement with experimental results—which is surprising considering the basic drastic assumptions.

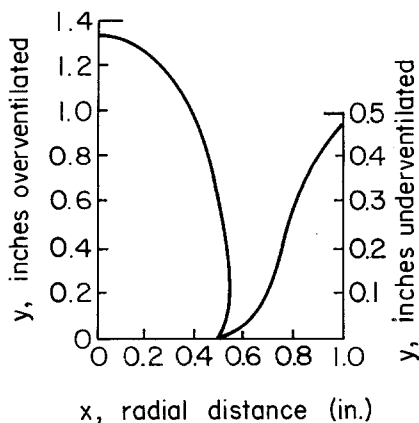


Fig. 9. Flame shapes as predicted by Burke-Schumann theory for cylindrical fuel jet systems (after Burke and Schumann [11]).

Indeed it should be noted that Eq. (21) specifies that the dimensionless flame height can be written as

$$\eta = f(c, v) \quad (22)$$

and, thus, the flame height can also be represented by

$$y_F = \frac{vr_j^2}{Dc^2} f(c, v) = \frac{\pi r_j^2 v}{\pi D} f'(c, v) = \frac{Q}{\pi D} f'(c, v) \quad (23)$$

where Q is the volumetric flow rate of the fuel and $f' = (f/c^2)$. Thus, one observes that the flame height of a circular fuel jet is directly proportional to the volumetric flow rate of the fuel.

Roper [3] in a pioneering paper has vastly improved on the Burke-Schumann approach to determine flame heights not only for circular ports, but also for square ports and slot burners. The significance of this work is that it uses the fact that the Burke-Schumann approach neglects buoyancy and assumes the mass velocity should everywhere be constant and parallel to the flame axis to satisfy continuity [9] and then points out that resulting errors cancel for the flame height of a circular port burner, but not for the other geometries [3,4]. The major assumption in the Burke-Schumann analyses is that the velocities are everywhere constant and parallel to the flame axis. Roper considers the case in which buoyancy forces increase the mass velocity after the fuel leaves the burner port and shows that continuity requires that the streamline spacing must decrease as the mass velocity increases. Consequently, all volume elements move closer to the flame axis, the width of the concentration profiles are reduced and the diffusion rates increased.

Roper [3] also considered that the velocity of the fuel gases is increased due to heating and that the gases leaving the burner port at temperature T_0 rapidly attained a constant value T_f in the flame regions controlling diffusion and that the diffusivity in the same region was

$$D = D_0(T_f/T_0)^{1.67}$$

where D_0 is the ambient value of the diffusivity. He then developed, considering the effect of temperature on the velocity, the following relationship for the flame height:

$$y_F = \frac{Q}{4\pi D_0} \frac{1}{\ln[1 + (1/S)]} \left(\frac{T_0}{T_f} \right)^{0.67} \quad (24)$$

where S is the stoichiometric volume rate of air to volume rate of fuel. Although Roper's analysis does not permit calculation of the flame shape, it does produce for the flame height a much simpler expression than Eq. (21).

If due to buoyancy the fuel gases attain a velocity v_b in the flame zone after leaving the port exit, then continuity requires that the effective radial

diffusion distance be some value r_b . Obviously, continuity requires that ρ be the same for both cases, so that

$$r_j^2 v = r_b^2 v_b$$

Thus, one observes that regardless whether the fuel jet is momentum or buoyancy controlled, the flame height y_F is directly proportional to the volumetric flow leaving the port exit.

Given the condition that buoyancy can play a significant role, then the fuel gases start with an axial velocity and continue with a mean upwards acceleration g due to buoyancy. The velocity of the fuel gases v is then given by

$$v = (v_o^2 + v_b^2)^{1/2} \quad (25)$$

where now v is the actual velocity, v_o is the momentum driven velocity at the port, and v_b is the velocity due to buoyancy. However, the buoyancy term can be closely approximated by

$$v_b^2 = 2gy_F \quad (26)$$

where g is the acceleration due to buoyancy. If one substitutes Eq. (26) into Eq. (25) and expands the result in terms of a binomial expression, one obtains

$$v = v_o \left[1 + \left(\frac{gy_F}{v_o^2} \right) - \frac{1}{2} \left(\frac{gy_F}{v_o^2} \right)^2 + \dots \right] \quad (27)$$

where the term in parentheses is the inverse of the modified Froude number

$$Fr \equiv (v_o^2 / gy_F) \quad (28)$$

Thus, Eq. (27) can be written as

$$v = v_o [1 + (1/Fr) - (1/2Fr^2) + \dots] \quad (29)$$

For large Froude numbers, the diffusion flame height is momentum controlled and $v = v_o$. However, most laminar burning fuel jets will have very small Froude numbers and $v = v_b$; that is, most laminar fuel jets are buoyancy controlled.

Although the flame height is proportional to the fuel volumetric flow rate whether the flame is momentum or buoyancy controlled, the time to the flame tip does depend on what the controlling force is. The characteristic time for diffusion (t_D) must be equal to the time (t_s) for a fluid element to travel from the port to the flame tip; i.e., if momentum controlled,

$$t_D \sim (r_j^2 / D) = (y_F / v) \sim t_s \quad (30)$$

It follows from Eq. (30), of course, that

$$y_F \sim r_j^2 v / D \sim \pi r_j^2 v / \pi D \sim \frac{Q}{\pi D} \quad (31)$$

Equation (31) shows the same dependency on Q as that developed from the Burke-Schumann approach [Eqs. (21)–(23)]. For a momentum controlled fuel jet flame, the diffusion distance is r_j , the jet port radius, and from Eq. (30) it is obvious that the time to the flame tip is independent of the fuel volumetric flow rate. For a buoyancy controlled flame t_s remains proportional to (y_F/v) ; however, since $v = (2gy_F)^{1/2}$ then

$$t \sim y_F/v \sim y_F/(y_F)^{1/2} \sim y_F^{1/2} \sim Q^{1/2} \quad (32)$$

Thus, the stay time of a fuel element in a buoyancy controlled laminar diffusion flame is proportional to the square root of the fuel volumetric flow rate. This conclusion is significant with respect to the soot smoke height tests to be discussed in Chapter 8.

The analyses above hold only for circular fuel jets. Roper [3] has shown as experimental evidence verifies [4] for a slot burner that the flame height is not the same for momentum and buoyancy controlled jets. Consider a slot burner of the Wolfhard-Parker type in which the width of the slot is x and the length L . As discussed earlier for a buoyancy controlled situation, the diffusive distance would not be x , but some smaller width, say x_b . Following the terminology of Eq. (25), for a momentum controlled slot burner,

$$t \sim x^2/D \sim y_F/v_o \quad (33)$$

and

$$y_F \sim (v_o x^2/D)/(L/L) \sim (Q/D)(x/L) \quad (34)$$

For buoyancy controlled slot burner,

$$t \sim (x_b)^2/D \sim y_F/v_b \quad (35)$$

$$y_F \sim [v_b(x_b)^2/D]/(L/L) \sim (Q/D)(x_b/L) \quad (36)$$

Since

$$\begin{aligned} x_b L v_b &\sim Q \\ x &\sim \frac{Q}{v_b L} \sim Q/(2gy_F)^{1/2} L \end{aligned}$$

Equation (36) becomes

$$y_F \sim \left(\frac{Q^2}{DL^2(2g)^{1/2}} \right)^{2/3} \sim \left(\frac{Q^4}{D^2 L^4 2g} \right)^{1/3} \quad (37)$$

Comparing Eqs. (34) and (37), one notes that under momentum controlled conditions for a given Q the flame height is directly proportional to the slot width and that under buoyancy controlled conditions for a given Q the flame

height is independent of the slot width. Roper *et al.* [4] have verified these conclusions experimentally.

5. Turbulent Fuel Jets

The previous section considered the burning of a laminar fuel jet and the essential result with respect to flame height was that

$$y_{F,L} \sim (r_j^2 v / D) \sim (Q/D) \quad (38)$$

where $y_{F,L}$ specifies that flame height of a laminar fuel jet. When the fuel jet velocity is increased to the extent that the flow is turbulent, not only does the Froude number become large and the system momentum controlled, but also molecular diffusion considerations are no longer valid. Thus, the simple phenomenological approach which led to Eq. (21) must be modified to account for the turbulent diffusion. The modification is accomplished by simply replacing the molecular diffusivity D with the turbulent eddy diffusivity ε . Consequently, the turbulent form of Eq. (28) becomes

$$y_{F,T} \sim (r_j^2 v / \varepsilon)$$

where $y_{F,T}$ is the flame height of a turbulent fuel jet. But $\varepsilon \sim lv'$, where l is the scale of the turbulence and proportional to the tube diameter (or radius) and v' is the intensity of turbulence, which is approximately proportional to the mean flow velocity at the axis. Thus, it may be assumed that

$$\varepsilon \sim r_j v \quad (39)$$

Combining Eqs. (38) and (39), one obtains

$$y_{F,T} \sim r_j^2 v / r_j v \sim r_j \quad (40)$$

This expression reveals that the height of a turbulent diffusion flame is proportional to the port radius (or diameter) alone, irrespective of the volumetric fuel flow rate or fuel velocity issuing from the burner! This

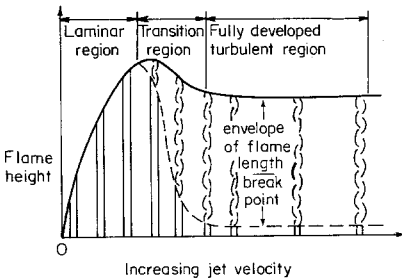


Fig. 10. Variations of the character of a diffusion flame as a function of fuel jet velocity (after Hawthorne *et al.* [12a]).

important practical conclusion has been verified by many investigators. Particularly the results of Hawthorne *et al.* [12a] have characteristically been shown. These results are depicted in Fig. 10, which reports the variation of flame height as a function of port velocity as it is raised from a laminar to turbulent state.

C. BURNING OF CONDENSED PHASES

When most liquids or solids are projected into an atmosphere so that a combustible mixture is formed and when this mixture is ignited, a flame surrounds the liquid or solid phase. Except at the very lowest of pressures, around 10^{-6} torr, this flame is a diffusion flame. If the condensed phase is considered as a liquid fuel and the gaseous oxidizer as oxygen, then fuel is evaporated from the liquid surface and diffuses to the flame front as the oxygen moves from the surroundings to the burning front. This picture of condensed phase burning is most readily and usually applied to droplet burning, but can also be applied to any liquid surface.

The rate at which the droplet evaporates and burns is generally considered to be determined by the rate of heat transfer from the flame front to the fuel surface. Here, as in the case of gaseous diffusion flames, chemical processes are assumed to occur so rapidly that the burning rates are determined solely by mass and heat transfer rates.

Many of the early analytical models of this burning process considered a double-film model for the combustion of the liquid fuel. One film separated the droplet surface from the flame front and the other separated the flame front from the surrounding oxidizer atmosphere as depicted in Fig. 11.

In some analytical developments the liquid surface was assumed to be at the normal boiling point temperature of the fuel. Surveys of the temperature field by Khudyakov [13] in burning liquids indicated that the temperature is only a few degrees below the boiling temperature. In the approach to be employed here, all that is required is that the droplet be at a uniform temperature at or below the normal boiling point. In the *sf* region of Fig. 11, fuel evaporates at the drop surface and diffuses toward the flame front where it is consumed. Heat is conducted from the flame front to the liquid and vaporizes the fuel. Many analyses assume that the fuel is heated to the flame temperature before it chemically reacts and that the fuel does not react until it reaches the flame front. This latter assumption implies that the flame front is a mathematically thin surface where the fuel and oxidizer meet in stoichiometric proportions. Some early investigators first determined T_f in order to calculate the fuel burning rate. However, in order to determine a T_f , the infinitely thin reaction zone at the stoichiometric position must be assumed.

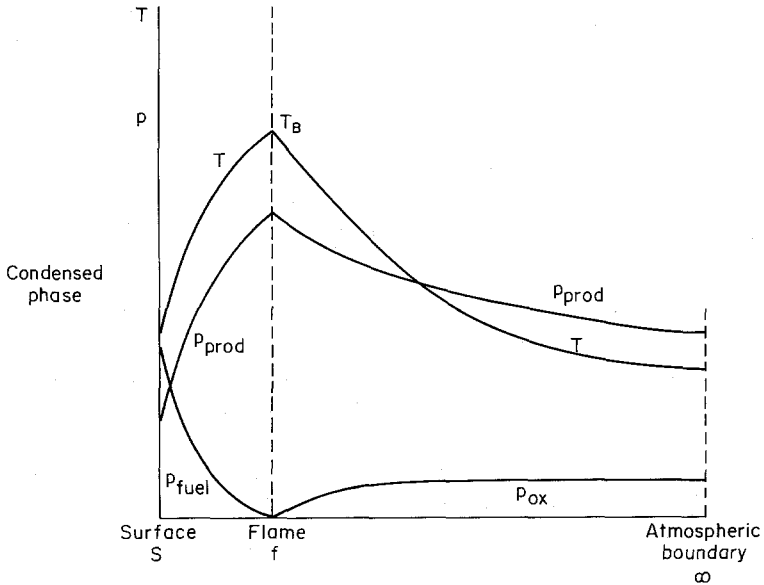


Fig. 11. Parameter variation along a radius of a droplet diffusion flame.

In the film $f \rightarrow \infty$, oxygen diffuses to the flame front and combustion products and heat are transported to the surrounding atmosphere. The position of the boundary designated by ∞ is determined by convection. A stagnant atmosphere places the boundary at an infinite distance from the fuel surface.

Although most analyses assumed no radiant energy transfer, as will be shown subsequently, the addition of radiation poses no mathematical difficulty in the solution to the mass burning rate problem.

1. General Mass Burning Considerations and the Evaporation Coefficient

Three parameters are generally evaluated: the mass burning rate (evaporation), the flame position above the fuel surface, and the flame temperature. The most important parameter is the mass burning rate, for it permits the evaluation of the so-called evaporation coefficient, which is most readily measured experimentally.

The use of the term *evaporation coefficient* comes about from mass and heat transfer experiments without combustion; i.e., evaporation, generally as used in spray drying and humidification. Basically the evaporation coefficient β is defined by the following expression, which has been verified experimentally:

$$d^2 = d_0^2 - \beta t \quad (41)$$

where d_0 is the original drop diameter and d is the drop diameter after the time t . It will be shown later that the same expression must hold for mass and heat transfer with chemical reaction (combustion).

The combustion of droplets is one aspect of a much broader problem, which involves the gasification of a condensed phase, i.e., a liquid or a solid. In this sense, the field of diffusion flames is rightfully broken down into gases and condensed phases. Here the concern is with the burning of droplets, but the concepts to be used are just as applicable to other practical experimental products such as the evaporation of liquids, sublimation of solids, hybrid burning rates, ablation heat transfer, solid propellant burning, transpiration cooling, etc. In all categories the interest is the mass consumption, or the rate of regression, of a condensed phase material. Whereas in gaseous diffusion flames, there was no specific property to measure and the flame height was evaluated; in condensed phase diffusion flames a specific quantity is measurable. This quantity is some representation of the mass consumption rate of the condensed phase. The similarity of the case just mentioned arises due to the fact that the condensed phase must be gasified, and consequently there must be an energy input into the condensed material. What determines the rate of regression or evolution of material is the heat flux at the surface. Thus, in all the processes mentioned,

$$q = \dot{r}\rho_f L'_v \quad (42)$$

where q is the heat flux to the surface in calories per square centimeter per second, \dot{r} is the regression rate in centimeters per second; ρ_f is the density of the condensed phase; and L'_v is the overall energy per unit mass required to gasify the material. Usually L'_v is the sum of two terms—the heat of vaporization, sublimation, or gasification plus the enthalpy required to bring the surface to the temperature of vaporization, sublimation, or gasification.

From the foregoing discussion, it is seen that the heat flux q , L'_v , and the density determine the regression rate, but it must also be realized that this statement does not mean the heat flux is the controlling or rate-determining step in each case. The fact is that it is generally not the controlling step. The controlling step and the heat flux are always interrelated, however. Regardless of the process of concern (assuming no radiation),

$$q = -\lambda(\partial T/\partial y)_s \quad (43)$$

where λ is the thermal conductivity and the subscript s designates the surface. This simple statement of the Fourier heat conduction law is of such great significance that its importance cannot be overstated.

This same equation holds regardless if there is mass evolution from the surface and regardless if convective effects prevail in the gaseous stream. For even in convective atmospheres in which one is interested in the heat transfer

to a surface (without mass addition of any kind, i.e., in the heat transfer situation generally encountered), one writes the heat transfer equation as

$$q = h(T_\infty - T_s) \quad (44)$$

Obviously, this statement is shorthand for

$$q = -\lambda(\partial T/\partial y)_s = h(T_\infty - T_s) \quad (45)$$

where T_∞ and T_s are the free-stream and surface temperatures, respectively; the heat transfer coefficient h is by definition

$$h \equiv \lambda/\delta \quad (46)$$

where δ is the boundary layer thickness. Again by definition, the boundary layer is the distance between the surface and free-stream condition, thus, as an approximation

$$q = \lambda(T_\infty - T_s)/\delta \quad (47)$$

The $(T_\infty - T_s)/\delta$ term is the temperature gradient, which correlates $(\partial T/\partial y)_s$ through the boundary layer thickness. The fact that δ can be correlated with the Reynold's number and that the Colburn analogy can be applied is what leads to the correlations of the form

$$\text{Nu} = f(\text{Re}, \text{Pr}) \quad (48)$$

where Nu is the Nusselt number hx/λ ; Pr is the Prandtl number $c_p\mu/\lambda$; and Re is the Reynold's number $\rho vx/\mu$, where x is the critical dimension—the distance from the leading edge of a flat plate or the diameter of a tube.

Although the correlations given by Eq. (48) are useful for practical evaluation of heat transfer to a wall, one must not lose sight of the fact that it is the temperature gradient at the wall that actually determines the heat flux there. In transpiration cooling problems, it is not so much that the injection of the transpiring fluid increases the boundary layer thickness and, thus, decreases the heat flux, but rather that the temperature gradient at the surface is decreased by the heat absorbing capacity of the injected fluid. What Eq. (43) specifies is that regardless of the processes taking place, the temperature profile at the surface determines the regression rate—whether it be evaporation, solid propellant burning, etc. Thus, all the mathematical approaches used in the type of problems mentioned simply seek to evaluate the temperature gradient at the surface. The temperature gradient at the surface is different for the various processes discussed. Thus, the temperature profile from the surface to the source of energy will be different for evaporation than for the burning of a liquid fuel, which releases energy when oxidized in a flame structure.

Nevertheless, a diffusion mechanism generally prevails, is the slowest step, and, thus, determines the regression rate. In evaporation, it is the conduction of heat from the surrounding atmosphere to the surface; in ablation it is the conduction of heat through the boundary layer; in droplet burning it is the diffusion rates of the fuel as it diffuses to approach the oxidizer, etc.

It is interesting from a mathematical sense to realize that the gradient at the surface will always be a boundary condition to the mathematical statement of the problem. Thus, the mathematical solution is necessary simply to evaluate the boundary condition.

Furthermore, it should be emphasized that the absence of radiation has been assumed. To incorporate radiation transfer is not difficult if the assumption is made that the radiant intensity of the emitters is known and there is no absorption between the emitters and the vaporizing surfaces; i.e., it can be assumed that q_r , the radiant heat flux to the surface, is known. Then Eq. (43) becomes

$$q + q_r = -\lambda(\partial T/\partial)_s + q_r = \dot{r}\rho L'_v \quad (49)$$

It is interesting to note that for the assumptions above the mathematical solution of the problem does not become significantly more difficult, for again q_r and, thus, radiation transfer is a known constant and enters only in the boundary condition. The differential equations describing the processes are not altered.

First the evaporation rate of a single fuel droplet is calculated before considering the combustion of this fuel droplet, or, to say it more exactly, the evaporation of a fuel droplet in the presence of combustion. Since the concern is with diffusional processes, it is best to start by reconsidering the laws that hold for diffusional processes.

Fick's law states that if a gradient in concentration of species A exists, say (dn_A/dy) , then there is found a flow or flux of A say j_A across a unit area in the y direction proportional to the flux so that

$$j_A = -D dn_A/dy \quad (50)$$

where D is the proportionality constant and called the molecular diffusion coefficient or more simply the diffusion coefficient, n_A is the number concentration of molecules per cubic centimeter, and j is the flux of molecules, number of molecules per square centimeter per second. Thus, the units of D are square centimeters per second.

The Fourier law of heat conduction relates the flux of heat q per unit area, as a result of a temperature gradient, such that

$$q = -\lambda dT/dy$$

The units of q are calories per square centimeter per second and those of λ , the thermal conductivity, are calories per centimeter per second per degree kelvin. It is not the temperature, an intensive thermodynamic property, that is exchanged, but energy content, an extensive property. In this case, the energy density and the exchange reaction, which show similarity, are written as

$$q = -\frac{\lambda}{\rho c_p} \rho c_p \frac{dT}{dy} = -\frac{\lambda}{\rho c_p} \frac{d(\rho c_p T)}{dy} = -\alpha \frac{dH}{dy} \quad (51)$$

where α is called the thermal diffusivity and has units square centimeters per second since $\lambda = \text{cal/cm sec K}$, $c_p = \text{cal/gm K}$, and $\rho = \text{gm/cm}^3$; H is the energy concentration in calories per cubic centimeter. Thus, the similarity of Fick's and Fourier's laws is apparent. One arises due to a number concentration gradient and the other due to an energy concentration gradient.

A similar law to these two diffusional processes is Newton's law of viscosity, which relates the flux (or shear stress) τ_{yx} of the x component of momentum u_x due to a gradient in u_x , and is written as

$$\tau_{yx} = -\mu du_x/dy \quad (52)$$

where the units of the stress τ are dynes per square centimeter and of the viscosity are grams per centimeter per second. Again, it is not velocity that is exchanged, but momentum and when the exchange of momentum density is written, similarity is again noted

$$\tau_{yx} = -(\mu/\rho)[d(\rho u_x)/dy] = -\nu[d(\rho u_x)/dy] \quad (53)$$

where ν is the momentum diffusion coefficient or more acceptably, the kinematic viscosity; ν is a diffusivity and its units are also square centimeters per second. Since Eq. (53) relates the momentum gradient to a flux, its similarity to Eqs. (50) and (51) is seen readily. Recall, as stated earlier in Chapter 4, the simple kinetic theory of gases predicts $\alpha = D = \nu$. The ratios of these three diffusivities give some familiar dimensionless similarity parameters

$$\text{Pr} = \nu/\alpha, \quad \text{Sc} = \nu/D, \quad \text{Le} = D/\alpha$$

where Pr, Sc, and Le are Prandtl, Schmidt, and Lewis numbers, respectively. Thus, for gases simple kinetic theory gives as a first approximation

$$\text{Pr} = \text{Sc} = \text{Le} = 1$$

2. Single Fuel Droplets in Quiescent Atmospheres

Since Fick's law will be used in many different forms in the ensuing development, it is best to develop those forms so that the later developments need not be interrupted.

Consider the diffusion of molecules A into an atmosphere of B molecules, i.e., a binary system. For a concentration gradient in A molecules alone, the future developments can be simplified readily if Fick's law is now written

$$j_A = -D_{AB} dn_A/dy \quad (54)$$

where D_{AB} is the binary diffusion coefficient, n_A is now considered in number of moles per unit volume since one could always multiply Eq. (50) through by Avogadro's number; j_A is now expressed in number of moles as well.

Multiplying through Eq. (39) by MW_A the molecular weight of A, one obtains

$$(j_A MW_A) = -D_{AB} d(n_A MW_A)/dy = -D_{AB} d\rho_A/dy \quad (55)$$

ρ_A is the mass density of A, ρ_B mass density of B, and n total number of moles is constant

$$n = n_A + n_B \quad (56)$$

and

$$dn/dy = 0, \quad dn_A/dy = -dn_B/dy, \quad j_A = -j_B \quad (57)$$

Thus, there will result a net flux of mass by diffusion equal to

$$\rho v = j_A MW_A + j_B MW_B \quad (58)$$

$$= j_A (MW_A - MW_B) \quad (59)$$

where v is the bulk direction velocity established by diffusion.

In problems dealing with the combustion of condensed matter and, thus, regressing surfaces, there is always a bulk velocity movement in the gases. Thus, the situation exists in which there are species diffusing while the bulk gases are moving at a finite velocity. The diffusion of the species can be against or with the bulk flow (velocity). For mathematical convenience it is best to decompose flows in which there is diffusion into a flow with an average mass velocity v and a diffusive velocity relative to v .

When one gas diffuses into another, as A into B, even without the quasi-steady-flow component imposed by the burning, the mass transport of a species, say A, is made up of two components—the normal diffusion component and the component related to the bulk movement established by the diffusion process. This mass transport flow has a velocity Δ_A and the mass of A transported per unit area is $\rho_A \Delta_A$. The bulk velocity established by the diffusive flow is given by Eq. (58). The fraction of the flow is Eq. (58) multiplied by the mass fraction of A, ρ_A/ρ . Thus,

$$\rho_A \Delta_A = -D_{AB} (d\rho_A/dy) \{1 - [1 - (MW_B/MW_A)](\rho_A/\rho)\} \quad (60)$$

Since $j_A = j_B$

$$MW_A j_A = -MW_B j_B = -(MW_B j_B)(MW_A/MW_B) \quad (61)$$

and

$$-d\rho_A/dy = (MW_A/MW_B)(d\rho_B/dy) \quad (62)$$

However,

$$(d\rho_A/dy) + (d\rho_B/dy) = d\rho/dy \quad (63)$$

which gives with Eq. (62)

$$(d\rho_A/dy) - (MW_B/MW_A)(d\rho_A/dy) = d\rho/dy \quad (64)$$

Multiplying through by ρ_A/ρ , one obtains

$$(\rho_A/\rho)[1 - (MW_B/MW_A)](d\rho_A/dy) = (\rho_A/\rho)(d\rho/dy) \quad (65)$$

Substituting Eq. (65) into Eq. (60), one finds

$$\rho_A \Delta_A = -D_{AB}[(d\rho_A/dy) - (\rho_A/\rho)(d\rho/dy)] \quad (66)$$

or

$$\rho_A \Delta_A = -\rho D_{AB} d(\rho_A/\rho)/dy \quad (67)$$

Defining m_A as the mass fraction of A, one obtains the following proper form for the diffusion of species A in terms of mass fraction.

$$\rho_A \Delta_A = -\rho D_{AB} d(\rho_A/\rho)/dy \quad (68)$$

This form is that most commonly used in the conservation equation.

The total mass flux of A under the condition of the burning of a condensed phase, which imposes a bulk velocity developed from the mass burned, is then

$$\rho_A v_A = \rho_A v + \rho_A \Delta_A = \rho_A v - \rho D_{AB} dm_A/dy \quad (69)$$

$\rho_A v$ is the bulk transport part and $\rho_A \Delta_A$ is the diffusive transport part. Indeed, in the developments of Chapter 4, the correct diffusion term was used without the proof just completed.

a. Heat and Mass Transfer without Chemical Reaction (Evaporation)—the Transfer Number B

Following Blackshear's [14] adaptation of Spalding's approach [15,16], consideration will now be given to the calculation of the evaporation of a single fuel droplet in a nonconvective atmosphere at a given temperature and pressure. A major assumption is now made in that the problem is considered as a quasi-steady one. Thus, the droplet is of fixed size and retains that size by a steady flux of fuel. One can consider the regression as being constant or even better to think of the droplet as a porous sphere being fed from a very thin tube at a rate equal to the mass evaporation so that the surface of the sphere is always wet and immediately replaces any liquid evaporated. The

porous sphere approach shows that for the diffusion flame a bulk gaseous velocity outward must exist and that this velocity in the spherical geometry will vary radially, but must always be the value given by $\dot{m} = 4\pi r_2 \rho v$. This velocity is the one referred to in the last section. With this physical picture, the important assumption is made that the temperature throughout the droplet is constant and equal to the surface temperature.

In developing the problem, a differential volume in the vapor above the liquid droplet is chosen as shown in Fig. 12. The surface area of a sphere is $4\pi r^2$. Since mass cannot accumulate in the element,

$$d(\rho Av) = 0, \quad (d/dr)(4\pi r^2 \rho v) = 0 \quad (70)$$

which is essentially the continuity equation.

Consider now the energy equation of the evaporating drop in spherical-symmetric coordinates in which c_p and λ are taken independent of temperature. The heat entering at the surface (i.e., the amount of heat convected in) is $\dot{m} c_p T$ or $(4\pi r^2 \rho v) c_p T$ (see Fig. 12). The heat leaving after $r + \Delta r$ is $\dot{m} c_p [T + (dT/dr) \Delta r]$ or $(4\pi r^2 \rho v) c_p [T + (dT/dr) \Delta r]$. The difference then is

$$-4\pi r^2 \rho v c_p (dT/dr) \Delta r$$

The heat diffusing from r toward the drop (out of the element) is

$$-\lambda 4\pi r^2 (dT/dr)$$

The heat diffusing into the element is

$$-\lambda 4\pi (r + \Delta r)^2 (d/dr) [T + (dT/dr) \Delta r]$$

or

$$-[\lambda 4\pi r^2 (dT/dr) + \lambda 4\pi r^2 (d^2 T/dr^2) \Delta r + \lambda 8\pi r^2 \Delta r (dT/dr)]$$

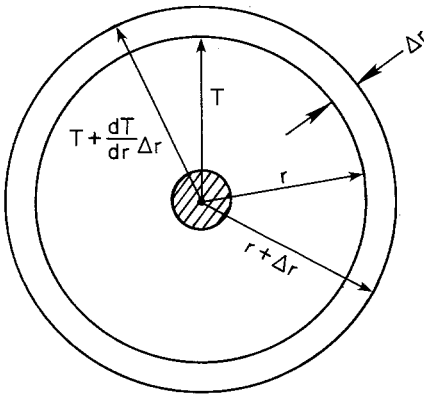


Fig. 12. Temperature balance across a differential element of a diffusion flame in spherical symmetry.

plus two terms in Δr^2 and one in Δr^3 which are negligible. The difference in the two terms is

$$+[\lambda 4\pi r^2(d^2T/dr^2)\Delta r + 8\lambda\pi r(dT/dr)]$$

Heat could be generated in the volume element defined by Δr and one has

$$-(4\pi r^2 \Delta r)\dot{H}$$

where \dot{H} is the rate of enthalpy change per unit volume. Thus, for the energy balance

$$4\pi r^2 \rho v c_p (dT/dr) - \lambda 4\pi r^2 (d^2T/dr^2) \Delta r + \lambda 8\pi r \Delta r (dT/dr) = 4\pi r^2 \Delta r \dot{H} \quad (71)$$

$$4\pi r^2 \rho v c_p (dT/dr) = \lambda 4\pi r^2 (d^2T/dr^2) + 2\lambda 4\pi r^2 (dT/dr) - 4\pi r^2 \dot{H} \quad (72)$$

or

$$4\pi r^2 (\rho v) (dc_p T/dr) = d/dr[(\lambda 4\pi r^2/c_p)(dc_p T/dr)] - 4\pi r^2 \dot{H} \quad (73)$$

Similarly, the conservation of the A th species can be written as

$$4\pi r^2 \rho v (dm_A/dr) = (d/dr)[4\pi r^2 \rho D(dm_A/dr)] + 4\pi r^2 \dot{m}_A \quad (74)$$

where \dot{m}_A is the generation or disappearance rate of A due to reaction in the unit volume. The kinetic theory of gases gives to a first approximation that the product $D\rho$ (and, thus, λ/c_p) is independent of temperature and pressure; consequently $D_s\rho_s = D\rho$, where the subscript s designates the condition at the droplet surface.

Consider a droplet of radius r . If the droplet is vaporizing, then the fluid will leave the surface by convection and diffusion. Since at the liquid droplet surface only A exists, then the boundary condition at the surface is

$$\underbrace{\rho_s v_s}_{\substack{\text{amount of material} \\ \text{leaving the surface}}} = \rho m_{As} v_s - \rho D(dm_A/dr)_s \quad (75)$$

Equation (75) is, of course, explicitly Eq. (69), when $\rho_s v_s$ is the bulk mass movement, which at the surface is exactly the amount of A that is being convected (evaporated) written in terms of a gaseous density and velocity plus the amount of gaseous A that diffuses to or from the surface. Equation (75), then, is written as

$$v_s = \frac{D(dm_A/dr)_s}{(m_{As} - 1)}$$

In the sense of Spalding, a new parameter is defined

$$b \equiv m_A/(m_{As} - 1) \quad (76)$$

Equation (76), thus, becomes

$$v_s = D(db/dr)_s \quad (77)$$

and Eq. (74) written in terms of the new variable b and for the evaporation condition (i.e., $\dot{m}_A = 0$) is

$$r^2 \rho v (db/dr) = (d/dr)[r^2 \rho D (db/dr)] \quad (78)$$

The boundary conditions at $r = \infty$ is $m_A = m_{A\infty}$ or

$$b = b_\infty \quad \text{at} \quad r \rightarrow \infty \quad (79)$$

From continuity

$$r^2 \rho v = r_s^2 \rho_s v_s \quad (80)$$

Integration of Eq. (78) proceeds simply since $r^2 \rho v = \text{constant}$ on the left-hand side of the equation and yields

$$r^2 \rho v b = r^2 \rho D (db/dr) + \text{const} \quad (81)$$

Evaluating the constant at $r = r_s$, one obtains

$$r_s^2 \rho_s v_s b_s = r_s^2 \rho_s v_s + \text{const}$$

since from Eq. (77), $v_s = D(db/dr)_s$. Or, one has from Eq. (81)

$$r_s^2 \rho_s v_s (b - b_s + 1) = r^2 \rho D (db/dr) \quad (82)$$

By separating variables,

$$(r_s^2 \rho_s v_s / r^2 \rho D) dr = db / (b - b_s + 1) \quad (83)$$

assuming ρD constant and integrating (recall $\rho D = \rho_s D_s$)

$$-(r_s^2 v_s / r D_s) = \ln(b - b_s + 1) + \text{const} \quad (84)$$

Evaluating the constant at $r \rightarrow \infty$, one obtains

$$\text{const} = -\ln(b_\infty - b_s + 1)$$

or Eq. (84) becomes

$$r_s^2 v_s / r D_s = \ln[(b_\infty - b_s + 1) / (b - b_s + 1)] \quad (85)$$

The left-hand term of Eq. (84) goes to zero as $r \rightarrow \infty$. This point is significant because it shows that the spherical-symmetric case is the only mathematically tractable quiescent one. No other quiescent case such as that for cylindrical symmetry or any other symmetry is tractable. Evaluating Eq. (85) at $r = r_s$ results in

$$\begin{aligned} (r_s v_s / D) &= \ln(b_\infty - b_s + 1) = \ln(1 + B) \\ r_s v_s &= D_s \ln(b_\infty - b_s + 1) = D_s \ln(1 + B) \end{aligned} \quad (86)$$

where $B \equiv b_\infty - b_s$ and is generally referred to as the Spalding transfer number. The mass consumption rate per unit area $G_A = \dot{m}_A/4\pi r_s^2$, where $\dot{m}_A = \rho_s v_s 4\pi r_s^2$, is then

$$4\pi r_s^2 \rho_s v_s / 4\pi r_s^2 = (D_s \rho_s / r_s) \ln(1 + B)$$

$$G_A = \dot{m}_A / 4\pi r_s^2 = (\rho_s D_s / r_s) \ln(1 + B) = (D\rho / r_s) \ln(1 + B) \quad (87)$$

Since the product $D\rho$ is independent of pressure, the evaporation rate is also independent of pressure. In order to find a solution for Eq. (87), or more rightly to evaluate B , m_{A_s} must be determined. A reasonable assumption would be that the gas that surrounds the droplet surface is saturated at the surface temperature T_s . Since vapor pressure data are available, the problem then is to determine T_s .

For the case of evaporation, Eq. (73) becomes

$$r_s^2 \rho_s v_s c_p \, dT/dr = (d/dr)[r^2 \lambda (dT/dr)] \quad (88)$$

Integrating,

$$r_s^2 \rho_s v_s c_p T = r^2 \lambda (dT/dr) + \text{const} \quad (89)$$

The boundary condition at the surface is

$$[\lambda (dT/\partial r)]_s = \rho_s v_s L_v \quad (90)$$

where L_v is the latent heat of vaporization at the temperature T_s . Recall that the droplet is considered uniform throughout at the temperature T_s . Substituting Eq. (90) into Eq. (89)

$$\text{const} = r_s^2 \rho_s v_s [c_p T_s - L_v]$$

Thus, Eq. (89) becomes

$$r_s^2 \rho_s v_s c_p [T - T_s + (L_v/c_p)] = r^2 \lambda (dT/dr) \quad (91)$$

Integrating Eq. (91),

$$-r_s^2 \rho_s v_s c_p / r \lambda = \ln[T - T_s + (L_v/c_p)] + \text{const} \quad (92)$$

After evaluating the constant at $r \rightarrow \infty$, one obtains

$$\frac{r_s^2 \rho_s v_s c_p}{r \lambda} = \ln \left[\frac{T_\infty - T_s + (L_v/c_p)}{T - T_s + (L_v/c_p)} \right] \quad (93)$$

Evaluating Eq. (93) at the surface,

$$\frac{r_s \rho_s v_s c_p}{\lambda} = \ln \left(\frac{c_p (T_\infty - T_s)}{L_v} + 1 \right) \quad (94)$$

Since $\alpha = \lambda/c_p\rho$,

$$r_s v_s = \alpha_s \ln\left(1 + \frac{c_p(T_\infty - T_s)}{L_v}\right) \quad (95)$$

Comparing Eqs. (86) and (95), one can write

$$r_s v_s = \alpha_s \ln\left(\frac{c_p(T_\infty - T_s)}{L_v} + 1\right) = D_s \left(\frac{m_{A\infty} - m_{As}}{m_{As} - 1} + 1\right)$$

or

$$r_s v_s = \alpha_s \ln(1 + B_T) = D_s \ln(1 + B_M) \quad (96)$$

where

$$B_T \equiv \frac{c_p(T_\infty - T_s)}{L_v}, \quad B_M \equiv \frac{m_{A\infty} - m_{As}}{m_{As} - 1}$$

Again, since $\alpha = D$,

$$B_T = B_M$$

and

$$c_p(T_\infty - T_s)/L_v = (m_{A\infty} - m_{As})/(m_{As} - 1) \quad (97)$$

m_{As} is determined from the vapor pressure of A or the fuel; however, it must be realized that m_{As} is a function of the total pressure since

$$m_{As} \equiv \rho_{As}/\rho = n_A MW_A/nMW = (P_A/P)(MW_A/MW) \quad (98)$$

where n_A and n are the number of moles of A and the total number of moles, respectively, MW_A and MW are the molecular weight of A and the average molecular weight of the mixture, respectively, and P_A and P are the vapor pressure of A and the total pressure, respectively.

In order to obtain the solution desired, a value of T_s is assumed, the vapor pressure of A determined from tables, and m_{As} calculated from Eq. (98). This value of m_{As} and the assumed value of T_s are inserted in Eq. (97). If this equation is satisfied, then the correct T_s was chosen. If not then one must reiterate. When the correct value of T_s and m_{As} are found, then B_T or B_M are determined for the given initial conditions T_∞ or $m_{A\infty}$. For fuel combustion problems, $m_{A\infty}$ is usually zero, however, for evaporation, say of water, there is humidity in the atmosphere and this humidity must be represented as $m_{A\infty}$. With B_T and B_M determined, the mass evaporation rate is determined from Eq. (87) for a fixed droplet size. It is, of course, much more preferable to know the evaporation coefficient β from which the total evaporation time can be determined. Once B is known, the evaporation coefficient can be determined readily as will be shown later.

b. Heat and Mass Transfer with Chemical Reaction (Droplet Burning Rates)

The previous developments also can be used to determine the burning rate, or evaporation coefficient, of a single droplet of fuel burning in a quiescent atmosphere. In this case, the mass fraction of the fuel, which is always considered to be the condensed phase, will be designated m_f and the mass fraction of the oxidizer m_o . m_o is the oxidant mass fraction exclusive of inerts and i is used as the mass stoichiometric fuel-oxidant ratio, also exclusive of inerts. The same assumptions hold as those for evaporation from a porous sphere. Recall that the temperature throughout the droplet is considered to be the same and equal to the surface temperature T_s . This assumption is sometimes referred to as one of infinite condensed phase thermal conductivity. For liquid fuels, this temperature is generally near, but slightly less than, the saturation temperature for the prevailing ambient pressure.

As in the case of burning gaseous fuel jets, it is assumed that the fuel and oxidant approach each other in stoichiometric proportions. The stoichiometric relations are written as

$$\dot{m}_f = \dot{m}_o i, \quad \dot{m}_f H = \dot{m}_o H i = \dot{H} \quad (99)$$

where \dot{m}_f and \dot{m}_o refer to the mass consumption rates per unit volume, H is the heat of reaction of the fuel per unit mass, and \dot{H} is the heat release rate per unit volume.

There are now three fundamental diffusion equations: one for the fuel, one for the oxidizer, and one for the heat. Equation (59) is then written as two equations: one in terms of m_f and the other in terms of m_o . Equation (58) remains the same for the consideration here. As seen in the case of the evaporation, the solution to the equations becomes quite simple when written in terms of the b variable, which led to the Spalding transfer number B . As noted in this case the b variable was obtained from the boundary condition. Indeed another b variable could have been obtained for the energy equation [Eq. (73)] and would have had the form

$$b = (c_p T/L_v)$$

As in the case of burning gaseous fuel jets, the diffusion equations are combined readily by the assuming $D\rho = (\lambda/c_p)$; i.e., $Le = 1$. The same procedure can be followed in combining the boundary conditions for the three droplet burning equations to determine the appropriate b variables to simplify the solution for the mass consumption rate.

The surface boundary condition for the diffusion of fuel is the same as that for pure evaporation [Eq. (75)] and takes the form

$$\rho_s v_s (m_{fs} - 1) = D\rho (dm_f/dr)_s \quad (100)$$

Since there is no oxidizer leaving the surface, the surface boundary condition for diffusion of oxidizer is

$$o = \rho_s v_s m_{os} - D\rho(dm_o/dr)_s \quad \text{or} \quad \rho_s v_s m_{os} = D\rho(dm_o/dr)_s \quad (101)$$

The boundary condition for the energy equation is also the same as that for the evaporation case [Eq. (75)] and is written as

$$\rho_s v_s L_v = (\lambda/c_p)[d(c_p T)/dr]_s \quad (102)$$

By multiplying Eq. (100) by H and Eq. (101) by iH , they take the new form

$$H[\rho_s v_s (m_{fs} - 1)] = [D_\rho(dm_f/dr)_s]H \quad (103)$$

and

$$H[i\{\rho_s v_s m_{os}\}] = [\{D_\rho(dm_o/dr)_s\}i]H \quad (104)$$

By adding Eqs. (102) and (103) and recalling $D\rho = (\lambda/c_p)$, one obtains

$$\rho_s v_s [H(m_{fs} - 1) + L_v] = D_\rho [d(m_f H + c_p T)/dr]_s$$

and the transposing

$$\rho_s v_s = D_\rho \left\{ d \left[\frac{m_f H + c_p T}{H(m_{fs} - 1) + L_v} \right] / dr \right\}_s \quad (105)$$

Similarly by adding Eqs. (102) and (104), one obtains

$$\rho_s v_s (L_v + H_i m_{os}) = D_\rho [(d/dr)(c_p T + m_o iH)]_s$$

or

$$\rho_s v_s = D_\rho \left[d \left(\frac{m_o iH + c_p T}{H_i m_{os} + L_v} \right) / dr \right]_s \quad (106)$$

And, lastly, by subtracting Eq. (104) from (103), one obtains

$$\rho_s v_s [(m_{fs} - 1) - i m_{os}] = D_\rho [d(m_f - i m_o)/dr]_s$$

or

$$\rho_s v_s = D_\rho \left\{ d \left[\frac{m_f - i m_o}{(m_{fs} - 1) - i m_{os}} \right] / dr \right\}_s \quad (107)$$

Thus, the new b variables are defined as

$$b_{fq} \equiv \frac{m_f H + c_p T}{H(m_{fs} - 1) + L_v}, \quad b_{oq} \equiv \frac{m_o iH + c_p T}{H_i m_{os} + L_v} \quad (108)$$

$$b_{fo} \equiv \frac{m_f - i m_o}{(m_{fs} - 1) - i m_{os}}$$

The denominators of each of these three b variables are constants. The three diffusion equations are transformed readily in terms of these variables by multiplying the fuel diffusion equation by H and the oxygen diffusion equation by iH . By use of the stoichiometric relations [Eq. (98)] and combining the equations in the same manner as the boundary conditions, the nonhomogeneous terms \dot{m}_f , \dot{m}_o , and \dot{H} can be eliminated. Again, it is assumed that $D\rho = (\lambda/c_p)$. The combined equations are then divided by the appropriate denominators from the b variables so that all equations become similar in form. Explicitly then, one has the following developments:

$$r^2\rho v \frac{d(c_p T)}{dr} = \frac{d}{dr} \left[r^2 \frac{\lambda}{c_p} \frac{d(c_p T)}{dr} \right] - r^2 \dot{H} \quad (109)$$

$$H \left\{ r^2\rho v \frac{dm_f}{dr} = \frac{d}{dr} \left[r^2 D\rho \frac{dm_f}{dr} \right] + r^2 \dot{m}_f \right\} \quad (110)$$

$$Hi \left\{ r^2\rho v \frac{dm_o}{dr} = \frac{d}{dr} \left[r^2 D\rho \frac{dm_o}{dr} \right] + r^2 \dot{m}_o \right\} \quad (111)$$

$$\dot{m}_f H = \dot{m}_o Hi = \dot{H} \quad (99)$$

Adding Eqs. (109) and (110) and dividing the resultant equation through by $[H(m_{fs} - 1) + L_v]$, one obtains

$$r^2\rho v \frac{d}{dr} \left(\frac{m_f H + c_p T}{H(m_{fs} - 1) + L_v} \right) = \frac{d}{dr} \left[r^2 D\rho \frac{d}{dr} \left(\frac{m_f H + c_p T}{H(m_{fs} - 1) + L_v} \right) \right] \quad (112)$$

which is then written as

$$r^2\rho v (db_{fq}/dr) = (d/dr)[r^2 D\rho (db_{fq}/dr)] \quad (113)$$

By adding Eqs. (109) and (111) and dividing the resultant equation through by $[Him_{os} + L_v]$, one obtains

$$r^2\rho v \frac{d}{dr} \left(\frac{m_o iH + c_p T}{Him_{os} + L_v} \right) = \frac{d}{dr} \left[r^2 D\rho \frac{d}{dr} \left(\frac{m_o iH + c_p T}{Him_{os} + L_v} \right) \right] \quad (114)$$

or

$$r^2\rho v \frac{d}{dr} (b_{oq}) = \frac{d}{dr} \left[r^2 D\rho \frac{d}{dr} (b_{oq}) \right] \quad (115)$$

Following the same procedures by subtracting Eq. (111) from Eq. (110), one obtains

$$r^2\rho v \frac{d}{dr} (b_{fo}) = \frac{d}{dr} \left[r^2 D\rho \frac{d}{dr} (b_{fo}) \right] \quad (116)$$

Obviously, all the combined equations have the same form and boundary conditions, i.e.,

$$r^2 \rho v \frac{d}{dr} (b)_{f_o, f_q, o_q} = \frac{d}{dr} \left[r^2 \rho D \frac{d}{dr} (b)_{f_o, f_q, o_q} \right] \quad (117)$$

$$\rho_s v_s = D_\rho \left[\frac{d}{dr} (b)_{f_o, f_q, o_q} \right]_s \quad \text{at } r = r_s$$

$$b = b_\infty \quad \text{at } r \rightarrow \infty$$

The equation and boundary conditions are the same as those obtained for the pure evaporation problem and consequently the solution is the same. Thus, one writes

$$G_f = \dot{m}_f / 4\pi r_s^2 = (D\rho/r_s) \ln(1 + B) \quad \text{where } B = b_\infty - b_s \quad (118)$$

It should be recognized that since $Le = Sc = Pr$, Eq. (118) can also be written as

$$G_f = (\lambda/c_p r_s) \ln(1 + B) = (\mu/r_s) \ln(1 + B) \quad (119)$$

As in the case of evaporation, it is important to note that since $D\rho$ is independent of pressure, the burning rate of a droplet in a quiescent atmosphere is also independent of the pressure. In Eq. (118) the transfer number B can take any of the following forms:

Without combustion assumption	With complete combustion assumption	
$B_{f_o} = \frac{(m_{f_\infty} - m_{f_s}) + (m_{o_s} - m_{o_\infty})i}{(m_{f_s} - 1) - im_{o_s}}$	$= \frac{im_{o_\infty} + m_{f_s}}{1 - m_{f_s}}$	
$B_{f_q} = \frac{H(m_{f_\infty} - m_{f_s}) + c_p(T_\infty - T_s)}{L_v + H(m_{f_s} - 1)}$	$= \frac{c_p(T_\infty - T_s) - m_{f_s}H}{L_v + H(m_{f_s} - 1)}$	(120)
$B_{o_q} = \frac{Hi(m_{o_\infty} - m_{o_s}) + c_p(T_\infty - T_s)}{L_v + im_{o_s}H}$	$= \frac{c_p(T_\infty - T_s) + im_{o_\infty}H}{L_v}$	

The combustion assumption in Eq. (120) is that $m_{o_s} = m_{f_\infty} = 0$ since it is assumed that neither the fuel or oxidizer can penetrate the flame zone. This requirement is not that the flame zone be infinitely thin, but that all the oxidizer must be consumed before it reaches the fuel surface and that there be no fuel in the quiescent atmosphere.

Similar to the evaporation case, in order to solve Eq. (118), it is necessary to proceed by first equating $B_{f_o} = B_{o_q}$. This expression

$$\frac{im_{o_\infty} + m_{f_s}}{1 - m_{f_s}} = \frac{c_p(T_\infty - T_s) + im_{o_\infty}H}{L_v} \quad (121)$$

is solved with the use of the vapor pressure data for the fuel. The iteration process described in the solution of $B_M = B_T$ in the evaporation problem is used. The solution of Eq. (121) gives T_s and m_{fs} and, thus, individually B_{fo} and B_{oq} . With B known, then the burning rate is obtained from Eq. (118).

For the combustion systems, B_{oq} is the most convenient form of B ; $c_p(T_\infty - T_s)$ is usually much less than $im_{o\infty}H$ and to a close approximation $B_{oq} \cong (im_{o\infty}H/L_v)$, and the burning rate (and as will be shown later the evaporation coefficient β) is readily determined; it is not necessary to solve for m_{fs} and T_s .

The form of B_{oq} and B_{fq} presented in Eq. (120) is for the assumption that the fuel droplet has infinite thermal conductivity, i.e., the temperature of the droplet is T_s throughout. In an actual porous sphere experiment the fuel enters the center of the sphere at some temperature T_1 and reaches T_s at the sphere surface. For a large sphere, the enthalpy required to raise the cool entering liquid to the surface temperature is $c_{pl}(T_s - T_1)$ where c_{pl} is the specific heat of the liquid fuel. For this type of condition an estimate of B that would give a conservative (lower) result of the burning rate could be obtained by replacing L_v by

$$L'_v = L_v + c_p(T_s - T_1) \quad (122)$$

in the forms of B represented by Eq. (120).

Table I, extracted from Kanury [17], lists various values of B for many condensed phase combustible substances burning in air. Examination of this table reveals that variation of B for different combustible liquids is not great; rarely does one liquid fuel have a value of B a factor of 2 greater than another. Since the transfer number always enters the burning rate expression as a $\ln(1 + B)$ term, one may conclude that as long as the oxidizing atmosphere is kept the same, there will not be a great variation in the burning rate or evaporation coefficient of liquid fuels. The diffusivities and gas density dominate the burning rate. A tenfold variation in B results in an approximately twofold variation in burning rate. A tenfold variation of the diffusivity or gas density would result in a tenfold variation in burning rate.

Furthermore, it is most interesting to note that the burning rate has been determined without determining the flame temperature or the position of the flame. In the approach attributed to Godsave [18], and developed further by others [19,20], it was necessary to find the flame temperature, and much of the early burning rate developments followed this procedure. In the early literature there are frequent comparisons not only of the calculated and experimental burning rates (or β), but also of the flame temperature and position. To their surprise, most experimenters found good agreement with respect to burning rate but poorer agreement in flame temperature and position. What they failed to realize is that, as shown by the developments

TABLE I

Transfer Numbers of Various Liquids in Air^a
 $T_\infty = 20^\circ\text{C}$

	B	B'	B''	B'''
<i>n</i> -Pentane	8.94	8.15	8.19	9.00
<i>n</i> -Hexane	8.76	6.70	6.82	8.83
<i>n</i> -Heptane	8.56	5.82	6.00	8.84
<i>n</i> -Octane	8.59	5.24	5.46	8.97
<i>i</i> -Octane	9.43	5.56	5.82	9.84
<i>n</i> -Decane	8.40	4.34	4.62	8.95
<i>n</i> -Dodcane	8.40	4.00	4.30	9.05
Octene	9.33	5.64	5.86	9.72
Benzene	7.47	6.05	6.18	7.65
Methanol	2.95	2.70	2.74	3.00
Ethanol	3.79	3.25	3.34	3.88
Gasoline	9.03	4.98	5.25	9.55
Kerosene	9.78	3.86	4.26	10.80
Light diesel	10.39	3.96	4.40	11.50
Medium diesel	11.18	3.94	4.38	12.45
Heavy diesel	11.60	3.91	4.40	13.00
Acetone	6.70	5.10	5.19	6.16
Toluene	8.59	6.06	6.30	8.92
Xylene	9.05	5.76	6.04	9.43

$${}^a B = [im_0H + c_p(T_\infty - T_s)]/Lv; B' = \{im_0H + c_p(T_\infty - T_s)\}/L'v; \\ B'' = (im_0H/L'v); B''' = (im_0H/L'v)$$

here, the burning rate is independent of the flame temperature. As long as an integrated approach is used and the gradients of temperature and product concentration must be zero at the outer boundary, then it does not matter what or where the reactions take place so long as they take place within the boundaries of the integration.

It is possible to determine the flame temperature T_f and position r_s that would correspond to the Godsave-type calculations, simply by assuming the flame exists at the position where $im_0 = m_f$. Equation (87) is written in terms of b_{f_0} as

$$\frac{r_s^2 \rho_s v_s}{D_s \rho_s r} = \ln \left[\frac{m_{f_\infty} - m_{f_s} - i(m_{o_\infty} - m_{o_s}) + (m_{f_s} - 1)}{m_f - m_{f_s} - i(m_o - m_{o_s}) + (m_{f_s} - 1)} \right] \quad (123)$$

At the flame surface, $m_f = m_o = 0$ and $m_{f_\infty} = m_{o_\infty} = 0$, thus Eq. (123) becomes

$$r^2 \rho_s v_s / D_s \rho_s r_f = \ln(1 + im_{o_\infty}) \quad (124)$$

Since $\dot{m} = 4\pi r_s^2 \rho_s v_s$ is known, r_f can be determined. Combining Eqs. (118) and (124) results in the ratio of the radii

$$\frac{r_f}{r_s} = \frac{\ln(1+B)}{\ln(1+im_{\infty})}$$

which indicates that for most fuel droplets burning in air, the flame standoff distance should be about 30 times the droplet radius. This value is much larger than that which is observed experimentally due to the assumption of equal diffusivities [see Section C,2,c, Eq. (131)].

The flame temperature T_f at r_f can be obtained by writing Eq. (85) with $b = b_{\text{oq}}$. Making use of Eq. (124)

$$1 + im_{\infty} = [(b_{\infty} - b_s + 1)/(b_f - b_s + 1)]$$

$$1 + im_{\infty} = [Him_{\infty} + c_p(T_{\infty} - T_s) + L_v]/[c_p(T_f - T_s) + L_v]$$

or

$$c_p(T_f - T_s) = \{[Him_{\infty} + c_p(T_{\infty} - T_s) + L_v]/(1 + im_{\infty})\} - L_v \quad (125)$$

Although it is now possible to calculate the burning rate of a droplet under the quasi-steady conditions outlined and to estimate as well the flame temperature and position, the only means to estimate the burning time of an actual droplet is to calculate the evaporation coefficient for burning β . From the mass burning results obtained, β may be readily determined. For a liquid droplet, the relation

$$dm/dt = -\dot{m}_f = 4\pi\rho_l r_s^2 (dr_s/dt) \quad (126)$$

gives the mass rate in terms of the rate of change of radius with time; ρ_l is the density of the liquid fuel. It should be evaluated at T_s .

Many experimenters have obtained results similar to those given in Fig. 13. These results confirm that the variation of droplet diameter during burning follows the same "law" as that for evaporation

$$d^2 = d_0^2 - \beta t \quad (127)$$

Since $d = 2r_s$,

$$dr_s/dt = -\beta/8r_s$$

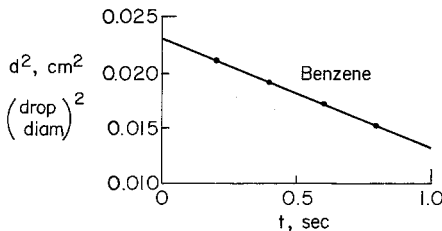


Fig. 13. Benzene droplet burning in quiescent air showing diameter-squared time dependency (after Godsave [18]).

It is readily shown that Eqs. (118) and (126) verify that a “ d^2 ” law should exist. Equation (126) is rewritten as

$$\dot{m} = -2\pi\rho_1 r_s (dr_s^2/dt) = -(\pi\rho_1 r_s/2)[d(d^2)/dt]$$

Making use of Eq. (118)

$$\dot{m}/4\pi r_s = (\lambda/c_p) \ln(1 + B) = -(\rho_1/8)[d(d^2)/dt] = +(\rho_1/8)\beta$$

shows that

$$d(d^2)/dt = \text{const}, \quad \beta = (8/\rho_1)(\lambda/c_p) \ln(1 + B) \quad (128)$$

which is a convenient form since λ/c_p is temperature insensitive. Sometimes β is written as

$$\beta = 8(\rho_s/\rho_1)\alpha \ln(1 + B)$$

to correspond more closely to expressions given by Eqs. (96) and (118).

c. Refinements of the Mass Burning Rate Expression

Some major assumptions were made in the derivation of Eqs. (118) and (128). First, it was assumed that the specific heat, thermal conductivity, and the product $D\rho$ were constants and that the Lewis number was equal to one. Second, it was assumed that there was no transient heating of the droplet. Furthermore, the role of finite reaction kinetics was not addressed adequately. These points will be given consideration in this section.

Variation of Transport Properties. The transport properties used throughout the previous developments are normally strong functions of both temperature and species concentration. The temperatures in a droplet diffusion flame as depicted in Fig. 11 vary from a few hundred degrees Kelvin to a few thousand. In the regions of the droplet flame one essentially has fuel, nitrogen, and products. However, since under steady-state conditions the nitrogen does not diffuse and the major constituent in the sf region is the fuel, it is most appropriate to use the specific heat of the fuel and its binary diffusion coefficient. In the region $f\infty$, the constituents are oxygen, nitrogen, and products. With similar reasoning one essentially considers the properties of the oxygen and products to be dominant and as the properties of fuel are used in the sf region, so the properties of oxygen are appropriate to use in the $f\infty$ region. To illustrate the importance of variable properties, Law [21] presented a simplified model in which the temperature dependence was suppressed, but the concentration dependence was represented by using λ , c_p and $D\rho$ to have constant, but different, values in the sf and $f\infty$ regions. The burning rate result of this model was

$$\frac{\dot{m}}{4\pi r_s} = \ln \left\{ \left[1 + \frac{c_{pf}(T_f - T_s)}{L_v} \right]^{(\lambda/c_{psf})} [1 + im_{o\infty}]^{(D\rho)_{f\infty}} \right\} \quad (129)$$

where T_f is obtained from expressions similar to Eq. (125) and found to be

$$(c_p)_{sf}(T_f - T_s) + \frac{(c_p)_{f\infty}(T_f - T_\infty)}{[(1 + im_{o\infty})^{1/Le_{f\infty}} - 1]} = H - L'_v \quad (130)$$

(r_f/r_s) was found to be

$$\frac{r_f}{r_s} = 1 + \left[\frac{(\lambda/c_p)_{sf} \ln[1 + (c_p)_{fs}(T_f - T_s)/L'_v]}{(D\rho)_{f\infty} \ln(1 + im_{o\infty})} \right] \quad (131)$$

Law [21] points out that since $im_{o\infty}$ is generally much less than one, the denominator of the second term in Eq. (130) becomes $[im_{o\infty}/(Le)_{f\infty}]$, which indicates that the effect of $(Le)_{f\infty}$ is to change the oxygen concentration by a factor $(Le)_{f\infty}^{-1}$ as experienced by the flame. Obviously, then for $(Le)_{f\infty} > 1$, the oxidizer concentration is effectively reduced and the flame temperature is also reduced from the adiabatic value obtained for $Le = 1$, the value given by Eq. (125). The effective Le for the mass burning rate [Eq. (129)] is

$$Le = (\lambda/c_p)_{sf}/(D\rho)_{f\infty}$$

which reveals that the individual Lewis numbers in the two regions play no role in determining \dot{m} . Law and Law [22] estimated that for heptane burning in air the effective Lewis number was between $\frac{1}{3}$ and $\frac{1}{2}$. Such values in Eq. (131) predict values of (r_f/r_s) in the right range of experimental values [21].

The question remains as to the temperature at which to evaluate the physical properties discussed. One could use an arithmetic mean for the two regions [23] or Sparrow's $\frac{1}{3}$ rule [24], which gives

$$T_{sf} = \frac{1}{3}T_s + \frac{2}{3}T_f; \quad T_{f\infty} = \frac{1}{3}T_f + \frac{2}{3}T_\infty$$

Transient Heating of Droplets. When a cold liquid fuel droplet is injected into a hot stream or ignited by some other source, it must be heated to its steady-state temperature T_s derived in the last section. Since the heat-up time can influence the " d^2 " law, particularly for high-boiling-point fuels, it is of interest to examine the effect of the droplet heating mode on the main bulk combustion characteristic, the burning time.

For this case, the boundary condition corresponding to Eq. (102) becomes

$$\begin{aligned} \dot{m}L_v + \left(4\pi\rho^2\lambda_l \frac{\partial T}{\partial r} \right)_{s^-} &= \left(4\pi r^2\lambda_g \frac{\partial T}{\partial r} \right)_{s^+} = \dot{m}L'_v \\ \dot{m}L_v + \left(4\pi r^2\lambda_l \frac{\partial T}{\partial r} \right)_{s^-} &= \left(4\pi r^2\lambda_g \frac{\partial T}{\partial r} \right)_{s^+} = \dot{m}L'_v \end{aligned} \quad (131a)$$

where the subscript s^- designates the liquid side of the liquid-surface-gas interface and s^+ the gas side. The subscripts l and g refer to liquid and gas, respectively.

At the initiation of combustion, the heat-up term (second) of Eq. (131) can be substantially larger than the vaporization term (first). Throughout combustion the third term is fixed. Thus, some [25,26] have postulated that droplet combustion can be considered to consist of two periods, namely an initial droplet heating period of slow vaporization with

$$\dot{m}L'_v \approx \left(4\pi r^2 \lambda_1 \frac{\partial T}{\partial r} \right)_{s^-}$$

followed by fast vaporization with almost no droplet heating and then

$$\dot{m}L'_v \approx \dot{m}L_v$$

The extent of the droplet heating time depends on the mode of ignition and the fuel volatility. If a spark is used then the droplet heating time can be a reasonable percentage (10–20%) of the total burning time [24]. Indeed the burning time would be 10–20% longer, if the value of B used to calculate β was calculated with $L'_v = L_v$; i.e., on the basis of the latent heat of vaporization. If the droplet is ignited by injection into a heated gas atmosphere, there will be a long heating time before ignition and after ignition the droplet will be near its saturation temperature and the heat-up time after ignition contributes little to the total burn-up time.

To study the effects due to droplet heating the temperature distribution $T(r, t)$ within the droplet would have to be determined. In absence of any internal motion, the unsteady heat transfer process within the droplet is simply described by the heat conduction equation and its boundary conditions

$$\frac{\partial T}{\partial t} = \frac{\alpha_1}{r^2} \frac{\partial}{\partial r} \left(r^2 \frac{\partial T}{\partial r} \right), \quad T(r, t = 0) = T_1(r), \quad \left(\frac{\partial T}{\partial r} \right)_{r=0} \quad (132)$$

The solution of Eq. (132) must be combined with the nonsteady equations for the diffusion of heat and mass. This system can only be solved numerically and the computing time is substantial. Therefore, an alternate simpler, droplet heating model is adopted [24,25]. In this model, the droplet temperature is assumed to be spatially uniform at T_s and temporally varying. With this assumption Eq. (131) becomes

$$\dot{m}L'_v = \left(4\pi r_s^2 \lambda_g \frac{\partial T}{\partial r} \right)_{s^+} = \dot{m}L_v + \left(\frac{4}{3} \right) \pi r_s^2 \rho_l (c_p)_l \frac{\partial T_s}{\partial t} \quad (133)$$

But since

$$\dot{m} = -(d/dt)[(4/3)\pi r_s^2 \rho_l]$$

Eq. (133) integrates to

$$\left(\frac{r_s}{r_{so}}\right)^3 = \exp\left\{-c_{pl} \int_{T_{so}}^{T_s} \left(\frac{dT_s}{L_v^1 - L_v}\right)\right\} \quad (134)$$

where $L_v' = L_v(T_s)$ is given by

$$L_v' = \frac{(1 - m_{fs})[im_{o\infty}H + c_p(T_{\infty} - T_s)]}{(m_{fs} + im_{o\infty})} \quad (135)$$

and r_{so} is the original droplet radius.

Figure 14 taken from Law [26] is a plot of the nondimensional radius squared as a function of a nondimensional time for an octane droplet initially at 300 K burning under ambient condition. Shown in this figure are the droplet histories calculated using Eqs. (132) and (133). Sirignano and Law [25] refer to the use of Eq. (132) as the diffusion limit and Eq. (133) as the distillation limit, respectively. Equation (132) allows for diffusion of heat into the droplet whereas Eq. (133) essentially assumes infinite thermal conductivity of the liquid and has vaporization at T_s as a function of time. Thus, one should expect Eq. (132) should give a slower burning time.

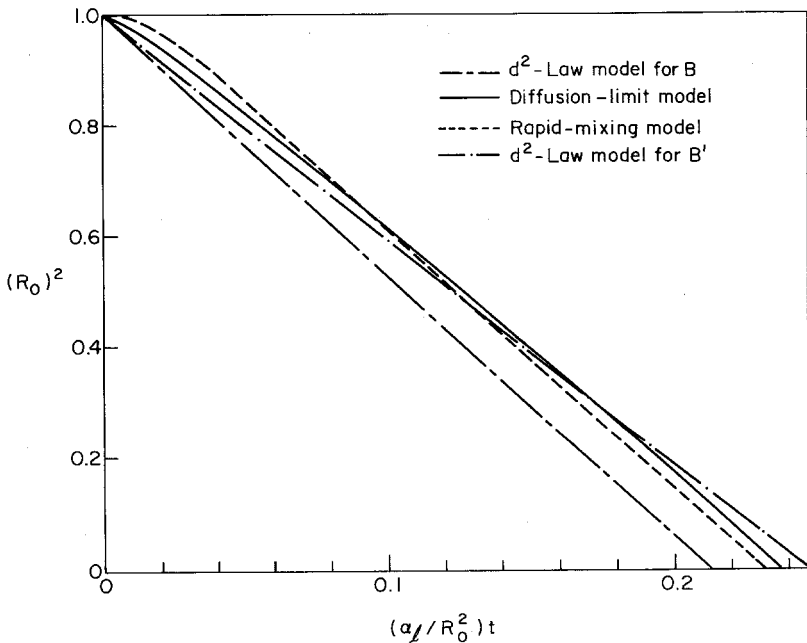


Fig. 14. Variations of nondimensional droplet radius as a function of nondimensional time for droplet heating and steady-state models (from Law [26]).

Also plotted in Fig. 14 are the results from using Eq. (128) in which the transfer number was calculated with $L'_v = L_v$ and $L'_v = L_v + c_p(T_s - T_i)$, Eq. (122). As one would expect $L'_v = L_v$ gives the shortest burning time and use of Eq. (122) gives the longest burning time since it does not allow storage of heat in the droplet as it burns. All four results are remarkably close for octane. The spread could be greater for a heavier fuel. For a conservative estimate of the burning time, use of B with L'_v evaluated by Eq. (122) is recommended.

The Effect of Finite Reaction Rates. When the fuel and oxidizer react at a finite rate, the flame front can no longer be considered infinitely thin. The reaction rate is then such that oxidizer and fuel can diffuse through each other and the reaction zone is spread over some distance. However, it must be realized that although the reaction rates are considered finite the characteristic time for the reaction is also considered to be much shorter than the characteristic time for the diffusional processes, particularly the diffusion of heat from the reaction zone to the droplet surface.

The development of the mass burning rate [Eq. (118)] in terms of the transfer number B [Eq. (120)] was made with the assumption that no oxygen reaches the fuel surface and no fuel reaches ∞ , the ambient atmosphere. In essence, the only assumption that was made was that the chemical reactions in the gas-phase flame zone were fast enough so that the conditions $m_{os} = 0 = m_{f\infty}$ could be met. The beauty of the transfer number approach, given that the kinetics are finite, but faster than diffusion, and the Lewis number is equal to one is its great simplicity compared to the more complex endeavors [18,19].

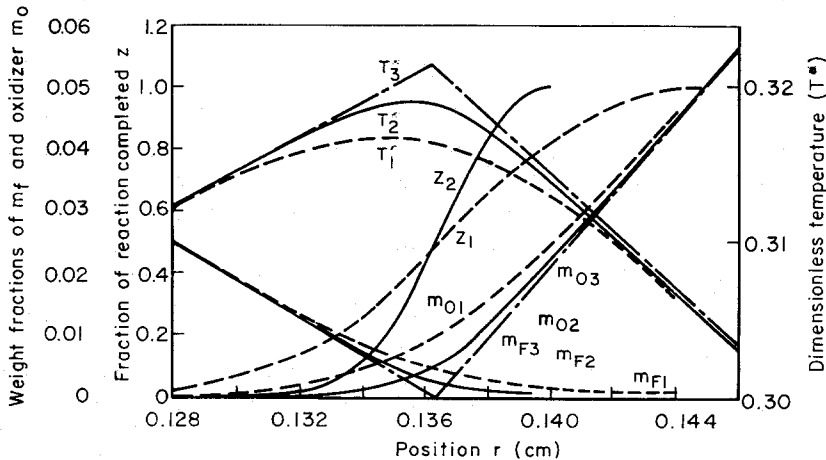


Fig. 15. Effect of chemical rate pressures on the structure of a diffusion controlled droplet flame (after Lorell *et al.* [20]).

Then for infinitely fast kinetics, the temperature profiles form a discontinuity at the infinitely thin reaction zone (see Fig. 11). With the realization that the mass burning rate must remain the same for either infinite or finite reaction rates, then there are three aspects dictated by physical insight to be considered when the kinetics are finite: first, the temperature gradient at $r = r_s$ must be the same in both cases; second, the maximum temperature reached when the kinetics are finite must be less than that for the infinite kinetics case; and, lastly, if the temperature is lower in the finite case, then the maximum must be closer to the droplet in order that the first aspect be met. Lorell *et al.* [20] have shown analytically that these physical insights as depicted in Fig. 15 are correct.

D. BURNING OF DROPLET CLOUDS

The understanding as to how particle clouds and sprays burn is still in its infancy. Many studies, both analytical and experimental, of burning droplet arrays have been made. The main consideration in most studies has been the effect of droplet separation on the overall burning rate. It is questionable whether study of simple arrays will reveal much insight into the burning of particle clouds or sprays.

An interesting approach to the spray problem has been made by Chiu and Liu [27] who consider a quasi-steady vaporization and diffusion process with infinite reaction kinetics. They show the importance of a group combustion number (G), which is derived from extensive mathematical analyses and which takes the form

$$G = 3(1 + 0.276 \text{Re}^{1/2} \text{Sc}^{1/2} \text{Le}^{2/3})(R/S) \quad (136)$$

where Re , Sc , and Le are the Reynolds, Schmidt, and Lewis numbers, respectively, N is the total number of droplets in the cloud, R the instantaneous average radius, and S the average spacing of the droplets.

The value of G was shown to have a profound effect upon the flame location and distribution of temperature, fuel vapor, and oxygen. Four types of behaviors were found for large G numbers. External heat combustion occurs for the largest value, and as G is decreased there is external group combustion, internal group combustion, and isolated droplet combustion.

Isolated droplet combustion obviously is the condition for a separate flame envelope for each droplet. Typically a group number less than 10^{-2} is required. Internal group combustion involves a core with a cloud where vaporization exists and in which the core is totally surrounded by flame. This condition occurs for G values above 10^{-2} and somewhere below 1. As G

increases, the size of the core increases. When a single flame envelopes all droplets, external group combustion exists. This phenomenon begins with G values close to unity and it is to be noted that many industrial burners and most gas turbine combustors are in this range. With external group combustion, the vaporization of individual droplets increases with distance from the center of the core. At very high G values (above 10^{-2}), only droplets in a thin layer at the edge of the cloud are vaporizing. This regime is called the external sheath condition.

E. BURNING IN CONVECTIVE ATMOSPHERES

1. The Stagnant Film Case

A spherical-symmetric fuel droplet burning problem is the only quiescent case that is mathematically tractable. However, the equations for mass burning may be readily solved in one-dimensional form for what may be considered the stagnant film case. If the stagnant film is of thickness δ , then the free-stream conditions are thought to exist at some distance δ from the fuel surface (see Fig. 16).

Within the stagnant film, the energy equation can be written as

$$\rho v c_p (dT/dy) = \lambda (d^2T/dy^2) + \dot{H} \quad (137)$$

Defining b as before, the solution of this equation and case proceeds as follows. Analogous to Eq. (117), for the one-dimensional case

$$\rho v (db/dy) = \rho D (d^2b/dy^2) \quad (138)$$

Integrating Eq. (98)

$$\rho v b = \rho D db/dy + \text{const} \quad (139)$$

The boundary condition is

$$\rho D (db/dy)_0 = \rho_s v_s = \rho v \quad (140)$$

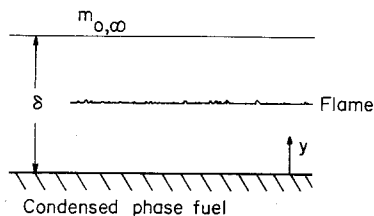


Fig. 16. Stagnant film height for condensed phase burning.

Substituting this boundary condition into Eq. (139)

$$\rho v b_0 = \rho v + \text{const}, \quad \rho v (b_0 - 1) = \text{const}$$

The integrated equation now becomes

$$\rho v (b - b_0 + 1) = \rho D \, db/dy \quad (141)$$

which upon second integration becomes

$$\rho v y = \rho D \ln(b - b_0 + 1) + \text{const} \quad (142)$$

At $y = 0$, $b = b_0$, therefore the constant equals zero so that

$$\rho v y = \rho D \ln(b - b_0 + 1) \quad (143)$$

Since δ is the stagnant film thickness,

$$\rho v \delta = \rho D \ln(b_\delta - b_0 + 1) \quad (144)$$

Thus,

$$G_f = (\rho D / \delta) \ln(1 + B) \quad (145)$$

where, as before,

$$B = b_{\delta \text{ or } \infty} - b_0 \quad (146)$$

Since the Prandtl number $c_p \mu / \lambda$ is equal to 1, Eq. (145) may be written as

$$G_f = (\rho D / \delta) \ln(1 + B) = (\lambda / c_p \delta) \ln(1 + B) = (\mu / \delta) \ln(1 + B) \quad (147)$$

A burning pool of liquid or a volatile solid fuel will establish a stagnant film height due to the natural convection which ensues. From analogies to heat transfer without mass transfer, a first approximation to the liquid pool burning rate may be written as

$$G_f d / \mu \ln(1 + B) \sim \text{Gr}^a \quad (148)$$

where a equals $\frac{1}{4}$ for laminar conditions and $\frac{1}{3}$ for turbulent conditions, d is the critical dimension of the pool, and Gr is the Grashof number.

$$\text{Gr} = (g d^3 \beta_1 / \alpha^2) \Delta T \quad (149)$$

where g is the gravitational constant and β_1 the coefficient of expansion.

Whenever the free stream, whether forced or due to buoyancy effects, is transverse to the mass evolution from the regressing fuel surface, a stagnant film does not exist, and the correlation given by Eq. (148) would not be explicitly correct.

2. The Longitudinally Burning Surface

Many practical cases of burning in convective atmospheres may be approximated by consideration of a burning longitudinal surface. This problem is similar to what could be called the burning flat plate case and has application to such problems as that which occur in the hybrid rocket. It differs from the stagnant film case in that there are gradients in the x -direction as well as the y -direction. This configuration is depicted in Fig. 17.

For the case of Schmidt number equal to 1, it can be shown (see [9]) that the conservation equations [in terms of Ω , see Eq. (17)] can be transposed into the form as the momentum equation for the boundary layer. Indeed, the transformations give the same form as the incompressible boundary layer equations developed and solved by Blasius. The important difference between this problem and the Blasius [28] problem is the boundary condition at the surface. The Blasius equation takes the form

$$f''' + ff'' = 0 \quad (150)$$

where f is a modified stream function and the primes designate differentiation with respect to a transformed coordinate. The boundary conditions at the surface for the Blasius problem are

$$\begin{aligned} \eta = 0, \quad f(0) = 0 \quad \text{and} \quad f'(0) = 0 \\ \eta = \infty, \quad f'(\infty) = 1 \end{aligned} \quad (151)$$

For the mass burning problem, the boundary conditions at the surface are

$$\begin{aligned} \eta = 0, \quad f(0) = 0 \quad \text{and} \quad Bf''(0) = -f'(0) \\ \eta = \infty, \quad f'(\infty) = 1 \end{aligned} \quad (152)$$

where η is the transformed distance normal to the plate. The second of these conditions contains the transfer number B and is of the same form as the boundary condition in the stagnant film case [Eq. (140)].

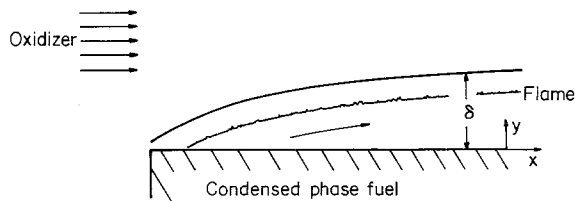


Fig. 17. Burning of a flat fuel surface in a one-dimensional flow field.

Emmons [29] solved this burning problem and his results can be shown to be of the form

$$G_f = (\lambda/c_p)(\text{Re}_x^{1/2}/x\sqrt{2})[-f(0)] \tag{153}$$

where Re_x is the Reynold's number based on the distance x from the leading edge of the flat plate. For Prandtl number equal to 1, Eq. (153) can be written in the form

$$G_f x/\mu = \text{Re}_x^{1/2}[-f(0)]/\sqrt{2} \tag{154}$$

It is particularly important to note that $[-f(0)]$ is a function of the transfer number B . This dependency as determined by Emmons is shown in Fig. 18.

An interesting approximation to this result [Eq. (154)] can be made from the stagnant film result of the last section, i.e.,

$$G_f = (D\rho/\delta) \ln(1 + B) = (\lambda/c_p \delta) \ln(1 + B) = (\mu/\delta) \ln(1 + B) \tag{147}$$

If δ were assumed to be the Blasius boundary layer thickness δ_x , then

$$\delta_x = 5.2x \text{Re}_x^{1/2} \tag{155}$$

Substituting Eq. (155) into Eq. (107),

$$G_f x/\mu = (\text{Re}_x^{1/2}/5.2) \ln(1 + B) \tag{156}$$

The values predicted by Eq. (156) are somewhat high compared to those predicted by Eq. (154). If Eq. (156) is divided by $B^{0.15}/2$ to give

$$G_f x/\mu = (\text{Re}_x^{1/2}/2.6)[\ln(1 + B)/B^{0.15}] \tag{157}$$

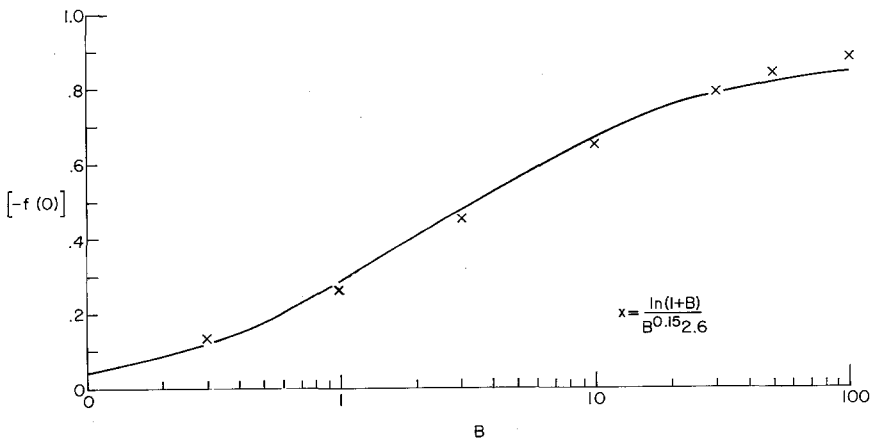


Fig. 18. $[-f'(0)]$ as a function of the transfer number B .

then the agreement is very good over a wide range of B values. To show the extent of the agreement, the function

$$\ln(1 + B)/B^{0.152.6} \quad (158)$$

is plotted on Fig. 11 as well.

Obviously these results do not hold at very low Reynold's number. As Re approaches zero, the boundary layer thickness approaches infinity. However, the burning rate is bounded by the quiescent results.

3. The Flowing Droplet Case

When droplets are not at rest relative to the oxidizing atmosphere, the quiescent results no longer hold and forced convection must again be considered. No one has solved this complex case. As discussed in Section 4.E, flow around a sphere can be complex, and at relatively high Re (>20), there is a boundary layer flow around the front of the sphere and a wake or eddy region behind it.

For this burning droplet case, an overall heat transfer relationship could be written to define the boundary condition given by Eq. (90)

$$h(\Delta T) = G_f L_v \quad (159)$$

The thermal driving force is represented by a temperature gradient ΔT which is the ambient temperature T_∞ plus the rise in this temperature due to the energy release minus the temperature at the surface T_s or

$$\Delta T = T_\infty + (im_{0\infty} H/c_p) - T_s = [im_{0\infty} H + c_p(T_\infty - T_s)]/c_p \quad (160)$$

Substituting Eq. (160) and Eq. (118) for G_f into Eq. (159),

$$h[im_{0\infty} H + c_p(T_\infty - T_s)]/c_p = [(D\rho/r) \ln(1 + B)]L_v = [(\lambda/c_p) \ln(1 + B)]L \quad (161)$$

where r is now the radius of the droplet. Cross-multiplying, Eq. (161) becomes

$$hr/\lambda = \ln(1 + B)/B = Nu \quad (162)$$

since

$$B = [im_{0\infty} H + c_p(T_\infty - T_s)]/L_v$$

Since Eq. (118) was used for G_f , this Nusselt number (Eq. (162)) is for the quiescent case ($Re \rightarrow 0$). For small B , $\ln(1 + B) \approx B$ and the $Nu = 1$, the classical result for heat transfer without mass addition.

The term $[\ln(1 + B)]/B$ has been used as an empirical correction for higher Reynold's number problems and a classical expression for Nu with mass transfer is

$$\text{Nu}_r = [\ln(1 + B)/B](1 + 0.39 \text{Pr}^{1/3} \text{Re}_r^{1/2}) \quad (163)$$

As $\text{Re} \rightarrow 0$, Eq. (163) approaches Eq. (162). For the case $\text{Pr} = 1$ and $\text{Re} \gg 1$, Eq. (163) becomes

$$\text{Nu}_r = (0.39)[\ln(1 + B)/B]\text{Re}_r^{1/2} \quad (164)$$

The flat plate result of the preceding section could have been written in terms of a Nusselt number as well. In that case

$$\text{Nu}_x = [-f(0)] \text{Re}_x^{1/2} / \sqrt{2B} \quad (165)$$

Thus, the burning rate expressions related to Eqs. (164) and (165) are, respectively,

$$G_f r / \mu = 0.39 \text{Re}_r^{1/2} \ln(1 + B) \quad (166)$$

$$= \text{Re}_r^{1/2} [-f(0)] / \sqrt{2} \quad (167)$$

Since in convective flow a wake exists behind the droplet and droplet heat transfer in the wake may be minimal, these equations are not likely to predict quantitative results. It is again interesting to note that if the right-hand side of Eq. (166) is divided by $B^{0.15}$, then the expression given by Eqs. (166) and (167) follow identical trends and thus data can be correlated as

$$(G_f r / \mu) \{ B^{0.15} / \ln(1 + B) \} \text{vs } \text{Re}^{1/2} \quad (168)$$

If turbulent boundary layer conditions are achieved under certain conditions, then the same type of expression should hold and Re should be raised to the 0.8 power.

If, indeed, Eqs. (166) and (167) adequately predict the burning rate of a droplet in laminar convective flow, then for a given relative velocity between the gas and the droplet, the droplet will follow a " $d^{3/2}$ " burning rate law. β in this case will be a function of the relative velocity as well as B and other physical parameters of the system. This result should be compared to the " d^2 " law [Eq. (127)] for droplet burning in quiescent atmospheres. In turbulent flow, droplets will appear to follow a burning rate law in which the power of the diameter is close to one.

4. Burning Rates of Plastics; The Small B Assumption and Radiation Effects

There is great interest in the fire safety of polymeric (plastic) materials and in determining the mass burning rate of plastics. For plastics whose burning rate measurements are made so that there is no melting, or for nonmelting

plastics, the developments just obtained should hold well. For the burning of some plastics in air or at low oxygen concentrations, the transfer number may be considered small compared to 1. For this condition, which of course would hold for any system in which $B \ll 1$,

$$\ln(1 + B) \cong B \quad (169)$$

and the mass burning rate expression may be written for nontransverse movement of the air case

$$G_f \cong (\lambda/c_p \delta) B \quad (170)$$

Recall that for these considerations the most convenient expression for B is

$$B = im_{0\infty} H + c_p(T_\infty - T_s)/L_v \quad (171)$$

In most cases

$$im_{0\infty} H \gg c_p(T_\infty - T_s) \quad (172)$$

so

$$B \cong im_{0\infty} H/L_v \quad (173)$$

and

$$G_f \cong (\lambda/c_p \delta)(im_{0\infty} H/L_v) \quad (174)$$

Equation (174) shows the reason that for burning rate experiments in which the dynamics of the air are constant or well controlled (i.e., δ is known or constant), then good straightline correlations are obtained when G_f is plotted as a function of $m_{0\infty}$. One should realize that

$$G_f \sim m_{0\infty} \quad (175)$$

holds only for small B .

The consequence of this small B assumption may not at first be apparent. A physical interpretation can be obtained from again writing the mass burning rate expression for the two assumptions made; i.e., $B \ll 1$ and $B \cong (im_{0\infty} H/L_v)$:

$$G_f \cong (\lambda/c_p \delta)(im_{0\infty} H/L_v) \quad (176)$$

and realizing that as an approximation

$$H \cong c_p(T_f - T_s) \quad (177)$$

where T_f is the diffusion flame temperature. Thus, the burning rate expression becomes

$$G_f \cong (\lambda/c_p \delta)[c_p(T_f - T_s)/L_v] \quad (178)$$

Cross-multiplying, one obtains

$$G_f L_v \cong \lambda(T_f - T_s)/\delta \quad (179)$$

which says that the energy required to gasify the surface at a given rate per unit area is supplied by the heat flux established by the flame. Equation (179) is simply another form of Eq. (159). Thus, the significance of the small B assumption is that the gasification from the surface is so small that it does not alter the gaseous temperature gradient determining the heat flux to the surface. This result is different from that obtained earlier and which stated that the stagnant film thickness was not affected by the surface gasification rate. The small B assumption goes one step further and reveals that under this condition the temperature profile in the boundary layer is not affected by the small amount of gasification.

If in the mass burning process there is flame radiation, or any other imposed radiation, as is frequently used in plastic flammability tests, then a convenient expression for the mass burning rate can be obtained provided it is assumed that only the gasifying surface and not any of the gases between the radiation source and the surface absorbs radiation. In this case Fineman [30] showed that the stagnant film expression for the burning rate can be approximated by

$$G_f = (\lambda/c_p \delta) \ln[1 + B/(1 - E)] \quad \text{where} \quad E \equiv Q_R/G_f L_v$$

and Q_R is the radiative heat transfer flux.

This simple form for the burning rate expression arises because the equations are developed for the conditions in the gas phase and the mass burning rate arises explicitly in the boundary condition to the problem. Since the assumption is made that no radiation is absorbed by the gases, the radiation term appears only in the boundary condition to the problem.

Notice that as the radiant flux Q_R increases, E and the term $B/(1 - E)$ increase. When $E = 1$, the problem disintegrates because the equation was developed in the framework of a diffusion analysis. $E = 1$ means that the solid is gasified by the radiant flux alone.

PROBLEMS

1. A laminar fuel jet issues from a tube into air and is ignited to form a flame. The height of the flame is 8 cm. With the same fuel the diameter of the jet is increased 50% and the laminar velocity leaving the jet decreased by 50%. What is the height of the flame after the changes are made? Suppose the experiments are repeated but that grids are inserted in the fuel tube so that all flows are turbulent. Again for the initial turbulent condition it is assumed the flame height is 8 cm. What is the height after the same changes are made as in the previous part?

2. An ethylene oxide monopropellant rocket motor is considered part of a ram rocket power plant in which the turbulent exhaust of the rocket reacts with induced air in an afterburner. The exit area of the rocket motor is 8 cm^2 . After testing it is found that it is necessary to reduce the afterburner length by 42.3%. What size must the exit port of the new rocket have to be to accomplish this reduction with the same afterburner combustion efficiency? The new rocket would operate at the same chamber pressure and area ratio. How many of the new rockets would be required to maintain the same level of thrust as the original power plant?
3. A spray of benzene fuel is burned in quiescent air at 1 atm and 298 K. The burning of the spray can be assumed to be characterized by single droplet burning. The (Sauter) mean diameter of the spray is $100 \mu\text{m}$; that is, the burning time of the spray is the same as a single droplet of $100 \mu\text{m}$. Calculate a mean burning time for the spray. For calculation purposes, assume whatever mean properties of the fuel, air and product mixture that are required. Generally for some properties those of nitrogen would suffice. Also assume the droplet is essentially of infinite conductivity. Report, as well, the steady-state temperature of the fuel droplet as it is being consumed.
4. Repeat the calculation of the previous problem for the initial condition that the air is at an initial temperature of 1000 K. Further calculate the burning time if the benzene were burned in pure oxygen at 298 K. Repeat all calculations with ethanol as the fuel. Then discuss the dependence of the results obtained on ambient conditions and fuel type.
5. Two liquid sprays are evaluated in a single cylinder test engine. The first is liquid methanol which has a transfer number $B = 2.9$. The second is a regular diesel fuel which has a transfer number $B = 3.9$. The two fuels have approximately the same liquid density, however the other physical characteristics of the diesel spray is such that its Sauter mean diameter is 1.5 times that of the methanol. Both are burning in air. Which spray requires the longer burning time and how much longer is it than the other?
6. Consider each of the condensed phase fuels listed to be a spherical particle burning with a perfect spherical flame front in air. From the properties of the fuels given, estimate the order of the fuels with respect to mass burning rate per unit area. List the fastest burning fuel first, etc.

	Latent heat of vaporization (cal/gm)	Density (gm/cm ³)	Thermal conductivity (cal/sec cm K)	Stoichiometric heat evolution in air per unit weight of fuel (cal/gm)	Heat capacity (cal/gm K)
Aluminum	2570	2.7	0.48	1392	0.28
Methanol	263	0.8	0.51×10^{-3}	792	0.53
Octane	87	0.7	0.33×10^{-3}	775	0.51
Sulfur	420	2.1	0.60×10^{-3}	515	0.24

7. Suppose various size fuel droplets are formed at one end of a combustor and move with the gas through the combustor at a velocity of 30 m/sec. It is known that the $50 \mu\text{m}$ droplets completely vaporize in 5 msec. It is desired to vaporize completely each droplet of $100 \mu\text{m}$ and less before they exit the combustion chamber. What is the minimum length of the combustion chamber allowable in design to achieve this goal?

8. A radiative flux Q_r is imposed on a solid fuel burning in air in a stagnation film mode. The expression for the burning rate is

$$G_r = (D\rho/\delta) \ln[1 + B/(1 - E)]$$

Where $E = Q_r/G_r L_v$. Develop this expression. It is a one-dimensional problem as described.

9. Experimental evidence from a porous sphere burning rate measurement in a low Reynold's number laminar flow condition confirms that the mass burning rate per unit area can be represented by

$$G_r r/\mu = f'(0, B)/\sqrt{2} \text{Re}_r^{1/2}$$

Would a real droplet of the same fuel follow a " d^2 " law under the same conditions? If not, what type of power law should it follow?

10. Write what would appear to be the most important physical result in each of the following areas:

- (a) laminar flame propagation
- (b) laminar diffusion flames
- (c) turbulent diffusion flames
- (d) detonation
- (e) droplet diffusion flames

Explain the physical significance of the answers. Do not develop equations.

REFERENCES

1. Gaydon, A. G., and Wolfhard, H., "Flames," Chapter VI, Macmillan, New York, 1960.
2. Smyth, K. C., Miller, J. H., Dorfman, R. C., Mallard, W. G., and Santoro, R. J., *Combust. Flame* **62**, 157 (1985).
3. Roper, F. G. *Combust. Flame* **29**, 219 (1977).
4. Roper, F. G., Smith, C., and Cunningham, A. C., *Combust. Flame* **29**, 227 (1977).
5. Spengler, G., and Kern, J., *Brennst. Chem.* **50**, 321 (1969).
6. Gomez, A., Sidebotham, G., and Glassman, I., *Combust. Flame* **58**, 45 (1984).
7. Hottel, H. C., and Hawthorne, W. R., *Int. Symp. Combust.*, 3rd, p. 255, Williams and Wilkins, Baltimore, 1949.
8. Boedecker, L. R., and Dobbs, G. M., *Combust. Sci. Technol.* **46**, 301 (1986).
9. Williams, F. A., "Combustion Theory," 2nd ed., Chapter 3, Benjamin-Cummins, Menlo Park, California, 1985.
10. Lewis, B., and von Elbe, G., "Combustion, Flames and Explosion of Gases," 2nd ed., Academic Press, New York, 1961.
11. Burke, S. P., and Schumann, T. E. W., *Ind. Eng. Chem.* **20**, 998 (1928).
12. Fristrom, R. M., and Westenberg, A. A., "Flame Structure," McGraw-Hill, New York, 1965.
- 12a. Hawthorne, W. R., Weddell, D. B., and Hottel, H. C., *Int. Symp. Combust.*, 3rd, p. 266, Williams and Wilkins, Baltimore, 1946.
13. Khudyakov, L., *Chem. Abst.* **46**, 10844e, 1955.
14. Blackshear, P. L., Jr., "An Introduction to Combustion," Chapter IV, Dept. of Mech. Eng., Univ. of Minnesota, Minneapolis, 1960.
15. Spalding, D. B., *Int. Symp. Combust.*, 4th, p. 846, Williams and Wilkins, Baltimore, 1953.

16. Spalding, D. B., "Some Fundamentals of Combustion," Chapter 4, Butterworth, London, 1955.
17. Kanury, A. M., "Introduction to Combustion Phenomena," Chapter 5, Gordon and Breach, New York, 1975.
18. Godsave, G. A. E., *Int. Symp. Combust., 4th*, p. 818, Williams and Wilkins, Baltimore, 1953.
19. Goldsmith, M., and Penner, S. S., *Jet Propul.* **24**, 245 (1954).
20. Lorell, J., Wise, H., and Carr, R. E., *J. Chem. Phys.* **25**, 325 (1956).
21. Law, C. K., *Prog. Energy Combust. Sci.* **8**, 169 (1982).
22. Law, C. K., and Law, A. V., *Combust. Sci. Technol.* **12**, 207 (1976).
23. Law, C. K., and Williams, F. A., *Combust. Flame* **19**, 393 (1972).
24. Hubbard, G. L., Denny, V. E., and Mills, A. F., *Int. J. Heat Mass Transfer* **18**, 1003 (1975).
25. Sirignano, W. A., and Law, C. K., *Adv. Chem. Ser. No. 166*, 1 (1978).
26. Law, C. K., *Combust. Flame* **26**, 17 (1976).
27. Chiu, H. H., and Lui, T. M., *Combust. Sci. Technol.* **17**, 127 (1977).
28. Blasius, H., *Z. Math. Phys.* **56**, 1 (1956).
29. Emmons, H. W., *Z. Angew. Math. Mech.* **36**, 60 (1956).
30. Fineman, S., M.S.E. Thesis, Dept. of Aero. Eng., Princeton University, Princeton, New Jersey, 1962.

Ignition

A. CONCEPTS

If the concept of ignition were purely a chemical phenomenon, then it should be treated more appropriately prior to the discussion of gaseous explosions (Chapter 3). However, thermal considerations are crucial to the concept of ignition. Indeed, thermal considerations play the key role in consideration of the ignition of condensed phases. The problem of storage of wet coal or large concentrations of solid materials that can undergo slow exothermic decomposition is also one of ignition, i.e., the concept of spontaneous combustion is an element of the theory of thermal ignition.

It is appropriate to consider again the elements discussed in analysis of the explosion limits of hydrocarbons. The explosion limits shown in Fig. 5 of Chapter 3 exist for particular conditions of pressure and temperature. When the thermal conditions for point 1 in this figure exist, some reaction begins and, thus, some heat must be evolved. The experimental configuration is assumed to be such that the heat of reaction is dissipated infinitely fast at the walls of the containing vessel to retain the temperature at the initial value T_1 . Then steady reaction prevails and a slight pressure rise can be noticed. When the conditions such as those at point 2 prevail, as discussed in Chapter 3, the rate of chain carrier generation exceeds the rate of chain termination, the reaction rate becomes progressively greater, and subsequently one has an explosion, i.e., in the context here, ignition. Generally, pressure is used as a measure of the extent of reaction; of course, other measures can be used as

well. The sensitivity of the measuring device determines when a change in initial conditions first exists. Essentially, this change in initial conditions (pressure) is not noted until after some time interval and as discussed in Chapter 3, this time interval can be related to that required to reach the degenerate branching stage, or some stage in which chain branching begins to show its effect on the overall reaction. This time interval is considered as an induction period and to correspond to the ignition concept. This induction period will vary considerably with temperature. Increasing the temperature increases the rates of the reactions leading to branching and, thus, shortens the induction period. The isothermal events discussed in this paragraph essentially define chemical chain ignition.

Now if one begins at conditions similar to point 1 (Fig. 5, Chapter 3), except that the experimental configuration is such that the heat of reaction is not dissipated at the walls of the vessel, i.e., the system is adiabatic, the reaction will self-heat until the temperature of the mixture moves the system into the explosive reaction regime. This type of event is called two-stage ignition and there are two induction periods, or ignition times, associated with it. The first is associated with the time (τ_c , chemical time) to build to the degenerate branching step or the critical concentration of radicals (or for that matter any other chain carriers) and the second (τ_t , thermal time) is associated with the subsequent steady reaction step and is the time it takes for the system to reach the thermal explosion (ignition) condition. Generally $\tau_c \gg \tau_t$.

If the initial thermal condition were to begin in the chain explosive regime, such as point 2, then the induction period τ_c still exists, there is no requirement for self-heating, and the mixture immediately explodes. In essence $\tau_c \rightarrow 0$.

In many practical systems, one cannot distinguish the two stages in the ignition process since $\tau_c \gg \tau_t$, and essentially one measures a time that is predominantly the chemical induction period. Any errors in correlating experimental ignition data in this low-temperature regime are due to small changes in τ_t .

Sometimes point 2 will exist in the cool-flame regime. Again, the physical conditions of the nonadiabatic experiment can be such that the heat rise due to the passage of the cool flame can raise the temperature such that it moves from a position characterized by point 1 to one characterized by point 4. This phenomenon is also referred to as two-stage ignition. The region of point 4 is not a chain branching explosion, but a self-heating explosion. Again, there is an induction period τ_c associated with the initial cool-flame stage and a subsequent time (τ_t) associated with the self-heating aspect.

If one initiates the reacting system under conditions similar to point 4, one develops pure thermal explosions and these explosions have associated with them thermal induction or ignition times. As will be discussed in subsequent

paragraphs, even at low temperatures under both nonadiabatic conditions as utilized in obtaining hydrocarbon-air explosion limits and adiabatic conditions, thermal explosion (ignition) is possible.

The above concepts were concerned with premixed fuel-oxidizer situations. In reality these ignition types described do not arise too frequently in practical systems; however, the concepts can be used for better understanding of many practical combustion systems as, for example, the ignition of liquid fuels.

Many ignition experiments have been performed by projecting liquid and gaseous fuels into heated stagnant and flowing air streams [1,2]. It is possible from such experiments to relate an ignition delay (or time) to the temperature of the air. If this temperature is reduced below a certain value, no ignition occurs even after an extended period of time. This temperature is one of

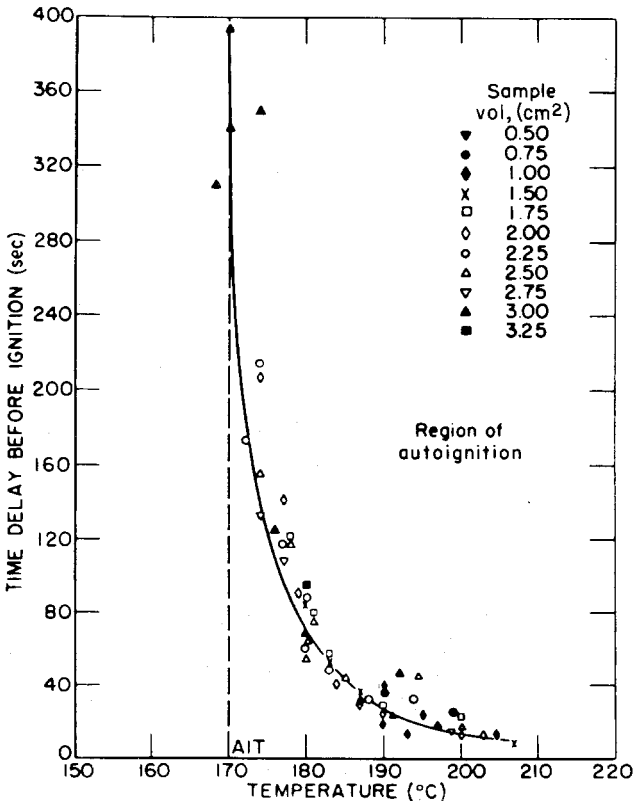


Fig. 1. Time delay before ignition of normal propyl nitrate at 1000 psig (from Zabetakis [2]).

interest in fire safety and is referred to as the spontaneous or autoignition temperature (AIT). Figure 1 shows some typical data from which the spontaneous ignition temperature is obtained. The AIT is fundamentally the temperature at which elements of the fuel-air system enters the explosion regime. Thus, the AIT must be a function of pressure as well; however, most reported data, such as that given in Appendix F are for 1-atm pressure. As will be shown later, a plot of the data in Fig. 1 in the form of $\log(\text{time})$ versus $(1/T)$ will give a straight line. In the experiments mentioned, in the case of liquid fuels, the fuel droplet attains a vapor pressure corresponding to the temperature of the heated air. A combustible mixture close to stoichiometric forms irrespective of the fuel. It is this mixture that enters the explosive regime, which in actuality has an induction period associated with it. Approximate measurements of this induction period can be made in a flowing system by observing the distance from point of injection of the fuel to the point of first visible radiation and relating this distance to the time through knowledge of the stream velocity.

In essence, droplet ignition was brought about by the heated flowing air stream. This type of ignition is called "forced ignition" in contrast to the "self-ignition" conditions of chain and thermal explosions. The terms self-ignition, spontaneous ignition and autoignition are used synonymously. Obviously, forced ignition also may be the result of electrical discharges (sparks), heated surfaces, shock waves, flames, etc. Forced ignition is usually considered a local initiation of a flame that will propagate; however, in certain instances, a true explosion is initiated. After examination of an analytical analysis of chain spontaneous ignition and its associated induction time, this chapter will concentrate on the fundamental concepts of self- or spontaneous ignition and then will encompass aspects of forced ignition.

B. CHAIN SPONTANEOUS IGNITION

In Chapter 3 the conditions for a chain branching explosion were developed on the basis of a steady-state analysis. It was shown that when the chain branching factor α at a given temperature and pressure was greater than some critical value α_{crit} at which the reacting system exploded. Obviously in the development no induction period or critical chain ignition time τ_c evolved.

In this section consideration is given to an analytical development of this chain explosion induction period that has its roots in the early work on chain reactions by Semenov [3] and Hinshelwood [4] and which has been reviewed by Zeldovich *et al.* [5].

The approach considered as a starting point is a generalized form of Eq. (6) of Chapter 3, except not as a steady-state expression. Thus, the overall rate of change of the concentration of chain carriers (R) is expressed by the equation

$$d(R)/dt = \dot{w}_0 + k_b + k_t(R) = \dot{w}_0 + \phi(R) \quad (1)$$

where \dot{w}_0 is the initiation rate of a very small concentration of carriers. Such initiation rates are usually very slow. Rate expressions k_b and k_t are for the overall chain branching and termination steps, respectively, and ϕ is simply the difference $k_b - k_t$.

Constants k_b , k_t , and obviously, ϕ are dependent on the physical conditions of the system and, in particular, temperature and pressure are major factors in their explicit values. However, it is to be realized that k_b is much more temperature dependent than k_t . The rates included in k_t are due to very low activation energy recombination reactions and essentially have no temperature dependency, whereas most chain branching and propagating reactions can have significant values of activation energy. One can conclude then that ϕ changes sign as the temperature is raised. At low temperatures it is negative and at high temperatures it is positive. Then at high temperatures $d(R)/dt$ is a continuously and rapidly increasing function. At low temperature as $[d(R)/dt] \rightarrow 0$, (R) approaches a fixed limit $[\dot{w}_0/\phi]$, hence there is no runaway and no explosion. The temperature corresponding to $\phi = 0$ is the critical temperature below which no explosion can take place.

At time zero the carrier concentration is essentially zero and (R) = 0 at $t = 0$ serves as the boundary condition for Eq. (1). Integrating Eq. (1) results in the following expression for (R)

$$(R) = (\dot{w}_0/\phi)[\exp(\phi t) - 1] \quad (2)$$

If as a result of the chain system the formation of every new carrier is accompanied by the formation of j molecules of final product (P), the expression for the rate of formation of the final product becomes

$$\dot{w} = [d(P)/dt] = jk_b(R) = (jk_b \dot{w}_0/\phi)[\exp(\phi t) - 1] \quad (3)$$

An analogous result is obtained if the rate of formation of carriers is equal to zero ($\dot{w}_0 = 0$) and the chain system is initiated due to the presence of some initial concentration (R)₀. Then for the initial condition that at $t = 0$, (R) = (R)₀, Eq. (1) becomes

$$(R) = (R)_0 \exp(\phi t) \quad (4)$$

The derivations of Eqs. (1)–(4) are only valid at the initiation of the reaction system; k_b and k_t were considered constant when the equations were integrated. Even for constant temperature k_b and k_t will change because the

concentration of the original reactants would appear in some form in these expressions.

Equations (2) and (4) are referred to as Semenov's law, which states that in the initial period of a chain reaction the chain carrier concentration increases exponentially with time when $k_b > k_t$.

During the very early stages of the reaction the rate of formation of carriers begins to rise, but it can be below the limits of measurability. After a period of time, the rate becomes measurable and continues to rise until the system becomes explosive. The explosive reaction only ceases when the reactants are consumed. The time to the small measurable rate \dot{w}_{ms} corresponds to the induction period τ_c .

For the time close to τ_c , \dot{w}_{ms} will be much larger than \dot{w}_0 and $\exp(\phi t)$ much greater than 1, so that Eq. (3) becomes

$$\dot{w}_{ms} = (jk_b \dot{w}_0 / \phi) \exp(\phi \tau) \quad (5)$$

The induction period then becomes

$$\tau_c \simeq (1/\phi) \ln(\dot{w}_{ms} \phi / jk_b \dot{w}_0) \quad (6)$$

Considering either the argument of the logarithm in Eq. (6) as a nearly constant term or k_b much larger than k_t so that $\phi \cong k_b$, gives the result that

$$\tau_c = \text{const}/\phi \quad (7)$$

so that the induction time depends on the relative rates of branching and termination. The time decreases as the branching rate increases.

C. THERMAL SPONTANEOUS IGNITION

The theory of thermal ignition is based upon a very simple concept. When the rate of thermal energy release is greater than the rate of thermal energy dissipation (loss), an explosive condition exists. When the contra condition exists, thermal explosion is impossible. When the two rates are equal, the critical conditions for ignition (explosion) are specified. Essentially, the same type of concept holds for the chain explosions discussed. When the rate of chain branching becomes greater than the rate of chain termination ($\alpha > \alpha_{crit}$), there is an explosive condition; $\alpha < \alpha_{crit}$ specifies steady reaction. Thus, when the external effects of heat loss or chain termination are considered, there is a great deal of commonality between chain and thermal explosions.

In consideration of external effects, it is essential to emphasize that there are conditions under which the thermal induction period could last several hours. This condition arises when the vessel walls are thermally insulated. In

this case even with a very low initial temperature, the heat of the corresponding slow reaction remains in the system and gradually self-heats the reactive components until ignition (explosion) takes place. If the vessel were not insulated and heat transferred to the external atmosphere, equilibrium is rapidly reached between the heat release and heat loss and thermal explosion is impossible.

It is possible to conclude from the preceding that the study of the laws governing thermal explosions will make it possible to better understand the phenomena controlling the spontaneous ignition of combustible mixtures and forced ignition in general.

The concepts discussed were first presented in analytical forms by Semenov [3] and later in more exact form by Frank-Kamenetskii [6]. Since the Semenov approach offers easier physical insight, it will be considered first and then the details of the Frank-Kamenetskii approach will be presented.

1. Semenov Approach to Thermal Ignition

Semenov first considered the progress of the reaction of a combustible gaseous mixture that had an initial temperature T_0 in a vessel whose walls were maintained at the same temperature. The amount of heat released due to chemical reaction per unit time (\dot{q}_r) then can be represented in simplified overall form as

$$\begin{aligned}\dot{q}_r &= V\dot{w}Q = VQc^n A \exp(-E/RT) \\ &= VQ\rho^n \varepsilon^n A \exp(-E/RT)\end{aligned}\quad (8)$$

where V is the volume of the vessel, \dot{w} the reaction rate, Q the thermal energy release of the reactions, c the overall concentration, n the overall reaction order, A is the pre-exponential in the simple rate constant expression, and T the temperature that exists in the gaseous mixture after reaction commences. As in Chapter 2, the concentration can be represented in terms of the total density ρ and the mass fraction ε of the reacting species. Since the interest in ignition is in the effect of the total pressure, all concentrations are treated as being equal to $\rho\varepsilon$.

The overall heat loss (\dot{q}_1) to the walls of the vessel, and, thus, to that medium that maintains the walls of the vessel at T_0 can be represented by the expression

$$\dot{q}_1 = hS(T - T_0) \quad (9)$$

where h is the heat transfer coefficient and S the surface area of the walls of the containing vessel.

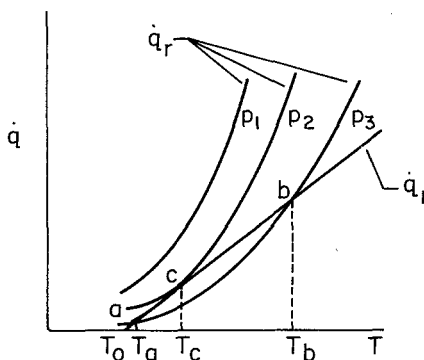


Fig. 2. Heat generation and heat loss of reacting mixture in a vessel with pressure and thermal bath variations.

Heat release \dot{q}_r is a function of pressure through the density term and \dot{q}_1 is a less sensitive function of pressure through h , which according to the heat transfer method by which the vessel walls are maintained at T_0 can be a function of the Reynold's number.

Shown in Fig. 2 is the relationship between \dot{q}_r and \dot{q}_1 for various initial pressures and values of the heat transfer coefficient h and for a constant wall temperature of T_0 . In Eq. (8) \dot{q}_r takes the usual exponential shape due to the Arrhenius term and \dot{q}_1 is obviously a linear function of the mixture temperature T . The \dot{q}_1 line for $h = h_3$ intersects the \dot{q}_r curve for an initial pressure p_3 at two points, a and b . For a system where there is simultaneous heat generation and heat loss the overall energy conservation equation takes the form

$$c_v V(dT/dt) = \dot{q}_r - \dot{q}_1 \quad (10)$$

where the term on the left-hand side is the rate of energy accumulation in the containing vessel and c_v is the molar constant volume heat capacity of the gas mixture. Thus, a system whose initial temperature is T_0 will rise to point a spontaneously. Since $\dot{q}_r = \dot{q}_1$ and the mixture attains the steady, slow-reaction rate $\dot{w}(T_i)$, this point is an equilibrium point. If the conditions of the mixture are somehow perturbed so that the temperature reaches a value greater than T_i , then \dot{q}_1 becomes greater than \dot{q}_r and the system moves back to the equilibrium condition represented by point a . Only if there is a very great perturbation so that the mixture temperature becomes a value greater than that represented by point b will the system self-heat to explosion. Under this condition $\dot{q}_r > \dot{q}_1$.

If the initial pressure is increased to some value p_2 , the heat release curve shifts to higher values, which are proportional to p^n (or ρ^n). The assumption is made that h is not affected by this pressure increase. The value of p_2 is selected so that the \dot{q}_1 becomes tangent to the \dot{q}_r curve at some point c . If the value of

p_2 were raised to some value p_1 , then q_r is everywhere greater than \dot{q}_1 and all initial temperatures give explosive conditions. It is obvious, then, that, when the \dot{q}_1 line is tangent to the \dot{q}_r curve, the critical condition for mixture self-ignition exists.

The point c represents an ignition temperature T_i (or T_c) and from the conditions there, Semenov showed that one could obtain a relationship between this ignition temperature and the initial temperature of the mixture or the temperature of the wall (T_0). Recall the initial temperature of the mixture and the temperature at which the vessel's wall is maintained are the same (T_0). It is important to emphasize that T_0 is a wall temperature that may cause a fuel-oxidizer mixture to ignite. T_0 can be hundreds of degrees greater than ambient and should not be confused with reference temperature taken as the ambient (298 K) in Chapter 1.

The conditions at c are

$$\dot{q}_r = \dot{q}_1, \quad (d\dot{q}_r/dT) = (d\dot{q}_1/dT) \quad (11)$$

or

$$VQ\rho^n e^n A \exp(-E/RT_i) = hS(T_i - T_0) \quad (12)$$

$$(d\dot{q}_r/dT) = (E/RT_i^2)VQ\rho^n e^n A \exp(-E/RT_i) = (d\dot{q}_1/dT) = hS \quad (13)$$

Since the variation in T is small, the effect of this variation on the density is ignored for simplicity sake. Dividing Eq. (12) by Eq. (13), one obtains

$$(RT_i^2/E) = (T_i - T_0) \quad (14)$$

Equation (14) is rewritten as

$$T_i^2 - (E/R)T_i + (E/R)T_0 = 0 \quad (15)$$

whose solutions are

$$T_i = (E/2R) \pm [(E/2R)^2 - (E/R)T_0]^{1/2} \quad (16)$$

The solution with the positive sign gives extremely high temperatures and does not correspond to any physically real situation. Rewriting Eq. (16)

$$T_i = (E/2R) - (E/2R)[1 - (4RT_0/E)]^{1/2} \quad (17)$$

and expanding one obtains

$$T_i = (E/2R) - (E/2R)[1 - (2RT_0/E) - 2(RT_0/E)^2 - \dots]$$

Since (RT_0/E) is a small number, the higher-order terms may be neglected and one obtains

$$T_i = T_0 + (RT_0^2/E), \quad (T_i - T_0) = (RT_0^2/E) \quad (18)$$

For a hydrocarbon-air mixture initially at a temperature of 900 K and considered to have an overall activation energy of about 40 kcal/mole, the temperature rise given in Eq. (18) is approximately 20°. Thus, for many cases it is possible to take T_i as being equal to T_0 or $T_0 + (RT_0^2/E)$ with only small error in the final result. Thus, if

$$\dot{w}(T_i) = \rho^n \varepsilon^n A \exp(-E/RT_i) \quad (19)$$

and

$$\dot{w}(T_0) = \rho^n \varepsilon^n A \exp(-E/RT_0) \quad (20)$$

and the approximation given by Eq. (18) is used in Eq. (19), one obtains

$$\begin{aligned} \dot{w}(T_i) &= \rho^n \varepsilon^n A \exp\{-E/R[T_0 + (RT_0^2/E)]\} \\ &= \rho^n \varepsilon^n A \exp\{-E/RT_0[1 + (RT_0/E)]\} \\ &= \rho^n \varepsilon^n A \exp\{-(E/RT_0)[1 - (RT_0/E)]\} \\ &= \rho^n \varepsilon^n A \exp[-(E/RT_0) + 1] \\ &= \rho^n \varepsilon^n A [\exp(-E/RT_0)]e \\ &= [\dot{w}(T_0)]e \end{aligned} \quad (21)$$

that is, the rate of chemical reaction at the critical ignition condition is equal to the rate at the initial temperature times the number e . Substituting this result and the approximation given by Eq. (18) into Eq. (12), one obtains

$$eVQ\rho^n \varepsilon^n A \exp(-E/RT_0) = hSR T_0^2/E \quad (22)$$

Representing ρ in terms of the perfect gas law and using the logarithmic form, one obtains

$$\ln(P^n/T_0^{n+2}) = +(E/RT_0) + \ln(hSR^{n+1}/eVQe^n AE) \quad (23)$$

Since the overall order of most hydrocarbon oxidation reactions can be considered to be approximately 2, Eq. (23) takes the form of the so-called Semenov expression

$$\ln(P/T_0^2) = +(E/2RT_0) + B \quad (24)$$

Equations (23) and (24) define the thermal explosion limits and a plot of $\ln(P/T_0^2)$ versus $(1/T_0)$ gives a straight line as is found for many gaseous hydrocarbons. A plot of P versus T_0 takes the form given in Fig. 3 and shows the similarity of this result to the thermal explosion limit (point 3 to point 4, Fig. 5, Chapter 3) of hydrocarbons. The variation of the correlation with the chemical and physical terms in B should not be overlooked. Indeed the explosion limits are a function of the surface area to volume ratio (S/V) of the containing vessel.

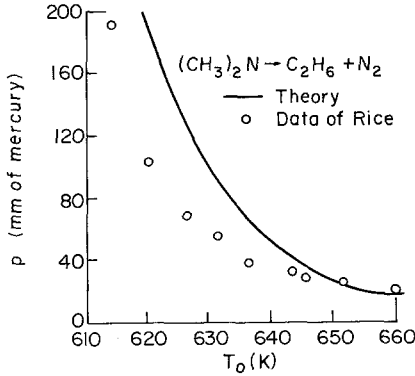


Fig. 3. Critical pressure-temperature relationship for ignition of a chemical process.

Under the inherent assumption made that the mass fractions of the reactants were not changing, further interesting insights can be obtained from rearrangement of Eq. (22). If the reaction proceeded at a constant rate corresponding to T_0 , a characteristic reaction time τ_r can be defined as

$$\tau_r = \rho / [\rho^n e^n A \exp(-E/RT_0)] \quad (25)$$

A characteristic heat loss time τ_1 can be obtained from the cooling rate of the gas as if it were not reacting by the expression

$$Vc_v\rho(dT/dt) = -hS(T - T_0) \quad (26)$$

The characteristic heat loss time is generally defined as the time it takes to cool the gas from the temperature $(T - T_0)$ to $[(T - T_0)/e]$ and is found to be

$$\tau_1 = (V\rho c_v/hS) \quad (27)$$

By substituting Eqs. (18), (25), and (27) into Eq. (22), and realizing that (Q/C_v) can be approximated by $(T_f - T_0)$, the adiabatic explosion temperature rise, the following expression is obtained

$$\begin{aligned} (\tau_r/\tau_1) &= e(T_f - T_0)/(T_f - T_0) = e(\Delta T_f/\Delta T_i) = e \Delta T_f/(RT_0^2/E) \\ &= e(Q/c_v)/(RT_0^2/E) \end{aligned} \quad (28)$$

Thus, if (τ_r/τ_1) is greater than the value obtained from Eq. (28), thermal explosion is not possible and the reaction proceeds at a steady low rate given by point *a* in Fig. 2. If $(\tau_r/\tau_1) > (e \Delta T_f/\Delta T_i)$ and ignition still takes place, then the explosion proceeds by a chain rather than a thermal mechanism.

With the physical insights developed from this qualitative approach to the thermal ignition problem, it is appropriate to consider the more quantitative approach of Frank-Kamenetskii [6].

2. Frank-Kamenetskii Theory of Thermal Ignition

Frank-Kamenetskii first considers the nonsteady heat conduction equation. However, since the gaseous mixture, liquid, or solid energetic fuel can undergo exothermic transformations, a chemical reaction rate term is included. This term specifies a continuously distributed source of heat throughout the containing vessel boundaries. The heat conduction equation for the vessel is then

$$c_v \rho \, dT/dt = \text{div}(\lambda \, \text{grad } T) + \dot{q}' \quad (29)$$

in which the nomenclature is apparent perhaps except for q' , which represents the heat release density.

The solution of this equation would give the temperature distribution as a function of the spatial distance and the time. At the ignition condition, the character of this temperature distribution changes sharply. There should be an abrupt transition from a small stationary rise to a large and rapid rise. The difficulties in solving this partial differential equation are great and attempts have been made. But much insight into overall practical ignition phenomena can be gained by considering the two approximate methods as Frank-Kamenetskii has done. The two approximate methods are referred to as the stationary and nonstationary solutions. In the stationary theory, only the temperature distribution throughout the vessel is considered and the time variation is ignored. In the nonstationary theory, the spatial temperature variation is not taken into account, a mean temperature value throughout the vessel is used, and the variation of this mean temperature with time is examined. The nonstationary problem is the same as that posed by Semenov; the only difference is in the mathematical treatment.

a. The Stationary Solution—The Critical Mass and Spontaneous Ignition Problems

The stationary theory deals with time-independent equations of heat conduction with distributed sources of heat. Its solution gives the stationary temperature distribution in the reacting mixture. The initial conditions under which such a stationary distribution becomes impossible are the critical conditions for ignition.

Under this steady assumption, Eq. (29) becomes

$$\text{div}(\lambda \, \text{grad } T) = -\dot{q}' \quad (30)$$

and if the temperature dependency of the thermal conductivity is neglected,

$$\lambda \, \nabla^2 T = -\dot{q}' \quad (31)$$

It is important to consider the definition of q' . It is the amount of heat evolved by chemical reaction in a unit volume and in unit time. It is the product of the terms involving the energy content of the fuel and its rate of reaction. The rate of the reaction can be written as $Ze^{-E/RT}$. Recall Z is different from the normal Arrhenius pre-exponential term in that it contains the concentration terms and thus can be dependent on the mixture composition and the pressure. Thus,

$$\dot{q}' = QZe^{-E/RT} \quad (32)$$

where Q is the volumetric energy release of the combustible mixture. It follows then that

$$\nabla^2 T = -(Q/\lambda)Ze^{-E/RT} \quad (33)$$

and the problem resolves itself in solving this equation under the boundary condition that $T = T_0$ at the wall of the vessel.

Since the stationary temperature distribution below the explosion limit is sought and, thus, the temperature rise throughout the vessel is to be small, it is best to introduce a new variable

$$v = T - T_0$$

in which $v \ll T_0$. Under this condition, it is possible to describe the cumbersome exponential term as

$$\exp(-E/RT) = \exp[-E/R(T_0 + v)] = \exp\left\{-\frac{E}{RT_0} \left[\frac{1}{1 + (v/T_0)}\right]\right\}$$

If the term in brackets is expanded and the higher-order terms are eliminated, the expression simplifies to

$$\exp[-E/RT] \cong \exp\left[-\frac{E}{RT_0} \left(1 - \frac{v}{T_0}\right)\right] = \exp\left[-\frac{E}{RT_0}\right] \exp\left[\frac{E}{RT_0^2} v\right]$$

and (Eq. 33) becomes

$$\nabla^2 v = -\frac{Q}{\lambda} Z \exp\left[-\frac{E}{RT_0}\right] \exp\left[\frac{E}{RT_0^2} v\right] \quad (34)$$

In order to solve Eq. (34), new variables are defined

$$\theta = (E/RT_0^2)v, \quad \eta_x = x/r$$

where r is the radius of the vessel and x the distance from the center. Equation (34) then becomes

$$\nabla_\eta^2 \theta = -(Q/\lambda)(E/RT_0^2)r^2 Z e^{-(E/RT_0)} e^\theta \quad (35)$$

and the boundary conditions are $\eta = 1$, $\theta = 0$, and $\eta = 0$, $d\theta/d\eta = 0$.

Both Eq. (35) and the boundary condition contain only one nondimensional parameter δ :

$$\delta = (Q/\lambda)(E/RT_0^2)r^2Ze^{-E/RT_0} \quad (36)$$

The solution of Eq. (35), which represents the stationary temperature distribution, should be of the form $\theta = f(\eta, \delta)$ with one parameter, i.e., δ . The condition under which such a stationary temperature distribution ceases to be possible; i.e., the critical condition of ignition, is of the form $\delta = \text{const} = \delta_{\text{crit}}$. The critical value depends upon T_0 , the geometry (if the vessel is nonspherical), and the pressure through Z . Numerical integration of Eq. (35) for various δ 's determines the critical δ . For a spherical vessel $\delta_{\text{crit}} = 3.32$; for an infinite cylindrical vessel, $\delta_{\text{crit}} = 2.00$; and for infinite parallel plates, $\delta_{\text{crit}} = 0.88$.

As in the discussion of flame propagation, the stoichiometry and pressure dependency are in Z and $Z \sim P^n$, where n is the order of the reaction. Equation (36) expressed in terms of δ_{crit} permits the relationship between the critical parameters to be determined. Taking logarithms,

$$\ln rP^n \sim (E/RT)$$

If the reacting medium is a solid or liquid undergoing exothermic decomposition, then the pressure term is omitted and

$$\ln r \sim (+E/RT_0)$$

These results define the conditions for the critical size of storage for compounds such as ammonium nitrate as a function of the ambient temperature T_0 (see Hainer [7]). Similarly it represents the variation of a size of combustible material that will spontaneously ignite as a function of the ambient temperature T_0 . The higher the ambient temperature, the smaller the critical mass has to be to prevent disaster.

b. The Nonstationary Solution

The nonstationary theory deals with the thermal balance of the whole reaction vessel and assumes the temperature to be the same at all points. This assumption is of course incorrect in the conduction range where the temperature gradient is by no means localized at the wall. It is, however, equivalent to a replacement of the mean values of all temperature-dependent magnitudes by their values at a mean temperature, and involves relatively minor error.

If the volume of the vessel is designated by V , its surface area by S , and if a heat transfer coefficient h is defined, then the amount of heat evolved over the whole volume per unit time by the chemical reaction is

$$VQZe^{-E/RT} \quad (37)$$

and the amount of heat carried away from the wall is

$$hS(T - T_0) \quad (38)$$

Thus, the problem is now essentially nonadiabatic. The difference between the two heat terms is the heat that causes the temperature within the vessel to rise a given amount per unit time, i.e.,

$$c_v \rho V dT/dt \quad (39)$$

These terms can be expressed as an equality,

$$c_v \rho V dT/dt = VQZe^{-E/RT} - hS(T - T_0) \quad (40)$$

or

$$dT/dt = (Q/c_v \rho)Ze^{-E/RT} - (hS/c_v \rho V)(T - T_0) \quad (41)$$

Equations (40) and (41) are forms of Eq. (29) with a heat loss term. Nondimensionalizing the temperature and linearizing in the exponent in the same manner as in the previous section, one obtains

$$d\theta/dt = (Q/c_v \rho)(E/RT_0^2)Ze^{-E/RT_0}e^\theta - (hS/c_v \rho V)\theta \quad (42)$$

with the boundary condition $\theta = 0$ at $t = 0$.

The equation is not in dimensionless form. Each term has the dimension of reciprocal time. In order to make the equation completely dimensionless, it is necessary to introduce a time parameter. Equation (42) contains two such time parameters

$$\tau_1 = [(Q/c_v \rho)(E/RT_0^2)Ze^{-E/RT_0}]^{-1}, \quad \tau_2 = (hA/c_v \rho V)^{-1}$$

Consequently, the solution of Eq. (14) should be in the form

$$\theta = f(t/\tau_{1,2}, \tau_2/\tau_1)$$

where $\tau_{1,2}$ implies either τ_1 or τ_2 .

Thus, the dependence of dimensionless temperature θ on dimensionless time $t/\tau_{1,2}$ contains one dimensionless parameter τ_2/τ_1 . Consequently, a sharp rise in temperature can occur for a critical value of τ_2/τ_1 .

It is best to examine Eq. (42) written in terms of these parameters,

$$d\theta/dt = (e^\theta/\tau_1) - (\theta/\tau_2) \quad (43)$$

In the ignition range the rate of energy release is much greater than the rate of heat loss; that is, the first term on the right-hand side of Eq. (43) is much greater than the second. Under these conditions it is possible to disregard the removal of heat and view the thermal explosion as adiabatic.

Then for an adiabatic thermal explosion, the time dependence of the temperature should be of the form

$$\theta = f(t/\tau_1) \quad (44)$$

Under these conditions the time within which a given value of θ is attained is proportional to the magnitude τ_1 . Consequently, the induction period in the instance of adiabatic explosion is proportional to τ_1 . The proportionality constant has been shown to be unity. Conceptually this induction period can be related to the time period for the ignition of droplets for different air (or ambient) temperatures. This τ can be the adiabatic induction time and is simply

$$\tau = \frac{c_v \rho}{Q} \frac{RT_0^2}{E} \frac{1}{Z} e^{(+E/RT_0)} \quad (45)$$

Again the expression can be related to the critical conditions of time, pressure, and ambient temperature T_0 by taking logarithms,

$$\ln(\tau P^{n-1}) \sim (+E/RT_0) \quad (46)$$

The pressure dependency, as before, is derived at not only from the perfect gas law for ρ , but also from the density–pressure relationship in Z . Also the effect of the stoichiometry of a reacting gas mixture would be in Z . But the mole fraction terms would be in the logarithm and, therefore, have only a mild effect on the induction time. For hydrocarbon–air mixtures, the overall order is approximately 2, so Eq. (46) becomes

$$\ln(\tau P) \sim (E/RT_0) \quad (47)$$

which is essentially the conditions used in bluff-body stabilization considerations in Section 4.F. This result gives the intuitively expected answer that the higher the ambient temperature the shorter the ignition time. Hydrocarbon droplet and gas fuel injection ignition data correlate well with the dependencies as shown in Eq. (47) [8,9].

Todes [10] (see Jost [11]) in a less elegant fashion obtained the same expression as represented by Eq. (45). As Semenov [3] has shown by use of Eq. (25), Eq. (45) can be written as

$$\tau_i = \tau_r (c_v RT_0^2 / QE) \quad (48)$$

Since $(E/RT_0)^{-1}$ is a small quantity not exceeding 0.05 for most cases of interest and $(c_v T_0 / Q)$ is also a small quantity of the order 0.1, the quantity $(c_v RT_0^2 / QE)$ may be considered to have a range from 0.01 to 0.001. Thus, the thermal ignition time for a given initial temperature T_0 is from a 100th to a

1000th of the reaction time evaluated at T_0 . Since from Eq.(28) and the discussion following this equation,

$$\tau_r \leq (Q/c_v)(E/RT_0^2)e\tau_i \quad (49)$$

then

$$\tau_i \leq e\tau_1 \quad (50)$$

which signifies that the induction period is of the same order of magnitude as the thermal relaxation time.

Since it takes only a very small fraction of the reaction time to reach the end of the induction period, at the moment of the sudden rapid rise in temperature (i.e., when explosion begins), not more than 1% of the original mixture has reacted. This result justifies the inherent approximation developed and used that the reaction rate remains constant until explosion occurs. Further justified is also the earlier assumption made that the original mixture concentration remains the same from T_0 to T_i . This observation is important in that it reveals that no significantly different results would have been obtained if the more complex approach using both variations in temperature and concentration were used.

D. FORCED IGNITION

Contrary to the concept of spontaneous ignition of a large condensed phase mass of a reactive material, forced ignition is essentially a concept associated with gaseous materials. The energy input into a condensed phase reactive mass may be such that the material vaporizes and then ignites, but the phenomena that lead to ignition are associated with the gas phase reactions. There are many means to force ignition of a reactive material or mixture, but it is rather interesting that the most commonly used concepts are associated with various processes that take place in the spark-ignition automotive engine.

The spark is the first and most prevalent form of forced ignition. In the automotive cylinder it initiates a flame that travels across the cylinder. The spark is fired before the piston reaches top dead center and as the flame is travelling the combustible mixture ahead of this flame is being compressed. Under certain circumstances the mixture ahead of the flame explodes and the phenomena of knock is said to exist. The gases ahead of the flame are usually ignited by the compression or some hot spot on the metallic surfaces in the cylinder. The phenomena of knock is most likely an explosion, or possibly

very rapid flame spread, but is not likely to be a detonation. The physical configuration would not permit the transformation from a deflagration to a detonation. Nevertheless, the knock, or premature forced ignition, can occur due to compressively heating a fuel-air mixture or to a heated object such as a hot spot. Consequently, it is not surprising that the ignitability of a gaseous fuel-air mixture, or for that matter any exoergic system, has been studied experimentally by means approaching adiabatic compression to high temperature and pressure, by shock waves, which also raise the material to a high temperature and pressure, or by propelling hot metallic spheres or incandescent particles into a cold reactive mixture.

Forced ignition can also be brought about by pilot flames, flowing hot gases, which act as a jet into the cold mixture to be ignited, or by creating a boundary layer flow parallel to the cold mixture, which may also be flowing. Indeed, there are probably other possibilities that one can evoke. For consideration of these systems the reader is referred to Ref. [12].

It is apparent then that an ignition source can lead to either a pure explosion or to a flame (deflagration) that propagates. The geometric configuration in which the flame has been initiated can be conducive for the flame transforming into a detonation. There are many elements of fire and industrial safety in these considerations. Thus, a concept of a minimum ignition energy has been introduced as a test method for evaluating the ignitability of various fuel-air mixtures or any system that has exoergic characteristics.

Ignition by near adiabatic compression or shock wave techniques creates explosions that are most likely chain carrier rather than thermal initiated. This aspect of the subject will be treated at the end of this chapter. The main concentration in this section will be on ignition by sparks based on a thermal approach by Zeldovich [13,14]. This approach gives insights into the parameters, which not only give spark ignition, but other forced ignition systems that lead to flames, and has applicability to the minimum ignition energy.

1. Spark Ignition and Minimum Ignition Energy

The most commonly used spark systems for mobile power plants are those developed from discharged condensers and are referred to as capacitance sparks. The duration of these discharges can be as short as 0.01 μ sec or as long as 100 μ sec for larger engines. Research techniques generally employ two circular electrodes with flanges at the tips. The flanges have a parallel orientation and have a separation distance greater than the quenching distance for the mixture to be ignited. Reference [12] reports most extensive

details about spark and all other types of forced ignition. The energy in a capacitance spark is given by

$$E = \frac{1}{2}c_f(v_2^2 - v_1^2) \quad (51)$$

where E is the electrical energy obtained in joules, c_f is the capacitance of the condenser in farads, v_2 the voltage on the condenser just before the spark occurs, and v_1 the voltage at the instance the spark ceases.

In the Zeldovich method of spark ignition, the spark is replaced by a point heat source, which releases a quantity of heat. The time-dependent distribution of this heat is obtained from the energy equation

$$(\partial T/\partial t) = \alpha \nabla^2 T \quad (52)$$

Transforming this equation into spherical coordinates, its boundary conditions become

$$r = \infty, \quad T = T_0, \quad \text{and} \quad (\partial T/\partial r) = 0$$

The distribution of the input energy at any time must obey the equality

$$Q'_v = 4\pi c_p \rho \int_0^\infty (T - T_0)r^2 dr \quad (53)$$

The solution of Eq. (52) then becomes

$$(T - T_0) = \{Q'_v/[c_p \rho (4\pi\alpha t)^{3/2}]\} \exp(-r^2/4\alpha t) \quad (54)$$

The maximum temperature (T_M) must occur at $r \rightarrow 0$, so that

$$(T_M - T_0) = Q'_v/[c_p \rho (4\pi\alpha t)^{3/2}] \quad (55)$$

Considering that the gaseous system to be ignited exists everywhere from $r = 0$ to $r = \infty$, the condition for ignition is specified when the cooling time (τ_c) associated with T_M is greater than the reaction duration time τ_r in the combustion zone of a laminar flame.

This characteristic cooling time is for the period in which the temperature at $r = 0$ changes by the value θ . This small temperature difference θ is taken as (RT_M^2/E) ; i.e.,

$$\theta = RT_M^2/E \quad (56)$$

This expression results from the same type of analysis that led to Eq. (18). A plot of T_M versus t [Eq. (55)] is shown in Fig. 4. From this figure the characteristic cooling time can be taken to a close approximation as

$$\tau_c = \theta/|dT_M/dt|_{T_M=T_r} \quad (57)$$

The slope is taken at a time at which the temperature at $r = 0$ is close to the adiabatic flame temperature of the mixture to be ignited. By differentiating

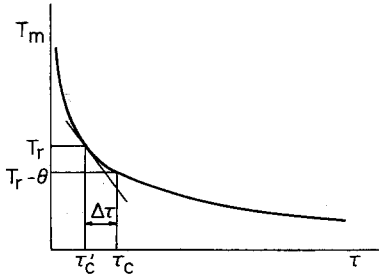


Fig. 4. Variation of the maximum temperature with time for energy input into a spherical volume of fuel-air mixture.

Eq. (55), the denominator of Eq. (57) can be evaluated to give

$$\tau_c = [\theta/6\pi\alpha(T_f - T_0)]\{Q'_v/[c_p\rho(T_f - T_0)]\}^{2/3} \quad (58)$$

where Q'_v is now given a specific definition as the amount of external input energy required to heat a spherical volume of radius r_f uniformly from T_0 to T_f ; i.e.,

$$Q'_v = \left(\frac{4}{3}\right)\pi r_f^3 c_p \rho (T_f - T_0) \quad (59)$$

Thus, Eq. (58) becomes

$$\tau_c = 0.14[\theta/(T_f - T_0)](r_f^2/\alpha) \quad (60)$$

Considering that the temperature difference θ must be equivalent to $T_f - T_i$ in the Zeldovich-Frank-Kamenetskii-Semenov thermal flame theory, than the reaction time corresponding to the reaction zone δ in the flame can also be approximated by

$$\tau_r \cong [2\theta/(T_f - T_0)](\alpha/S_L^2) \quad (61)$$

where (α/S_L^2) is the characteristic time associated with the flame and

$$a = (\alpha/S_L) \quad (62)$$

specifies the thermal width of the flame.

Combining Eqs. (60), (61), and (62) for the condition $\tau_c \geq \tau_r$ yields the condition for ignition as

$$r_f \geq 3.7a \quad (63)$$

Physically, Eq. (63) specifies that for a spark to lead to ignition of an exoergic system the corresponding equivalent heat input radius must be several times the characteristic width of the laminar flame zone. Under this condition, the nearby layers of the combustible material will further ignite before the volume heated by the spark cools.

The above developments are for an idealized spark ignition system. In actual systems much of the electrical energy is expended in radiative losses,

shock wave formation, and convective and conductive heat losses to the electrodes and flanges. Zeldovich [13] has reported for mixtures that the efficiency

$$\eta_s = (Q'_v/E) \quad (64)$$

can vary from 2-16%. Furthermore, the development was idealized by assuming consistency of the thermophysical properties and the specific heat. Nevertheless, experimental results taking all these factors into account [13,14] reveal relationships very close to

$$r_f \geq 3a \quad (65)$$

The further importance of Eqs. (63) and (65) is in the determination of the important parameters that govern the minimum ignition energy. By substituting Eqs. (62) and (63) into Eq. (59), one obtains the proportionality

$$Q'_{v,\min} \sim (\alpha/S_L)^3 c_p \rho (T_f - T_0) \quad (66)$$

Considering $\alpha = (\lambda/\rho c_p)$ and applying the perfect gas law, the dependence of $Q'_{v,\min}$ on P and T is found to be

$$Q'_{v,\min} \sim [\lambda^3 T_0^2 (T_f - T_0)] / S_L^3 P^2 c_p^2 \quad (67)$$

The minimum ignition energy is also a function of the electrode spacing. It becomes asymptotic to a very small spacing below which no ignition is possible. This spacing is the quenching distance discussed in Chapter 4. The minimum ignition energy decreases as the electrode spacing is increased, reaches its lowest value at some spacing and begins to rise again. At small spacings the electrode removes large amounts of heat from the incipient flame and, thus, a large minimum ignition energy is required. As the spacing increases, the surface area to volume ratio decreases, and, consequently, the ignition energy required increases. Most experimental investigations [12,15] report the minimum ignition energy for the electrode spacing that gives the lowest value.

An interesting experimental observation is that there appears to be an almost direct relation between the minimum ignition energy and the quenching distance [15,16]. Calcote *et al.* [15] have reported significant data in this regard and their results are shown in Fig. 5. These data are for stoichiometric mixtures with air at 1 atm pressure.

The general variation of minimum ignition energy with pressure and temperature would be as that given in Eq. (67) in which one must recall that S_L is also a function of the pressure and T_f of the mixture. Figure 6 from Blanc *et al.* [14] shows the variation of Q'_v as a function of equivalence ratio. The variation is very similar to the variation of quenching distance with the equivalence ratio ϕ [11] and to a degree appears like the inverse of S_L versus

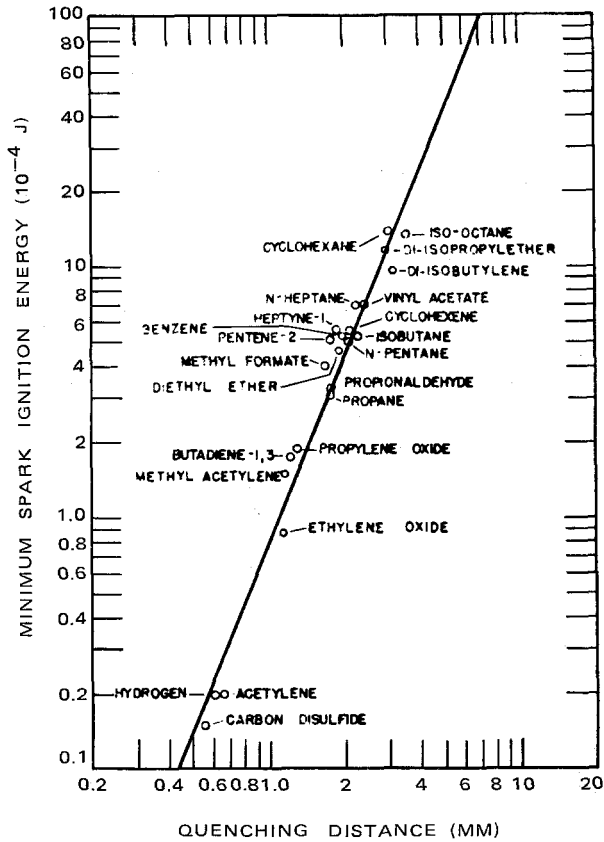


Fig. 5. Correlation of minimum spark ignition energy with quenching diameter (after Calcote *et al.* [15]).

ϕ . However, the increase of Q'_v from its lowest value for a given ϕ is much steeper than the decay of S_L from its maximum value. The rapid increase in Q'_v must be due to the fact that S_L is a cubed term in the denominator of Eq. (67). Furthermore, the lowest Q'_v is always found on the fuel-rich side of stoichiometric except for methane [13,15]. This trend is apparently due to the difference in the mass diffusivities of the fuel and oxygen.

Many [12,15] have tried to determine the effect of molecular structure on Q'_v . Generally, the dominant effect of molecular structure would be through its effect on T_f (in S_L) and α .

Appendix G lists minimum ignition energies of many fuels for the stoichiometric mixture and a pressure of 1 atm. The Blanc data in this

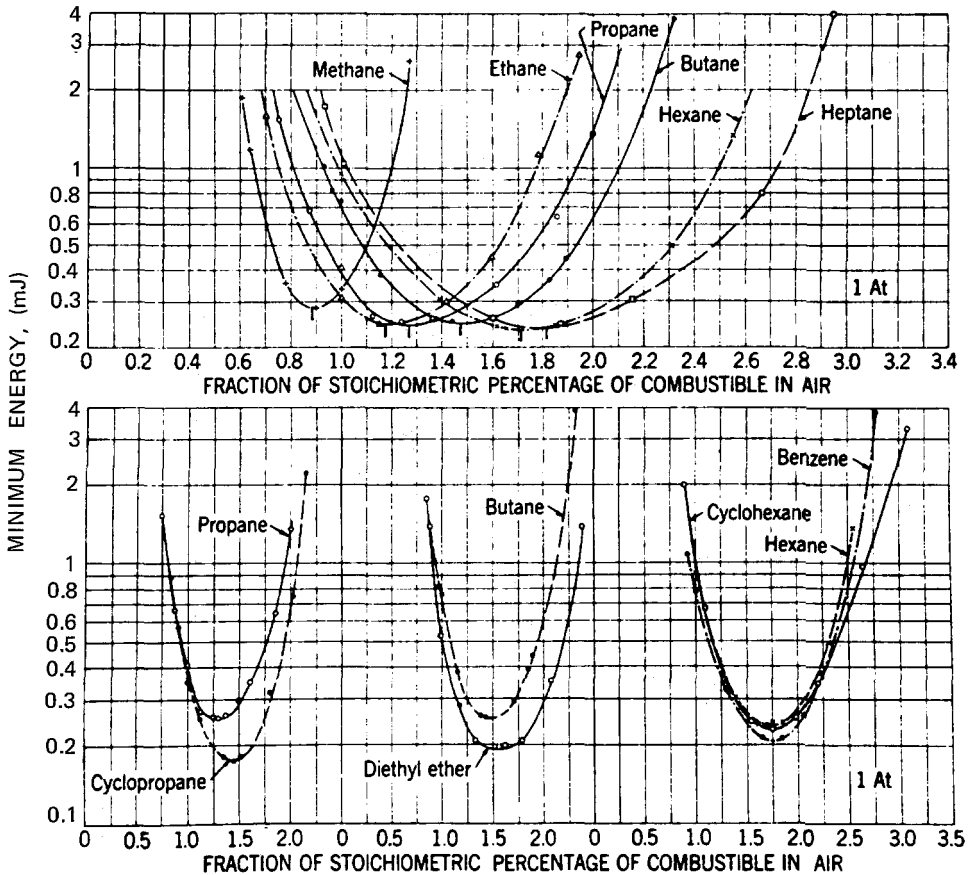


Fig. 6. Minimum ignition energies of fuel-air mixtures as a function of stoichiometry (after Blanc *et al.* [14]).

appendix are taken from Fig. 6. It is remarkable that the minimum of the energy curves for the various compounds occur at nearly identical values.

In many practical applications sparks are used to ignite flowing combustible mixtures. Increasing the flow velocity past the electrodes increases the energy required for ignition. The flow blows the spark downstream, lengthens the spark path, and causes the energy input to be distributed over a much larger volume [12]. Thus, the minimum energy in a flow system is greater than in a stagnant one.

From a safety point of view, one is also interested in grain elevator and coal dust explosions. Analysis of such explosions are not covered in this text and the reader is referred to the literature [17]. However, many of the thermal

concepts discussed for homogeneous gas-phase ignition will be fruitful in understanding the phenomena that control dust ignition and explosions.

2. Ignition by Adiabatic Compression and Shock Waves

Ignition by sparks occurs in a very local region and spreads by flame characteristics throughout the combustible system. If an exoergic system at standard conditions is adiabatically compressed to a higher pressure and, thus, to a higher temperature, the gas phase system will explode. There is little likelihood that there will be flame propagation in this situation. Similarly, a shock wave can propagate through the same type mixture and rapidly compress and heat the mixture to an explosive condition. A detonation will develop under such conditions only if the test section is sufficiently long.

Ignition by compression is similar to the conditions that generate "knock" in a spark ignited automotive engine. Thus, it would appear that compression ignition and "knock" are chain initiated explosions. Many have established the onset of ignition with a rapid temperature rise over and above that expected due to compression. Others have used the onset of some visible radiation or in the case of shock tubes, a certain limit concentration of hydroxyl radical formation identified by spectroscopic absorption techniques. The observations and measurement techniques are interrelated. Ignition occurs in such systems in the 1000 K temperature range. However, it must be realized that in hydrocarbon-air systems, the rise in temperature due to exothermic energy release of the reacting mixture occurs most sharply when the carbon monoxide, which eventually forms, is converted to carbon dioxide. This step is the most exothermic of all the conversion steps of the fuel-air mixture to products [18]. Indeed the early steps of the process are overall isoergic due to the simultaneous oxidative pyrolysis of the fuel, which is endothermic, and the conversion of some of the hydrogen formed to water, which is an exothermic process [18]. Analyses by Dryer and Brezinsky [19] in consideration of the knock problem have shown that in hydrocarbon oxidation processes, the chain carrying radicals, particularly hydroxyl, reach large concentrations well before significant quantities of carbon monoxide are oxidized; that is, before there is a rapid energy release or a noticeable temperature rise. Thus, the chain induction time occurs at a time prior to that for significant energy release. In the automotive cylinder it is the temperature rise which rapidly increases the cylinder pressure and gives the "knock" effect.

Shock waves are an ideal way of obtaining induction periods for high-temperature-high-pressure conditions. Since a shock system is nonisentropic, a system at some initial temperature and pressure condition brought to a

TABLE I
Compression versus shock-induced temperature^a

Shock and adiabatic compressure ratio	Shock wave velocity (m/sec)	T (°C) behind shock	T (°C) after compression
2	452	63	57
5	698	209	153
10	978	432	242
50	2149	1988	521
100	3021	3588	677
1000	9205	18816	1438
2000	12893	25704	1799

^a Initial temperature is 0°C.

final pressure by the shock wave will have a higher temperature than if the same mixture at the same initial conditions were brought by adiabatic compression to the same pressure. Table 1 compares the final temperature for the same compression ratio of a shock and an adiabatic compression.

PROBLEMS

1. The reported decomposition of ammonium nitrate stated that the reaction was unimolecular and that the rate constant had an A factor of $10^{13.8}$ and an activation energy of 40.5 kcal/mole. Using this information, determine the critical storage radius at 16°C. Report the calculation so that a plot of r_{crit} versus t can be obtained. Take a temperature range from 8 to 32°C.
2. Concisely explain the difference between chain and thermal explosions.
3. Are liquid droplet ignition times appreciably affected by droplet size? Explain.

REFERENCES

1. Mullins, B. P., "Spontaneous Ignition of Liquid Fuels," Chapter 11, Agardograph No. 4, Butterworth, London, 1955.
2. Zabetakis, M. G., *U. S. Bur. Mines Bull.* **627**, 1965.
3. Semenov, N. N., "Chemical Kinetics and Chain Reactions," Oxford Univ. Press, London, 1935.
4. Hinshelwood, C. N., "The Kinetics of Chemical Change," Oxford Univ. Press, London, 1940.
5. Zeldovich, Ya., B., Barenblatt, G. I., Librovich, V. B., and Makhviladze, G. M., "The Mathematical Theory of Combustion and Explosions," Chapter 1, Consultants Bureau, New York, 1985.

6. Frank-Kamenetskii, D. A., "Diffusion and Heat Exchange in Chemical Kinetics," Princeton Univ. Press, Princeton, New Jersey.
7. Hainer, R. M., *Int. Symp. Combust., 5th*, p. 224, Van Nostrand-Reinhold, Princeton, New Jersey, 1955.
8. Mullins, B. P., *Fuel* **32**, 343 (1953).
9. Mullins, B. P., *Fuel* **32**, 363 (1953).
10. Todes, O. M., *Acta Physicochem URSS* **5**, 785 (1936).
11. Jost, W., "Explosions and Combustion Processes in Gases," Chapter I, McGraw-Hill, New York, 1946.
12. Belles, F. E., and Swett, C. C., Ignition and flammability of hydrocarbon fuels in "Basic Considerations in the Combustion of Hydrocarbon Fuels with Air," Chapter III, *NACA Rep. No. 1300*, 1959.
13. Zeldovich, Ya. B., *Zh. Eksp. Teor. Fiz.* **11**, 159 (1941). See Shchetinkov, Ye. S., "The Physics of the Combustion of Gases," Chapter 5, Edited Translation FTD-HT-23-496-68, Translation Revision, Foreign Technology Division, Wright-Patterson AFB, Ohio, 1969.
14. Blanc, M. V., Guest, P. G., von Elbe, G., and Lewis, B., *Int. Symp. Combust. 3rd*, p. 363, Williams and Wilkens, Baltimore, 1949.
15. Calcote, H. F., Gregory, C. A., Jr., Barnett, C. M., and Gilmer, R. B., *Ind. Eng. Chem.* **44**, 2656 (1952).
16. Kanury, A. M., "Introduction to Combustion Phenomena," Chapter 4, Gordon and Breach Science, New York, 1975.
17. Hertzberg, M., Cashdollar, K. L., Contic, R. S., and Welsch, L. M., *Bur. Mines Rep.*, 1984.
18. Dryer, F. L., and Glassman, I., *Prog. Astronaut. Aeronaut.* **26**, 255 (1978).
19. Dryer, F. L., and Brezinsky, K., *Mech. and Aero. Eng. Rep. No. 1656*, Princeton Univ., Princeton, New Jersey (1984).

Environmental Combustion Considerations

A. INTRODUCTION

In the mid-1940s symptoms now recognized as being due to photochemical air pollution were first encountered in Los Angeles. Several researchers identified that the conditions in the Los Angeles area were a new kind of smog caused by the action of sunlight on the oxides of nitrogen and subsequent reactions with hydrocarbons. This smog was to be contrasted with the conditions in London in the early part of this century and the polluted air disaster that struck Donora, Pennsylvania. In these latter cases, particulates and sulfur oxides from the burning of coal created the unhealthy conditions. In Los Angeles the primary source of nitrogen oxides and hydrocarbons was readily identified to be the automobile. The burgeoning population and industrial growth in this and other areas led to controls not only on automobiles, but other mobile and stationary sources.

Atmosphere pollution symptoms became a concern all over the world and a much greater sensitivity to environmental conditions arose when supersonic transport developments began as part of the air transport era. Questions arose as to how the water vapor ejected by the power plants of these planes would affect the stratosphere in which they were to fly. This suggestion led to the consideration of the effects of injecting large amounts of any species on the ozone balance in the stratosphere. It is interesting that the major

species now thought to affect the ozone balances are again the oxides of nitrogen.

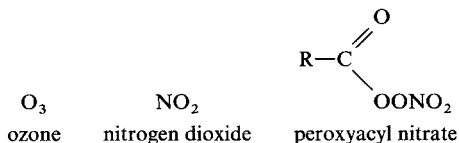
In the case of automobiles and stationary and jet power plants, it may be possible to reduce the extent of the emissions, particularly the nitrogen oxides and hydrocarbons, so that there is no severe damage to the troposphere and stratosphere. Indeed, the fluorocarbons used in aerosol spray cans may have a more devastating effect on the stratosphere than any of the other chemical species noticed.

Other factors have compounded the environmental emissions problem. A shortage of sulfur-free fossil fuels has arisen. Energy crises demand the development of fossil fuel resources from coal, shale, and secondary and tertiary oil schemes. Fuels from these sources are known to contain fuel-bound nitrogen and sulfur. Indeed the key in the more rapid development of coal usage may be the sulfur problem. Further, the fraction of aromatics in liquid fuels derived from these new sources or synthetically developed is found to be large and, in general, such fuels have serious sooting characteristics.

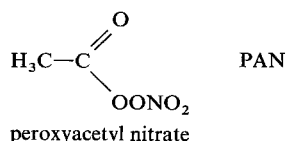
This chapter seeks not only to provide better understanding of the oxidation processes of sulfur and nitrogen and the processes leading to particulate (soot) formation, but also to make use of many of the chemical concepts developed so that it is possible to analyze how these pollutants affect the atmosphere.

B. THE NATURE OF PHOTOCHEMICAL SMOG

Photochemical air pollution consists of a complex mixture of gaseous pollutants and aerosols, some of which are photochemically produced. Among the gaseous compounds are the oxidizing species



The member of this last series most commonly found in the atmosphere is



The three compounds, ozone, NO_2 , and PAN are often grouped together and called photochemical oxidant.

In photochemical smog, one has mixtures of particulate matter and noxious gases, just as those which occur in the typical London-type smog. The London smog is a mixture of particulates and oxides of sulfur, chiefly sulfur dioxide. But the overall system is chemically reducing in nature.

This difference in redox chemistry between photochemical oxidant and SO_x -particulate smog is quite important from several aspects. In particular the problem of quantitatively detecting oxidant in the presence of sulfur dioxide is to be noted. The SO_x being a reducing agent tends to reduce the oxidizing effects of ozone and results in low quantities of the oxidant.

In dealing with the heterogeneous gas-liquid-solid mixture characterized as photochemical smog, it is important to realize from a chemical, as well as biological point of view, that synergistic effects may occur.

1. Primary and Secondary Pollutants

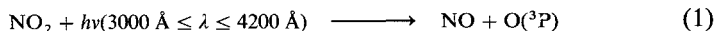
Primary pollutants are those emitted directly to the atmosphere and secondary pollutants are formed by chemical or photochemical reactions of primary pollutants after they have been admitted to the atmosphere and exposed to sunlight.

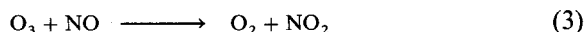
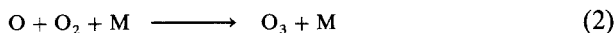
Unburned hydrocarbons, NO, particulates, and the oxides of sulfur are examples of primary pollutants. The particulates may be lead oxide from the oxidation of tetraethyl lead in automobiles, fly ash, and various types of carbon formations. Peroryocyl nitrate and ozone are examples of secondary pollutants.

Some pollutants fall in both categories. NO_2 , which is emitted directly from auto exhaust, is formed also in the atmosphere photochemically from NO. Aldehydes, which are released in auto exhausts, are also formed in the photochemical oxidation of hydrocarbons. CO, which arises primarily from autos and stationary sources, is again a product of atmospheric hydrocarbon oxidation.

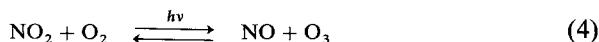
2. The Effect of NO_x

It has been well established that if a laboratory chamber containing NO, a trace of NO_2 , and air is irradiated with ultraviolet light, the following reactions occur:





The net effect of irradiation on this inorganic system is to establish the dynamic equilibrium



However, if a hydrocarbon, particularly an olefin or an alkylated benzene, is added to the chamber, the equilibrium represented by Eq. (4) is unbalanced and the following events take place:

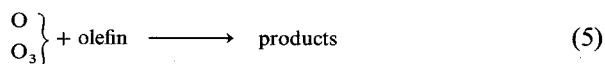
- a. The hydrocarbons are oxidized and disappear.
- b. Reaction products such as aldehydes, nitrates, PAN, etc., are formed.
- c. NO is converted to NO₂.
- d. When all the NO is consumed, ozone begins to appear. On the other hand, PAN and other aldehydes are formed from the beginning.

Basic rate information permits one to examine these phenomena in detail. Leighton [1] in his excellent book "Photochemistry of Air Pollution" gives numerous tables of rates and products of photochemical nitrogen oxide-hydrocarbon reactions in air. The data in these tables show low rates of photochemical consumption of the saturated hydrocarbons, as compared to the unsaturates, and the absence of aldehydes in the products of the saturated hydrocarbon reactions. These data conform to the relatively low rate of reaction of the saturated hydrocarbons with oxygen atoms and their inertness with respect to ozone.

Among the major products in the olefin reactions are aldehydes and ketones. Such results correspond to the splitting of the double bond and the addition of an oxygen atom to one end of the olefin.

Irradiation of mixtures of an olefin with nitric oxide and nitrogen dioxide in air shows that the nitrogen dioxide rises in concentration before it is eventually consumed by reaction. Since it is the photodissociation of the nitrogen dioxide that initiates the reaction, it would appear that a negative quantum yield results. More likely, the nitrogen dioxide is being formed by secondary reactions more rapidly than it is being photodissociated.

The important point to realize is that this negative quantum yield is only recognized when an olefin (hydrocarbon) is present. Thus adding the overall step

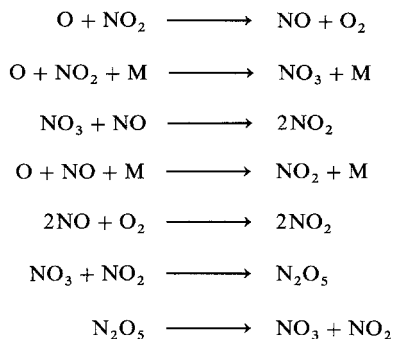


to reactions (1)–(3) would not be an adequate representation of the atmosphere photochemical reactions. However, if it is assumed that O_3 attains a steady-state concentration in the atmosphere, then a steady-state analysis (see Section 2.B) with respect to O_3 can be performed. Furthermore, if it is assumed that O_3 is largely destroyed by reaction (3), then a very useful approximate relationship is attained.

$$O_3 = -(j_1/k_3)(NO_2)/(NO)$$

where j is the rate constant for the photochemical reaction. Thus, the O_3 steady-state concentration in a polluted atmosphere is seen to increase with decreasing concentration of nitric oxide and vice versa. The ratio of j_1/k_3 approximately equals 1.2 ppm for the Los Angeles noonday condition [1].

Reactions such as



do not play a part. They are generally too slow to be important.

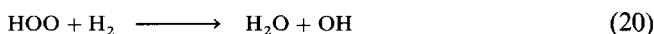
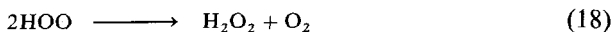
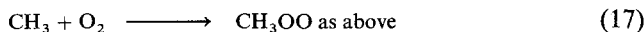
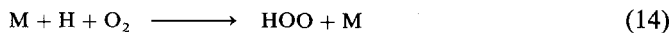
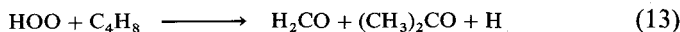
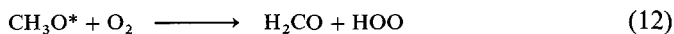
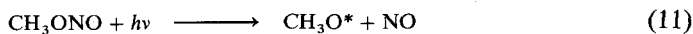
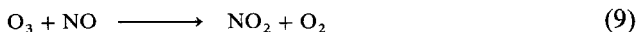
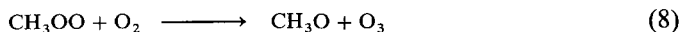
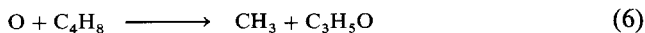
Furthermore, it has been noted that when the rate of the oxygen atom–olefin reaction and the rate of the ozone–olefin reaction are totaled, they do not give the complete hydrocarbon consumption. This anomaly is also an indication of an additional process.

An induction period with respect to olefin consumption is also noted in the photochemical laboratory experiments and indicates the buildup of an intermediate. When illumination is terminated in these experiments, the excess rate over the total of the O and O_3 reactions disappears. These and other results indicate that the intermediate formed is photolyzed and contributes to the concentration of the major species of concern.

Possible intermediates which fulfill the requirements of the laboratory experiments are alkyl and acyl nitrites and pernitrites. The second photolysis effect eliminates the possibility of aldehydes being the intermediate.

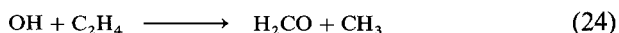
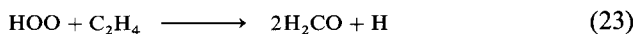
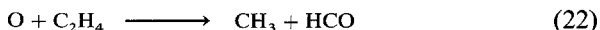
Various mechanisms have been proposed to explain the laboratory results discussed above. The following low- (atmospheric) temperature sequence

based on isobutene as the initial fuel has been proposed by Leighton [1] and appears to account for most of what has been observed:



There are two chain-propagating sequences [reactions (13) and (14) and reactions (15)–(17)] and one chain-breaking sequence [reactions (18)–(19)]. The intermediate is the nitrite as shown in reaction (10). Reaction (11) is the required additional photochemical step. For every NO_2 used to create the O atom of reaction (6), one is formed by reaction (9). However, reactions (10), (11), and (15) reveal that for every two molecules of NO consumed, one NO and one NO_2 form; thus, the negative quantum yield of NO_2 .

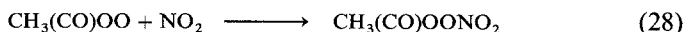
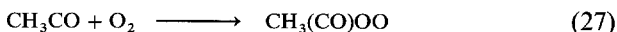
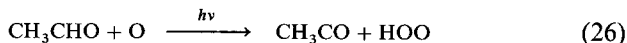
With other olefins, other appropriate reactions may be substituted. Ethylene would give



Propylene would add



Thus, PAN would form from



An acid could form from the overall reaction



Since pollutant concentrations are generally in the parts per million range, it is not difficult to postulate many types of reactions and possible products.

3. The Effect of SO_x

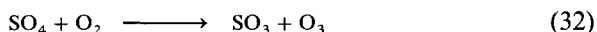
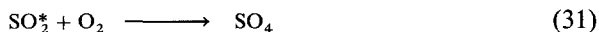
Historically the sulfur oxides were always known to have had a deleterious effect on the atmosphere. Sulfuric acid mist and other sulfate particulate matter have long been recognized as important sources of atmospheric contamination; however, the atmospheric chemistry is probably not as well understood as the gas-phase photooxidation reactions of the nitrogen oxides-hydrocarbon system. The pollutants form originally from the SO_2 emitted to the air. Just as mobile and stationary combustion sources emit some small quantities of NO_2 as well as NO , so do they emit some small quantities of SO_3 when they burn sulfur-containing fuels. Leighton [1] also discusses the oxidation of SO_2 in polluted atmospheres and an excellent review by Bulfalini [2] has appeared. This section draws heavily from these sources.

The chemical problem here involves the photochemical and catalytic oxidation of SO_2 and its mixtures with the hydrocarbons and NO , but primarily the concern is with the photochemical reactions, both gas phase and aerosol forming.

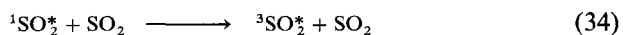
The photodissociation of SO_2 into SO and O atoms is quite different from the photodissociation of NO_2 . The bond to be broken in the sulfur compound requires 135 kcal/mole. Thus, wavelengths greater than 2180 Å do not have sufficient energy to initiate dissociation. This fact is significant in that only solar radiation greater than 2900 Å reaches the lower atmosphere. If there is to be a photochemical effect in the SO_2 - O_2 atmospheric system, then it must be that the radiation electronically excites the SO_2 molecule but does not dissociate it.

There are two absorption bands of SO_2 within the 3000–4000 Å range. The first is a weak absorption band and corresponds to the transition to the first excited state (a triplet). This band originates at 3880 Å and has a maximum around 3840 Å. The second is a strong absorption band and corresponds to the excitation to the second excited state (a singlet). This band originates at 3376 Å and has a maximum around 2940 Å.

Blacet [3] carrying out experiments in high O_2 concentrations reported that ozone and SO_3 appeared to be the only products of the photochemically induced reaction. The essential steps were postulated to be

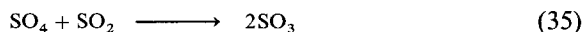


The radiation used was at 3130 Å, and it would appear that the excited SO_2^* in reaction (30) would be a singlet. The precise roles of the excited singlet and triplet states in the photochemistry of SO_2 are still unclear [2]. Nevertheless, for purposes here, this point need not be of too great concern since it is possible to write the reaction sequence

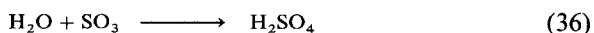


Thus, reaction (30) could specify either an excited singlet or triplet SO_2^* . The excited state may, of course, degrade by internal transfer to a vibrationally excited ground state which is later deactivated by collision or it may be degraded directly by collisions. Fluorescence of SO_2 has not been observed above 2100 Å. The collisional deactivation steps known to exist in laboratory experiments are not listed here in order to minimize the writing of reaction steps.

Since they involve one specie in large concentrations, reactions (30)–(32) are the primary ones for the photochemical oxidation of SO_2 to SO_3 . A secondary reaction route to SO_3 could be



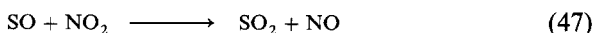
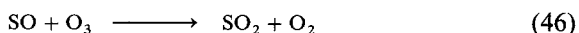
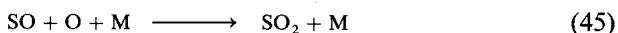
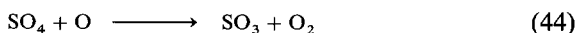
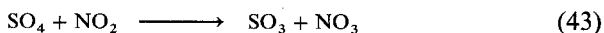
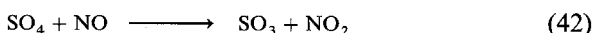
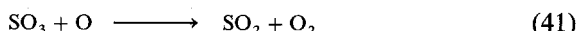
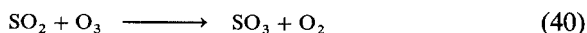
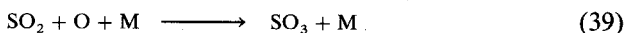
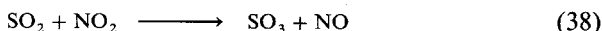
In the presence of water a sulfuric acid mist forms according to



The SO_4 molecule formed by Reaction (31) would probably have a peroxy structure and if SO_2^* were a triplet it might be a biradical.

There is conflicting evidence with respect to the results of the photolysis of mixtures of SO_2 , NO_x , and O_2 . However, many believe that the following

should be considered with the NO_x photolysis reactions:



The reducing effect of the SO_2 mentioned in the introduction of this section becomes evident from these reactions.

Some work [4] has been performed on the photochemical reaction between sulfur dioxide and hydrocarbons, both paraffins and olefins. In all cases, mists were found, and these mists settled out in the reaction vessels as oils which had the characteristics of sulfinic acids. Because of the small amounts of materials formed there are great problems in elucidating particular steps. When NO_x and O_2 are added to this system, the situation is most complex. Bufalini [2] sums up the status in this way, "... work indicates that the aerosol formed from mixtures of the lower hydrocarbons with NO_x and SO_2 is predominantly sulfuric acid, whereas the higher olefin hydrocarbons appear to produce carbonaceous aerosols also, possibly organic acids, sulfinic or sulfonic acids, nitrate-esters, etc."

C. NO_x FORMATION AND REDUCTION

The previous section established the great importance of NO_x in the photochemical smog reaction cycles. Strong evidence exists that the major producer of NO_x has been the automobile. But as automobile emissions' standards are enforced and electricity-generating plants turn from natural gas to coal and oil as fuels, there is no doubt that stationary sources will contribute a heavier fraction of the total NO_x emitted to the atmosphere. Consequently there has been great interest in predicting NO_x emissions and this interest has led to the formulation of various analytical models to predict specifically NO formation in combustion systems.

The greatest number of analytical and experimental studies have been focused on NO formation alone and not on NO₂. Indeed the major portion of NO_x has been found to be NO. Recent measurements in practical combustion systems, particularly those used to simulate aircraft gas turbine conditions, have shown larger amounts of NO₂ than one would expect. Controversy surrounds this question of NO₂ formation, and many believe that the NO₂ measured in some experiments actually formed in the probe systems used to remove a sample of gas.

Another controversy which has made the study of the NO_x chemistry confusing revolved around the question of "prompt" NO postulated to form in the flame zone by mechanisms other than those thought to hold exclusively for NO formation from atmospheric nitrogen. Although the amount of NO formed by the so-called "prompt" condition is usually very small, the fundamental studies into this problem have helped clarify much about NO_x formation both from atmospheric and fuel-bound nitrogen.

Nitrogen oxide formation from atmospheric nitrogen is meant to specify the NO formed in combustion systems in which the original fuel contains no nitrogen atoms which are chemically bound to other elements such as carbon and hydrogen. Generally it is thought to be the NO formed from the nitrogen in air. Since this NO forms only at high temperatures, it is sometimes called the thermal NO. The "prompt" NO work has shown, however, that in the flame zone the nitrogen in the air can form small quantities of CN compounds, which are subsequently oxidized to NO. The stable compound HCN has been found as a product in very fuel-rich flames.

NO_x formation from fuel-bound nitrogen is meant to specify the NO formed from fuel compounds that contain nitrogen atoms bound to other atoms. Generally these nitrogen atoms are bound to carbon or hydrogen atoms. Fuel-bound nitrogen compounds are ammonia, pyridine, and many other amines. The amines can be designated as the other organic compounds have in Chapter 3 as R—NH₂, where R is an organic radical or H atom. The NO formed from HCN and the fuel fragments from the nitrogen compounds are sometimes referred to as chemical NO in an analogous terminology to the thermal NO mentioned in the last paragraph.

1. The Structure of the Nitrogen Oxides

Many investigators have attempted to investigate analytically the formation of NO in fuel-air systems. Because of the availability of an enormous computer capacity, they have written all the possible reactions of the nitrogen oxides which they thought possible. Unfortunately some of these investigators have ignored the fact that some of the reactions written could have been eliminated because of steric considerations. Since the structure of the various

nitrogen oxides can be important, their formulas and structures are given in Table 1.

2. The Effect of Flame Structure

As the important effect of temperature on NO formation is discussed in the following sections, it is well to remember that flame structure can play a most significant role in determining the overall NO_x emitted. For premixed systems such as that obtained on Bunsen and flat flame burners and almost obtained in carbureted spark-ignition engines, the temperature, and thus the mixture ratio, is the prime parameter in determining the quantities of NO_x formed. Ideally, as in equilibrium systems, the NO formation should peak at

TABLE 1

Structure of gaseous nitrogen compounds	
Nitrogen N_2	$\text{N}\equiv\text{N}$
Nitrous oxide N_2O	$^-\text{N}=\text{N}^+=\text{O}$ $\text{N}\equiv\text{N}^+-\text{O}^-$
Nitric oxide NO	$\text{N}=\text{O}$
Nitrogen dioxide NO_2	
Nitrate ion NO_3^-	
Nitrogen tetroxide N_2O_4	
Nitrogen pentoxide	

the stoichiometric value and decline on both the fuel-rich and fuel-lean sides, just as the temperature does. Actually because of kinetic (nonequilibrium) effects, the peak is found somewhat on the lean (oxygen-rich) side of stoichiometric.

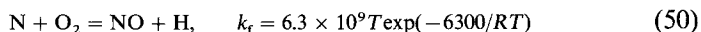
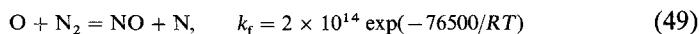
However in fuel injection systems, even though the overall mixture ratio may be lean and the final temperature could correspond to this overall mixture ratio, the fuel droplets or fuel jets burn as diffusion flames. The temperature of these diffusion flames are at the stoichiometric values during part of the burning time, even though the excess species will eventually dilute the products of the flame to reach the true equilibrium final temperature. Thus, in diffusion flames, more NO_x forms than would be expected from a calculation of an equilibrium temperature based on the overall mixture ratio. The reduction reactions of NO are so slow that in most practical systems the amount of NO formed in diffusion flames is unaffected by the subsequent drop in temperature caused by dilution of the excess species.

3. Atmospheric Nitrogen Kinetics

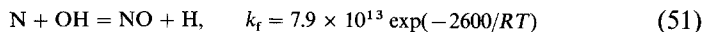
For premixed systems a conservative estimate can be made of the NO formation from consideration of the equilibrium given by reaction (48)



However, the kinetic route of NO formation is not the attack of an oxygen molecule on a nitrogen molecule. Mechanistically, oxygen atoms form from the H₂-O₂ radical pool, or possibly from the dissociation of O₂, and these oxygen atoms attack nitrogen molecules to start the simple chain shown by reactions (49) and (50).

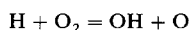


This chain was first postulated by Zeldovich [6] and is referred to as the Zeldovich or thermal mechanism. It is thought to be the main source of NO in combustion systems. However, emission standards on NO_x have been so stringent that in analyses some have included the fast reaction



even though the reacting species are both radicals and, therefore, are present in only relatively small amounts.

If one evokes the steady-state approximation for the N atom concentration and makes the partial equilibrium assumption for the reaction



then one obtains for the rate of formation of NO [5]

$$\frac{d(\text{NO})}{dt} = 2k_{49f}(\text{O})(\text{N}_2) \left\{ \frac{1 - [(\text{NO})^2/K'(\text{O}_2)(\text{N}_2)]}{1 + [k_{49b}(\text{NO})/k_{50f}(\text{O}_2)]} + k_{51f}[\text{OH}] \right\},$$

$$K' = (K_{51}/K_{52}) = K_{c, f, \text{NO}} \quad (52)$$

where K is the concentration equilibrium constant for the specified reaction system and K' the equilibrium constant of formation of NO.

In order to calculate the thermal NO formation rate, it is required to know the concentrations of O_2 , N_2 , O , and OH . But, the characteristic times for the forward reaction (49) always exceeds the characteristic time for the flame process so that it is often feasible to decouple the thermal NO process from the combustion process. Using such an assumption, the NO formation is calculated from Eq. (52) using local equilibrium values of temperature and concentrations of O_2 , N_2 , O , and H .

From examination of Eq. (52) it is seen that the maximum rate is given by

$$d(\text{NO})/dt = 2k_{49f}(\text{O})(\text{N}_2) \quad (53)$$

which corresponds to the condition that $(\text{NO}) \ll (\text{NO})_{\text{eq}}$. Due to the assumed equilibrium condition, the (O) can be related to the (O_2) via

$$\frac{1}{2}\text{O}_2 = \text{O}$$

$$K_{c, f, o, T_{\text{eq}}} = (\text{O})_{\text{eq}}/(\text{O}_2)_{\text{eq}}^{1/2}$$

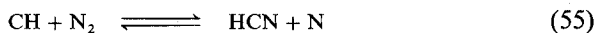
and Eq. (53) becomes

$$d(\text{NO})/dt = 2k_1 K_{c, f, o, T_{\text{eq}}} (\text{O}_2)_{\text{eq}}^{1/2} (\text{N}_2)_{\text{eq}} \quad (54)$$

The strong dependence of thermal NO formation on the combustion gas temperature and the lesser dependence on the oxygen concentration is evident from Eq. (54). Thus, the best practical means of controlling NO is to reduce either the combustion gas temperature or the oxygen concentration.

In essence the forward rate of reaction (49) controls the system due to its high activation energy. Thus, many investigators believed that in premixed flame systems, the NO would form only in the post-flame or burned gas zone. Thus, it was thought that it would be possible to determine the rate of formation and the rate constant of NO by measurements of the NO concentration profiles past the flame in the post-flame zone. Such measurements can be obtained readily on flat flame burners. In order to make these determinations, it is necessary to know the O atom concentrations. The nitrogen concentration was always in large excess. The oxygen atom concentration was taken as the equilibrium concentration at the flame temperature. The thought is that all other reactions are very fast compared to the Zeldovich mechanism.

Experimental measurements on flat flame burners showed that when the NO concentration profiles were extrapolated to the flame-front position, the NO concentration did not go to zero, but some finite value. Such results were most prevalent with fuel-rich flames. Fenimore [7] argued that reactions other than the Zeldovich mechanism were playing a role in the flame and that some NO was being formed in the flame region. He called this NO, "prompt" NO. He noted that "prompt" NO was not found in nonhydrocarbon CO-air and H₂-air flames, which were analyzed experimentally in the same manner as the hydrocarbon flames. The reaction scheme he suggested to explain the NO found in the flame zone involved a hydrocarbon species and atmospheric nitrogen. The nitrogen compound formed via the following mechanism



The N atoms could form NO, in part at least, by reactions (50) and (51), and the CN could yield NO by oxygen or oxygen atom attack. It is well known that CH exists in flames and indeed, as stated in Chapter 4, is the molecule that gives the deep violet color to a Bunsen flame.

In order to verify whether reactions other than the Zeldovich mechanism were effective in NO formation, various investigators undertook the study of NO formation kinetics by use of shock tubes. Some of the best work in this area was that of Bowman and Seery [8] who studied the CH₄-O₂-N₂ system. Complex kinetic calculations of the CH₄-O₂-N₂ reacting system at a fixed high temperature and pressure similar to those obtained in a shock tube [9] for $T = 2477$ K and $P = 10$ atm are shown in Fig. 1. These results are worth considering in their own right for they show explicitly much that has been inferred. Examination of Fig. 1 shows that at about 5×10^{-5} sec, all the energy release reactions have equilibrated before any significant amounts of

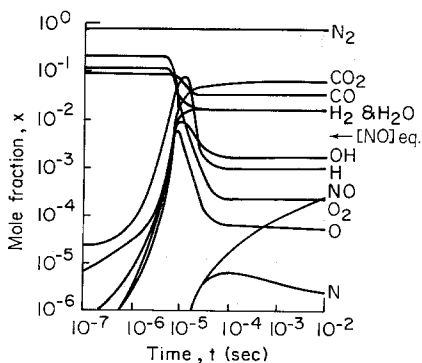


Fig. 1. Concentration-time profiles in the kinetic calculation of the methane-air reaction at inlet temperature of 1000 K, $P_2 = 10$ atm, $\phi = 1.0$, and $T_c = 2477$ K (after Martenay [9]).

NO have formed and, indeed, even at 10^{-2} sec the NO has not reached its equilibrium concentration for $T = 2477$ K. These results show that for such homogeneous, or near-homogeneous, reacting systems it would be possible to quench the NO reactions, obtain the chemical heat release and prevent NO formation. In certain combustion schemes, this procedure has been put in practice.

Figure 1 also shows a large oxygen radical overshoot within the reaction zone. It was thought that, if within the reaction zone, the O atom concentration could be orders of magnitude greater than its equilibrium value, then this condition could lead to the "prompt" NO found in flames. The mechanism analyzed to obtain the results depicted in Fig. 1 was essentially that given in Section 3.D.3a with the Zeldovich reactions. Thus it was thought possible that the Zeldovich mechanism could account for the "prompt" NO.

The experiments of Bowman and Seery appeared to confirm this conclusion. Some of Bowman's results are shown in Fig. 2. In this figure the experimental points correlated very well with the analytical calculations based on the Zeldovich mechanisms alone. Bowman and Seery used the same computational program as Martenay. Figure 2 also depicts another frequent result which is that fuel-rich systems approach NO equilibrium much faster than fuel-lean systems.

Although Bowman and Seery's results would seem to refute the suggestion by Fenimore that "prompt" NO forms by reactions other than the Zeldovich mechanism, one must remember that flames and shock tube initiated reacting systems are distinctively different processes. In a flame there is a temperature profile which begins at the ambient temperature and proceeds to the flame temperature. Thus although flame temperatures may be simulated in shock tubes, the reactions in flames are initiated at much lower temperatures than those in shock tubes. As stressed many times before, the temperature history frequently determines the kinetic route and the products. Thus the shock tube results do not prove that the Zeldovich mechanism alone determines NO

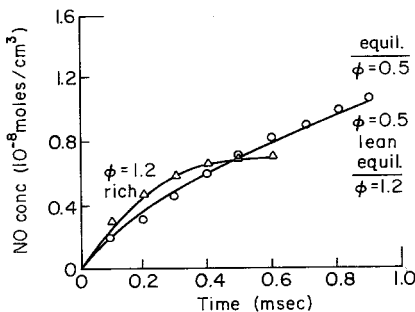


Fig. 2. Comparison of measured and calculated NO concentration profiles for $\text{CH}_4\text{-O}_2\text{-N}_2$ mixture behind reflected shocks. Initial post shock conditions $T = 2960$ K, $P = 3.2$ atm (after Bowman [10]).

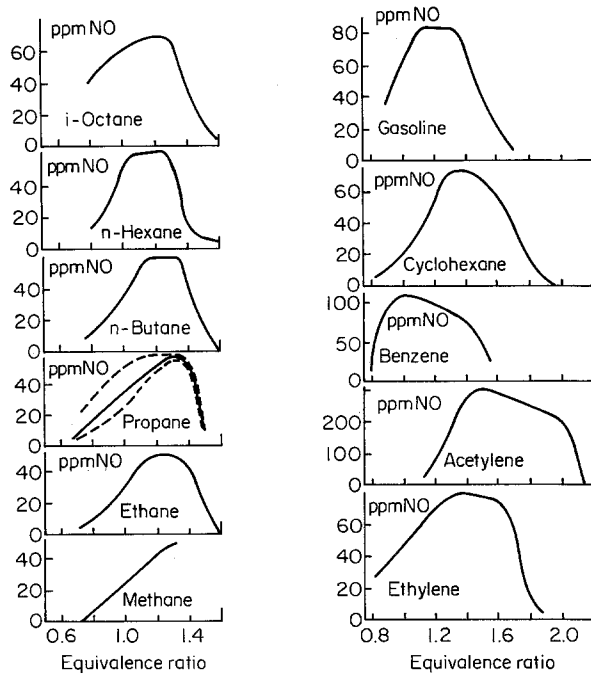


Fig. 3. “Prompt” NO as a function of mixture strength and fuel. The dotted lines show the uncertainty of the extrapolation at the determination of “prompt” NO in propane flames; similar curves were obtained for the other hydrocarbons (after Bachmeier *et al.* [11]).

formation. The “prompt” NO could arise from other reactions in flames as suggested by Fenimore.

Bachmeier *et al.* [11] appear to substantiate Fenimore’s postulates and to give greater insight to the flame NO problem. They measured the “prompt” NO formed as a function of equivalence ratio for many hydrocarbon compounds. These results are shown in Fig. 3. What is significant about these results is that the maximum “prompt” NO is reached on the fuel-rich side of stoichiometric, remains at a high level through a fuel-rich region, and then drops off sharply about an equivalence ratio of 1.4.

Bachmeier *et al.* also measured the HCN concentrations through propane-air flames. These results, which are shown in Fig. 4, show that HCN concentrations rise sharply somewhere in the flame, reach a maximum and then decrease sharply. However, for an equivalence ratio of 1.5, a fuel-rich condition for which little “prompt” NO is found, the HCN continues to rise and is not depleted. The explanation offered for this trend is that HCN forms in all the rich hydrocarbon flames; however, below an equivalence ratio of 1.4

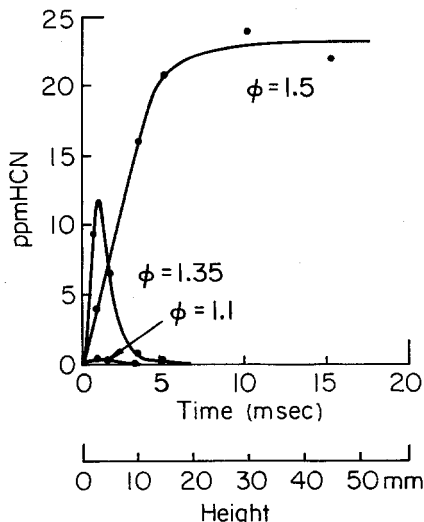
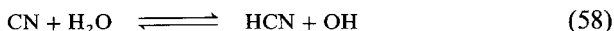
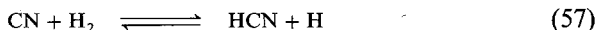


Fig. 4. HCN profiles of fuel-rich propane-air flames (after Bachmeier *et al.* [11]).

there are still sufficient O radicals present to react with HCN to deplete it and to form the NO. Since the sampling and analysis techniques used by Bachmeier *et al.* [11] would not permit the identity of CN, the cyanogen radical, the HCN concentrations probably represent the sum of CN and HCN as they exist in the flame. The CN and HCN in the flame are related through the rapid equilibrium reactions [12]



The HCN concentration is most likely reduced mainly by the oxidation of the CN radicals [12,13].

From other more recent studies of NO formation in the combustion of lean and slightly rich methane-oxygen-nitrogen mixtures and lean and very rich hydrocarbon-oxygen-nitrogen mixtures, it must be concluded that some of the prompt NO is due to the overshoot of O and OH radicals above their equilibrium values, as Bowman and Seery initially thought. However, even though there can be O radical overshoot on the fuel-rich side of stoichiometric, this overshoot cannot explain the "prompt" NO formation in fuel-rich systems. It would appear that both the Zeldovich and Fenimore mechanisms could hold. Some very interesting experiments by Eberius and Just [14] would seem to clarify what is happening in the flame zone with regard to NO formation.

Eberius and Just's experiments were performed on a flat flame burner with propane as the fuel. Measurements were made of the "prompt" NO at

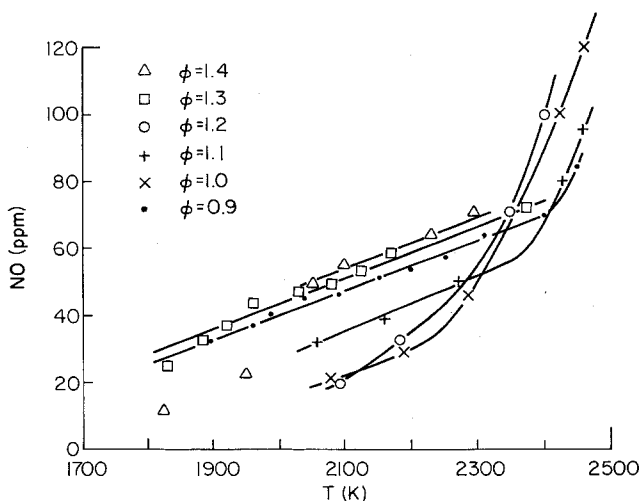


Fig. 5. "Prompt" NO as a function of the temperature at various mixture strengths ϕ in adiabatic propane-synthetic air flames (after Eberius and Just [14]).

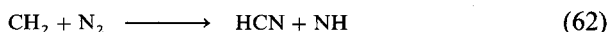
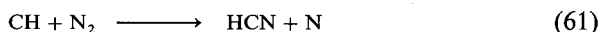
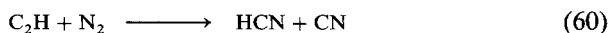
various fuel-oxygen equivalence ratios whose flame temperatures were controlled by dilution with nitrogen. Thus a range of temperatures could be obtained for a given propane-oxygen equivalence ratio. The results obtained are shown in Fig. 5. The highest temperature point for each equivalence ratio corresponds to zero dilution.

The shape of the plots in Fig. 5 are revealing. At both the low- and higher-temperature ends, all plots seem nearly parallel. The slopes at the low-temperature end are very much less than the slopes at the high-temperature end and would indicate that there are indeed two mechanisms for the formation of "prompt" NO. The two mechanisms are not related solely to the fuel-rich and fuel-lean stoichiometry as many investigators thought, but to the flame temperature. These results indicate that there is a high temperature, high-activation route and a lower-temperature, low-activation route.

The systematic appearance of these data led Eberius and Just to estimate the activation energy for the two regions. Without correcting for diffusion, they obtained an activation energy of the order of 65 kcal/mole for the high temperature zone. This value is remarkably close to the 75 kcal/mole activation energy for the initiating step in the Zeldovich mechanism. Furthermore, diffusion corrections would raise the experimental value somewhat. The low-temperature region has an activation energy of the order of 12-16 kcal/mole. As will be shown later, radical attack on the cyano species is faster than oxygen radical attack on hydrogen. The activation energy of $O + H_2$ is about 8 kcal/mole, thus the HCN reaction should be less. Again, diffusion

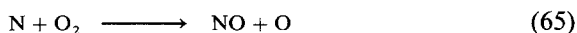
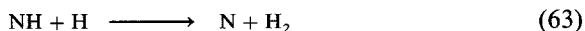
corrections for the oxygen atom concentration could lower the apparent activities of 12–16 kcal/mole to below 8 kcal/mole. It would appear that even this crude estimate of the activation energy from Eberius and Just's low-temperature region and the formation of HCN found by the same group [11], in their other flame studies with propane (Fig. 4) would indicate that the Fenimore mechanism would hold in the lower-temperature region.

The kinetic details for "prompt" NO formation must begin with the possible reactions between N_2 and hydrocarbon fragments as Fenimore originally suggested. Hayhurst and Vance [15] suggest that there are two other likely candidate reactions to be added to those stated by Fenimore. The four candidate reactions would then be

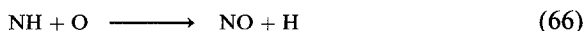


As discussed in the introduction to Chapter 4, the existence of C_2 and CH in hydrocarbon-air flames is well established.

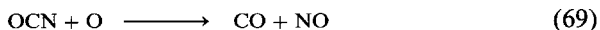
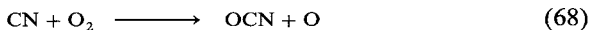
In each case for the reactions above the products are HCN and CN, which in hydrocarbon flames are indistinguishable because of their equilibrium reactions mentioned earlier. The NH species readily yield NO by



Also possible are



Equations (63)–(67) are all exothermic and spin allowed. In addition to be considered are



which are also exothermic. Reactions of HCN with the various oxidizing species, except OH, are very endothermic and not likely to proceed.

The subsequent CN reactions to yield NO is relatively straightforward. What remains to be decided is which of the four reactions forming CN (or HCN) are the more probable. Hayhurst and Vance [15] established that the amount of "prompt" NO in moderately fuel-rich systems is proportional to

the number of carbon atoms present per unit volume and is independent of the original parent hydrocarbon identity. This result indicates that reactions (59)–(60) are not the primary system because it is unlikely that C₂ or C₂H could derive from CH₄ with an efficiency one-half that of C₂H₂ or one-third that from C₃H₄ or C₃H₈. Consequently, one concludes that reactions (61) and (62) and the equilibrium represented by the reaction (57) system are the most likely initiating steps for “prompt” NO.

4. Fuel-Bound Nitrogen Kinetics

In several recent experiments, it has been shown that NO emissions from combustion devices that operated with nitrogen-containing compounds in the fuel were high or, in other words, fuel-bound nitrogen is an important source of NO. The initial experiments of Martin and Berkau [16] commanded the greatest interest. These investigators added 0.5% pyridine to base oil and found almost an order of magnitude increase over the NO formed from base oil alone. Their results are shown in Fig. 6.

During the combustion of fuels containing bound nitrogen compounds, the nitrogen compounds will most likely undergo some thermal decomposition

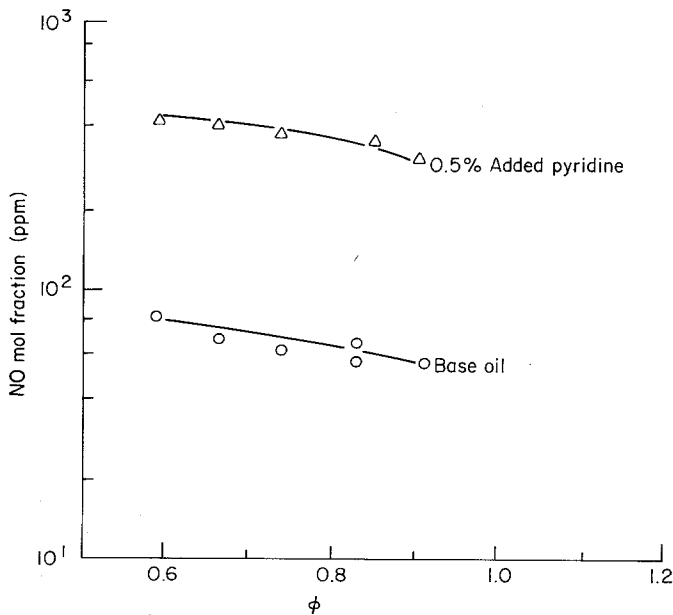


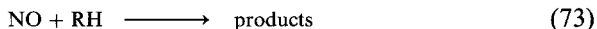
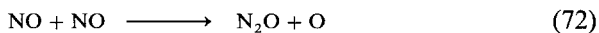
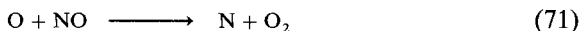
Fig. 6. Nitric oxide emissions from an oil-fired laboratory furnace (after Martin and Berkau [16]).

prior to entering the combustion zone. Hence, the precursors to NO formation will, in general, be low molecular weight nitrogen-containing compounds or radicals (NH_3 , NH_2 , NH , HCN , CN , etc.). All indications are that the oxidation of fuel-bound nitrogen compounds to NO is rapid and occurs on a time scale comparable to the energy release reactions in the combustion systems. This conclusion arises from the fact that the NH and CN oxidation reactions discussed in the previous section are faster [17, 18] than the important chain branching reaction



Thus, it is not possible to quench the reaction system to prevent NO formation from fuel-bound nitrogen as it is for atmospheric nitrogen. In fact, in the vicinity of the combustion zone, observed NO concentrations significantly exceed calculated equilibrium values. In the postcombustion zone, the NO concentration decreases relatively slowly for fuel-lean mixtures and more rapidly for fuel-rich mixtures. Recall Bowman and Seery's results (Fig. 2) showing that fuel-rich systems approach equilibrium faster. When fuel nitrogen compounds are present, high NO yields are obtained for lean and stoichiometric mixtures and relatively lower yields are found for fuel-rich mixtures. The NO yields appear to be only slightly dependent on temperature and, thus, indicate a low-activation energy step. This result should be compared to the strong temperature dependence of NO formation from atmospheric nitrogen.

The high yields on the lean side of stoichiometric pose a dilemma. It is desirable to operate lean to reduce hydrocarbon and carbon monoxide emissions, but with fuel containing bound nitrogen high NO yields would be obtained. The reason for the superequilibrium yields is that the reactions leading to the reduction of NO to its equilibrium concentration, namely,

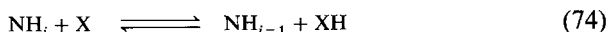


are very slow. NO can be reduced under certain conditions by CH and NH radicals, which can be present in relatively large concentrations in fuel-rich systems. These reduction steps and their application will be discussed later.

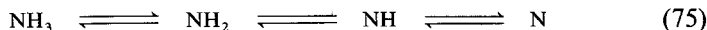
The extent of conversion of fuel nitrogen to NO is nearly independent of the parent fuel molecule, but is strongly dependent on the local combustion environment and on the initial fuel nitrogen in the reactant. Unlike sulfur in the fuel molecule, nitrogen is much more tightly bound in the molecule and for the most part in an aromatic ring [19]. Regardless, in all fuel-nitrogen compounds there are solely carbon-nitrogen or nitrogen-hydrogen bonding. Thus, it is not surprising that in the oxidation of fuel nitrogen compounds the

major intermediates are HCN and CN and amine radicals stemming from an ammonia structure, i.e., NH₂, NH, and N.

In a large radical pool, there exists an equilibrium



which essentially establishes an equilibrium between all NH compounds, i.e.,



Consequently, reactions (61) and (62) can be written as a generalized reaction

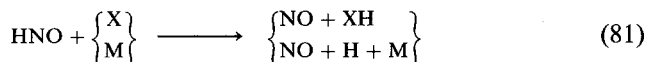
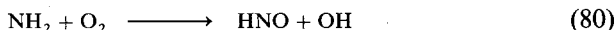
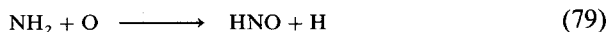


Thus, there is great similarity between the "prompt" NO reactions discussed and the fuel-nitrogen reactions.

Since certainly in the combustion of fuel-nitrogen compounds the equilibrium



will exist, then the conversion of all relevant intermediates to NO has essentially been discussed and only the NH₂ reactions remain to be considered. These reactions follow the sequence



In fuel-rich systems, there is evidence [20, 21, 5] that the fuel-nitrogen intermediate reacts not only with oxidizing species in the manner represented, but also in a competitive manner with NO (or another nitrogen intermediate) to form N₂. This second step, of course, is the reason that there are lower NO yields in fuel-rich systems. The fraction of fuel-nitrogen converted to NO in fuel-rich systems can be as much as an order of magnitude less than that of lean or near-stoichiometric systems. One should realize, however, that even in fuel-rich systems the exhaust NO concentration is substantially greater than its equilibrium value at the combustion temperature.

Haynes *et al.* [12] have shown that when small amounts of pyridine are added to a premixed rich ($\phi = 1.68$; $T = 2030$ K) ethylene-air flame, the amount of NO increases with little decay of NO in the post-flame gases. However, when larger amounts of the pyridine are added, significant decay of NO is observed after the reaction zone. Increasingly higher pyridine additions result in high NO concentrations leaving the reaction zone, but this

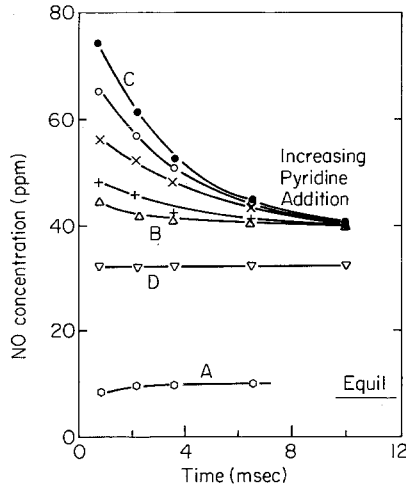
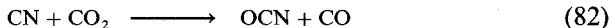


Fig. 7. Effect of NO concentrations leaving the reaction zone of an ethylene-air flame ($\phi = 1.68$, $T = 2030$ K) with various pyridine additions. Curve A, no pyridine addition; curves B and C, 0.1–0.5% N by weight of fuel; and curve D, NO addition to fuel-air mixture (after Haynes *et al.* [12]).

concentration drops appreciably in the post-flame gases to a value characteristic of the flame, but well above the calculated equilibrium value. Actual experimental results are shown in Fig. 7.

In fuel-rich systems, the conversion reactions of the fuel-nitrogen intermediates must be considered in doubt, mainly because the normal oxidizing species O_2 , O , and OH are present only in very small concentrations, particularly near the end of the reaction zone. Haynes *et al.* [12] offer the interesting suggestion that the CN can be oxidized by CO_2 since the reaction



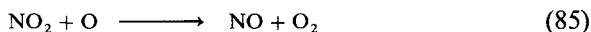
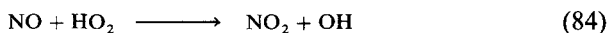
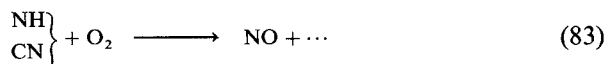
is 20 kcal/mole exothermic and is estimated to be reasonably fast.

5. The Formation of NO_2

Significant concentrations of NO_2 have been reported in the exhaust of gas turbines and in the products of range top burners [19]. These results are surprising in that chemical equilibrium considerations reveal that for typical flame temperatures the NO_2/NO ratio should be negligibly small. Furthermore, kinetic models when modified to include NO_2 formation and reduction show that in practical devices the conversion of NO to NO_2 can be neglected.

However, in the case of sampling from gas turbines and depending on the NO level, NO₂ can vary from 15–50% of the total NO_x [19,22,23]. In the case of range type burners, the NO_x has been reported as high as 15 to 20 times the NO levels in parts of the flame surrounding the burner top [24,25].

Merryman and Levy [26] examined both NO and NO₂ formation in a flat flame burner operated near stoichiometric. Their measurements showed that NO₂ is produced in the visible regime of all air flames (with and without fuel-bound nitrogen) and that NO is only observed in the visible when there is fuel-bound nitrogen. Furthermore, these investigators found that NO₂ is consumed rapidly in the near-post-flame zone and the NO concentration rises correspondingly. They postulated the following scheme to represent their findings:



The significant step is represented by reaction (84). One should recall that in the early parts of a flame there can be appreciable amounts of HO₂. The appearance of the NO₂ is supported further by the fact that reaction (84) is two-orders of magnitude faster than reaction (85). The importance of the hydroperoxy radical attack on NO appeared to be verified further by adding NO to the cold-fuel mixtures in some experiments. In these tests the NO disappeared before the visible region was reached in oxygen-rich and stoichiometric flames, i.e., flames that would produce HO₂. The NO₂ persists because, as mentioned previously, its reduction to N₂ and O₂ is very slow. The role of HO₂ would not normally be observed in shock tube experiments because of the high temperatures at which they usually operate.

The Merryman–Levy sequence could explain the experimental results that show high NO₂/NO ratios. In the experiments in which these high ratios were found, it is quite possible that reaction (85) is quenched and the NO₂ is not reduced.

Cernansky and Sawyer [27] in experiments with turbulent diffusion flames also concluded that the high NO₂ levels found were due to the reactions of NO with HO₂ and O atoms.

The experimental efforts reporting high NO₂ levels have come under question because of the possibility that much of the NO₂ actually forms in sampling tubes [28,29]. Optical techniques are now being applied, but unfortunately the low concentrations of NO₂ existing makes resolution of the controversy very difficult.

6. The Reduction of NO_x

Because of the stringent emission standards imposed on both mobile and stationary power sources, methods for reducing NO_x must be found, and these methods should not impair the efficiency of the device. The simplest method of reducing NO_x , particularly from gas turbines, is by water addition to the combustor can. Water vapor can reduce the O radical concentration by the following scavenging reaction



Fortunately OH radicals do not attack N_2 efficiently. However, it is more likely that the effect of water on NO_x emissions is through the attendant reduction in combustion temperature. NO_x formation from atmospheric nitrogen arises primarily from the very temperature sensitive Zeldovich mechanism.

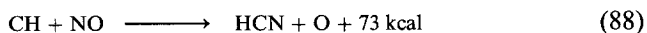
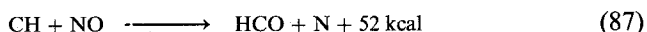
In heterogeneous systems such as those which arise due to direct liquid fuel injection and which are known to burn as diffusion flames, the problem of NO_x reduction is more difficult. One possible means is to decrease the average droplet size formed from injection. Kesten [30] and Bracco [31], have shown that the amount of NO formed from droplet diffusion flames can be related to the droplet size, in that a large droplet will give more NO than that obtained from a group of smaller droplets equal to the mass of the larger droplet. Any means of decreasing the heterogeneity of a flame system will decrease the NO_x . Another possible practical scheme is to emulsify the fuel with a higher vapor pressure, nonsoluble component such as water. It has been shown [32] that droplets from such emulsified fuels explode after combustion has been initiated. These microexplosions occur when the superheated water within the fuel droplet vaporizes and appreciably decreases the heterogeneity of the system. A further benefit is obtained by not only having water present for dilution, but also having the water present in the intimate vicinity of the diffusion flame.

If it is impossible to reduce the amount of NO_x in the combustion section of a device, then the NO_x must be removed somewhere in the exhaust. Myerson [33] has shown that it is possible to reduce NO_x by adding small concentrations of fuel and oxygen. The addition of about 0.1% hydrocarbon (isobutane) and 0.4% O_2 to a NO_x -containing system at 1260 K reduced the NO_x concentration by a factor of two in about 125 msec. Myerson found that the ratio of O_2/HC was most important. At large concentrations of O_2 and the hydrocarbon, an HCN formation problem could arise. This procedure will only hold for slightly fuel-lean or fuel-rich systems. The oxygen is the creator and the destroyer of other species involved in the NO reduction. This fact in turn means that the initial addition of O_2 to the hydrocarbon-NO

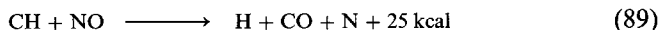
mixture promotes the production of the strongly reducing species CH and CH₂ and similar substituted free radicals that otherwise must be produced by slower pyrolysis reactions.

Continued addition of O₂ beyond one-half the stoichiometric value with the hydrocarbons present encourages a net destruction of the hydrocarbon radicals. For the temperature range 1200–1300 K, production of the hydrocarbon radicals via hydrogen abstraction by O₂ is rapid, even assuming an activation energy of 45 kcal/mole, and more than adequate to provide sufficient radicals for NO reduction in the stay time range of 125 msec.

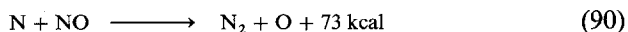
The reactions postulated by Myerson to be involved are



The exothermicity of reaction (87) is sufficient to fragment the formyl radical and could be written as

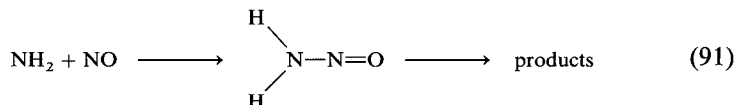


The N radicals in the absence of O₂ in these fuel-rich systems can react rapidly with NO via



Another technique for NO_x reduction is by addition of ammonia to the exhaust of a combustion system. This technique is known as EXXON's Thermal DeNO_x process [34]. Nitrogen reduction by ammonia also is effective only in a narrow temperature range about $T \sim 1250$ K. Below 1000 K the reaction takes place too slowly to be of value and above 1500 K the more NO is found to be formed in the system. Miller *et al.* [35] found that if H₂ is added to the system the center of the temperature window moves to a lower value without changing the width of the window. They also found that slightly lean combustion products appeared to be required to cause the reduction reaction to take place effectively. This group then proposed the following analysis of the NH₃–NO reduction system.

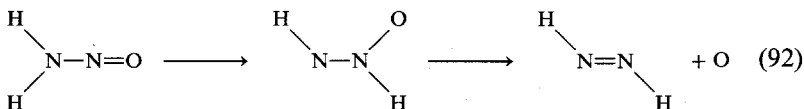
The ammonia added in the process is considered to form the NH₂ radical that reacts with the NO to form an intermediate, which decays into products



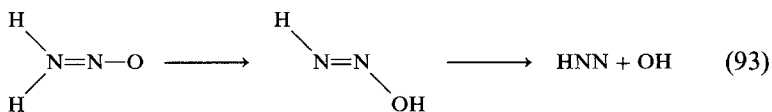
There are various possibilities as to the fate of the intermediate. It could form HNNO + H, but this route is not likely because at low temperatures no H is found, nor any N₂O that inevitably would have to form. In addition this decay step is endothermic.

Another consideration is the formation of N_2O and H_2 , which is exothermic, but would require a large energy barrier to form the H_2 . Also, of course, no N_2O is found. The formation of $H_2N=N$ and O is very endothermic and is not conceivable.

The possibility exists of a migration of a H atom. The following migration step



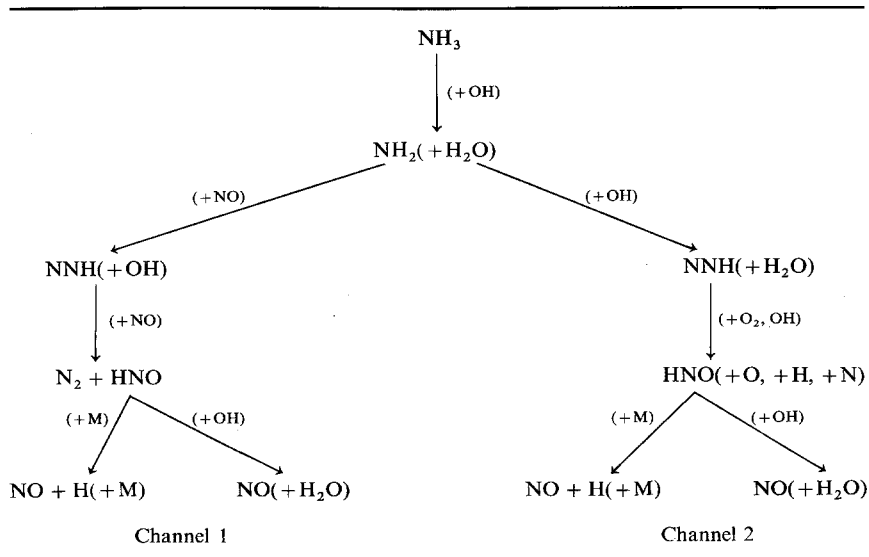
is also very endothermic and is thus ruled out. What appears most feasible is the migration of H to the O atom in the following step



The product HNN provides a feasible route for the overall NO reduction mechanism and for the determination of the temperature window. Miller *et al.* [35] proposed the following competitive channels in Table 2 as the explanation

TABLE 2

NO reduction scheme



At temperatures before 1000 K, hydrogen abstraction by OH is too slow so that little NH₂ forms. In the temperature range 1000–1500 K, the mix of branching and termination is proper for the conversion of NH₃ to NH₂ at a sufficiently rapid rate. In this range the initial steps of channel 1 are faster than those of channel 2. However, above 1500 K channel 2 becomes dominant since at higher temperatures there is more chain branching, which leads to higher concentration of OH and, thus, a route favoring channel 2. The reactions NH₂ + NO and NH₂ + OH are competitive around 1250 K; however, OH attack becomes dominant about 1500 K. Note that in channel 1, two NO are used to form one N₂ and NO and, thus, an overall reduction in NO is obtained.

D. SO_x EMISSIONS

Sulphur compounds pose a dual problem. Not only do their combustion products contribute to atmospheric pollution, as described in a previous section, but these products are also very corrosive in nature and cause severe physical problems in gas turbines and industrial power plants. Sulfur pollution and corrosion were problems long before the nitrogen oxides were known to affect the atmosphere. However, the general availability of low sulfur fuels diminished the concern with respect to the sulfur. Now that the availability of low sulfur crude oil is somewhat restricted, greater attention is being given to the use of coal and those crudes which have "appreciable" sulfur content. Costs for removing sulfur from residual oils by catalytic hydrodesulfurization techniques remain high, and the desulfurized residual oil have a tendency to become "waxy" at low temperatures. To remove sulfur from coal is an even more imposing problem. It is possible to remove pyrites from coal, but this approach is limited by the size of the pyrite particles. Unfortunately, pyrite sulfur makes up only half the sulfur content of coal, whereas the other half is organically bound. Coal gasification is the only means by which this sulfur mode could be removed. Of course, it is always possible to eliminate the deleterious effects of sulfur by removing the major product oxide SO₂ by absorption processes. These processes impose large initial capital investments and most industries believe these are too costly for implementation.

nitrogen oxides as well. Thus, a study of sulfur compound oxidation is not only important from the point of view of possibly offering alternate or new means of controlling the emission of the objectionable sulfur oxide, but also with regard to their effect on the formation and concentration of other pollutants.

There are some very basic differences between the sulfur problem and that posed by the formation of the nitrogen oxides. The two possible sources of nitrogen in any combustion process are either atmospheric or organically bound. Sulfur can be present in elemental form, organically bound, or as a species in various inorganic compounds. Once it enters the combustion process it is very reactive with oxidizing species, and similar to fuel nitrogen, its conversion to the sulfurous oxides is fast compared to the other energy releasing reactions.

Even though sulfur oxides posed a problem in combustion processes well before the concern for photochemical smog and the role of the nitrogen oxides in creating this smog, much less is understood about the mechanisms of sulfur oxidation. Indeed the amount of recent work on sulfur oxidation has been minimal. The status of the field has been reviewed by Levy *et al.* [36] and Cullis and Mulcahy [37] and much of the material from the following subsections has been drawn from Cullis and Mulcahy's article.

1. The Product Composition and Structure of Sulfur Compounds

In any combustion system in which elemental sulfur or a sulfur bearing compound is present, the predominant product is sulfur dioxide. The concentration of sulfur trioxide found in combustion systems is most interesting. Even under very lean conditions, the amount of sulfur trioxide formed is only a few percent of that of sulfur dioxide. However, generally the sulfur trioxide concentration is higher than its equilibrium value, as would be expected from the reactions



These higher than equilibrium concentrations appear to be due to the fact that the homogeneous reactions which would reduce the SO_3 to SO_2 and O_2 are known to be slow. This point will be discussed later in this section.

It is well known that SO_3 has a great affinity for water and that at low temperatures it appears as sulfuric acid. Above 500°C , sulfuric acid dissociates almost completely into sulfur trioxide and water.

Under fuel-rich conditions, in addition to sulfur dioxide, the stable products are found to be hydrogen sulfide, carbonyl sulfide, and elemental sulfur.

There are other oxides of sulfur which, due to their reactivity, appear only as intermediates in various oxidation reactions. These are sulfur monoxide SO , its dimer $(\text{SO})_2$, and disulfur monoxide S_2O . There has been a great deal of confusion with respect to these oxides and what is now known to be S_2O was thought to be SO or $(\text{SO})_2$. The most important of these oxides is sulfur

monoxide, which is the crucial intermediate in all high-temperature systems. SO is a highly reactive radical whose ground state is a triplet and electronically analogous to O₂. According to Cullis and Mulcahy [37], its lifetime is seldom longer than a few milliseconds.

Spectroscopic studies have revealed other species in flames such as: CS, a singlet molecule analogous to CO and much more reactive; S₂, a triplet analogous to O₂ and the main constituent of sulfur vapor above 600°C; and the radical HS.

Johnson *et al.* [38] calculated the equilibrium concentration of the various sulfur species for the equivalent of 1% SO₂ in propane-air flames. Their results, as a function of fuel-air ratio, are shown in Fig. 7. The dominance of SO₂ in the product composition for these equilibria calculations, even under deficient air conditions, should be noted. As reported earlier, practical systems reveal SO₃ concentrations (1–2%) that are higher than those depicted in Fig. 8.

Insight into much that will be discussed and that which has been discussed can be obtained by the study of the structure of the various sulfur compounds given in Table 3.

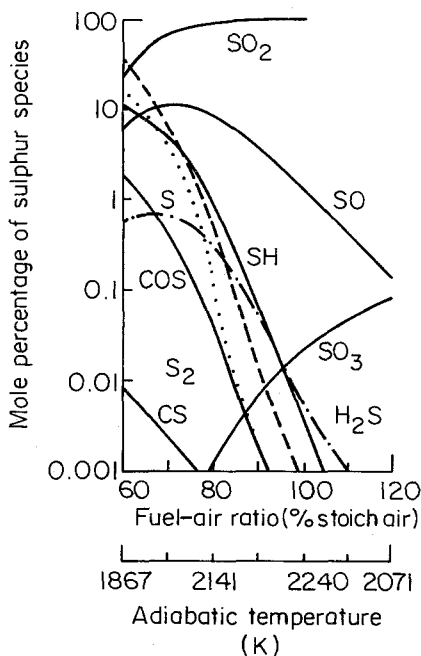
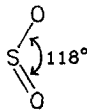
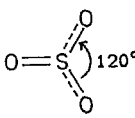


Fig. 8. Equilibrium distribution of sulfur-containing species in propane-air flames with unburned gases initially containing 1% SO₂.

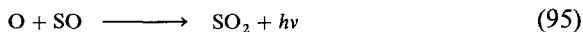
TABLE 3

Structure of gaseous sulfur compounds

Sulfur S_8	Rhombic	
Sulfur monoxide SO	$S=O$	
Sulfur dioxide SO_2 (OSO)		$+S \begin{matrix} O^- \\ \\ O \end{matrix}$
Sulfur superoxide $SO_2(SOO)$	$+S \equiv O - O^-$	
Sulfur trioxide SO_3		$O=S^{++} \begin{matrix} O^- \\ \\ O^- \end{matrix}$
Sulfur suboxide S_2O	$S=S=O$	
Carbonyl sulfide COS	$S=C=O$	$-S-C \equiv O^+ \quad +S \equiv C-O^-$
Carbon disulfide CS_2	$S=C=S \quad -S-C \equiv S^+$	
Organic thiols	$R'-SH$	
Organic sulfides	$R'-S-R'$	
Organic disulfides	$R'-S-S-R'$	

2. Oxidative Mechanisms of Sulfur Fuels

Sulfur fuels characteristically burn with flames that are pale blue, sometimes very intensely so. This color comes about from emissions as a result of the reaction



and since it is found in all sulfur-fuel flames, this blue color serves to identify SO as an important reaction intermediate in all cases.

Most studies of sulfur-fuel oxidation have been performed using H_2S as the fuel. Consequently, the following material will concentrate on under-

standing the H₂S oxidation mechanism. Much of what is learned from these mechanisms can be applied to understanding the combustion of COS, CS₂, elemental and organically bound sulfur.

a. H₂S

Figure 9 is a general representation of the explosion limits of H₂S/O₂ mixtures. This three limit curve is very similar to that shown for H₂/O₂ mixtures. However, there is an important difference in the character of the experimental data which determine the H₂S/O₂ limits. In the H₂S/O₂ peninsula and in the third limit region, explosion occurs after an induction period of several seconds.

The main reaction scheme for the low-temperature oxidation of H₂S, although explicitly not known, would appear to be



The addition of reaction (98) to this scheme is necessary because of the identification of S₂O in explosion limit studies. More importantly, Merryman

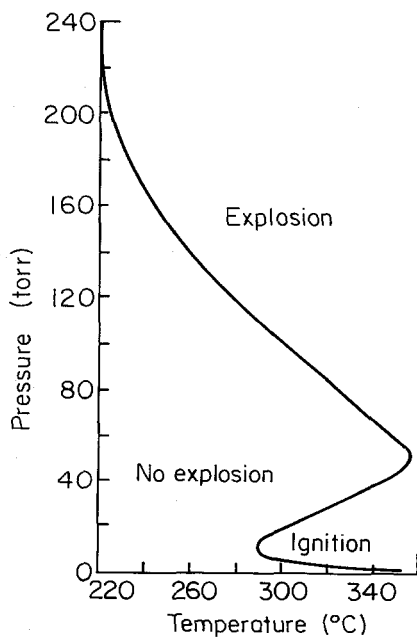
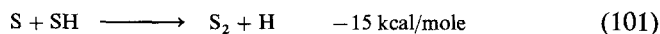


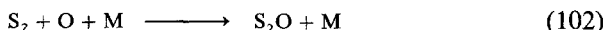
Fig. 9. Approximate explosion limits for stoichiometric mixtures of hydrogen sulfide and oxygen.

and Levy [39] in burner studies showed that S_2O occurs upstream from the peak of the SO concentration and that elemental sulfur was present still further upstream in the preignition zone.

The most probably system for the introduction of elemental sulfur is

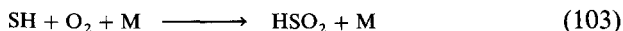


It does not seem feasible kinetically at the temperatures in the preignition zone and at the overall pressures that the flame studies were carried out that the reaction

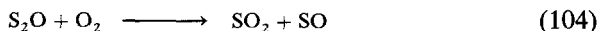


could account for the presence of S_2O . The disproportion of SO would have to give SO_2 as well as S_2O . Since SO_2 is not found in certain experiments where S_2O can be identified, then disproportion would not be feasible and reaction (98) appears to be the best candidate for the presence of S_2O .

Reaction (97) is the branching step in the mechanism. It has been suggested that

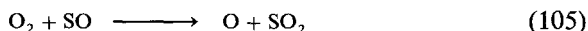


competes with reaction (97), and determines the second limit. Cullis and Mulcahy [37] suggest the reaction



as the degenerate branching step. The explicit mechanism for forming S_2O and its role in flame processes must be considered a great uncertainty.

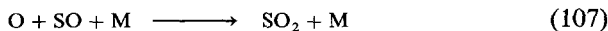
At higher temperatures the reaction



becomes competitive with reaction (98) and introduces O radicals into the system. The presence of O radicals gives another branching reaction, namely,



The branching is held in check by reaction (98), which removes SO, and the fast termolecular reaction

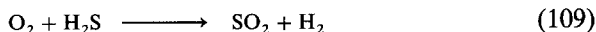


which removes both O radicals and SO.

In shock tube studies, SO_2 is formed before OH radicals appear. To explain this result it has been postulated that the reaction

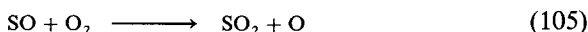
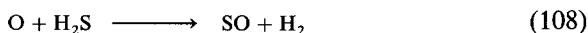


is possible. This reaction and reaction (98) give the overall step



Detailed sampling in flames by Sachjan *et al.* [40] indicates that the H₂S is oxidized in a three-step process. During the first stage, most of the H₂S is consumed, and the products are mainly sulfur monoxide and water. In the second stage, the concentration of SO decreases, the concentration of OH reaches its maximum value, the SO₂ reaches its final concentration, and the concentration of the water begins to build as the hydrogen passes through a maximum.

The interpretation given to these results is that during the first stage the H₂S and O₂ are consumed mainly by reactions (108) and (105)



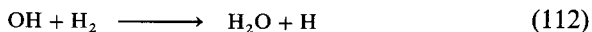
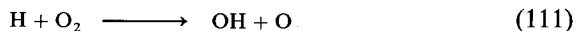
with some degree of chain branching by reaction (106).



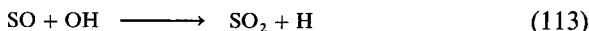
In the second stage, reaction (105) predominates over reaction (108) because of the depletion of the H₂S and the OH concentration rises via reaction (106) and begins the oxidation of the hydrogen



Of course the complete flame mechanism must include



Reactions (108) and (110) together with the fast reaction at the higher temperature

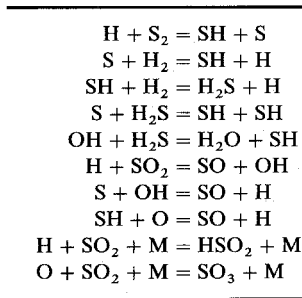


explain the known fact that H₂S inhibits the oxidation of hydrogen.

Using laser fluorescence measurements on fuel-rich H₂/O₂/N₂ flames seeded with H₂S, Muller *et al.* [41] determined the concentrations of SH, S₂, SO, SO₂, and OH in the post-flame gases. From their results and evaluation of rate constants they postulated that the flame chemistry of sulfur under rich

TABLE 4

Major flame chemistry reactions
of sulfur under rich conditions



conditions could be described by the eight fast bimolecular reactions and the two three-body recombination reactions given in Table 4.

Reactions 1 and 6 in Table 4 were identified to control the S_2 and SO_2 concentrations, respectively, and reaction 2 and 4 to control the S concentration with some contribution from reaction 1. Reaction 6 was the major one for the SO flux rate. The three reactions involving H_2S were said to play an important role. SH was found to be controlled by reactions (1)–(5). Because the first eight reactions were found to be fast, it was concluded that they rapidly establish and maintain equilibrium so that the species S, S_2 , H_2S , SH, SO, and SO_2 are efficiently interrelated and relative concentrations, such as those of SO and SO_2 , can be calculated from thermodynamic considerations at the local gas temperature from the system of reactions,



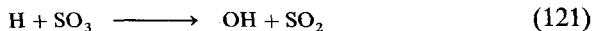
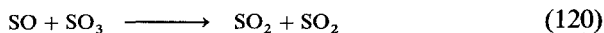
The three-body recombination reactions listed in Table 4 are significant in sulfur containing flames because one provides the homogeneous catalytic recombination of the important $\text{H}_2\text{-O}_2$ chain carriers H and OH via



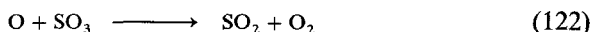
and the other



is the only major source of SO₃ in flames. Under such conditions the SO₃ concentration is controlled by other reactions with H and SO, i.e.,



and under lean conditions by

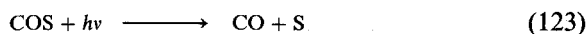


b. COS and CS₂

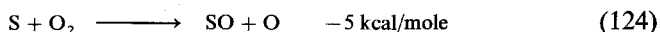
Even though there have been appreciably more studies of CS₂, COS is known to exist as an intermediate in CS₂ flames. Thus it appears logical to analyze the COS oxidation mechanisms first. Both substances show explosion limit curves which indicate that branched chain mechanisms exist. Most of the reaction studies used flash photolysis and very little information exists on what the chain initiating mechanism for thermal conditions would be.

COS flames exhibit two zones. In the first zone carbon monoxide and sulfur dioxide form, and in the second zone the carbon monoxide is converted into carbon dioxide. Since these flames are hydrogen free, it is not surprising to note that the CO conversion in the second zone is rapidly accelerated by adding a very small concentration of water to the system.

Photolysis initiates the reaction by creating sulfur atoms



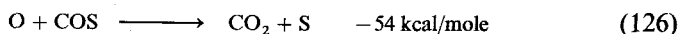
The S atom then creates the chain branching step



which is followed by



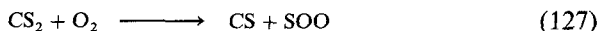
At high temperatures the slow reaction



must also be considered.

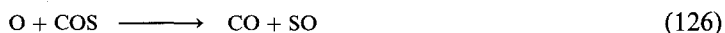
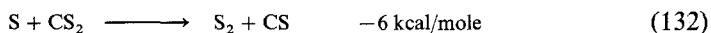
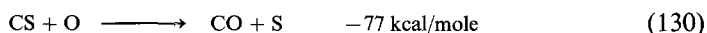
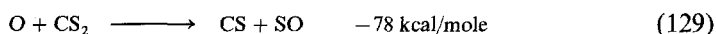
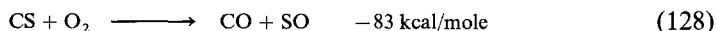
The initiation step under purely thermally induced conditions such as those imposed by shocks has not been postulated, but is simply thought to be a reaction which produces O atoms. The high-temperature mechanism would then be reactions (105), (124)–(126), with termination by the elimination of the O atoms.

For the explosive reaction of CS_2 , Myerson *et al.* [42], suggest

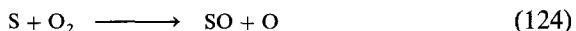


as the chain initiating step. Although the existence of the superoxide, SOO is not universally accepted, it is difficult to conceive a more logical thermal initiating step, particularly when the reaction can be induced in the 200–300°C range.

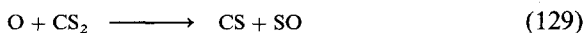
The introduction of the CS by reaction (127) starts the following chain scheme



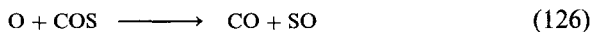
The high flammability of CS_2 in comparison to COS is thought to be brought about by the greater availability of S atoms. At low-temperatures, branching occurs in both systems via



Even greater branching occurs since in CS_2 one has



The comparable reaction for COS is reaction (110)

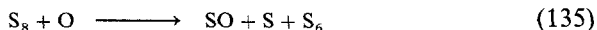


which is not chain branching.

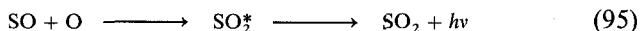
c. Elemental Sulfur

Elemental sulfur is found in all the flames of sulfur-bearing compounds discussed in the previous subsections. Generally this sulfur appears as atoms or the dimer S_2 . When pure sulfur is vaporized at low temperatures, the vapor molecules are polymeric in nature and have the formula S_8 . Vapor phase studies of pure sulfur oxidation around 100°C have shown that the oxidation reaction has the characteristics of a chain reaction. It is interesting to note that in the explosive studies the reaction must be stimulated by the

introduction of O atoms (spark, ozone) in order for the explosion to proceed. Levy *et al.* [36] report that Semenov suggests the following initiation and branching reactions:



with the products produced by

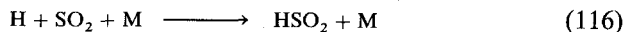


A unique feature of oxidation of pure sulfur is that the percent of SO₃ formed is a very much larger (about 20%) fraction of the SO_x than is generally found in the oxidation of sulfur compounds.

d. Organic Sulfur Compounds

It is more than likely that when sulfur is contained in a crude oil or in coal (other than the pyrites) it is organically bound in one of the three forms listed in Table 3—the thiols, sulfides, or disulfides. The combustion of these compounds is very much different than the other sulfur compounds studied in that a large portion of the fuel element is a pure hydrocarbon fragment. Thus in explosion or flame studies, the branched chain reactions which determine the overall consumption rate or flame speed would characteristically follow those chains described in hydrocarbon combustion and not the CS, SO, and S radical chains which dominate in H₂S, CO, COS, and S₈ combustion.

A major product in the combustion of all organic sulfur compounds is sulfur dioxide. Sulfur dioxide has a well-known inhibiting effect on hydrocarbon and hydrogen oxidation and, indeed, is responsible for a self-inhibition in the oxidation of organic sulfur compounds. This inhibition most likely arises from its role in the removal of H atoms by the termolecular reaction



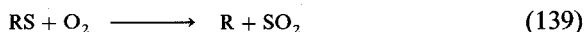
HSO₂ is a known radical which has been found in H₂-O₂-SO₂ systems and is sufficiently inert to be destroyed without reforming any active chain carrier.

In the lean oxidation of the thiols, even at temperatures around 300°C, all the sulfur is converted to SO₂. At lower temperatures and under rich conditions, disulfides form and other products such as aldehydes and

methanol are found. The presence of the disulfides suggests a chain-initiating step very much similar to low-temperature hydrocarbon oxidation

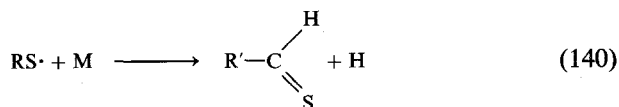


Cullis and Mulcahy report this step to be followed by

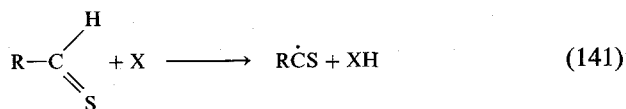


to form the hydrocarbon radical and sulfur dioxide. One must question whether the SO_2 in reaction (139) is sulfur dioxide or not. If the O_2 strips the sulfur from the RS radical, then it is more likely the SO_2 is the sulfur superoxide, which would decompose or react to form SO. The SO is then oxidized to sulfur dioxide as described previously. The organic radical is oxidized, as discussed in Chapter 3. The radicals formed in the subsequent oxidation, of course, attack the original fuel to give the RS radical, and the initiating step is no longer needed.

The SH bond strength is sufficiently weaker than the CH bonds so that the RS radical would be the dominant one formed. At high temperatures, it is likely that the RS decay could lead to the thioaldehyde



The disappearance of the thioaldehyde at these temperatures would be very much like that of the aldehydes; namely,



Then the CS radical is oxidized as in the previous discussion on CS_2 .

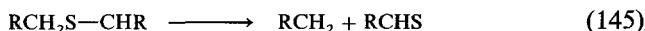
The disulfide forms in the thiol oxidation from the recombination of the two RS radicals



The principal products in the oxidation of the sulfides are sulfur dioxide and aldehydes. The low-temperature initiating step is similar to reaction (138), except the hydrogen abstraction is known to be from the carbon atom next to the sulfur atom, i.e.



The radical formed in reaction (144) then decomposes to form an alkyl radical and a thioaldehyde molecule, i.e.,



Both products in reaction (145) are then oxidized as discussed.

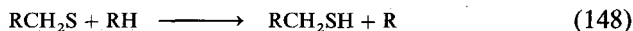
The oxidation of the disulfides follow a similar route to the sulfide with an initiating step



followed by radical decomposition



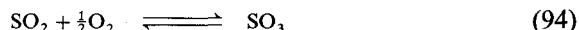
The thiol is then formed by hydrogen abstraction



and the oxidation proceeds as described previously.

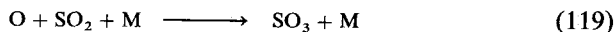
e. Sulfur Trioxide and Sulfates

Earlier it was pointed out that the concentration of sulfur trioxide found in the combustion gases of flames, though small, is greater than that which would have been expected from equilibrium calculations. Indeed this same phenomenon exists in large combustors, such as furnaces, in which there is a sulfur component in the fuel used. The equilibrium represented by Eq. (94)



is shifted strongly to the left at high temperatures and one would expect very little SO₃ in a real combustion environment. It is very apparent, then, that the combustion chemistry involved in oxidizing sulfur dioxide to the trioxide is such that equilibrium cannot be obtained.

Truly the most interesting finding is that the superequilibrium concentrations of SO₃ are very sensitive to the original oxygen concentration. Under fuel-rich conditions approaching even stoichiometric conditions, practically no SO₃ is found. In proceeding from stoichiometric to 1% excess air, a sharp increase in the conversion of SO₂ to SO₃ is found. Further addition of air only causes a slight increase, however, the effect of the excess nitrogen in reducing the temperature could be a moderating factor in the rate of increase. Figure 10, taken from the work of Barrett *et al.* [43] on hydrocarbon flames characterizes the results generally found not only in flame studies but also with furnaces. Such results strongly indicate that the SO₂ is converted into SO₃ in a termolecular reaction with oxygen atoms



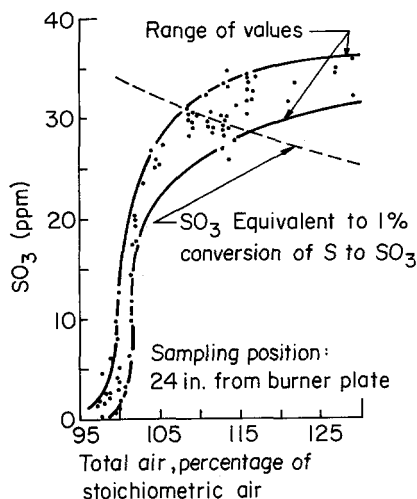


Fig. 10. Effect of excess air on the formation of SO₃ in a hydrocarbon-air flame (after Barrett *et al.* [43]).

It is important to note that the superequilibrium results are obtained with either sulfur fuels, small concentration of sulfur fuels added to hydrocarbons, SO₂ added to hydrocarbon, etc. Further confirmation supporting reaction (119) as the conversion route comes from the observation that in carbon monoxide flames the amount of SO₃ produced was substantially higher than in all other cases. It is well known that since O atom cannot attack CO directly, the SO₃ concentration is much higher in CO flames than any other flames. The fact that in all cases the SO₃ concentration also increases with pressure supports a termolecular route such as reaction (119).

It is well known that the thermal dissociation of SO₃ is slow and that the concentration of SO₃ is then frozen within its stay time in flames and furnaces. The thermal dissociation rates are known, but one can also calculate the superequilibrium concentration of oxygen atom in flames. If so, then the SO₃ concentration should correspond to the equilibrium concentration given by reaction (119), in which the oxygen atom superequilibrium concentration is used. However, the SO₃ concentrations are never this high, thus one must conclude that some SO₃ is being reduced by routes other than thermal decomposition. The two most likely routes are by oxygen and hydrogen atom attack on the sulfur trioxide via



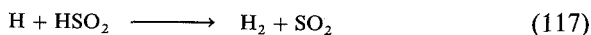
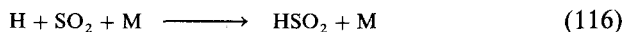
Evidence supports this contention, and it would appear that reaction (122) would be more important than reaction (121) in controlling the SO₃ concentration with reaction (119). Furthermore, it is important to note that

reactions (119) and (120) are effective means of reducing O radical concentration. Since reaction (116) has been shown to be an effective means of reducing H radical concentrations, one can draw the general conclusion that sulfur compounds reduce the extent of superequilibrium concentration of the characteristic chain carrying radicals which exist in hydrocarbon flames.

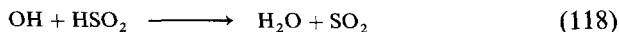
In dealing with furnaces using residual oils, one must recognize heterogeneous catalysis as a possible route for the conversion of SO₂ to SO₃. Sulfur dioxide and molecular oxygen will react catalytically on steel surfaces and vanadium pentoxide (deposited from vanadium compounds in the fuel) and at lower temperatures where the equilibrium represented by reaction (94) favors the formation of SO₃.

If indeed SO₂ and SO₃ are effective in reducing the superequilibrium concentration of radicals in flames, then it is apparent that sulfur compounds should play a role in NO formation from atmospheric nitrogen in flame systems. Since no matter what type of sulfur compounds is added to combustion systems SO₂ and SO₃ form, these species reduce the oxygen atom concentration and thus should reduce NO formation. Wendt and Ekman [45] have reported flame data which appear to substantiate this conclusion.

In examining reactions (121) and (122), one realizes that SO₂ plays a role in catalyzing the recombination of oxygen atoms. Indeed this homogeneous catalytic recombination of oxygen atoms causes the decrease in the super-equilibrium concentration of the oxygen atoms. SO₂ also plays a role in the recombination of hydrogen radicals through the route



and the recombination of hydrogen and hydroxyl radicals through the route of reaction (116) and



With the above considerations of SO₃ formation and the realization that SO₂ and SO are the major sulfur oxide species in flames, the use of the term SO_x is then meant to specify the sum of SO, SO₂, and SO₃. Also considering the fact that in any combustion system sulfur can appear in the parent hydrocarbon fuel in various forms makes it evident that the details of the reaction mechanism for SO_x formation are virtually impossible to specify. By virtue of the rapidity of the SO_x formation process, Bowman [44] has suggested that approximate models that by-pass the need for a detailed fuel-sulfur oxidation model may be postulated to estimate the gaseous SO_x product distribution in the exhaust products. It is suggested [45] that three principal assumptions would be involved in the proposed model: (1) the

fuel-sulfur compounds would be considered minor species so that major stable species concentrations are those due to combustion of the hydrocarbon fuel; (2) the bimolecular H_2-O_2 reactions and reaction (115) are partially equilibrated in the post-flame gases; and (3) the SO_3 concentration may be calculated from reactions (119), (121), and (122). The SO_x pool then will vary as the overall reaction approaches equilibrium by means of the H_2-O_2 radical recombination reactions and the reactions that determine the equilibrium between SO_2 and SO_3 and those that affect the catalytic recombination of H, O, and OH.

f. SO_x - NO_x Interactions

It is to be realized that reactions of fuel-sulfur and fuel-nitrogen are closely coupled to the fuel oxidation and that both sulfur-containing radicals and nitrogen-containing radicals compete for the available H, O, OH radicals with the hydrocarbons [19]. Because of the close coupling of the sulfur and nitrogen chemistry and the H, O, OH radical pool in flames, interactions between fuel-sulfur and fuel-nitrogen chemistry is to be expected.

The catalytic reduction of the radicals by sulfur compounds, particularly the O atom, will generally reduce the rates of reactions converting atmospheric nitrogen to NO by the thermal mechanism. However, experiments do not permit explicit conclusions [19]. Wendt and Eckmann [45] showed an inhibiting effect of high concentrations of SO_2 and H_2S on thermal NO in premixed methane-air flames. DeSoete [46] showed the opposite effect. To resolve this conflict, Wendt *et al.* [45] studied the influence of fuel sulfur on fuel NO in rich flames and found both enhancement and inhibition.

E. PARTICULATE FORMATION

In earlier sections of this chapter, the role that particulates play in a given environmental scenario was identified. This section will be devoted exclusively to those particulates that form in combustion processes and have carbon as the main constituent. Those carbonaceous particulates that form from gas phase processes are generally referred to as soot and those that develop from pyrolysis of liquid hydrocarbon fuels are generally referred to as coke or cenospheres.

Although there are various restrictions on carbon particulate emissions from different types of power plants, these particles can play both a beneficial and detrimental role in the overall plant process. The presence of particulates in gas turbines can severely affect the lifetime of the blades; soot particulates in diesel engines absorb carcinogenic materials and thus can have a health

effect. After a nuclear blast, it has been postulated that the subsequent fires would create enormous amounts of soot, which when dispersed in the atmosphere would absorb sufficient amount of the sun's radiation to create a "nuclear winter" on Earth. However, in many industrial furnaces the presence of carbon particulates increases the radiative power of the flame and, thus, can increase appreciably the heat transfer rates.

The last point is worth considering in more detail. Most hydrocarbon diffusion flames are luminous and, thus, luminosity arises due to carbon particulates that radiate strongly at the high combustion gas temperatures. The solid phase particulate cloud has a very high emissivity compared to a pure gaseous system and, thus, soot laden flames appreciably increase the radiant heat transfer. In fact some systems can approach black-body conditions. As discussed in Chapter 6 most flames appear yellow when there is particulate formation. Thus, in certain industrial furnaces in which the rate of heat transfer from the combustion gases to some surface, such as a melt, is important, it is beneficial to operate the system in a particular diffusion flames mode to assure formation of carbon particles. The particles formed are later burned off with additional air to meet emission standards. Some flames are not as luminous as others since conditions can prevail so that the very small particles formed are oxidized in the flame front and do not create a particulate cloud.

It is well known that the extent of soot formation is related to the type of flame existing in a given process. Diesel exhausts are known to be more smoky than spark-ignition engines. Diffusion flame conditions prevail in fuel-injected diesel engines, but carburetted spark-ignition engines entail the combustion of nearly homogeneous premixed fuel-air systems.

The various phenomena involved in carbon particulate formation have been under extensive study. There is an abundant literature and some extensive review articles [43-55]. Most of the subsequent material in this chapter will deal with soot formation and at the end a brief commentary on the coke-like formation from liquid fuels will be given.

1. Characteristics of Soot

The characteristics of soot are well described in the article by Palmer and Cullis [48] who give detailed references on the subject matter. Aspects of their review are worth summarizing directly.

Investigators have used the words "carbon" and "soot" to describe a wide variety of solid materials, many of which contain appreciable amounts of hydrogen and other elements and compounds that may have been present in the original hydrocarbon fuel. The properties of the solids change markedly with the conditions of formation and indeed several quite well-defined

varieties of solid carbon may be distinguished. One of the most obvious and important differences depend on whether the carbon is formed by a homogeneous vapor-phase reaction or whether the carbon is deposited on a solid surface, which may be present in or near the reaction zone.

The existence of two distinct types of carbon, which arise due to the presence or absence of a surface, was first noted on studies of acetylene decomposition flames. It was further noted that the presence of small amounts of oxygen or water vapor in the decomposing gases largely suppresses the formation of the gas-phase carbon.

Investigations have been made both on the properties of the carbon formed and the extent of the carbon formation for various experimental conditions and for both diffusion and premixed flames. In general, however, the properties of the carbon particulates formed in flames are remarkably little affected by the type of the flame, and nature of the fuel being burned and the other conditions under which they may have been produced. The extent of carbon particulates does vary appreciably with flame type. Diffusion flames invariably give more carbon than premixed flames. Theories must be able to explain these experimental findings.

Palmer and Cullis [48] report the detailed physical characteristics of soot as follows.

The carbon formed in flames generally contains at least 1% by weight of hydrogen. On an atomic basis this represents quite a considerable proportion of this element and corresponds approximately to an empirical formula of C_8H . When examined under the electron microscope, the deposited carbon appears to consist of a number of roughly spherical particles, strung together rather like pearls on a necklace. The diameters of these particles vary from 100 to 2000 Å and most commonly lie between 100 and 500 Å. The smallest particles are found in luminous but nonsooting flames, while the largest are obtained in heavily sooting flames. X-ray diffraction shows that each particle is made up of a large number (10^4) of crystallites. Each crystallite is shown by electron diffraction to consist of 5–10 sheets of carbon atoms (of the basic type existing in ideal graphite), each containing about 100 carbon atoms and thus having length and breadth of the order of 20–30 Å; but the layer planes, although parallel to one another and at the same distance apart, have a turbostratic structure, i.e., they are randomly stacked in relation to one another, with the result that the interlayer spacing (3.44 Å) is considerably greater than in ideal graphite (3.35 Å). It may readily be calculated on this picture of dispersed carbon deposits that an 'average' spherical particle contains from 10^5 to 10^6 carbon atoms.

The actual chemical structure is that of a multiple ring polynuclear aromatic compound.

2. Soot Formation Processes

The history of those fuel components that eventually form the polynuclear aromatic compound called soot and those that can survive the combustion environment is most complex. Many sequential and overlapping steps are in

the overall soot forming system. Initially, depending on whether premixed or diffusion flame conditions prevail, there is the pure or oxidative pyrolysis of the fuel. There can then be the creation of a precursor monoelement from the pyrolysis components. These elements then form some key precursors that could be aromatic in nature. There is growth in the aromatic structure as the nucleation reaction proceeds to form the condensed phase material and subsequent absorption of high-molecular-weight hydrocarbon compounds. Dehydrogenation of the virgin soot particles and cyclization and dehydrogenation of the absorbed hydrocarbons can then take place. Simultaneously there can be agglomeration, conglomeration, and thermal ionization of the small particles, and particle repulsion. Oxidation at every stage can occur in premixed flames and at all stages after the particles leave the flame front in a diffusion flame. There can also be the oxidation of the final aged particle in the last stages of the combustion system.

That the properties of the soot found in most cases are the same, may be due to the fact that, as is now known [56], the carbon-hydrogen ratio of virgin soot particles increases as the particles pass through the hot burned gases of a combustor.

A key element of the soot formation process, which has intrigued many investigators, is the rapidity with which soot particles form in flames. The particles would appear to form in less than 1 msec and reach diameters of 500–1000 Å in less than 10 msec [50]. There still exists great controversy about the various reaction steps leading to chemical nucleation of the soot particle. Irrespective of the specific steps, it is apparent that, as the various precursors build, they must have conjugated structures. Such structures are resonance stabilized at high temperatures. Normally, the larger a gaseous molecule, the more likely it is to fracture at high temperatures. Aromatic structures are so stabilized and, besides having an elemental form of the final soot structure, this resonance is the reason aromatic fuels have a great tendency to soot. It is not surprising then that it has been suggested [51] that resonance stabilized butadiene, diacetylene, methyl and vinyl acetylene, and ion or radical forms of these compounds may be important precursors in the soot formation process. Since it is extremely difficult to form polynuclear aromatic structures from phenyl radicals alone, aliphatic fragments such as acetylene or vinyl acetylene may be necessary intermediates, even when the initial fuel is aromatic in nature [52].

One early soot model described in a review [53] suggested that the precursors are acetylenic in character and that these acetylenes polymerize and go through a cyclization process to form the virgin soot particle. This free-radical mechanism would appear to be too slow to be consistent with experimental observations of soot formation. There has been a school of thought [55] that ions in flames permit a series of much faster ion-neutral

reactions that account for the rapid soot production under appropriate stoichiometric conditions. However, ion theories have not gained much acceptance. A model proposed by Frenklach *et al.* [57] appears to explain the time scale of soot formation and soot yields obtained in shock-tube pyrolysis of acetylene and to be in accord with product distributions observed in flames. The model, which is shown in Table 5, could have greater applicability than to acetylene as the fuel alone in that the major additive component need not be acetylene, but perhaps could be vinyl acetylene, butadienyl radical, or butadiene. The main controlling (slowest) element in the overall system is the formation of the first aromatic ring. This model would confirm earlier suggestions [51,58] that fuel pyrolysis rates control the overall soot formation process and be consistent with the fact that aromatic fuels have the greatest tendency to soot.

Indeed, there appears to be substantial evidence [51,58,59] that fuel pyrolysis rates and mechanisms control the tendency of a given fuel to soot. Those which pyrolyze the fastest and form the important conjugated procurors (butadienyl radical, butadiene, vinyl acetylene, and phenyl radicals, or any aromatic) will have the greatest tendency to soot.

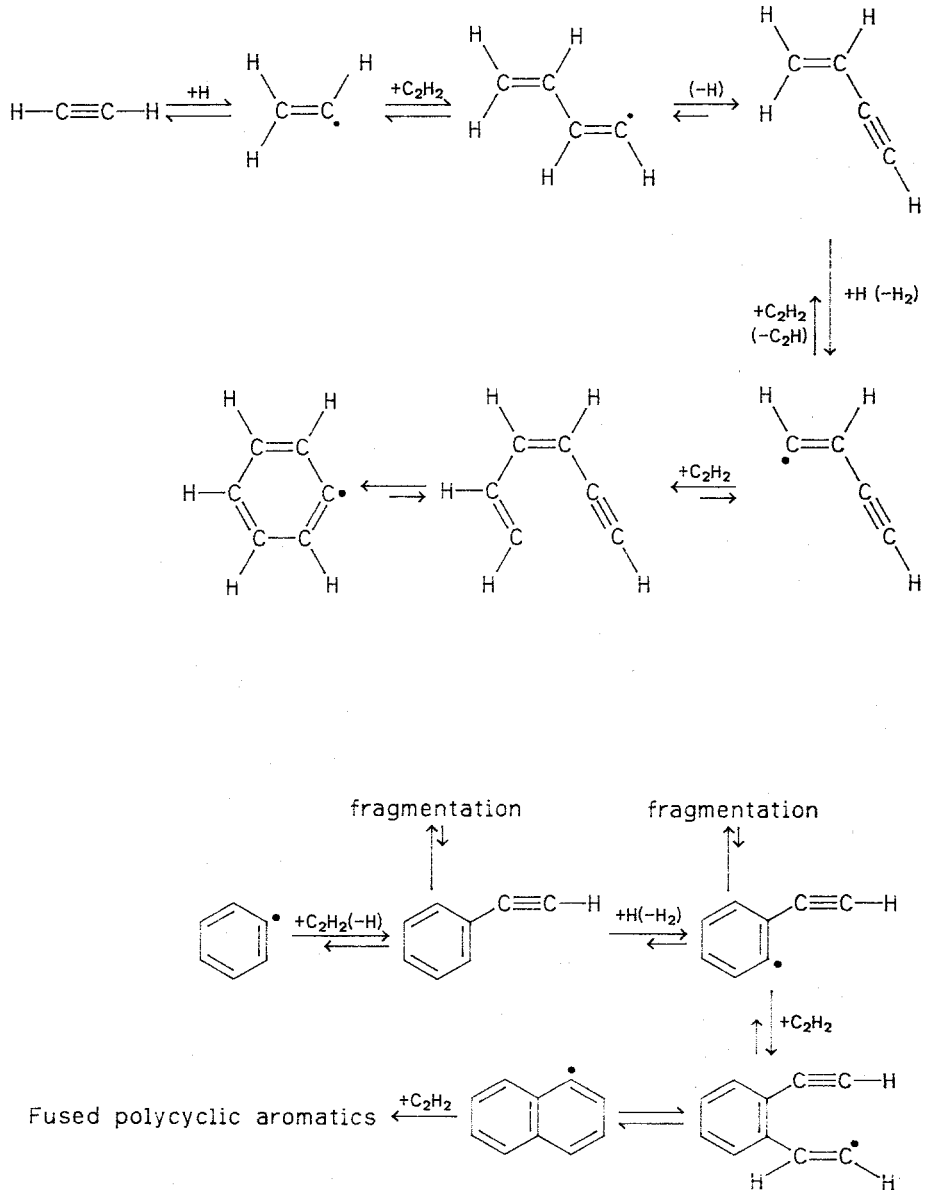
3. The Use of Flames in Soot Formation Analyses

The tendency of fuels to soot has been measured by various means: laminar premixed flames [60,61], laminar diffusion flames [62-64], turbulent diffusion flames [65], and stirred reactors [66-67]. As discussed earlier, the amount of soot that will form from a particular combustion process is the result of a series of sequential and overlapping steps. It is well to note, however, that in laminar flame processes the spacial distribution of the steps is such that they are essentially noninterfering. Thus, from a given laminar flow experiment one is more likely to determine which step is affected by a change in a given physical or chemical variable. In turbulent flames and stirred reactors, the processes are mixed and although these types of experiments probably approach more realistic practical conditions, it is more difficult to compare results of various investigators because of the lack of detailed turbulence and degree-of-mixing measurements. The fact that stirred reactions give the same tendency to soot trends as do premixed flames [51,66,67], but somewhat different quantitative results, points again to the dominance of a step or steps not affected by backmixing. Indeed, the step must be related to fuel pyrolysis.

In premixed flames the tendency to soot is correlated with the equivalence ratio at which luminosity just begins. The luminosity is attributed to the formation of soot. When the equivalence ratio is defined as the actual fuel-air

TABLE 5

Acetylene Soot Formation Mechanism



ratio to the stoichiometric value, the smaller the equivalence ratio at the sooting point the greater the tendency to soot [60,61]. In diffusion flame tests, the tendency to soot is measured by the height of an overventilated gaseous (or vaporized fuel) jet [62,63], or the fuel mass flow at this height [58,62], at which the luminous diffusion flame breaks opens near its apex and emits a stream of particles.

The sooting tendency as measured by the techniques described above shows very different effects for fuel structure and depends upon whether premixed or diffusion flame conditions prevailed. For premixed fuel-air flames, the literature [60] reported the following descending tendency to soot according to fuel type

aromatics > alcohols > paraffins > olefins > acetylene

For diffusion flames, the order that had been reported is

aromatics > acetylenes > olefins > paraffins > alcohols

Unfortunately, reporting such trends is misleading in understanding how fuel structure affects sooting tendency. The essential reason is that the flame temperature plays an extremely important role.

Using a cooled flat flame burner with premixed ethene-air, Milliken [68] showed that as the flame temperature was lowered by plug cooling, the flame emitted soot at a lower equivalence ratio; that is, it had a greater tendency to soot. Milliken proposed that the fate of the acetylene under the rich operating condition determined the tendency to soot. He showed that although the rate of pyrolysis increased with temperature, the rate of hydroxyl radical attack on the acetylene precursors increased even faster with temperature. Thus, the higher the premixed flame temperature, the less is the tendency to soot. This conclusion is very important, for the same type of reasoning can be applied to diffusion flames [51]. In diffusion flames there is no oxidizer present on the fuel side where pyrolysis takes place. Since the higher the flame temperature, the greater is the rate of pyrolysis, the greater is the tendency to soot [51,58]. Thus, the temperature has opposite effects depending on the type of flame.

a. Premixed Flames

Listed in Table 6 are the critical sooting equivalence ratio (ϕ_c) for numerous hydrocarbon fuels mixed with air. The trend according to class of hydrocarbon follows that given previously. However, such trends are inconsistent with observation of fuel-rich oxidation kinetics in that it is well known under such conditions ethane is converted to ethene and then to acetylene [69]. Thus, it is not likely that acetylene would have a lesser tendency to soot than ethane. The anomaly has to do with the temperature.

TABLE 6
Critical sooting equivalence ratios (ϕ_c) of various
fuels premixed with air

Fuel	ϕ_c			
	60	61	67	70
Ethane	1.67			1.70
Propane	1.56	1.73		
<i>n</i> -pentane	1.47			
Iso-pentane	1.49			
<i>N</i> -hexane	1.45		1.61	
Iso-hexane	1.45	1.73		
<i>N</i> -octane	1.39	1.73		
Iso-octane	1.45		1.70	
Iso-dodecane	1.41			
<i>N</i> -Cetane	1.35			
Acetylene	2.08	2.00		2.00
Ethylene	1.82		2.00	1.75
Propylene	1.67			
Butylene	1.56			
Amylene	1.54			
Cyclohexane	1.52	1.74	1.70	
<i>N</i> -heptene	1.45			
Ethyl alcohol	1.52			
Propyl alcohol	1.37			
Isopropyl alcohol	1.39			
Isoamyl alcohol	1.54			
Acetaldehyde	1.82			
Propionaldehyde	1.75			
Methyl ethyl ketone	1.69			
Diethyl ether	1.72			
Di-isopropyl ether	1.56			
Benzene	1.43	1.54		
Toluene	1.33	1.46	1.39	
Eylene	1.27	1.45	1.30	
Cumene	1.28	1.56	1.40	
Methyl naphthalene	1.03		1.21	

Much of the early work on sooting premixed flames was repeated at Princeton [70] with the flame temperature controlled by the amount of nitrogen in the system. Thus, the critical equivalence ratio (ϕ_c) could be obtained as a function of the calculated adiabatic flame temperature for the particular fuel-oxygen-nitrogen mixture. Results are shown in Fig. 11. To be noted in Fig. 11 is that the points with crosses are values for air and that the results are in good agreement with the values of other investigators listed in

Table 6. However, these results are consistent with knowledge of oxidation kinetics in that at a constant flame temperature acetylene has a lower ϕ_c than ethene or ethane.

Figure 11 also indicates that the C_2 hydrocarbons have a lesser tendency to soot than the C_3 's, etc. Since the sooting equivalence ratio is normally obtained in the fuel-rich region, it is unlikely that all the CO formed is converted to CO_2 . Consequently, the data were replotted as critical sooting equivalence ratio (ψ_c) based on the actual fuel-oxidizer ratio to that for conversion to CO and H_2O rather than CO_2 and water. These results are shown in Fig. 12 and the trends are much more appealing.

All the fuels are compared at a fixed temperature (2200 K) and the corresponding ψ_c is plotted as a function of the number of CC bonds in the given fuel molecule (Fig. 13); that is, a double bond is counted as two. The choice of number of CC bonds as a correlating parameter has been shown to have physical significance [69]. This analysis [69] equates the rate of fuel pyrolysis and rate of hydroxyl radical attack on the precursors at the critical condition. Thus, it can be seen that the number of CC bonds is a measure of

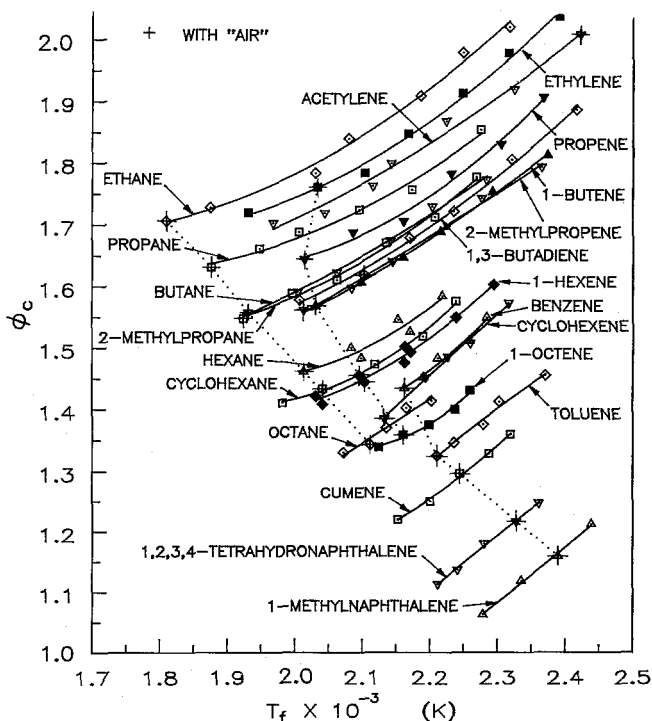


Fig. 11. Critical sooting equivalence ratios (ϕ_c) of various hydrocarbon fuels as a function of calculated adiabatic flame temperature.

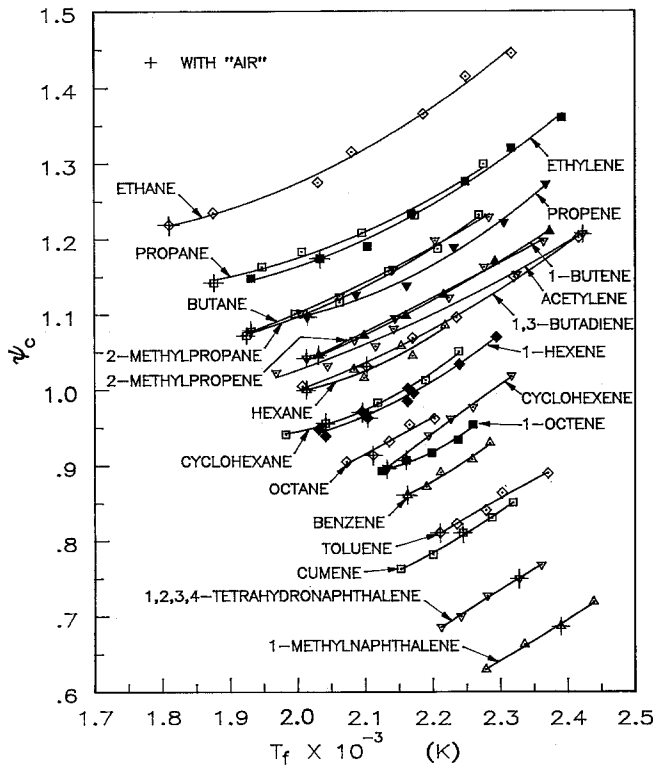


Fig. 12. Same as Fig. 11 on basis of critical sooting equivalence ratio ψ_c .

the size of the molecule and the carbon-hydrogen ratio. The larger the molecule, the greater is the pyrolysis rate and the larger the carbon-hydrogen ratio, the lesser is the OH concentration. The significance of the results in Fig. 12 is that irrespective of the fuel structure, all fuels and fuel mixtures [71] fit the same correlation. Thus, in premixed sooting flames all fuels must break down to the same precursor element and then build to the soot in a postflame regime. The precursor element is most likely acetylene.

The above conclusions would be consistent with the quantitative results of Harris and Weiner [72], who have shown that the increments of carbon introduced as ethylene in premixed flames were just as effective in measuring soot formation as increments of carbon introduced as toluene. These investigators also have shown [73] that the greatest mass of soot came about by growth on particles and that the dominant species contributing to this particle growth was acetylene.

If a premixed flame is made very fuel-rich and operated well past its critical sooting equivalence ratio, then the sooting characteristic will change in that

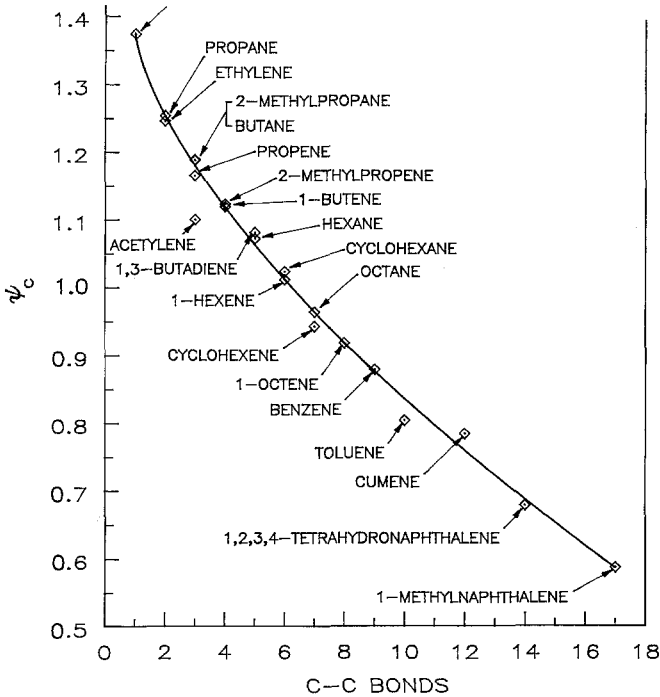


Fig. 13. Critical sooting equivalence ratio ψ_c at 2200 K as a function of “number of C—C bonds” in hydrocarbon fuel.

the fuel structure begins to play a role as the system approaches that of a diffusion flame.

b. Diffusion Flames

The sooting tendency under diffusion controlled conditions is usually determined by the smoke height method. Although the standard ASTM test [74] uses a fuel wick, the most common research procedure has been to work in a concentric configuration with a fuel jet in the center and air surrounding the jet. For consistent results the system is run in a highly overventilated system [58,62]. The liquid fuels are vaporized to create a gaseous jet. The mass flow of the fuel jet is increased until soot breaks through the top of the flame. This point is called the sooting or smoke height and data are reported in terms of the fuel mass flow at this height.

If nitrogen, or any other inert species is added to the fuel jet, the flame closes and soot no longer emanates from the top of the flame [58,75]. As the fuel-inert mass flow is increased, another smoke height is reached. Additional inert again suppresses the soot formation and additional flow is necessary for

the flame to soot. In this manner the smoke height, or mass flow at the smoke height, may be obtained at different flame temperatures.

If the original hypothesis put forth [51] that in diffusion flames the fuel pyrolysis controls the overall sooting tendency, then the smoke height test is an indirect measurement of the fuel pyrolysis rate. Smoke height data taken with inert addition should then be plotted as the log of the reciprocal of the fuel mass flow rate at the smoke height ($1/\text{FFM}$) versus the reciprocal of the calculated adiabatic flame temperature. The calculated adiabatic flame temperature has been found to be good surrogate temperature for the pyrolysis field within the fuel jet [59]. Actual data for some fuels are reported in Fig. 13, and the summary of data for 29 fuels are shown in Fig. 14 [58,59].

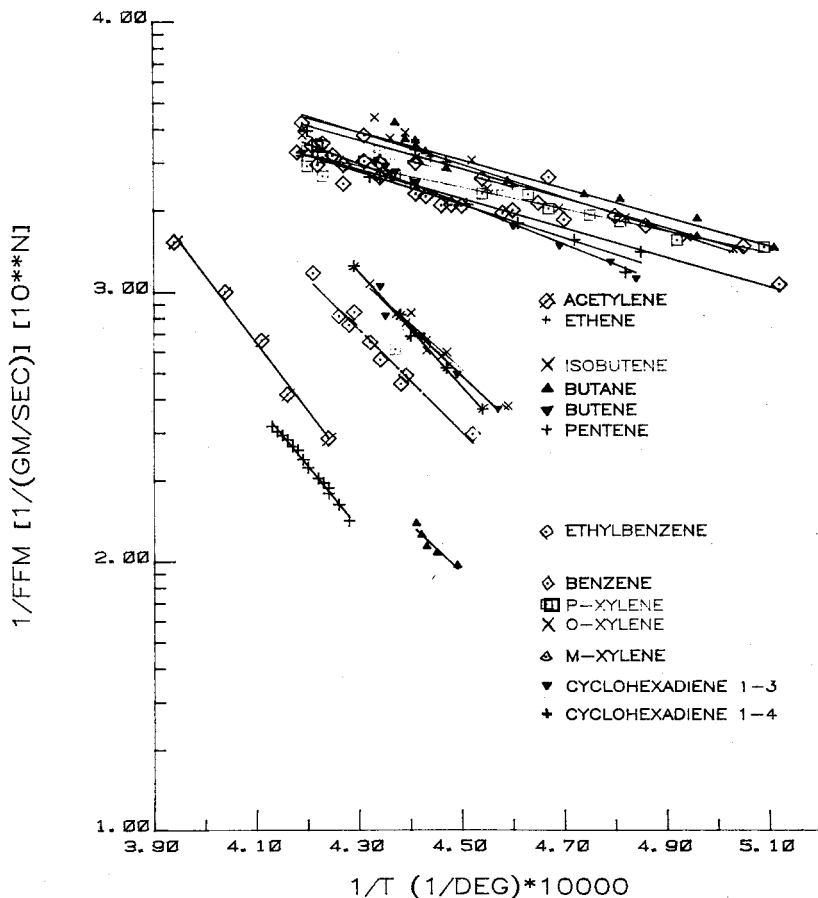


Fig. 14. Sooting tendency of some hydrocarbon fuels plotted as the log of the reciprocal of the fuel mass flow at the smoke height versus the reciprocal of the calculated adiabatic flame temperature.

Frenklach *et al.* [76], evaluated the sooting tendency of fuels by shock tube pyrolysis at various temperatures. They found that the sooting rate increased with temperature, reached a maximum, and then decreased. The maxima occur in the range 1900–2300 K. In air flames the flow configuration is such that the pyrolysis is initiated at temperatures much lower than the stoichiometric temperature so that the soot forms prior to reaching the maxima temperatures Frenklach *et al.* observed. In the shock tube when the fuel is instantaneously exposed to very high temperatures, intermediates shown in Table 5 begin to decompose and the soot rates slow. What is most important is that the shock tube pyrolysis data show the same general sooting trends as the diffusion flame results shown in Fig. 15. For example, both groups of investigators [58,59,76] show the following sooting tendency

benzene > allene > butadiene > butene > acetylene

It is most interesting to note that at a fixed flame temperature butane has a greater tendency to soot than acetylene.

The fact that fuels fall in bands according to their structure signifies that not only does the pyrolysis rate play a role, but also the pyrolysis mechanism. Those fuels that most readily form the soot precursor element have the greatest tendency to soot. According to the data presented in Figs. 14 and 15, the aromatics have the greatest tendency to soot and the most moderate temperature dependence; next are the olefins that show a greater temperature dependency, and last the paraffins. Acetylene falls between most of the olefins and ethene and shows a strong temperature dependency.

A knowledge of fuel pyrolysis characteristics of a fuel permits one to estimate its tendency to soot from Fig. 15. During pyrolysis, cyclohexadienes are known to dehydrogenate to benzene and indeed, the sooting data in Fig. 15 show almost exact correspondence for the cyclohexadienes and benzene. Cyclopropane is known to pyrolyze to propane, again correspondence with smoke height data. Similar correspondence of many other fuels is discussed in Ref. [59]. Thus, the conclusion is reached that the fuel pyrolysis rate and its pyrolysis mechanism determines its tendency to soot.

Again, it must be recognized that the smoke height measurement comparisons are qualitative ones. Laser diagnostic developments [77] have permitted extensive analysis of the structure of the sooting diffusion flame and the processes taking place therein [78–82]. Measurements of soot volume fraction, number density, mean particle size, and temperature throughout the flame permits an understanding of the different soot events. In a concentric flame arrangement soot is first observed to form low in the flame in an annular region about 1–2 mm inside the main reaction zone [78,79]. At higher locations the annular region widens until the entire flame is observed to contain soot particles [79]. Then particle oxidation begins. When the

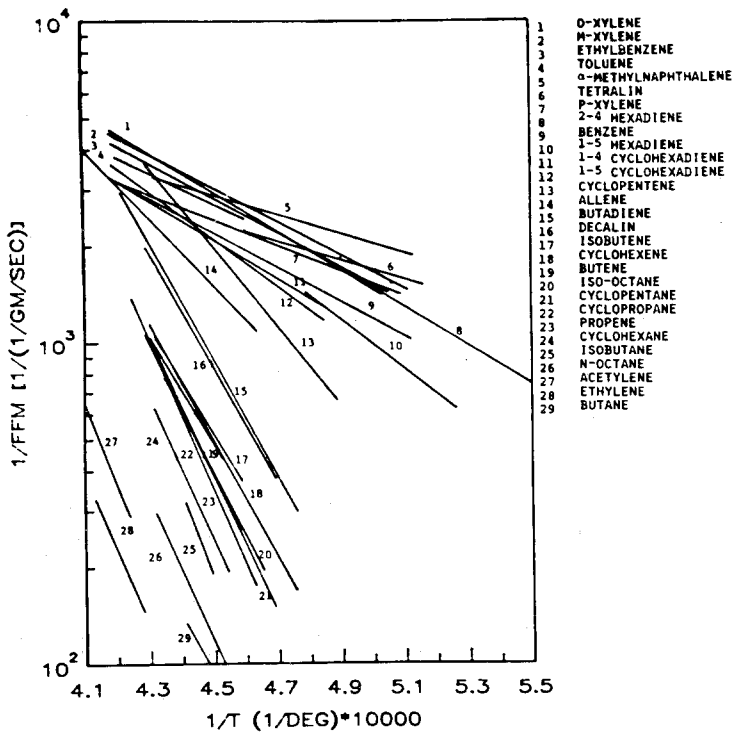


Fig. 15. Same plot as Fig. 14 for 29 hydrocarbon fuels.

temperature in the upper region falls below about 1300 K, soot oxidation appears to stop [83].

These optical measurements confirm for diffusion flames [79,82], as has been shown for premixed flames [73], that the greatest contribution to the mass of soot formed is due to surface growth rather than incipient particle formation. However, it must be realized that the initial number density determines the total surface growth and, thus, the mass of soot formed [82,84].

4. The Influence of Physical and Chemical Parameters on Soot Formation

As discussed in the previous sections, the major physical effect on soot formation is the temperature. Increasing the temperature under premixed conditions increases soot production, whereas the opposite is true for diffusion flames. The main effect of varying pressure must be felt through the

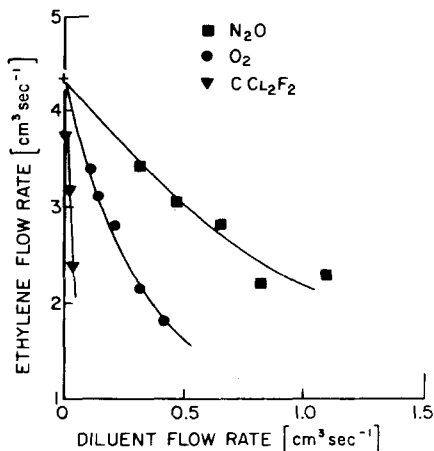
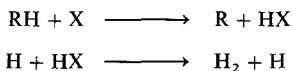


Fig. 16. The effect of catalytic additives on the volumetric flow rate at the smoke height of ethylene diffusion flames.

effect on the system temperature. Soot does not undergo a physical nucleation as occurs for water molecules. There have been some diffusion flame results that would indicate increased soot yields with increased pressure over what one would expect just due to a temperature increase [85].

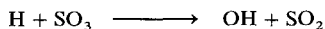
Addition of inerts to the fuel stream is effective only through the temperature and the greater the inert specific heat, the greater their effectiveness [74].

Chemical additives, which are known to increase the pyrolysis rates, increase sooting tendencies in diffusion flames substantially. Figure 16 shows the effect of three pyrolysis promoters [75]. The strong effect of halogens must be due to a catalytic sequence

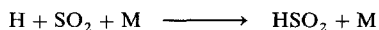


where X is the halogen atom.

Sulfur trioxide is known to suppress soot in diffusion flames and increase soot in premixed flames. These opposite effects can be explained in the context of the previous section on sulfur oxidation. In diffusion flames the slight suppression could come about by the H atoms, which form during fuel pyrolysis reacting with the SO₃ to form hydroxyl radicals



which attack the soot precursors. In premixed flames the SO₃ must dissociate into SO₂, which removes H radicals by



The reduction in H leads to a reduction in OH and, thus, greater soot production.

The most striking effect of additives are those exhibited by various metals, particularly nickel, manganese, and the alkaline earth metals [53]. A reasonable explanation of the effect in diffusion flames is that metals with low ionization potentials cause the soot particles to become charged and agglomeration is reduced. The smaller particles that then exist are more readily burned. For premixed flames, Feugier [86,87] has also shown reduction in soot formation with alkaline earth metal addition and attributes the reduction to both a charge and chemical effect. The chemical reaction leads to an increase in the hydroxyl radical concentration. Some experimenters have found anomalous results when metal compounds are added [53].

For information on agglomeration and conglomeration one is referred to the review in Ref. [53]. Discussion of soot particle burn-up is considered with the topic of pulverized coal combustion in Chapter 9.

5. Particulates from Liquid Hydrocarbon Pyrolysis

The effluent from many liquid-fueled combustion systems contains, in many instances, not only soot formed by the gas phase process described in the previous subsections, but also carbon particulates that are formed from the liquid hydrocarbon itself. If a liquid spray is allowed to impinge directly on a very hot wall before it is appreciably oxidized then the hydrocarbon is known to undergo liquid-phase cracking, subsequent pyrolysis, and finally coking. The resulting carbon particulate called petroleum coke is a harder material than the soot formed from gas-phase processes. Experiments burning heavy multicomponent residual fuels have shown that, in the latter stages of burning of these fuel droplets, a coke will form. These coke particles have been referred to as cenospheres and can be difficult to burn. They are very much like, if not the same as, petroleum coke. Unfortunately, compared to gas-phase soot formation, much less work has been done to understand coke formation. Early work [88] shows the following possible sequence of reactions to form this petroleum coke:

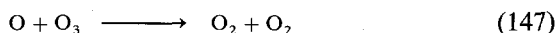
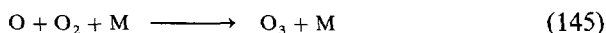
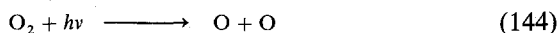
paraffins → olefins → aromatics with side chain →
condensed ring systems → asphalt → pitch →
semipitch → asphaltic coke → carboid coke

As one would readily realize, the fuels containing aromatics form petroleum coke more readily than other fuels. In regenerative cooled liquid propellant rockets, one must remove the aromatics from the fuel or coke will form in the cooling passage at the wall near the injector. This thermal insulating coke formation can cause burn-out of the rocket wall. Indeed, rocket propulsion fuels differ from the jet propulsion fuels mainly in aromatic content.

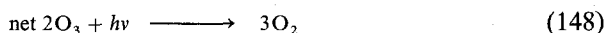
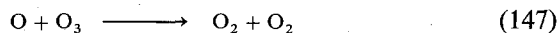
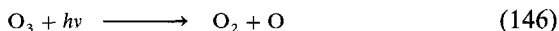
F. STRATOSPHERIC OZONE

The nature of the ozone balance in the stratosphere is determined through complex interactions of solar radiation, meteorological movements within the stratosphere, transport to and from the troposphere, and the concentration of species, which based on elements other than oxygen and which arrive into the stratosphere by natural or artificial means (such as flight of aircraft).

It is not difficult to perceive that ozone initially forms from the oxygen present in the air. Chapman [89] initially developed the photochemical model of stratospheric ozone and suggested that the ozone mechanism depended on two photochemical and two chemical reactions:



Reactions (144) and (145) are the reactions by which the ozone is created. Reactions (146) and (147) establish the balance which is the ozone concentration in the troposphere. If one adds reactions (146) and (147), the overall rate of destruction of the ozone is obtained, namely,

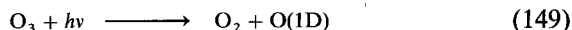


The rates of reactions (144)–(147) vary with the altitude. The rate constants of reactions (144) and (146) are determined by the solar flux at a given altitude and rate constants of the other reactions by the temperature at that altitude. Precise solar data obtained from rocket experiments and better kinetic data for reactions (145)–(147) coupled with recent meteorological analysis showed that the Chapman model was in serious error. The concentrations predicted by the model were essentially too high. Something else was affecting the ozone.

1. The HO_x Catalytic Cycle

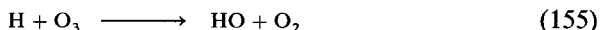
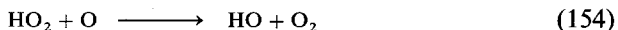
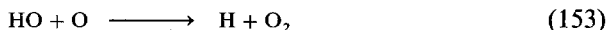
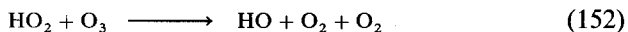
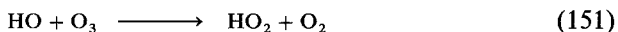
Hunt [90,91] suggested that perhaps excited electronic states of O atoms and O₂ could account for the discrepancy between the Chapman model and the measured meteorological ozone distributions. But he showed that reactions based on these excited species were too slow to account for the

differences sought. Realizing that water could enter the stratosphere, Hunt considered the reactions of free radicals (H, HO, HOO) derived from water. Consistent with the shorthand developed for the oxides of nitrogen, these radicals are specified by the chemical formula HO_x . The mechanism that Hunt postulated was predicated on the formation of hydroxyl radicals. The photolysis of ozone by ultraviolet radiation below 310 nm produces excited singlet oxygen atoms which react rapidly with water to form hydroxyl radicals:

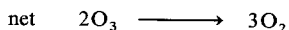
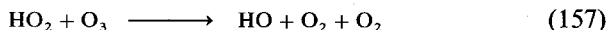
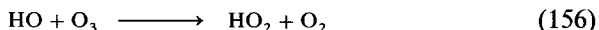


Only an excited singlet oxygen atom could react with water at stratospheric temperatures to form hydroxyl radicals.

At these temperatures, singlet oxygen atoms could also react with hydrogen or methane to form OH. The OH reacts with O_3 to produce hydroperoxy radicals HO_2 . Both HO and HO_2 destroy ozone by an indirect reaction which sometimes involves O atoms:



There are numerous reactions of HO_2 radicals possible in the stratosphere. The essential reactions for the discussion of the ozone balance are

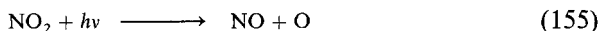
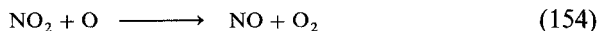
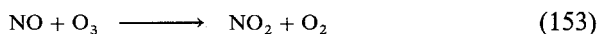


The reaction sequence (151)–(152) is a catalytic chain for ozone destruction and contributes to the net destruction. However, even given the uncertainty possible in the rates of these reactions and the uncertainty of the air motions, this system could not explain the imbalance in the ozone throughout the stratosphere.

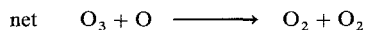
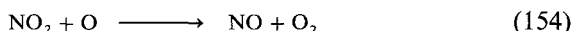
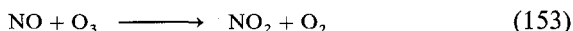
2. The NO_x Catalytic Cycle

In the late 1960s, direct observations of substantial amounts (3 ppb) of nitric acid vapor in the stratosphere were reported. Crutzen [92] reasoned that if HNO_3 vapor is present in the stratosphere it could be broken down to

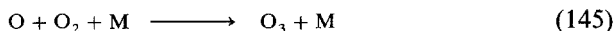
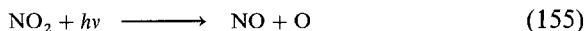
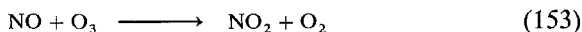
a degree to the active oxides of nitrogen (NO_x -NO and NO_2) and that these oxides could form a catalytic cycle for the destruction of the ozone. Johnston [93] first realized that if this were so, then supersonic aircraft flying in the stratosphere could wrought serious harm to the ozone balance in the stratosphere. Much of what appears in this section is drawn from an excellent review by Johnston and Whitten [94]. The most important of the possible NO_x reactions in the atmosphere for purposes here are:



whose rate constants are now quite well known. The reactions combine in two different competing cycles. The first is catalytic destructive



and the second parallel one is essentially a "do-nothing" one:



net no chemical change

The rate of destruction of ozone with the oxides of nitrogen relative to the rate in "pure air" (Chapman model) is defined as the catalytic ratio, which may be expressed either in terms of the variables NO_2 and O_3 or NO and O. These ratio expressions are

$$\beta = \frac{\text{rate of ozone destruction with } \text{NO}_x}{\text{rate of ozone destruction in pure air}} \quad (156)$$

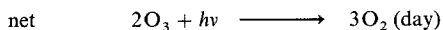
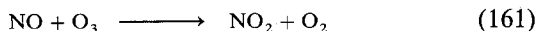
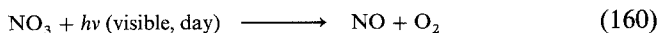
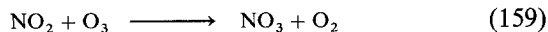
$$\beta = 1 + \{k_{156}(\text{NO}_2)/k_{147}(\text{O}_3)\} \quad (157)$$

$$\beta = 1 + \{(k_{153}k_{154}/k_{147}j_{155})(\text{NO})\}/\{1 + k_{154}(\text{O})/j_{155}\} \quad (158)$$

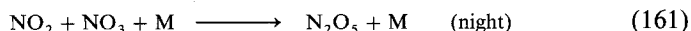
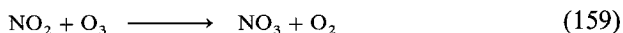
As throughout this book, the k 's are the specific rate constants of the chemical reactions. The j 's are the specific rate constants of the photochemical reactions.

At low elevations where the oxygen atom concentration is low and the

NO_2 cycle slow, another catalytic cycle derived from the oxides of nitrogen may be important:

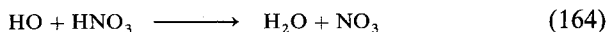
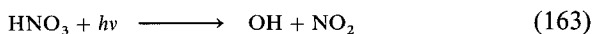


The radiation involved here is red light, which is abundant at all elevations. Reaction (152) permits another route at night (including the polar night) which converts a few percent of NO_2 to N_2O_5 :



The rate of reaction (152) is only known accurately at room temperature, and extrapolation to stratospheric temperature is uncertain; nevertheless, the extrapolated values indicate the NO_3 catalytic cycle (reactions 159 and 160) destroys ozone faster than the NO_2 cycle below 22 km and in the region where the temperature is at least 220 K.

The nitric acid cycle is established by the reaction



The steady-state concentration of nitrogen dioxide to nitric acid can be readily found to be

$$[(\text{NO}_2)/(\text{HNO}_3)]_{\text{SS}} = [k_{164}/k_{162}] + [j_{162}/k_{162}(\text{OH})] \quad (165)$$

For the best data available for the hydroxyl radical concentration and the rate constants, the ratio has the values

$$0.1 \text{ at } 15 \text{ km}, \quad 1 \text{ at } 25 \text{ km}, \quad \geq 1 \text{ at } 35 \text{ km}$$

Thus it can be seen that nitric acid is a significant reservoir or sink for the oxides of nitrogen. In the lowest stratosphere, the nitric acid predominates over the NO_2 and there is a major loss of NO_x from the stratosphere by diffusion of the acid into the troposphere where it is rained out.

By using the HO_x and NO_x cycles discussed and by assuming NO_x concentration 4.2×10^9 molecules/cm³ distributed uniformly through the stratosphere, Johnston and Whitten [94] were able to make the most reasonable prediction of the ozone balance in the stratosphere. The only

measurements of the concentration of NO_x in the stratosphere show a range of $2-8 \times 10^9$ molecules/cm³.

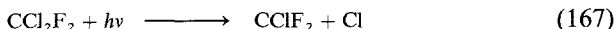
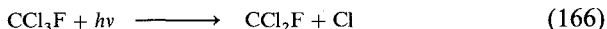
It is possible to similarly estimate the effect of the various cycles for ozone destruction. The results can be summarized as follows: between 15 and 20 km, the NO_3 catalytic cycle dominates; between 20 and 40 km, the NO_2 cycle; between 40 and 45 km the NO_2 , HO_x , and O_x mechanisms are about equal; and above 45 km, the HO_x reactions control.

It appears that between 15 and 35 km, the oxides of nitrogen are by far the most important agent for maintaining the natural ozone balance. Calculations show that the natural NO_x should be about 4×10^9 molecules/cm³. The extent to which this concentration would be modified by man-made sources such as supersonic aircraft determines the extent of the danger to the normal ozone balance. It must be stressed that this question is a complex one since both concentration and distribution are involved (see Johnston and Whitten [94]).

3. The ClO_x Catalytic Cycle

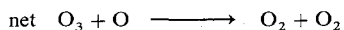
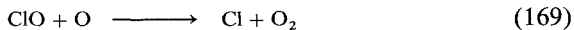
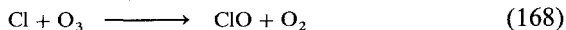
Molina and Rowland [95] pointed out that fluorocarbons could diffuse into the stratosphere and also act as a potential sink for ozone. Cicerone *et al.* [96], show that the effect of these man-made chemicals could last for decades. This possible major source of atmospheric contamination arises because of the use of fluorocarbons as propellants and refrigerants. Approximately 80% of all fluorocarbons released to the atmosphere come from these sources. There is no natural source. 85% of all fluorocarbons are F11 (CCl_3F) or F12 (CCl_2F_2).

According to Molina and Rowland [95] these fluorocarbons are removed from the stratosphere by photolysis above altitudes of 25 km. The primary reactions are

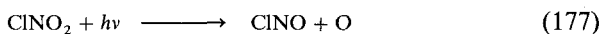
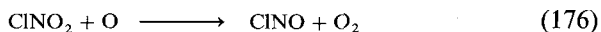
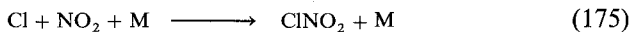
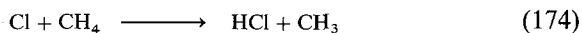
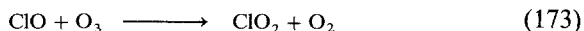
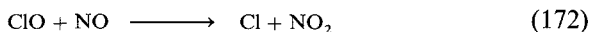
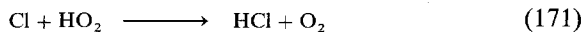
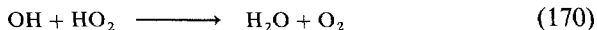


Subsequent chemistry leads to release of additional chlorine, and for purposes here it is assumed that all of the available chlorine is eventually liberated to form compounds such as HCl , ClO , ClO_2 , and Cl_2 .

The catalytic chain for ozone which develops is



Other reactions which are important in affecting the chain are



The unique problem that arises here is that F11 and F12 are relatively inert chemically and have no natural sources or sinks such as CCl_4 does. The lifetimes of these fluorocarbons are controlled by diffusion to the stratosphere where photodissociation takes place as designated by reactions (166) and (167). Lifetimes of halogen species in the atmosphere have been given in "Fluorocarbons and the Environment" [97]. These values are reproduced in Table 7. The incredibly long lifetimes of F11 and F12 and their gradual diffusion into the stratosphere pose the problem. Even if use of these materials were stopped today, their effects are likely to be felt for decades.

Some recent results indicate, however, that the rate of reaction (178) may be much greater than initially thought. If so, the depletion of ClO by this route could reduce the effectiveness of this catalytic cycle in reducing the O_3 concentration in the stratosphere.

TABLE 7

Residence time of halocarbons in the troposphere^a

Halocarbon	Average residence time in years
Chloroform (CHCl_3)	0.19
Methylene chloride (CH_2Cl_2)	0.30
Methyl chloride (CH_3Cl)	0.37
1,1,1-Trichloroethane (CH_3CCl_3)	1.1
F12	330 or more
Carbon tetrachloride (CCl_4)	330 or more
F11	1000 or more

^a Based on reaction with OH radicals.

PROBLEMS

1. Explain what is meant by atmospheric, "prompt" and fuel NO.
2. Does prompt NO form in carbon monoxide-air flames? Why or why not?
3. Which is most sensitive to temperature—the formation of atmospheric, "prompt" or fuel NO?
4. Order the tendency to soot of the following fuels under premixed combustion with air: hexadecane, ethyl benzene, cycloheptane, heptane, and heptene.

REFERENCES

1. Leighton, P. A., "Photochemistry of Air Pollution," Chapter 10, Academic Press, New York, 1961.
2. Bulfalini, M., *Environ. Sci. Technol.* **8**, 685 (1971).
3. Blacet, F. R., *Ind. Eng. Chem.* **44**, 1339 (1952).
4. Dainton, F. S., and Irvin, K. J., *Trans. Faraday Soc.* **46**, 374, 382 (1950).
5. Bowman, C. T., *Progr. Energy Combust. Sci.* **1**, 33 (1975).
6. Zeldovich, Ya. B., *Acta Physicochem USSR* **21**, 557 (1946).
7. Fenimore, C. P., *Int. Symp. Combust., 13th*, p. 373, Combustion Inst., Pittsburgh, Pennsylvania, 1971.
8. Bowman, C. T., and Seery, D. V., "Emissions from Continuous Combustion Systems," p. 123, Plenum Press, New York, 1972.
9. Martenay, P. J., *Combust. Sci. Technol.* **1**, 461 (1970).
10. Bowman, C. T., *Int. Symp. Combust., 14th*, p. 729, Combustion Inst., Pittsburgh, Pennsylvania, 1973.
11. Bachmeier, F., Eberius, K. H., and Just, Th., *Combust. Sci. Technol.* **7**, 77 (1973).
12. Haynes, D. S., Iverach, D., and Kirov, N. Y., *Int. Symp. Combust., 15th*, p. 1103, The Combustion Inst., Pittsburgh, Pennsylvania, 1975.
13. Leonard, R. A., Plee, S. L., and Mellor, A. M., *Combust. Sci. Technol.* **14**, 183 (1976).
14. Eberius, K. H., and Just, Th., Atmospheric Pollution by Jet Engines, *AGARD Conf. Proc.* No. 125, p. 16-1 (1973).
15. Hayhurst, A. N., and Vance, I. M., *Combust. Flame* **50**, 41 (1983).
16. Martin, G. B., and Berkau, E. E., AIChE Meeting, San Francisco, California, 1971.
17. Flagan, R. C., Galant, S., and Appleton, J. P., *Combust. Flame* **22**, 299 (1974).
18. Mulvihill, J. N., and Phillips, L. F., *Int. Symp. Combust., 15th*, p. 1113, Combustion Inst., Pittsburgh, Pennsylvania, 1975.
19. Levy, A., *Int. Symp. Combust., 19th*, p. 1223, Combustion Inst., Pittsburgh, Pennsylvania, 1982.
20. Fenimore, C. P., *Combust. Flame* **19**, 289 (1972).
21. deSoete, C. C., *Int. Symp. Combust., 15th*, p. 1093, Combustion Inst., Pittsburgh, Pennsylvania, 1975.
22. Diehl, L. A., NASA TMX-2726 (March, 1973).
23. Hazard, H. R., *J. Eng. Power, Trans. ASME* **96**, 235 (1974).
24. Hargraves, K. J. A., Harvey, R., Roper, F. G., and Smith, D. B., *Int. Symp. Combust., 18th*, p. 133, Combustion Inst., Pittsburgh, Pennsylvania, 1981.

25. Courant, R. W., Merryman, E. L., and Levy, A., *Int. Symp. Air Pollut., Health Energy Conserv.*, Univ. of Massachusetts, October (1981).
26. Merryman, E. L., and Levy, A., *Int. Symp. Combust., 15th*, p. 1073, Combustion Inst., Pittsburgh, Pennsylvania, 1975.
27. Cernansky, N. P., and Sawyer, R. F., *Int. Symp. Combust., 15th*, p. 1039, Combustion Inst., Pittsburgh, Pennsylvania, 1975.
28. Allen, J. P., *Combust. Flame* **24**, 133 (1975).
29. Johnson, G. M., Smith, M. Y., and Mulcahy, M. F. R., *Int. Symp. Combust., 17th*, p. 647, Combustion Inst., Pittsburgh, Pennsylvania, 1979.
30. Kesten, A. S., *Combust. Sci. Technol.* **6**, 115 (1972).
31. Bracco, F. V., *Int. Symp. Combust., 14th*, p. 831, Combustion Inst., Pittsburgh, Pennsylvania, 1973.
32. Dryer, F. L., Princeton Univ., Princeton, New Jersey, (1975). *Mech. and Aerosp. Sci. Rep. No. 1224*.
33. Myerson, A. L., *Int. Symp. Combust., 15th*, p. 1085, Combustion Inst., Pittsburgh, Pennsylvania, 1975.
34. Lyon, R. K., U.S. Patent 3,900,554; *Int. J. Chem. Kinet.* **8**, 315 (1976).
35. Miller, J. A., Branch, M. C., and Kee, R. J., *Combust. Flame* **43**, (1981).
36. Levy, A., Merryman, E. L., and Ried, W. T., *Environ. Sci. Technol.* **4**, 653 (1970).
37. Cullis, C. F., and Mulcahy, M. F. R., *Combust. Flame* **18**, 222 (1972).
38. Johnson, G. M., Matthews, C. J., Smith, M. Y., and Williams, D. V., *Combust. Flame* **15**, 211 (1970).
39. Merryman, E. L., and Levy, A., *Int. Symp. Combust., 13th*, p. 427, Combustion Inst., Pittsburgh, Pennsylvania, 1971.
40. Sachjan, G. A., Gershenzen, Y. M., and Naltandyan, A. B., *Dokl. Akad. Nauk SSSR* **175**, 647 (1971).
41. Muller, C. H., Schofield, K., Steinberg, M., and Broida, H. P., *Int. Symp. Combust., 17th*, p. 687, Combustion Inst., Pittsburgh, Pennsylvania, 1979.
42. Myerson, A. L., Taylor, F. R., and Harst, P. L., *J. Chem. Phys.* **26**, 1309 (1957).
43. Barrett, R. E., Hummell, J. D., and Reid, W. T., *J. Eng. Power Ser. A, Trans. ASME* **88**, 165 (1966).
44. Wendt, J. O. L., and Ekmann, J. M., *Combust. Flame* **25**, 355 (1975).
45. Bowman, C. T., "Combustion Fundamentals," EXXON Course No. 632, EXXON Research and Engineering Corp., Linden, New Jersey (April 1981).
46. DeSoete, G. G., Inst. Francais du Petrole, Fuel Rep. No. 23306 (June, 1975).
47. Wendt, J. O. L., Morcomb, J. T., and Corley, T. L., *Int. Symp. Combust., 17th*, p. 671, Combustion Inst., Pittsburgh, Pennsylvania, 1979.
48. Palmer, H. B., and Cullis, H. F., "The Chemistry and Physics of Carbon," Vol. 1, p. 265, Marcel Dekker, New York, 1965.
49. Homan, K. H., and Wagner, H. Gg., *Int. Symp. Combust., 11th*, p. 371, Combustion Inst., Pittsburgh, Pennsylvania, 1967.
50. Wagner, H. Gg. *Int. Symp. Combust., 17th*, p. 3, Combustion Inst., Pittsburgh, Pennsylvania, 1979.
51. Glassman, I., *Mech. and Aero. Eng. Rep. 1450* Princeton Univ., Princeton, New Jersey, (1979); also AFOSR TR 79-2247 (1979).
52. Bittner, J. P., and Howard, J. B., *Prog. Astronaut. Aeronaut.* **62**, 335 (1978).
53. Haynes, B. S., and Wagner, H. Gg., *Prog. Energy Combust. Sci.*, **7**, 229 (1981).
54. Smith, O. I., *Prog. Energy Combust. Sci.* **7**, 275 (1981).
55. Calcote, H. F., *Combust. Flame* **42**, 215 (1981).
56. Homann, K. H., *U. S. Nat. Bur. Stand. Publ.* **357**, p. 143 (1972).

57. Frenklach, M., Clary, D. W., Gardiner, W. C., Jr., and Stein, S. E., *Int. Symp. Combust.*, 20th, p. 887, Combustion Inst., Pittsburgh, Pennsylvania, 1985.
58. Glassman, I., and Yaccarino, P., *Int. Symp. Combust.*, 18th, p. 1175, Combustion Inst., Pittsburgh, Pennsylvania, 1981.
59. Gomez, A., Sidebotham, G., and Glassman, I., *Combust. Flame* **58**, 45 (1984).
60. Street, J. C., and Thomas, A., *Fuel* **34**, (1955).
61. Miller, W. J., and Calcote, H. F., "Tonic Mechanisms of Carbon Formation in Flames," East. States Sect. Combust. Inst. Meet., East Hartford, Connecticut (November, 1971).
62. Schalla, R. L., and Hibbard, R. R., *NACA Rep. No. 1300*, Chapter 9 (1957).
63. Menchem, S. T., *World Pet. Cong. Proc.* **2**, 738 (1933).
64. Clarke, A. E., Hunter, T. C., and Garner, F. H., *J. Inst. Pet.* **32**, 627 (1946).
65. Magnussen, B. F., and Hjerhager, B. H., *Int. Symp. Combust.*, 15th, p. 1415, Combustion Inst., Pittsburgh, Pennsylvania, 1975.
66. Wright, F. J., *Int. Symp. Combust.*, 12th, p. 867, Combustion Inst., Pittsburgh, Pennsylvania, 1960.
67. Blazowski, W. S., *Combust. Sci. Technol.* **21**, 87 (1980).
68. Milliken, R. C., *J. Phys. Chem.*, **66**, 794 (1962).
69. Dryer, F. L., and Glassman, I., *Prog. Astronaut. Aeronaut.* **62**, 255 (1978).
70. Takahashi, F., and Glassman, I., *Combustion Sci. Technol.* **37**, 1 (1984).
71. Takahashi, F., Bonini, J., and Glassman, I., East. States Sect. Combust. Inst. Meet. Pap. No. 98 (December 1984).
72. Harris, S., and Weiner, A. M., *Int. Symp. Combust.*, 20th, p. 969, Combustion Inst., Pittsburgh, Pennsylvania, 1985.
73. Harris, S. J., and Weiner, A. M., *Combust. Sci. Technol.* **31**, 155 (1983).
74. ASTM Test D1322-75.
75. Schug, K. P., Mannheimer-Timnat, Y., Yaccarino, P., and Glassman, I., *Combust. Sci. Technol.* **22**, 235 (1980).
76. Frenklach, M., Clary, D. W., and Ramachandra, M. K., *NASA Contract. Rep. No. 174880* (May 1985).
77. D'Allesio, A., and Di Lorenzo, A., *Int. Symp. Combust.*, 14th, p. 941, Combustion Inst., Pittsburgh, Pennsylvania, 1973.
78. Haynes, B. S., and Wagner, H. Gg., *Ber. Bunsenges. Phys. Chem.* **84**, 499 (1980).
79. Santoro, R. J., Semerjian, H. G., and Dobbins, R. A., *Combust. Flame* **51**, 203 (1983).
80. Smyth, K. C., Miller, J. H., Dorfman, R. C., Mallard, W. G., and Santoro, R. J., *Combust. Flame* **62**, 157 (1985).
81. Boedecker, L. M., and Dobbs, G. M., *Combust. Sci. Technol.* **46**, 301 (1986).
82. Vandsburger, U., Ph.D. Thesis, Dept. of Mech. and Aero. Eng., Princeton Univ., Princeton, New Jersey (1986).
83. Kent, J., and Wagner, H. Gg., *Int. Symp. Combust.*, 20th, p. 1007, Combustion Inst., Pittsburgh, Pennsylvania, 1985.
84. Dasch, C. J., *Combust. Flame* **61**, 219 (1985).
85. Flower, W., and Bowman, C. T., *Combust. Sci., Technol.* **37**, 93 (1984).
86. Feugier, A., "Combustion Institute European Symposium," p. 406, Academic Press, London, 1973.
87. Feugier, A., "Deuxime Symposium European sur la Combustion," p. 362, Combustion Inst., Orleans, France, 1975.
88. Berry, A. G. U., and Edgeworth-Johnstone, R., *Ind. Eng. Chem.* **36**, 1140 (1944).
89. Chapman, S., *Phil. Mag.* **10**, 369 (1930).
90. Hunt, B. G., *J. Atmos. Sci.* **23**, 88 (1965).
91. Hunt, B. G., *J. Geophys. Res.* **71**, 1385 (1966).

92. Crutzen, P. J., *Roy. Meterol. Soc. Q. J.* **96**, 320 (1970).
93. Johnston, H., *Science* **173**, 517 (1971).
94. Johnston, H., and Whitten, G., Atmospheric Pollution by Aircraft Engines, AGARD Conf. Proc. No. 125, pp. 2-1 (1973).
95. Molina, M. I., and Rowland, F. S., *Nature* **249**, 810 (1974).
96. Cicerone, R. J., Stolarski, R. S., and Walters, S., *Science* **185**, 1165 (1974).
97. "Fluorocarbons and the Environment," Council on Environmental Quality, Washington, D.C., 1975.

Combustion of Nonvolatile Fuels

A. CARBON CHAR AND METAL COMBUSTION

In the final stages of coal combustion, a nonvolatile char exists and must be consumed to obtain good combustion efficiencies. The combustion of this char is a factor not considered to this point and is essentially a surface burning process similar to that which occurs when carbon graphite burns. Coal is a natural solid fuel that contains carbon, moisture, minerals that lead to an ash, and a large number of different hydrocarbons that volatilize when combustion is initiated. The volatiles in coal contribute a substantial amount to the overall energy release. They burn rapidly, however, compared to the solid carbonaceous char that remains after devolatilization. It is the surface burning rate of this remaining nonvolatile solid carbonaceous fuel that determines the efficiency of the coal process.

The importance of this type of heterogeneous surface burning also arises in the combustion of many metals. The combustion of metals is an important field in that many metals are used as additives to increase performance of fuel systems and in the presence of high oxygen concentrations, metal containers have been known to burn and to lead to serious conflagrations.

Not all metals burn heterogeneously. The determination of which metals will burn in a heterogeneous combustion mode has been developed from

knowledge of the thermodynamic and physical properties of the metal and its oxide product [1].

What is unique about metal particle burning is that the flame temperature developed is a specific known value—the boiling point of the metal oxide product. This interesting observation is due to the physical fact that the heat of vaporization or decomposition of the metal oxide formed is greater than the heat available to raise the condensed state of the oxide above its boiling point. That is, if Q_R is the heat of reaction of the metal at the reference temperature 298 K and $(H_{T, BP}^\circ - H_{298}^\circ)$ is the enthalpy required to raise the product oxide to its boiling point at the pressure of concern then

$$\Delta H_{\text{vap, dissoc}} > Q_R - (H_{T, BP}^\circ - H_{298}^\circ) = \Delta H_{\text{avail}}$$

where $\Delta H_{\text{vap, dissoc}}$ is the heat of vaporization or dissociation of the metal oxide [2]. Q_R is to be recognized as the negative of the heat of formation of the metal oxide. This equation assumes conservatively that no vaporization or decomposition takes place between the reference temperature and the boiling point.

The developments in Chapter 6 show that in the steady state the temperature of the fuel particle undergoing combustion approaches its boiling point (saturation) temperature at the given pressure. Characteristically, it is a few degrees less. For a condensed phase fuel to burn in the vapor phase, then the flame temperature must be greater than the fuel saturation temperature so that the fuel will vaporize and diffuse towards the oxidizing atmosphere to react. For liquid hydrocarbon fuels, the droplet flame temperature is substantially higher than the fuel saturation temperature. However, many metals have very high saturation temperatures. Thus, for a metal to burn as a vapor the temperature of the oxide boiling point must be greater than the temperature of the metal boiling point. This statement is known as Glassman's criterion for the vapor-phase combustion of metals.

Listed in Table 1 are the boiling points of some metals and their oxides at 1-atm pressure. To be noted from this table is that four elements; boron, silicon, titanium, and zirconium must burn heterogeneously. There is substantial experimental observations that indicate that metals such as aluminum, magnesium, calcium, and strontium burn in the vapor phase as liquid hydrocarbon fuels do and that boron, titanium, and zirconium burn heterogeneously on the metal surface [3-10]. As the pressure is raised both of the oxide and metal saturation temperatures change. However, the latent heats of these materials are such that vapor-pressure lines on a Clausius-Clapeyron plot never cross and, thus, materials which burn heterogeneously at 1-atm pressure burn so at all reasonable elevated pressures [2].

Consideration of the heterogeneous burning rate of carbonaceous materials such as carbon graphite, coal char or soot, and metallic substances such

TABLE 1

Normal boiling points of metals and their higher oxides^a

Element	Boiling point (K)	Oxide	Boiling point (K)
Li	1620	Li ₂ O	2836
B	3931	Be ₂ O ₃	2316
Na	1156	Na ₂ O	2223
Mg	1378	MgO	3533
Al	2768	Al ₂ O ₃	3800*
K	1037	K ₂ O	1154
Ca	1767	CaO	3800*
Ti	3591	Ti ₂ O ₃	3300*
Zr	4777	ZrO ₂	4548
Be	2757	BeO	4060
Si	3514	SiO ₂	2500*

^a All data from JANNAF Thermochemical Tables except those with asterisks which are estimates.

as boron, silicon, titanium, and zirconium form the subject matter of this chapter.

B. DIFFUSIONAL KINETICS

When there is heterogeneous surface burning of a particle, consideration must be given to whether diffusion rates or surface kinetic reaction rates are controlling the overall burning rate of the material. In many cases, it cannot be assumed that the surface oxidation kinetic rate is fast compared to the rate of diffusion of oxygen to the surface. The surface temperature determines the rate of oxidation and this temperature is not always known *a priori*. Thus, in surface combustion the assumption that chemical kinetic rates are very much faster than diffusion rates cannot be made.

Consider, for example, a carbon surface burning in a concentration of oxygen in the free stream specified C_∞ . The burning is at a steady mass rate. Then the concentration of oxygen at the surface is some value C_s . If the surface oxidation rate follows first-order kinetics as Frank-Kamenetskii [11] assumed, then

$$G_{\text{ox}} = G_f/i = kC_s \quad (1)$$

where G is the flux in gm/sec cm^2 , k is the heterogeneous specific reaction rate constant for surface oxidation in units reflecting a volume to surface area

ratio as well, i.e., centimeters per second; and i is the mass stoichiometric index. However, the problem is that C_s is unknown. But one also knows that the consumption rate of oxygen must be equal to the rate of diffusion of oxygen to the surface. Thus if h_D is designated the overall convective mass transfer coefficient (conductance), then one can write

$$G_{\text{ox}} = kC_s = h_D(C_\infty - C_s) \quad (2)$$

What is sought is the mass burning rate in terms of C_∞ . It follows then

$$kC_s = h_D C_\infty - h_D C_s \quad (3)$$

$$kC_s + h_D C_s = h_D C_\infty \quad (4)$$

$$C_s = \{h_D/(k + h_D)\}C_\infty \quad (5)$$

or

$$G_{\text{ox}} = [\{kh_D/(k + h_D)\}C_\infty] = KC_\infty \quad (6)$$

$$K \equiv kh_D/(k + h_D) \quad (7)$$

$$1/K = (k + h_D)/kh_D = (1/h_D) + (1/k) \quad (8)$$

When the kinetic rates are large compared to the diffusion rates, $K = h_D$; when the diffusion rates are large compared to the kinetic rates, $K = k$. When $k \ll h_D$, $C_s \cong C_\infty$ from Eq. (5), thus

$$G_{\text{ox}} = kC_\infty \quad (9)$$

When $k \gg h_D$, Eq. (5) gives

$$C_s = (h_D/k)C_\infty \quad (10)$$

But since $k \gg h_D$, it follows from Eq. (10) that

$$C_s \ll C_\infty \quad (11)$$

This result permits one to write Eq. (2) as

$$G_{\text{ox}} = h_D(C_\infty - C_s) \cong h_D C_\infty \quad (12)$$

Consider the case of rapid kinetics, $k \gg h_D$, further. In terms of Eq. (6), or examining Eq. (12) in light of K ,

$$K = h_D \quad (13)$$

Of course, Eq. (12) also gives us the mass burning rate of the fuel

$$G_f/i = G_{\text{ox}} = h_D C_\infty \quad (14)$$

h_D is the convective mass transfer coefficient for an unspecified geometry. For a given geometry, h_D would contain the appropriate boundary layer thickness

or would have to be determined by some independent measurements which would give correlations from which h_D could be determined from other parameters of the system.

C. DIFFUSION CONTROLLED BURNING RATE

This situation, as discussed in the last section, is then very much like the droplet diffusion flame discussed previously. The oxygen concentration approaches zero at the flame front, except now the flame front is at the particle surface and there is no fuel volatility. Of course, the droplet flame discussed before had a specified spherical geometry and was in a quiescent atmosphere. Thus h_D must contain the transfer number term because there is regression of the surface and the carbon oxide formed will diffuse away from the surface. However, for the diffusion-controlled case, there is no need to proceed through the conductance h_D , as the system developed earlier is superior.

Recall for the spherical symmetric case of particle burning in a quiescent atmosphere, one has

$$G_f = (D\rho/r_s) \ln(1 + B) \quad (15)$$

where D is the mass diffusivity, ρ the gaseous density, r_s the radius of the particle, and B the transfer number. The most convenient B in liquid droplet burning was

$$B_{oq} = [im_{0\infty}H + C_p(T_\infty - T_s)]/L_v \quad (16)$$

since even though T_s was not known directly, $C_p(T_\infty - T_s)$ could always be considered much less than $im_{0\infty}H$ and ignored. Another form of B is

$$B_{f0} = (im_{0\infty} + m_{fs})/(1 - m_{fs}) \quad (17)$$

Indeed this form of B was required in order to determine T_s and m_{fs} with the use of the Clausius-Clapeyron equation. This latter form is not frequently used because m_{fs} is essentially an unknown in the problem and cannot be ignored as the T_s term was in Eq. (16). It is, of course, readily determined and necessary in determining G_f . However, observe the convenience in the current problem. Since there is no volatility of the fuel, $m_{fs} = 0$, and one has from Eq. (17)

$$B_{f0} = im_{0\infty} \quad (18)$$

Thus, for surface burning with fast kinetics, a very simple expression is obtained:

$$G_f = (D\rho/r_s) \ln(1 + im_{0\infty}) \quad (19)$$

Notice whereas in liquid droplet burning B was not explicitly known because T_s is an unknown, in the problem of heterogeneous burning with fast surface reaction kinetics, B takes the simple form of $im_{0,\infty}$ and is known provided the mass stoichiometric coefficient i is known. For small values of $im_{0,\infty}$, Eq. (19) becomes very similar in form to Eq. (14).

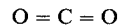
1. The Burning of Carbon Char Particles

The value of i for carbon, or for that matter any heterogeneous combustion system, depends on the surface chemistry and is thus not readily apparent.

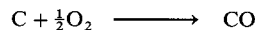
If the final product of the carbon surface reaction is carbon dioxide, then



and i the stoichiometric coefficient is defined as the number of grams of fuel that burns with one gram of oxidizer. Thus for this reaction, $i = 12/32$. From knowledge of the structure of CO_2 ,



it is not likely that CO_2 would form as a gaseous product on the surface. It is much more reasonable that CO would form and the correct value of i would be $i = 12/16$ as evaluated from



Indeed, experimental evidence appears to confirm that near the surface the product is CO and that the conversion of CO to CO_2 takes place in the gas phase in a thin reaction (flame) zone surrounding the particle.

Figure 1 details some of the evidence as reported by Coffin and Brokaw [4]. These results confirm what was inferred in the previous paragraph that carbon monoxide forms on the surface, diffuses away and reacts with the oxygen to form carbon dioxide. The carbon dioxide then diffuses in both directions—towards and away from the surface. When CO_2 reaches the carbon surface, it is reduced to CO by the reaction

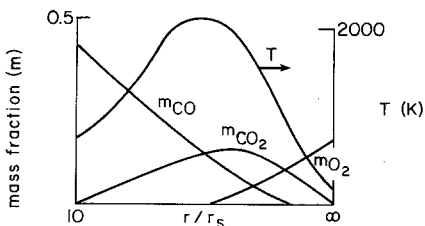


Fig. 1. Distribution of gaseous species and temperature above a carbon sphere burning on the surface (after Coffin and Brokaw [4]).

Thus actually little, if any, oxygen reaches the carbon surface. What depletes the carbon is its reduction of CO_2 into CO . Yet the stoichiometric coefficient in B is related to the free-stream mass fraction of oxygen. Since it is CO which forms at the surface, one would expect that the correct i is 12/16.

In order to verify that this value is the correct i for the sequence of reactions, one must proceed through the analytical development of the graphite particle burning. In this problem, because there is no combustion in the gas phase, one is required to deal only with the oxygen diffusion equation. Indeed this is the reason for the simple result that $B = im_{\text{O}_\infty}$. The procedure of Blackshear [12] is followed.

The mass diffusion equation developed earlier for droplet evaporation alone

$$4\pi r^2 \rho v \, dm_{\text{ox}}/dr = (d/dr)(4\pi r^2 \rho D \, dm_{\text{ox}}/dr) \quad (20)$$

now holds for the case where there is combustion on the surface, i.e., there is no reaction rate term in Eq. (20). In the gas phase i' grams of CO react with one gram of O_2 to give $(1 + i')$ grams of CO_2 , therefore,

$$m_{\text{O}_2} = -[1/(1 + i')]m_{\text{CO}_2} \quad (21)$$

A new variable, physically symbolizing and allowing for the diffusing of both the oxygen and CO_2 ,

$$m_{\text{H}} = m_{\text{O}_2} + [1/(1 + i')]m_{\text{CO}_2} \quad (22)$$

satisfies the fundamental differential equation for diffusion:

$$\rho v \, dm_{\text{H}}/dr = (d/dr)(\rho D \, dm_{\text{H}}/dr) \quad (23)$$

When this equation is integrated and evaluated at $r = r_s$, one obtains

$$\text{const} = r_s^2 [\rho_s v_s (m_{\text{H}})_s - D_s \rho_s (dm_{\text{H}}/dr)_s] \quad (24)$$

$4\pi r_s^2 \rho_s v_s$ is the mass consumption rate of the fuel and is a constant. At $r = r_s$, $m_{\text{H}} = [1/(1 + i')]m_{\text{CO}_2}$ since $m_{\text{O}_2} = 0$. Thus, the term in brackets is the flux of m_{H} into the surface, but it is, of course, also $(1/1 + i')$ times the negative flux of CO_2 into the surface as well. But, by realizing that the statement that 1 gm of CO_2 can combine with i'' gm of C to form $(1 + i'')$ gm of CO can be written, then the flux of CO_2 can be written in terms of the flux of carbon. Thus, the flux of CO_2 must be $(1/i'')$ times the flux of C . The flux of carbon comes from the basic consumption rate of the carbon and the form is very much like that of liquid droplet consumption, i.e.,

$$\rho_s v_s (m_{\text{H}})_s = D \rho [d(m_{\text{H}})/dr]_s \quad (25)$$

which is correct for solid or gas as long as consistent values of density and velocity are chosen. Then the flux of CO_2 must be

$$\rho_s v_s (1/i'') \quad (26)$$

But the term in the brackets of Eq. (24) is $(1/1 + i)$ times the flux of CO_2 . Then the term in the brackets is

$$-\rho_s v_s (1/i'') [1/(1 + i)] \quad (27)$$

and the equation is written

$$\text{const} = -r_s^2 \rho_s v_s (1/i'') [1/(1 + i)] \quad (28)$$

Integrating the second time, one has

$$\frac{r_s^2 \rho_s v_s}{rD\rho} = \ln \left(\frac{m_{\text{H}\infty} + [1/i''(1 + i)]}{m_{\text{H}} + [1/i''(1 + i)]} \right) \quad (29)$$

However both CO_2 and O_2 must approach zero at $r = r_s$, therefore $m_{\text{H}} = 0$ at $r = r_s$ and, of course, $m_{\text{H}} = m_{\text{O}_2\infty}$ at $r = \infty$. Therefore

$$r_s \rho_s v_s / \rho D = \ln [m_{\text{O}_2\infty} i''(1 + i) + 1] \quad (30)$$

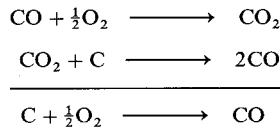
Comparing this equation with the many forms that were obtained previously, one then has that

$$B = i''(1 + i)m_{\text{O}_2\infty} \quad (31)$$

The values of i' and i'' are $i'' = 12/44$ and $i' = 28/16$. Then

$$\begin{aligned} i''(1 + i) &= (12/44)(1 + 28/16) = (12/44)(44/16) = 12/16 \\ i''(1 + i) &= 12/16 = i \end{aligned} \quad (32)$$

Thus irrespective of the mechanism of removing carbon from the surface, the main consideration is that only CO forms on the surface and the flux of oxygen from the quiescent atmosphere must be stoichiometric with respect to CO formation regardless of the intermediate reactions which take place. The same point can be seen by simple addition of the two primary reactions considered



Recall this discussion has been for $k \gg h_D$, which in the context of combustion reactions means high-temperature particles. Of course, such high temperatures are created at the surface by accelerating the mass burning rate by increasing the convective rates. The convective expression for the burning of the carbon particle is of the same form as that of the burning liquid droplet, except that the expression for B is simpler in this case.

Various investigators have shown for relatively large particles that the combustion of carbon above 1200 K exhibits rates that are strictly proportional to the diffusional characteristics. For the small particles one finds that in pulverized coal or as metallic additives in fuels, the Reynold's number are so small that the particles may be considered to burn under ambient conditions and, again, the above analyses apply. However, very small particles may have their burning rates controlled by chemical oxidation kinetics as will be discussed later. The work of Dryer *et al.* [13] shows that above 1100 K, CO oxidation to CO_2 is very rapid. Thus, it would appear that all the assumptions made above are self-consistent. If the CO rates were not rapid, one would have to be concerned with oxygen penetrating to the carbon surface, and the overall analysis would become more complex algebraically, but the same overall result obtained nevertheless. Indeed, for the combustion of small pulverized coal particles, CO appears not to be converted to carbon dioxide because of the low temperatures found and oxygen does penetrate to the char surface.

2. The Burning of Boron Particles

In certain aspects the combustion of boron is different from that of carbon in that under normal conditions of temperature and pressure the product oxide B_2O_3 is not a gas. Thus, there normally exists on a boron particle an oxide coat that thickens as the particle is heated in an oxidizing atmosphere. This condition is characteristic of most metals, even those that will burn in the vapor phase. For the efficient combustion of the boron particle, the oxide coat must be removed. The practical means for removing the coat is to undertake the oxidation at temperatures greater than the saturation temperature of the boron oxide B_2O_3 . This temperature is about 2300 K at 1 atm pressure.

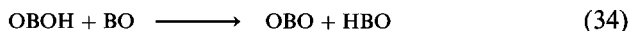
The temperature at which sufficient oxide is removed so that oxidation can take place rapidly is referred to as the metal ignition temperature. The rate of oxidation when the oxide coat persists has been discussed extensively in Refs. [14] and [15]. Nevertheless, what does control the burning time of a boron particle is the heterogeneous oxidation of the clean particle after the oxide has been evaporated. Thus, for efficient burning the particle temperature and that of the oxidizing medium must be close to the saturation temperature of the B_2O_3 . Then the burning rate of the particle is given by Eq. (19), the same as that used for carbon except the mass stoichiometric coefficient i is different. Even though the chemical reaction steps for boron are quite different from those of carbon, since i is a thermodynamic quantity and the atomic weight of boron is 10 compared to 12 for carbon, it is not surprising that the i values for both materials are nearly the same.

Just as discussed for carbon that it is not likely that the surface oxidation chemistry would yield CO_2 , so it is not likely that boron would yield B_2O_3 . Gaseous boron monoxide BO forms at the surface and this product is oxidized further to gaseous B_2O_3 by vapor-phase reactions. The gaseous B_2O_3 diffuses back to the clean boron surface and reacts to form three molecules of BO . The actual reaction sequence is most likely given by the sequence of reactions [15] discussed in the following paragraphs.

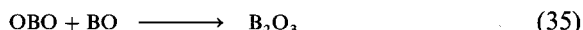
In a high-temperature atmosphere created by the combustion of a host hydrocarbon fuel there will be an abundance of hydroxyl radicals. Thus, boron monoxide reacts with hydroxyl radicals to form gaseous metaboric oxide HOBO ,



It is postulated that HOBO then reacts with BO to form gaseous boron oxide hydride HBO and boron dioxide BO_2 (OBO),

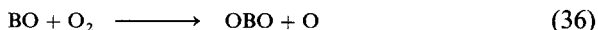


The boron dioxide then reacts with another BO to form boron oxide



This route chosen is consistent with the structure of the various boron oxide compounds in the system [15].

In a hydrogen-free oxidizing atmosphere, a slower step forms the boron dioxide,

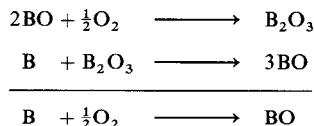


and then B_2O_3 again forms via reaction (35).

After the gaseous reaction system is established, the B_2O_3 diffuses back to the nascent boron surface to form BO similar to CO_2 diffusing back to the carbon surface to form CO . The reaction is



Thus, the overall thermodynamic steps required to calculate the mass stoichiometric index in Eq. (19) are



and

$$i = (10/16) = 0.625$$

compared to the value of 0.75 obtained for the carbon system.

3. The Role of Gaseous Inerts in Heterogeneous Diffusional Burning

In solving the vapor phase burning rate of a liquid particle burning in Chapter 6, no consideration was given to the concentration profiles of inerts, for example that of the nitrogen in air. As will be discussed later in this section the role of inerts can be of importance during heterogeneous burning when small amounts are added to pure oxygen. It is interesting to examine the concentration trend of the inert in a particle burning in an ambient atmosphere. Considering first the case of vapor phase combustion of a particle as analyzed in Chapter 6, the equation describing the diffusion of the inert simplifies to

$$(4r^2\rho v)m_i = 4r^2D(dm_i/dr) \quad (38)$$

when m_i is the mass fraction of the inert species. The boundary condition at $r = \infty$ is

$$m_i = m_{i\infty}$$

and the solution to Eq. (38) is

$$-[(4r^2\rho v)/4\pi](1/r) = D\rho \ln(m_i/m_{i\infty}) \quad (39)$$

Substituting for $4\pi r^2\rho v$ by using Eq. (118) in Chapter 6, one obtains

$$-[4\pi r_s \rho D \ln(1 + B)]/4\pi \cdot (1/r) = D\rho \ln(m_i/m_{i\infty}) \quad (40)$$

that simplifies to

$$-(r_s/r) \ln(1 + B) = \ln(m_i/m_{i\infty}) \quad (41)$$

Evaluating Eq. (41) at $r = r_s$ give

$$(1 + B) = (m_{i\infty}/m_{is}) \quad (42)$$

Since B is always a positive value m_{is} will always be less than m_i . For hydrocarbon fuels that have values of B about 6, then

$$m_{is} = (m_{i\infty}/7)$$

and for air at which $m_{i\infty} = 0.77$, $m_{is} = 0.11$.

The inert mass fraction is readily determined at the flame front as well. Equation (41) is written as

$$-(r_s/r_f) \ln(1 + B) = \ln(m_i/m_{i\infty}) \quad (43)$$

where m_{if} is the inert mass fraction at the flame radius r_f . Using the value of (r_s/r_{stoich}) given by Eq. (124) of Chapter 6, Eq. (43) becomes

$$-\ln(1 + im_{0\infty}) = \ln(m_{if}/m_{i\infty})$$

or

$$1 + im_{0\infty} = (m_{if}/m_{i\infty}) \quad (44)$$

For octane burning in air, the mass stoichiometric index $i = 0.28$, and

$$m_{if} = 0.77/1.064 = 0.72$$

Thus, during the vapor-phase combustion of a fuel droplet in air the nitrogen mass fraction falls slowly from the ambient value of 0.77 to a value of about 0.72 at the flame front and then drops rapidly as it approaches the droplet surface, where it attains a value of about 0.11.

Considering the case of the heterogeneous combustion of a carbon particle, it is apparent that the "flame front" is at the surface, so Eq. (41) is applicable and since $B = im_{0\infty}$, Eq. (44) is also obtained. Indeed the same result could be obtained from Eq. (42) setting $B = im_{0\infty}$. In this case $i = 0.75$ and

$$m_{is} = (0.77/1.73) = 0.657 \quad (45)$$

If there is no evolution of product gases for the surface burning case, i.e., only molten oxide forms, then, since the oxygen concentration must approach zero at the surface, the inert mass fraction must always approach one there regardless of its concentration in the ambient atmosphere. For the case of burning in pure oxygen under these same conditions, the rate must then be controlled by the surface oxidation kinetics.

4. Oxidation of Very Small Particles—Pulverized Coal and Soot

Equation (19) shows that the rate of fuel consumption in a diffusion controlled system is inversely proportional to the radius of the fuel particle. Hence, below some critical particle size, other conditions being constant, the rate of mass (oxygen) transfer will become faster than the rate of the surface chemical reaction. When this condition prevails, the kinetic rate controls the

mass consumption rate of the fuel and the concentration of the oxidant close to the surface does not differ appreciably from its bulk (ambient) concentration. If the fuel particle is porous, the essential assumption is always that the chemical rate is fast enough that it is possible to assume that the particle is impervious to the oxygen concentration.

The surface chemical reaction rate is different from that of ordinary gaseous reactions. It is considered to be a two-step physical process; that is, the attachment of the oxygen chemically to the fuel surface (absorption) and desorption of the oxygen with the attached fuel component from the surface as a product. In the discussion to follow it will be tacitly assumed that the fuel is carbonaceous. In principle then, either adsorption of the oxygen or desorption of the gaseous fuel oxide can be controlling. Realizing that these physical processes actually govern the chemical conversion rate and that the particular fuel atoms to which the oxygen attaches are the ones that produce the products, then in actuality it is either adsorption or desorption that controls the number of active sites that will produce products.

This concept has been applied by Mulcahy and Smith [16] to determine whether the burning process of pulverized coal particles is controlled by chemical kinetic or diffusion rates. It is their work which is followed in the subsequent paragraphs.

The maximum rate of absorption-controlled step may be calculated by assuming every oxygen molecule, which has the necessary activation energy E_{ads} and strikes the fuel surface reacts immediately to form two molecules of the product CO. It makes no significant difference whether the oxidant molecule is O_2 or CO_2 since in either case the product evolved is two molecules of CO.

This rate of chemical adsorption is given by

$$R_{\text{ads}} = (2Z/N) \exp(-E_{\text{ads}}/RT) \quad (\text{gm atm of carbon/cm}^2 \text{ sec}) \quad (46)$$

where N is Avogadro's number and Z is the number of collisions per square centimeter per second and can be calculated from the kinetic theory of gases. Thus, the adsorption rate expression becomes

$$R_{\text{ads}} = [2MW_{\text{O}_2} P_{\text{O}_2}/(2RTMW_{\text{O}_2})^{0.5}] \exp(-E_{\text{ads}}/RT) \quad (47)$$

where MW_{O_2} is the molecular weight of oxygen. Thus, the adsorption rate is seen to be proportional to the oxygen particle pressure (or concentration) and is thus first order with respect to the oxygen.

The maximum rate of the desorption process can be estimated by assuming, in the steady state, an oxygen atom is attached to every carbon atom on the surface. The rate at which carbon evolves from the surface as CO is found to be

$$R_{\text{des}} = (12RTC_A/N^2h) \exp(-E_{\text{des}}/RT) \quad (48)$$

where C_A is assumed to be the number of carbon atoms per square centimeter of the carbon lattice and h is Planck's constant. Thus, the desorption rate is seen to be independent of the oxygen concentration; that is, zero order with respect to the oxygen consideration.

For a fixed fuel particle size whether the fuel consumption rate is controlled by the diffusional or chemical rate is a matter of the temperature range. Since the diffusion rate is essentially independent of temperature and Eqs. (47) and (48) show that the possible controlling chemical rates follow an exponential dependence, the overall rate of fuel consumption as a function of temperature can be represented in the form of an Arrhenius plot as shown in Fig. 2. It should be realized that the diffusional and kinetic processes in heterogeneous burning are sequential and thus it is apparent from Fig. 2 that even for a small particle, if the temperature is high enough, the kinetic rates will again become

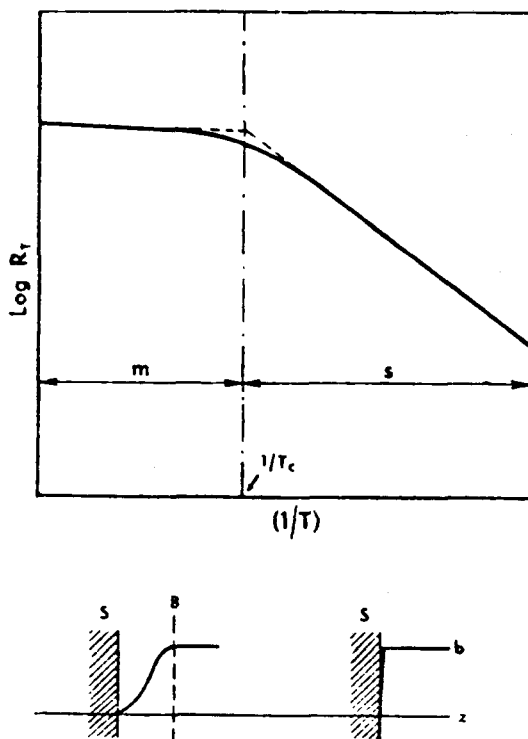


Fig. 2. Rate-controlling regimes in gas-solid reactions for an impervious solid. Where m is rate controlled by mass transfer to solid; s , rate controlled by surface reaction; S , solid; B , boundary layer; b , bulk concentration of oxidant; z , zero concentration of oxidant (after Mulcahy and Smith [16]).

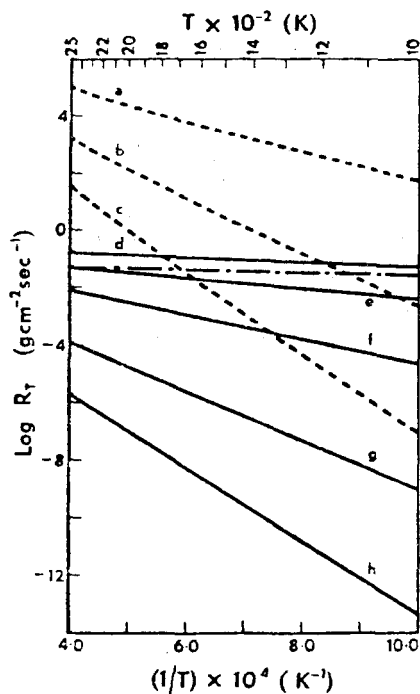


Fig. 3. Theoretical combustion rates for various mechanisms of rate control. R_{MT} , (-----) ($40 \mu\text{m}$ particle); $R_{\text{Chem,ads}}$, (—); $R_{\text{Chem,Des}}$, (-----). E (kcal/mole): (a) = 20, (b) = 40, (c) = 60, (d) = 5, (e) = 10, (f) = 20, (g) = 40, (h) = 60 (after Mulcahy and Smith [16]).

faster than the diffusion rates. Shown in Fig. 2 are also the oxygen concentration profiles for each case controlling.

Mulcahy and Smith [16] have shown how the transition temperature is determined for $40 \mu\text{m}$ particle burning at one atom presence under an oxygen partial pressure of 0.1 atm. These results are shown in Fig. 3 and the chemical rates are those represented by Eqs. (47) and (48). Figure 3 reveals that the particle burning rate is controlled chemically when $E_{\text{ads}} \geq 10$ kcal/mole. It is also interesting to note that for $E_{\text{ads}} < 5$ kcal/mole mass transfer to a $40 \mu\text{m}$ particle is unable to sustain the maximum chemical rate. For $E_{\text{ads}} = 40$ and 60 kcal/mole, the transition from chemical to mass transfer control takes place at 1150 and 1700 K, respectively.

Thus, if the true E_{act} for the reaction is greater than a few kilocalories per mole, the observation (or assumption) of first-order kinetic is compatible only with chemical control in the range of particle sizes found in pulverized coal.

Since the mass diffusion rate varies inversely with the particle radius and the chemical rate is independent of diameter, the temperature at which the transition from one to the other takes place is a function of the particle size. A graphical representation of this approach [16] is given in Fig. 4. Considering

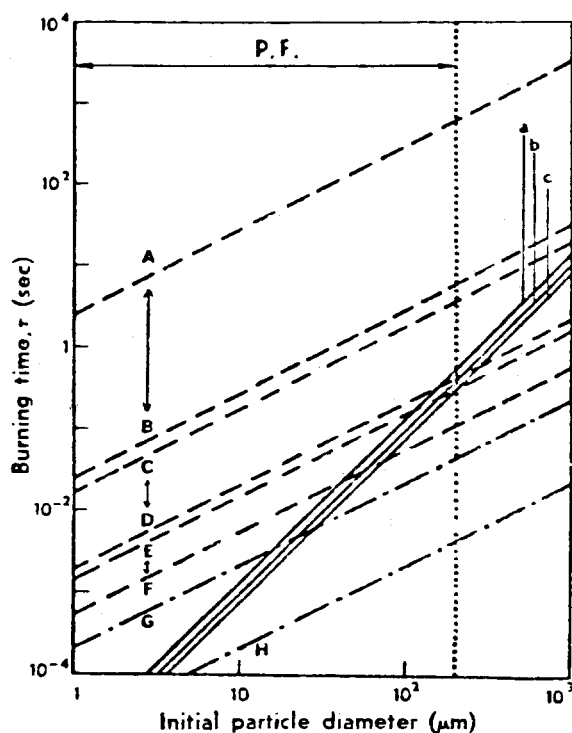


Fig. 4. Theoretical particle burning times showing effects of particle diameter, temperature, and pressure (after Mulcahy and Smith [16]).

	T (K)	E (kcal/mole)	P (atm)
A	1000	20	1
B	2000	20	1
C	1000	10	1
D	2000	10	1
E	1000	5	1
F	2000	5	1
G	2000	10	10
H	2000	10	100

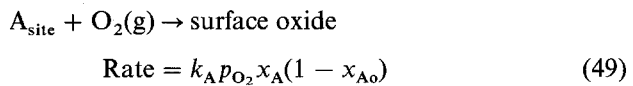
Solid lines indicate mass transfer control, all pressures; (a) 1000K; (b) 1600 K; (c) 2000 K.

that the pulverized coal particle range ends at $200 \mu\text{m}$, one will note from Fig. 4 that pulverized coal particles have their rate of burning controlled by heterogeneous oxidation kinetics.

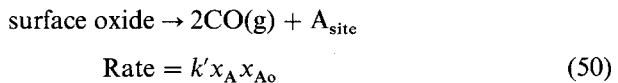
Inherent in the developments given is the assumption that all adsorption sites lead to a product oxide. In particular consideration of the heterogeneous oxidation of coal char or soot particles, it is most apparent not all sites are reactive or have the same reactivity. In an effort to obtain a more detailed

analysis of the burning rates of such materials as a function of temperature, Appleton [17] proposed a mechanism that leads to the development of the semi-empirical correlation of Nagle and Strickland-Constable [18]. In this mechanism of surface oxidation it is assumed that there are two types of reaction sites in the exposed area of the particle; namely an A site, which is reactive, and a B site, which is much less reactive. The fraction of the surface covered by A sites is assumed to be x and the remaining fraction $(1 - x)$ is assumed to be covered by B sites.

It is proposed that a steady-state fraction of the A sites are covered by a surface oxide and that this fraction, x_{A_0} , is given by a balance between the rate of activated adsorption of oxygen from the gas phase on the A sites to produce the surface oxide, i.e.,



and the rate of activated desorption of CO from the surface, i.e.,



It follows then

$$k_A p_{\text{O}_2} x_A (1 - x_{A_0}) = k' x_{A_0} \quad (51)$$

which gives

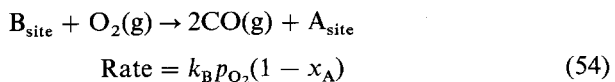
$$x_{A_0} = (k_A p_{\text{O}_2}) / (k' + k_A p_{\text{O}_2}) \quad (52)$$

Therefore, the rate at which carbon leaves the surface is given by the substitution of Eq. (52) into Eq. (50) to yield

$$\text{Rate} = x_A [k_A p_{\text{O}_2} / (1 + k_z p_{\text{O}_2})] \quad (53)$$

where $k_z = (k_A/k')$.

The model further assumes that oxygen reacts with B sites in a slow endothermic first-order reaction to yield an A site and CO which is then desorbed from the surface, i.e.,



Finally, it is assumed that A sites undergo a slow process of active thermal rearrangement to yield B sites, i.e.,



For a steady-state value of x_A , one obtains

$$x_A = [1 + (k_T/p_{O_2}k_B)]^{-1} \tag{56}$$

and the overall specific surface reaction rate is then given by

$$(w/MW_C) = x_A[k_A p_{O_2}/(1 + k_z p_{O_2})] + k_B p_{O_2}(1 - x_A) \tag{57}$$

where w is the specific reaction rate and MW_C is the atomic weight of carbon-12. This expression is the semi-empirical correlation developed by Nagle and Strickland-Constable [18].

Nagle and Strickland-Constable [18] chose the following values for the rate constants:

$$k_A = 20 \exp(-30/RT) \text{ (gm cm}^{-2} \text{ sec}^{-1} \text{ atm}^{-1}\text{)}$$

$$k_B = (4.46)10^{-3} \exp(-15.2/RT) \text{ (gm cm}^{-2} \text{ sec}^{-1} \text{ atm}^{-1}\text{)}$$

$$k_T = (1.51)10^{-5} \exp(-97/RT) \text{ (gm cm}^{-2} \text{ sec}^{-1}\text{)}$$

$$k_z = 21.3 \exp(4.1/RT) \text{ (atm}^{-1}\text{)}$$

where all activation energies are in kilocalories per mole. Their results are depicted in Fig. 5 and have served as the standard for comparison of experimental burning rates of small carbonaceous particles including soot.

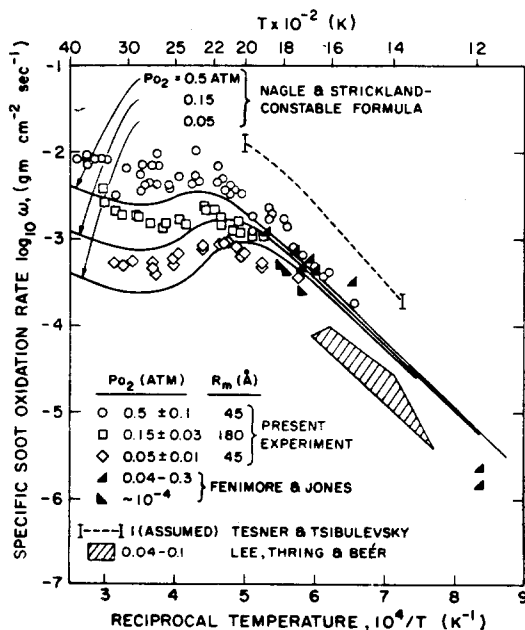


Fig. 5. Log of specific soot oxidation rate measurements versus reciprocal temperature and oxygen partial pressure (after Appleton [17]).

Using the values chosen by Nagle and Strickland-Constable, it is possible to explain the trends given in Fig. 5. One observes that at low temperatures $k_T \rightarrow 0$ and $x_A \rightarrow 1$ and for low O_2 partial pressure,

$$\dot{w} \cong (2.4)10^2 p_{O_2} \exp(-30/RT)$$

At high O_2 partial pressures, $x \rightarrow 1$ and the second term of Eq. (57) approaches zero and the rate becomes zero order with respect to p_{O_2} ;

$$\dot{w} \cong 11.3 \exp(-34/RT)$$

At even higher temperatures where thermal rearrangements produce an increasing number of B sites and

$$x_A = (3)10^{-8} p_{O_2} \exp(81.8/RT)$$

which means that the apparent activation energy of the A site oxidation term in the rate equation changes sign and value with the net result that for a fixed p_{O_2} , the rate decreases with increasing temperature. At still higher temperatures the A site oxidation term in the rate equation becomes negligibly small by comparison with the B site term and again the rate begins to increase with temperature for the k_B term takes over to give

$$\dot{w} = (5.35)10^{-2} p_{O_2} \exp(-15.2/RT)$$

D. THE BURNING OF POROUS CHARs

Real coal particles have pores and thus are not like the ideal carbon particles discussed in the last sections. Indeed, one could analyze the pore situation by assuming that pores give increased surface area to the particle. Of course, if diffusion rates to the particle are controlling, then the surface area of the particle does not play a significant role. What does play a role is the rate at which the oxygen reaches the surface, i.e., the molecular or convective diffusion rate as discussed.

Physically it is better to consider a large surface area particle as one that has a great deal of pores. However, one can use physical arguments to distinguish between ranges of applicability when there are deep pores and a large, rough external surface area. Following the pore concept, it must be realized that there is penetration of oxygen into these pores, and the reaction or depletion of carbon takes place within these pores as well.

Consider now, as Knorre *et al.* [19] have, the situation in which diffusion to the particle is sufficiently fast that it is not the controlling rate. For the porous medium, carbon is being consumed within the pores as well as on the surface. The surface consumption rates are therefore controlled by the kinetic

rates; however, the consumption rates in the pores are controlled by the diffusion of oxygen into the pore. Thus the mass consumption rate of oxygen in terms of a flux of oxygen must be that which is consumed at the surface and that which diffused into the pores

$$G_{\text{ox}} = k(C_{\text{O}_2})_s + D_i(\partial C_{i,\text{O}_2}/\partial n)_s \quad (58)$$

where D_i is the internal diffusion coefficient and C_{i,O_2} the oxygen concentration within the particle.

Following a convention established earlier, this equation is written in the form

$$G_{\text{ox}} = k(C_{\text{O}_2})_s + D_i(\partial C_{i,\text{O}_2}/\partial n)_s = k'(C_{\text{O}_2})_s \quad (59)$$

The easiest manner to consider the problem is that the pore is one of spherical symmetry and thus the internal oxygen diffusion process is described by the equation

$$D_i \left(\frac{d^2 C_i}{dr^2} + \frac{2}{r} \frac{dC_i}{dr} \right) - q_{\text{O}_2} = 0 \quad (60)$$

where q_{O_2} is the oxygen requirement (consumption) rate per unit particle volume.

It is possible to express the quantity q_{O_2} as

$$q_{\text{O}_2} = k S_i C_i \quad (61)$$

where S_i is the internal surface area in a unit particle volume m^2/m^3 which for a very porous particle would approximate the total surface area per unit volume.

The solution of Eq. (60) in terms of the expression as given in Eq. (59) results in the following expression for k' :

$$k' = k + \lambda D_i [\coth(\lambda R) - 1/\lambda R] \quad (62)$$

where R is the particle radius and

$$\lambda = (S_i k)^{1/2} / D_i \quad (63)$$

For the case of small values of λR ($\lambda R < 0.55$) which physically is representative of burning at low temperatures or the burning of small particles, the $\coth(\lambda R)$ can be expanded into a series in which only the first two terms can be considered significant, i.e.,

$$\coth(\lambda R) \cong (1/\lambda R) + (\lambda R/3) \quad (64)$$

Substituting Eq. (64) in (62), one obtains

$$k' = k \{1 + (S_i R/3)\} \quad (65)$$

This expression then is the rate constant when the inner surface of the pores participate.

If the second term in the parenthesis of Eq. (65) is small compared to unity, i.e., if the internal surface area is small with respect to the external surface area of the particle, then

$$k' = k \quad (66)$$

Since S_i can be a very large number, tens of thousands of m^2/m^3 , the condition $(S_i/R/3) < 1$ may be satisfied only for very small particles which have radii of the order of tens of microns. Physically one would not expect that for very small particles there would be a large internal surface area compared to an external surface.

For large values of λR which correspond to high temperatures and large particles

$$\coth(\lambda R) \approx 1 \quad (67)$$

and Eq. (67) becomes

$$k' = k + (S_i D k)^{1/2} \quad (68)$$

As the temperature increases, the first term in Eq. (68) increases more rapidly than the second because the temperature dependency is only in k . Therefore at high temperatures

$$k' = k \quad (69)$$

which simply means that the oxygen is completely consumed at the external surface. For moderate temperatures, it is found that

$$k' \approx (S_i D_i k)^{1/2} \quad (70)$$

or

$$k'/k \approx (S_i D_i/k)^{1/2} \quad (71)$$

$S_i D_i/k$ is a dimensionless number which arises in diffusional kinetics problems. In reality the best form for k' is Eq. (70), since Eq. (59) may now be written as

$$G_{\text{ox}} \approx (S_i D_i k)^{1/2} (C_{\text{O}_2})_s \approx (S_i D_i k)^{1/2} C_{\infty} \quad (72)$$

because external diffusion is fast and thus $(C_{\text{O}_2})_s \approx C_{\infty}$.

To this point the limit conditions have been handled but one can make some experimental headway by recalling Eq. (6),

$$G_{\text{ox}} = (k h_D / (k + h_D)) C_{\infty} = K C_{\infty} \quad (73)$$

and Eq. (7)

$$K = k h_D / (k + h_D) \quad (74)$$

But, more generally for the possible porous problem, Eq. (74) can be written as

$$K = k'h_D/(k' + h_D)$$

where k' can take the values

$$\begin{aligned} k' &= k[1 + (S_1R/3)] && \left\{ \begin{array}{l} \text{low temperature} \\ \text{or small particles} \end{array} \right. \\ &= k(\text{high temperature}) && \left\{ \begin{array}{l} \text{all particles} \end{array} \right. \\ &= k + (S_1D_1k)^{1/2} && \left\{ \begin{array}{l} \text{high temperatures and} \\ \text{large porous particles} \end{array} \right. \\ &= (S_1D_1k)^{1/2} && \left\{ \begin{array}{l} \text{moderate temperatures and} \\ \text{large porous particles} \end{array} \right. \end{aligned}$$

according to the various limit conditions defined.

E. THE BURNING RATE OF ASH-FORMING COAL

Some coals contain an ash in addition to carbon, moisture, and volatiles. To obtain a conservative estimate one should assume that a porous ash shell is retained during the burning of the combustible material. This ash may, of course, have a catalytic effect on the heterogeneous carbon combustion reactions but it is a cause, however, for additional diffusion resistance.

It is apparent that this shell offers great resistance to oxygen diffusion from the free stream to reach the combustible material. It does not matter whether the oxygen actually diffuses to the carbonaceous surface. The actual mechanism by which the carbonaceous material is consumed is probably very much like that for the pure carbon particle except that the CO to CO₂ conversion is largely heterogeneous. In this problem, diffusion of oxygen to the particle is very much faster than diffusion through the ash; hence, one can assume that the oxygen concentration at the edge of the shell is the same as the atmospheric concentration. The oxygen (or CO₂) concentration at the fuel surface approaches zero.

As a first approximation and realizing from the previous discussion that it does not matter whether O₂ or CO₂ gets to the surface, one can assume that a simple linear oxygen gradient determines the oxygen flux. Since it is not a convective problem, one can write a simplified expression as

$$G_{\text{ox}} = D_1(C_{\text{O}_2, \infty}/x) \quad (75)$$

where x is the thickness of the ash as shown in Fig. 6, and D_1 is a diffusion coefficient through the ash.

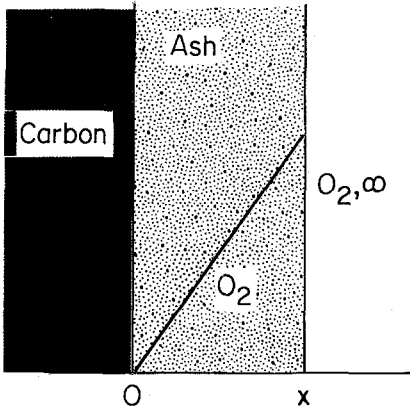


Fig. 6. Thickness of ash shell in diffusion combustion of high-ash fuel.

The fuel recedes at a rate dx/dt and is related to the oxygen flux by the expression

$$G_{O_2} = (\rho_C/i)(dx/dt) \quad (76)$$

where ρ_C is the density of the carbonaceous material and i the mass stoichiometric index. Thus at any given instant

$$(\rho_C/i)(dx/dt) = D_i C_{O_2, \infty} / x \quad (77)$$

If one takes $x = 0$ at $t = 0$, the solution of Eq. (77) is

$$x = \{(2D_i C_{O_2, \infty} i / \rho_C) t\}^{1/2} \quad (78)$$

Substituting in Eq. (75)

$$G_{O_2} = (D_i C_{O_2, \infty} \rho_C / i)^{1/2} (1/t)^{1/2} \quad (79)$$

or

$$G_f \sim (C_{O_2, \infty})^{1/2} \quad (80)$$

It is not such a surprising solution that the oxygen flux decreases or that the consumption of fuel decreases with time as the ash thickness increases. What one obtains, however, is the inverse square root dependency with time and the square root dependency with concentration. Thus for an ash-forming fuel in which ash remains firm throughout the combustion process, the burning rate is proportional to the square root of the oxygen concentration and is independent of the convective nature of the oxidizer stream.

For nonash-forming coals, the burning rate according to Eq. (19) is

$$G_f \sim \ln(1 + im_{O_2}) \quad (81)$$

However, the mass fraction of oxygen in air is 0.23 and i is 0.75, and the product is 0.172. Thus im_{O_2} is small compared to 1 and

$$G_f \sim m_{O_2, \infty} \sim C_{O_2, \infty} \quad (82)$$

i.e., the burning rate is directly proportional to the oxygen concentration.

PROBLEMS

1. Consider a spherical metal particle that is undergoing a high-temperature surface oxidation process. The product of this reaction is a nonvolatile oxide that immediately dissolves in the metal itself. The surface reaction and oxide dissolving rates are very fast compared to the oxidizer diffusion rate. Calculate an expression for the burning rate of this metal.
2. Calculate the value of the transfer number for silicon combustion in air. Show all the stoichiometric relationships in the calculation.
3. A carbon particle is large enough so that the burning rate is diffusion controlled. In one case the carbon monoxide leaving the surface burns to carbon dioxide in the gas phase; in another, no further carbon monoxide combustion takes place. Is the burning rate of the particle different in the two cases? If so, which is larger? Explain.

REFERENCES

1. Glassman, I., Am. Rocket Soc. Preprint 938-59 (November 1959).
2. Glassman, I., in "Solid Propellant Rocket Research, ARS Progress in Astronautics and Rocketry," Vol. 1, p. 253, Academic Press, New York, 1960.
3. Brzustowski, T. A., Ph.D. Thesis, Dept. of Aero. Eng., Princeton Univ., Princeton, New Jersey (1963).
4. Coffin, K. P., NACA TN 3332 (1954); Coffin, K. P., and Brokaw, R. S., NACA TN 3929 (1957).
5. Harrison, P. L., *Int. Symp. Combust.*, 7th, p. 931, Rhenhold, New York, 1959.
6. Talley, C. P., *Aerosp. Eng.* **18**, 37 (1959).
7. Mellor, A. M., and Glassman, I., *Pyrodynamics* **3**, 43 (1965).
8. Sullivan, H. F., and Glassman, I., *Combust. Sci. Technol.* **4**, 241 (1972).
9. Macek, A., *Int. Symp. Combust.*, 11th, p. 203, Combustion Inst., Pittsburgh, Pennsylvania, 1967.
10. Grosse, A. V., and Conway, J. B., *Ind. Eng. Chem.* **50**, 663 (1958).
11. Frank-Kamenetskii, D. A., "Diffusion and Heat Exchange in Chemical Kinetics," Chapter II, Princeton Univ. Press, Princeton, New Jersey, 1955.
12. Blackshear, P. L., Jr., "An Introduction to Combustion," Chapter V, Dept. of Mech. Eng., Univ. of Minnesota, Minneapolis, Minnesota, 1960.
13. Dyer, F. L., Naegeli, D. W., and Glassman, I., *Combust. Flame* **17**, 270 (1971).
14. Glassman, I., Williams, F. A., and Antaki, P., *Int. Symp. Combust.*, 20th, p. 2057, Combustion Inst., Pittsburgh, Pennsylvania, 1985.

15. King, M. K., *J. Spacecr. Rockets* **19**, 294 (1982).
16. Mulcahy, M. F. R., and Smith, I. W., *Rev. Pure Appl. Chem.* **19**, 81 (1969).
17. Appleton, J. P., Conf. Proc. AGARD Propulsion and Energetics Panel, 41st, AGARD/NATO, Paris, 1973.
18. Nagle, J., and Strickland-Constable, R. F., *Proc. Carbon Conf.*, 5th, **1**, 154 (1962).
19. Knorre, G. F., Aref'yev, K. M., and Blokh, A. G., "Theory of Combustion Processes," Chapter 24, WPAFB Report FTD-HT-23-495-68, Wright-Patterson Air Force Base, Ohio, 1968.

Appendixes

The data presented in the appendixes that follow are provided as a convenience to assist in solving some of the problems in the text, to meet preliminary research needs, to make rapid estimates in evaluating physical concepts, etc. Such data are constantly appearing in the literature and thus those presented are subject to change. Although judgment was used in selecting the data, it is important to note further that those presented are not the result of a critical survey. The reader is cautioned to use the data with care and to seek out original sources when a given datum value is crucial to a research result.

Thermochemical Data and Conversion Factors

The thermochemical data for the chemical compounds which follow in this appendix are extracted directly from the JANAF tables. The compounds chosen from the numerous ones given are those believed to be most frequently used and those required to solve some of the problem sets given in Chapter 1. Since cgs units have been used in the JANAF tables, these units were chosen as the standard throughout. Conversion to SI units is readily accomplished by use of the Table 1 in this appendix. Table 2 contains the thermochemical data.

The ordered listing of the chemical compounds in Table 2 is the same as that in the JANAF tables and is alphabetical according to the chemical formula with the lowest order letter in the formula determining the position. The thermochemical tables have the following order:

BHO₂ (metaboric acid)
BO (boron monoxide)
B₂O₃ (boron oxide)
C graphite (carbon)
CH₄ (methane)
CO (carbon monoxide)
CO₂ (carbon dioxide)
C₂H₄ (ethene)
H (hydrogen atom)
OH (hydroxyl)
HO₂ (hydroperoxyl)
H₂ (hydrogen)
H₂O (water)

NH_3 (ammonia)
 N (nitrogen atom)
 NO (nitric oxide)
 NO^+ (nitric oxide ion)
 NO_2 (nitrogen dioxide)
 N_2 (nitrogen)
 O (oxygen atom)
 O_2 (oxygen)
 O_3 (ozone)
 SO (sulfur monoxide)
 SO_2 (sulfur dioxide)
 SO_3 (sulfur trioxide)
 S (sulfur)

The reader should refer to the original tables for the reference material on which the thermochemical data are based. The reference state used in Chapter 1 was chosen as 298 K; consequently, the thermochemical values at this temperature are underlined and the reference heat of formation of the compound is determined from this listing. The logarithm of the equilibrium constant is to the base 10.

Detailed data on the higher-order hydrocarbons are not presented. Such data are obtained readily from NBS Circular C 461, "Selected Values of Properties of Hydrocarbons," 1947 or from the more recent work of Stull and co-workers, Stull, D. R., Westrum, E. F., Jr., and Sinke, G. C., "The Chemical Thermodynamics of Organic Compounds," Wiley, New York, 1969. Burcat ["Thermochemical Data for Combustion Calculations" in "Combustion Chemistry," (W. C. Gardener, Jr., Ed., Chapter 8. Wiley, New York, 1984)] discusses in detail the various sources of thermochemical data and their adaptation for computer usage.

TABLE 1

Conversion factors in SI units

$1 \text{ J} = 1 \text{ W sec} = 1 \text{ N m} = 10^7 \text{ erg}$
$1 \text{ cal} = 4.1868 \text{ J}$
$1 \text{ cal/g K} = 1 \text{ kcal/kg K} = 4.18669 \text{ kJ/kg K}$
$1 \text{ N} = 1 \text{ kg m/sec}^2 = 10^5 \text{ dyn}$
$1 \text{ Pa} = 1 \text{ N/m}^2$
$1 \text{ atm} = 1.0132 \times 10^5 \text{ N/m}^2$
$1 \text{ bar} = 10^5 \text{ N/m}^2 = 10^5 \text{ Pa}$
$g_c = \text{gravitational acceleration conversion factor}$ $= 1 \text{ kg m/(N sec}^2)$
$R = \text{universal gas constant} = 8.314 \text{ J/(g mol K)}$
$\sigma = \text{Stefan-Boltzmann constant} = 5.6697 \times 10^{-8} \text{ W/(m}^2 \text{ K}^4)$

TABLE 2
Thermochemical data of selected chemical compounds
Metaboric acid (HBO_2) (ideal gas) mol. wt. = 43.828

T. °K.	cal. mole ⁻¹ deg. ⁻¹			kcal. mole ⁻¹			Log K _p
	C _p	S°	-(F°-H° ₂₉₈)/T	H°-H° ₂₉₈	ΔH _f °	ΔF _f °	
0	.000	.000	INFINITE	- 2.554	- 133.175	- 133.175	INFINITE
100	7.984	47.787	65.377	- 1.759	- 133.478	- 132.878	200.390
200	8.816	53.517	58.155	- .928	- 133.709	- 132.196	144.450
298	10.094	57.273	57.273	.000	- 134.000	- 131.395	96.310
300	10.118	57.334	57.273	.019	- 134.006	- 131.379	95.705
400	11.366	60.420	57.486	1.094	- 134.311	- 130.457	71.275
500	12.466	63.078	58.504	2.287	- 134.611	- 129.459	56.584
600	13.402	65.436	59.466	3.582	- 134.896	- 128.401	46.768
700	14.189	67.562	60.474	4.962	- 135.161	- 127.297	39.742
800	14.851	69.502	61.483	6.415	- 135.404	- 126.159	34.463
900	15.414	71.284	62.474	7.929	- 135.626	- 124.989	30.350
1000	15.895	72.934	63.438	9.495	- 135.831	- 123.795	27.054
1100	16.311	74.469	64.372	11.106	- 136.026	- 122.583	24.354
1200	16.671	75.904	65.274	12.756	- 136.210	- 121.351	22.100
1300	16.986	77.251	66.144	14.439	- 136.390	- 120.106	20.191
1400	17.260	78.520	66.983	16.151	- 136.566	- 118.847	18.552
1500	17.501	79.719	67.793	17.890	- 136.742	- 117.575	17.130
1600	17.713	80.856	68.574	19.651	- 136.920	- 116.292	15.884
1700	17.901	81.935	69.328	21.432	- 137.100	- 114.996	14.783
1800	18.066	82.963	70.057	23.230	- 137.284	- 113.696	13.803
1900	18.214	83.944	70.763	25.044	- 137.471	- 112.376	12.926
2000	18.345	84.882	71.445	26.872	- 137.659	- 111.051	12.135
2100	18.462	85.779	72.107	28.713	- 137.851	- 109.713	11.417
2200	18.567	86.641	72.748	30.564	- 138.047	- 108.370	10.765
2300	18.661	87.468	73.370	32.426	- 138.246	- 107.017	10.168
2400	18.748	88.264	73.974	34.296	- 138.451	- 105.652	9.620
2500	18.822	89.031	74.561	36.175	- 138.660	- 104.276	9.107
2600	18.892	89.771	75.132	38.060	- 138.876	- 102.876	8.622
2700	18.955	90.485	75.688	39.953	- 139.093	- 101.468	8.172
2800	19.012	91.175	76.228	41.851	- 139.320	- 99.954	7.755
2900	19.065	91.843	76.755	43.755	- 139.559	- 98.426	7.364
3000	19.113	92.490	77.269	45.664	- 139.805	- 96.899	7.000
3100	19.156	93.118	77.770	47.577	- 140.052	- 95.364	6.659
3200	19.197	93.727	78.260	49.495	- 140.304	- 92.821	6.339
3300	19.234	94.318	78.737	51.417	- 140.560	- 91.268	6.037
3400	19.268	94.893	79.204	53.342	- 140.825	- 89.711	5.753
3500	19.300	95.452	79.660	55.270	- 141.095	- 88.149	5.485
3600	19.329	95.996	80.107	57.202	- 141.366	- 86.575	5.231
3700	19.356	96.526	80.543	59.136	- 141.640	- 84.997	4.991
3800	19.381	97.042	80.971	61.073	- 141.915	- 83.408	4.762
3900	19.404	97.546	81.389	63.012	- 142.195	- 81.813	4.546
4000	19.426	98.038	81.799	64.954	- 142.475	- 80.213	4.322
4100	19.447	98.518	82.201	66.897	- 142.755	- 78.600	4.106
4200	19.466	98.986	82.595	68.843	- 143.035	- 76.975	3.893
4300	19.483	99.445	82.982	70.790	- 143.315	- 75.342	3.682
4400	19.500	99.893	83.361	72.739	- 143.595	- 73.694	3.472
4500	19.516	100.331	83.733	74.690	- 143.875	- 72.035	3.262
4600	19.530	100.760	84.099	76.643	- 144.155	- 70.362	3.052
4700	19.544	101.180	84.458	78.596	- 144.435	- 68.675	2.842
4800	19.557	101.592	84.810	80.551	- 144.715	- 66.975	2.632
4900	19.569	101.995	85.157	82.508	- 144.995	- 65.262	2.422
5000	19.581	102.391	85.498	84.465	- 145.275	- 63.535	2.212
5100	19.592	102.770	85.833	86.424	- 145.555	- 61.795	1.995
5200	19.602	103.159	86.162	88.384	- 145.835	- 60.045	1.775
5300	19.612	103.533	86.487	90.344	- 146.115	- 58.285	1.555
5400	19.621	103.899	86.806	92.306	- 146.395	- 56.515	1.335
5500	19.630	104.260	87.120	94.268	- 146.675	- 54.735	1.115
5600	19.638	104.613	87.429	96.232	- 146.955	- 52.945	0.895
5700	19.646	104.961	87.734	98.196	- 147.235	- 51.135	0.675
5800	19.654	105.303	88.034	100.161	- 147.515	- 49.305	0.455
5900	19.661	105.639	88.329	102.127	- 147.795	- 47.455	0.235
6000	19.668	105.969	88.620	104.093	- 148.075	- 45.585	0.015

(continues)

TABLE 2 (continued)

Thermochemical data of selected chemical compounds
Boron Monoxide (BO) (ideal gas) GF_W = 26.8104

T, °K	gibbs/mol			kcal/mol			Log K _p
	C _p ^o	S ^o	-(G ^o -H ^o _{298})/T	H ^o -H ^o _{298}	ΔH _F ^o	ΔG _F ^o	
0	.000	.000	INFINITE	- 2.073	- .744	- .744	INFINITE
100	6.956	41.001	54.794	- 1.379	- .403	- 2.425	5.300
200	6.958	45.824	49.241	- .684	- .135	- 4.560	4.983
298	6.978	48.604	48.604	.000	.000	- 6.768	4.961
300	6.979	48.647	48.604	.013	.001	- 6.810	4.961
400	7.068	50.665	48.879	.715	.026	- 9.087	4.965
500	7.230	52.259	49.401	1.429	.038	- 11.359	4.965
600	7.427	53.594	49.991	2.162	.158	- 13.612	4.958
700	7.627	54.754	50.596	2.914	.311	- 15.842	4.956
800	7.810	55.785	51.176	3.687	.482	- 18.051	4.951
900	7.971	56.714	51.741	4.476	.666	- 20.236	4.944
1000	8.108	57.561	52.281	5.280	.861	- 22.399	4.895
1100	8.225	58.340	52.797	6.097	1.067	- 24.544	4.876
1200	8.324	59.060	53.289	6.924	1.283	- 26.668	4.857
1300	8.408	59.729	53.756	7.761	1.508	- 28.774	4.837
1400	8.480	60.355	54.208	8.606	1.743	- 30.862	4.818
1500	8.542	60.942	54.638	9.457	1.988	- 32.935	4.799
1600	8.595	61.495	55.049	10.314	2.243	- 34.989	4.779
1700	8.641	62.018	55.444	11.175	2.507	- 37.028	4.760
1800	8.682	62.513	55.823	12.042	2.780	- 39.051	4.741
1900	8.717	62.983	56.188	12.912	3.061	- 41.058	4.723
2000	8.749	63.431	56.539	13.785	3.347	- 43.051	4.704
2100	8.777	63.859	56.877	14.661	3.638	- 45.028	4.686
2200	8.803	64.268	57.204	15.540	3.935	- 46.992	4.668
2300	8.826	64.660	57.520	16.422	4.236	- 48.948	4.651
2400	8.847	65.036	57.825	17.305	4.544	- 50.879	4.633
2500	8.866	65.397	58.121	18.191	4.858	- 52.696	4.607
2600	8.884	65.745	58.407	19.079	5.155	- 54.388	4.572
2700	8.901	66.081	58.685	19.968	5.461	- 56.067	4.538
2800	8.917	66.405	58.955	20.859	5.772	- 57.737	4.507
2900	8.932	66.718	59.218	21.751	6.083	- 59.391	4.476
3000	8.947	67.021	59.473	22.645	6.396	- 61.039	4.447
3100	8.961	67.315	59.721	23.541	6.710	- 62.677	4.419
3200	8.976	67.599	59.963	24.438	7.023	- 64.303	4.392
3300	8.990	67.876	60.198	25.336	7.338	- 65.918	4.366
3400	8.004	68.144	60.428	26.236	7.653	- 67.525	4.340
3500	8.018	68.406	60.652	27.137	7.969	- 69.125	4.316
3600	9.032	68.660	60.871	28.039	8.286	- 70.711	4.293
3700	9.047	68.908	61.085	28.943	8.603	- 72.291	4.270
3800	9.063	69.149	61.294	29.849	8.920	- 73.860	4.248
3900	9.079	69.385	61.499	30.756	9.237	- 75.427	4.227
4000	9.096	69.615	61.699	31.664	9.554	- 77.000	4.208
4100	9.113	69.840	61.894	32.575	9.871	- 78.567	3.907
4200	9.131	70.059	62.086	33.487	10.188	- 80.133	3.734
4300	9.150	70.274	62.274	34.401	10.505	- 81.698	3.569
4400	9.170	70.485	62.458	35.317	10.822	- 83.268	3.412
4500	9.191	70.691	62.639	36.235	11.139	- 84.847	3.261
4600	9.212	70.894	62.816	37.155	11.456	- 86.422	3.117
4700	9.235	71.092	62.990	38.078	11.772	- 88.000	2.979
4800	9.258	71.287	63.161	39.002	12.088	- 89.577	2.846
4900	9.283	71.478	63.329	39.929	12.403	- 91.158	2.719
5000	9.308	71.666	63.494	40.859	12.718	- 92.742	2.597
5100	9.334	71.850	63.656	41.791	13.033	- 94.330	2.479
5200	9.361	72.032	63.815	42.726	13.348	- 95.920	2.367
5300	9.389	72.210	63.972	43.663	13.663	- 97.512	2.258
5400	9.418	72.386	64.126	44.604	13.978	- 99.107	2.153
5500	9.448	72.559	64.278	45.547	14.293	- 100.705	2.052
5600	9.478	72.730	64.427	46.493	14.608	- 102.305	1.954
5700	9.509	72.898	64.574	47.443	14.923	- 103.908	1.860
5800	9.541	73.063	64.719	48.395	15.238	- 105.514	1.769
5900	9.573	73.227	64.862	49.351	15.553	- 107.122	1.681
6000	9.606	73.388	65.003	50.310	15.868	- 108.732	1.596

TABLE 2 (continued)

Thermochemical data of selected chemical compounds
 Boron Monoxide, Dimeric $[(BO)_2]$ (ideal gas) mol. wt. = 53.64

T, °K.	cal. mole ⁻¹ deg. ⁻¹			kcal. mole ⁻¹			Log K _p
	C _p	S°	-(F°-H° ₂₉₈)/T	H°-H° ₂₉₈	ΔH _f °	ΔF _f °	
0	.000	.000	INFINITE	- 2.963	= 109.304	= 109.304	INFINITE
100	8.214	46.175	68,564	- 2.239	= 109.305	= 109.754	239,856
200	11.528	52,912	59,150	- 1.248	= 109.154	= 110.254	120,474
298	13.695	57,958	57,958	.000	= 109.000	= 110.833	81.239
300	13.725	58,043	57,959	.025	= 108.998	= 110.845	80.747
400	15.027	62,184	58,514	1.468	= 108.910	= 111.476	60.905
500	15.947	65.640	59,603	3.018	= 108.917	= 112.119	49.005
600	16.688	68,615	60,863	4.651	= 108.989	= 112.752	41.068
700	17.307	71,307	62,161	6.352	= 109.098	= 113.371	35.394
800	17.824	73,581	63,445	8.109	= 109.229	= 113.974	31.135
900	18.255	75,706	64,691	9.914	= 109.370	= 114.559	27.818
1000	18.613	77,649	65,891	11.758	= 109.523	= 115.126	25.160
1100	18,910	79,437	67,042	13,634	= 109,694	= 115,680	22,982
1200	19,157	81,093	68,145	15,538	= 109,876	= 116,214	21,164
1300	19,363	82,635	69,201	17,464	= 110,075	= 116,736	19,424
1400	19,537	84,077	70,213	19,410	= 110,287	= 117,240	18,301
1500	19,683	85,430	71,182	21,371	= 110,519	= 117,731	17,153
1600	19,808	86,704	72,113	23,346	= 110,767	= 118,201	16,145
1700	19,915	87,908	73,007	25,332	= 111,033	= 118,658	15,254
1800	20,007	89,049	73,867	27,328	= 111,316	= 119,099	14,460
1900	20,087	90,133	74,695	29,333	= 111,612	= 119,524	13,748
2000	20,157	91,165	75,493	31,345	= 111,918	= 119,932	13,105
2100	20,218	92,150	76,263	33,364	= 112,234	= 120,323	12,522
2200	20,271	93,092	77,006	35,389	= 112,561	= 120,701	11,990
2300	20,318	93,994	77,726	37,418	= 112,898	= 121,065	11,503
2400	20,360	94,860	78,422	39,452	= 113,246	= 121,411	11,055
2500	20,398	95,692	79,096	41,490	= 124,378	= 121,528	10,623
2600	20,431	96,493	79,750	43,532	= 124,728	= 121,408	10,205
2700	20,462	97,264	80,384	45,576	= 125,082	= 121,269	9,816
2800	20,489	98,009	81,000	47,624	= 125,437	= 121,125	9,454
2900	20,513	98,728	81,599	49,674	= 125,795	= 120,958	9,115
3000	20,535	99,424	82,182	51,726	= 126,156	= 120,789	8,799
3100	20,556	100,098	82,749	53,781	= 126,518	= 120,606	8,502
3200	20,574	100,751	83,301	55,837	= 126,884	= 120,410	8,223
3300	20,591	101,384	83,840	57,896	= 127,251	= 120,199	7,960
3400	20,606	101,999	84,365	59,956	= 127,622	= 119,979	7,712
3500	20,621	102,596	84,877	62,017	= 127,995	= 119,753	7,477
3600	20,634	103,178	85,378	64,080	= 128,370	= 119,511	7,255
3700	20,646	103,743	85,866	66,144	= 128,748	= 119,258	7,044
3800	20,657	104,294	86,344	68,209	= 129,128	= 118,994	6,843
3900	20,667	104,831	86,811	70,275	= 129,510	= 118,730	6,653
4000	20,677	105,354	87,268	72,342	= 129,893	= 118,457	6,477
4100	20,686	105,865	87,716	74,410	= 130,278	= 118,177	6,312
4200	20,694	106,363	88,154	76,479	= 130,665	= 117,891	6,156
4300	20,702	106,850	88,583	78,549	= 131,053	= 117,600	6,008
4400	20,709	107,326	89,004	80,620	= 131,442	= 117,304	5,868
4500	20,716	107,792	89,416	82,691	= 131,832	= 117,011	5,733
4600	20,722	108,247	89,820	84,763	= 132,223	= 116,713	5,602
4700	20,728	108,693	90,217	86,835	= 132,615	= 116,410	5,476
4800	20,734	109,129	90,607	88,908	= 133,008	= 116,103	5,354
4900	20,739	109,557	90,989	90,982	= 133,402	= 115,792	5,236
5000	20,744	109,976	91,365	93,056	= 133,797	= 115,477	5,121
5100	20,749	110,387	91,734	95,131	= 134,193	= 115,158	5,008
5200	20,753	110,790	92,096	97,208	= 134,590	= 114,835	4,898
5300	20,757	111,185	92,453	99,282	= 134,988	= 114,508	4,790
5400	20,761	111,573	92,803	101,357	= 135,387	= 114,177	4,684
5500	20,765	111,954	93,148	103,434	= 135,787	= 113,842	4,580
5600	20,769	112,328	93,487	105,510	= 136,188	= 113,503	4,478
5700	20,772	112,696	93,821	107,588	= 136,590	= 113,160	4,378
5800	20,775	113,057	94,149	109,665	= 136,993	= 112,814	4,279
5900	20,778	113,412	94,473	111,743	= 137,397	= 112,465	4,181
6000	20,781	113,761	94,791	113,820	= 137,802	= 112,113	4,084

(continues)

TABLE 2 (continued)

Thermochemical data of selected chemical compounds
Boron Dioxide (BO₂) (ideal gas) GFW = 42.8098

T, °K	gibbs/mol			kcal/mol			Log Kp
	Cp°	S°	-(G°-H° ₂₉₈)/T	H°-H° ₂₉₈	ΔHf°	ΔGf°	
0	.000	.000	INFINITE	- 2.565	- 68.198	- 68.198	INFINITE
100	8.060	45.089	63.300	- 1.821	- 68.154	- 68.515	149.740
200	9.208	51.007	55.810	- .961	- 68.070	- 68.910	75.301
298	10.343	54.900	54.900	.000	- 68.000	- 69.339	50.827
300	10.363	54.964	54.900	.019	- 67.999	- 69.348	50.520
400	11.351	58.085	55.319	1.106	- 67.945	- 69.806	38.140
500	12.137	60.706	56.141	2.283	- 67.912	- 70.276	30.718
600	12.730	62.974	57.095	3.527	- 67.898	- 70.750	25.771
700	13.171	64.971	58.080	4.824	- 67.895	- 71.225	22.238
800	13.501	66.752	59.055	6.158	- 67.904	- 71.702	19.588
900	13.750	68.358	60.001	7.521	- 67.921	- 72.176	17.527
1000	13.942	69.817	60.911	8.906	- 67.948	- 72.646	15.877
1100	14.091	71.153	61.782	10.308	- 67.989	- 73.115	14.527
1200	14.209	72.384	62.615	11.723	- 68.041	- 73.578	13.400
1300	14.304	73.525	63.411	13.149	- 68.106	- 74.037	12.447
1400	14.381	74.588	64.172	14.583	- 68.183	- 74.490	11.628
1500	14.444	75.583	64.899	16.025	- 68.273	- 74.939	10.919
1600	14.497	76.517	65.597	17.472	- 68.376	- 75.379	10.296
1700	14.541	77.397	66.265	18.924	- 68.491	- 75.813	9.746
1800	14.579	78.229	66.907	20.380	- 68.619	- 76.240	9.257
1900	14.611	79.018	67.524	21.839	- 68.758	- 76.660	8.818
2000	14.639	79.768	68.117	23.302	- 68.904	- 77.073	8.422
2100	14.663	80.483	68.689	24.767	- 69.059	- 77.476	8.063
2200	14.685	81.166	69.241	26.234	- 69.224	- 77.873	7.736
2300	14.704	81.819	69.774	27.704	- 69.395	- 78.264	7.437
2400	14.722	82.445	70.289	29.175	- 69.576	- 78.663	7.161
2500	14.738	83.047	70.787	30.648	- 69.752	- 78.910	6.898
2600	14.753	83.625	71.270	32.123	- 69.939	- 79.057	6.643
2700	14.768	84.182	71.738	33.599	- 70.131	- 79.195	6.410
2800	14.781	84.719	72.192	35.076	- 70.327	- 79.328	6.192
2900	14.795	85.238	72.633	36.555	- 70.525	- 79.450	5.987
3000	14.809	85.740	73.061	38.035	- 70.724	- 79.569	5.797
3100	14.823	86.226	73.478	39.517	- 70.934	- 79.681	5.618
3200	14.837	86.697	73.884	41.000	- 71.143	- 79.786	5.449
3300	14.851	87.153	74.279	42.484	- 71.355	- 79.884	5.291
3400	14.864	87.597	74.665	43.970	- 71.567	- 79.975	5.141
3500	14.882	88.028	75.040	45.458	- 71.786	- 80.064	4.999
3600	14.898	88.448	75.407	46.946	- 72.006	- 80.140	4.865
3700	14.914	88.856	75.765	48.437	- 72.227	- 80.213	4.738
3800	14.932	89.254	76.115	49.929	- 72.447	- 80.277	4.617
3900	14.950	89.642	76.456	51.423	- 72.667	- 80.343	4.502
4000	14.969	90.021	76.791	52.919	- 72.887	- 80.403	4.376
4100	14.988	90.391	77.118	54.417	- 73.107	- 80.460	4.260
4200	15.008	90.752	77.438	55.917	- 73.327	- 80.514	4.152
4300	15.029	91.105	77.752	57.419	- 73.547	- 80.565	4.051
4400	15.050	91.451	78.060	58.923	- 73.767	- 80.613	3.955
4500	15.072	91.790	78.361	60.429	- 73.987	- 80.658	3.865
4600	15.095	92.121	78.656	61.937	- 74.207	- 80.700	3.780
4700	15.117	92.446	78.946	63.448	- 74.427	- 80.739	3.700
4800	15.141	92.765	79.231	64.961	- 74.647	- 80.775	3.625
4900	15.164	93.077	79.510	66.476	- 74.867	- 80.808	3.555
5000	15.188	93.384	79.785	67.994	- 75.087	- 80.838	3.490
5100	15.213	93.685	80.054	69.514	- 75.307	- 80.865	3.425
5200	15.237	93.980	80.319	71.036	- 75.527	- 80.888	3.365
5300	15.262	94.271	80.580	72.561	- 75.747	- 80.908	3.305
5400	15.287	94.556	80.836	74.089	- 75.967	- 80.925	3.250
5500	15.312	94.837	81.088	75.618	- 76.187	- 80.939	3.200
5600	15.337	95.113	81.336	77.151	- 76.407	- 80.950	3.155
5700	15.361	95.385	81.580	78.686	- 76.627	- 80.958	3.115
5800	15.386	95.652	81.820	80.223	- 76.847	- 80.963	3.075
5900	15.411	95.915	82.057	81.763	- 77.067	- 80.965	3.035
6000	15.435	96.175	82.290	83.305	- 77.287	- 80.965	3.000

TABLE 2 (continued)

Thermochemical data of selected chemical compounds
 Boron Oxide (B_2O_3) (crystal) mol wt. = 69.64

T. °K.	cal. mole ⁻¹ deg. ⁻¹			kcal. mole ⁻¹			Log K _p
	C _p	S°	-(F°-H° ₂₉₈)/T	H°-H° ₂₉₈	ΔH _f °	ΔF _f °	
0	.000	.000	INFINITE	- 2.218	- 302.162	- 302.162	INFINITE
100	4.987	2.624	22.994	- 2.037	- 303.062	- 297.080	649.236
200	10.499	7.850	14.105	- 1.251	- 303.456	- 290.921	317.888
298	15.050	12.870	12.870	.000	- 303.640	- 284.725	208.699
300	15.140	12.963	12.870	.028	- 303.642	- 284.608	207.327
400	18.350	17.787	13.506	1.712	- 303.668	- 278.257	152.025
500	20.800	22.148	14.806	3.671	- 303.631	- 271.907	118.845
600	23.250	26.153	16.367	5.872	- 303.513	- 265.571	96.729
700	26.200	29.951	18.038	8.339	- 303.245	- 259.265	80.942
800	29.650	33.875	19.760	11.131	- 302.740	- 253.015	69.117
900	32.050	37.316	21.510	14.226	- 301.998	- 246.843	59.939
1000	33.450	40.769	23.265	17.504	- 301.130	- 240.757	52.615
1100	34.300	44.000	25.005	20.895	- 300.204	- 234.766	46.642
1200	34.700	47.003	26.714	24.347	- 299.264	- 228.857	41.479
1300	34.900	49.789	28.383	27.827	- 298.337	- 223.029	37.493
1400	35.000	52.379	30.006	31.323	- 297.432	- 217.268	33.915
1500	35.000	54.794	31.579	34.823	- 296.560	- 211.576	30.825
1600	35.000	57.053	33.101	38.323	- 295.722	- 205.936	28.128
1700	35.000	59.175	34.573	41.823	- 294.915	- 200.350	25.755
1800	35.000	61.175	35.996	45.323	- 294.138	- 194.810	23.652
1900	35.000	63.068	37.372	48.823	- 293.387	- 189.313	21.775
2000	35.000	64.863	38.702	52.323	- 292.655	- 183.855	20.090

(continues)

TABLE 2 (continued)

Thermochemical data of selected chemical compounds
 Boron Oxide (B₂O₃) (liquid) mol. wt. = 69.64

T, °K.	cal. mole ⁻¹ deg. ⁻¹			kcal. mole ⁻¹			Log K _p
	C _p	S°	-(F°-H° ₂₉₈)/T	H°-H° ₂₉₈	ΔH _f °	ΔF _f °	
0							
100							
200							
298	15.050	16.739	16.739	0.000	-209.280	-282.115	206.786
300	15.140	16.832	16.739	.028	-209.282	-282.009	205.433
400	18.350	23.656	19.175	1.712	-209.308	-276.244	190.926
500	20.800	28.017	20.675	3.671	-209.271	-270.481	118.222
600	28.600	32.354	22.248	6.064	-208.961	-264.739	96.426
700	31.700	37.060	24.091	9.120	-208.104	-259.100	80.891
800	31.950	41.375	25.642	12.313	-207.198	-253.593	68.275
900	31.650	44.068	27.494	15.493	-206.371	-248.192	60.266
1000	31.400	48.391	29.744	18.646	-205.628	-242.877	53.078
1100	31.050	51.367	31.478	21.768	-204.973	-237.637	47.212
1200	30.750	54.055	33.341	24.857	-204.394	-232.449	42.333
1300	30.600	56.510	35.030	27.924	-203.881	-227.310	38.212
1400	30.540	58.775	36.646	30.980	-203.414	-222.205	34.686
1500	30.540	60.882	38.193	34.034	-202.989	-217.137	31.635
1600	30.540	62.853	39.673	37.088	-202.596	-212.091	28.969
1700	30.540	64.705	41.091	40.143	-202.234	-207.070	26.619
1800	30.540	66.446	42.452	43.189	-201.912	-202.071	24.534
1900	30.540	68.097	43.759	46.243	-201.606	-197.088	22.669
2000	30.540	69.663	45.015	49.297	-201.320	-192.120	20.993
2100	30.540	71.153	46.224	52.351	-201.054	-187.165	19.478
2200	30.540	72.574	47.390	55.405	-200.808	-182.225	18.101
2300	30.540	73.932	48.515	58.459	-200.578	-177.297	16.846
2400	30.540	75.232	49.601	61.513	-200.367	-172.373	15.696
2500	30.540	76.479	50.652	64.567	-200.174	-167.447	14.620
2600	30.540	77.677	51.669	67.621	-200.751	-161.903	13.609
2700	30.540	78.830	52.654	70.675	-200.564	-156.565	12.672
2800	30.540	79.941	53.609	73.729	-200.384	-151.238	11.804
2900	30.540	81.013	54.536	76.783	-200.212	-145.909	10.995
3000	30.540	82.048	55.436	79.837	-200.048	-140.593	10.242
3100	30.540	83.049	56.310	82.891	-200.889	-135.281	9.537
3200	30.540	84.019	57.161	85.945	-200.738	-129.975	8.876
3300	30.540	84.959	57.989	88.999	-200.593	-124.672	8.256
3400	30.540	85.871	58.796	92.053	-200.456	-119.373	7.673
3500	30.540	86.756	59.583	95.107	-200.323	-114.084	7.123
3600	30.540	87.616	60.349	98.161	-200.196	-108.787	6.604
3700	30.540	88.453	61.097	101.215	-200.075	-103.500	6.113
3800	30.540	89.267	61.828	104.269	-200.958	-98.210	5.648
3900	30.540	90.060	62.542	107.323	-200.846	-92.936	5.208
4000	30.540	90.833	63.239	110.377	-200.098	-87.666	4.755

TABLE 2 (continued)

Thermochemical data of selected chemical compounds
Boron Oxide (B₂O₃) (ideal gas) mol wt. = 69.64

T, °K.	cal. mole ⁻¹ deg. ⁻¹			kcal. mole ⁻¹			Log K _p
	C _p	S°	-(F° - H° ₂₉₈)/T	H° - H° ₂₉₈	ΔH _f °	ΔF _f °	
0	.000	.000	INFINITE	- 3.427	- 198.870	- 198.870	INFINITE
100	9.570	54.227	86.034	- 2.581	- 199.106	- 198.284	433.328
200	13.224	61.965	69.180	- 1.443	- 199.148	- 197.436	215.738
298	15.979	67.798	67.798	.000	- 199.140	- 196.602	144.106
300	16.020	67.897	67.799	.030	- 199.140	- 196.586	143.206
400	17.861	72.774	64.451	1.729	- 199.151	- 195.735	106.939
500	19.207	76.911	69.740	3.586	- 199.217	- 194.874	85.175
600	20.272	80.510	71.241	5.561	- 199.324	- 193.995	70.659
700	21.136	83.703	72.798	7.433	- 199.451	- 193.097	60.285
800	21.846	86.573	74.343	9.784	- 199.587	- 192.182	52.499
900	22.427	89.181	75.849	11.998	- 199.726	- 191.248	46.439
1000	22.903	91.569	77.303	14.266	- 199.869	- 190.296	41.587
1100	23.295	93.771	78.702	16.576	- 200.025	- 189.333	37.615
1200	23.619	95.812	80.044	18.922	- 200.189	- 188.352	34.302
1300	23.889	97.714	81.330	21.298	- 200.366	- 187.360	31.487
1400	24.116	99.493	82.565	23.699	- 200.554	- 186.352	29.089
1500	24.307	101.163	83.750	26.120	- 200.743	- 185.332	27.002
1600	24.469	102.737	84.888	28.559	- 200.985	- 184.294	25.172
1700	24.608	104.225	85.982	31.013	- 201.224	- 183.244	23.537
1800	24.727	105.635	87.035	33.480	- 201.481	- 182.181	22.119
1900	24.830	106.975	88.049	35.958	- 201.752	- 181.101	20.830
2000	24.920	108.251	89.028	38.446	- 202.032	- 180.008	19.669
2100	24.999	109.468	89.972	40.942	- 202.323	- 178.896	18.617
2200	25.068	110.633	90.885	43.445	- 202.628	- 177.775	17.659
2300	25.129	111.749	91.766	45.955	- 202.942	- 176.640	16.784
2400	25.183	112.819	92.623	48.471	- 203.269	- 175.485	15.979
2500	25.231	113.848	93.452	50.991	- 203.603	- 174.315	15.220
2600	25.275	114.839	94.255	53.517	- 203.945	- 173.129	14.498
2700	25.313	115.793	95.035	56.046	- 204.295	- 171.924	13.829
2800	25.348	116.715	95.793	58.579	- 204.654	- 170.695	13.207
2900	25.380	117.605	96.530	61.116	- 205.022	- 169.443	12.627
3000	25.409	118.466	97.247	63.655	- 205.399	- 168.168	12.084
3100	25.435	119.299	97.945	66.197	- 205.783	- 166.871	11.576
3200	25.458	120.107	98.625	68.742	- 206.174	- 165.551	11.099
3300	25.480	120.891	99.288	71.289	- 206.572	- 164.208	10.650
3400	25.500	121.652	99.935	73.838	- 206.977	- 162.844	10.227
3500	25.518	122.391	100.566	76.389	- 207.389	- 161.458	9.827
3600	25.535	123.110	101.182	78.942	- 207.807	- 160.051	9.448
3700	25.551	123.810	101.784	81.496	- 208.231	- 158.624	9.090
3800	25.565	124.492	102.373	84.052	- 208.661	- 157.178	8.750
3900	25.578	125.156	102.949	86.609	- 209.097	- 155.713	8.427
4000	25.591	125.804	103.512	89.167	- 209.539	- 154.229	8.125
4100	25.602	126.436	104.063	91.727	- 210.000	- 152.724	7.840
4200	25.613	127.053	104.603	94.288	- 210.468	- 151.198	7.570
4300	25.623	127.656	105.132	96.850	- 210.943	- 149.651	7.313
4400	25.632	128.245	105.651	99.412	- 211.425	- 148.084	7.068
4500	25.641	128.821	106.160	101.976	- 211.914	- 146.497	6.833
4600	25.649	129.385	106.658	104.541	- 212.409	- 144.890	6.607
4700	25.657	129.936	107.148	107.106	- 212.911	- 143.263	6.390
4800	25.664	130.477	107.628	109.672	- 213.419	- 141.617	6.181
4900	25.671	131.006	108.100	112.239	- 213.934	- 139.952	5.978
5000	25.677	131.524	108.563	114.806	- 214.455	- 138.267	5.780
5100	25.683	132.033	109.018	117.374	- 214.982	- 136.562	5.587
5200	25.689	132.532	109.464	119.943	- 215.515	- 134.837	5.400
5300	25.694	133.021	109.906	122.512	- 216.054	- 133.092	5.218
5400	25.699	133.501	110.338	125.082	- 216.598	- 131.327	5.041
5500	25.704	133.973	110.764	127.652	- 217.148	- 129.542	4.869
5600	25.709	134.436	111.182	130.223	- 217.703	- 127.737	4.701
5700	25.713	134.891	111.594	132.794	- 218.264	- 125.912	4.538
5800	25.717	135.339	112.000	135.365	- 218.831	- 124.067	4.380
5900	25.721	135.776	112.399	137.937	- 219.403	- 122.202	4.227
6000	25.725	136.211	112.792	140.509	- 220.000	- 120.317	4.079

(continues)

TABLE 2 (continued)

Thermochemical data of selected chemical compounds
Carbon (C) (reference state—graphite) mol. wt. = 12.011

T, °K.	cal. mole ⁻¹ deg. ⁻¹			kcal. mole ⁻¹			Log K _p
	C _p ^o	S ^o	-(F ^o -H _{298^o})/T}	H ^o -H _{298^o}	ΔH _f ^o	ΔF _f ^o	
0	.000	.000	INFINITE	-.252	.000	.000	.000
100	.393	.210	2.591	-.238	.000	.000	.000
200	1.202	.720	1.520	-.160	.000	.000	.000
298	2.038	1.359	1.359	.000	.000	.000	.000
300	2.054	1.372	1.359	.008	.000	.000	.000
400	2.851	2.075	1.450	.250	.000	.000	.000
500	3.496	2.784	1.644	.569	.000	.000	.000
600	4.038	3.471	1.893	.947	.000	.000	.000
700	4.440	4.124	2.144	1.372	.000	.000	.000
800	4.740	4.739	2.449	1.831	.000	.000	.000
900	4.970	5.311	2.736	2.318	.000	.000	.000
1000	5.149	5.844	3.020	2.824	.000	.000	.000
1100	5.304	6.342	3.300	3.347	.000	.000	.000
1200	5.430	6.809	3.573	3.883	.000	.000	.000
1300	5.527	7.248	3.839	4.432	.000	.000	.000
1400	5.605	7.661	4.098	4.988	.000	.000	.000
1500	5.669	8.050	4.348	5.552	.000	.000	.000
1600	5.721	8.417	4.591	6.122	.000	.000	.000
1700	5.765	8.765	4.827	6.696	.000	.000	.000
1800	5.803	9.094	5.055	7.275	.000	.000	.000
1900	5.836	9.411	5.274	7.857	.000	.000	.000
2000	5.865	9.711	5.490	8.442	.000	.000	.000
2100	5.891	9.998	5.698	9.029	.000	.000	.000
2200	5.914	10.272	5.900	9.620	.000	.000	.000
2300	5.936	10.536	6.095	10.212	.000	.000	.000
2400	5.956	10.789	6.284	10.807	.000	.000	.000
2500	5.974	11.032	6.471	11.403	.000	.000	.000
2600	5.992	11.267	6.651	12.002	.000	.000	.000
2700	6.009	11.493	6.826	12.602	.000	.000	.000
2800	6.026	11.712	6.997	13.203	.000	.000	.000
2900	6.042	11.924	7.163	13.807	.000	.000	.000
3000	6.057	12.129	7.325	14.412	.000	.000	.000
3100	6.073	12.328	7.483	15.018	.000	.000	.000
3200	6.088	12.521	7.638	15.626	.000	.000	.000
3300	6.103	12.708	7.788	16.236	.000	.000	.000
3400	6.119	12.891	7.936	16.847	.000	.000	.000
3500	6.134	13.068	8.080	17.460	.000	.000	.000
3600	6.150	13.241	8.221	18.074	.000	.000	.000
3700	6.165	13.410	8.359	18.690	.000	.000	.000
3800	6.181	13.575	8.494	19.307	.000	.000	.000
3900	6.197	13.736	8.626	19.926	.000	.000	.000
4000	6.213	13.893	8.756	20.546	.000	.000	.000
4100	6.230	14.046	8.883	21.168	.000	.000	.000
4200	6.247	14.197	9.008	21.792	.000	.000	.000
4300	6.264	14.344	9.130	22.418	.000	.000	.000
4400	6.281	14.488	9.250	23.045	.000	.000	.000
4500	6.299	14.629	9.368	23.674	.000	.000	.000
4600	6.317	14.768	9.484	24.305	.000	.000	.000
4700	6.335	14.904	9.598	24.937	.000	.000	.000
4800	6.354	15.038	9.710	25.572	.000	.000	.000
4900	6.373	15.169	9.820	26.208	.000	.000	.000
5000	6.392	15.298	9.928	26.846	.000	.000	.000
5100	6.412	15.424	10.035	27.487	.000	.000	.000
5200	6.432	15.549	10.140	28.129	.000	.000	.000
5300	6.452	15.672	10.243	28.773	.000	.000	.000
5400	6.473	15.793	10.345	29.419	.000	.000	.000
5500	6.494	15.912	10.445	30.068	.000	.000	.000
5600	6.516	16.029	10.543	30.718	.000	.000	.000
5700	6.538	16.144	10.641	31.371	.000	.000	.000
5800	6.560	16.258	10.737	32.024	.000	.000	.000
5900	6.583	16.371	10.831	32.683	.000	.000	.000
6000	6.606	16.481	10.924	33.342	.000	.000	.000

TABLE 2 (continued)

Thermochemical data of selected chemical compounds
Carbon, Monatomic (C) (ideal gas) at. wt. = 12.011

T, °K.	cal. mole ⁻¹ deg. ⁻¹			kcal. mole ⁻¹			Log K _p
	C _g	S°	-(F°-H° ₂₉₈)/T	H°-H° ₂₉₈	ΔH _f °	ΔF _f °	
0	.000	.000	INFINITE	- 1.362	169.376	169.376	INFINITE
100	5.085	32.283	42.203	- .992	170.132	166.925	- 366.798
200	4.997	35.770	38.217	- .489	170.537	163.547	- 178.707
298	4.981	37.761	37.761	.000	170.686	160.033	- 117.302
300	4.981	37.792	37.761	.009	170.691	159.965	- 116.529
400	4.975	39.224	37.956	.507	171.143	156.283	- 85.385
500	4.973	40.338	38.325	1.004	171.321	152.546	- 66.675
600	4.971	41.240	38.738	1.502	171.441	148.779	- 54.190
700	4.970	42.006	39.151	1.999	171.513	144.996	- 45.268
800	4.970	42.670	39.551	2.496	171.551	141.204	- 38.574
900	4.970	43.255	39.930	2.992	171.561	137.411	- 33.366
1000	4.969	43.779	40.290	3.489	171.552	133.616	- 29.200
1100	4.969	44.253	40.629	3.986	171.525	129.824	- 25.792
1200	4.970	44.685	40.949	4.483	171.486	126.035	- 22.953
1300	4.971	45.083	41.252	4.980	171.434	122.249	- 20.551
1400	4.972	45.451	41.539	5.478	171.376	118.469	- 18.493
1500	4.975	45.794	41.811	5.975	171.309	114.692	- 16.710
1600	4.978	46.116	42.070	6.473	171.237	110.919	- 15.150
1700	4.984	46.418	42.317	6.971	171.161	107.151	- 13.775
1800	4.990	46.703	42.553	7.469	171.080	103.388	- 12.552
1900	4.998	46.973	42.779	7.969	170.998	99.631	- 11.460
2000	5.008	47.229	42.995	8.469	170.913	95.876	- 10.476
2100	5.019	47.474	43.202	8.970	170.827	92.128	- 9.587
2200	5.032	47.708	43.402	9.473	170.739	88.380	- 8.779
2300	5.046	47.932	43.594	9.977	170.651	84.641	- 8.042
2400	5.061	48.147	43.779	10.482	170.561	80.903	- 7.367
2500	5.077	48.354	43.958	10.989	170.472	77.168	- 6.746
2600	5.094	48.553	44.131	11.497	170.381	73.438	- 6.173
2700	5.112	48.746	44.298	12.008	170.292	69.710	- 5.642
2800	5.130	48.932	44.460	12.520	170.203	65.987	- 5.150
2900	5.149	49.112	44.618	13.034	170.113	62.267	- 4.692
3000	5.168	49.287	44.771	13.550	170.024	58.549	- 4.265
3100	5.187	49.457	44.919	14.067	169.935	54.836	- 3.866
3200	5.206	49.622	45.063	14.587	169.847	51.124	- 3.491
3300	5.224	49.782	45.204	15.108	169.758	47.413	- 3.140
3400	5.243	49.938	45.341	15.632	169.671	43.709	- 2.809
3500	5.261	50.091	45.474	16.157	169.583	40.003	- 2.498
3600	5.279	50.239	45.605	16.684	169.496	36.303	- 2.204
3700	5.296	50.384	45.732	17.213	169.409	32.605	- 1.926
3800	5.313	50.526	45.856	17.743	169.322	28.910	- 1.663
3900	5.329	50.664	45.978	18.275	169.235	25.217	- 1.413
4000	5.345	50.799	46.097	18.809	169.149	21.526	- 1.176
4100	5.360	50.931	46.213	19.344	169.062	17.834	- .951
4200	5.375	51.060	46.327	19.881	168.975	14.149	- .736
4300	5.388	51.187	46.438	20.419	168.887	10.462	- .532
4400	5.402	51.311	46.548	20.959	168.800	6.776	- .337
4500	5.414	51.433	46.655	21.499	168.711	3.096	- .150
4600	5.426	51.552	46.760	22.041	168.622	- .582	.028
4700	5.437	51.668	46.863	22.585	168.534	- 4.259	.198
4800	5.448	51.783	46.965	23.129	168.445	- 7.933	.361
4900	5.459	51.896	47.064	23.674	168.357	- 11.608	.518
5000	5.468	52.006	47.162	24.221	168.261	- 15.279	.668
5100	5.477	52.114	47.258	24.768	168.167	- 18.954	.812
5200	5.486	52.221	47.352	25.316	168.073	- 22.620	.951
5300	5.494	52.325	47.445	25.865	167.978	- 26.284	1.084
5400	5.502	52.428	47.536	26.415	167.882	- 29.947	1.212
5500	5.509	52.529	47.626	26.966	167.784	- 33.611	1.335
5600	5.516	52.628	47.715	27.517	167.685	- 37.272	1.455
5700	5.523	52.726	47.802	28.069	167.584	- 40.934	1.569
5800	5.529	52.822	47.888	28.621	167.481	- 44.591	1.680
5900	5.535	52.917	47.972	29.175	167.378	- 48.243	1.787
6000	5.541	53.010	48.055	29.728	167.272	- 51.901	1.890

(continues)

TABLE 2 (continued)

Thermochemical data of selected chemical compounds
Methane (CH₄) (ideal gas) mol. wt. = 16.043

T, °K.	cal. mole ⁻¹ deg. ⁻¹			kcal. mole ⁻¹			Log K _p
	C _p	S°	-(F°-H° ₂₉₈)/T	H°-H° ₂₉₈	ΔH _f °	ΔF _f °	
0	.000	.000	INFINITE	- 2.386	- 15.991	- 15.991	INFINITE
100	7.949	35.704	51.716	- 1.401	- 16.728	- 15.800	33.656
200	8.001	37.222	45.287	.805	- 17.216	- 13.509	15.188
298	8.518	44.490	44.490	.000	- 17.895	- 12.145	8.902
300	8.535	44.543	44.490	.016	- 17.909	- 12.110	8.822
400	9.680	47.144	44.837	.923	- 18.436	- 10.066	5.900
500	11.076	49.453	45.533	1.960	- 19.316	- 7.845	3.429
600	12.483	51.597	46.367	3.138	- 19.916	- 5.493	2.001
700	13.813	53.622	47.260	4.454	- 20.429	- 3.046	.951
800	15.041	55.548	48.174	5.897	- 20.857	- .533	.146
900	16.157	57.385	49.098	7.458	- 21.207	2.029	.493
1000	17.160	59.141	50.016	9.125	- 21.482	4.625	1.011
1100	18.052	60.819	50.922	10.887	- 21.696	7.247	1.440
1200	18.842	62.424	51.814	12.732	- 21.854	9.887	1.801
1300	19.538	63.960	52.690	14.652	- 21.971	12.535	2.107
1400	20.150	65.431	53.548	16.637	- 22.050	15.195	2.372
1500	20.688	66.840	54.387	18.679	- 22.104	17.859	2.602
1600	21.161	68.191	55.208	20.772	- 22.137	20.520	2.803
1700	21.579	69.486	56.010	22.910	- 22.148	23.189	2.981
1800	21.947	70.730	56.794	25.086	- 22.144	25.854	3.139
1900	22.273	71.928	57.559	27.298	- 22.127	28.522	3.281
2000	22.562	73.076	58.306	29.540	- 22.099	31.187	3.408
2100	22.820	74.183	59.036	31.809	- 22.065	33.851	3.523
2200	23.050	75.250	59.749	34.103	- 22.026	36.511	3.627
2300	23.254	76.279	60.445	36.418	- 21.981	39.173	3.722
2400	23.441	77.273	61.126	38.753	- 21.935	41.833	3.809
2500	23.608	78.233	61.791	41.106	- 21.888	44.483	3.889
2600	23.756	79.162	62.441	43.474	- 21.839	47.141	3.962
2700	23.894	80.062	63.077	45.857	- 21.790	49.791	4.030
2800	24.018	80.933	63.700	48.253	- 21.741	52.440	4.093
2900	24.131	81.778	64.309	50.660	- 21.694	55.093	4.152
3000	24.233	82.597	64.905	53.079	- 21.649	57.736	4.206
3100	24.327	83.394	65.488	55.507	- 21.602	60.381	4.257
3200	24.413	84.167	66.060	57.944	- 21.561	63.026	4.304
3300	24.493	84.920	66.620	60.389	- 21.524	65.669	4.349
3400	24.565	85.652	67.169	62.842	- 21.488	68.309	4.391
3500	24.633	86.365	67.707	65.302	- 21.459	70.951	4.430
3600	24.695	87.060	68.235	67.768	- 21.433	73.589	4.467
3700	24.752	87.737	68.753	70.241	- 21.414	76.231	4.503
3800	24.806	88.398	69.262	72.719	- 21.397	78.872	4.536
3900	24.855	89.043	69.761	75.202	- 21.389	81.511	4.568
4000	24.901	89.673	70.251	77.690	- 21.386	84.150	4.598
4100	24.944	90.288	70.732	80.182	- 21.387	86.785	4.626
4200	24.984	90.890	71.205	82.678	- 21.397	89.429	4.653
4300	25.022	91.478	71.669	85.179	- 21.412	92.063	4.679
4400	25.057	92.054	72.126	87.683	- 21.434	94.700	4.704
4500	25.090	92.617	72.575	90.190	- 21.463	97.335	4.727
4600	25.121	93.169	73.017	92.701	- 21.498	99.983	4.750
4700	25.150	93.710	73.452	95.214	- 21.540	102.625	4.772
4800	25.177	94.240	73.879	97.730	- 21.589	105.268	4.793
4900	25.203	94.759	74.300	100.249	- 21.644	107.912	4.813
5000	25.227	95.268	74.714	102.771	- 21.706	110.552	4.832
5100	25.250	95.768	75.122	105.295	- 21.777	113.198	4.851
5200	25.272	96.259	75.524	107.821	- 21.853	115.844	4.869
5300	25.292	96.740	75.920	110.349	- 21.937	118.501	4.886
5400	25.311	97.213	76.310	112.879	- 22.029	121.145	4.903
5500	25.330	97.678	76.694	115.411	- 22.128	123.799	4.919
5600	25.347	98.134	77.073	117.945	- 22.234	126.449	4.935
5700	25.364	98.583	77.446	120.481	- 22.348	129.106	4.950
5800	25.379	99.024	77.814	123.018	- 22.469	131.762	4.965
5900	25.394	99.458	78.178	125.557	- 22.596	134.428	4.979
6000	25.409	99.885	78.536	128.097	- 22.732	137.081	4.993

TABLE 2 (continued)

Thermochemical data of selected chemical compounds
Carbon Monoxide (CO) (ideal gas) mol. wt. = 28.01055

T, °K.	cal. mole ⁻¹ deg. ⁻¹			kcal. mole ⁻¹			Log K _p
	C _p	S°	-(F°-H° ₂₉₈)/T	H°-H° ₂₉₈	ΔH _f °	ΔF _f °	
0	0.000	0.000	INFINITE	2.072	-27.200	-27.200	INFINITE
100	6.956	39.613	53.601	1.379	-26.876	-28.741	62.809
200	6.957	44.653	47.651	0.683	-26.599	-30.718	33.566
298	6.965	47.214	47.000	0.000	-26.417	-32.783	24.029
300	6.965	47.257	47.000	0.013	-26.414	-32.823	23.910
400	7.013	49.265	47.488	0.711	-26.310	-34.975	19.109
500	7.121	50.841	48.006	1.417	-26.298	-37.144	16.235
600	7.276	52.152	48.591	2.137	-26.332	-39.311	14.318
700	7.450	53.287	49.182	2.873	-26.409	-41.468	12.946
800	7.624	54.293	49.759	3.627	-26.514	-43.612	11.914
900	7.786	55.200	50.314	4.397	-26.637	-45.744	11.108
1000	7.931	56.028	50.845	5.183	-26.771	-47.859	10.459
1100	8.057	56.790	51.351	5.983	-26.914	-49.962	9.926
1200	8.168	57.496	51.834	6.704	-27.062	-52.049	9.479
1300	8.263	58.154	52.295	7.346	-27.218	-54.126	9.099
1400	8.346	58.769	52.736	8.006	-27.376	-56.189	8.771
1500	8.417	59.348	53.158	8.685	-27.537	-58.241	8.485
1600	8.480	59.894	53.562	9.380	-27.700	-60.284	8.234
1700	8.535	60.409	53.950	10.090	-27.865	-62.315	8.011
1800	8.583	60.898	54.322	11.816	-28.032	-64.337	7.811
1900	8.626	61.363	54.681	12.697	-28.201	-66.349	7.631
2000	8.664	61.807	55.026	13.661	-28.372	-68.353	7.469
2100	8.698	62.230	55.359	14.630	-28.543	-70.346	7.321
2200	8.728	62.635	55.680	15.601	-28.719	-72.335	7.185
2300	8.756	63.024	55.991	16.575	-28.894	-74.311	7.061
2400	8.781	63.397	56.292	17.552	-29.074	-76.282	6.946
2500	8.804	63.756	56.584	17.931	-29.254	-78.247	6.840
2600	8.825	64.102	56.866	18.813	-29.438	-80.202	6.741
2700	8.844	64.435	57.140	19.696	-29.623	-82.153	6.649
2800	8.863	64.757	57.407	20.582	-29.810	-84.093	6.563
2900	8.879	65.069	57.666	21.469	-30.001	-86.028	6.483
3000	8.895	65.370	57.917	22.357	-30.194	-87.957	6.407
3100	8.910	65.662	58.163	23.248	-30.388	-89.878	6.336
3200	8.924	65.945	58.401	24.139	-30.586	-91.795	6.269
3300	8.937	66.220	58.634	25.032	-30.786	-93.707	6.206
3400	8.949	66.487	58.861	25.927	-30.988	-95.609	6.145
3500	8.961	66.746	59.083	26.822	-31.192	-97.509	6.088
3600	8.973	66.990	59.299	27.719	-31.399	-99.400	6.034
3700	8.984	67.245	59.511	28.617	-31.608	-101.286	5.982
3800	8.994	67.485	59.717	29.516	-31.818	-103.164	5.933
3900	9.004	67.718	59.919	30.416	-32.031	-105.039	5.886
4000	9.014	67.946	60.117	31.316	-32.247	-106.908	5.841
4100	9.024	68.169	60.311	32.218	-32.464	-108.774	5.798
4200	9.033	68.387	60.501	33.121	-32.684	-110.630	5.756
4300	9.042	68.599	60.687	34.025	-32.906	-112.483	5.717
4400	9.051	68.807	60.869	34.930	-33.130	-114.333	5.679
4500	9.059	69.011	61.047	35.835	-33.356	-116.177	5.642
4600	9.068	69.210	61.223	36.741	-33.584	-118.012	5.607
4700	9.076	69.405	61.395	37.649	-33.814	-119.845	5.573
4800	9.084	69.596	61.564	38.557	-34.046	-121.672	5.540
4900	9.092	69.784	61.729	39.465	-34.280	-123.497	5.508
5000	9.100	69.967	61.892	40.375	-34.516	-125.315	5.477
5100	9.107	70.148	62.052	41.285	-34.755	-127.132	5.448
5200	9.115	70.325	62.210	42.196	-34.995	-128.941	5.419
5300	9.123	70.498	62.365	43.108	-35.237	-130.741	5.391
5400	9.130	70.669	62.517	44.021	-35.480	-132.542	5.364
5500	9.138	70.836	62.667	44.934	-35.727	-134.336	5.338
5600	9.145	71.001	62.814	45.849	-35.974	-136.129	5.312
5700	9.153	71.163	62.959	46.763	-36.225	-137.919	5.288
5800	9.160	71.322	63.102	47.679	-36.476	-139.698	5.264
5900	9.167	71.479	63.242	48.595	-36.730	-141.473	5.240
6000	9.175	71.633	63.381	49.513	-36.985	-143.249	5.218

(continues)

TABLE 2 (continued)

Thermochemical data of selected chemical compounds
Carbon Dioxide (CO₂) (ideal gas) mol. wt. = 44.0095

T, °K.	cal. mole ⁻¹ deg. ⁻¹			kcal. mole ⁻¹			Log K _p
	C _p	S°	-(F°-H° ₂₉₈)/T	H°-H° ₂₉₈	ΔH _f °	ΔF _f °	
0	0.00	0.00	INFINITE	- 2.238	- 93.965	- 93.965	INFINITE
100	6.981	42.758	58.188	- 1.543	- 93.997	- 94.100	205.645
200	7.734	47.769	51.849	- .816	- 94.028	- 94.191	102.922
298	8.874	51.072	51.072	.000	- 94.054	- 94.265	69.095
300	8.896	51.127	51.072	.016	- 94.055	- 94.267	68.670
400	9.877	53.830	51.474	.958	- 94.070	- 94.335	51.540
500	10.666	56.122	52.148	1.987	- 94.091	- 94.399	41.260
600	11.310	58.126	52.981	3.087	- 94.124	- 94.458	34.405
700	11.846	59.910	53.845	4.245	- 94.169	- 94.510	29.506
800	12.293	61.522	54.706	5.453	- 94.218	- 94.556	25.830
900	12.667	62.947	55.544	6.707	- 94.270	- 94.596	22.970
1000	12.980	64.344	56.359	7.984	- 94.321	- 94.628	20.680
1100	13.243	65.594	57.143	9.296	- 94.371	- 94.658	18.806
1200	13.466	66.756	57.896	10.632	- 94.419	- 94.681	17.243
1300	13.656	67.841	58.620	11.988	- 94.469	- 94.701	15.920
1400	13.815	68.859	59.315	13.362	- 94.515	- 94.716	14.785
1500	13.953	69.817	59.984	14.740	- 94.562	- 94.728	13.801
1600	14.074	70.722	60.627	16.122	- 94.607	- 94.739	12.940
1700	14.177	71.578	61.244	17.505	- 94.650	- 94.746	12.180
1800	14.260	72.391	61.843	18.897	- 94.696	- 94.750	11.504
1900	14.332	73.165	62.418	20.298	- 94.742	- 94.751	10.898
2000	14.424	73.900	62.974	21.857	- 94.788	- 94.752	10.353
2100	14.489	74.608	63.512	23.303	- 94.834	- 94.746	9.860
2200	14.547	75.284	64.031	24.755	- 94.885	- 94.744	9.411
2300	14.600	75.931	64.535	26.212	- 94.936	- 94.735	9.001
2400	14.649	76.554	65.023	27.674	- 94.991	- 94.724	8.625
2500	14.692	77.153	65.496	29.141	- 95.048	- 94.714	8.280
2600	14.734	77.730	65.956	30.613	- 95.107	- 94.698	7.960
2700	14.771	78.284	66.402	32.088	- 95.170	- 94.683	7.664
2800	14.807	78.824	66.836	33.567	- 95.235	- 94.662	7.388
2900	14.841	79.344	67.259	35.049	- 95.305	- 94.639	7.132
3000	14.873	79.848	67.670	36.535	- 95.377	- 94.615	6.892
3100	14.902	80.334	68.071	38.024	- 95.451	- 94.587	6.668
3200	14.930	80.810	68.461	39.515	- 95.530	- 94.560	6.458
3300	14.956	81.270	68.843	41.010	- 95.611	- 94.531	6.260
3400	14.982	81.717	69.215	42.507	- 95.696	- 94.495	6.074
3500	15.006	82.151	69.578	44.006	- 95.784	- 94.462	5.898
3600	15.030	82.574	69.933	45.508	- 95.874	- 94.421	5.732
3700	15.053	82.986	70.280	47.012	- 95.968	- 94.379	5.574
3800	15.075	83.388	70.620	48.518	- 96.064	- 94.331	5.425
3900	15.097	83.780	70.953	50.027	- 96.162	- 94.286	5.283
4000	15.119	84.162	71.278	51.538	- 96.263	- 94.237	5.149
4100	15.139	84.535	71.597	53.051	- 96.367	- 94.186	5.020
4200	15.159	84.901	71.909	54.566	- 96.473	- 94.130	4.898
4300	15.179	85.258	72.216	56.082	- 96.583	- 94.072	4.781
4400	15.197	85.607	72.516	57.601	- 96.694	- 94.015	4.670
4500	15.216	85.949	72.811	59.122	- 96.807	- 93.954	4.563
4600	15.234	86.284	73.100	60.644	- 96.923	- 93.885	4.460
4700	15.254	86.611	73.384	62.169	- 97.040	- 93.818	4.362
4800	15.272	86.933	73.663	63.695	- 97.160	- 93.746	4.268
4900	15.290	87.248	73.937	65.223	- 97.281	- 93.678	4.178
5000	15.306	87.557	74.206	66.753	- 97.404	- 93.603	4.091
5100	15.327	87.860	74.471	68.285	- 97.530	- 93.528	4.008
5200	15.349	88.158	74.731	69.819	- 97.656	- 93.450	3.927
5300	15.371	88.451	74.988	71.355	- 97.783	- 93.361	3.850
5400	15.393	88.738	75.239	72.893	- 97.912	- 93.280	3.775
5500	15.415	89.021	75.488	74.433	- 98.042	- 93.190	3.703
5600	15.437	89.299	75.732	75.976	- 98.173	- 93.104	3.633
5700	15.459	89.572	75.972	77.521	- 98.305	- 93.017	3.566
5800	15.481	89.841	76.209	79.068	- 98.438	- 92.918	3.501
5900	15.503	90.106	76.442	80.617	- 98.572	- 92.820	3.438
6000	15.525	90.367	76.672	82.168	- 98.707	- 92.724	3.377

TABLE 2 (continued)

Thermochemical data of selected chemical compounds
Acetylene (C_2H_2) (ideal gas) mol. wt. = 26.038

T. °K.	cal. mole ⁻¹ deg. ⁻¹			kcal. mole ⁻¹			Log K _p
	C _p ^o	S ^o	-(F ^o -H ₂₉₈ ^o)/T	H ^o -H ₂₉₈ ^o	ΔH _f ^o	ΔF _f ^o	
0	.000	.000	INFINITE	2.393	54.325	54.325	INFINITE
100	7.014	39.002	55.982	1.498	54.211	52.614	115.418
200	6.505	44.213	48.003	.938	54.234	51.383	56.146
298	10.539	48.004	48.004	.000	54.190	49.993	36.644
300	10.571	48.069	48.004	.020	54.189	49.966	36.399
400	12.065	51.324	48.438	1.155	54.138	48.567	26.534
500	13.114	54.139	49.303	2.418	54.064	47.181	20.622
600	13.931	56.604	50.319	3.771	53.961	45.813	16.687
700	14.615	58.805	51.377	5.199	53.837	44.466	13.882
800	15.239	60.798	52.432	6.693	53.707	43.137	11.784
900	15.801	62.625	53.484	8.245	53.573	41.821	10.155
1000	16.318	64.317	54.486	9.852	53.450	40.522	8.856
1100	16.789	65.895	55.434	11.507	53.333	39.234	7.795
1200	17.221	67.375	56.368	13.208	53.228	37.960	6.913
1300	17.613	68.769	57.269	14.950	53.128	36.690	6.166
1400	17.968	70.087	58.138	16.729	53.041	35.432	5.531
1500	18.291	71.338	58.977	18.543	52.961	34.177	4.979
1600	18.582	72.528	59.787	20.387	52.887	32.923	4.497
1700	18.845	73.663	60.570	22.258	52.823	31.679	4.072
1800	19.085	74.747	61.327	24.155	52.765	30.436	3.695
1900	19.302	75.785	62.061	26.074	52.714	29.199	3.358
2000	19.504	76.780	62.772	28.015	52.670	27.962	3.055
2100	19.684	77.736	63.462	29.974	52.631	26.730	2.782
2200	19.853	78.656	64.132	31.951	52.594	25.493	2.532
2300	20.004	79.541	64.783	33.944	52.564	24.266	2.306
2400	20.151	80.396	65.416	35.952	52.535	23.037	2.098
2500	20.282	81.221	66.032	37.974	52.510	21.804	1.906
2600	20.404	82.019	66.631	40.008	52.486	20.579	1.730
2700	20.519	82.791	67.216	42.055	52.466	19.349	1.566
2800	20.625	83.540	67.785	44.112	52.448	18.124	1.415
2900	20.726	84.265	68.341	46.179	52.429	16.901	1.274
3000	20.820	84.969	68.884	48.257	52.413	15.674	1.142
3100	20.910	85.654	69.414	50.343	52.399	14.451	1.019
3200	20.996	86.319	69.932	52.439	52.385	13.227	.903
3300	21.078	86.966	70.438	54.542	52.369	12.000	.795
3400	21.154	87.596	70.934	56.654	52.356	10.779	.693
3500	21.225	88.211	71.418	58.773	52.340	9.554	.597
3600	21.297	88.810	71.893	60.899	52.325	8.331	.506
3700	21.367	89.394	72.358	63.032	52.307	7.111	.420
3800	21.431	89.965	72.814	65.172	52.291	5.894	.339
3900	21.494	90.522	73.261	67.319	52.272	4.675	.262
4000	21.557	91.067	73.699	69.471	52.252	3.455	.189
4100	21.615	91.600	74.130	71.630	52.231	2.230	.119
4200	21.670	92.122	74.552	73.794	52.208	1.017	.053
4300	21.728	92.632	74.966	75.964	52.179	.205	.010
4400	21.782	93.133	75.374	78.139	52.151	-1.425	.071
4500	21.835	93.623	75.774	80.320	52.120	-2.648	.129
4600	21.883	94.103	76.167	82.506	52.087	-3.858	.183
4700	21.935	94.574	76.554	84.697	52.052	-5.073	.236
4800	21.985	95.037	76.934	86.893	52.013	-6.286	.286
4900	22.036	95.490	77.308	89.094	51.973	-7.500	.335
5000	22.077	95.936	77.676	91.300	51.930	-8.715	.381
5100	22.129	96.374	78.038	93.510	51.881	-9.935	.426
5200	22.174	96.804	78.395	95.725	51.832	-11.144	.468
5300	22.219	97.227	78.746	97.945	51.780	-12.348	.509
5400	22.263	97.642	79.093	100.169	51.724	-13.559	.549
5500	22.309	98.051	79.434	102.397	51.663	-14.767	.587
5600	22.349	98.454	79.770	104.630	51.601	-15.977	.624
5700	22.393	98.850	80.101	106.867	51.534	-17.188	.659
5800	22.433	99.239	80.428	109.108	51.463	-18.394	.693
5900	22.474	99.623	80.750	111.354	51.390	-19.588	.726
6000	22.521	100.001	81.067	113.603	51.313	-20.802	.758

(continues)

TABLE 2 (continued)

Thermochemical data of selected chemical compounds
Ethylene (C₂H₄) (ideal gas) mol. wt. = 28.05418

T, °K.	cal. mole ⁻¹ deg. ⁻¹			kcal. mole ⁻¹			Log K _p
	C _p ^o	S ^o	-(F ^o -H ₂₉₈ ^o)/T	H ^o -H ₂₉₈ ^o	ΔH _f ^o	ΔF _f ^o	
0	.000	.000	INFINITE	- 2.514	14.578	14.578	INFINITE
100	7.952	43.125	60.316	- 1.719	13.827	14.434	- 31.544
200	8.451	48.721	53.267	- .909	13.275	15.227	- 16.638
298	10.250	52.396	52.396	.000	12.540	16.338	- 11.975
300	10.292	52.459	52.396	.019	12.525	16.361	- 11.918
400	12.679	55.745	52.628	1.167	11.793	17.752	- 9.699
500	14.933	58.821	53.722	2.550	11.140	19.319	- 8.444
600	16.889	61.721	54.816	4.143	10.577	21.008	- 7.652
700	18.574	64.454	55.999	5.918	10.098	22.788	- 7.114
800	20.039	67.033	57.219	7.851	9.701	24.628	- 6.728
900	21.320	69.468	58.446	9.920	9.372	26.514	- 6.438
1000	22.443	71.774	59.665	12.109	9.113	28.431	- 6.213
1100	23.427	73.960	60.866	14.404	8.910	30.373	- 6.034
1200	24.290	76.036	62.044	16.791	8.757	32.334	- 5.889
1300	25.044	78.011	63.197	19.258	8.638	34.302	- 5.766
1400	25.706	79.892	64.323	21.797	8.557	36.282	- 5.664
1500	26.285	81.686	65.421	24.397	8.497	38.266	- 5.575
1600	26.794	83.399	66.492	27.051	8.455	40.246	- 5.497
1700	27.242	85.037	67.535	29.753	8.435	42.237	- 5.430
1800	27.636	86.605	68.551	32.498	8.428	44.224	- 5.369
1900	27.986	88.109	69.541	35.279	8.433	46.215	- 5.316
2000	28.296	89.552	70.506	38.094	8.448	48.204	- 5.275
2100	28.571	90.940	71.446	40.937	8.469	50.192	- 5.223
2200	28.818	92.275	72.362	43.807	8.493	52.174	- 5.183
2300	29.038	93.561	73.256	46.700	8.524	54.163	- 5.146
2400	29.236	94.801	74.128	49.614	8.554	56.148	- 5.113
2500	29.414	95.998	74.979	52.546	8.584	58.124	- 5.081
2600	29.575	97.155	75.810	55.496	8.616	60.109	- 5.052
2700	29.721	98.274	76.621	58.461	8.647	62.085	- 5.025
2800	29.853	99.357	77.414	61.440	8.678	64.064	- 5.000
2900	29.973	100.407	78.189	64.431	8.705	66.047	- 4.977
3000	30.083	101.425	78.947	67.434	8.730	68.019	- 4.955
3100	30.184	102.413	79.688	70.447	8.755	69.996	- 4.934
3200	30.276	103.373	80.413	73.470	8.774	71.971	- 4.915
3300	30.360	104.305	81.123	76.502	8.788	73.947	- 4.897
3400	30.438	105.213	81.818	79.542	8.800	75.920	- 4.880
3500	30.510	106.096	82.499	82.590	8.804	77.894	- 4.864
3600	30.577	106.957	83.167	85.644	8.804	79.864	- 4.848
3700	30.638	107.795	83.821	88.705	8.795	81.844	- 4.834
3800	30.695	108.613	84.463	91.772	8.784	83.822	- 4.821
3900	30.748	109.411	85.092	94.844	8.762	85.798	- 4.808
4000	30.797	110.190	85.710	97.921	8.735	87.775	- 4.796
4100	30.843	110.951	86.317	101.003	8.701	89.746	- 4.784
4200	30.886	111.695	86.912	104.090	8.658	91.729	- 4.773
4300	30.926	112.422	87.497	107.180	8.606	93.703	- 4.762
4400	30.964	113.134	88.071	110.275	8.549	95.678	- 4.752
4500	30.999	113.830	88.636	113.373	8.481	97.653	- 4.742
4600	31.032	114.512	89.191	116.475	8.407	99.643	- 4.734
4700	31.063	115.180	89.737	119.579	8.323	101.628	- 4.725
4800	31.093	115.834	90.274	122.687	8.231	103.617	- 4.718
4900	31.120	116.475	90.802	125.798	8.132	105.608	- 4.710
5000	31.146	117.104	91.322	128.911	8.023	107.593	- 4.703
5100	31.171	117.721	91.834	132.027	7.903	109.582	- 4.696
5200	31.194	118.327	92.337	135.145	7.777	111.574	- 4.689
5300	31.216	118.921	92.833	138.266	7.642	113.583	- 4.683
5400	31.236	119.505	93.322	141.388	7.496	115.577	- 4.677
5500	31.256	120.078	93.803	144.513	7.341	117.593	- 4.672
5600	31.275	120.641	94.277	147.639	7.177	119.586	- 4.667
5700	31.292	121.195	94.745	150.768	7.004	121.591	- 4.662
5800	31.309	121.740	95.205	153.898	6.820	123.597	- 4.657
5900	31.325	122.275	95.660	157.030	6.628	125.625	- 4.653
6000	31.340	122.802	96.108	160.163	6.427	127.627	- 4.649

TABLE 2 (continued)

Thermochemical data of selected chemical compounds
Hydrogen, Monatomic (H) (ideal gas) at. wt. = 1.00797

T, °K.	cal. mole ⁻¹ deg. ⁻¹			kcal. mole ⁻¹			Log K _p
	C _p	S°	-(F°-H° ₂₉₈)/T	H°-H° ₂₉₈	ΔH _f °	ΔF _f °	
0	.000	.000	INFINITE	- 1.481	51.631	51.631	INFINITE
100	4.968	21.965	31.809	- .984	51.748	50.771	- 110.954
200	4.968	25.408	27.847	- .488	51.943	49.714	- 54.322
298	4.968	27.392	27.392	.000	52.100	48.585	- 35.612
300	4.968	27.423	27.392	.009	52.103	48.563	- 35.377
400	4.968	28.852	27.587	.506	52.253	47.361	- 25.876
500	4.968	29.961	27.955	1.003	52.400	46.121	- 20.158
600	4.968	30.867	28.367	1.500	52.547	44.851	- 16.336
700	4.968	31.632	28.780	1.996	52.692	43.558	- 13.599
800	4.968	32.296	29.179	2.493	52.836	42.242	- 11.539
900	4.968	32.881	29.559	2.990	52.977	40.910	- 9.934
1000	4.968	33.404	29.917	3.487	53.115	39.562	- 8.646
1100	4.968	33.878	30.256	3.984	53.249	38.200	- 7.589
1200	4.968	34.310	30.576	4.481	53.379	36.826	- 6.707
1300	4.968	34.708	30.879	4.977	53.503	35.441	- 5.958
1400	4.968	35.076	31.166	5.474	53.623	34.048	- 5.315
1500	4.968	35.419	31.438	5.971	53.737	32.645	- 4.776
1600	4.968	35.739	31.697	6.468	53.845	31.236	- 4.266
1700	4.968	36.041	31.944	6.965	53.948	29.819	- 3.823
1800	4.968	36.325	32.179	7.461	54.046	28.396	- 3.448
1900	4.968	36.593	32.405	7.958	54.140	26.970	- 3.102
2000	4.968	36.848	32.621	8.455	54.230	25.538	- 2.790
2100	4.968	37.090	32.828	8.952	54.314	24.102	- 2.508
2200	4.968	37.322	33.027	9.449	54.395	22.659	- 2.251
2300	4.968	37.542	33.216	9.945	54.472	21.217	- 2.016
2400	4.968	37.754	33.403	10.442	54.546	19.769	- 1.800
2500	4.968	37.957	33.581	10.939	54.615	18.316	- 1.601
2600	4.968	38.152	33.753	11.436	54.682	16.864	- 1.417
2700	4.968	38.339	33.919	11.933	54.745	15.409	- 1.247
2800	4.968	38.520	34.081	12.430	54.806	13.949	- 1.089
2900	4.968	38.694	34.237	12.926	54.863	12.491	- .941
3000	4.968	38.862	34.388	13.423	54.918	11.030	- .803
3100	4.968	39.025	34.535	13.920	54.971	9.565	- .674
3200	4.968	39.183	34.678	14.417	55.021	8.099	- .553
3300	4.968	39.336	34.817	14.914	55.068	6.632	- .439
3400	4.968	39.484	34.952	15.410	55.113	5.164	- .332
3500	4.968	39.628	35.083	15.907	55.156	3.695	- .231
3600	4.968	39.768	35.212	16.404	55.196	2.224	- .135
3700	4.968	39.904	35.337	16.901	55.233	.753	- .044
3800	4.968	40.037	35.459	17.398	55.269	-.722	-.042
3900	4.968	40.166	35.578	17.895	55.302	- 2.196	-.123
4000	4.968	40.292	35.694	18.391	55.333	- 3.671	-.201
4100	4.968	40.414	35.808	18.888	55.362	- 5.144	-.274
4200	4.968	40.534	35.919	19.385	55.388	- 6.621	-.345
4300	4.968	40.651	36.027	19.882	55.412	- 8.099	-.412
4400	4.968	40.765	36.134	20.379	55.435	- 9.575	-.476
4500	4.968	40.877	36.238	20.875	55.454	- 11.056	-.537
4600	4.968	40.986	36.340	21.372	55.473	- 12.531	-.595
4700	4.968	41.093	36.440	21.869	55.489	- 14.010	-.651
4800	4.968	41.198	36.538	22.366	55.503	- 15.492	-.705
4900	4.968	41.300	36.634	22.863	55.515	- 16.968	-.757
5000	4.968	41.400	36.728	23.359	55.525	- 18.447	-.806
5100	4.968	41.499	36.821	23.856	55.534	- 19.928	-.854
5200	4.968	41.595	36.912	24.353	55.541	- 21.406	-.900
5300	4.968	41.690	37.001	24.850	55.546	- 22.887	-.944
5400	4.968	41.783	37.089	25.347	55.548	- 24.369	-.986
5500	4.968	41.874	37.175	25.844	55.550	- 25.848	- 1.027
5600	4.968	41.963	37.260	26.340	55.549	- 27.326	- 1.066
5700	4.968	42.051	37.343	26.837	55.547	- 28.805	- 1.104
5800	4.968	42.138	37.425	27.334	55.543	- 30.289	- 1.141
5900	4.968	42.223	37.506	27.831	55.537	- 31.768	- 1.177
6000	4.968	42.306	37.585	28.328	55.530	- 33.246	- 1.211

(continues)

TABLE 2 (continued)

Thermochemical data of selected chemical compounds
Hydroxyl (OH) (ideal gas) mol. wt. = 17.0074

T, °K.	cal. mole ⁻¹ deg. ⁻¹			kcal. mole ⁻¹			Log K _p
	C _p	S°	-(F°-H° ₂₉₈)/T	H°-H° ₂₉₈	ΔH _f °	ΔF _f °	
0	.000	.000	INFINITE	- 2.192	9.289	9.289	INFINITE
100	7.798	35.726	50.398	- 1.467	9.278	9.001	- 19.672
200	7.356	40.985	44.541	- .711	9.393	8.671	- 9.475
298	7.167	43.880	43.880	.000	9.432	8.307	- 6.089
300	7.165	43.925	43.881	.013	9.432	8.299	- 6.046
400	7.087	45.974	44.160	.725	9.442	7.920	- 4.327
500	7.055	47.551	44.687	1.432	9.434	7.540	- 3.296
600	7.057	48.837	45.275	2.137	9.411	7.163	- 2.609
700	7.090	49.927	45.863	2.845	9.379	6.791	- 2.120
800	7.150	50.877	46.432	3.556	9.338	6.424	- 1.755
900	7.233	51.724	46.974	4.275	9.294	6.062	- 1.472
1000	7.332	52.491	47.488	5.003	9.250	5.706	- 1.247
1100	7.439	53.195	47.975	5.742	9.206	5.353	- 1.064
1200	7.549	53.847	48.437	6.491	9.164	5.005	- .912
1300	7.659	54.455	48.877	7.252	9.124	4.661	- .784
1400	7.766	55.027	49.296	8.023	9.086	4.318	- .674
1500	7.867	55.566	49.696	8.805	9.050	3.980	- .580
1600	7.963	56.077	50.079	9.596	9.014	3.642	- .497
1700	8.053	56.563	50.447	10.397	8.980	3.307	- .425
1800	8.137	57.025	50.799	11.207	8.947	2.975	- .361
1900	8.214	57.467	51.139	12.024	8.914	2.645	- .304
2000	8.286	57.891	51.466	12.849	8.881	2.313	- .253
2100	8.353	58.296	51.782	13.681	8.849	1.988	- .207
2200	8.414	58.686	52.087	14.520	8.815	1.662	- .165
2300	8.472	59.062	52.382	15.364	8.782	1.336	- .127
2400	8.526	59.424	52.668	16.214	8.748	1.014	- .092
2500	8.576	59.773	52.945	17.069	8.711	.690	- .060
2600	8.622	60.110	53.214	17.929	8.675	.372	- .031
2700	8.665	60.436	53.476	18.794	8.637	.054	- .004
2800	8.706	60.752	53.730	19.662	8.598	-.264	-.021
2900	8.744	61.058	53.977	20.535	8.557	-.578	-.044
3000	8.780	61.355	54.218	21.411	8.515	-.893	-.065
3100	8.814	61.644	54.453	22.291	8.472	- 1.208	-.085
3200	8.846	61.924	54.682	23.174	8.427	- 1.519	-.104
3300	8.876	62.197	54.906	24.060	8.381	- 1.829	-.121
3400	8.905	62.462	55.124	24.949	8.333	- 2.137	-.137
3500	8.933	62.721	55.338	25.841	8.283	- 2.446	-.153
3600	8.959	62.973	55.546	26.735	8.232	- 2.751	-.167
3700	8.984	63.218	55.750	27.632	8.179	- 3.052	-.180
3800	9.008	63.458	55.950	28.532	8.125	- 3.355	-.193
3900	9.031	63.693	56.145	29.434	8.069	- 3.660	-.205
4000	9.053	63.922	56.337	30.338	8.011	- 3.961	-.216
4100	9.074	64.145	56.525	31.245	7.952	- 4.256	-.227
4200	9.095	64.364	56.709	32.153	7.892	- 4.553	-.237
4300	9.115	64.579	56.889	33.064	7.830	- 4.851	-.247
4400	9.134	64.788	57.066	33.976	7.766	- 5.144	-.255
4500	9.153	64.994	57.240	34.890	7.701	- 5.439	-.264
4600	9.171	65.195	57.411	35.807	7.635	- 5.726	-.272
4700	9.189	65.393	57.579	36.725	7.567	- 6.018	-.280
4800	9.206	65.586	57.744	37.644	7.499	- 6.304	-.287
4900	9.223	65.776	57.906	38.566	7.429	- 6.592	-.294
5000	9.239	65.963	58.065	39.489	7.358	- 6.882	-.301
5100	9.255	66.146	58.222	40.414	7.286	- 7.162	-.307
5200	9.271	66.326	58.376	41.340	7.213	- 7.448	-.313
5300	9.286	66.502	58.527	42.268	7.140	- 7.722	-.318
5400	9.301	66.676	58.677	43.197	7.065	- 8.007	-.324
5500	9.316	66.847	58.824	44.128	6.989	- 8.284	-.329
5600	9.330	67.015	58.968	45.060	6.912	- 8.563	-.334
5700	9.344	67.180	59.111	45.994	6.835	- 8.837	-.339
5800	9.358	67.343	59.252	46.929	6.757	- 9.112	-.343
5900	9.372	67.503	59.390	47.866	6.678	- 9.385	-.348
6000	9.386	67.661	59.527	48.803	6.598	- 9.659	-.352

TABLE 2 (continued)

Thermochemical data of selected chemical compounds
Hydroperoxyl (HO₂) (ideal gas) mol. wt. = 33.008

T, °K.	cal. mole ⁻¹ deg. ⁻¹				kcal. mole ⁻¹			Log K _p
	C _p ^o	S ^o	-(F ^o -H _{298^o})/T}	H ^o -H _{298^o}	ΔH _f ^o	ΔF _f ^o		
0	.000	.000	INFINITE	- 2.390	5.697	5.697	INFINITE	
100	7.949	45.618	61.574	- 1.596	5.399	6.209	- 13.568	
200	8.003	51.136	55.132	- .799	5.214	7.085	- 7.742	
298	8.338	54.383	54.183	.000	5.000	8.049	- 5.900	
300	8.347	54.434	54.183	.015	4.996	8.067	- 5.877	
400	8.907	56.910	54.717	.877	4.800	9.122	- 4.984	
500	9.479	58.960	55.166	1.797	4.639	10.222	- 4.468	
600	9.980	60.734	56.116	2.771	4.508	11.351	- 4.134	
700	10.405	62.305	56.890	3.791	4.399	12.501	- 3.903	
800	10.769	63.719	57.657	4.850	4.307	13.663	- 3.732	
900	11.087	65.006	58.403	5.943	4.230	14.838	- 3.603	
1000	11.365	66.189	59.123	7.066	4.167	16.021	- 3.501	
1100	11.612	67.284	59.816	8.215	4.114	17.209	- 3.419	
1200	11.831	68.304	60.481	9.387	4.071	18.401	- 3.351	
1300	12.025	69.258	61.120	10.580	4.035	19.597	- 3.294	
1400	12.197	70.156	61.734	11.791	4.005	20.795	- 3.246	
1500	12.350	71.003	62.323	13.019	3.979	21.996	- 3.205	
1600	12.485	71.804	62.891	14.261	3.955	23.197	- 3.168	
1700	12.606	72.565	63.438	15.515	3.934	24.401	- 3.137	
1800	12.714	73.288	63.965	16.782	3.913	25.605	- 3.109	
1900	12.810	73.979	64.474	18.058	3.891	26.812	- 3.084	
2000	12.895	74.638	64.966	19.343	3.869	28.017	- 3.061	
2100	12.972	75.269	65.442	20.637	3.845	29.226	- 3.041	
2200	13.041	75.874	65.902	21.937	3.818	30.435	- 3.023	
2300	13.104	76.455	66.349	23.245	3.790	31.645	- 3.007	
2400	13.160	77.014	66.781	24.558	3.757	32.859	- 2.992	
2500	13.210	77.552	67.202	25.876	3.720	34.069	- 2.978	
2600	13.256	78.071	67.610	27.200	3.682	35.286	- 2.966	
2700	13.298	78.572	68.007	28.528	3.638	36.502	- 2.954	
2800	13.336	79.057	68.393	29.859	3.590	37.719	- 2.944	
2900	13.371	79.525	68.768	31.195	3.539	38.941	- 2.935	
3000	13.403	79.979	69.135	32.534	3.483	40.162	- 2.926	
3100	13.432	80.419	69.492	33.875	3.423	41.386	- 2.918	
3200	13.459	80.844	69.840	35.220	3.359	42.610	- 2.910	
3300	13.484	81.261	70.180	36.567	3.291	43.838	- 2.903	
3400	13.507	81.663	70.511	37.917	3.218	45.067	- 2.897	
3500	13.528	82.055	70.836	39.268	3.141	46.299	- 2.891	
3600	13.547	82.437	71.153	40.622	3.060	47.534	- 2.886	
3700	13.565	82.808	71.463	41.978	2.974	48.771	- 2.881	
3800	13.582	83.170	71.766	43.335	2.886	50.011	- 2.876	
3900	13.598	83.523	72.063	44.694	2.793	51.250	- 2.872	
4000	13.612	83.867	72.354	46.055	2.695	52.493	- 2.868	
4100	13.626	84.204	72.639	47.417	2.594	53.741	- 2.864	
4200	13.638	84.532	72.918	48.780	2.490	54.989	- 2.861	
4300	13.650	84.853	73.192	50.144	2.382	56.242	- 2.858	
4400	13.662	85.167	73.460	51.510	2.270	57.493	- 2.856	
4500	13.672	85.474	73.724	52.876	2.154	58.749	- 2.853	
4600	13.682	85.775	73.983	54.244	2.037	60.013	- 2.851	
4700	13.691	86.069	74.237	55.613	1.916	61.274	- 2.849	
4800	13.700	86.358	74.486	56.982	1.790	62.538	- 2.847	
4900	13.708	86.640	74.731	58.353	1.663	63.802	- 2.846	
5000	13.716	86.917	74.972	59.724	1.533	65.069	- 2.844	
5100	13.723	87.189	75.209	61.096	1.399	66.346	- 2.843	
5200	13.730	87.455	75.442	62.468	1.264	67.616	- 2.842	
5300	13.736	87.717	75.671	63.842	1.126	68.890	- 2.841	
5400	13.743	87.974	75.897	65.216	.985	70.174	- 2.840	
5500	13.748	88.226	76.119	66.590	.843	71.460	- 2.839	
5600	13.754	88.474	76.337	67.965	.697	72.742	- 2.839	
5700	13.759	88.717	76.552	69.341	.550	74.029	- 2.838	
5800	13.764	88.957	76.764	70.717	.400	75.323	- 2.838	
5900	13.769	89.192	76.973	72.094	.248	76.615	- 2.838	
6000	13.774	89.423	77.178	73.471	.094	77.911	- 2.838	

(continues)

TABLE 2 (continued)

Thermochemical data of selected chemical compounds
 Hydrogen (H₂) (ideal gas—reference state) mol. wt. = 2.016

T, °K.	cal. mole ⁻¹ deg. ⁻¹			kcal. mole ⁻¹			Log K _p
	C _p	S°	-(F°-H° ₂₉₈)/T	H°-H° ₂₉₈	ΔH _f °	ΔF _f °	
0	0.000	0.000	INFINITE	-2.024	0.000	0.000	0.000
100	5.193	24.387	37.035	-1.265	0.000	0.000	0.000
200	6.510	24.570	31.831	.662	0.000	0.000	0.000
298	6.492	31.204	31.208	0.000	0.000	0.000	0.000
300	6.494	31.251	31.208	.013	0.000	0.000	0.000
400	6.475	33.247	31.480	.707	0.000	0.000	0.000
500	6.493	34.406	31.995	1.406	0.000	0.000	0.000
600	7.004	36.082	32.573	2.105	0.000	0.000	0.000
700	7.036	37.165	33.153	2.804	0.000	0.000	0.000
800	7.087	38.107	33.715	3.514	0.000	0.000	0.000
900	7.144	38.944	34.250	4.226	0.000	0.000	0.000
1000	7.219	39.702	34.756	4.944	0.000	0.000	0.000
1100	7.300	40.384	35.240	5.670	0.000	0.000	0.000
1200	7.390	41.033	35.696	6.404	0.000	0.000	0.000
1300	7.480	41.628	36.130	7.144	0.000	0.000	0.000
1400	7.580	42.187	36.543	7.902	0.000	0.000	0.000
1500	7.700	42.716	36.937	8.668	0.000	0.000	0.000
1600	7.823	43.217	37.314	9.446	0.000	0.000	0.000
1700	7.971	43.695	37.675	10.233	0.000	0.000	0.000
1800	8.110	44.150	38.022	11.030	0.000	0.000	0.000
1900	8.190	44.586	38.356	11.836	0.000	0.000	0.000
2000	8.195	45.004	38.678	12.651	0.000	0.000	0.000
2100	8.279	45.404	38.989	13.475	0.000	0.000	0.000
2200	8.356	45.793	39.290	14.307	0.000	0.000	0.000
2300	8.434	46.166	39.581	15.146	0.000	0.000	0.000
2400	8.504	46.527	39.863	15.993	0.000	0.000	0.000
2500	8.575	46.875	40.136	16.848	0.000	0.000	0.000
2600	8.639	47.213	40.402	17.704	0.000	0.000	0.000
2700	8.700	47.540	40.660	18.575	0.000	0.000	0.000
2800	8.757	47.857	40.912	19.448	0.000	0.000	0.000
2900	8.810	48.166	41.157	20.326	0.000	0.000	0.000
3000	8.859	48.465	41.395	21.210	0.000	0.000	0.000
3100	8.911	48.756	41.628	22.098	0.000	0.000	0.000
3200	8.962	49.040	41.855	22.992	0.000	0.000	0.000
3300	9.012	49.317	42.077	23.891	0.000	0.000	0.000
3400	9.061	49.586	42.294	24.794	0.000	0.000	0.000
3500	9.110	49.850	42.506	25.703	0.000	0.000	0.000
3600	9.158	50.107	42.714	26.616	0.000	0.000	0.000
3700	9.205	50.359	42.917	27.535	0.000	0.000	0.000
3800	9.252	50.605	43.116	28.457	0.000	0.000	0.000
3900	9.297	50.846	43.311	29.385	0.000	0.000	0.000
4000	9.342	51.082	43.502	30.317	0.000	0.000	0.000
4100	9.386	51.313	43.690	31.253	0.000	0.000	0.000
4200	9.429	51.540	43.874	32.194	0.000	0.000	0.000
4300	9.472	51.762	44.055	33.139	0.000	0.000	0.000
4400	9.514	51.980	44.233	34.088	0.000	0.000	0.000
4500	9.555	52.194	44.407	35.042	0.000	0.000	0.000
4600	9.595	52.405	44.579	35.999	0.000	0.000	0.000
4700	9.634	52.612	44.748	36.961	0.000	0.000	0.000
4800	9.673	52.815	44.914	37.924	0.000	0.000	0.000
4900	9.711	53.015	45.077	38.895	0.000	0.000	0.000
5000	9.748	53.211	45.238	39.864	0.000	0.000	0.000
5100	9.785	53.405	45.396	40.845	0.000	0.000	0.000
5200	9.822	53.595	45.552	41.825	0.000	0.000	0.000
5300	9.859	53.783	45.705	42.809	0.000	0.000	0.000
5400	9.895	53.967	45.857	43.797	0.000	0.000	0.000
5500	9.930	54.149	46.006	44.788	0.000	0.000	0.000
5600	9.965	54.328	46.153	45.783	0.000	0.000	0.000
5700	10.000	54.505	46.296	46.781	0.000	0.000	0.000
5800	10.034	54.679	46.441	47.783	0.000	0.000	0.000
5900	10.067	54.851	46.582	48.788	0.000	0.000	0.000
6000	10.100	55.020	46.721	49.796	0.000	0.000	0.000

TABLE 2 (continued)

Thermochemical data of selected chemical compounds
Water (H₂O) (ideal gas) mol. wt. = 18.016

T, °K.	cal. mole ⁻¹ deg. ⁻¹			kcal. mole ⁻¹			Log K _p
	C _p	S°	-(F°-H° ₂₉₈)/T	H°-H° ₂₉₈	ΔH _f °	ΔF _f °	
0	.000	.000	INFINITE	- 2.367	- 57.103	- 57.103	INFINITE
100	7.961	36.396	52.202	- 1.581	- 57.433	- 56.557	123.600
200	17.969	61.916	45.837	- .766	- 57.579	- 55.635	60.792
298	25.106	65.106	45.106	.000	- 57.798	- 54.636	40.008
300	0.027	45.155	45.106	.015	- 57.803	- 54.617	39.786
400	0.186	47.484	45.422	.825	- 58.042	- 53.519	29.240
500	0.415	49.334	44.026	1.654	- 58.277	- 52.361	22.886
600	0.676	50.891	44.710	2.509	- 58.500	- 51.156	18.633
700	0.954	52.249	47.406	3.390	- 58.710	- 49.915	15.583
800	1.246	53.464	48.089	4.300	- 58.905	- 48.646	13.289
900	1.547	54.570	48.749	5.240	- 59.084	- 47.352	11.498
1000	1.851	55.592	49.382	6.209	- 59.246	- 46.040	10.062
1100	10.152	56.545	49.991	7.210	- 59.391	- 44.712	8.883
1200	10.444	57.441	50.575	8.240	- 59.519	- 43.371	7.899
1300	10.723	58.286	51.138	9.298	- 59.634	- 42.022	7.064
1400	10.987	59.092	51.675	10.384	- 59.734	- 40.663	6.347
1500	11.233	59.859	52.196	11.495	- 59.824	- 39.297	5.725
1600	11.462	60.591	52.698	12.630	- 59.906	- 37.927	5.180
1700	11.674	61.293	53.183	13.787	- 59.977	- 36.549	4.699
1800	11.869	61.965	53.652	14.964	- 60.041	- 35.170	4.270
1900	12.048	62.612	54.107	16.160	- 60.099	- 33.786	3.886
2000	12.214	63.234	54.548	17.373	- 60.150	- 32.401	3.540
2100	12.366	63.834	54.976	18.602	- 60.198	- 31.012	3.227
2200	12.505	64.412	55.392	19.846	- 60.242	- 29.621	2.942
2300	12.634	64.971	55.796	21.103	- 60.282	- 28.229	2.682
2400	12.753	65.511	56.190	22.372	- 60.321	- 26.832	2.443
2500	12.863	66.034	56.573	23.653	- 60.359	- 25.439	2.224
2600	12.965	66.541	56.947	24.945	- 60.393	- 24.040	2.021
2700	13.059	67.032	57.311	26.246	- 60.422	- 22.641	1.833
2800	13.146	67.508	57.667	27.556	- 60.447	- 21.242	1.658
2900	13.226	67.971	58.014	28.875	- 60.466	- 19.838	1.495
3000	13.304	68.421	58.354	30.201	- 60.530	- 18.438	1.343
3100	13.378	68.858	58.685	31.535	- 60.562	- 17.034	1.201
3200	13.448	69.284	59.010	32.876	- 60.596	- 15.630	1.067
3300	13.513	69.698	59.328	34.223	- 60.631	- 14.223	.942
3400	13.574	70.102	59.639	35.577	- 60.666	- 12.818	.824
3500	13.631	70.496	59.943	36.936	- 60.703	- 11.409	.712
3600	13.689	70.881	60.242	38.300	- 60.741	- 10.000	.607
3700	13.748	71.256	60.534	39.669	- 60.782	- 8.589	.507
3800	13.798	71.622	60.821	41.043	- 60.822	- 7.177	.413
3900	13.848	71.980	61.103	42.422	- 60.865	- 5.766	.323
4000	13.890	72.331	61.379	43.805	- 60.910	- 4.353	.238
4100	13.930	72.673	61.651	45.192	- 60.957	- 2.938	.157
4200	13.977	73.008	61.917	46.583	- 61.006	- 1.522	.079
4300	13.993	73.336	62.179	47.977	- 61.056	- .105	.005
4400	13.997	73.659	62.436	49.375	- 61.109	1.311	.065
4500	14.000	73.973	62.689	50.777	- 61.164	2.729	.133
4600	14.001	74.281	62.938	52.181	- 61.220	4.154	.197
4700	14.001	74.584	63.182	53.589	- 61.279	5.576	.259
4800	14.120	74.881	63.423	55.000	- 61.339	6.998	.319
4900	14.184	75.172	63.660	56.413	- 61.401	8.422	.376
5000	14.174	75.459	63.893	57.829	- 61.465	9.844	.430
5100	14.201	75.740	64.122	59.246	- 61.532	11.275	.483
5200	14.228	76.016	64.348	60.669	- 61.600	12.700	.534
5300	14.254	76.287	64.571	62.093	- 61.669	14.135	.583
5400	14.279	76.553	64.791	63.520	- 61.741	15.560	.630
5500	14.303	76.816	65.007	64.949	- 61.813	16.995	.675
5600	14.328	77.074	65.220	66.381	- 61.889	18.426	.719
5700	14.351	77.327	65.430	67.815	- 61.965	19.862	.762
5800	14.374	77.577	65.637	69.251	- 62.043	21.299	.803
5900	14.396	77.823	65.842	70.690	- 62.122	22.736	.842
6000	14.422	78.065	66.044	72.131	- 62.203	24.174	.880

(continues)

TABLE 2 (continued)

Thermochemical data of selected chemical compounds
Ammonia (NH₃) (ideal gas) mol. wt. = 17.03061

T, °K.	cal. mole ⁻¹ deg. ⁻¹			kcal. mole ⁻¹			Log K _p
	C _p	S°	-(F°-H° ₂₉₈)/T	H°-H° ₂₉₈	ΔH _f °	ΔF _f °	
0	.000	.000	INFINITE	- 2.404	- 9.302	- 9.302	INFINITE
100	7.950	37.210	53.303	- 1.609	- 9.988	- 8.146	17.401
200	8.064	42.740	46.794	- .811	- 10.446	- 6.139	6.708
298	8.515	46.033	46.033	.000	- 10.970	- 3.915	2.869
300	8.526	46.085	46.033	.016	- 10.980	- 3.871	2.820
400	9.241	48.633	46.375	.903	- 11.482	- 1.424	.778
500	10.036	50.780	47.047	1.867	- 11.919	1.142	-.499
600	10.808	52.679	47.830	2.709	- 12.282	3.790	- 1.380
700	11.538	54.400	48.647	4.027	- 12.582	6.494	- 2.027
800	12.225	55.986	49.467	5.215	- 12.824	9.235	- 2.523
900	12.868	57.464	50.274	6.470	- 13.016	12.005	- 2.915
1000	13.467	58.851	51.063	7.787	- 13.163	14.792	- 3.233
1100	14.030	60.161	51.831	9.163	- 13.271	17.594	- 3.495
1200	14.550	61.404	52.578	10.592	- 13.343	20.405	- 3.716
1300	15.030	62.588	53.303	12.071	- 13.385	23.218	- 3.903
1400	15.460	63.718	54.007	13.596	- 13.402	26.034	- 4.064
1500	15.850	64.798	54.690	15.162	- 13.399	28.853	- 4.204
1600	16.205	65.833	55.355	16.765	- 13.381	31.666	- 4.325
1700	16.520	66.825	56.000	18.402	- 13.347	34.483	- 4.433
1800	16.762	67.776	56.628	20.066	- 13.303	37.294	- 4.528
1900	16.995	68.689	57.239	21.754	- 13.250	40.104	- 4.613
2000	17.220	69.566	57.834	23.465	- 13.191	42.911	- 4.689
2100	17.429	70.411	58.413	25.197	- 13.125	45.715	- 4.757
2200	17.630	71.227	58.977	26.950	- 13.053	48.514	- 4.819
2300	17.825	72.015	59.527	28.723	- 12.973	51.310	- 4.875
2400	18.014	72.777	60.063	30.515	- 12.887	54.107	- 4.927
2500	18.195	73.516	60.586	32.326	- 12.797	56.893	- 4.973
2600	18.370	74.234	61.097	34.154	- 12.697	59.679	- 5.016
2700	18.537	74.930	61.597	35.999	- 12.592	62.461	- 5.056
2800	18.698	75.607	62.085	37.861	- 12.480	65.237	- 5.092
2900	18.853	76.266	62.563	39.739	- 12.360	68.015	- 5.125
3000	19.000	76.908	63.030	41.631	- 12.236	70.780	- 5.156
3100	19.115	77.532	63.488	43.537	- 12.105	73.546	- 5.185
3200	19.228	78.141	63.937	45.454	- 11.973	76.307	- 5.211
3300	19.341	78.734	64.376	47.383	- 11.838	79.067	- 5.236
3400	19.452	79.314	64.807	49.322	- 11.698	81.814	- 5.259
3500	19.563	79.879	65.230	51.273	- 11.557	84.565	- 5.280
3600	19.672	80.432	65.644	53.235	- 11.412	87.307	- 5.300
3700	19.781	80.972	66.051	55.207	- 11.265	90.051	- 5.319
3800	19.888	81.501	66.451	57.191	- 11.112	92.787	- 5.336
3900	19.994	82.019	66.843	59.185	- 10.958	95.520	- 5.353
4000	20.100	82.527	67.229	61.190	- 10.800	98.246	- 5.368
4100	20.205	83.024	67.608	63.205	- 10.639	100.972	- 5.382
4200	20.308	83.512	67.981	65.231	- 10.474	103.694	- 5.396
4300	20.411	83.991	68.348	67.267	- 10.306	106.409	- 5.408
4400	20.512	84.462	68.709	69.313	- 10.134	109.117	- 5.420
4500	20.613	84.924	69.064	71.369	- 9.961	111.823	- 5.431
4600	20.712	85.378	69.414	73.435	- 9.781	114.534	- 5.441
4700	20.811	85.824	69.758	75.511	- 9.600	117.236	- 5.451
4800	20.908	86.264	70.098	77.597	- 9.415	119.928	- 5.460
4900	21.005	86.696	70.432	79.693	- 9.226	122.621	- 5.469
5000	21.100	87.121	70.761	81.798	- 9.033	125.309	- 5.477
5100	21.195	87.540	71.086	83.913	- 8.838	127.995	- 5.485
5200	21.288	87.952	71.407	86.037	- 8.638	130.678	- 5.492
5300	21.381	88.359	71.723	88.170	- 8.436	133.355	- 5.499
5400	21.472	88.759	72.035	90.313	- 8.231	136.026	- 5.505
5500	21.563	89.154	72.342	92.465	- 8.020	138.697	- 5.511
5600	21.652	89.543	72.646	94.625	- 7.809	141.361	- 5.517
5700	21.740	89.927	72.946	96.795	- 7.592	144.028	- 5.522
5800	21.828	90.306	73.242	98.974	- 7.374	146.683	- 5.527
5900	21.914	90.680	73.534	101.161	- 7.152	149.337	- 5.532
6000	22.000	91.049	73.823	103.356	- 6.926	151.984	- 5.536

TABLE 2 (continued)

Thermochemical data of selected chemical compounds
 Nitrogen, Monatomic (N) (ideal gas) at wt. = 14.008

T, °K.	cal. mole ⁻¹ deg. ⁻¹				kcal. mole ⁻¹			Log K _p
	C _p	S°	-(F°-H° ₂₉₈)/T	H°-H° ₂₉₈	ΔH _f °	ΔF _f °		
0	.000	.000	INFINITE	-	1.461	112.520	112.520	INFINITE
100	4.966	31.187	41.031	-	.984	112.670	111.459	- 243.583
200	4.966	34.631	37.069	-	.488	112.819	110.191	- 120.405
298	4.966	36.614	36.614	-	.000	112.965	108.670	- 79.800
300	4.966	36.645	36.614	.009		112.968	108.645	- 79.289
400	4.966	38.074	36.809	.504		113.116	107.448	- 58.704
500	4.966	39.163	37.177	1.003		113.261	106.014	- 46.336
600	4.966	40.069	37.569	1.500		113.402	104.551	- 38.081
700	4.966	40.855	38.002	1.996		113.535	103.066	- 32.177
800	4.966	41.518	38.401	2.493		113.660	101.562	- 27.744
900	4.966	42.103	38.781	2.990		113.778	100.042	- 24.292
1000	4.966	42.627	39.140	3.487		113.887	98.510	- 21.528
1100	4.966	43.100	39.479	3.984		113.990	96.967	- 19.265
1200	4.966	43.532	39.799	4.481		114.087	95.415	- 17.377
1300	4.966	43.930	40.101	4.977		114.178	93.856	- 15.778
1400	4.966	44.298	40.388	5.474		114.264	92.289	- 14.406
1500	4.966	44.641	40.660	5.971		114.346	90.716	- 13.217
1600	4.966	44.962	40.919	6.468		114.425	89.139	- 12.175
1700	4.966	45.263	41.166	6.965		114.501	87.556	- 11.256
1800	4.966	45.547	41.402	7.461		114.573	85.968	- 10.437
1900	4.966	45.815	41.627	7.958		114.644	84.378	- 9.705
2000	4.966	46.070	41.843	8.455		114.712	82.784	- 9.046
2100	4.970	46.313	42.050	8.952		114.778	81.185	- 8.449
2200	4.971	46.544	42.249	9.449		114.843	79.583	- 7.905
2300	4.972	46.765	42.440	9.946		114.906	77.979	- 7.409
2400	4.975	46.977	42.625	10.444		114.968	76.373	- 6.954
2500	4.978	47.180	42.803	10.941		115.028	74.763	- 6.535
2600	4.982	47.375	42.975	11.439		115.088	73.151	- 6.149
2700	4.987	47.563	43.142	11.938		115.148	71.537	- 5.790
2800	4.993	47.745	43.303	12.437		115.207	69.922	- 5.457
2900	5.001	47.920	43.459	12.936		115.265	68.303	- 5.147
3000	5.011	48.090	43.611	13.437		115.324	66.683	- 4.858
3100	5.022	48.254	43.758	13.939		115.383	65.060	- 4.587
3200	5.035	48.414	43.901	14.441		115.442	63.435	- 4.332
3300	5.050	48.569	44.040	14.946		115.503	61.810	- 4.093
3400	5.067	48.720	44.175	15.451		115.564	60.181	- 3.868
3500	5.086	48.867	44.307	15.959		115.626	58.551	- 3.656
3600	5.107	49.011	44.436	16.469		115.690	56.921	- 3.455
3700	5.130	49.151	44.562	16.980		115.755	55.287	- 3.265
3800	5.154	49.288	44.684	17.495		115.823	53.653	- 3.086
3900	5.183	49.422	44.804	18.012		115.892	52.015	- 2.915
4000	5.213	49.554	44.921	18.531		115.964	50.376	- 2.752
4100	5.245	49.683	45.036	19.054		116.038	48.735	- 2.598
4200	5.278	49.810	45.148	19.580		116.116	47.094	- 2.450
4300	5.314	49.934	45.258	20.110		116.196	45.449	- 2.310
4400	5.351	50.057	45.365	20.643		116.280	43.803	- 2.176
4500	5.390	50.178	45.471	21.180		116.367	42.154	- 2.047
4600	5.431	50.297	45.575	21.721		116.458	40.505	- 1.924
4700	5.473	50.414	45.676	22.266		116.552	38.853	- 1.807
4800	5.517	50.530	45.776	22.816		116.651	37.199	- 1.694
4900	5.562	50.644	45.874	23.370		116.753	35.542	- 1.585
5000	5.608	50.757	45.971	23.928		116.860	33.883	- 1.481
5100	5.655	50.868	46.066	24.491		116.971	32.222	- 1.381
5200	5.703	50.978	46.159	25.059		117.087	30.560	- 1.284
5300	5.751	51.087	46.251	25.632		117.207	28.894	- 1.191
5400	5.800	51.195	46.342	26.210		117.332	27.228	- 1.102
5500	5.850	51.302	46.431	26.792		117.461	25.557	- 1.016
5600	5.900	51.408	46.519	27.380		117.595	23.884	- .932
5700	5.950	51.513	46.606	27.972		117.734	22.211	- .852
5800	6.000	51.617	46.691	28.570		117.878	20.534	- .774
5900	6.050	51.720	46.775	29.172		118.026	18.853	- .698
6000	6.100	51.822	46.859	29.780		118.179	17.172	- .625

(continues)

TABLE 2 (continued)

Thermochemical data of selected chemical compounds
Nitric Oxide (NO) (ideal gas) mol wt. = 30.008

T, °K.	cal. mole ⁻¹ deg. ⁻¹			kcal. mole ⁻¹			Log K _p
	C _p	S°	-(F°-H° ₂₉₈)/T	H°-H° ₂₉₈	ΔH _f	ΔF _f	
0	.000	.000	INFINITE	- 2.197	21.456	21.456	INFINITE
100	7.721	42.286	56.801	- 1.451	21.503	21.256	- 46.453
200	7.271	47.477	51.003	- .705	21.558	20.984	- 22.929
298	7.133	50.347	50.347	.000	21.580	20.697	- 15.171
300	7.132	50.392	50.348	.013	21.580	20.692	- 15.073
400	7.157	52.644	50.627	.727	21.590	20.904	- 11.142
500	7.287	54.053	51.157	1.448	21.594	20.995	- 8.783
600	7.466	55.397	51.755	2.186	21.598	19.795	- 7.210
700	7.655	46.562	47.360	2.942	21.601	19.494	- 6.086
800	7.832	57.596	52.941	3.716	21.605	19.192	- 5.243
900	7.988	58.528	53.520	4.507	21.610	18.890	- 4.587
1000	8.123	59.377	54.064	5.313	21.615	18.588	- 4.062
1100	8.238	60.157	54.583	6.131	21.620	18.285	- 3.633
1200	8.336	60.878	55.078	6.960	21.624	17.981	- 3.275
1300	8.419	61.548	55.550	7.798	21.628	17.678	- 2.972
1400	8.491	62.175	56.001	8.644	21.631	17.373	- 2.712
1500	8.552	62.763	56.432	9.496	21.633	17.069	- 2.487
1600	8.605	63.317	56.845	10.354	21.635	16.765	- 2.290
1700	8.651	63.840	57.242	11.217	21.635	16.461	- 2.116
1800	8.692	64.335	57.622	12.084	21.633	16.156	- 1.962
1900	8.727	64.806	57.988	12.955	21.630	15.853	- 1.823
2000	8.759	65.254	58.340	13.829	21.626	15.548	- 1.699
2100	8.788	65.683	58.680	14.706	21.619	15.244	- 1.586
2200	8.813	66.092	59.007	15.587	21.611	14.941	- 1.484
2300	8.837	66.484	59.324	16.469	21.601	14.637	- 1.391
2400	8.858	66.861	59.630	17.354	21.589	14.336	- 1.305
2500	8.877	67.223	59.927	18.241	21.574	14.033	- 1.227
2600	8.895	67.571	60.214	19.129	21.558	13.732	- 1.154
2700	8.912	67.908	60.493	20.020	21.540	13.432	- 1.087
2800	8.927	68.232	60.763	20.911	21.520	13.132	- 1.025
2900	8.941	68.545	61.026	21.805	21.498	12.834	- .967
3000	8.955	68.849	61.282	22.700	21.474	12.535	- .913
3100	8.968	69.143	61.531	23.596	21.449	12.237	- .863
3200	8.980	69.427	61.773	24.493	21.421	11.940	- .815
3300	8.991	69.704	62.010	25.392	21.392	11.644	- .771
3400	9.002	69.973	62.240	26.291	21.361	11.349	- .729
3500	9.012	70.234	62.464	27.192	21.329	11.054	- .690
3600	9.022	70.488	62.684	28.094	21.294	10.762	- .653
3700	9.032	70.735	62.898	28.997	21.259	10.470	- .618
3800	9.041	70.976	63.108	29.900	21.222	10.179	- .585
3900	9.050	71.211	63.312	30.805	21.185	9.889	- .554
4000	9.058	71.440	63.513	31.710	21.145	9.598	- .524
4100	9.066	71.664	63.709	32.616	21.104	9.311	- .496
4200	9.074	71.882	63.901	33.523	21.063	9.024	- .470
4300	9.082	72.096	64.089	34.431	21.021	8.739	- .444
4400	9.090	72.305	64.273	35.340	20.977	8.452	- .420
4500	9.097	72.509	64.454	36.249	20.932	8.169	- .397
4600	9.105	72.709	64.631	37.159	20.887	7.888	- .375
4700	9.112	72.905	64.805	38.070	20.841	7.605	- .354
4800	9.119	73.097	64.976	38.982	20.794	7.324	- .333
4900	9.125	73.285	65.144	39.894	20.747	7.040	- .314
5000	9.132	73.470	65.308	40.807	20.699	6.763	- .296
5100	9.139	73.651	65.470	41.720	20.650	6.484	- .278
5200	9.145	73.828	65.629	42.634	20.601	6.207	- .261
5300	9.152	74.002	65.786	43.549	20.551	5.932	- .245
5400	9.158	74.173	65.939	44.465	20.501	5.654	- .229
5500	9.164	74.342	66.091	45.381	20.451	5.383	- .214
5600	9.170	74.507	66.239	46.298	20.400	5.107	- .199
5700	9.176	74.669	66.386	47.215	20.348	4.835	- .185
5800	9.182	74.829	66.530	48.133	20.297	4.566	- .172
5900	9.188	74.986	66.672	49.051	20.245	4.292	- .159
6000	9.194	75.140	66.812	49.970	20.192	4.024	- .147

TABLE 2 (continued)

Thermochemical data of selected chemical compounds
Nitric Oxide Unipositive Ion (NO⁺) (ideal gas) GFW = 30.00555

T, °K	gibbs/mol			kcal/mol			Log Kp
	C _p ^o	S ^o	-(G ^o -H ^o) ₂₉₈ /T	H ^o -H ^o ₂₉₈	ΔH ^o	ΔG ^o	
0							
100							
200							
298	6.961	47.349	47.349	.000	236.660	235.184	- 172.395
300	6.961	47.349	47.349	.013	236.669	235.175	- 171.324
400	6.989	49.307	47.622	.710	247.159	234.603	- 128.181
500	7.067	50.964	48.139	1.412	257.641	233.908	- 102.741
600	7.191	52.263	48.721	2.125	268.117	233.117	- 84.913
700	7.344	53.383	49.109	2.852	278.587	232.245	- 72.510
800	7.505	54.374	49.481	3.504	289.056	231.307	- 63.190
900	7.682	55.267	49.841	4.153	299.525	230.311	- 55.927
1000	7.807	56.082	50.096	4.726	309.995	229.262	- 50.105
1100	7.938	56.832	51.456	5.213	320.466	228.166	- 45.332
1200	8.054	57.528	51.934	6.713	340.938	227.028	- 41.347
1300	8.156	58.177	52.369	7.524	361.411	225.848	- 37.908
1400	8.245	58.784	52.825	8.344	381.885	224.634	- 35.067
1500	8.323	59.356	53.241	9.172	402.361	223.384	- 32.547
1600	8.392	59.895	53.640	10.008	422.837	222.104	- 30.338
1700	8.452	60.406	54.023	10.850	443.314	220.794	- 28.385
1800	8.506	60.891	54.392	11.698	463.789	219.454	- 26.645
1900	8.553	61.352	54.746	12.551	484.265	218.091	- 25.086
2000	8.595	61.792	55.087	13.409	504.740	216.700	- 23.680
2100	8.633	62.212	55.417	14.270	525.215	215.286	- 22.405
2200	8.667	62.614	55.735	15.135	545.688	213.851	- 21.264
2300	8.697	63.000	56.042	16.004	566.160	212.391	- 20.182
2400	8.725	63.371	56.340	16.875	586.632	210.915	- 19.206
2500	8.750	63.728	56.628	17.749	607.101	209.415	- 18.307
2600	8.774	64.071	56.908	18.625	627.570	207.900	- 17.476
2700	8.795	64.403	57.180	19.503	648.037	206.366	- 16.704
2800	8.814	64.723	57.443	20.384	668.502	204.814	- 15.986
2900	8.832	65.033	57.700	21.266	688.965	203.246	- 15.317
3000	8.849	65.332	57.949	22.150	709.428	201.667	- 14.691
3100	8.865	65.623	58.192	23.036	729.889	200.059	- 14.104
3200	8.879	65.905	58.429	23.923	750.348	198.446	- 13.553
3300	8.893	66.178	58.659	24.812	770.806	196.818	- 13.035
3400	8.906	66.444	58.884	25.702	791.261	195.175	- 12.546
3500	8.918	66.702	59.104	26.593	811.716	193.518	- 12.084
3600	8.929	66.953	59.319	27.485	832.170	191.852	- 11.647
3700	8.940	67.198	59.528	28.379	852.622	190.166	- 11.233
3800	8.951	67.437	59.733	29.273	873.073	188.473	- 10.840
3900	8.961	67.669	59.934	30.169	893.524	186.769	- 10.466
4000	8.970	67.896	60.130	31.065	913.971	185.049	- 10.111
4100	8.979	68.118	60.322	31.963	934.419	183.319	- 9.772
4200	8.988	68.334	60.510	32.861	954.866	181.584	- 9.449
4300	8.996	68.546	60.695	33.760	975.312	179.834	- 9.140
4400	9.004	68.753	60.876	34.660	995.756	178.072	- 8.845
4500	9.012	68.955	61.053	35.561	1016.199	176.302	- 8.562
4600	9.019	69.154	61.227	36.463	1036.643	174.521	- 8.292
4700	9.026	69.348	61.398	37.365	1057.085	172.729	- 8.032
4800	9.033	69.538	61.565	38.268	1077.526	170.930	- 7.783
4900	9.040	69.724	61.730	39.172	1097.968	169.121	- 7.543
5000	9.047	69.907	61.892	40.076	1118.407	167.304	- 7.313
5100	9.053	70.086	62.050	40.981	1138.846	165.476	- 7.091
5200	9.060	70.262	62.207	41.887	1159.286	163.642	- 6.878
5300	9.066	70.434	62.360	42.793	1179.725	161.802	- 6.672
5400	9.072	70.604	62.511	43.700	1200.163	159.945	- 6.473
5500	9.078	70.770	62.660	44.607	1220.601	158.092	- 6.282
5600	9.084	70.934	62.806	45.515	1241.037	156.216	- 6.097
5700	9.089	71.095	62.950	46.424	1261.474	154.346	- 5.918
5800	9.095	71.253	63.092	47.333	1281.911	152.462	- 5.745
5900	9.100	71.409	63.232	48.243	1302.347	150.566	- 5.577
6000	9.106	71.562	63.369	49.153	1322.783	148.672	- 5.415

(continues)

TABLE 2 (continued)

Thermochemical data of selected chemical compounds
 Nitrogen Dioxide (NO₂) (ideal gas) mol. wt. = 46.008

T, °K.	cal. mole ⁻¹ deg. ⁻¹			kcal. mole ⁻¹			Log K _p
	C _p	S°	-(F°-H° ₂₉₈)/T	H°-H° ₂₉₈	ΔH _f °	ΔF _f °	
0	.000	.000	INFINITE	- 2.435	8.586	8.586	INFINITE
100	7.953	48.387	64.785	- 1.640	8.326	9.545	20.859
200	8.218	53.954	58.130	- .835	8.099	10.853	11.859
298	8.837	57.343	57.343	.000	7.910	12.247	8.977
300	8.850	57.398	57.344	.016	7.907	12.274	8.941
400	9.601	60.046	57.700	.939	7.770	13.751	7.513
500	10.327	62.268	58.197	1.936	7.684	15.258	6.669
600	10.955	64.208	59.207	3.001	7.638	16.778	6.111
700	11.469	65.937	60.047	4.123	7.618	18.302	5.714
800	11.881	67.496	60.882	5.291	7.617	19.828	5.417
900	12.208	68.915	61.697	6.496	7.629	21.355	5.185
1000	12.468	70.215	62.485	7.730	7.649	22.879	5.000
1100	12.677	71.414	63.243	8.988	7.674	24.400	4.848
1200	12.847	72.524	63.971	10.265	7.702	25.921	4.721
1300	12.985	73.558	64.669	11.556	7.731	27.438	4.612
1400	13.099	74.525	65.339	12.861	7.761	28.951	4.510
1500	13.193	75.432	65.982	14.176	7.790	30.464	4.428
1600	13.273	76.286	66.599	15.499	7.818	31.975	4.367
1700	13.340	77.093	67.193	16.830	7.846	33.484	4.304
1800	13.398	77.857	67.764	18.167	7.869	34.992	4.248
1900	13.447	78.583	68.315	19.509	7.890	36.498	4.198
2000	13.490	79.274	68.846	20.856	7.908	38.002	4.152
2100	13.527	79.933	69.358	22.207	7.923	39.507	4.111
2200	13.560	80.563	69.853	23.561	7.932	41.010	4.074
2300	13.588	81.166	70.332	24.919	7.939	42.514	4.040
2400	13.614	81.745	70.796	26.279	7.942	44.019	4.008
2500	13.636	82.301	71.245	27.641	7.939	45.520	3.979
2600	13.656	82.836	71.680	29.006	7.933	47.025	3.953
2700	13.674	83.352	72.103	30.373	7.922	48.529	3.928
2800	13.690	83.850	72.514	31.741	7.907	50.031	3.905
2900	13.705	84.330	72.913	33.111	7.888	51.540	3.884
3000	13.718	84.795	73.301	34.482	7.863	53.045	3.864
3100	13.730	85.245	73.679	35.854	7.836	54.551	3.846
3200	13.741	85.681	74.048	37.228	7.803	56.058	3.828
3300	13.751	86.104	74.407	38.602	7.767	57.565	3.812
3400	13.760	86.515	74.757	39.976	7.726	59.075	3.797
3500	13.768	86.914	75.099	41.354	7.683	60.583	3.783
3600	13.776	87.302	75.432	42.731	7.635	62.097	3.770
3700	13.783	87.679	75.758	44.109	7.584	63.613	3.757
3800	13.790	88.047	76.077	45.488	7.529	65.128	3.746
3900	13.796	88.405	76.388	46.867	7.473	66.643	3.734
4000	13.801	88.755	76.693	48.247	7.412	68.158	3.724
4100	13.806	89.096	76.991	49.627	7.347	69.678	3.714
4200	13.811	89.428	77.284	51.008	7.281	71.201	3.705
4300	13.816	89.753	77.570	52.390	7.213	72.727	3.696
4400	13.820	90.071	77.850	53.771	7.140	74.247	3.688
4500	13.824	90.382	78.125	55.154	7.066	75.772	3.680
4600	13.828	90.686	78.395	56.536	6.990	77.304	3.673
4700	13.831	90.983	78.660	57.919	6.911	78.833	3.666
4800	13.834	91.274	78.920	59.302	6.830	80.366	3.659
4900	13.837	91.559	79.175	60.686	6.748	81.894	3.652
5000	13.840	91.839	79.425	62.070	6.663	83.428	3.646
5100	13.843	92.113	79.671	63.454	6.577	84.966	3.641
5200	13.846	92.382	79.913	64.838	6.489	86.501	3.635
5300	13.848	92.646	80.151	66.223	6.400	88.044	3.630
5400	13.850	92.905	80.385	67.608	6.309	89.579	3.625
5500	13.852	93.159	80.615	68.993	6.217	91.128	3.621
5600	13.854	93.408	80.841	70.379	6.122	92.673	3.617
5700	13.856	93.654	81.063	71.764	6.027	94.215	3.612
5800	13.858	93.895	81.283	73.140	5.931	95.767	3.608
5900	13.860	94.132	81.498	74.516	5.833	97.313	3.605
6000	13.862	94.365	81.711	75.892	5.734	98.866	3.601

TABLE 2 (continued)

Thermochemical data of selected chemical compounds
 Nitrogen, Diatomic (N_2) (reference state—ideal gas) mol. wt. = 28.0134

T, °K.	cal. mole ⁻¹ deg. ⁻¹			kcal. mole ⁻¹			Log K_p
	C_p°	S°	$-(F^\circ - H_{298}^\circ)/T$	$H^\circ - H_{298}^\circ$	ΔH_f°	ΔF_f°	
0	.000	.000	INFINITE	- 2.072	.000	.000	.000
100	6.956	38.170	51.957	- 1.379	.000	.000	.000
200	6.957	42.992	46.407	.683	.000	.000	.000
298	6.961	45.770	45.770	.000	.000	.000	.000
300	6.961	45.813	45.770	.013	.000	.000	.000
400	6.990	47.818	46.043	.710	.000	.000	.000
500	7.069	49.386	46.561	1.413	.000	.000	.000
600	7.196	50.685	47.143	2.125	.000	.000	.000
700	7.350	51.806	47.731	2.853	.000	.000	.000
800	7.512	52.798	48.303	3.596	.000	.000	.000
900	7.670	53.692	48.853	4.355	.000	.000	.000
1000	7.815	54.507	49.378	5.129	.000	.000	.000
1100	7.945	55.258	49.879	5.917	.000	.000	.000
1200	8.061	55.955	50.357	6.718	.000	.000	.000
1300	8.162	56.604	50.813	7.529	.000	.000	.000
1400	8.252	57.212	51.248	8.350	.000	.000	.000
1500	8.330	57.784	51.665	9.179	.000	.000	.000
1600	8.398	58.324	52.065	10.015	.000	.000	.000
1700	8.458	58.835	52.448	10.858	.000	.000	.000
1800	8.512	59.320	52.816	11.707	.000	.000	.000
1900	8.559	59.782	53.171	12.560	.000	.000	.000
2000	8.601	60.222	53.513	13.418	.000	.000	.000
2100	8.638	60.642	53.842	14.280	.000	.000	.000
2200	8.672	61.045	54.160	15.146	.000	.000	.000
2300	8.703	61.431	54.468	16.015	.000	.000	.000
2400	8.731	61.802	54.766	16.886	.000	.000	.000
2500	8.756	62.159	55.055	17.761	.000	.000	.000
2600	8.779	62.503	55.335	18.638	.000	.000	.000
2700	8.800	62.835	55.606	19.517	.000	.000	.000
2800	8.820	63.155	55.870	20.398	.000	.000	.000
2900	8.838	63.465	56.127	21.280	.000	.000	.000
3000	8.855	63.765	56.376	22.165	.000	.000	.000
3100	8.871	64.055	56.619	23.051	.000	.000	.000
3200	8.886	64.337	56.856	23.939	.000	.000	.000
3300	8.900	64.611	57.087	24.829	.000	.000	.000
3400	8.914	64.877	57.312	25.719	.000	.000	.000
3500	8.927	65.135	57.532	26.611	.000	.000	.000
3600	8.939	65.387	57.747	27.505	.000	.000	.000
3700	8.950	65.632	57.957	28.399	.000	.000	.000
3800	8.962	65.871	58.162	29.295	.000	.000	.000
3900	8.972	66.104	58.362	30.191	.000	.000	.000
4000	8.983	66.331	58.559	31.089	.000	.000	.000
4100	8.993	66.553	58.751	31.988	.000	.000	.000
4200	9.002	66.770	58.940	32.888	.000	.000	.000
4300	9.012	66.982	59.124	33.788	.000	.000	.000
4400	9.021	67.189	59.305	34.690	.000	.000	.000
4500	9.030	67.392	59.482	35.593	.000	.000	.000
4600	9.039	67.591	59.657	36.496	.000	.000	.000
4700	9.048	67.785	59.827	37.400	.000	.000	.000
4800	9.057	67.976	59.995	38.306	.000	.000	.000
4900	9.066	68.162	60.160	39.212	.000	.000	.000
5000	9.074	68.346	60.322	40.119	.000	.000	.000
5100	9.083	68.525	60.481	41.027	.000	.000	.000
5200	9.091	68.702	60.637	41.935	.000	.000	.000
5300	9.100	68.875	60.791	42.845	.000	.000	.000
5400	9.109	69.045	60.942	43.755	.000	.000	.000
5500	9.118	69.213	61.091	44.667	.000	.000	.000
5600	9.127	69.377	61.238	45.579	.000	.000	.000
5700	9.136	69.539	61.382	46.492	.000	.000	.000
5800	9.145	69.698	61.524	47.406	.000	.000	.000
5900	9.155	69.854	61.664	48.321	.000	.000	.000
6000	9.165	70.008	61.802	49.237	.000	.000	.000

(continues)

TABLE 2 (continued)

Thermochemical data of selected chemical compounds
Oxygen, Monatomic (O) (ideal gas) at. wt. = 16.000

T, °K.	cal. mole ⁻¹ deg. ⁻¹				kcal. mole ⁻¹			Log K _p
	C _p	S°	-(F°-H ₂₉₈ °)/T	H°-H ₂₉₈ °	ΔH _f °	ΔF _f °		
0	.000	.000	INFINITE	- 1.608	58.989	58.989	INFINITE	
100	5.666	37.466	43.266	- 1.080	59.160	57.989	= 126.730	
200	5.434	38.340	38.953	.523	59.377	56.733	= 61.992	
298	5.237	38.468	38.468	.000	59.559	55.395	= 40.804	
300	5.235	38.501	38.468	.010	59.562	55.369	= 40.334	
400	5.135	39.991	38.672	.528	59.725	53.946	= 29.473	
500	5.081	41.131	39.055	1.038	59.870	52.485	= 22.940	
600	5.049	42.054	39.480	1.544	59.998	50.995	= 18.574	
700	5.029	42.431	39.805	2.048	60.113	49.486	= 15.449	
800	5.015	43.501	40.313	2.550	60.216	47.960	= 13.101	
900	5.006	44.092	40.701	3.052	60.311	46.422	= 11.272	
1000	4.994	44.614	41.067	3.552	60.397	44.875	= 9.807	
1100	4.984	45.095	41.412	4.051	60.477	43.318	= 8.406	
1200	4.976	45.528	41.737	4.551	60.553	41.755	= 7.604	
1300	4.967	45.920	42.044	5.049	60.623	40.186	= 6.755	
1400	4.964	46.298	42.335	5.548	60.689	38.611	= 6.027	
1500	4.962	46.642	42.611	6.046	60.752	37.032	= 5.395	
1600	4.961	46.963	42.873	6.544	60.812	35.446	= 4.842	
1700	4.979	47.265	43.123	7.042	60.869	33.862	= 4.353	
1800	4.979	47.550	43.361	7.540	60.922	32.271	= 3.918	
1900	4.976	47.819	43.588	8.038	60.973	30.678	= 3.529	
2000	4.978	48.074	43.806	8.536	61.020	29.082	= 3.178	
2100	4.976	48.317	44.015	9.034	61.066	27.484	= 2.860	
2200	4.979	48.549	44.216	9.532	61.108	25.884	= 2.571	
2300	4.980	48.770	44.409	10.029	61.147	24.282	= 2.307	
2400	4.981	48.987	44.596	10.527	61.184	22.679	= 2.065	
2500	4.984	49.195	44.775	11.026	61.219	21.073	= 1.842	
2600	4.986	49.381	44.948	11.524	61.251	19.467	= 1.636	
2700	4.990	49.549	45.116	12.023	61.281	17.859	= 1.446	
2800	4.994	49.751	45.278	12.522	61.309	16.251	= 1.268	
2900	4.999	49.926	45.436	13.022	61.334	14.642	= 1.103	
3000	5.004	50.096	45.588	13.522	61.358	13.031	= .949	
3100	5.010	50.260	45.736	14.023	61.380	11.420	= .805	
3200	5.017	50.419	45.880	14.524	61.401	9.807	= .670	
3300	5.025	50.573	46.020	15.026	61.420	8.194	= .543	
3400	5.033	50.724	46.156	15.529	61.437	6.581	= .423	
3500	5.041	50.870	46.289	16.033	61.454	4.967	= .310	
3600	5.050	51.012	46.418	16.537	61.469	3.354	= .204	
3700	5.060	51.150	46.544	17.043	61.484	1.739	= .103	
3800	5.070	51.285	46.667	17.549	61.498	.125	= .007	
3900	5.081	51.417	46.787	18.057	61.511	- 1.492	= .084	
4000	5.091	51.546	46.904	18.565	61.524	- 3.107	= .170	
4100	5.103	51.672	47.019	19.075	61.536	- 4.723	= .252	
4200	5.114	51.795	47.131	19.586	61.549	- 6.339	= .330	
4300	5.128	51.915	47.241	20.098	61.561	- 7.955	= .404	
4400	5.138	52.033	47.349	20.611	61.572	- 9.573	= .475	
4500	5.150	52.149	47.454	21.126	61.584	- 11.189	= .543	
4600	5.162	52.262	47.558	21.641	61.596	- 12.805	= .608	
4700	5.174	52.373	47.659	22.156	61.608	- 14.423	= .671	
4800	5.186	52.482	47.758	22.676	61.620	- 16.041	= .730	
4900	5.196	52.589	47.856	23.195	61.633	- 17.661	= .788	
5000	5.210	52.695	47.951	23.715	61.646	- 19.279	= .843	
5100	5.222	52.798	48.045	24.237	61.659	- 20.896	= .895	
5200	5.234	52.899	48.138	24.760	61.673	- 22.517	= .946	
5300	5.246	52.999	48.229	25.284	61.687	- 24.134	= .995	
5400	5.258	53.097	48.318	25.809	61.702	- 25.755	= 1.042	
5500	5.269	53.194	48.406	26.335	61.718	- 27.373	= 1.088	
5600	5.280	53.289	48.492	26.863	61.733	- 28.995	= 1.132	
5700	5.292	53.383	48.577	27.392	61.750	- 30.616	= 1.174	
5800	5.302	53.475	48.661	27.921	61.767	- 32.234	= 1.215	
5900	5.313	53.565	48.743	28.452	61.785	- 33.856	= 1.254	
6000	5.323	53.655	48.824	28.984	61.803	- 35.476	= 1.292	

TABLE 2 (continued)

Thermochemical data of selected chemical compounds
 Oxygen, Diatomic (O₂) (reference state—ideal gas) mol. wt. = 31.9988

T, °K.	cal. mole ⁻¹ deg. ⁻¹			kcal. mole ⁻¹			Log K _p
	C _p	S°	-(F°-H° ₂₉₈)/T	H°-H° ₂₉₈	ΔH _f °	ΔF _f °	
0	.000	.000	INFINITE	- 2.075	.000	.000	.000
100	6.958	41.395	55.705	- 1.381	.000	.000	.000
200	6.961	46.218	49.643	- .685	.000	.000	.000
298	7.020	49.004	49.004	.000	.000	.000	.000
300	7.023	49.047	49.004	.013	.000	.000	.000
400	7.196	51.091	49.782	.724	.000	.000	.000
500	7.431	52.722	49.812	1.455	.000	.000	.000
600	7.670	54.098	50.414	2.410	.000	.000	.000
700	7.883	55.297	51.028	2.988	.000	.000	.000
800	8.063	56.361	51.629	3.786	.000	.000	.000
900	8.212	57.320	52.209	4.600	.000	.000	.000
1000	8.336	58.192	52.765	5.427	.000	.000	.000
1100	8.439	58.991	53.295	6.266	.000	.000	.000
1200	8.527	59.720	53.801	7.114	.000	.000	.000
1300	8.604	60.415	54.283	7.971	.000	.000	.000
1400	8.674	61.055	54.744	8.835	.000	.000	.000
1500	8.738	61.656	55.185	9.706	.000	.000	.000
1600	8.800	62.222	55.608	10.583	.000	.000	.000
1700	8.858	62.757	56.013	11.465	.000	.000	.000
1800	8.916	63.265	56.401	12.354	.000	.000	.000
1900	8.973	63.749	56.776	13.249	.000	.000	.000
2000	9.029	64.210	57.136	14.149	.000	.000	.000
2100	9.084	64.652	57.483	15.054	.000	.000	.000
2200	9.139	65.076	57.819	15.966	.000	.000	.000
2300	9.194	65.483	58.143	16.882	.000	.000	.000
2400	9.248	65.876	58.457	17.804	.000	.000	.000
2500	9.301	66.254	58.762	18.732	.000	.000	.000
2600	9.354	66.620	59.057	19.664	.000	.000	.000
2700	9.405	66.974	59.344	20.602	.000	.000	.000
2800	9.455	67.317	59.622	21.545	.000	.000	.000
2900	9.503	67.650	59.893	22.493	.000	.000	.000
3000	9.551	67.973	60.157	23.446	.000	.000	.000
3100	9.596	68.287	60.415	24.403	.000	.000	.000
3200	9.640	68.592	60.665	25.365	.000	.000	.000
3300	9.682	68.889	60.910	26.331	.000	.000	.000
3400	9.723	69.179	61.149	27.302	.000	.000	.000
3500	9.762	69.461	61.383	28.276	.000	.000	.000
3600	9.799	69.737	61.611	29.254	.000	.000	.000
3700	9.835	70.006	61.834	30.236	.000	.000	.000
3800	9.869	70.269	62.053	31.221	.000	.000	.000
3900	9.901	70.525	62.267	32.209	.000	.000	.000
4000	9.932	70.776	62.476	33.201	.000	.000	.000
4100	9.961	71.022	62.682	34.196	.000	.000	.000
4200	9.988	71.262	62.883	35.193	.000	.000	.000
4300	10.015	71.498	63.081	36.193	.000	.000	.000
4400	10.039	71.728	63.275	37.196	.000	.000	.000
4500	10.062	71.954	63.465	38.201	.000	.000	.000
4600	10.084	72.176	63.652	39.208	.000	.000	.000
4700	10.104	72.393	63.836	40.218	.000	.000	.000
4800	10.123	72.606	64.016	41.229	.000	.000	.000
4900	10.140	72.814	64.194	42.242	.000	.000	.000
5000	10.156	73.019	64.368	43.257	.000	.000	.000
5100	10.172	73.221	64.540	44.274	.000	.000	.000
5200	10.187	73.418	64.708	45.292	.000	.000	.000
5300	10.200	73.613	64.875	46.311	.000	.000	.000
5400	10.213	73.803	65.038	47.332	.000	.000	.000
5500	10.225	73.991	65.199	48.353	.000	.000	.000
5600	10.237	74.175	65.358	49.377	.000	.000	.000
5700	10.247	74.356	65.514	50.401	.000	.000	.000
5800	10.258	74.535	65.668	51.426	.000	.000	.000
5900	10.267	74.710	65.820	52.452	.000	.000	.000
6000	10.276	74.883	65.970	53.479	.000	.000	.000

(continues)

TABLE 2 (continued)

Thermochemical data of selected chemical compounds
Sulfur Dioxide (SO₂) (ideal gas) mol. wt. = 64.066

T, °K.	cal. mole ⁻¹ deg. ⁻¹			kcal. mole ⁻¹			Log K _p
	C _p	S°	-(F°-H° ₂₉₈)/T	H°-H° ₂₉₈	ΔH _f	ΔF _f	
0	.000	.000	INFINITE	- 2.522	- 70.341	- 70.341	INFINITE
100	6.013	49.932	67.182	- 1.725	- 70.421	- 70.966	155.088
200	8.693	55.770	60.135	- .893	- 70.662	- 71.425	78.044
298	9.530	59.298	59.298	.000	- 70.947	- 71.741	52.595
300	9.547	59.357	59.298	.018	- 70.952	- 71.746	52.264
400	10.395	62.222	59.683	1.016	- 71.764	- 71.947	39.308
500	11.132	64.423	60.437	2.093	- 72.356	- 71.923	31.436
600	11.793	66.707	61.312	3.237	- 72.824	- 71.790	26.148
700	12.180	68.550	62.217	4.433	- 73.206	- 71.562	22.342
800	12.532	70.200	63.114	5.669	- 73.593	- 72.574	19.825
900	12.806	71.693	63.985	6.937	- 73.977	- 73.022	17.197
1000	13.022	73.054	64.825	8.229	- 74.353	- 73.071	15.095
1100	13.194	74.303	65.631	9.540	- 74.724	- 67.326	13.376
1200	13.335	75.458	66.402	10.866	- 75.090	- 65.582	11.943
1300	13.451	76.530	67.141	12.206	- 75.452	- 63.840	10.732
1400	13.549	77.530	67.847	13.556	- 75.813	- 62.102	9.694
1500	13.632	78.468	68.524	14.915	- 76.173	- 60.369	8.795
1600	13.704	79.350	69.174	16.282	- 76.531	- 58.635	8.009
1700	13.767	80.183	69.797	17.656	- 76.888	- 56.905	7.315
1800	13.822	80.971	70.396	19.035	- 77.248	- 55.178	6.699
1900	13.872	81.720	70.973	20.420	- 77.608	- 53.452	6.148
2000	13.917	82.433	71.528	21.809	- 77.967	- 51.731	5.653
2100	13.958	83.113	72.064	23.203	- 78.323	- 50.010	5.204
2200	13.995	83.743	72.581	24.601	- 78.679	- 48.290	4.797
2300	14.030	84.386	73.080	26.002	- 79.037	- 46.573	4.425
2400	14.063	84.984	73.564	27.407	- 79.397	- 44.855	4.084
2500	14.093	85.558	74.032	28.815	- 79.758	- 43.141	3.771
2600	14.122	86.112	74.486	30.225	- 80.116	- 41.426	3.482
2700	14.149	86.645	74.927	31.639	- 80.474	- 39.713	3.214
2800	14.175	87.160	75.355	33.055	- 80.833	- 38.002	2.966
2900	14.200	87.658	75.770	34.474	- 81.193	- 36.288	2.735
3000	14.224	88.140	76.175	35.895	- 81.553	- 34.575	2.519
3100	14.247	88.607	76.568	37.319	- 81.913	- 32.864	2.317
3200	14.270	89.059	76.952	38.745	- 82.273	- 31.154	2.128
3300	14.291	89.499	77.325	40.173	- 82.633	- 29.446	1.950
3400	14.312	89.926	77.689	41.603	- 82.993	- 27.733	1.783
3500	14.333	90.341	78.045	43.035	- 83.353	- 26.026	1.625
3600	14.353	90.745	78.392	44.469	- 83.713	- 24.313	1.476
3700	14.373	91.136	78.731	45.906	- 84.073	- 22.602	1.335
3800	14.392	91.522	79.063	47.344	- 84.433	- 20.890	1.201
3900	14.411	91.896	79.387	48.784	- 84.793	- 19.183	1.075
4000	14.430	92.261	79.705	50.226	- 85.153	- 17.469	.954
4100	14.448	92.618	80.015	51.670	- 85.513	- 15.758	.840
4200	14.467	92.966	80.319	53.114	- 85.873	- 14.047	.731
4300	14.485	93.307	80.617	54.563	- 86.233	- 12.333	.627
4400	14.502	93.640	80.910	56.013	- 86.593	- 10.623	.528
4500	14.520	93.966	81.196	57.464	- 86.953	- 8.908	.433
4600	14.537	94.285	81.477	58.917	- 87.313	- 7.194	.342
4700	14.554	94.598	81.753	60.371	- 87.673	- 5.482	.255
4800	14.572	94.905	82.024	61.828	- 88.033	- 3.769	.172
4900	14.588	95.205	82.290	63.286	- 88.393	- 2.056	.092
5000	14.605	95.500	82.551	64.745	- 88.753	- .345	.015
5100	14.622	95.790	82.808	66.207	- 89.113	1.375	-.059
5200	14.639	96.074	83.060	67.670	- 89.473	3.087	-.130
5300	14.655	96.353	83.308	69.134	- 89.833	4.806	-.198
5400	14.672	96.627	83.553	70.601	- 90.193	6.518	-.264
5500	14.688	96.896	83.793	72.069	- 90.553	8.237	-.327
5600	14.704	97.161	84.029	73.538	- 90.913	9.952	-.388
5700	14.720	97.421	84.262	75.010	- 91.273	11.665	-.447
5800	14.736	97.677	84.491	76.482	- 91.633	13.387	-.504
5900	14.753	97.930	84.717	77.957	- 91.993	15.099	-.559
6000	14.769	98.178	84.939	79.433	- 92.353	16.823	-.613

TABLE 2 (continued)

Thermochemical data of selected chemical compounds
Ozone (O₃) (ideal gas) mol. wt. = 48.000

T, °K.	cal. mole ⁻¹ deg. ⁻¹			kcal. mole ⁻¹			Log K _p
	C _p	S°	-(F°-H° ₂₉₈)/T	H°-H° ₂₉₈	ΔH _f °	ΔF _f °	
0	.000	.000	INFINITE	= 2.474	34.739	34.739	INFINITE
100	7.957	47.289	47.981	= .002	36.141	37.573	82.112
200	6.379	53.564	57.909	= .889	34.254	37.411	40.879
298	9.376	57.080	57.080	.000	34.100	36.997	28.585
300	9.400	57.138	57.080	.017	34.098	39.028	28.430
400	10.455	59.992	57.462	1.012	34.026	40.684	22.227
500	11.296	62.419	54.217	2.101	34.019	42.351	18.511
600	11.916	64.536	59.097	3.243	34.048	44.015	16.032
700	12.369	66.409	60.011	4.479	34.097	45.672	14.259
800	12.704	68.083	60.917	5.733	34.154	47.321	12.927
900	12.956	69.595	61.799	7.017	34.217	48.963	11.889
1000	13.151	70.971	62.648	8.323	34.282	50.599	11.058
1100	13.303	72.232	63.463	9.646	34.347	52.227	10.376
1200	13.426	73.395	64.243	10.982	34.411	53.850	9.807
1300	13.526	74.473	64.989	12.330	34.474	55.468	9.324
1400	13.611	75.479	65.702	13.687	34.535	57.080	8.910
1500	13.682	76.420	66.386	15.052	34.593	58.688	8.550
1600	13.743	77.395	67.041	16.423	34.649	60.293	8.235
1700	13.796	78.140	67.670	17.800	34.703	61.895	7.957
1800	13.843	78.930	68.273	19.182	34.751	63.492	7.709
1900	13.885	79.680	68.854	20.569	34.795	65.088	7.486
2000	13.922	80.393	69.413	21.959	34.835	66.680	7.286
2100	13.957	81.073	69.953	23.353	34.872	68.272	7.105
2200	13.988	81.723	70.473	24.750	34.901	69.861	6.940
2300	14.017	82.345	70.976	26.150	34.927	71.449	6.789
2400	14.045	82.943	71.462	27.554	34.948	73.039	6.651
2500	14.070	83.516	71.933	28.959	34.961	74.623	6.523
2600	14.094	84.069	72.389	30.368	34.972	76.211	6.406
2700	14.117	84.601	72.831	31.778	34.975	77.797	6.297
2800	14.139	85.115	73.261	33.191	34.973	79.383	6.196
2900	14.160	85.611	73.678	34.604	34.966	80.971	6.102
3000	14.180	86.092	74.084	36.023	34.954	82.557	6.014
3100	14.199	86.557	74.479	37.442	34.937	84.145	5.932
3200	14.216	87.008	74.864	38.863	34.915	85.731	5.855
3300	14.231	87.444	75.238	40.285	34.889	87.314	5.783
3400	14.254	87.871	75.604	41.710	34.857	88.908	5.715
3500	14.272	88.285	75.960	43.136	34.822	90.496	5.651
3600	14.288	88.687	76.308	44.564	34.783	92.090	5.590
3700	14.305	89.079	76.648	45.994	34.740	93.682	5.533
3800	14.321	89.460	76.980	47.425	34.694	95.278	5.479
3900	14.337	89.833	77.305	48.858	34.645	96.869	5.428
4000	14.353	90.196	77.623	50.293	34.591	98.464	5.380
4100	14.369	90.550	77.934	51.729	34.535	100.064	5.334
4200	14.384	90.897	78.236	53.166	34.477	101.661	5.290
4300	14.399	91.235	78.536	54.605	34.416	103.266	5.248
4400	14.414	91.567	78.829	56.046	34.352	104.864	5.208
4500	14.429	91.891	79.116	57.488	34.287	106.468	5.171
4600	14.444	92.208	79.397	58.932	34.220	108.078	5.135
4700	14.458	92.519	79.673	60.377	34.150	109.682	5.100
4800	14.473	92.823	79.943	61.824	34.080	111.291	5.067
4900	14.487	93.122	80.209	63.272	34.009	112.894	5.035
5000	14.501	93.415	80.471	64.721	33.935	114.504	5.005
5100	14.515	93.702	80.727	66.172	33.861	116.121	4.976
5200	14.529	93.984	80.979	67.624	33.786	117.730	4.948
5300	14.543	94.261	81.227	69.078	33.711	119.352	4.921
5400	14.557	94.533	81.471	70.533	33.635	120.962	4.895
5500	14.571	94.800	81.711	71.989	33.559	122.585	4.871
5600	14.585	95.063	81.947	73.447	33.481	124.200	4.847
5700	14.598	95.321	82.180	74.906	33.404	125.818	4.824
5800	14.612	95.575	82.408	76.366	33.327	127.447	4.802
5900	14.625	95.825	82.634	77.828	33.250	129.077	4.781
6000	14.639	96.071	82.856	79.292	33.173	130.695	4.760

(continues)

TABLE 2 (continued)

Thermochemical data of selected chemical compounds
Sulfur Trioxide (SO₃) (ideal gas) mol. wt. = 80.0622

T, °K.	cal. mole ⁻¹ deg. ⁻¹			kcal. mole ⁻¹			Log K _p
	C _p	S°	-(F°-H° ₂₉₈)/T	H°-H° ₂₉₈	ΔH _f °	ΔF _f °	
0	.000	.000	INFINITE	- 2.796	- 93.220	- 93.220	INFINITE
100	8.145	50.733	70.715	- 1.998	- 93.656	- 92.205	201.504
200	10.119	56.920	62.390	- 1.094	- 94.165	- 90.555	98.949
298	12.108	61.344	61.344	.000	- 94.590	- 88.689	65.007
300	12.142	61.419	61.345	.022	- 94.597	- 88.652	64.580
400	13.784	65.146	61.842	1.322	- 95.463	- 86.597	47.312
500	15.082	68.367	62.832	2.768	- 96.052	- 84.310	36.850
600	16.075	71.209	63.996	4.328	- 96.481	- 81.919	29.837
700	16.824	73.746	65.211	5.975	- 96.801	- 79.441	24.801
800	17.391	76.031	66.423	7.687	- 110.111	- 78.213	21.366
900	17.823	78.105	67.607	9.448	- 110.009	- 74.230	18.025
1000	18.157	80.001	68.753	11.248	- 109.891	- 70.260	15.154
1100	18.419	81.745	69.856	13.077	- 109.763	- 66.306	13.173
1200	18.628	83.357	70.915	14.930	- 109.626	- 62.360	11.357
1300	18.796	84.855	71.930	16.802	- 109.485	- 58.426	9.822
1400	18.933	86.253	72.904	18.688	- 109.341	- 54.504	8.508
1500	19.046	87.563	73.838	20.587	- 109.197	- 50.593	7.371
1600	19.140	88.795	74.735	22.497	- 109.051	- 46.689	6.377
1700	19.219	89.958	75.596	24.415	- 108.905	- 42.796	5.502
1800	19.286	91.058	76.425	26.340	- 108.763	- 38.911	4.724
1900	19.344	92.103	77.223	28.272	- 108.624	- 35.034	4.030
2000	19.393	93.096	77.992	30.209	- 108.488	- 31.166	3.405
2100	19.436	94.044	78.734	32.150	- 108.356	- 27.304	2.841
2200	19.474	94.949	79.451	34.096	- 108.230	- 23.447	2.329
2300	19.507	95.815	80.143	36.045	- 108.108	- 19.596	1.862
2400	19.536	96.646	80.814	37.997	- 107.992	- 15.748	1.434
2500	19.562	97.444	81.463	39.952	- 107.882	- 11.910	1.041
2600	19.585	98.212	82.093	41.909	- 107.777	- 8.072	.678
2700	19.605	98.951	82.703	43.869	- 107.678	- 4.239	.343
2800	19.623	99.664	83.296	45.830	- 107.586	- .409	.032
2900	19.640	100.353	83.873	47.793	- 107.500	3.419	-.258
3000	19.655	101.019	84.433	49.758	- 107.421	7.244	-.528
3100	19.669	101.664	84.979	51.724	- 107.345	11.064	-.780
3200	19.681	102.289	85.510	53.692	- 107.278	14.879	- 1.016
3300	19.692	102.895	86.028	55.660	- 107.214	18.693	- 1.238
3400	19.702	103.483	86.532	57.630	- 107.158	22.510	- 1.447
3500	19.712	104.054	87.025	59.601	- 107.106	26.319	- 1.643
3600	19.721	104.609	87.506	61.573	- 107.058	30.136	- 1.829
3700	19.729	105.150	87.975	63.545	- 107.018	33.945	- 2.005
3800	19.736	105.676	88.434	65.518	- 106.980	37.756	- 2.171
3900	19.743	106.189	88.883	67.492	- 106.947	41.559	- 2.329
4000	19.749	106.689	89.322	69.467	- 106.920	45.368	- 2.479
4100	19.755	107.176	89.751	71.442	- 106.896	49.179	- 2.621
4200	19.761	107.652	90.172	73.418	- 106.876	52.985	- 2.757
4300	19.766	108.117	90.584	75.394	- 106.859	56.794	- 2.886
4400	19.770	108.572	90.988	77.371	- 106.848	60.594	- 3.010
4500	19.775	109.016	91.383	79.348	- 106.839	64.404	- 3.128
4600	19.779	109.451	91.771	81.326	- 106.833	68.211	- 3.241
4700	19.783	109.876	92.152	83.304	- 106.831	72.016	- 3.349
4800	19.787	110.293	92.526	85.283	- 106.831	75.819	- 3.452
4900	19.790	110.701	92.892	87.261	- 106.834	79.621	- 3.551
5000	19.793	111.101	93.253	89.241	- 106.840	83.423	- 3.646
5100	19.796	111.493	93.606	91.220	- 106.849	87.234	- 3.738
5200	19.799	111.877	93.954	93.200	- 106.859	91.037	- 3.826
5300	19.802	112.254	94.296	95.180	- 106.871	94.850	- 3.911
5400	19.805	112.625	94.632	97.160	- 106.886	98.664	- 3.992
5500	19.807	112.988	94.962	99.141	- 106.901	102.460	- 4.071
5600	19.809	113.345	95.287	101.122	- 106.921	106.263	- 4.147
5700	19.812	113.695	95.607	103.103	- 106.941	110.070	- 4.220
5800	19.814	114.040	95.922	105.084	- 106.962	113.882	- 4.291
5900	19.816	114.379	96.232	107.065	- 106.985	117.682	- 4.359
6000	19.817	114.712	96.537	109.047	- 107.009	121.498	- 4.425

TABLE 2 (continued)

Thermochemical data of selected chemical compounds
Sulfur (S) (crystal) at. wt. = 32.064

T, °K.	cal. mole ⁻¹ deg. ⁻¹			kcal. mole ⁻¹			Log K _p
	C _p ^o	S ^o	-(F ^o -H _{298^o^o)/T}	H ^o -H _{298^o^o}	ΔH _f ^o	ΔF _f ^o	
0	.000	.000	INFINITE	- 1.053	.000	.000	.000
100	3.060	2.965	11.855	- .889	.000	.000	.000
200	4.634	5.622	8.104	- .469	.000	.000	.000
298	5.401	7.631	7.631	.000	.000	.000	.000
300	5.412	7.665	7.632	.010	.000	.000	.000
400	6.133	9.571	7.871	.680	- .429	.012	-.007
500	6.819	11.013	8.358	1.327	- .720	.158	-.069
600	7.504	12.317	8.911	2.044	- .860	.349	-.127
700	8.190	13.525	9.485	2.828	- .876	.577	-.180
800	8.876	14.664	10.062	3.682	- 13.847	.488	-.133
900	9.561	15.749	10.634	4.603	- 13.364	1.154	-.280
1000	10.247	16.792	11.198	5.594	- 12.814	2.738	-.598
1100	10.933	17.800	11.752	6.653	- 12.198	4.263	-.847
1200	11.619	18.781	12.297	7.780	- 11.515	5.731	- 1.044
1300	12.304	19.738	12.833	8.977	- 10.763	7.139	- 1.200
1400	12.990	20.675	13.360	10.241	- 9.946	8.485	- 1.325
1500	13.676	21.595	13.878	11.575	- 9.060	9.770	- 1.423
1600	14.361	22.499	14.389	12.976	- 8.107	10.996	- 1.502
1700	15.047	23.390	14.892	14.447	- 7.085	12.158	- 1.563
1800	15.733	24.270	15.389	15.986	- 5.996	13.259	- 1.610
1900	16.418	25.139	15.879	17.593	- 4.839	14.298	- 1.645
2000	17.104	25.998	16.364	19.270	- 3.613	15.274	- 1.669

(continues)

TABLE 2 (continued)

Thermochemical data of selected chemical compounds
Sulfur (S) (liquid) at. wt. = 32.064

T, °K.	cal. mole ⁻¹ deg. ⁻¹			kcal. mole ⁻¹			Log K _p
	C _p	S°	-(E°-H° ₂₉₈)/T	H°-H° ₂₉₈	ΔH _f	ΔF _f	
0							
100							
200							
298	7.579	8.444	8.444	.000	.338	.093	.068
300	7.579	8.444	8.444	.014	.340	.092	.067
400	7.734	10.674	8.741	.773	.000	.000	.000
500	9.081	12.766	9.746	1.711	.000	.000	.000
600	8.200	14.333	10.053	2.568	.000	.000	.000
700	7.799	15.601	10.700	3.368	.000	.000	.000
800	7.694	16.634	11.457	4.147	- 13.051	1.769	.347
900	7.694	17.540	12.084	4.911	- 12.721	.185	.045
1000	7.694	18.350	12.671	5.680	- 12.393	1.601	.350
1100	7.694	19.084	13.221	6.449	- 12.066	2.983	.593
1200	7.694	19.753	13.738	7.218	- 11.741	4.338	.790
1300	7.694	20.369	14.224	7.988	- 11.416	5.666	.952
1400	7.694	20.939	14.684	8.757	- 11.094	6.967	1.088
1500	7.694	21.470	15.119	9.527	- 10.773	8.245	1.201
1600	7.694	21.966	15.531	10.296	- 10.451	9.503	1.298
1700	7.694	22.433	15.924	11.065	- 10.131	10.740	1.381
1800	7.694	22.873	16.298	11.835	- 9.811	11.959	1.452
1900	7.694	23.289	16.655	12.604	- 9.492	13.161	1.514
2000	7.694	23.683	16.998	13.374	- 9.174	14.344	1.567

TABLE 2 (continued)

Thermochemical data of selected chemical compounds
Sulfur, Monatomic (S) (ideal gas) at. wt. = 32.064

T, °K.	cal. mole ⁻¹ deg. ⁻¹			kcal. mole ⁻¹			Log K _p
	C _p	S°	-(F°-H° ₂₉₈)/T	H°-H° ₂₉₈	ΔH _f °	ΔF _f °	
0	.000	.000	INFINITE	- 1.591	66.142	66.142	INFINITE
100	5.103	34.127	45.046	- 1.092	66.477	63.361	- 138.468
200	5.589	37.831	40.604	- .555	66.621	60.180	- 65.758
298	5.659	40.086	40.086	.000	66.680	57.004	- 41.783
300	5.658	40.121	40.086	.010	66.680	56.944	- 41.481
400	5.554	41.736	40.307	.572	66.143	53.718	- 29.349
500	5.436	42.962	40.720	1.421	65.754	50.657	- 22.141
600	5.340	43.944	41.178	1.659	65.435	47.669	- 17.363
700	5.266	44.762	41.634	2.490	65.166	44.753	- 13.972
800	5.211	45.461	42.069	2.713	51.864	40.586	- 11.087
900	5.169	46.072	42.481	3.232	51.945	39.172	- 9.512
1000	5.137	46.615	42.868	3.747	52.019	37.748	- 8.250
1100	5.112	47.103	43.231	4.260	52.089	36.317	- 7.215
1200	5.093	47.547	43.572	4.770	52.155	34.881	- 6.352
1300	5.079	47.954	43.894	5.279	52.219	33.440	- 5.622
1400	5.070	48.331	44.198	5.786	52.279	31.992	- 4.994
1500	5.064	48.680	44.485	6.293	52.338	30.540	- 4.449
1600	5.062	49.007	44.758	6.799	52.396	29.085	- 3.973
1700	5.063	49.314	45.017	7.305	52.453	27.626	- 3.551
1800	5.068	49.603	45.263	7.812	52.510	26.165	- 3.177
1900	5.075	49.877	45.499	8.319	52.567	24.701	- 2.841
2000	5.085	50.138	45.725	8.827	52.624	23.232	- 2.539
2100	5.097	50.386	45.941	9.336	52.681	21.761	- 2.265
2200	5.112	50.624	46.148	9.846	52.739	20.287	- 2.015
2300	5.127	50.851	46.348	10.358	52.798	18.811	- 1.787
2400	5.144	51.070	46.540	10.872	52.859	17.332	- 1.578
2500	5.162	51.280	46.725	11.387	52.921	15.851	- 1.386
2600	5.181	51.483	46.905	11.904	52.984	14.367	- 1.208
2700	5.200	51.679	47.078	12.423	53.049	12.879	- 1.042
2800	5.219	51.869	47.246	12.944	53.115	11.387	- .889
2900	5.239	52.052	47.408	13.467	53.183	9.898	- .746
3000	5.258	52.230	47.566	13.992	53.252	8.405	- .612
3100	5.277	52.403	47.719	14.519	53.324	6.908	- .487
3200	5.295	52.571	47.868	15.048	53.396	5.408	- .369
3300	5.313	52.734	48.013	15.578	53.470	3.907	- .259
3400	5.331	52.893	48.154	16.110	53.545	2.406	- .155
3500	5.347	53.047	48.292	16.644	53.621	.901	- .056
3600	5.363	53.198	48.426	17.180	53.700	-.606	.037
3700	5.378	53.345	48.557	17.717	53.778	- 2.115	.125
3800	5.392	53.489	48.685	18.255	53.858	- 3.628	.209
3900	5.406	53.629	48.810	18.795	53.939	- 5.142	.288
4000	5.419	53.766	48.932	19.336	54.021	- 6.655	.364
4100	5.430	53.900	49.052	19.879	54.105	- 8.174	.436
4200	5.441	54.031	49.169	20.422	54.188	- 9.694	.504
4300	5.451	54.159	49.283	20.967	54.273	- 11.216	.570
4400	5.461	54.285	49.396	21.513	54.358	- 12.742	.633
4500	5.470	54.408	49.506	22.059	54.443	- 14.267	.693
4600	5.477	54.528	49.613	22.607	54.530	- 15.795	.750
4700	5.485	54.646	49.719	23.155	54.617	- 17.326	.806
4800	5.491	54.761	49.823	23.703	54.703	- 18.857	.859
4900	5.497	54.875	49.925	24.253	54.791	- 20.390	.909
5000	5.502	54.986	50.025	24.803	54.878	- 21.927	.958
5100	5.507	55.095	50.124	25.353	54.965	- 23.462	1.005
5200	5.511	55.202	50.220	25.904	55.053	- 25.001	1.051
5300	5.515	55.307	50.315	26.456	55.142	- 26.542	1.094
5400	5.518	55.410	50.409	27.007	55.229	- 28.082	1.136
5500	5.521	55.511	50.500	27.559	55.317	- 29.625	1.177
5600	5.523	55.611	50.591	28.111	55.404	- 31.172	1.216
5700	5.525	55.708	50.680	28.664	55.492	- 32.716	1.254
5800	5.526	55.805	50.767	29.216	55.579	- 34.269	1.291
5900	5.528	55.899	50.853	29.769	55.667	- 35.818	1.327
6000	5.529	55.997	50.938	30.322	55.754	- 37.366	1.361

Specific Reaction Rate Constants

The reaction rate data presented in Table 1 are taken from the listing given by Westbrook and Dryer [*Prog. Energy Combust. Sci.* **10**, 1 (1984)]. The reader should refer to this reference for the original source of each rate constant quoted. The backward rate at a given temperature is determined through the value of the equilibrium constant at the temperature. The units are in $\text{cm}^3 \text{ mol sec kcal}$ for the expression $k = AT^n \exp(-E_A/RT)$.

TABLE 1

Hydrocarbon oxidation mechanism, reaction rates in $\text{cm}^3 \text{ mol sec kcal}$ units,
 $k = AT^n \exp(-E_A/RT)$

Reaction	Forward rate		
	log A	n	E_a
1. $\text{H} + \text{O}_2 \rightarrow \text{O} + \text{OH}$	16.71	-0.816	16.51
2. $\text{O} + \text{H}_2 \rightarrow \text{H} + \text{OH}$	10.26	1.0	8.90
3. $\text{H}_2 + \text{OH} \rightarrow \text{H}_2\text{O} + \text{H}$	13.34	0.0	5.15
4. $\text{O} + \text{H}_2\text{O} \rightarrow \text{OH} + \text{OH}$	13.83	0.0	18.36
5. $\text{H} + \text{H} + \text{M} \rightarrow \text{H}_2 + \text{M}$	15.48	0.0	0.00
6. $\text{O} + \text{O} + \text{M} \rightarrow \text{O}_2 + \text{M}$	13.28	0.0	-1.79
7. $\text{O} + \text{H} + \text{M} \rightarrow \text{OH} + \text{M}$	16.00	0.0	0.00
8. $\text{H} + \text{OH} + \text{M} \rightarrow \text{H}_2\text{O} + \text{M}$	23.15	-2.0	0.00
9. $\text{H} + \text{O}_2 + \text{M} \rightarrow \text{HO}_2 + \text{M}$	15.18	0.0	-1.00

TABLE 1 (continued)

Reaction	Forward rate		
	log <i>A</i>	<i>n</i>	<i>E_a</i>
10. H + HO ₂ → H ₂ + O ₂	13.40	0.0	0.70
11. H + HO ₂ → OH + OH	14.40	0.0	1.90
12. H + HO ₂ → H ₂ O + O	13.70	0.0	1.00
13. HO ₂ + OH → H ₂ O + O ₂	13.70	0.0	1.00
14. HO ₂ + O → O ₂ + OH	13.70	0.0	1.00
15. HO ₂ + HO ₂ → H ₂ O ₂ + O ₂	13.00	0.0	1.00
16. H ₂ O ₂ + OH → H ₂ O + HO ₂	13.00	0.0	1.80
17. H ₂ O ₂ + H → H ₂ O + OH	14.50	0.0	8.94
18. H ₂ O ₂ + H → HO ₂ + H ₂	12.23	0.0	3.75
19. H ₂ O ₂ + M → OH + OH + M	17.08	0.0	45.50
20. O + OH + M → HO ₂ + M	17.00	0.0	0.00
21. H ₂ + O ₂ → OH + OH	12.40	0.0	38.95
22. O ₃ + M → O ₂ + O + M	14.63	0.0	22.18
23. O ₃ + O → O ₂ + O ₂	13.06	0.0	4.57
24. H + O ₃ → O ₂ + OH	13.90	0.0	0.89
25. OH + O ₃ → HO ₂ + O ₂	12.04	0.0	18.48
26. CO + O + M → CO ₂ + M	15.77	0.0	4.10
27. CO + O ₂ → CO ₂ + O	12.40	0.0	47.69
28. CO + OH → CO ₂ + H	7.18	1.3	-0.77
29. CO + HO ₂ → CO ₂ + OH	13.76	0.0	22.93
30. CH ₂ O + M → HCO + H + M	16.52	0.0	81.00
31. CH ₂ O + OH → HCO + H ₂ O	12.88	0.0	0.17
32. CH ₂ O + H → HCO + H ₂	14.52	0.0	10.50
33. CH ₂ O + O → HCO + OH	13.70	0.0	4.60
34. CH ₂ O + HO ₂ → HCO + H ₂ O ₂	12.00	0.0	8.00
35. HCO + M → H + CO + M	14.16	0.0	19.00
36. HCO + O ₂ → CO + HO ₂	12.52	0.0	7.00
37. HCO + OH → CO + H ₂ O	14.00	0.0	0.00
38. HCO + H → CO + H ₂	14.30	0.0	0.00
39. HCO + O → CO + OH	14.00	0.0	0.00
40. CH ₄ + M → CH ₃ + H + M	17.30	0.0	88.00
41. CH ₄ + O ₂ → CH ₃ + HO ₂	13.90	0.0	56.00
42. CH ₄ + H → CH ₃ + H ₂	4.35	3.0	8.75
43. CH ₄ + OH → CH ₃ + H ₂ O	3.54	3.08	2.00
44. CH ₄ + O → CH ₃ + OH	7.07	2.08	7.63
45. CH ₄ + HO ₂ → CH ₃ + H ₂ O ₂	13.30	0.0	18.00
46. CH ₃ + O ₂ → CH ₃ O + O	13.68	0.0	29.00
47. CH ₃ + CH ₃ → C ₂ H ₆	13.00	0.0	0.00
48. CH ₃ + CH ₃ → C ₂ H ₄ + H	14.90	0.0	26.52
49. CH ₃ + CH ₃ → C ₂ H ₄ + H ₂	16.00	0.0	32.00
50. CH ₃ + O → CH ₂ O + H	14.11	0.0	2.00
51. CH ₃ + OH → CH ₂ O + H ₂	12.60	0.0	0.00
52. CH ₃ + OH → CH ₃ O + H	16.30	0.0	27.41
53. CH ₃ + CH ₂ O → CH ₄ + HCO	10.00	0.5	6.00
54. CH ₃ + HCO → CH ₄ + CO	11.48	0.5	0.00
55. CH ₃ + HO ₂ → CH ₃ O + OH	13.30	0.0	0.00
56. CH ₃ + M → CH ₃ + H + M	16.29	0.0	91.60
57. CH ₃ O + M → CH ₂ O + H + M	13.70	0.0	21.00
58. CH ₃ O + O ₂ → CH ₂ O + HO ₂	12.00	0.0	6.00
59. CH ₃ O + H → CH ₂ O + H ₂	13.30	0.0	0.00
60. C ₂ H ₆ + O ₂ → C ₂ H ₄ + HO ₂	13.00	0.0	51.00
61. C ₂ H ₆ + CH ₃ → C ₂ H ₅ + CH ₄	-0.26	4.0	8.28
62. C ₂ H ₆ + H → C ₂ H ₅ + H ₂	2.73	3.5	5.20

(continues)

TABLE 1 (continued)

Reaction	Forward rate		
	log <i>A</i>	<i>n</i>	<i>E_a</i>
63. C ₂ H ₆ + O → C ₂ H ₅ + OH	13.40	0.0	6.36
64. C ₂ H ₆ + OH → C ₂ H ₅ + H ₂ O	9.94	1.05	1.81
65. C ₂ H ₅ + M → C ₂ H ₄ + H + M	15.30	0.0	30.00
66. C ₂ H ₅ + O ₂ → C ₂ H ₄ + HO ₂	12.00	0.0	5.00
67. C ₂ H ₅ + O → CH ₃ CHO + H	13.70	0.0	0.00
68. C ₂ H ₅ + O → CH ₂ O + CH ₃	13.00	0.0	0.00
69. C ₂ H ₅ + C ₂ H ₅ → C ₄ H ₁₀	12.90	0.0	0.00
70. C ₃ H ₈ → C ₂ H ₅ + CH ₃	16.23	0.0	84.84
71. C ₃ H ₈ → C ₂ H ₄ + CH ₄	15.80	0.0	85.80
72. C ₂ H ₅ + C ₂ H ₃ → C ₄ H ₈	12.95	0.0	0.00
73. C ₂ H ₃ + C ₂ H ₃ → C ₄ H ₆	12.95	0.0	0.00
74. C ₂ H ₄ + M → C ₂ H ₂ + H ₂ + M	16.97	0.0	77.20
75. C ₂ H ₄ + M → C ₂ H ₃ + H + M	18.80	0.0	108.72
76. C ₂ H ₄ + C ₂ H ₄ → C ₂ H ₃ + C ₂ H ₅	14.70	0.0	64.70
77. C ₂ H ₃ + M → C ₂ H ₂ + H + M	14.90	0.0	31.50
78. C ₂ H ₃ + O ₂ → C ₂ H ₂ + HO ₂	12.00	0.0	10.00
79. C ₂ H ₄ + H → C ₂ H ₃ + H ₂	7.18	2.0	6.00
80. C ₂ H ₄ + OH → C ₂ H ₃ + H ₂ O	12.68	0.0	1.23
81. C ₂ H ₄ + O → CH ₃ + HCO	12.52	0.0	1.13
82. C ₂ H ₄ + O → CH ₂ O + CH ₂	13.40	0.0	5.00
83. C ₂ H ₄ + OH → CH ₃ + CH ₂ O	12.30	0.0	0.96
84. C ₂ H ₃ + H → C ₂ H ₂ + H ₂	13.30	0.0	2.50
85. C ₂ H ₃ + O → CH ₂ CO + H	13.52	0.0	0.00
86. C ₂ H ₃ + OH → C ₂ H ₂ + H ₂ O	12.70	0.0	0.00
87. C ₂ H ₃ + C ₂ H ₄ → C ₄ H ₆ + H	12.00	0.0	7.30
88. C ₂ H ₂ + M → C ₂ H + H + M	16.62	0.0	107.00
89. C ₂ H ₂ + C ₂ H ₂ → C ₄ H ₂ + H	13.00	0.0	45.00
90. C ₂ H ₂ + O ₂ → HCCO + OH	12.70	0.0	23.50
91. C ₂ H ₂ + O ₂ → HCO + HCO	12.60	0.0	28.00
92. C ₂ H ₂ + H → C ₂ H + H ₂	14.30	0.0	19.00
93. C ₂ H ₂ + O → C ₂ H + OH	15.50	-0.6	15.00
94. C ₂ H ₂ + O → CH ₂ + CO	10.34	1.0	2.58
95. C ₂ H ₂ + O → HCCO + H	4.55	2.7	1.39
96. C ₂ H ₂ + OH → CH ₂ CO + H	11.51	0.0	0.20
97. C ₂ H ₂ + OH → C ₂ H + H ₂ O	12.80	0.0	7.00
98. C ₂ H ₂ + OH → CH ₃ + CO	12.08	0.0	0.50
99. C ₂ H ₂ + OH → C ₂ H ₂ OH	11.83	0.0	0.23
100. C ₂ H ₂ OH + H → CH ₂ CO + H ₂	13.30	0.0	4.00
101. C ₂ H ₂ OH + O → CH ₂ CO + OH	13.30	0.0	4.00
102. C ₂ H ₂ OH + OH → CH ₂ CO + H ₂ O	13.00	0.0	2.00
103. C ₂ H ₂ OH + O ₂ → CH ₂ CO + HO ₂	12.30	0.0	10.00
104. C ₂ H ₂ OH + M → CH ₂ CO + H + M	15.70	0.0	28.00
105. C ₂ H ₂ + C ₂ H → C ₄ H ₂ + H	13.60	0.0	0.00
106. C ₄ H ₂ + OH → C ₃ H ₂ + HCO	12.81	0.0	1.00
107. CH ₂ CO + M → CH ₂ + CO + M	16.30	0.0	60.00
108. CH ₂ CO → OH + CH ₂ O + HCO	13.45	0.0	0.00
109. CH ₂ CO + OH → HCCO + H ₂ O	13.00	0.0	0.00
110. CH ₂ CO + O → HCCO + OH	13.00	0.0	0.00
111. CH ₂ CO + O → HCO + HCO	13.00	0.0	2.41
112. CH ₂ CO + H → HCCO + H ₂	13.00	0.0	0.00
113. CH ₂ CO + H → CH ₂ + CO	13.04	0.0	3.40
114. HCCO + O ₂ → CO + CO + OH	11.80	0.0	2.00
115. HCCO + O → CO + CO + H	12.08	0.0	0.00
116. HCCO + H → CH ₂ + CO	12.70	0.0	0.00
117. HCCO + OH → HCO + H + CO	12.30	0.0	0.00
118. HCCO + CH ₂ → C ₂ H ₃ + CO	13.48	0.0	0.00
119. CH ₂ + O ₂ → CO ₂ + H ₂	12.21	0.0	1.00

TABLE 1 (continued)

Reaction	Forward rate		
	log <i>A</i>	<i>n</i>	<i>E_a</i>
120. CH ₂ + O ₂ → CO ₂ + H + H	12.57	0.0	1.50
121. CH ₂ + O ₂ → CO + H ₂ O	11.00	0.0	0.00
122. CH ₂ + O ₂ → CO + OH + H	11.30	0.0	0.00
123. CH ₂ + O ₂ → HCO + OH	14.00	0.0	3.70
124. CH ₂ + O → CH + OH	11.30	0.68	25.00
125. CH ₂ + O → CO + H + H	12.70	0.0	0.00
126. CH ₂ + O → CO + H ₂	12.70	0.0	0.00
127. CH ₂ + OH → CH + H ₂ O	11.40	0.67	25.70
128. CH ₂ + H → CH + H ₂	11.40	0.67	25.70
129. CH ₂ + CH ₂ → C ₂ H ₄ + H	12.70	0.0	0.00
130. CH ₂ + CH ₂ → C ₂ H ₂ + H ₂	13.50	0.0	0.00
131. CH ₂ + C ₂ H ₂ → CH ₃ + C ₂ H ₂	13.48	0.0	0.00
132. C ₂ H + O ₂ → HCCO + O	12.52	0.0	0.00
133. C ₂ H + O ₂ → HCO + CO	13.00	0.0	7.00
134. C ₂ H + O → CO + CH	13.70	0.0	0.00
135. C ₂ H + C ₂ H ₂ → C ₂ H ₂ + C ₂ H ₂	13.48	0.0	0.00
136. CH + O ₂ → HCO + O	13.00	0.0	0.00
137. CH + O ₂ → CO + OH	11.13	0.67	25.70
138. C ₄ H ₃ + M → C ₄ H ₂ + H + M	16.00	0.0	60.00
139. C ₂ H ₂ + C ₂ H → C ₄ H ₂ + H	13.60	0.0	0.00
140. C ₄ H ₂ + M → C ₄ H + H + M	17.54	0.0	80.00
141. CH ₃ OH + M → CH ₃ + OH + M	18.48	0.0	80.00
142. CH ₃ OH + O ₂ → CH ₂ OH + HO ₂	10.60	0.0	50.91
143. CH ₃ OH + H → CH ₃ + H ₂ O	12.72	0.0	5.34
144. CH ₃ OH + H → CH ₂ OH + H ₂	13.48	0.0	7.00
145. CH ₃ OH + OH → CH ₂ OH + H ₂ O	12.60	0.0	2.00
146. CH ₃ OH + O → CH ₂ OH + OH	12.23	0.0	2.29
147. CH ₃ OH + CH ₃ → CH ₂ OH + CH ₄	11.26	0.0	9.80
148. CH ₃ OH + HO ₂ → CH ₂ OH + H ₂ O ₂	12.80	0.0	19.36
149. CH ₂ OH + M → CH ₂ O + H + M	13.40	0.0	29.00
150. CH ₂ OH + O ₂ → CH ₂ O + HO ₂	12.00	0.0	6.00
151. CH ₂ OH + H → CH ₂ O + H ₂	12.48	0.0	0.00
152. C ₂ H ₅ OH + M → CH ₃ + CH ₂ OH + M	18.48	0.0	75.47
153. C ₂ H ₅ OH + O ₂ → CH ₃ CHOH + HO ₂	10.60	0.0	50.00
154. C ₂ H ₅ OH + OH → CH ₃ CHOH + H ₂ O	13.48	0.0	5.96
155. C ₂ H ₅ OH + H → CH ₃ CHOH + H ₂	12.64	0.0	4.57
156. C ₂ H ₅ OH + O → CH ₃ CHOH + OH	12.83	0.0	1.51
157. C ₂ H ₅ OH + HO ₂ → CH ₃ CHOH + H ₂ O ₂	12.80	0.0	15.00
158. C ₂ H ₅ OH + CH ₃ → CH ₃ CHOH + CH ₄	12.60	0.0	9.69
159. CH ₃ CHOH + M → CH ₃ CHO + H + M	13.70	0.0	21.85
160. CH ₃ CHOH + O ₂ → CH ₃ CHO + HO ₂	13.00	0.0	5.56
161. C ₂ H ₅ OH + H → C ₂ H ₄ + H ₂ O	12.72	0.0	5.00
162. CH ₃ CHO → CH ₃ + HCO	15.85	0.0	81.76
163. CH ₃ CHO → CH ₃ CO + H	14.70	0.0	87.86
164. CH ₃ CHO + O ₂ → CH ₃ CO + HO ₂	13.30	0.5	42.20
165. CH ₃ CHO + H → CH ₃ CO + H ₂	13.60	0.0	4.20
166. CH ₃ CHO + OH → CH ₃ CO + H ₂ O	13.00	0.0	0.00
167. CH ₃ CHO + O → CH ₃ CO + OH	12.70	0.0	1.79
168. CH ₃ CHO + CH ₃ → CH ₃ CO + CH ₄	12.23	0.0	8.43
169. CH ₃ CHO + HO ₂ → CH ₃ CO + H ₂ O ₂	12.23	0.0	10.70
170. CH ₃ CO → CH ₃ + CO	13.48	0.0	17.24
171. C ₃ H ₈ + O ₂ → <i>i</i> C ₃ H ₇ + HO ₂	13.60	0.0	47.50
172. C ₃ H ₈ + O ₂ → <i>n</i> C ₃ H ₇ + HO ₂	13.60	0.0	47.50
173. <i>i</i> C ₃ H ₇ + C ₃ H ₈ → <i>n</i> C ₃ H ₇ + C ₃ H ₈	10.50	0.0	12.90
174. C ₃ H ₈ + H → <i>i</i> C ₃ H ₇ + H ₂	6.94	2.0	5.00
175. C ₃ H ₈ + H → <i>n</i> C ₃ H ₇ + H ₂	7.75	2.0	7.70

(continues)

TABLE 1 (continued)

Reaction	Forward rate		
	log <i>A</i>	<i>n</i>	<i>E_a</i>
176. $C_3H_8 + CH_3 \rightarrow iC_3H_7 + CH_4$	15.04	0.0	25.14
177. $C_3H_8 + CH_3 \rightarrow nC_3H_7 + CH_4$	15.04	0.0	25.14
178. $C_3H_8 + C_2H_5 \rightarrow iC_3H_7 + C_2H_4$	11.30	0.0	10.40
179. $C_3H_8 + C_2H_5 \rightarrow nC_3H_7 + C_2H_4$	11.30	0.0	10.40
180. $C_3H_8 + C_2H_6 \rightarrow iC_3H_7 + C_2H_6$	11.30	0.0	10.40
181. $C_3H_8 + C_2H_6 \rightarrow nC_3H_7 + C_2H_6$	11.30	0.0	10.40
182. $C_3H_8 + C_3H_8 \rightarrow iC_3H_7 + C_3H_8$	11.90	0.0	16.20
183. $C_3H_8 + C_3H_8 \rightarrow nC_3H_7 + C_3H_8$	11.90	0.0	16.20
184. $C_3H_8 + O \rightarrow iC_3H_7 + OH$	6.70	2.0	3.00
185. $C_3H_8 + O \rightarrow nC_3H_7 + OH$	6.70	2.0	3.00
186. $C_3H_8 + OH \rightarrow iC_3H_7 + H_2O$	8.68	1.4	0.85
187. $C_3H_8 + OH \rightarrow nC_3H_7 + H_2O$	8.76	1.4	0.85
188. $C_3H_8 + HO_2 \rightarrow iC_3H_7 + H_2O_2$	12.70	0.0	18.00
189. $C_3H_8 + HO_2 \rightarrow nC_3H_7 + H_2O_2$	12.70	0.0	18.00
190. $nC_3H_7 \rightarrow C_3H_4 + CH_3$	13.98	0.0	31.00
191. $nC_3H_7 \rightarrow C_3H_6 + H$	14.10	0.0	37.00
192. $iC_3H_7 \rightarrow C_3H_4 + CH_3$	10.30	0.0	29.50
193. $iC_3H_7 \rightarrow C_3H_6 + H$	13.80	0.0	36.90
194. $nC_3H_7 + O_2 \rightarrow C_3H_6 + HO_2$	12.00	0.0	5.00
195. $iC_3H_7 + O_2 \rightarrow C_3H_6 + HO_2$	12.00	0.0	5.00
196. $C_3H_6 \rightarrow C_3H_5 + H$	13.00	0.0	78.00
197. $C_3H_6 + O \rightarrow CH_2O + C_2H_4$	13.77	0.0	5.00
198. $C_3H_6 + O \rightarrow CH_3 + CH_2CO$	12.70	0.0	0.60
199. $C_3H_6 + OH \rightarrow CH_3 + CH_2CHO$	12.85	0.0	0.00
200. $C_3H_6 + O \rightarrow C_2H_5 + HCO$	12.55	0.0	0.00
201. $C_3H_6 + OH \rightarrow C_3H_5 + H_2O$	12.60	0.0	0.00
202. $C_3H_6 + OH \rightarrow C_2H_5 + CH_2O$	12.90	0.0	0.00
203. $C_3H_6 + H \rightarrow C_3H_5 + H_2$	12.70	0.0	1.50
204. $C_3H_6 + CH_3 \rightarrow C_3H_5 + CH_4$	10.95	0.0	8.50
205. $C_3H_6 + HO_2 \rightarrow C_3H_6O + OH$	7.30	0.0	0.00
206. $C_3H_6 + C_2H_6 \rightarrow C_3H_5 + C_2H_6$	11.00	0.0	9.20
207. $C_3H_5 \rightarrow C_3H_4 + H$	13.60	0.0	70.00
208. $C_3H_5 + O_2 \rightarrow C_3H_4 + HO_2$	11.78	0.0	10.00
209. $C_3H_5 + CH_3 \rightarrow C_2H_8$	13.13	0.0	0.00
210. $C_3H_5 + H \rightarrow C_3H_4 + H_2$	13.00	0.0	0.00
211. $C_3H_5 + CH_3 \rightarrow C_3H_4 + CH_4$	12.00	0.0	0.00
212. $C_3H_4 + O \rightarrow CH_2O + C_2H_2$	12.00	0.0	0.00
213. $C_3H_4 + OH \rightarrow CH_2O + C_2H_3$	12.00	0.0	0.00
214. $C_3H_4 + O \rightarrow HCO + C_2H_3$	12.00	0.0	0.00
215. $C_3H_4 + OH \rightarrow HCO + C_2H_4$	12.00	0.0	0.00
216. $C_4H_{10} \rightarrow C_2H_5 + C_2H_5$	16.30	0.0	81.40
217. $C_4H_{10} \rightarrow nC_3H_7 + CH_3$	17.00	0.0	85.40
218. $C_4H_{10} + O_2 \rightarrow sC_4H_9 + HO_2$	13.60	0.0	47.60
219. $C_4H_{10} + H \rightarrow pC_4H_9 + H_2$	14.11	0.0	9.70
220. $C_4H_{10} + H \rightarrow sC_4H_9 + H_2$	14.30	0.0	8.30
221. $C_4H_{10} + O \rightarrow pC_4H_9 + OH$	13.48	0.0	5.80
222. $C_4H_{10} + O \rightarrow sC_4H_9 + OH$	13.72	0.0	4.50
223. $C_4H_{10} + OH \rightarrow pC_4H_9 + H_2O$	12.57	0.0	1.65
224. $C_4H_{10} + OH \rightarrow sC_4H_9 + H_2O$	12.75	0.0	0.86
225. $C_4H_{10} + HO_2 \rightarrow pC_4H_9 + H_2O_2$	11.47	0.0	14.90
226. $C_4H_{10} + HO_2 \rightarrow sC_4H_9 + H_2O_2$	11.30	0.0	12.60
227. $C_4H_{10} + CH_3 \rightarrow pC_4H_9 + CH_4$	12.47	0.0	11.70
228. $C_4H_{10} + CH_3 \rightarrow sC_4H_9 + CH_4$	12.12	0.0	10.10
229. $C_4H_{10} + C_2H_3 \rightarrow pC_4H_9 + C_2H_4$	12.00	0.0	18.00
230. $C_4H_{10} + C_2H_3 \rightarrow sC_4H_9 + C_2H_4$	11.90	0.0	16.80
231. $C_4H_{10} + C_2H_5 \rightarrow pC_4H_9 + C_2H_6$	11.00	0.0	13.40
232. $C_4H_{10} + C_2H_5 \rightarrow sC_4H_9 + C_2H_6$	11.00	0.0	10.40

TABLE 1 (continued)

Reaction	Forward rate		
	log <i>A</i>	<i>n</i>	<i>E_a</i>
233. $C_4H_{10} + C_3H_5 \rightarrow pC_4H_9 + C_3H_6$	11.60	0.0	18.80
234. $C_4H_{10} + C_3H_5 \rightarrow sC_4H_9 + C_3H_6$	11.90	0.0	16.80
235. $nC_4H_9 \rightarrow C_2H_5 + C_2H_4$	12.20	0.0	28.00
236. $sC_4H_9 \rightarrow C_3H_6 + CH_3$	13.45	0.0	31.90
237. $nC_4H_9 \rightarrow {}_1C_4H_8 + H$	13.00	0.0	36.00
238. $sC_4H_9 \rightarrow {}_2C_4H_8 + H$	13.30	0.0	39.80
239. $nC_4H_9 + O_2 \rightarrow {}_1C_4H_8 + HO_2$	12.00	0.0	2.00
240. $sC_4H_9 + O_2 \rightarrow {}_1C_4H_8 + HO_2$	12.00	0.0	4.50
241. $sC_4H_9 + O_2 \rightarrow {}_2C_4H_8 + HO_2$	12.30	0.0	4.25
242. ${}_1C_4H_8 + H \rightarrow C_4H_7 + H_2$	13.70	0.0	3.90
243. ${}_2C_4H_8 + H \rightarrow C_4H_7 + H_2$	13.70	0.0	3.80
244. ${}_1C_4H_8 + O \rightarrow C_3H_6 + CH_2O$	12.70	0.0	0.00
245. ${}_2C_4H_8 + O \rightarrow nC_3H_7 + HCO$	12.78	0.0	0.00
246. ${}_1C_4H_8 + OH \rightarrow nC_3H_7 + CH_2O$	13.26	0.0	0.00
247. ${}_2C_4H_8 + OH \rightarrow C_2H_5 + CH_3CHO$	13.41	0.0	0.00
248. ${}_1C_4H_8 + CH_3 \rightarrow {}_1C_4H_7 + CH_4$	11.00	0.0	7.30
249. ${}_2C_4H_8 + CH_3 \rightarrow C_4H_7 + CH_4$	11.00	0.0	8.20
250. ${}_2C_4H_8 + O \rightarrow C_2H_5 + CH_3CO$	12.70	0.0	0.00
251. $C_4H_7 \rightarrow C_4H_6 + H$	14.08	0.0	49.30
252. $C_4H_7 \rightarrow C_3H_4 + C_2H_3$	11.00	0.0	37.00
253. $C_4H_7 + C_4H_7 \rightarrow {}_1C_4H_8 + C_4H_6$	12.20	0.0	0.00
254. $C_4H_7 + C_4H_7 \rightarrow {}_2C_4H_8 + C_4H_6$	12.20	0.0	0.00
255. $C_4H_7 + CH_3 \rightarrow C_4H_6 + CH_4$	12.90	0.0	0.00

Bond Dissociation Energies of Hydrocarbons

The bond dissociation energies which follow are taken from the review of McMillan and Golden [*Amer. Rev. Phys. Chem.* **33**, 493 (1982)]. The reader should refer to this publication for the methods of determining the values presented, their uncertainty, and original sources. In the tables presented, all bond energies and heats of formation are in kcal/mole. The values listed in the first column are the heats of formation at 298 K for the reference radical and those above the column heading for the associated radical. Thus, the tables presented are not only a source of bond energies, but also of heats of formation of radicals.

McMillen and Golden employ the commonly invoked uncertainty of ± 1 kcal/mole for the dissociation energies and most of the uncertainties for the heats of formation fall in the same range. The reader is urged to refer to the McMillen and Golden reference for the specific uncertainty values.

TABLE 1

Bond dissociation energies of alkanes^a

$H_f^0(\text{R})$	R	(52.1) H	CH ₃	C ₂ H ₅	iC ₃ H ₇	tC ₄ H ₉	(78.6) C ₆ H ₅	(47.8) PhCH ₂
35.1	CH ₃	105.1	90.4	85.8	85.7	84.1	101.8	75.8
25.9	C ₂ H ₂	98.2	85.8	82.2	81	79.1	97.4	71.8
21.0	nC ₃ H ₇	97.9	86.5	82.1	80.4	78.9	97.7	72.1
18.2	iC ₃ H ₇	95.1	85.7	81	79.0	75.6	95.9	71.3
13.0	sC ₄ H ₉	95.5	85.0	80.0	78.5	—	—	—
8.7	tC ₄ H ₉	93.2	84.1	79.1	75.6	71.2	—	69.6
8.7	CH ₂ C(CH ₃) ₃	100	87.2	82.7	—	—	—	—
66.9	cyclopropyl	106.3						
51.1	cyclopropyl	97.4						
51.2	cyclopentyl	96.5						
25.3	cyclopentyl	94.5						
13.9	cyclohexyl	95.5						
12.1	cycloheptyl	92.5						

^a Note that in alkanes values of 98, 95, and 93 kcal/mole characterize primary, secondary, and tertiary C—H bonds, respectively.

TABLE 2

Bond dissociation energies for alkenes, alkynes, and aromatics

$H_f^0(\text{R})$	R	H	CH ₃
70.4	·C=C	110	100.6
78.6	·C=C	110.9	101.8
135	·C=C	132	125.7
-130.9	·C ₆ F ₅	113.9	—
139.1	·C—C=C	86.3	74.4
30.0	·C—C=C C	85.6	72.9
30.4	·C—C=C C	82.5	—
18.5	·C—C=C C	77.2	—
9.0	·C—C=C C C	76.3	—

(continues)

TABLE 2 (continued)

H_f^0 (R)	R	H	CH ₃
9.5	$\begin{array}{c} \text{C} \quad \text{C} \\ \quad \\ \cdot\text{C}-\text{C}=\text{C} \\ \\ \text{C} \end{array}$	78.0	
38.4	$\begin{array}{c} \text{Cl} \\ \\ \cdot\text{C}-\text{C}=\text{C} \end{array}$	88.6 82.3	— —
49	$\begin{array}{c} \text{C}=\text{C} \\ / \\ \cdot\text{C} \\ \backslash \\ \text{C}=\text{C} \end{array}$	76	
49	$\cdot\text{C}-\text{C}=\text{C}-\text{C}=\text{C}$	83	
57.9		71.1	
47		73	
47.8		88.0	75.8
60.4	$\begin{array}{c} \text{C}\cdot \\ \\ \text{O}-\text{O} \end{array}$	85.1	72.9
80.7	$\begin{array}{c} \text{C}\cdot \\ \\ \text{O}-\text{O}-\text{O} \end{array}$	81.8	67.6
74.4	$\begin{array}{c} \text{C} \\ \\ \text{O}-\text{O} \end{array}$	85.1	72.9
40.4	$\begin{array}{c} \text{O} \\ \\ \cdot\text{C}-\text{C} \\ \\ \text{O} \\ \\ \text{C}-\dot{\text{C}}-\text{C} \end{array}$	85.4	74.6
33.2	$\begin{array}{c} \text{O} \\ \\ \cdot\text{C}-\text{C}=\text{C} \end{array}$	84.4	73.7
81.4	$\cdot\text{C}-\text{C}=\text{C}$	89.4	76.0
70.2	$\cdot\text{C}-\text{C}=\text{C}-\text{C}$	87.2	73.7
65.2	$\begin{array}{c} \text{C} \\ \\ \cdot\text{C}-\text{C}=\text{C}-\text{C} \end{array}$	87.3	76.7
53.0	$\begin{array}{c} \text{C} \\ \\ \cdot\text{C}-\text{C}=\text{C}-\text{C} \\ \\ \text{C} \end{array}$	82.3	72.5
61.3	$\begin{array}{c} \text{C} \\ \\ \cdot\text{C}-\text{C}=\text{C} \end{array}$	81.0	70.7
70.5	$\begin{array}{c} \text{C} \\ \\ \cdot\text{C}-\text{C}=\text{C} \\ \\ \text{C} \end{array}$	83.1	73.0

TABLE 3

Bond dissociation energies of C—H—O compounds

ΔH_f^0 (R)	R ₁	(52.1) H	R ₁	(9.4) OH	(35.1) CH ₃	(25.9) C ₂ H ₅
9.43	OH	119	51	51	92.3	91.5
4.2	OCH ₃	104.4	37.6	—	83.3	81.8
-4.1	OC ₂ H ₅	104.2	37.9	—	82.7	82.1
-9.9	O— <i>n</i> C ₃ H ₇	103.4	37.1	—	82.0	—
-15.0	O— <i>n</i> C ₄ H ₉	102.9	—	—	—	—
-12.5	O— <i>i</i> C ₃ H ₇	104.7	37.7	—	82.8	—
-16.6	O— <i>s</i> C ₄ H ₉	105.5	36.4	—	—	—
-21.7	O— <i>t</i> C ₄ H ₉	105.1	38.0	—	83.1	—
—	O— <i>t</i> C ₅ H ₁₁	—	39.3	—	—	—
—	OCH ₂ C(CH ₃) ₃	102.3	36.4	46.3	—	—
11.4	OC ₆ H ₅	86.5	—	—	63.8	63
—	OCF ₃	—	46.2	—	—	—
—	OC(CF ₃) ₃	—	35.5	—	—	—
2.5	O ₂ H	87.2	—	—	—	—
-49.6	O ₂ CCH ₃	105.8	30.4	—	—	82.6
-54.6	O ₂ CC ₂ H ₅	106.4	30.4	—	—	—
-59.6	O ₂ C— <i>n</i> C ₃ H ₇	105.9	30.4	—	—	—

Carbon-centered radicals

ΔH_f^0 (R)	R ₁	H	CH ₃	C ₆ H ₅	R ₁
8.9	CHO	87	82.5	96.3	68.4
-5.8	COCH ₃	86.0	81.2	93.5	67.4
17.3	COCH=CH ₂	87.1	—	—	—
-10.2	COC ₂ H ₅	87.4	80.6	94.4	—
26.1	COC ₆ H ₅	86.9	81.9	90.1	66.4
—	COCF ₃	91.0	—	—	—
-5.7	CH ₂ COCH ₃	98.3	86.4	—	—
-16.8	CH(CH ₃)COCH ₃	92.3	—	—	—
-6.2	CH ₂ OH	94	—	96.4	80.2
-15.2	CH(OH)CH ₃	93	—	—	84.9
-26.6	C(OH)(CH ₃) ₂	91	—	—	—
-2.8	CH ₂ OCH ₃	93	86.4	—	—
-4.3	Tetrahydrofuran-2-yl	92	—	—	—
0.0	CH(OH)CH=CH ₂	81.6	—	—	—
-40.4	COOCH ₃	92.7	—	—	—
-16.7	CH ₂ OCOC ₆ H ₅	100.2	—	—	—
-53.3	COOH—CH ₂ C ₆ H ₅	67	—	—	—
59.2	(C ₆ H ₅) ₂ CH—COOH	59.4	—	—	—
—	C ₆ H ₅ CH ₂ CO—CH ₂ C ₆ H ₅	65.4	—	—	—
47.8	C ₆ H ₅ CH ₂ —OH	81.2	—	—	—
11.4	C ₆ H ₅ —CO—CH ₃	73.8	—	—	—

TABLE 4

Bond dissociation energies of sulfur-containing compounds

R_1-R_2	D_{298}^0	$\Delta H_f^0 (R_1)$
HS—H	91.1	33.6
CH ₃ S—H	90.7	32.2
RS—H	91	—
CH ₃ —SH	74	—
C ₂ H ₅ —SH	70.5	—
<i>t</i> Bu—SH	68.4	—
C ₆ H ₅ —SH	86.5	—
CH ₃ S—CH ₃	77.2	—
CH ₃ S—C ₂ H ₅	73.3	—
CH ₃ S— <i>n</i> C ₃ H ₇	73.78	—
PhS—H	83.3	—
PhS—CH ₃	69.4	54.9
PhCH ₂ —SCH ₃	61.4	—
CS—S	102.9	65.0
OS—O	130.1	—
CH ₃ SO ₂ —CH ₃	66.8	—
CH ₃ SO ₂ —CH ₂ C ₆ H ₅	52.9	—
RS ₂ —H	70	—
RS ₂ —CH ₃	57	—
HS—SH	66	—
RS—SR	72	—

TABLE 5

Bond dissociation energies of nitrogen-containing compounds amines and nitriles

$\Delta H_f^0 (R)$	R	(52.1) H	(35.1) CH ₃	(25.9) C ₂ H ₅	(47.8) PLCH ₂	(78.6) C ₆ H ₅	(44.3) NH ₂
44.3	NH ₂	107.4	84.9	81.6	71.1	102	65.8
42.4	NHCH ₃	100.0	82.2	79.8	68.7	100.6	64.1
34.7	N(CH ₃) ₂	91.5	75.5	72.3	62.1	93.2	59.0
56.7	NHC ₆ H ₅	88.0	71.4	69.1	—	81.1	52.3
55.8	N(CH ₃)C ₆ H ₅	87.5	70.8	—	—	—	—
8	NF ₂	75.7	—	—	—	—	—
112	N ₃	92	—	—	—	—	—
35.7	CH ₂ NH ₂	93.3	82.2	79.4	68.0	93.3	—
30	CH ₂ NHCH ₃	87	76.6	—	—	87.8	—
26	CH ₂ N(CH ₃) ₂	84	73.7	—	—	84.2	—
104	CN	123.8	121.8	118.2	—	131	—
58.5	CH ₂ CN	93	81.3	76.9	—	—	—
50.0	CH(CH ₃)CN	89.9	78.8	—	—	—	—
39.8	C(CH ₃) ₂ CN	86.5	74.7	—	—	—	—
59.4	C(CH ₃)(CN)C ₆ H ₅	—	59.9	—	—	—	—

TABLE 5 (continued)

		(21.6)	(7.9)	(17)
		NO	NO ₂	ONO ₂
52.1	H	—	78.3	101.2
9.4	OH	49.3	49.4	39
35.1	CH ₃	40.0	60.8	—
25.9	iC ₃ H ₅	—	58.6	—
18.2	iC ₃ H ₇	36.5	59.0	—
8.7	iC ₄ H ₉	39.5	58.5	—
-117.7	CH ₃	42.8	—	—
19	CCl ₃	32	—	—
79	C ₆ H ₅	50.8	71.3	—
-130.9	C ₆ F ₅	49.8	—	—
—	C(NO ₂)R ₂	—	48.8	—
—	C(NO ₂) ₂ R	—	40.5	—
—	RO	40.8	49.7	—
7.9	NO ₂	9.7	13.6	—

TABLE 6

Bond dissociation energies of halocarbons

ΔH_f° (R)	R	H	CH ₃	F	Cl	Br	I	CF ₃
35.1	CH ₃	105.1	90.4	109.9	84.6	70.9	57.2	101.6
29.9	C ₂ H ₅	98.2	—	107.7	79.9	67.8	53.4	—
18.2	iC ₃ H ₇	95.1	85.7	106.5	80.7	68.4	53.5	—
47.8	CH ₂ C ₆ H ₅	88.0	75.8	—	72.2	57.6	48.2	—
-7.8	CH ₂ F	100	119	85.3	85.3	—	—	94.6
-59.2	CHF ₂	101	95.6	126	—	69	—	—
-111.7	CF ₃	106.7	101.6	130.5	86.2	70.6	55.0	98.7
28.3	CH ₂ Cl	100.9	—	—	80.1	—	—	—
24.1	CHCl ₂	99.0	—	—	77.6	—	—	—
19	CCl ₃	95.8	—	101.9	73.1	55.3	—	—
-64.3	CF ₃ Cl	101.6	—	123	76	64.5	—	—
23	CFCl ₂	—	—	110	73	—	—	—
41.5	CH ₂ Br	102.0	—	—	—	—	—	—
54.3	CHBr ₂	103.7	—	—	—	—	—	—
—	CBr ₃	96.0	—	—	—	56.2	—	—
-213.4	C ₂ F ₅	102.7	—	126.8	82.7	68.7	51.2	—
—	nC ₃ F ₇	104	—	—	—	66.5	49.8	—
—	iC ₃ F ₇	103	—	—	—	66.5	—	—
-72.3	CF ₂ CH ₃	99.5	—	124.8	—	—	52.1	—
-123.6	CH ₂ CF ₃	106.7	—	109.4	—	—	56.3	—
—	CHClF ₂	101.8	—	—	—	65.7	—	—
—	CClBrCF ₃	96.6	—	—	—	60.0	—	—
104	CN	123.8	121.8	112.3	100.8	87.8	72.5	134.1
9.4	OH	119	92.6	—	60	56	56	—
79	C ₆ H ₅	111.3	102.2	125.7	95.7	80.5	65.4	—
-130.9	C ₆ F ₅	116.5	—	—	91.6	—	66.2	—

Laminar Flame Speeds

The compilation of laminar flame speed data given in Tables 1 and 2 is due to Gibbs and Calcote [*J. Chem. Eng. Data* **4**, 2226 (1959)]. The reader is referred to the quoted paper for details on the chosen values. The data are for premixed fuel-air mixtures at 25 and 100°C and 1 atm pressure.

TABLE 1

Burning velocities of various fuels at 25°C air-fuel temperature (0.31 mole-% H₂O in air)
 Burning velocity *S* as a function of equivalence ratio ϕ in cm sec⁻¹

	$\phi = 0.7$	0.8	0.9	1.0	1.1	1.2	1.3	1.4	<i>S</i> _{max}	ϕ at <i>S</i> _{max}
Saturated hydrocarbons										
Ethane	30.6	36.0	40.6	44.5	47.3	47.3	47.3	44.4	37.4	47.6
Propane			42.3	45.6	46.2	46.2	42.4	34.3		46.4
n-Butane		38.0	42.6	44.8	44.2	44.2	41.2	34.4	25.0	44.9
Methane		30.0	38.3	43.4	44.7	39.8	31.2			44.8
n-Pentane		35.0	40.5	42.7	42.7	39.3		33.9		43.1
n-Heptane		37.0	39.8	42.2	42.0	35.5	29.4			42.8
2, 2, 4-Trimethylpentane		37.5	40.2	41.0	37.2	31.0	23.5			41.0
2, 2, 3-Trimethylpentane		37.8	39.5	40.1	39.5	36.2				40.1
2, 2-Dimethylbutane		33.5	38.3	39.9	37.0	33.5				40.0
Isopentane		33.0	37.6	39.8	38.4	33.4	24.8			39.9
2, 2-Dimethylpropane			31.0	34.8	36.0	35.2	33.5	31.2		36.0
Unsaturated hydrocarbons										
Acetylene		107	130	144	151	154	154	154	152	155
Ethylene		37.0	50.0	60.0	68.0	73.0	72.0	66.5	60.0	73.5
Propyne			62.0	66.6	70.2	72.2	71.2	61.0		72.5
1, 3-Butadiene			42.6	49.6	55.0	57.0	57.0	56.9	55.4	57.2
n-1-Heptyne		46.8	50.7	52.3	50.9	47.4	41.6			52.3
Propylene			48.4	51.2	49.9	46.4	40.8			51.2
n-2-Pentene		35.1	42.6	47.8	46.9	42.6	34.9			48.0
2, 2, 4-Trimethyl-1,3-pentene		34.6	41.3	42.2	37.4	33.0				42.5

(continues)

TABLE 1 (continued)

	$\phi = 0.7$	0.8	0.9	1.0	1.1	1.2	1.3	1.4	S_{\max} ϕ at S_{\max}
Substituted alcohols									
Methanol		34.5	42.0	48.0	50.2	47.5	44.4	42.2	50.4 1.08
Isopropyl alcohol		34.4	39.2	41.3	40.6	38.2	36.0	34.2	41.4 1.04
Triethylamine		32.5	36.7	38.5	38.7	36.2	28.6		38.8 1.06
n-Butyl chloride	24.0	30.7	33.8	34.5	32.5	26.9	20.0		34.5 1.00
Allyl chloride	30.6	33.0	33.7	32.4	29.6				33.8 0.89
Isopropyl mercaptan		30.0	33.5	33.0	26.6				33.8 0.94
Ethylamine		28.7	31.4	32.4	31.8	29.4	25.3		32.4 1.00
Isopropylamine		27.0	29.5	30.6	29.8	27.7			30.6 1.01
n-Propyl chloride		24.7	28.3	27.5	24.1				28.5 0.93
Isopropyl chloride		24.8	27.0	27.4	25.3				27.6 0.97
n-Propyl bromide									
	No ignition								
Silanes									
Tetramethylsilane	39.5	49.5	57.3	58.2	57.7	54.5	47.5		58.2 1.01
Trimethylthoxysilane	34.7	41.0	47.4	50.3	46.5	41.0	35.0		50.3 1.00
Aldehydes									
Acrolein	47.0	58.0	66.6	65.9	56.5				67.2 0.95
Propionaldehyde		37.5	44.3	49.0	49.5	46.0	41.6	37.2	50.0 1.06
Acetaldehyde		26.6	35.0	41.4	41.4	36.0	30.0		42.2 1.05
Ketones									
Acetone		40.4	44.2	42.6	38.2				44.4 0.93
Methyl ethyl ketone		36.0	42.0	43.3	41.5	37.7	33.2		43.4 0.99
Esters									
Vinyl acetate	29.0	36.6	39.8	41.4	42.1	41.6	35.2		42.2 1.13
Ethyl acetate		30.7	35.2	37.0	35.6	30.0			37.0 1.00

Ethers										
Dimethyl ether		44.8	47.6	48.4	47.5	45.4	42.6		48.6	0.99
Diethyl ether	30.6	37.0	43.4	48.0	47.6	40.4	32.0		48.2	1.05
Dimethoxymethane	32.5	38.2	43.2	46.6	48.0	46.6	43.3		48.0	1.10
Dioisopropyl ether		30.7	35.5	38.3	38.6	36.0	31.2		38.9	1.06
Thio ethers										
Dimethyl sulfide		29.9	31.9	33.0	30.1	24.8			33.0	1.00
Peroxides										
Di- <i>tert</i> -butyl peroxide		41.0	46.8	50.0	49.6	46.5	42.0	35.5	50.4	1.04
Aromatic compounds										
Furan	48.0	55.0	60.0	62.5	62.4	60.0			62.9	1.05
Benzene		39.4	45.6	47.6	44.8	40.2	35.6		47.6	1.00
Thiophene	33.8	37.4	40.6	43.0	42.2	37.2	24.6		43.2	1.03
Cyclic compounds										
Ethylene oxide	57.2	70.7	83.0	88.8	89.5	87.2	81.0	73.0	89.5	1.07
Butadiene monoxide		36.6	47.4	57.8	64.0	66.9	66.8	64.5	67.1	1.24
Propylene oxide	41.6	53.3	62.6	66.5	66.4	62.5	53.8		67.0	1.05
Dihydrofuran	39.0	45.7	51.0	54.5	55.6	52.6	44.3	32.0	55.7	1.08
Cyclopropane		40.6	49.0	54.2	55.6	53.5	44.0		55.6	1.10
Tetrahydrofuran	44.8	51.0	53.6	51.5	42.3				53.7	0.93
Cyclic compounds										
Tetrahydrofuran			43.2	48.0	50.8	51.5	49.2	44.0	51.6	1.19
Cyclopentadiene	36.0	41.8	45.7	47.2	45.5	40.6	32.0		47.2	1.00
Ethylenimine		37.6	43.4	46.0	45.8	43.4	38.9		46.4	1.04
Cyclopentane	31.0	38.4	43.2	45.3	44.6	41.0	34.0		45.4	1.03
Cyclohexane			41.3	43.5	43.9	38.0			44.0	1.08
Inorganic compounds										
Hydrogen	102	120	145	170	204	245	213	290	325	1.80
Carbon disulfide	50.6	58.0	59.4	58.8	57.0	55.0	52.8	51.6	59.4	0.91
Carbon monoxide					28.5	32.0	34.8	38.0	52.0	2.05
Hydrogen sulfide	34.8	39.2	40.9	39.1	32.3				40.9	0.90

TABLE 2

Burning velocities of various fuels at 100°C air-fuel temperature (0.31 mole-% H₂O in air)
 Burning velocity S as a function of equivalence ratio ϕ in cm sec⁻¹

	$\phi = 0.7$	0.8	0.9	1.0	1.1	1.2	1.3	1.4	S_{mix}	ϕ at S_{max}
Propargyl alcohol		76.8	100.0	110.0	110.5	108.8	105.0	85.0	110.5	1.08
Propylene oxide	74.0	86.2	93.0	96.6	97.8	94.0	84.0	71.5	97.9	1.09
Hydrazine ^c	87.3	90.5	93.2	94.3	93.0	90.7	87.4	83.7	94.4	0.98
Furfural	62.0	73.0	83.3	87.0	87.0	84.0	77.0	65.5	87.3	1.05
Ethyl nitrate	70.2	77.3	84.0	86.4	83.0	72.3			86.4	1.00
Butadiene monoxide	51.4	57.0	64.5	73.0	79.3	81.0	80.4	76.7	81.1	1.23
Carbon disulfide	64.0	72.5	76.8	78.4	75.5	71.0	66.0	62.2	78.4	1.00
n-Butyl ether		67.0	72.6	70.3	65.0				72.7	0.91
Methanol	50.0	58.5	66.9	71.2	72.0	66.4	58.0	48.8	72.2	1.08
Diethyl cellosolve	49.5	56.0	63.0	69.0	69.7	65.2			70.4	1.05
Cyclohexene monoxide	54.5	59.0	63.5	67.7	70.0	64.0			70.0	1.10
Epichlorohydrin	53.0	59.5	65.0	68.6	70.0	66.0	58.2		70.0	1.10
n-Pentane		50.0	55.0	61.0	62.0	57.0	49.3	42.4	62.9	1.05
n-Propyl alcohol	49.0	56.6	62.0	64.6	63.0	50.0	37.4		64.8	1.03
n-Heptane	41.5	50.0	58.5	63.8	59.5	53.8	46.2	38.8	63.8	1.00
Ethyl nitrite	54.0	58.8	62.6	63.5	59.0	49.5	42.0	36.7	63.5	1.00
Pinene	48.5	58.3	62.5	62.1	56.6	50.0			63.0	0.95
Nitroethane	51.5	57.8	61.4	57.2	46.0	28.0			61.4	0.92
Iso-octane		50.2	56.8	57.8	53.3	50.5			58.2	0.98
Pyrrrole		52.0	55.6	56.6	56.1	52.8	48.0	43.1	56.7	1.00
Aniline		41.5	45.4	46.6	42.9	37.7	32.0		46.8	0.98
Dimethyl formamide		40.0	43.6	45.8	45.5	40.7	30.7		46.1	1.04

^cResults questionable because of an indication of decomposition in the stainless-steel feed system

Flammability Limits in Air

The data presented in Table 1 are for fuel gases and vapors and are taken almost exclusively from Zabetakis [U.S. Bur. Mines Bulletin 627 (1965)]. The conditions are for the fuel-air mixture at 25°C and 1 atm unless otherwise specified. As noted in the text, most fuels have a rich limit at approximately $\phi = 3.3$ and a lean limit at approximately $\phi = 0.5$. The fuels which vary most from the rich limit are those that are either very tightly bound as ammonia is or which can decompose as hydrazine or any monopropellant does.

There can also be a flammability limit associated with dust clouds. The flammability limits of combustible dusts are reported as the minimum explosion concentrations. The upper explosion limits for dust clouds have not been determined due to experimental difficulties. In the 14th edition of the Fire Protection Handbook (National Fire Protection Association, Boston, MA, 1975), numerous results from the US Bureau of Mines reports are listed. These results were obtained with dusts 74 μm or smaller. It should be noted that variations in minimum explosive concentrations will occur with change in particle diameter, i.e., the minimum explosive concentration is lowered as the diameter of the particle decreases. Other conditions which affect this limit are sample purity, oxygen concentration, strength of ignition source, turbulence, and uniformity of the dispersion. The NFPA tabulation is most extensive and includes data for dusts from agricultural materials, carbonaceous matter, chemicals, drugs, dyes, metals, pesticides, and various plastic resins and molding compounds. Except for metal dusts, it is rather remarkable that most materials have a minimum explosive concentration in the range 0.03–0.05 kg/m^3 . It should be noted, however, that the variation according to the specific compound can range from 0.01 to 0.50 kg/m^3 . For a specific value the reader should refer to the NFPA handbook.

TABLE 1

Flammability limits of fuel gases and vapors in air at 25°C and 1 atm

Fuel	Lean limit		Rich limit	
	Vol. %	ϕ	Vol. %	ϕ
Acetal	1.6		10	
Acetaldehyde	4.0	0.59	60	28
Acetic acid	5.4 (100°C)			
Acetic anhydride	2.7 (47°C)		10 (75°C)	
Acetanilide	1.0 (calc)			
Acetone	2.6	0.52	13	2.6
Acetophenone	1.1 (calc)			
Acetylacetone	1.7 (calc)			
Acetyl chloride	5.0 (calc)			
Acetylene	2.5		100	
Acrolein	2.8		31	
Acrylonitrile	3.0			
Acetone cyanohydrin	2.2		12	
Adipic acid	1.6 (calc)			
Aldol	2.0 (calc)			
Allyl alcohol	2.5		18	
Allyl amine	2.2		22	
Allyl bromide	2.7 (calc)			
Allyl chloride	2.9			
<i>o</i> -Aminodiphenyl	0.66		4.1	
Ammonia	15	0.69	28	1.3
<i>n</i> -Amyl acetate	1.0 (100°C)	0.51	7.1 (100°C)	3.3
<i>n</i> -Amyl alcohol	1.4 (100°C)	0.51	10 (100°C)	
<i>t</i> -Amyl alcohol	1.4 (calc)			
<i>n</i> -Amyl chloride	1.6 (50°C)		8.6 (100°C)	
<i>t</i> -Amyl chloride	1.5 (85°C)			
<i>n</i> -Amyl ether	0.7 (calc)			
Amyl nitrite	1.0 (calc)			
<i>n</i> -Amyl propionate	1.0 (calc)			
Amylene	1.4		8.7	
Aniline	1.2 (140°C)		8.3 (140°C)	
Anthracene	0.65 (calc)			
<i>n</i> -Amyl nitrate	1.1			
Benzene	1.3 (100°C)	0.48	7.9 (100°C)	2.9
Benzyl benzoate	0.7 (calc)			
Benzyl chloride	1.2 (calc)			
Bicyclohexyl	0.65 (100°C)		5.1 (150°C)	
Biphenyl	0.70 (110°C)			
2-Biphenyl amine	0.8 (calc)			
Bromobenzene	1.6 (calc)			
Butadiene(1,3)	2.0		12	
<i>n</i> -Butane	1.8	0.58	8.4	2.7

TABLE 1 (continued)

Fuel	Lean limit		Rich limit	
	Vol. %	ϕ	Vol. %	ϕ
1,3-Butandiol	1.9 (calc)			
Butene-1	1.6		10	
Butene-2	1.7		9.7	
<i>n</i> -Butyl acetate	1.4 (50°C)	0.55	8.0 (100°C)	3.1
<i>n</i> -Butyl alcohol	1.7 (100°C)	0.50	12 (100°C)	
<i>s</i> -Butyl alcohol	1.7 (100°C)		9.8 (100°C)	
<i>t</i> -Butyl alcohol	1.9 (100°C)		9.8 (100°C)	
<i>t</i> -Butyl amine	1.7 (100°C)		8.9 (200°C)	
<i>n</i> -Butyl benzene	0.82 (100°C)		5.8 (100°C)	
<i>s</i> -Butyl benzene	0.77 (100°C)		5.8 (100°C)	
<i>t</i> -Butyl benzene	0.77 (100°C)		5.8 (100°C)	
<i>n</i> -Butyl bromide	2.5 (100°C)			
Butyl cellosolve	1.1 (150°C)		11 (175°C)	
<i>n</i> -Butyl chloride	1.8		10 (100°C)	
<i>n</i> -Butyl formate	1.7	0.54	8.2	2.6
<i>n</i> -Butyl stearate	0.3 (calc)			
Butyric acid	2.1 (calc)			
γ -Butyrolactone	2.0 (150°C)			
Carbon disulfide	1.3	0.20	50	7.7
Carbon monoxide	12.5		74	
Chlorobenzene	1.4			
<i>m</i> -Cresol	1.1 (150°C)			
Crotonaldehyde	2.1		16 (60°C)	
Cumene	0.88 (100°C)	0.51	6.5 (100°C)	3.8
Cyanogen	6.6			
Cyclobutane	1.8	0.56		
Cycloheptane	1.1	0.56	6.7	3.4
Cyclohexane	1.3	0.57	7.8	3.4
Cyclohexanol	1.2 (calc)			
Cyclohexene	1.2 (100°C)			
Cyclohexylacetate	1.0 (calc)			
Cyclopentane	1.5	0.55		
Cyclopropane	2.4	0.54	10.4	2.3
Cymene	0.85 (100°C)	0.56	6.5 (100°C)	3.6
Decaborane	0.2	0.11		
Decalin	0.74 (100°C)		4.9 (100°C)	
<i>n</i> -Decane	0.75 (53°C)	0.56	5.6 (86°C)	4.2
Deuterium	4.9		75	
Diborane	0.8	0.12	88	13.5
Diethyl amine	1.8		10	
Diethyl aniline	0.8 (calc)			
1,4-Diethyl benzene	0.8 (100°C)			

(continues)

TABLE 1 (continued)

Fuel	Lean limit		Rich limit	
	Vol. %	ϕ	Vol. %	ϕ
Diethyl cyclohexane	0.75			
Diethyl ether	1.9		36	
3,3-Diethyl pentane	0.7 (100°C)			
Diethyl ketone	1.6	0.55		
Diisobutyl carbinol	0.82 (100°C)		6.1 (175°C)	
Diisobutyl ketone	0.79 (100°C)		6.2 (100°C)	
Diisopropyl ether	1.4		7.9	
Diethyl amine	2.8			
2,2-Dimethyl butane	1.2		7.0	
2,3-Dimethyl butane	1.2		7.0	
Dimethyl decalin	0.69 (100°C)		5.3 (110°C)	
Dimethyl dichlorosilane	3.4			
Dimethyl ether	3.4		27	
N,N-Dimethyl formamide	1.8 (100°C)		14 (100°C)	
2,3-Dimethyl pentane	1.1		6.8	
2,2-Dimethyl propane	1.4		7.5	
Dimethyl sulfide	2.2	0.50	20	4.5
Dioxane	2.0		22	
Dipentene	0.75 (150°C)		6.1 (150°C)	
Diphenylamine	0.7 (calc)			
Diphenyl ether	0.8 (calc)			
Diphenyl methane	0.7 (calc)			
Divinyl ether	1.7		27	
n-Dodecane	0.60 (calc)	0.56		
Ethane	3.0	0.53	12.4	2.2
Ethyl acetate	2.2	0.55	11	2.7
Ethyl alcohol	3.3	0.50	19 (60°C)	2.9
Ethyl amine	3.5			
Ethyl benzene	1.0 (100°C)	0.51	6.7 (100°C)	3.4
Ethyl chloride	3.8			
Ethyl cyclobutane	1.2	0.53	7.7	3.4
Ethyl cyclohexane	2.0 (130°C)	0.56	6.6 (130°C)	3.9
Ethyl cyclopentane	1.1	0.56	6.7	3.4
Ethyl formate	2.8	0.50	16	2.8
Ethyl lactate	1.5			
Ethyl mercaptan	2.8	0.63	18	4.4
Ethyl nitrate	4.0			
Ethyl nitrite	3.0		50	
Ethyl propionate	1.8	0.58	11	3.5
Ethyl propyl ether	1.7		9	
Ethylene	2.7		36	
Ethyleneimine	3.6		46	
Ethylene glycol	3.5 (calc)			

TABLE 1 (continued)

Fuel	Lean limit		Rich limit	
	Vol. %	ϕ	Vol. %	ϕ
Ethylene oxide	3.6		100	
Furfural alcohol	1.8 (72°C)		16 (117°C)	
Gasoline (100/130)	1.3		7.1	
Gasoline (115/145)	1.2		7.1	
<i>n</i> -Heptane	1.0	0.56	6.7	3.6
<i>n</i> -Hexadecane	0.43 (calc)			
<i>n</i> -Hexane	1.2	0.56	7.4	3.4
<i>n</i> -Hexyl alcohol	1.2 (100°C)	0.53		
<i>n</i> -Hexyl ether	0.6 (calc)			
Hydrazine	4.7	0.27	100	
Hydrogen	4.0	0.14	75	2.54
Hydrogen cyanide	5.6		40	
Hydrogen sulfide	4.0	0.33	44	3.6
Isoamyl acetate	1.1 (100°C)		7.0 (100°C)	
Isoamyl alcohol	1.4 (100°C)		9.0 (100°C)	
Isobutane	1.8		8.4	
Isobutyl alcohol	1.7 (100°C)		11 (100°C)	
Isobutyl benzene	0.82 (100°C)		8.9	
Isobutylene	1.8		9.6	
Isopentane	1.4			
Isophorone	0.84			
Isopropylacetate	1.7 (calc)			
Isopropyl alcohol	2.2			
Isopropyl biphenyl	0.6 (calc)			
Jet Fuel (JP-4)	1.3		8	
Methane	5.0	0.53	15.0	1.6
Methyl acetate	3.2	0.57	16	2.8
Methyl acetylene	1.7	0.55		2.9
Methyl alcohol	6.7		36 (60°C)	
Methylamine	4.2 (calc)			
Methyl bromide	10		15	
3-Methyl-1-butene	1.5		9.1	
Methyl butyl ketone	1.2 (50°C)	0.58	8.0 (100°C)	3.3
Methyl cellosolve	2.5 (125°C)		20 (140°C)	
Methyl cellosolve acetate	1.7 (150°C)			
Methyl ethyl ether	2.2 (calc)			
Methyl chloride	7 (calc)			
Methyl cyclohexane	1.1	0.56	6.7	3.4
Methyl cyclopentadiene	1.3 (100°C)		7.6 (100°C)	
Methyl ethyl ketone	1.9	0.52	10	2.7
Methyl formate	5.0	0.58	23	2.4
Methyl cyclohexanol	1.0 (calc)			

(continues)

TABLE 1 (continued)

Fuel	Lean limit		Rich limit	
	Vol. %	ϕ	Vol. %	ϕ
Methyl isobutyl carbinol	1.2 (calc)			
Methyl isopropenyl ketone	1.8 (50°C)		9.0 (50°C)	
Methyl lactate	2.2 (100°C)			
Methyl mercaptan	3.9	0.60	2.2	3.4
1-Methyl naphthalene	0.8 (calc)			
2-Methyl pentane	1.2 (calc)			
Methyl propionate	2.4	0.60	13	3.2
Methyl propyl ketone	1.6	0.55	8.2	2.8
Methyl styrene	1.0 (calc)			
Methyl vinyl ether	2.6		39	
Monoisopropyl bicyclohexyl	0.52		4.1 (200°C)	
2-Monoisopropyl biphenyl	0.53 (175°C)		3.2 (200°C)	
Monomethylhydrazine	4	0.52		
Naphthalene	0.88 (78°C)		5.9 (122°C)	
Nicotine	0.75 (calc)			
Nitroethane	3.4			
Nitromethane	7.3			
1-Nitropropane	2.2			
2-Nitropropane	2.5			
<i>n</i> -Nonane	0.85 (43°C)	0.58		
<i>n</i> -Octane	0.95	0.58		
Paraldehyde	1.3	0.48		
Pentaborane	0.42	0.22		
<i>n</i> -Pentane	1.4	0.55	7.8	3.1
Phthalic anhydride	1.2 (140°C)		9.2 (195°C)	
3-Picoline	1.4 (calc)			
Pinane	0.74 (160°C)		7.2 (160°C)	
Propadiene	2.16			
Propane	2.1	0.52	9.5	2.4
1,2-Propendiol	2.5 (calc)			
β -Propiolactone	2.9 (75°C)			
Propionaldehyde	2.9		17	
<i>n</i> -Propyl acetate	1.8	0.58	8	2.6
<i>n</i> -Propyl alcohol	2.2 (53°C)	0.49	14 (100°C)	3.2
Propylamine	2.0			
Propyl chloride	2.4 (calc)			
<i>n</i> -Propyl nitrate	1.8 (126°C)		100 (125°C)	
Propylene	2.4		11	
Propylene dichloride	3.1 (calc)			
Propylene glycol	2.6 (96°C)			
Propylene oxide	2.8		37	
Pyridine	1.8 (60°C)		12 (70°C)	
Propargyl alcohol	2.4 (50°C)			

TABLE 1 (continued)

Fuel	Lean limit		Rich limit	
	Vol. %	ϕ	Vol. %	ϕ
Quinoline	1.0 (calc)			
Styrene	1.1 (19°C)			
Sulfur	2.0 (247°C)			
<i>p</i> -Terphenyl	0.96 (calc)			
Tertaborane	0.4 (calc)	0.11		
<i>n</i> -Tetradecane	0.5 (cal)	0.52		
Tetrahydrofuran	2.0			
Tetralin	0.84 (100°C)		50 (150°C)	
2,2,3,3-Tetramethyl pentane	0.8			
Toluene	1.2 (100°C)	0.53	7.1 (100°C)	3.1
Trichloroethylene	12 (30°C)		40 (70°C)	
Triethylamine	1.2		8.0	
Triethylene glycol	0.9 (150°C)		9.2 (203°C)	
2,2,3-Trimethyl butane	1.0			
Trimethyl amine	2.0		12	
2,2,4-Trimethyl pentane	0.95			
Trimethylene glycol	1.7 (calc)			
Trioxane	3.2 (calc)			
Turpentine	0.7 (100°C)			
UDMH	2.0	0.40	95	19.1
Vinyl acetate	2.6			
Vinyl chloride	3.6		33	
<i>m</i> -Xylene	1.1 (100°C)	0.56	6.4 (100°C)	3.3
<i>o</i> -Xylene	1.1 (100°C)	0.56	6.4 (100°C)	3.3
<i>p</i> -Xylene	1.1 (100°C)	0.56	6.4 (100°C)	3.3

Spontaneous Ignition Temperature Data

The greatest compilations of spontaneous ignition (autoignition) temperatures are those of Mullins [AGARDograph No. 4 (1955)] and Zabetakis [U.S. Bur. Mines Bulletin 627 (1965)]. These data have been collated and are given with permission in this appendix. The largest compilation is that of Mullins, and consequently his general format of presenting the data is followed. There have been many methods of measuring ignition temperatures and the results from different measurements have not necessarily been self-consistent. Mullins lists the various results, a reference to the technique used, and the reporting investigators. Since the various techniques have not been discussed in this text, these references have been omitted from the data which are reproduced here, and only the reported ignition temperatures are presented.

All temperatures are reported in degrees centigrade. The delay period, where known, is in milliseconds and follows the temperature in parentheses. If no delay time appears, then the spontaneous ignition time was either not specifiable, not specified or determined by the manner shown in Fig. 1 of Chapter 7, and probably always in excess of 1000 msec. All data are for atmospheric pressure with the exception of the vitiated air data for acetylene and hydrogen, which are for 0.9 atm. The data for oxygen, air, and vitiated air are given in this order following letters O, A, and V. When there was significant difference between the values reported by Mullins and Zabetakis, the values given by Zabetakis were added to the reorganized Mullins compilation. This value is designated by the letter z following the temperature. When the original Mullins listing reported two or more values within 2 degrees of each other, then only one value has been presented. If there are large differences between the reported values, the reader is urged to refer to Mullins and Zabetakis for the method and original source.

TABLE 1

Spontaneous ignition temperature data

Acetal O 174; A 230; V 768 (20); 957
Acetaldehyde O 140; 159; A 185, 275, 175; V869 (20), 1088 (1)
Acetanilide A 546
Acetic acid O 570; 490; A 599, 550, 566, 465z
Acetic anhydride O 361; A 392, 401
Acetone O 568, 485; A 700, 727, 561, 538, 569, 465z; V871 (20), 1046 (1)
Acetone cyanhydrin A 688
Acetonitrile V 1000 (20), 1059 (10)
Acetylacetone A 493, 340z; V 816 (10), 996 (1)
Acetophenone A 520z
Acetylchloride A 390z
Acetylene O 296; A 305, 335; V 623 (20), 826 (1)
Acetyl oxide (see Acetic anhydride)
Acrolein A 278, 235z; V 712 (10), 859 (1)
Acrylaldehyde (see Acrolein)
Acrylonitrile O 460; A 481
Adipic acid A 420z
Aldol A 277, 248
Allyl alcohol O 348; A 389; V 767 (20), 979 (1)
Allylamine A 374
Allyl bromide A 295
Allyl chloride O 404; A 487; 392
Allyl ether O 200; V 749 (10), 927 (1)
Aminobenzene (see Aniline)
Amenodyphenyl A 450z
2-Aminoethanol (see Monoethanolamine)
Aminoethylethanolamine A 360
Ammonia A 651
<i>n</i> -Amyl acetate A 399, 360z, 378
<i>i</i> -Amyl acetate A 379, 360z
<i>n</i> -Amyl alcohol O 390, 332; A 409, 427, 327; V 806 (20), 990 (1)
<i>i</i> -Amyl alcohol A 518, 343, 353; V 818 (20), 1013 (1)
<i>s</i> -Amyl alcohol 343-385
<i>t</i> -Amyl alcohol A 437; V 814 (20), 995 (1)
Amylbenzene O 255
<i>n</i> -Amyl chloride A 250
<i>t</i> -Amyl chloride A 343
<i>n</i> -Amylene A 273
<i>i</i> -Amyl ether A 428
Amylmethyl ketone A 311
Amyl nitrate A 210z; V 524 (20), 798 (1)
Amyl nitrite V 496 (20), 910 (1)
<i>i</i> -Amyl nitrite V 437 (10), 918 (1)
<i>n</i> -Amyl propionate A 380z
Aniline O 530; A 770, 628, 530, 617, 593 (6000); V 907 (20), 1065 (2)

(continues)

TABLE 1 (continued)

<i>o</i> -Anisidine V 787 (20), 1039 (1)
Anisole O 560; V 744 (20), 1025 (1)
Anthracene O 580; A 472
Antifebrin (see Acetanilide)
Banana Oil (see <i>i</i> -Amyl acetate)
Benzaldehyde O 168; A 180, 192; V 744 (20), 936 (1)
Benzene carbonal (see Benzaldehyde)
Benzoic acid O 475, 556; A 573
Benzyl acetate A 588, 461; V 767 (20), 1019 (1)
Benzyl alcohol O 373; A 502, 436; V 806 (20), 1007 (1)
Benzyl benzoate A 480z
Benzyl cellosolve (see Ethyleneglycolmonobenzyl ether)
Benzyl chloride A 627, 585z
Benzyl ethanoate (see Benzyl acetate)
Benzylethyl ether A 496
Bicyclohexyl A 245z
Biphenyl A 477 (36000), 540z
Bromobenzene A 688, 565z; V 858 (20), 1046 (1)
1-Bromobutane (see <i>n</i> -Butyl bromide)
Bromoethane (see Ethyl bromide)
1,3-Butadiene O 335; A 418
<i>n</i> -Butaldehyde (see <i>n</i> -Butyraldehyde)
<i>n</i> -Butane O 283; A 403, 430 (6000)
<i>i</i> -Butane O 319; A 462, 543, 477 (18000)
2,3-Butanedione (see Diacetyl)
1-Butanol (see Methyl ethyl ketone)
2-Butanol (see <i>sec</i> -Butyl alcohol)
2-Butanone (see Methyl ethyl ketone)
2-Butenal (see Crotonaldehyde)
1-Butene O 310z; A 384
2-Butene 325z, A 435
2-Butanol (see <i>sec</i> -Butyl alcohol)
2-Butoxyethanol (see Ethyleneglycolmonobutyl ether)
<i>n</i> -Butyl acetate A 423; V 793 (20), 1040 (1)
<i>n</i> -Butyl alcohol O 385, 328; A 450, 503, 367, 359 (18000); V 809 (20), 993 (1)
<i>i</i> -Butyl alcohol O 364; A 542, 441, 414; V 794 (20), 1010 (1)
<i>sec</i> -Butyl alcohol O 377; A 414; V 833 (20), 990 (1)
<i>t</i> -Butyl alcohol O 460; A 478, 483
<i>n</i> -Butylamine A 312
<i>i</i> -Butylamine A 374
<i>t</i> -Butylamine A 380z
<i>n</i> -Butylbenzene A 412, 444 (6000)
<i>i</i> -Butylbenzene A 428, 456 (12000)
<i>sec</i> -Butylbenzene A 443, 420z, 447 (18000)
<i>t</i> -Butylbenzene A 448, 477 (72000); V 779 (20), 1000 (1)
2-Butylbiphenyl A 433 (12000)
<i>n</i> -Butyl bromide A 483, 316, 265z

TABLE 1 (continued)

Butyl carbinol (see <i>i</i> -Amyl alcohol)
Butyl carbitol A 228
Butyl carbitol acetate A 299
Butyl cellosolve (see Ethyleneglycolmonobutyl ether)
<i>n</i> -Butyl chloride A 460
α -Butylene (see 1-Butene)
β -Butylene (see 2-Butene)
γ -Butylene (see 2-Methylpropene)
<i>i</i> -Butylene (see 2-Methylpropene)
β -Butylene glycol A 377
<i>n</i> -Butyl ether A 294
<i>n</i> -Butyl formate O 308; A 322
Butyl lactate A 382
<i>i</i> -Butylmethyl ketone A 459
<i>n</i> -Butyl nitrite V 400 (4), 490 (1)
Butylphthalate A 403; V 813 (20), 1021 (1)
<i>n</i> -Butyl propionate A 426
<i>n</i> -Butyl stearate A 355z
<i>n</i> -Butyraldehyde O 206; A 408, 230
<i>i</i> -Butyraldehyde A 254
<i>n</i> -Butyric acid A 552, 450z
Camphor A 466
Carbon disulfide O 107; A 149, 120, 125, 80z; v 610 (20), 842 (1)
Carbon monoxide O 588; A 609, 651; V 758 (20), 848 (1)
Castor oil A 449
Cellosolve (see Ethyleneglycolmonoethyl ether)
Cetane A 235
Cetene V 748 (20), 1036 (1)
<i>o</i> -Chloroaniline V 885 (20), 1084 (2)
<i>m</i> -Chloroaniline V 846 (20), 1080 (2)
Chlorobenzene A 674, 640z
Chloroethane (see Ethyl chloride)
2-Chloro-2-methyl chloride O 318; A 343
3-Chloro-(trifluoromethyl) benzene A 654
Creosote oil A 336
<i>o</i> -Cresol A 599, 599
<i>m</i> -Cresol A 626; V 836 (20), 110 (2)
Crotonaldehyde A 232; V 703 (20), 924 (1)
Cumene A 467 (6000), 425z; V 802 (20), 985 (1)
pseudo-Cumene V 770 (20), 1025 (2)
Cyanogen A 850
Cyclohexadiene O 360
Cyclohexane O 325, 296; A 259, 270 (102000), 245z; V 798 (20), 980 (1)
Cyclohexanol O 350; A 300z; V 814 (20), 1030 (1)
Cyclohexanone O 550; A 557, 453; V 816 (20), 1046 (1)
Cyclohexylamine A 293

(continues)

TABLE 1 (continued)

Cyclohexyl acetate A 355z
Cyclohexene O 325; V 781 (20); 972 (1)
Cyclopentadiene O 510
Cyclopropane O 545; A 498
<i>p</i> -Cymene A 466, 494, 445, 435z; V 807 (20), 1050 (1)
Decahydronaphthalene O 280; A 262, 272 (18000), 250z
<i>trans</i> -Decahydronaphthalene V 814 (20), 1002 (1)
Decalin (see Decahydronaphthalene)
<i>n</i> -Decane O 202; A 463, 425, 250, 210z; 232 (54000); 236
1-Decanol A 291
1-Decene A 244 (78000)
<i>n</i> -Decyl alcohol V 793 (20), 960 (1)
Diacetone alcohol A 603; V 805 (20), 1065
Diacetyl V 748 (20), 930 (1)
1,2-Diacetyethane (see Acetylacetone)
Diallyl O 330
Diallyl ether (see Allyl ether)
Dibutyl ether (see <i>n</i> -Butyl ether)
Dibutyl phthalate (see Butyl phthalate)
Di- <i>n</i> -butyl tartrate A 824
<i>o</i> -Dichlorobenzene A 648
1,2-Dichloro- <i>n</i> -butane O 250; A 276
Dichloro-1-(chlorotetrafluoroethyl)-4-(trifluoromethyl) benzene A 591
1,2-Dichloroethane (see Ethylene dichloride)
Dichloroethylene A 441, 458; V 738 (20), 1079 (1)
2,2-Dichloroethyl ether A 369; V 766 (20), 953 (1)
Dichloromethane (see Methylene chloride)
1,2-Dichloropropane (see Propylene dichloride)
Dicyclopentadiene O 510
Di- <i>n</i> -decyl ether A 217
Diesel fuel (60 cetone) A 225z
Diethanolamine A 662; V 823 (20), 1000 (2); V 754 (20), 977 (1)
Diethylaniline A 630z; V 762 (20), 965 (1)
1,2-Diethylbenzene A 404 (6000)
1,3-Diethylbenzene A 455 (12000)
1,4-Diethylbenzene A 430, 451 (12000)
Diethylcellosolve (see Ethyleneglycoldiethyl ether)
Dimethyl cyclohexane A 240z
1,4-Diethylene dioxide (see Dioxane)
Diethyl ether (see Ethylether)
Diethylene glycol A 229
Diethyleneglycolbenzoate-2-ethylhexoate A 340
Diethylene oxide (see Dioxane)
Diethylenetriamine A 399
Diethyl ketone A 608, 450z
3,3-Diethylpentane A 322, 290z
Diethyl peroxide A 189

TABLE 1 (continued)

Diethyl sulfate A 436
Dihexyl (see Dodecane)
Di-*n*-hexyl ether A 200
2,2'-Dihydroxyethylamine (see Diethanolamine)
Diisobutylenes A 470; V 799 (20), 1064 (1)
Diisooctyladipate A 366
Diisopropyl (see 2,3-Dimethylbutane)
Diisopropylbenzene A 449
Diisopropyl ether A 443, 416, 500; V 820 (20), 1037 (1)
Dimethylamine O 346; A 402
Dimethylaniline A 371; V 780 (20), 960 (1)
2,2-Dimethylbutane A 425, 440 (12000)
2,3-Dimethyl-1-butene A 369 (6000)
2,3-Dimethyl-2-butene A 407 (6000)
Dimethylchloroacetal A 232
Dimethyl decalin A 235z
2,4-Dimethyl-3-ethylpentane A 390 (12000), 520
Dimethyl ether O 252; A 350
trans-Dimethylethylene (see 2-Methyl propene)
Dimethyl formamide A 445, 435z
Dimethylhexane A 438
Dimethylketone (see Acetone)
2,3-Dimethyloctane A 231 (72000)
4,5-Dimethyloctane A 388
2,3-Dimethylpentane A 337, 338 (6000)
o-Dimethylphthalate A 556
2,2-Dimethylpropane A 450, 456 (3000)
Dimethyl sulfide A 206
1,1-Dineopentylethane A 500
1,1-Dineopentylethylene A 455
Diocetylbenzenephosphonate A 314
Di-*n*-octyl ether A 210
Diocetylisoctenephosphonate A 320
1,4-Dioxene A 266, 179; V 775 (20), 933 (1)
Dipentene A 237z
Diphenylamine A 452, 535z
1,1-Diphenylbutane A 462 (6000)
1,1-Diphenylethane A 487 (6000)
Diphenylether A 620z
Diphenylmethane A 517 (18000), 485z
Diphenyloxide A 646 (12000)
1,1-Diphenylpropane A 466 (6000)
Di-*n*-propyl ether A 189
Divinyl ether A 360
n-Dodecane A 232, 205z
i-Dodecane A 534, 500; V 827 (20), 1010 (1)

(continues)

TABLE 1 (continued)

1-Dodecanol A 283
<i>n</i> -Eicosane A 240
Ethanal (see Acetaldehyde)
Ethane A 472, 515; V 809 (20), 991 (1)
Ethanol (see Ethyl alcohol)
Ethene (see Ethylene)
Ether (see Ethylether)
<i>p</i> -Ethoxyaniline (see <i>p</i> -Phenetidine)
2-Ethoxyethanol (see Ethyleneglycolmonoethyl ether)
2-Ethoxyethanol acetate (see Ethyleneglycolmonoethyl ether monoacetate)
Ethyl acetate A 610, 486; V 804 (20), 1063 (1)
Ethyl alcohol O 425, 375; A 558, 426, 365z; V 814 (20), 1030 (1)
Ethylamine (70% aqueous solution) A 384
Ethylaniline A 479
Ethylbenzene O 468; A 460 (18000), 553, 477, 430z; V 785 (20), 996 (1)
Ethylbenzoate A 644
2-Ethylbiphenyl A 449 (18000)
Ethyl bromide A 533; 511; V 883 (20), 1055 (2)
2-Ethylbutane O 273
2-Ethyl-1-butanol (see <i>i</i> -Hexyl alcohol)
2-Ethyl-1-butene A 324 (6000)
Ethyl- <i>n</i> -butyrate O 351; A 612, 463
Ethyl caprate A 493
Ethyl- <i>n</i> -caproate A 582
Ethyl- <i>n</i> -caprylate A 571
Ethyl carbonate V 782 (20), 1013 (1)
Ethyl chloride O 463, A 516, 494
Ethylcyclobutane A 211
Ethylcyclohexane A 262 (114000)
Ethylcyclopentane A 262
Ethylene O 485; A 490, 543
Ethylene chlorhydrin O 400; A 425
Ethylene dichloride A 413
Ethylenglycol O 500; A 522, 413, 400z
Ethylenglycol diacetate A 635
Ethyleneglycoldiethyl ether A 208
Ethyleneglycolmonobenzyl ether A 352
Ethyleneglycolmonobutyl ether A 244; V 792 (20), 964 (1)
Ethyleneglycolmonoethyl ether A 238, 350z; V 790 (20), 954 (1)
Ethyleneglycolmonoethyl ether acetate A 379
Ethyleneglycolmonoethyl ether monoacetate V 744 (20), 960 (1)
Ethyleneglycolmonoethyl ether A 288, 382; V 780 (20), 933 (1)
Ethylene imine A 322
Ethylene oxide A 429
Ethyl ether O 178, 182; A 343, 491, 186, 193, 160z; V 794 (20), 947 (1)
Ethyl formate A 477, 455z; V 768 (20), 956 (1)
Bis-(2-ethylhexyl)-adipate A 262

TABLE 1 (continued)

Ethyl lactate A 400
Ethyl malonate A 541
Ethyl mercaptan O 261; A 299
Ethylmethyl ether (see Methyl ethyl ether)
Ethylmethyl ketone (see Methyleneethyl ketone)
1-Ethyl-naphthalene A 481 (6000)
Ethyl nitrate V 426, 562
Ethyl nitrite A 90; V 580 (20), 833 (1)
3-Ethyloctane A 235
4-Ethyloctane A 237 (54000)
Ethyloleate A 353
Ethyl oxalate V 742 (10), 880 (1)
Ethyl palmitate A 388
Ethyl pelargonate A 524
Ethyl propionate O 440; A 602, 476, 440z
Ethylpropyl ketone A 575
Ethyl- <i>n</i> -valerianate A 590
Formaldehyde (37% solution) A 430
Formamide V 969, 1032 (10)
Formic acid A 504
Furan V 783 (20), 982 (1)
2-Furancarboxal (see Furfuraldehyde)
Furfuraldehyde A 391, V 696 (20), 880 (1)
Furfuran (see Furan)
Furfuryl alcohol O 364, A 391, 491, V 775 (20), 944 (1)
Fusel oil (see <i>n</i> -Amyl alcohol)
Gas oil O 270
Gasoline (100/130) A 440Z
Gasoline (115/145) A 470Z
Glycerol O 414, 320, A 500, 523, 393
Glyceryl triacetate A 433
Glycol (see Ethylene glycol)
<i>n</i> -Heptane O 300, 214, A 451, 230, 233, 250, 247 (30000), V 806 (20), 950 (1)
<i>n</i> -Heptanoic acid A 523
1-Heptene A 332, 263 (66000)
α - <i>n</i> -Heptylene (see 1-Heptene)
Hexachlorobutadiene A 618 (6000)
Hexachlorodiphenyl oxide A 628
<i>n</i> -Hexadecane A 230 (66000), 232
<i>i</i> -Hexadecane A 484
1-Hexadecene A 240 (78000), 253
Hexahydrobenzene (see cyclohexane)
Hexahydrophenol (see cyclohexanol)
Hexamethylbenzene O 375
Hexamethylene (see cyclohexane)
<i>n</i> -Hexane O 296, A 487, 520, 248, 261, 225 Z, 261 (30000), V 820 (20), 1015 (1)

(continues)

TABLE 1 (continued)

<i>i</i> -Hexane O 268, 284
2,5-Hexanedione (see Acetylacetone)
1-Hexene A 272 (72000)
Hexone (see <i>i</i> -Butylmethyl ketone)
<i>n</i> -Hexyl alcohol O 300, V 801 (20), 970 (1)
<i>i</i> -Hexyl alcohol V 800 (20), 963 (1)
Hexylene O 325
<i>n</i> -Hexylether A 185z
Hydrazine A 270
Hydrocyanic acid A 538
Hydrogen O 560, A 572, 400z, V 610 (20), 700 (1)
Hydrogen sulfide O 220, A 292
Hydroquinone O 630
2-Hydroxyethylamine (see Monoethanolamine)
4-Hydroxy-4-methyl-2-pentanone (see Diacetone alcohol)
<i>o</i> -Hydroxytoluene (see Benzyl alcohol)
<i>m</i> -Hydroxytoluene (see <i>m</i> -Cresol)
Isophorone O 322, A 462
Isoprene O 440, JP4 A 240 Z, JPG A20 Z
Kerosine O 270, A 295, 254, 210 Z, 249 (66000), V 806 (20), 998 (1)
Ketohexahydrobenzene (see cyclohexanone)
<i>dl</i> -Limonene A 263 (30000)
Linseed oil A 438
Mesitylene A 621
Mesityl oxide A 344, V 823 (20), 1037 (1)
Methanamide (see Formamide)
Methane O 556, A 632, 537, 540 Z, V 961 (20), 1050 (10)
Methanol (see Methyl alcohol)
Methone A 506
<i>o</i> -Methoxyaniline (see <i>o</i> -Anisidine)
2-Methoxyethanol (see Ethyleneglycolmonomethyl ether)
Methyl acetate A 654, 502, V 816 (20), 1028 (2)
Methyl alcohol O 555, 500, 461, A 574, 470, 464, 385 Z, V 820 (20), 1040 (1)
Methylamine O 400, A 430
Methylaniline (see Toluidine)
2-Methylbiphenyl A 502 (12000)
Methyl bromide A 537
2-Methylbutane O 294, A 420, 427 (6000)
2-Methyl-2-butanol (see <i>t</i> -Amyl alcohol)
3-Methyl-1-butanol (see <i>i</i> -Amyl alcohol)
3-Methyl-1-butene A 374 (6000)
1-Methyl-2- <i>t</i> -butylcyclohexane A 314 (12000)
1-Methyl-3- <i>t</i> -butylcyclohexane (high boiling isomer) A 304 (12000)
1-Methyl-3- <i>t</i> -butylcyclohexane (low boiling isomer) A 291 (24000)
Methylbutyl ketone A 533
Methyl cellosolve (see Ethyleneglycolmonomethyl ether)
Methyl chloride A 632

TABLE 1 (continued)

Methyl cyanide (see Acetonitrile)
Methylcyclohexane O 285, A 265 (108000), 250z
Methylcyclohexanone A 598
Methylcyclopentane O 329, A 323 (6000), V 812 (20), 1013 (1)
Methyl cyclopentadiene A 445z
2-Methyldecane A 231
Methylenedichloride (see Methylene chloride)
1-Methyl-3,5-diethylbenzene A 461 (12000)
Methylene chloride O 606, A 642, 662, 615 Z, V 902 (20), 1085 (2)
Methyl ether (see Dimethyl ether)
1-Methyl-2-ethylbenzene A 447 (18000)
1-Methyl-3-ethylbenzene A 485 (18000)
1-Methyl-4-ethylbenzene A 483 (12000)
Methylethyl ether A 190
Methylethyl ketone A 514, 505, V 804 (20), 975 (!)
Methyl ethylketone peroxide A 390z
2-Methyl-3-ethylpentane A 461
Methylformate A 236, 449, 465z, V 797 (20), 1026 (2)
Methylheptenone A 534
Methylcyclohexanol A 295z
Methylhexyl ketone A 572
Methylisopropylcarbinol (see <i>s</i> -Amyl alcohol)
Methyl lactate A 385
1-Methylnaphthalene A 566, 547 (24000), 553, 530z
2-Methylnonane A 214 (102000)
2-Methylpropanal (see <i>iso</i> -Butyraldehyde)
2-Methyloctane A 227 (66000)
3-Methyloctane A 228 (60000)
4-Methyloctane A 232 (6000)
2-Methylpentane O 275, A 306, 306 (6000)
3-Methylpentane A 304 (12000)
2-Methyl-1-pentene A 306 (6000)
4-Methyl-1-pentene A 304 (12000)
4-Methyl-3-pentene-2-one (see Mesityl oxide)
2-Methyl-1-propanol (see <i>i</i> -Butyl alcohol)
α -Methylpropyl alcohol (see <i>s</i> -Butyl alcohol)
2-Methyl propane (see <i>i</i> -Butane)
2-Methylpropene A 465
Methylpropionate A 469
Methyl- <i>n</i> -propyl ketone A 505, V 832 (20), 1020 (1)
2-Methylpyridine (see α -Picoline)
Methyl salicylate A 544
2-Methyltetrahydrofuran (see tetrahydrofuran)
Methylstyrene A 495 Z
Monoethanolamine V 780 (20), 1006 (1)
Monoisopropyl bicyclohexyl A 230 A

(continues)

TABLE 1 (continued)

Monoisopropyl biphenyl A 435z
Monoisopropylxylenes V 798 (20), 1040 (1)
Naphthalene O 630, 560, A 587, 568, 526z
Neatsfoot oil A 442
Neohexane (see 2,2-Dimethylbutane)
Nicotene O 235, A 244
Nitrobenzene A 556, 482, V 706 (20), 884 (1)
Nitroethane A 415, V 623 (20), 762 (1)
Nitroglycerol A 270
Nitromethane A 415, V 684 (20), 784 (1)
1-Nitropropane A 417
2-Nitropropane A 428
<i>o</i> -Nitrotoluene V 672 (20), 837 (1)
<i>m</i> -Nitrotoluene V 711 (20), 911 (1)
<i>n</i> -Nonadecane A 237
<i>n</i> -Nonane A 285, 234 (6000), 205z
<i>n</i> -Octadecane A 235
1-Octadecene A 251
Octadecyl alcohol O 270
Octahydroanthracene O 315
<i>n</i> -Octane O 208, A 458, 218, 240 (54000)
<i>i</i> -Octane (see 2,2,4-Trimethylpentane)
1-Octene A 256 (72000)
Octyleneglycol A 335
Olive Oil A 441
Oxalic acid O 640
Oxybutyraldehyde (see Aldol)
Palm Oil A 343
Paraldehyde A 541, 424, V 846 (20), 1064 (1)
Pentanethylene glycol A 335z
<i>n</i> -Pentane O 300, 258, A 579, 290, 284 (24000)
<i>i</i> -Pentane (see 2-Methylbutane)
1-Pentene A 298 (18000)
1-Pentanol (see <i>n</i> -Amyl alcohol)
2-Pentanone (see Methylpropyl ketone)
γ -Pentylene oxide (see Tetrahydrofuran)
Perfluorodimethylcyclohexane A 651 (6000)
<i>p</i> -Phenetidine V 822 (20), 1004 (10)
Phenol O 574, 500, A 715
Phenylamine (see Aniline)
Phenylaniline (see Diphenylamine)
Phenylbromide (see Bromobenzene)
Phenyl carbinol (see Benzyl alcohol)
Phenyl chloride (see Chlorobenzene)
<i>N</i> -Phenyldiethylamine (see Diethylaniline)
Phenylethane (see Ethylbenzene)
Phenylethylene (see Styrene)

TABLE 1 (continued)

Phenylmethyl ether (see Anisole)
Phenylmethyl ketone (see Acetophenone)
Phosphorus (yellow) A 30
Phosphorus (red) A 260
Phosphorus sesquisulfide A 100
Phthalic anhydride A 584, 530z
α -Picolene A 538, 500 Z, V 846 (20), 1037 (20)
Picric acid A 300
Pinene O 275, A 263 (60000), V 797 (20), 1039 (1)
Propandiol A 410 Z
Propane O 468, A 493, 450z, 466, 504 (6000)
1-Propanol (see <i>n</i> -Propyl alcohol)
2-Propanol (see <i>i</i> -Propyl alcohol)
2-Propanone (see Acetone)
Propenal (see Acrolein)
Propene 423z, A 458
Propen-1-ol (see Allyl alcohol)
Propene oxide (see Propylene oxide)
Propionaldehyde A 419
<i>n</i> -Propionic acid A 596
<i>n</i> -Propyl acetate O 388, A 662, 450, V 828 (20), 1060 (2)
<i>i</i> -Propyl acetate O 448, A 572, 460, 476
<i>n</i> -Propyl alcohol O 445, 370, 328, A 505, 540, 439, 433, N (i3) V 811 (20), 1007 (1)
<i>i</i> -Propyl alcohol O 512, A 590, 620, 456, V 811 (20), 1050 (1)
<i>n</i> -Propylamine A 318
<i>i</i> -Propylamine A 402
<i>n</i> -Propylbenzene A 456 (12000)
<i>i</i> -Propylbenzene (see Cumene)
2-Propylbiphenyl A 452 (18000), 440 Z
Propyl bromide O 255, A 490
Propyl chloride A 520
<i>i</i> -Propyl chloride A 593
Propylcyclopentane A 285
Propylene (see Propene)
Propylenealdehyde (see Crotonaldehyde)
Propylene dichloride A 557, V 790 (20), 1012 (2)
Propylene glycol O 392, A 421
Propylene oxide V 748 (10), 870 (1)
<i>i</i> -Propyl ether (see Diisopropyl ether)
<i>n</i> -Propyl formate A 455
<i>n</i> -Propyl nitrate A 175 Z
<i>i</i> -Propyl formate A 485
4- <i>iso</i> -propylheptane A 288
<i>p</i> - <i>iso</i> -propyltoluene (see <i>p</i> -Cymene)
Pseudocumene (see pseudo-Cumene)
Pulegon A 426

(continues)

TABLE 1 (continued)

Pyridine A 482, 574, V 745 (20), 1014 (1)
Pyrogallol O 510
Quinoline A 480
Quinone O 575
Rape seed oil A 446
Rosin oil A 342
Salicylaldehyde V 772 (20), 1015 (1)
Soya bean oil A 445
Stearic acid O 250, A 395
Styrene O 450, A 490, V 777 (20), 1065 (1)
Sugar O 378, A 385
Sulfur A 232
Tannic acid A 527
Tartaric acid A 428
<i>p</i> -Tephenyl A 535 Z
Tetraaryl salicylate A 577 (6000)
<i>n</i> -Tetradecane A 232
1-Tetradecane A 239 (66000), 255
1,2,3,4-Tetrahydrobenzene (see Cyclohexene)
Tetrahydrofurfuryl alcohol O 273, A 282, V 793 (20) 980 (1)
Tetrahydronaphthalene O 420, A 423 (6000) 385z, V 819 (20), 1030 (1)
Tetrahydrosylvan V 794 (20), 1025 (1)
Tetraisobutylene A 415
<i>n</i> -Tetradecane A 200 Z
Tetralin (see Tetrahydronaphthalene)
Tetramethylbenzene V 791 (20), 1030 (1)
Tetramethylene glycol A 390z
2,2,3,4-Tetramethylpentane A 437 (24000), 514
Toluene O 552, 640, 516, A 810, 633, 552, 540, 480z, 568 (48000), 635, V 830 (20), 1057 (1)
<i>o</i> -Toluidine A 537, 482, V 832 (20), 1040 (3)
<i>m</i> -Toluidine A 580, V 846 (1), 1062 (2)
<i>p</i> -Toluidine A 482
Tributyl citrate A 368
Trichloroethylene O 419, A 463, 420 Z, V 771 (10), 950 (1)
Trichloro-1-(pentafluoroethyl)-4-(trifluoromethyl) benzene A 568
Tricresyl phosphate A 600
Triethyleneglycol O 244, A 371
Triethylenetetramine A 388
Triisobutylenes A 413, V 789 (20), 1060 (1)
1,2,3-Trimethylbenzene A 479 (24000), 510
1,2,4-Trimethylbenzene A 521 (24000), 528
1,3,5-Trimethylbenzene A 550 (48000), 577
2,2,3-Trimethylbutane A 454 (18000), 420 Z
2,3,3-Trimethyl-1-butene A 383 (12000)
Trimethylene glycol A 400 Z
2,5,5-Trimethylheptane A 485
2,2,3-Trimethylpentane A 436 (24000)

TABLE 1 (continued)

2,2,4-Trimethylpentane	O 283, A 561, 434, 447 (12000), 515, 415z, V 786 (20), 996 (2)
2,3,3-Trimethylpentane	A 430 (12000)
2,3,4-Trimethyl-1-pentene	A 257 (12000)
2,4,4-Trimethyl-1-pentene (cf. Diisobutylenes)	A 420 (12000)
2,4,4-Trimethyl-2-pentene (cf. Diisobutylenes)	A 308 (30000)
3,4,4-Trimethyl-2-pentene	A 330 (24000)
2,4,6-Trimethyl-1,3,5-trioxane (see Paraldehyde)	
Trinitrophenol (see Picric acid)	
Trioxane	A 424, 414
Tritolyl phosphate (see Tricresyl phosphate)	
Tung oil	A 456
Turkey red oil	A 445
Turpentine	A 252, 255, V 780 (20), 996 (1)
Vinyl acetate	A 427
Vinylcyclohexane	A 269
Vinyl ether (see Divinyl ether)	
Vinylethyl ether	A 201
Vinyl-2-ethylhexyl ether	A 201
Vinylisopropyl ether	A 272
<i>o</i> -Xylene	A 496, 465 Z, 501 (30000), 551
<i>m</i> -Xylene	A 563 (54000), 652, 530 Z
<i>p</i> -Xylene	A 618, 564 (42000), 657, 530 Z
Zinc stearate	A 421

Minimum Spark Ignition Energies and Quenching Distances

Most of the data presented in Table 1 are taken from Calcote *et al.* [*Ind. Eng. Chem.* **44**, 2656 (1952)]. Additional data by Blanc *et al.* [Third Symp. (Int'l) on Combustion, p. 363 (1949)] and Meltzer [NACA RM E53H31 (1953) and NACA RM E52 F27 (1952)] given in the table are designated by the letters b and m, respectively, in parentheses. Since the values for the least minimum ignition energy given by Meltzer were extrapolated from low pressures, these values were not given if a value by Calcote *et al.*, or Blanc *et al.* were available.

The column labeled plain contains data from $\frac{1}{8}$ inch rod electrodes and that labeled flange contains data for the negative electrode flanged on the other an $\frac{1}{8}$ inch rod. Values in parentheses are taken from a Calcote *et al.* correlation between the two different types of electrode sets.

Quenching distances can be obtained from the data presented in Table 1 and the correlation given as Fig. 5 of Chapter 7. It is interesting to note that most stable fuels have a least minimum ignition energy in the region of 0.2 mJ.

TABLE 1

Minimum spark ignition energy data fuels in air at 1 atm pressure

Fuel	Minimum ignition energy $\phi = 1 \times 10^{-4}$ J		Least minimum ignition energy ($\times 10^{-4}$ J)	ϕ Value for least minimum ignition energy
	Plain	Flange		
Acetaldehyde	3.76	(5.7)		
Acetone	11.5	(21.5)		
Acetylene	0.2	0.3	0.2	1.0
Acrolein	(1.37)	1.75	1.6 (m)	
Allyl chloride	7.75	13.5		
Benzene	5.5	(9.1) 7.8 (b)	2.25 (b)	1.8
1,3-Butadiene	(1.75)	(2.35)	1.25	1.4
<i>n</i> -Butane	7.6 (n)	7.0 (b)	2.6 (b)	1.5
Butane, 2,2-dimethyl-	16.4	(33)	2.5 (m)	1.4
Butane, 2-methyl-	7.0	9.6	2.1 (m)	1.3
<i>n</i> -Butyl chloride	(12.4)	23.5		
Carbon disulfide	0.15	0.39		
Cyclohexane	13.8	(26.5), 10 (b)	2.23 (m)	1.6
Cyclohexane, methyl-			2.7 (m)	1.8
Cyclohexene	(5.25)	8.6		
Cyclopentadiene	6.7	(11.4)		
Cyclopentane	(5.4)	8.3		
Cyclopropane	2.4	(3.4), 4.0 (b)	1.8 (b)	1.4
Diethylether	4.9	(7.9), 5.3 (b)	1.9 (b)	1.5
Dehydrogran	(3.65)	5.6		
Diisopropyl ether	11.4	(21.4)		
Dimethoxymethane	4.2	6.6		

(continues)

TABLE 1 (continued)

Fuel	Minimum ignition energy $\phi = 1 \times 10^{-4}$ J		Least minimum ignition energy ($\times 10^{-4}$ J)	ϕ Value for least minimum ignition energy
	Plain	Flange		
Dimethyl ether	(3.3) 2.9	4.5		
Dimethyl sulfide	(4.8)	7.6		
Di- <i>t</i> -butyl peroxide	(4.1)	6.5		
Ethane	(2.86)	4.2, 3.2 (b)	2.4 (b)	1.2
Ethene	0.96	(1.14)	1.24 (m)	1.1
Ethylacetate	14.2	(28)	4.8	1.2
Ethylamine	24	52		
Ethylene oxide	0.87	1.05	0.62	1.3
Ethylenimine	4.8	(7.8)		
Furan	2.25	(3.28)		
Furan, tetrahydro-	5.4 (n)			
Furan, thio- (Thiophene)	(3.9)	6		
<i>n</i> -Heptane	7.0	11.5, 11 (b)	2.4 (b)	1.8
1-Heptyne	(5.6)	9.31		
Hexane	9.5 (m)	9.7 (b)	2.48 (b)	1.7
Hydrogen	0.2	0.3	0.18	0.8
Hydrogen sulfide	(0.68)	0.77		

Isopropyl alcohol	6.5	(11.1)		
Isopropylamine	(20)	41		
Isopropyl chloride	(15.5)	31		
Isopropyl mercaptane	(5.3)	8.7		
Methane	4.7, 3.3 (m)	(7.1), 3.3 (b)	2.8 (b)	0.9
Methanol	2.15	(3.0)	1.4 (m)	1.3
Methyl acetylene	1.52	(2)	1.2	1.4
Methyl ethyl ketone	(6.8) 5.3	11	2.8	1.4
Methyl formate	(4.0)	6.2		
<i>n</i> -Pentane			2.2 (m)	1.3
<i>n</i> -Pentane, 2,4,4-trimethyl-(isooctane)	13.5	29	2.8 (m)	
1-Pentene, 2,4,4-trimethyl-(dissobutene)	(6)	17.5		
<i>n</i> -Pentane, 2,4,4-trimethyl- (isooctane)	13.5	29	2.8 (m)	
1-Pentene, 2,4,4-trimethyl- (dissobutene)	(6)	17.5		
2-Pentene	(5.1) 4.7		1.8 (m)	1.6
Propane	3.05	5, 4.0 (b)	2.5	1.3
Propane, 2,2-dimethyl- (neopentane)	15.7	(31)		
Propane, 2-methyl- (isobutane)	(5.2)	8.5		
Propene	2.82	(4.18) 4.1		
Propionaldehyde	(3.25)	4.9		
<i>n</i> -Propyl chloride	(10.8)	20		
Propylenoxide	1.9	2.1	1.4	1.4
Tetrahydropyran	12.1	(23)	2.2 (m)	1.7
Triethylamine	(7.5) 11.5	13		
Treptane	10	(18.2)		
Vinyl acetate	(7.0)	12.0		
Vinyl acetylene	0.822	(0.95)		

Author Index

A

Aders, W. K., 94, 106
Allen, J. P., 341, 383
Antaki, P., 394, 409
Appleton, J. P., 338, 382, 402, 403, 410,
Aref'yev, K. M., 404, 410
Aronowitz, D., 94, 106
Arrhenius, S., 34, 50
Astholz, D. C., 102, 106

B

Bachmeier, F., 333, 334, 336, 382
Baldwin, A. C., 82, 105
Barenblatt, G. I., 116, 195, 295, 316
Barnard, J. A., 96, 106
Barnett, C. M., 312, 313, 317
Barrett, R. E., 357, 358, 361, 383
Baulch, D. L., 59, 105
Belles, F. E., 231, 237, 309, 312, 313, 314,
317
Benson, S. W., 31, 33, 36, 50, 76, 77, 79,
82, 105
Berkau, E. E., 337, 382
Berry, A.G.U., 375, 384
Bettens, B., 101, 106
Bilger, R. W., 163, 196
Bird, R. B., 115, 116, 194
Bittner, J. D., 100, 106, 361, 363, 383

Blacet, F. R., 325, 382
Blackshear, P. L., Jr., 262, 290, 392, 409
Blanc, M. V., 309, 312, 314, 317
Blasius, H., 283, 291
Blazowski, W. S., 365, 384
Blokh, A. G., 404, 410
Blumenberg, B., 91, 92, 101, 105
Bodenstein, M., 41, 50
Boedecker, L. R., 245, 290, 371, 384
Bonini, J., 368, 384
Botha, J. P., 134, 195
Bowden, F. P., 235, 237
Bowman, C. T., 94, 106, 331, 332, 359, 361,
374, 382, 383
Brabbs, T. A., 83, 105
Bracco, F. V., 342, 383
Bradley, J. N., 42, 50, 57, 105, 108, 112,
150, 151, 156, 194
Branch, M. C., 343, 344, 383
Bray, K.N.C., 164, 195
Brezinsky, K., 88, 90, 94, 100, 102, 103,
104, 105, 106, 315, 317
Broida, H. P., 351, 383
Brokaw, R. S., 63, 65, 83, 105, 139, 195,
391, 409
Brzustowski, T. A., 387, 409
Buckmaster, J. D., 116, 195
Bulfalini, M., 324, 325, 326, 382
Bull, D. C., 228, 237
Burke, E. J., 94, 106, 116, 195, 248, 250,
290

C

- Calcote, H. F., 136, 195, 312, 313, 317, 361, 363, 365, 383
 Caldwell, F. R., 133, 195
 Cambel, A. B., 192, 196
 Carr, R. E., 272, 279, 280, 291
 Cashdollar, K. L., 314, 317
 Cernansky, N. P., 341, 383
 Chapman, D. L., 201, 207, 236
 Chapman, S., 376, 384
 Chiu, H. H., 280, 291
 Choudbury, A. P. R., 191, 192, 196
 Cicerone, R. J., 380, 385
 Clark, G., 21, 30
 Clarke, A. E., 365, 384
 Clary, D. W., 94, 100, 106, 364, 371, 384
 Clavin, P., 178, 195
 Clingman, W. H., Jr., 139, 195
 Coffin, K. P., 387, 391, 409
 Cole, J. A., 94, 105
 Colket, M. B., III, 95, 100, 106
 Contic, R. S., 314, 317
 Conway, J. B., 387, 409
 Cook, M. A., 235, 237
 Corley, T. L., 361, 383
 Courant, R. W., 341, 383
 Coward, H. J., 142, 195
 Crutzen, P. J., 377, 385
 Cullis, C. F., 346, 347, 350, 383
 Cullis, H. F., 361, 362, 383
 Cunningham, A. C., 241, 251, 253, 254, 290
 Curtiss, C. F., 115, 116, 194
 Cypres, R., 101, 106

D

- Dabora, E. K., 235, 237
 Dainton, F. S., 42, 50, 56, 105, 326, 382
 D'Allesio, A., 371, 384
 Damkohler, G. Z., 175, 195
 Darrieus, G., 172, 195
 Dasch, C. J., 373, 384
 Davis, W. C., 201, 236
 Denny, V. E., 276, 277, 291
 deSoete, C. C., 339, 360, 361, 382, 383
 Diehl, L. A., 341, 382
 Di Lorenzo, A., 371, 384
 Dobbins, R. A., 371, 373, 384

- Dobbs, G. M., 245, 290, 371, 384
 Dorfman, R. C., 240, 241, 242, 243, 244, 290, 371, 384
 Doring, W., 202, 223, 236
 Dryer, F. L., 38, 45, 48, 50, 57, 61, 62, 63, 66, 67, 83, 85, 86, 88, 89, 90, 91, 93, 94, 95, 96, 97, 105, 106, 113, 135, 136, 194, 223, 236, 315, 317, 342, 367, 383, 409
 Durant, J., 102, 106

E

- Eberius, K. H., 333, 334, 335, 336, 382
 Edelman, R. B., 182, 195
 Edgeworth-Johnstone, R., 375, 384
 Edwards, D. H., 231, 237
 Ekmann, J. M., 359, 360, 361, 383
 Elsworth, J. E., 228, 237
 Emmons, H. W., 284, 291
 Engel, C. D., 228, 237

F

- Fenimore, C. P., 331, 339, 382
 Fetting, F., 191, 196
 Feugier, A., 375, 384
 Fickett, W., 201, 236
 Fields, J. P., 183, 184, 188, 195
 Fineman, S., 288, 291
 Flagan, R. C., 338, 382
 Flock, E. S., 133, 195
 Flower, W., 374, 384
 Fontijn, A., 38, 50
 Frank-Kamenetskii, D. A., 298, 302, 317, 388, 409
 Frenklach, M., 94, 100, 106, 364, 371, 384
 Friedman, R., 116, 195, 198, 236
 Fristrom, R. M., 85, 105, 134, 195
 Frost, E. E., 188, 196

G

- Galant, S., 338, 382
 Gardiner, W. C., Jr., 57, 94, 100, 106, 364, 384
 Garner, F. H., 365, 384
 Gaydon, A. G., 239, 290

Gershenzen, Y. M., 351, 383
 Gerstein, M., 132, 195
 Gibbs, G. J., 136, 195
 Gilmer, R. B., 312, 313, 317
 Glassman, I., 19, 20, 21, 30, 38, 48, 50, 66,
 67, 85, 86, 88, 89, 90, 94, 95, 96, 97,
 101, 102, 103, 104, 105, 106, 223, 225,
 236, 241, 290, 315, 317, 361, 363, 365,
 366, 367, 368, 369, 370, 371, 374, 383,
 387, 394, 409
 Godsave, G. A. E., 272, 274, 279, 291
 Golden, D. M., 82, 90, 105
 Goldsmith, M., 272, 279, 291
 Gomez, A., 241, 290, 365, 370, 371, 384
 Gordon, A. S., 65, 105
 Gordon, S., 19, 20, 30, 218, 221, 236
 Grebe, J., 93, 94, 97, 105
 Gregory, C. A., Jr., 312, 313, 317
 Grosse, A. V., 387, 409
 Guest, P. G., 309, 312, 314, 317
 Guirao, C., 228, 237

H

Hainer, R. M., 305, 317
 Hargraves, K. J. A., 341, 382
 Harris, S. J., 368, 373, 384
 Harrison, P. L., 387, 409
 Harsha, P. T., 182, 195
 Harst, P. L., 354, 383
 Harvey, R., 341, 382
 Hawthorne, W. R., 242, 254, 255, 290
 Hayhurst, A. N., 336, 382
 Haynes, B. S., 334, 339, 340, 361, 363, 371,
 375, 382, 383, 384
 Hazard, H. R., 341, 382
 Hertzberg, M., 314, 317
 Hibbard, R. R., 365, 369, 384
 Hinshelwood, C. N., 295, 316
 Hirschfelder, J. O., 115, 116, 194
 Hjerhager, B. H., 365, 384
 Homann, K. H., 93, 94, 97, 105, 361, 362,
 363, 383
 Hottel, H. C., 48, 50, 135, 178, 195, 242,
 254, 255, 290
 Howard, J. B., 100, 106, 361, 363, 383
 Hoyer mann, K., 91, 92, 101, 105
 Hubbard, G. L., 276, 277, 291
 Huff, V. N., 9, 19, 30
 Hummell, J. D., 357, 358, 361, 383

Hunt, B. G., 376, 384
 Hunter, T. C., 365, 384
 Hunziker, H. E., 91, 92, 105

I

Ibberson, V. J., 96, 106
 Irvin, K. J., 326, 382
 Iverach, D., 334, 339, 340, 382

J

Johnson, G. M., 341, 347, 383
 Johnston, H., 378, 379, 380, 383
 Jones, A. J., 231, 237
 Jones, O. W., 142, 195
 Jost, W., 307, 312, 317
 Jouguet, E., 201, 210, 236
 Just, T., 333, 334, 335, 336, 382

K

Kanury, A. M., 272, 291, 312, 317
 Kaufman, F., 38, 50
 Kee, R. J., 92, 105, 343, 344, 383
 Kent, J., 373, 384
 Kern, J., 241, 290
 Kesten, A. S., 342, 383
 Khudyakov, L., 255, 290
 Kibeley, V., 176, 195
 King, M. K., 394, 395, 410
 Kirov, N. Y., 334, 339, 340, 382
 Klimov, A. M., 173, 195
 Knepe, H., 91, 92, 105
 Knipe, R., 65, 105
 Knorre, G. F., 404, 410
 Kompaneets, A. S., 201, 236
 Kruger, C. H., Jr., 36, 37, 39, 50
 Kynstantas, R., 228, 237

L

Landau, L., 39, 50, 172, 195
 Larson, C. W., 90, 105
 Law, A. V., 276, 291
 Law, C. K., 275, 276, 277, 278, 291

Leason, D. B., 139, 195
 Le Chateleier, H. L., 114, 194
 Lee, J. H., 199, 200, 201, 202, 226, 236,
 228, 230, 237
 Leighton, P. A., 321, 323, 324, 382
 Leonard, R. A., 334, 382
 Levine, O., 132, 195
 Levy, A., 338, 340, 341, 346, 350, 354, 355,
 360, 382, 383
 Lewis, B., 56, 57, 60, 63, 64, 105, 115, 147,
 148, 152, 153, 194, 220, 222, 232, 248,
 250, 290, 309, 312, 314, 317
 Libby, P. A., 164, 167, 195
 Libouton, J. C., 227, 237
 Librovich, V. B., 116, 195, 295, 316
 Lindemann, F. A., 33, 44, 50
 Litzinger, T. A., 88, 102, 103, 104, 105
 Longwell, J. P., 178, 188, 195
 Lorell, J., 272, 279, 280, 291
 Ludford, G. S. S., 116, 195
 Lui, T. M., 280, 291
 Lyon, R. K., 343, 383

M

Macek, A., 387, 409
 Magnussen, B. F., 365, 384
 Mahnen, G., 91, 105
 Makviladze, G. M., 116, 195, 295, 316
 Mallard, E., 114, 194
 Mallard, W. G., 240, 241, 242, 243, 244,
 290, 384
 Mannheimer-Timnat, Y., 369, 374, 384
 Marble, F. E., 187, 188, 195, 196
 Markstein, G. H., 172, 195
 Martenay, P. J., 331, 382
 Martin, G. B., 337, 382
 Marvin, C. S., Jr., 133, 195
 Mascolo, R. W., 176, 195
 McBride, B. J., 19, 20, 30, 218, 221, 236
 Mellor, A. M., 334, 382, 387, 409
 Menchem, S. T., 365, 384
 Merryman, E. L., 341, 346, 350, 354, 355,
 383
 Metcalfe, E., 228, 237
 Miller, J. A., 92, 105, 343, 344, 383
 Miller, J. H., 240, 241, 242, 243, 244, 290,
 371, 384
 Miller, W. J., 364, 384
 Milliken, R. C., 366, 384
 Mills, A. F., 276, 277, 291

Minkoff, G. J., 74, 105
 Mitchell, R. E., 92, 105
 Molina, M. I., 380, 385
 Morcomb, J. T., 361, 383
 Morell, V. E., 9, 19, 30
 Morgan, A. G., 48, 50
 Mulcahy, M. F. R., 341, 346, 347, 350, 383,
 398, 399, 400, 401, 410
 Muller, C. H., 351, 383
 Mullins, B. P., 294, 307, 316, 317
 Mulvihill, J. N., 338, 382
 Myerson, A. L., 342, 354, 383

N

Naegeli, D. W., 38, 50, 66, 95, 100, 105,
 106, 223, 236, 394, 409
 Nagle, J., 402, 403, 410
 Naltandyan, A. B., 351, 383
 Nerheim, N. M., 135, 178, 195
 Nicholson, H. M., 183, 184, 188, 195
 Norris, R. G. W., 96, 106
 Norton, T. S., 94, 95, 96, 106

O

Olson, D. B., 57, 105
 Oppenheim, A. K., 200, 236

P

Palmer, H. B., 361, 362, 383
 Palmer, K. N., 235, 237
 Pease, R. N., 115, 139, 194, 195
 Penner, S. S., 32, 50, 116, 195, 272, 279,
 291
 Peters, J., 91, 105
 Phillips, L. F., 338, 382
 Phillips, P. E., 231, 237
 Plee, S. L., 334, 382
 Powling, J., 133, 195
 Putnam, A. A., 192, 196

R

Rabitz, 45, 50
 Ramachandra, M. K., 371, 384
 Reid, W. T., 357, 358, 361, 383

Reiter, S. H., 176, 195
 Ried, W. T., 346, 354, 355, 383
 Roeder, C. H., 133, 195
 Roper, F. G., 241, 251, 253, 254, 290, 341,
 382
 Rowland, F. S., 380, 385

S

Sachjan, G. A., 351, 383
 Santoro, R. J., 94, 96, 101, 106, 240, 241,
 242, 243, 244, 290, 371, 373, 384
 Sawyer, R. F., 19, 20, 30, 223, 225, 236,
 341, 383
 Schalla, R. L., 365, 369, 384
 Schelkin, K. I., 177, 195, 229, 237
 Schneider, G. R., 135, 178, 195
 Schofield, K., 351, 383
 Schug, K. P., 369, 374, 384
 Schumann, T. E. W., 248, 250, 290
 Schwartz, H. A., 31, 33, 36, 50
 Scurlock, A. C., 186, 195
 Seery, D. V., 331, 382
 Semenov, N. N., 73, 75, 105, 115, 194, 295,
 298, 307, 316
 Semerjian, H. G., 371, 373, 384
 Sheinson, R. S., 75, 105
 Shuff, P. J., 228, 237
 Sichel, M., 235, 237
 Sidebotham, G., 241, 290, 365, 370, 371,
 384
 Sievert, R., 91, 92, 101, 105
 Sirignano, W. A., 277, 278, 291
 Smith, C., 241, 251, 253, 254, 290
 Smith, D. B., 341, 382
 Smith, I. W. M., 66, 105, 398, 399, 400,
 401, 410
 Smith, M. Y., 341, 347, 383
 Smith, O. I., 361, 383
 Smooke, M. D., 92, 105
 Smyth, K. C., 240, 241, 242, 243, 244, 290,
 371, 384
 Spalding, D. B., 134, 148, 149, 153, 188,
 189, 190, 195, 196, 262, 290, 291
 Spengler, G., 241, 290
 Stein, S. E., 94, 100, 106, 364, 384
 Steinberg, M., 351, 383
 Stolarski, R. S., 380, 385
 Strauss, W. A., 235, 237
 Street, J. C., 365, 384
 Strehlow, R. A., 220, 228, 236, 237

Strickland-Constable, R. F., 402, 403, 410
 Sullivan, H. F., 387, 409
 Sulmistras, A., 228, 237
 Summerfield, M., 176, 195
 Swett, C. C., 309, 312, 313, 314, 317

T

Takahashi, F., 366, 368, 384
 Talley, C. P., 387, 409
 Tanford, C., 115, 194
 Taylor, F. R., 354, 383
 Taylor, G. W., 96, 106
 Teller, E., 39, 50
 Thomas, A., 365, 384
 Tipper, C. F. H., 75, 105
 Todes, O. M., 307, 317
 Tonkin, P. S., 235, 237
 Troe, J., 45, 46, 50, 102, 106
 Troshin, Y. K., 229, 237
 Tsiang, W., 96, 106
 Tully, F. P., 91, 93, 105

U

Urtiew, P. A., 200, 229, 236

V

Vandooren, J., 94, 97, 99, 101, 106
 Vandsburger, U., 371, 373, 374, 383
 Van Tiggelen, P. J., 94, 97, 99, 101, 106,
 227, 237
 Venkat, C., 100, 103, 104, 106
 Vince, I. M., 336, 382
 Vincenti, W. G., 36, 37, 39, 50
 von Elbe, G., 56, 57, 60, 63, 64, 105, 115,
 147, 148, 152, 153, 194, 220, 223, 232,
 236, 248, 250, 290, 309, 312, 314, 317
 von Karman, T., 116, 195
 von Neumann, J., 202, 223, 236

W

Wagner, H., 361, 363, 371, 373, 375, 383,
 384
 Walters, S., 380, 385
 Warnatz, J., 84, 88, 105

Weddell, D. B., 254, 255, 290
 Weiner, A. M., 368, 373, 384
 Weiss, M. A., 178, 188, 195
 Welsch, L. M., 314, 317
 Wendt, H. R., 91, 92, 105, 359, 360, 361,
 383
 Westbrook, C. K., 38, 50, 57, 59, 61, 62,
 63, 66, 67, 83, 91, 93, 94, 105, 106, 113,
 135, 136, 194, 229, 237
 Westenberg, A. A., 85, 105, 134, 195
 Weston, R. E., 31, 33, 36, 50
 Whitten, G., 378, 379, 380, 385
 Wilhelm, R. H., 191, 196
 Williams, D. V., 341, 347, 383
 Williams, F. A., 32, 43, 50, 116, 164, 167,
 173, 178, 182, 183, 185, 192, 195, 201,
 230, 231, 236, 247, 251, 276, 283, 290,
 291, 394, 409
 Williams, F. W., 75, 105
 Williams, G. C., 48, 50, 135, 178, 195
 Wise, H., 272, 279, 280, 291

Wolfhard, H., 239, 290
 Wong, E. L., 132, 195
 Wright, F. J., 365, 384

Y

Yaccarino, P., 365, 366, 369, 370, 371, 384
 Yetter, R. A., 45, 50
 Yoffee, A. D., 235, 237

Z

Zabetakis, M. G., 294, 316
 Zebatakis, K. S., 136, 138, 142, 144, 195
 Zeldovich, Y. B., 116, 201, 202, 223, 236,
 295, 309, 312, 316, 329, 382
 Zellner, R., 38, 50, 66, 105
 Zukoski, E. E., 187, 188, 195, 196

Subject Index

A

Abstraction selectivity, 88
Acetaldehyde decomposition, 49
Acetaldehyde oxidation, 79
Acetylene, 69
 oxidation, 92
Activation energy, 34
Aerosols, 319
Air pollution, 318
Alcohol oxidation, 94
Aldehydes, 68, 70, 75
 oxidation, 79
Alkyl compounds, 68
Aromatics, 69
 oxidation, 96
Arrhenius reaction rate law, 33, 34, 38
Atmospheric nitrogen kinetics, 329
Autoignition temperature, 295

B

b variable, 264, 269
Benzaldehyde, 102
Benzene, 69
 oxidation, 96
Biradical, 41
Blowoff, 151
 gradient, 154, 155
Bluff body stabilization, 182
Boron combustion, 394

Boundary layer thickness, 284
Branched chain reaction, 41, 53, 54
Bunsen burner, 59, 112
 design, 157
Burke-Schumann development, 248
Burning of condensed phases, 255
Burning of plastics, 286
Butadiene, 101

C

C_2 , 112
CH, 112
Carbon burning rate, 391
Carbon disulfide (CS_2) oxidation, 353
Carbon monoxide oxidation and explosion
 limits, 63
Carbonyl sulfide (COS) oxidation, 353
Chain branching, 41, 51, 53, 73
Chain initiation, 41, 52, 54
Chain length, 56
Chain propagation, 41, 52, 54
Chain reactions, 41
Chain termination, 41, 52, 54
Chapman-Jouguet point, 110, 201
Characteristic time, 159, 160, 166
 chemical, 159, 166, 293
 cooling, 310
 diffusion, 252
 fluid mechanical, 160
 ignition, 188, 293

Char burning, 386, 391
 Chemical kinetics, 31
 Chemical potential, 9
 Chemical thermodynamics, 1
 Closed thermodynamic systems, 2
 Coke combustion, 386, 391, 404
 ash forming, 407
 oxygen concentration dependence, 408, 409
 Coke formation, 375
 Combustion wave, *see* Flame speed
 Compression ignition, 315
 Cool flames, 73, 74
 Critical mass, 305
 Cyanogen–oxygen flame, 115
 Cycloparaffins, 69
 Cyclopentadienyl radical, 100

D

“ d^2 ” law, 256, 274
 Damkohler number, 166, 173, 188
 Dark zone in flames, 58
 Deflagration, 208, *see also* Flame speed
 Degenerate branching, 75
 Detonation, 197
 cellular, 202, 226
 dynamic parameters, 202, 230
 experimental results, 220
 limits, 231
 nongaseous media, 235
 transition to, 200
 velocity, 202, 216
 wave structure, 223
 Diffusion flames, 197, 238
 appearance, 239
 buoyancy effects, 250
 species distribution, 396
 structure, 242
 theoretical considerations, 245
 Diffusional kinetics, 388
 Droplet burning, 255, 260
 clouds, 280
 convective conditions, 221, 285
 flame position, 273
 flame temperature, 273
 with radiation, 288
 rate, 271
 refinements, 275

E

Eddy viscosity, 176, 254
 Enthalpy, 2
 Equilibrium constant, 6, 11, 40
 of formation, 14
 Equilibrium of a chemical system, 8, 19
 Equivalence ratio, 20
 Ethane oxidation, 86
 Ethanol, 70
 oxidation, 91
 Ethene (ethylene), 69
 oxidation, 91
 Ethers, 71
 Evaporation coefficient, 256, 274
 Evaporation of liquids, 257
 Explosion, 51, 198, 292
 Explosion limits, 56, 63, 72
 Explosive mixtures, 52
 Explosive reaction, 31, 55, 107

F

“Fall-off” effect in rate expressions, 49
 Fick’s law, 246
 First Law of Thermodynamics, 3
 Flames, 107, 112
 Flame compression, 171
 Flame instability (hydrodynamic), 173
 Flame radiation, 112
 Flame speed, laminar, 114
 comprehensive theories, 115
 diffusion theories, 115
 experimental results, 137, 138, 139, 460
 physical and chemical effects, 134
 thermal theories, 114, 117, 119
 Flame speed measurements, 126
 Bunen burner method, 130
 closed spherical bomb method, 132
 cylindrical tube method, 131
 flat flame burner method, 133
 soap bubble method, 132
 Flame spreading behind baffles, 183, 185, 187
 Flame stabilization (*in high velocity streams*), 183
 Flame stabilization (*low velocity*), 150
 Flame stretch, 171
 Flame structure, 111
 Flame suppressants, 87

- Flame thickness, 166
- Flame temperature, 15, 20, 21
- Flammability limits, 107, 141, 142, 143, 465
 - chemical effects, 144
 - experimental values, 143, 465
 - physical effects, 147
- Flashback, 151
- Flashback gradient, 153, 154, 155
- Flat flame burner, 133
- Forced ignition, 308
- Formaldehyde, 67
 - oxidation, 80
- Formyl radical (HCO), 76, 79
 - reactions, 81
- Fourier law of heat conduction, 256, 259
- Frank-Kamenetskii numbers, 167

G

- Gaseous fuel jets, 239
 - appearance, 239
 - phenomenological analysis, 253
 - structure, 242
 - theoretical considerations, 248
 - turbulent, 254
- Gasification, 257
- Glassman's criterion, 387
- Grashof number, 282

H

- H atom recombination, 32
- H₂-Br₂ reaction, 41, 52
- H₂-Cl₂ reaction, 53
- H₂-I₂ reaction, 40, 53
- H₂-O₂ reaction, 56
 - explosion limits, 56, 72
- HCN in flames, 233
- Heat of vaporization, 257
- Heat transfer coefficient, 258
- Heats of formation, 4, 5, 21
- Heats of reaction, 1, 3, 6
- Heterogeneous reaction rates, 388
- Homogeneous catalytic recombination, 146, 374, 377, 378, 380
- Hugoniot curve, 130, 201
- Hugoniot relationship, 119, 203
 - variation of entropy, 211
- Hybrid burning rates, 283

- Hydrocarbon oxidation, 67
 - high temperature, 85
 - low temperature, 75
 - steady reaction, 75, 76
- Hydrogen peroxide, 67, 76, 113
- Hydrogen sulfide oxidation, 349
- Hydroperoxide, 71, 75
- Hydroperoxy radical (HO₂), 60, 76, 113

I

- Ignition, 293
 - chain, 295
 - thermal, 297
- Ignition temperature, 194
- Induction intervals, 72
- Interferometry, 128
- Internal energy, 2

K

- Karlovitz flame stretch factor, 171
- Ketones, 40, 48
- Kolmogorov length, 165
- Klimov-Williams criterion, 175
- Knock and anti-knocks, 140, 315

L

- Law of heat summation, 4, 5
- Law of mass action, 17
- Le Chatelier's principle, 16
- Lewis number, 120
- Lindemann's theory of first-order processes, 33
- Longitudinally burning surface, 283
- Luminous zone in flames, 58

M

- Mallard and Le Chatelier theory of flame speed, 114
- Mass burning, 225, *see also* Droplet burning
- Mass diffusivity, 119, 251, 260
- Mass transfer with chemical reaction (burning rates), 181

Mass transfer without chemical reaction
(evaporation), 176
Metal combustion, 386
Metastable molecules, 32, 37, 44
Methane flame velocities, 85
Methane oxidation, 81
Methanol, 70
 oxidation, 94
Methoxy radical, 83, 84
2-methylpentane oxidation, 78
Methyl peroxy radical, 82
Minimum ignition energy, 301
Mole fraction, 10
Momentum diffusivity, 120, 260
Monoradical, 40

N

Negative temperature coefficients of reaction rate, 73
Newton's law of viscosity, 260
Nitrogen dioxide (NO_2), 19, 328
 formation, 340
Nitrogen oxide (NO), 16
Nitrogen oxides, 318
 structure, 328
 NO_x , 321, 326
 NO_x formation and reduction, 326, 342
 effect of flame structure, 328
non-Arrhenius behavior, 38
Nusselt number, 258, 285, 286

O

Olefins, 69
 oxidation, 90
 reactions, 322
Open thermodynamic systems, 22
Order of the reaction, 33
Organic acids, 71
Organic nomenclature, 68
Organic sulfur compounds, 355
Ozone decomposition, 49
Ozone balance, 376
 ClO_x catalytic cycle and the effect of
 fluorocarbons, 380
 HO_x catalytic cycle, 376
 NO_x catalytic cycle, 377

P

Paraffins, 68
 oxidation of, 87
Partial equilibrium assumption, 47
Partial pressure, 10
Particulate formation, 360
 from liquid hydrocarbon pyrolysis,
 375
Partition function, 37
Peroxide bonding, 79
Peroxides, 75
Peroxyacetyl nitrate (PAN), 71, 319, 321
Peroxyl radical, 78, 79
Phenyl radical, 97
Photochemical initiation, 51, 321
Photochemical oxidant, 319
Photochemical smog, 312, 319
Photodissociation of nitrogen dioxide,
 321
Photoyield, 52, 53
Plug flow reactor, 86, 179
Pollutants, 320
Prandtl number, 120, 165
Preheat zone, 113
"Prompt" NO, 331, 333
Propane oxidation, 89
Pseudo-first-order reactions, 44, 46
Pulverized coal combustion, 397
Pyridine, 337, 339

Q

Quenching distance, 141, 148, 312

R

Radiant heat flux, 259, 288
Radical isomerization, 78
Radical recombination, 39
Rates of reactions, 32
Reaction rate constant, 32
 values, 62, 448
Reaction zone thickness, 117
Recess flame stabilization, 153, 192
Recombination zone, 112
Reference state, 2
Reynold's number, 164

S

Schlieren technique, 128
Schmidt number, 120, 165
Scission rule, 89
Shadowgraph, 128
Similarity parameters, 120
Simultaneous interdependent reactions, 40
SO₂ emissions, 324, 345
Solid propellant burning, 170
Soot characteristics, 361
Soot formation, 360, 362
 diffusion flames, 369
 influence of physical and chemical parameters, 373
 premixed flames, 366
Soot particle combustion, 397
Spontaneous combustion, 387
Spontaneous ignition, 295, 297
Stability limits of laminar flames, 141
Standard state, 2
Steady reaction, 76
Steady state assumption, 42, 47
Steric factor, 35
Stirred reactors, 178, 190
Strong deflagration, 209
Strong detonation, 209
Sublimation, 257
Sulfates, 357
Sulfur compound structures, 349
Sulfur monoxide (SO), 349
 dimer (SO)₂, 349
Sulfur compound oxidation, 349
 carbon disulfide, 353
 carbonyl sulfide, 353
 elemental sulfur, 354
 hydrogen sulfide, 349
 organic sulfides, 355
Sulfur suboxide (S₂O), 349, 351
Sulfur superoxide, 354
Sulfur trioxide, 357

Superequilibrium, 332, 359
Stagnant film burning, 281

T

Taylor length (microscale), 165
Thermal diffusivity, 119, 251, 260
Thermal ignition theory, 399
Transfer number, B, 262, 273
 small B assumption, 286, 409
Transition state theory, 36
Transportation cooling, 257, 258
Turbulent flames, 159
 Clavin-Williams result, 178
 Damkohler theory, 175
 Schelkin theory, 177
 velocity, 170, 175
Turbulent fuel jet, 254
Turbulent reacting flows, 159
 regimes, 163
Turbulent reaction rate, 161
Turbulent Reynold's number, 164
Two-stage ignition, 73

V

Vinylacetylene, 101
Viscosity, 260

W

Weak deflagration, 209
Weak detonation, 209

Z

Zeldovich, Frank-Kamenetskii, Semenov
 theory of flame speed, 119
Zeldovich NO mechanism, 329

**SECOND
EDITION**

COMBUSTION

Glassman



**ACADEMIC
PRESS**

ISBN 0-12-285851-4